TESIS DOCTORAL

DERIVATIZACIÓN DE TRITERPENOS NATURALES PARA LA OBTENCIÓN DE AGENTES ANTI-CANCERÍGENOS Y ANTI-VIRALES

Marta Medina O'Donnell

Granada, 2017

UNIVERSIDAD DE GRANADA

Editor: Universidad de Granada. Tesis Doctorales
Autora: Marta Medina O'Donnell
ISBN: 978-84-9163-564-2
URI: http://hdl.handle.net/10481/48438

UNIVERSIDAD DE GRANADA

PROGRAMA DE DOCTORADO EN QUÍMICA

FACULTAD DE CIENCIAS

Departamento de Química Orgánica

TESIS DOCTORAL

Derivatización de triterpenos naturales para la obtención de agentes anti-cancerígenos y anti-virales

Marta Medina O'Donnell

Granada, 2017

Derivatización de triterpenos naturales para la obtención de agentes anti-cancerígenos y anti-virales

Por

Marta Medina O'Donnell

Departamento de Química Orgánica

Memoria presentada para aspirar al grado de Doctor por la Universidad de Granada

Marta Medina O'Donnell

Los Directores de la Tesis Doctoral:

Dr.D.Andrés Parra Sánchez

Catedrático del Dpto. de Química Orgánica. Universidad de Granada

Dr.D.Francisco Rivas Sánchez

Profesor Titular del Dpto. de Química Orgánica. Universidad de Granada

Dr.D.Fernando J. Reyes Zurita

Profesor contratado Doctor del Dpto. de Bioquímica y Biología Molecular I. Universidad de Granada

La doctoranda Marta Medina O'Donnell y los directores de la Tesis Doctoral Dr. D. Andrés Parra Sánchez, Dr. D. Francisco Rivas Sánchez y Dr. D. Fernando J. Reyes Zurita garantizamos, al firmar esta Tesis Doctoral, que el trabajo que aquí se presenta ha sido realizado por la doctoranda bajo su dirección y hasta donde nuestro conocimiento alcanza, en la realización del trabajo, se han respetado los derechos de otros autores a ser citados, cuando se han utilizado sus resultados o publicaciones.

Granada, a

Directores de la Tesis Doctoral:

Fdo.: Dr. D. Andrés Parra Sánchez Fdo.: Dr. D. Francisco Rivas Sánchez

Fdo.: Dr. D. Fernando J. Reyes Zurita

Doctoranda:

Fdo.: Marta Medina O'Donnell

Esta Tesis Doctoral ha sido realizada gracias a una beca predoctoral asociada al proyecto de investigación:

"Incremento de la biodisponibilidad y la actividad biológica de ácido maslínico e hidroxitirosol, dos compuestos procedentes de los residuos de la molturación de la aceituna, por acilación y pegilación mediante técnicas de síntesis orgánica en fase sólida" (FQM-7372, Proyectos Investigación Excelencia, Junta de Andalucía, Consejería de Innovación, Ciencia y Empresa).

AGRADECIMIENTOS

Esta Tesis Doctoral se ha llevado a cabo gracias a la inestimable dirección y continuo apoyo del Catedrático D. Andrés Parra Sánchez y de los Doctores D. Francisco Rivas Sánchez y D. Fernando J. Reyes Zurita. En especial quiero agradecer a D. Andrés Parra, por iniciarme en el mundo de la Química Orgánica con esas clases magistrales que nunca olvidaré y que han hecho que la Química Orgánica forme parte de mi vida. También, agradecerle su labor como docente, investigador y la extraordinaria calidad humana que posee. A D. Francisco Rivas, por su esfuerzo para que saliera adelante esta Tesis Doctoral, y por sus sabios consejos y enseñanzas en el mundo de la docencia. A D. Fernando J. Reyes, por todo su conocimiento sobre Biología Molecular, gracias a los cuales han permitido poner a punto muchos de los ensayos biológicos que se presentan en esta Tesis Doctoral.

Quisiera expresar, así mismo, mi agradecimiento al Catedrático D. Andrés García-Granados López de Hierro por confiar en mi desde el primer momento, y darme la oportunidad de formar parte de este Grupo de Investigación. Al Dr. D. Antonio Martínez Rodríguez, por estar siempre dispuesto a resolver cualquier duda y por su compañía a lo largo de la escritura de esta memoria.

Me gustaría agradecer al Dr. D. Ali Haïdour y a la Dra. Dª Laura Méndez Liñán, por la realización de las experiencias de Resonancia Magnética Nuclear y a D. Juan Moliz Medina y Dª Yolanda Madrid Fernández, por la realización de los espectros de masas.

A los miembros del Grupo de Investigación del Catedrático D. José Antonio Lupiáñez Cara, por permitirme el uso de todas las instalaciones de su laboratorio para llevar a cabo los ensayos biológicos. Gracias Eva y Amalia por su ayuda, ánimo y consejos.

A mis compañeros de laboratorio Nacho, Samuel y Alberto por compartir todos estos años de innumerables experimentos. Sin olvidarme

de todos aquellos que han pasado por el laboratorio durante estos años. Gracias.

A mi familia. En especial a mi padre, el que me enseñó que la palabra "no puedo" no existe en el vocabulario, un ejemplo de fortaleza. A mi madre por enseñarme a luchar en la vida y apoyarme en todo momento, a la que le debo todo. A mi hermano por su apoyo. A mis suegros por considerarme como una hija, ayudándome en todo lo que necesitaba. Gracias.

Por último, me gustaría dar las gracias a mi marido Antonio por su ayuda en la maquetación de esta memoria, y porque desde el primer momento en que nos conocimos me apoyó y me animó a perseguir mis sueños, gracias a ti, estoy donde estoy.

GLOSARIO DE TÉRMINOS Y ABREVIATURAS

AO	Ácido oleanólico (ácido 3β-hidroxiolean-12-en-28-oico)
AM	Ácido maslínico
ADN	Ácido desoxirribonucleico
ARN	Ácido ribonucleico
Ac_2O	Anhídrido acético
$[\alpha]_D$	Poder rotatorio
BAS	Enzima β-amirina
BAX	Proteína X asociada a Bcl-2
Bcl-2	Proteína asociada al linfoma de células-B de tipo 2
Boc	Grupo protector terc-butiloxicarbonilo
Boc_2O	Dicarbonato de di-terc-butilo
Caspasa	Cisteinil aspartato proteasa
^{13}C RMN	Espectro de resonancia magnética nuclear de carbono
$CHCl_3$	Cloroformo
$CDCl_3$	Cloroformo deuterado
CD_3OD	Metanol deuterado
CDDO	Ácido 2-ciano-3,12-dioxooleana-1,9(11)-dien-28-oico
CDDO-Me	CDDO-metil éster
CDDO-im	CDDO-imidazol
CDDO-MA	CDDO- metilamida
CDDO-EA	CDDO-etilamida
CDDO-TFEA	CDDO-trifluoroetilamida
CD4	Cúmulo de diferenciación 4
CCR5	Quimiocina receptora de tipo 5

COX-2	Ciclooxigenasa 2
CXCR4	Quimiocina receptora de tipo 4
δ	desplazamiento químico
d	doblete
dd	doble doblete
ddd	doble doble doblete
DCM	Diclorometano
DEPT	Distortionless Enhancement by Polarization Transfer
DMA	*N,N*'-dimetilanilina
DMEM	*Dulbecco's Modified Eagle's medium*
DMAP	Dimetilaminopiridina
DMAPP	Pirofosfato de 2-isopentenilo o pirofosfato de Dimetilalilo
DMF	*N,N*'-dimetilformamida
DMSO	Dimetilsulfóxido
DHR	Dihidrorodamina
DIEA o DIPEA	*N,N*'-diisopropiletilamina
DIPCDI	*N,N*'-diisopropilcarbodiimida
Et_3N	Trietilamina
Et_2O	Dietil éter
EtOAc	Acetato de etilo
Fmoc	9-fluorenilmetoxicarbonil
FAS	Receptor de superficie de muerte celular
FADD	Proteína asociada a Fas con dominio de muerte
FCS	Fetal Calf Serum (suero bovino fetal)
g	gramo
Gag	*Gen*-specific antigen
$Pr55^{Gag}$	Poliproteína precursora Gag del VIH-1

Gag	*Gen*-specific antigen
Gp41	Glicoproteína 41
gp120	Glicoproteína 120
HOAt	1-hidroxi-7-azabenzotriazol
HepG2	Línea celular de hepatocarcinoma
HPLC	Cromatografía líquida de alta eficacia
^{1}H RMN	Espectro de resonancia magnética nuclear de protones
HT29	Línea celular de adenocarcinoma de colon humano
IC_{50}	Concentración que inhibe la proliferación celular al 50%
IC_{80}	Concentración que inhibe la proliferación celular al 80%
IL-6	Interleuquina-6
IP	Ioduro de propidio
IPP	Pirofosfato de 3-isopentenilo o pirofosfato de isopentenilo
IR	Espectro de infrarrojo
J	Constante de acoplamiento
KBr	Bromuro de potasio
m	multiplete
MDA	Malondialdehido (marcador de la peroxidación lipídica)
Me	Metilo
MeOH	Metanol
Me_2CO	Acetona
min	Minuto
MTT	Bromuro de 3-(4,5-dimetiltiazol-2-ilo)-2,5-difeniltetrazol
m/z	Relación masa/carga
nm	Nanómetros
NF-KB	Factor nuclear de las cadenas Kappa, células B activadas
p.f	punto de fusión

p.f	punto de fusión
p24	Proteína de la cápside del VIH
P450	Complejo enzimático de monooxigenasas
PBS	Phosphate buffert saline
pNL4.3	Clon recombinante que contiene el genoma completo del VIH-1, que genera una progenie infecciosa
pNL4.3-Luc	Clon proviral derivado de pNL4.3 que contiene el gen de la luciferasa
PyAOP	Hexafluorofosfato de(7-azabenzotriazol-1-iloxi)-tris(pirrolidin)fosfonio
PEG	Polietilenglicol
ppm	Partes por millón
Rpms	Revoluciones por minuto
rt	Room temperature
Rh	Rodamina
S	singlete
SAR	Relación estructura-actividad
SIDA	Síndrome de Inmunodeficiencia Adquirida
SOFS	Síntesis Orgánica en Fase Sólida
t	triplete
TBS	Tris-buffered saline
TBTU	2-(1H-benzotriazole-1-yl)-1,1,3,3-tetramethyluronium tetrafluoroborate
TFA	Ácido trifluoroacético
THF	Tetrahidrofurano
TLC	Cromatografía en capa fina
TRAILR	Receptor implicado en la inducción de la apoptosis
TNFa	Factor de necrosis tumoral tipo alfa

TNFR	Receptor del factor de necrosis tumoral
VIH	Virus de la inmunodeficiencia humana
VSV	Virus de la estomatitis vesicular
VSV-G	Vector de VSV usado para la producción de lentivirus

INDICE

I INTRODUCCIÓN

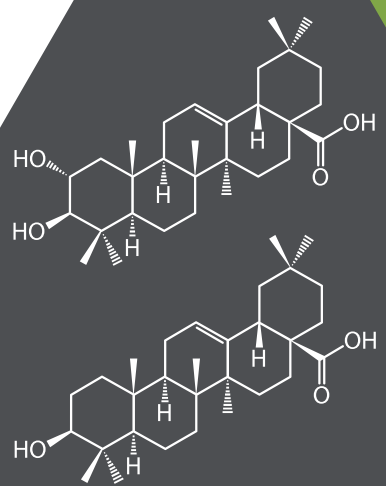

El hombre desde sus comienzos, ha estado utilizando las virtudes de las plantas para su beneficio, siendo el reino vegetal una fuente importante de nuevos agentes farmacológicos.

Una de las primeras obras de naturaleza científica, fue escrita por Dioscórides (40-90 d. c), médico militar griego y botánico considerado padre de la farmacognosia y que escribió el libro *De Materia Médica* en el cuál plasmó sus estudios sobre las propiedades de más de 900 plantas y de muchos principios activos químicos.[1] Este libro se convirtió en el principal manual de farmacopea durante toda la Edad Media y el Renacimiento.

Hoy en día el estudio de los Productos Naturales Orgánicos y sus derivados es uno de los objetivos de la Química Orgánica, representando una de las vías más eficaces para encontrar nuevos agentes terapéuticos, interrelacionando así la Química Biológica y la Médica con la Química Orgánica.[2]

Los productos naturales procedentes del reino vegetal usados con fines médicos, son en su mayoría metabolitos secundarios cuya función principal en la planta es la supervivencia, ya que muchos de ellos están implicados en los mecanismos de defensa frente al ataque de bacterias, virus y hongos, un sistema inmunitario análogo al de los animales.

Como metabolitos secundarios, los terpenos constituyen el grupo de productos naturales más extenso y diverso de terpenoides, con más de 25.000 compuestos.[3] Se les atribuye actividades farmacológicas importantes que los convierten en potenciales agentes terapéuticos. Entre ellos encontramos a los esteroles, saponinas, glucósidos cardiacos y terpenos modificados.

[1] Hassan, H. M. a. A Short History of the Use of Plants as Medicines from Ancient Times. *Chim. Int. J. Chem.* **69,** 622–623 (2015).
[2] Kumar, K. & Waldmann, H. Synthesis of natural product inspired compound collections. *Angew. Chemie - Int. Ed.* **48,** 3224–3242 (2009).
[3] Hill, R. A. & Connolly, J. D. Triterpenoids. *Nat. Prod. Rep.* **34**, 90–122 (2017).

Teniendo en cuenta los siguientes factores, como son: el extenso campo de aplicación de estos terpenos, el creciente interés en la utilización terapéutica y alimentaria, el uso abusivo o incorrecto de los medicamentos sintéticos que conlleva una terapia ineficaz y la aparición de efectos secundarios, se hace necesario el estudio y búsqueda de nuevas moléculas bioactivas.[4]

Nuestro grupo de investigación, "Biotecnología y Química de Productos Naturales", trabaja desde hace años con dos triterpenos naturales de importancia, dadas sus relevantes propiedades biológicas. A partir de estos compuestos se han realizado derivatizaciones con objeto de mejorar la bioactividad de dichas moléculas. Estos triterpenos son el ácido oleanólico (ácido 3β-hidroxiolean-12-en-28-oico, AO) y el ácido maslínico (ácido 2a,3β-dihidroxiolean-12-en-28-oico, AM), de los cuales hablaremos con mayor profundidad en apartados siguientes.

1. TRITERPENOS PENTACÍCLICOS. GENERALIDADES Y BIOGÉNESIS

Los terpenos son un grupo muy importante de productos naturales que tienen un origen biosintético común, derivan del ácido mevalónico y se clasifican según su estructura química en base al número de unidades de isopreno, (2-metil-1,3-butadieno) presentes en su esqueleto hidrocarbonado, de forma que podemos clasificarlos en monoterpenos (10 carbonos, 2 unidades), sesquiterpenos (15 carbonos, 3 unidades), diterpenos (20 carbonos, 4 unidades), sesterterpenos (25 carbonos, 5 unidades), triterpenos (30 carbonos, 6 unidades) y tetraterpenos (40 carbonos, 8 unidades).

[4] Jacob, D., Marrón, B., Rutherford, P. A. & Corporation, B. H. Pharmacovigilance as a tool for safety and monitoring : a review of general issues and the specific challenges with end-stage renal failure patients. *Drug. Healthc. Patient Saf.* **5**, 105–112 (2013).

Los terpenos no son exclusivos del reino vegetal, también se encuentran en animales, bacterias y algas, pero es en las plantas donde podemos encontrar una gran variedad y abundancia. La diferencia radica en la biosíntesis y en la participación de enzimas.

Dentro del grupo de los terpenos, se encuentran los triterpenos, objeto de nuestro estudio, que se distribuyen ampliamente por el reino vegetal, constituyendo el grupo más extenso de terpenoides, debido a su gran diversidad estructural. Hasta la fecha, se han identificado más de 20.000 estructuras triterpénicas distintas con más de 100 variaciones esqueléticas.[5] Este tipo de moléculas destacan por su gran variedad de aplicaciones en perfumería, cosmética, como fármacos, insecticidas, herbicidas, fitoreguladores, etc.

El químico Leopold Ružička, galardonado con el premio Nobel de Química en el año 1939, fue el que inició los estudios de las estructuras de los terpenos, siendo capaz de racionalizar la biogénesis de estos compuestos y desarrollarla (regla biogenética del isopreno): "*los esqueletos carbonados de los terpenos son divisibles en un número entero de unidades isoprénicas conectadas cabeza con cola*".[6]

Los triterpenos están formados por 30 carbonos y tienen su origen por ciclación directa de escualeno, alcohol triterpénico formado por condensación cola-cola del farnesol. Presentan un esqueleto policíclico formado por condensación de 6 unidades de isopreno. La mayoría de los triterpenos son tetracíclicos o pentacíclicos, aunque se encuentran excepciones con tres o menos ciclos.

[5] Ghosh, S. Biosynthesis of structurally diverse triterpenes in plants: The role of oxidosqualene cyclases. *Proc. Indian Natl. Sci. Acad.* **82,** 1189–1210 (2016).
[6] Ruzicka, L. The isoprene rule and the biogenesis of terpenic compounds. *Experientia* **9,** 357–367 (1953).

En las plantas, la biosíntesis de los compuestos terpénicos se inicia en el citosol, donde la condensación de 2 unidades de acetil-CoA conduce a la formación de acetoacetil-CoA, para posteriormente adicionarse una tercera molécula de acetil-CoA mediante una adición esteroespecífica de aldol, originando el éster 3-hidroxi-3-metilglutaril-CoA, que por acción de la enzima 3-hidroxi-3-metilglutaril CoA reductasa (HMG-CoA reductasa) conduce a la síntesis del ácido mevalónico. Este ácido sufre una activación por fosforilación y descarboxilación, formándose pirofosfato de 3-isopentenilo o pirofosfato de isopentenilo (IPP) que puede isomerizar a pirofosfato de 2-isopentenilo o pirofosfato de dimetilalilo (DMAPP) (Fig. 1).

IPP posee un doble enlace terminal, presentando una gran reactividad en procesos de sustitución nucleofílica, lo que permite la unión cabeza-cola con DMAPP. Tras la pérdida de un protón por parte del intermedio carbocatiónico de la reacción, da lugar a un monoterpeno lineal denominado pirofosfato de geranilo susceptible de transformarse en los más diversos esqueletos de diez átomos de carbonos, dependiendo de las enzimas que intervengan en los procesos, denominados monoterpenos (geraniol, limoneno, mentol).

El estudio de la ruta biogenética de los terpenos en general, ha dado lugar a la publicación de un gran número de trabajos.[7] Los esquemas y comentarios que se presentan a continuación tienen su base en todos ellos.

[7] a) Singh, B. & Sharma, R. a. Plant terpenes: defense responses, phylogenetic analysis, regulation and clinical applications. *Biotech* ***5,*** 129–151 (2015). b) Simonsen, E. Q. J., Ross, W. C. J. *The Terpenes*. Cambridge University Press, Cambridge, UK, Vol. ***4-5*** (1957). c) Devon, T. K., Scott, A. I. *Handbook of Naturally Occurring Compounds*. Academic Press, New York, US, Vol. **2** (1972). d) Coffey, S. *Rodd´s Chemistry of Carbon Compounds,* 2nd ed.; Coffey, S. Ed.; Elsevier, Amsterdam, NL, Part c Vol. **11** (1969); Part e Vol. **11** (1971). e) Overton, K. H. En *Terpenoids and Steroids. A Specialist Periodical Report*; Overton, K. H. Ed.; The Chemical Society, London, UK, Vol. **1-2** (1971, 1972). f) Revisiones periódicas en la revista *Natural Product Report*, Conolly, J. D., Hill, R. A. ***20***, 640-659 (2003); ***19***, 494-514 (2002); ***18***, 131-148 (2001); ***18***, 560-579 (2001); ***17***, 483-505 (2000); ***16***, 221-241 (1999); ***14***, 661-681 (1997); ***13***, 151-171 (1996); ***12***, 609-639 (1995).

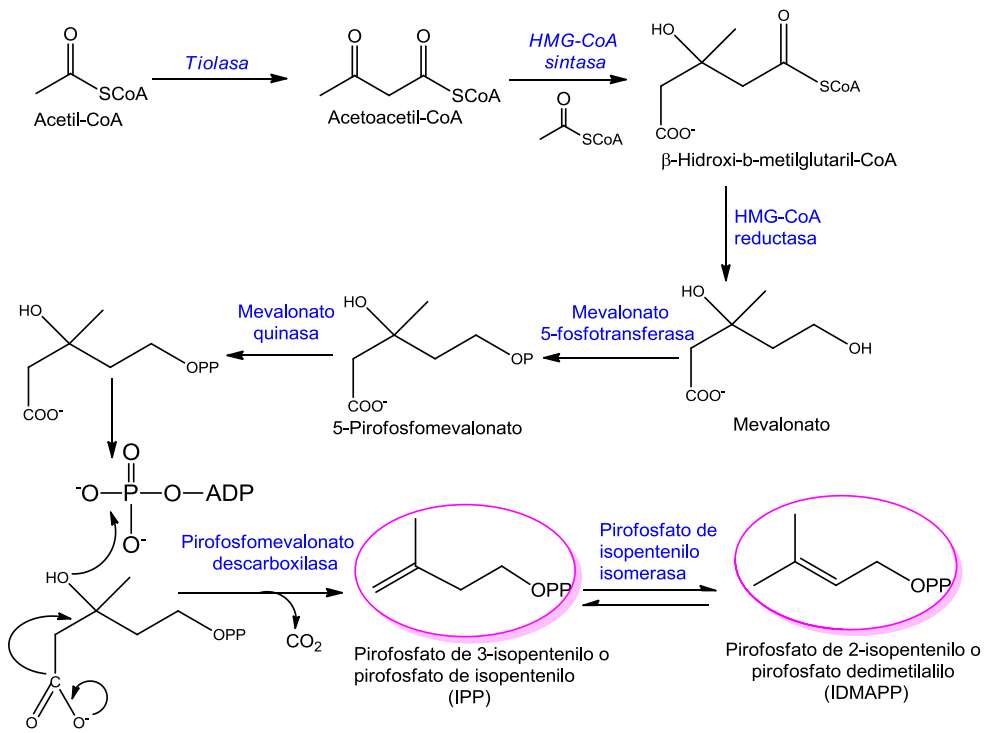

Figura 1. Biosíntesis de los precursores biológicos de los terpenos.

El pirofosfato de geranilo reacciona con una nueva unidad isoprénica (IPP) por la acción de la enzima geranil transferasa, obteniéndose el pirofosfato de farnesilo, que es el precursor de toda la gama de productos con quince átomos de carbono (sesquiterpenos) que presentan diferentes esqueletos carbonados (germacranos, eudesmanos, cariofilanos, etc.). Si el farnesil pirofosfato reacciona con otra molécula de IPP, dará lugar al pirofosfato de geranil-geraniol, precursor de los compuestos diterpénicos (kauranos, beyeranos, atisanos, etc.), pero, si se produce el acoplamiento cabeza-cabeza de dos unidades de pirofosfato de farnesilo conduce a la formación del escualeno, precursor de los triterpenos (dammarano, lupano, oleanano, ursano, etc.) (Fig. 2).

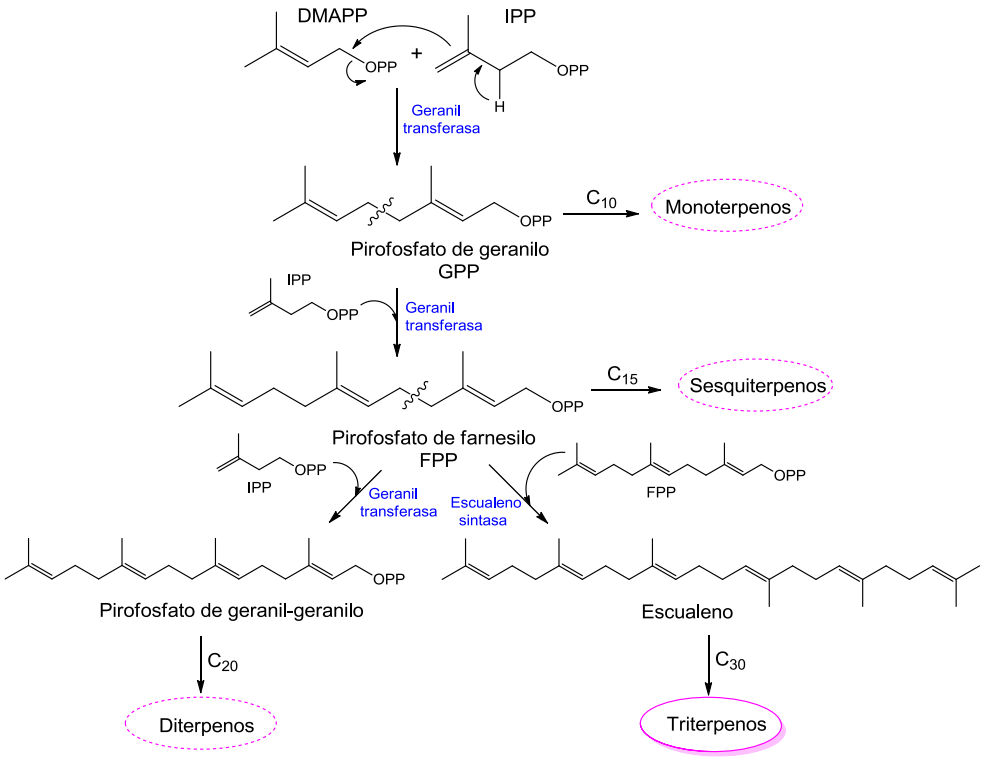

Figura 2. Biosíntesis del escualeno, precursor de los triterpenos.

A partir del escualeno, mediante diferentes carbocationes generados por ciclaciones y migraciones de metilo o hidruro, se obtienen los triterpenos pentacíclicos con esqueleto de lupano, ursano y oleanano. La ciclación del escualeno es a través de un intermedio denominado 2,3-oxidoescualeno, producido en una reacción de oxidación catalizada por la enzima escualeno epoxidasa, a partir del cual se formarán los distintos tipos de triterpenos según la geometría tridimensional del plegamiento y de las enzimas que participen (Fig. 3). Los esqueletos de lupano, ursano y oleanano son los más importantes dentro de los triterpenos,[8] y este hecho se debe al amplio espectro de actividades biológicas que presentan como agentes anti-tumorales, anti-inflamatoria, anti-VIH, anti-bacterianos, e inhibidores de enzimas implicadas en procesos degenerativos.

[8] Cano-flores, A. microorganismos Biotransformation of triterpene with diferent microorganisms **44**, 7–16 (2013).

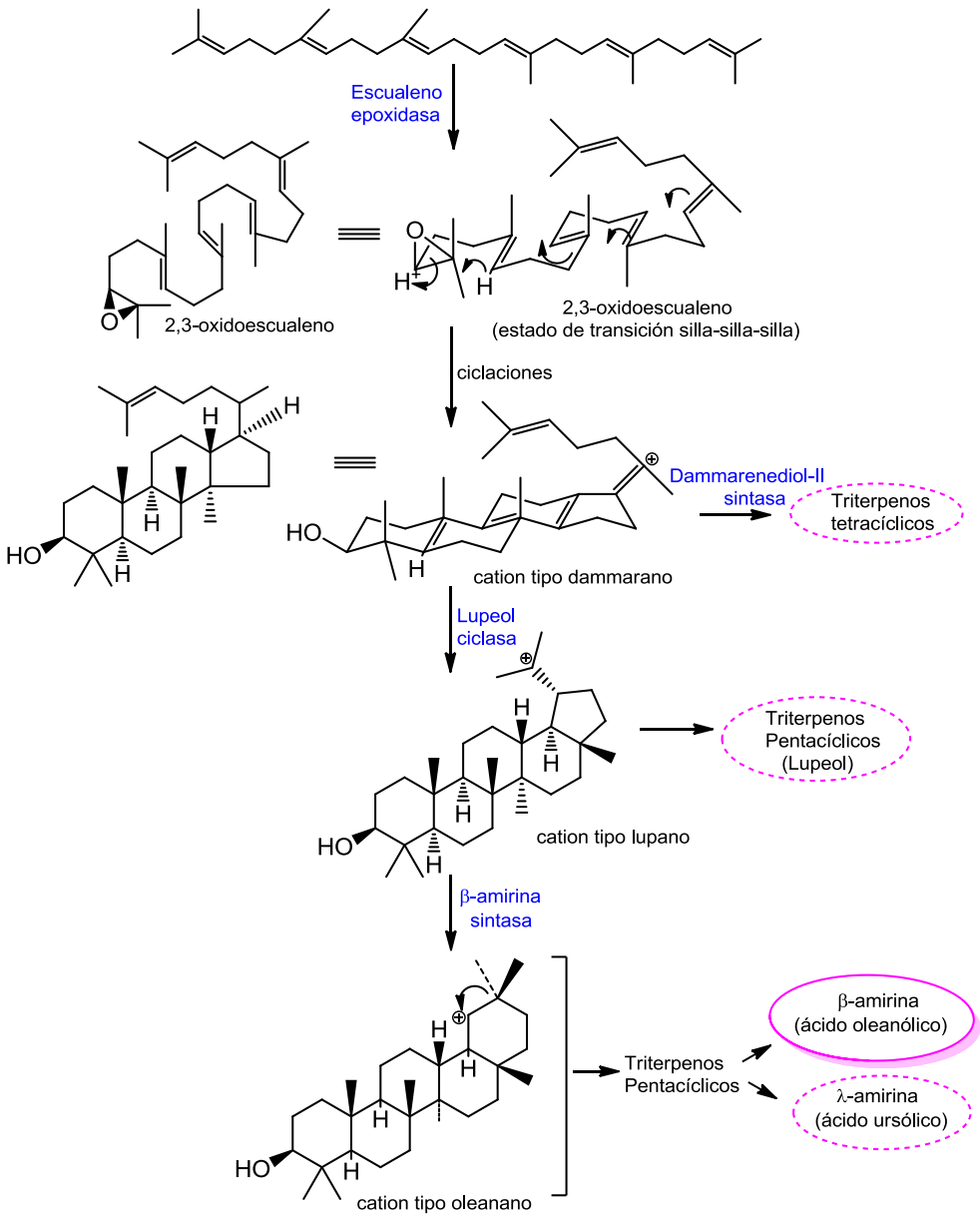

Figura 3. Biosíntesis de triterpenos.

Las modificaciones estructurales o funcionales en el esqueleto básico de estos triterpenos han producido nuevos derivados con mejores propiedades farmacocinéticas. Un ejemplo de ello son los derivados del ácido betulínico como el bevirimat, el cual se encuentra en evaluación en pacientes (fase clínica II) con VIH.[9]

2. BIOSÍNTESIS DE ÁCIDO OLEANÓLICO Y ÁCIDO MASLÍNICO

Como se vio anteriormente en las células vegetales, la molécula precursora de la síntesis de las estructuras de oleanano, el 2,3-oxidoesqualeno, se cicla gracias a la actuación de la enzima β-amirina sintetasa (BAS), formando la β-amirina. En la ruta biogenética del ácido oleanólico la β-amirina sufre una oxidación en tres etapas oxidativas sobre C-28, mediante un enzima del citocromo P450 (complejo enzimático de monooxigenasas), identificada como CYP716A12 y descubierta por primera vez en la planta *Medicago truncatula*,[10] produciéndose así el ácido oleanólico (Fig. 4). [11]

Las enzimas que puedan participar en la biosíntesis del ácido maslínico, no se conocen a día de hoy. En la actualidad, se realizan estudios genómicos (transcriptómicos, proteómicos y metabolónicos) para comprender mejor la actuación de las enzimas implicadas en la síntesis de triterpenos.[12]

[9] Smith, P. F. *et al.* Phase I and II study of the safety, virologic effect, and pharmacokinetics/pharmacodynamics of single-dose 3-O-(3',3- dimethylsuccinyl)betulinic acid (bevirimat) against human immunodeficiency virus Infection. *Antimicrob. Agents Chemother.* **51,** 3574–3581 (2007).
[10] Carelli, M. *et al.* Medicago truncatula CYP716A12 is a multifunctional oxidase involved in the biosynthesis of hemolytic saponins. *Plant Cell* **23,** 3070–81 (2011).
[11] Pollier, J. & Goossens, A. Oleanolic acid. *Phytochemistry* **77,** 10–15 (2012).
[12] Shah, Z. H. & Hamooh, B. T. Transcriptomics and Biochemical Profiling : Current Dynamics in Elucidating the Potential Attributes of Olive. Curr. Issues Mol. Biol. **21,** 73–98 (2017).

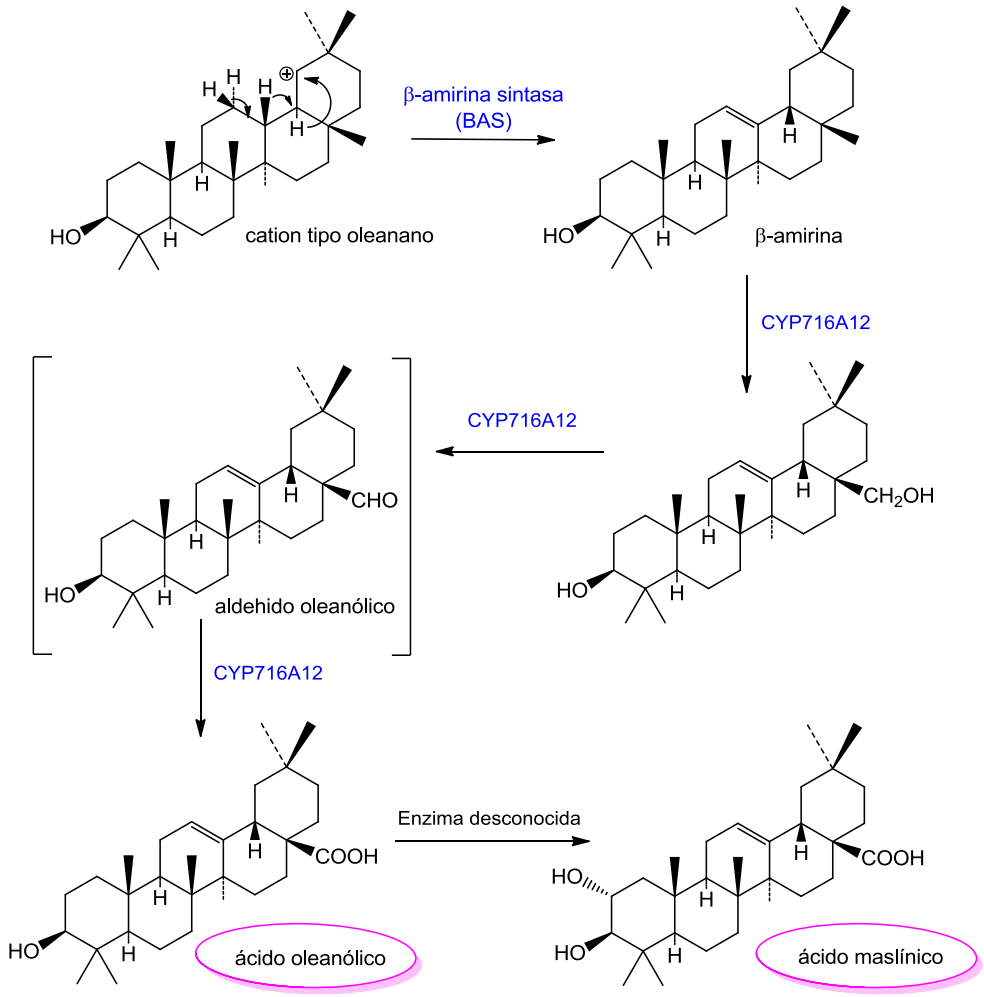

Figura 4. Biosíntesis de ácido oleanólico y ácido maslínico.

3. GENERALIDADES DE ÁCIDO OLEANÓLICO Y ÁCIDO MASLÍNICO

Los triterpenos pentacíclicos empleados para este trabajo, como se ha ido desarrollando a lo largo de esta introducción, son el ácido oleanólico (ácido 3β-hidroxiolean-12-en-28-oico, AO) y el ácido maslínico (ácido 2a,3β-dihidroxiolean-12-en-28-oico, AM). Ambos ácidos se encuentran ampliamente distribuidos por el reino vegetal, siendo particularmente abundante en la piel del fruto y hojas del olivo (*Olea europea*).

El ácido oleanólico ha sido aislado en más de 2000 especies vegetales,[13] de las cuales se incluyen frutas, hojas o raíces de plantas medicinales, entre las que destacamos *Calendula officinalis*, *Lavandula angustifolia*, *Melissa officinalis*, *Rosmarinus officinalis*, etc. En ellas se puede encontrar de forma libre o bien formando distintos derivados, glicósidos en su mayoría.

El ácido maslínico, de forma menos extendida, se encuentra distribuido en la naturaleza como tal, y formando ésteres metílicos o glicósidos, y está presente en plantas como: *Salvia officinallis*, *Zyziphus jujuba*, *Punica granatum*, etc.

Como se mencionó anteriormente, estos dos ácidos se encuentran en mayor cantidad en *Olea europea*, encontrándose de forma libre en la cera epicuticular de su fruto (aceituna). Nuestro grupo de investigación ha aislado estos ácidos a partir de los residuos de la molturación de la aceituna, obteniendo en torno al 0.4% en peso de ácido oleanólico y el 0.8% en peso de ácido maslínico, empleando métodos de extracción en Soxhlet que detallaremos más adelante. Estos porcentajes significan que, por cada kilogramo de materia prima que se procesa, se aíslan cuatro gramos de ácido oleanólico y ocho gramos de ácido maslínico. Esto supone una gran disponibilidad de materia prima, algo inusual cuando se trabaja con productos naturales. Además, el hecho de que se aíslen a partir de los residuos de la molturación de la aceituna (alpeorujo) permite minimizar el impacto contaminante con fines farmacológicos o de síntesis química.

[13] Jäger, S., Trojan, H., Kopp, T., Laszczyk, M. N. & Scheffler, A. Pentacyclic triterpene distribution in various plants - rich sources for a new group of multi-potent plant extracts. *Molecules* **14,** 2016–2031 (2009).

4. REACTIVIDAD Y DERIVATIZACIÓN DE LOS ÁCIDOS OLEANÓLICO Y MASLÍNICO

Se define reactividad química, como la capacidad que posee una sustancia para participar en las reacciones químicas. Algunos de los factores por los que la reactividad viene determinada es la presencia de grupos funcionales y tipos de enlaces (dobles o triples) que podemos encontrar en una molécula, constituyendo los puntos de ataque por los cuales podemos hacer reaccionar otras moléculas o reactivos.

Los triterpenos objeto de nuestro estudio poseen varios puntos en los que se encuentran funcionalizados y que serán zonas diana para la formación de derivados. Así, en el ácido oleanólico, encontramos un grupo hidroxilo β en el anillo A en C-3, un doble enlace en el anillo C (C-12/C-13) y un grupo carboxilo en C-28, mientras que la única diferencia con el ácido maslínico es la presencia de dos grupos hidroxilos en el anillo A en C-2 y C-3 (Fig. 5). La presencia de este grupo hidroxilo adicional en el ácido maslínico, hace que su reactividad y propiedades físico-químicas sean bastante distintas al ácido oleanólico.

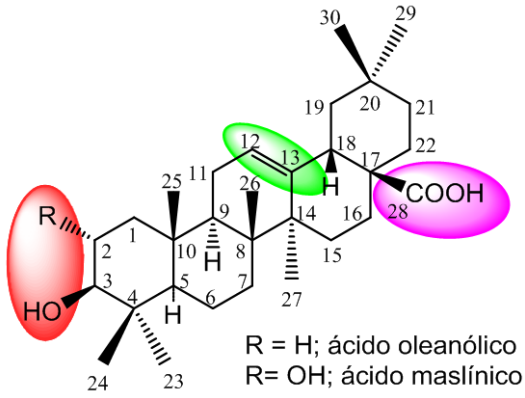

Figura 5. Zonas funcionalizadas de los ácidos oleanólico y maslínico.

Ambos ácidos presentan esqueleto de oleanano que se caracteriza por presentar una conformación de silla con uniones *trans* entre los distintos ciclos, a excepción de los ciclos D y E cuya unión interanular es *cis*. (Fig. 6).

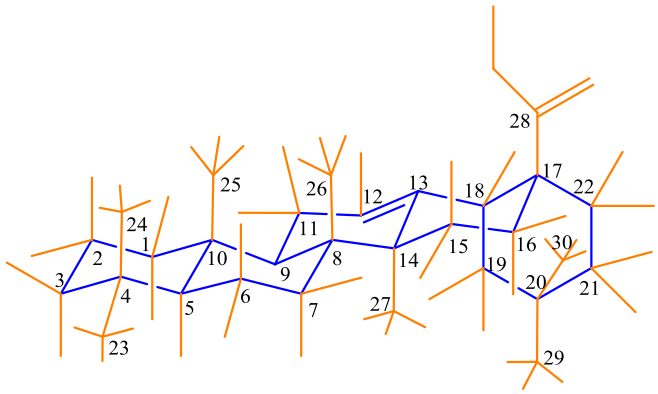

Figura 6. Representación estereoquímica del esqueleto de oleanano.

La disposición del esqueleto de oleanano conlleva una diferencia de la reactividad de los grupos presentes según tenga una disposición axial o ecuatorial, debido al impedimento estérico. En nuestro caso, el impedimento estérico del anillo A, se debe a la presencia de dos grupos metilo en C-4 y uno en C-10.

Como se indicó anteriormente, los triterpenos pentacíclicos poseen propiedades biológicas muy importantes. No obstante, y con el objeto de modificar las propiedades físico-químicas de estos compuestos naturales e incrementar su biodisponibilidad, se han desarrollado nuevos derivados de los mismos, que han resultado ser más efectivos desde el punto de vista biológico. La derivatización es una técnica química que permite modificar algunas propiedades físico-químicas, mediante la transformación de los grupos funcionales que presentan las moléculas, obteniendo así nuevos compuestos que difieren de su precursor en algún punto de su estructura.

Hoy en día, la derivatización permite crear librerías de compuestos a partir de un producto de partida, en su mayoría productos naturales con

una reconocida actividad biológica, con el objetivo de amplificar dicha actividad.[14]

Nuestro grupo de investigación, se ha dedicado en los últimos años al estudio de la reactividad de compuestos naturales con estructura de oleanano y la semisíntesis de derivados de los mismos, para su posterior evaluación terapéutica. Estudios similares también han sido realizados por distintos autores que han semisintetizado derivados de estos triterpenos con diferentes funcionalizaciones, modificando tanto el anillo A como el grupo carboxilo de C-28. A continuación se expondrá con más detalle los estudios previos realizados por nuestro grupo de investigación.

4.1. Reactividad del anillo A

Los primeros estudios que se realizaron en nuestro grupo de investigación fue sobre la reactividad del anillo A, obteniendo una serie de derivados sencillos por reacciones de acetilación, mesilación y tosilación, dando lugar a una serie de compuestos monofuncionalizados en el caso del ácido oleanólico y bifuncionalizados en el caso del ácido maslínico (Fig. 7).[15]

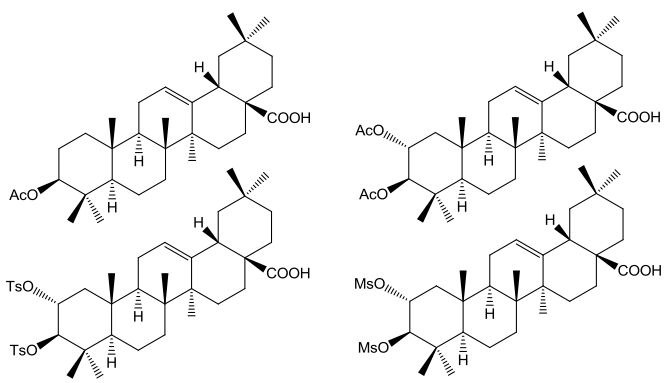

Figura 7. Derivados de los ácidos oleanólico y maslínico.

[14] Kingston, D. G. & Newman, D. J. Natural products as drug leads: an old process or the new hope for drug discovery?. *J. Med. Chem.* **51**, 2589–2599 (2008).
[15] García-Granados, A. *et al.* Semi-synthesis of triterpene A-ring derivatives from oleanolic and maslinic acids. Part II. Theoretical and experimental chemical shifts. *J. Chem. Res.* 211–212 (2000).

A raíz de estos estudios, se emprendieron otros más complejos mediante la desoxigenación del anillo A, a partir del oleanato de metilo tratado con cloruro de mesilo con piridina, obteniéndose una serie de compuestos con distintas insaturaciones y diferentes tamaños de anillo mediante un reagrupamiento que conduce a la contracción del anillo A (Fig. 8).[16]

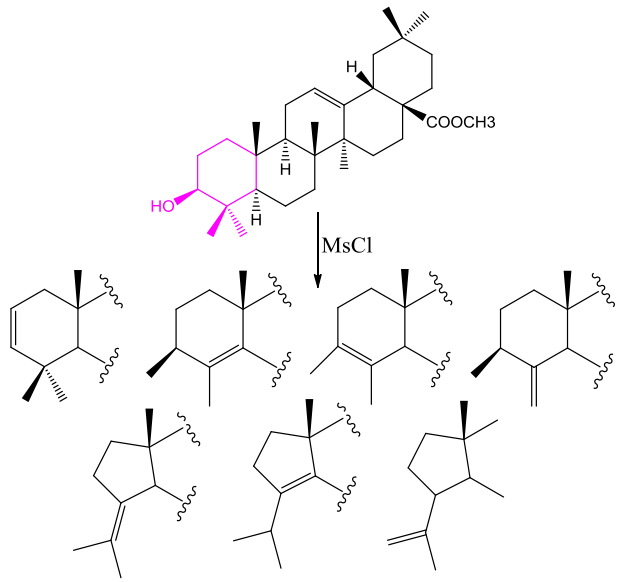

Figura 8. Desoxigenación del anillo A del oleanato de metilo.

En otros trabajos relevantes se realizó la hidroxilación remota de grupos metilo por ciclopaladación regioselectiva. La hidroxilación remota del metilo de C-4 permitió la obtención de derivados hidroxilados en los metilos angulares sobre C-4 (Fig. 9).[17]

[16] Parra, A., Lopez, P. E. & Garcia-Granados, A. Different pathways for the deoxygenation of the A-ring of natural triterpene compounds. *Nat. Prod. Res.* **24**, 177–96 (2010).
[17] García-Granados, A., López, P. E., Melguizo, E., Parra, A. & Simeó, Y. Remote hydroxylation of methyl groups by regioselective cyclopalladation. Partial synthesis of hyptatic acid-A. *J. Org. Chem.* **72**, 3500–3509 (2007).

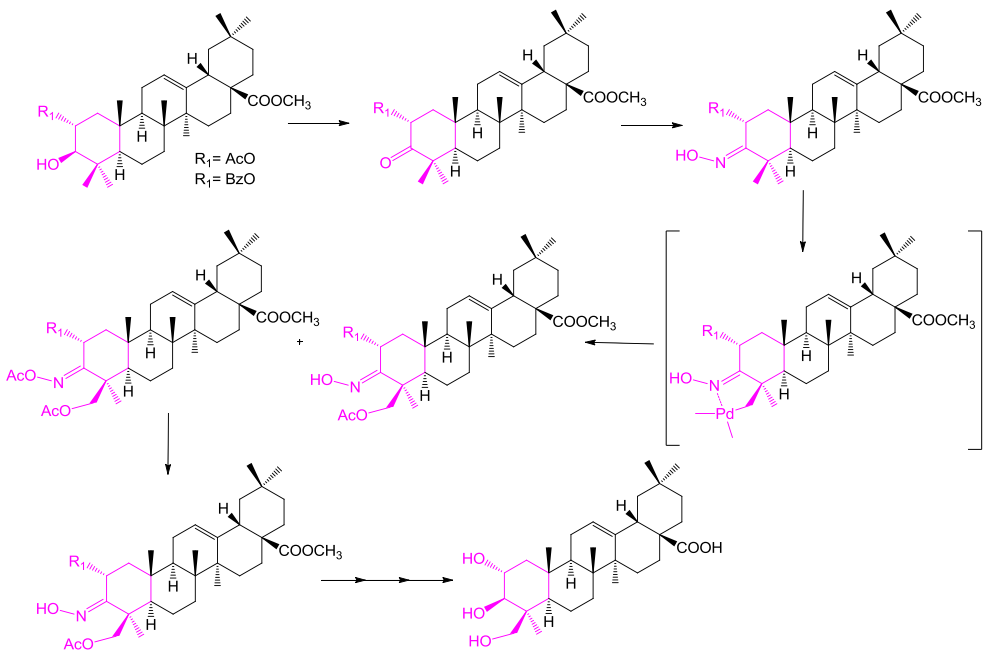

Figura 9. Hidroxilación remota de grupos metilo por ciclopaladación regioselectiva.

En el año 2014, nuestro grupo de investigación realizó un estudio sobre la reactividad del anillo A, sintetizando un amplio conjunto de compuestos bioactivos, a través de procedimientos de Síntesis Orgánica en Fase Sólida y en disolución, acoplando a los ácidos maslínico y oleanólico 10 grupos acilos diferentes sobre el C-3 ó C-2/C-3 de dicho anillo (Fig. 10).[18]

[18] Parra, A. *et al.* Semi-synthesis of acylated triterpenes from olive-oil industry wastes for the development of anticancer and anti-HIV agents. *Eur. J. Med. Chem.* **74,** 278–301 (2014).

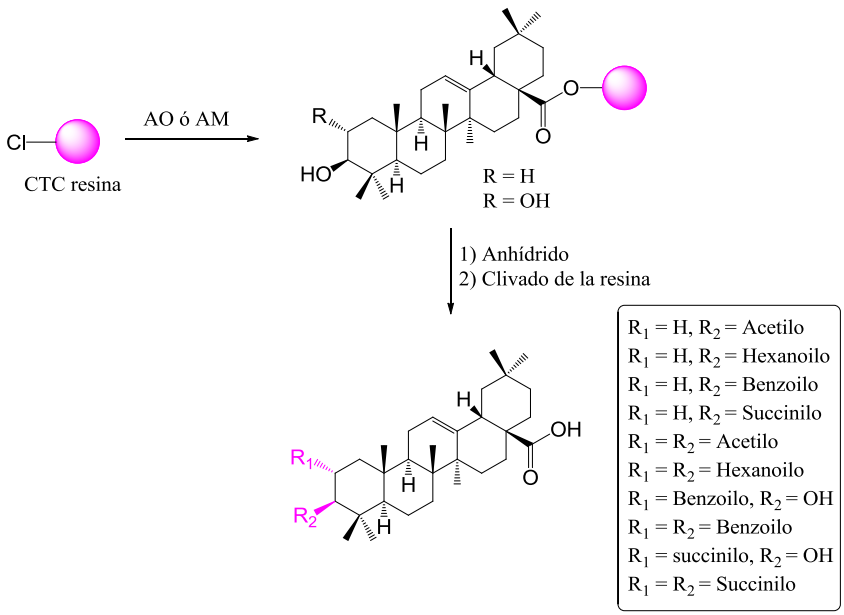

Figura 10. Obtención de derivados de los ácidos oleanólico y maslínico acilados mediante Síntesis Orgánica en Fase Sólida.

4.2. Reactividad del anillo C

Para el estudio de la reactividad del anillo C, nuestro grupo de investigación llevó a cabo una serie de oxidaciones con el objetivo de escindir la molécula triterpénica a través del anillo C y producir interesantes sintones quirales.[19]

El primer objetivo fue la obtención de varios dienos y trienos que se utilizaron como material de partida para llevar a cabo los procesos de rotura oxidativa (Fig.11).[20]

[19] García-Granados, A., López, P. E., Melguizo, E., Parra, A. & Simeó, Y. Oxidation of several triterpenic diene and triene systems. Oxidative cleavage to obtain chiral intermediates for drimane and phenanthrene semi-synthesis. *Tetrahedron* **60,** 3831–3845 (2004).

[20] García-Granados, A., López, P. E., Melguizo, E., Parra, A. & Simeó, Y. Degradation of triterpenic compounds from olive-pressing residues. Synthesis of trans-decalin type chiral synthons. *Tetrahedron Lett.* **44,** 6673–6677 (2003).

Los compuestos diénicos fueron tratados con ozono, dando como resultado epoxidaciones, hidroxilaciones y lactonizaciones sobre uno o dos dobles enlaces del anillo C, sin que se produjese la apertura del mismo. Un derivado con un grupo *cis*-trieno, también tratado con ozono, condujo al mismo tipo de derivados, mientras que la oxidación del derivado con un grupo *trans*-trieno produjo una mezcla de dos sesquiterpenos por la escisión del anillo C. Los compuestos que se obtuvieron son sintones relevantes ya que sirvieron de productos de partida para la obtención de otros productos naturales como elengasidiol, achilleoles A y B y camelliol A. Hay que destacar que las roturas llevadas a cabo sobre los trienos triterpénicos dieron lugar a una serie de *cis* y *trans* decalinas, que pueden ser sintones relevantes en la formación de esteroides (Fig. 12).

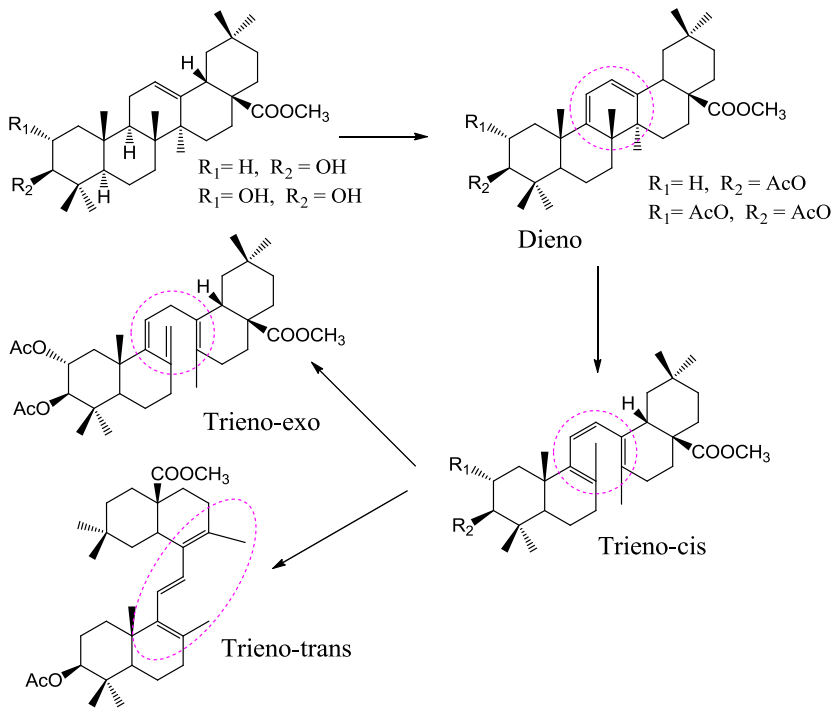

Figura 11. Formación de dienos y trienos.

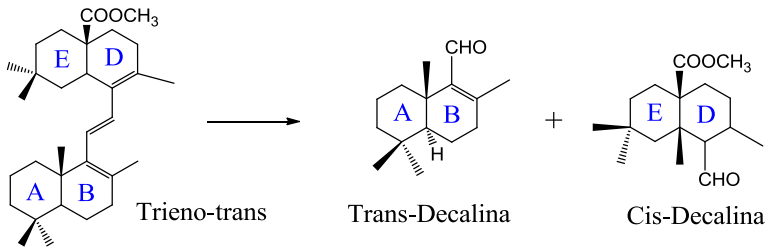

Figura 12. Degradación química del trieno-*trans* para formar decalinas.

4.3. Reactividad del grupo funcional carboxilo en C-28 de la estructura triterpénica

El grupo carboxilo situado sobre C-28 del esqueleto carbonado es uno de los más estudiados debido a que es un grupo frecuente en los triterpenos. En general la mayoría de los derivados que podemos encontrar son ésteres, amidas y derivados con aminoácidos. Nuestro grupo de investigación ha estudiado la modificación de este grupo en C-28 con dos fines; el primero ha sido bloquear dicho grupo carboxilo, lo que ha permitido obtener una serie de derivados nuevos en el anillo A; y el segundo ha sido la obtención de derivados con aminoácidos (Fig. 13) con el fin de conseguir una mejora tanto de su biodisponibilidad como de su actividad biológica.

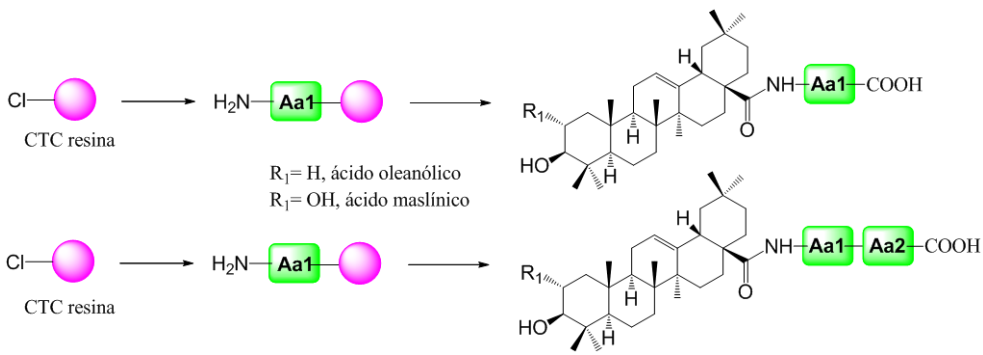

Figura 13. Obtención de derivados con uno o dos aminoácidos por técnica de Síntesis Orgánica en Fase Sólida.

Otro ejemplo de estudio realizado por nuestro grupo de investigación es el que se llevó a cabo sobre la reactividad en C-28 del ácido maslínico, acoplando varios aminoácidos mediante técnicas sintéticas en fase sólida y en disolución, obteniendo una serie de derivados con un solo aminoácido (monopéptidos), dos aminoácidos (dipéptidos) o tres aminoácidos (tripéptidos) (Fig. 14)).[21]

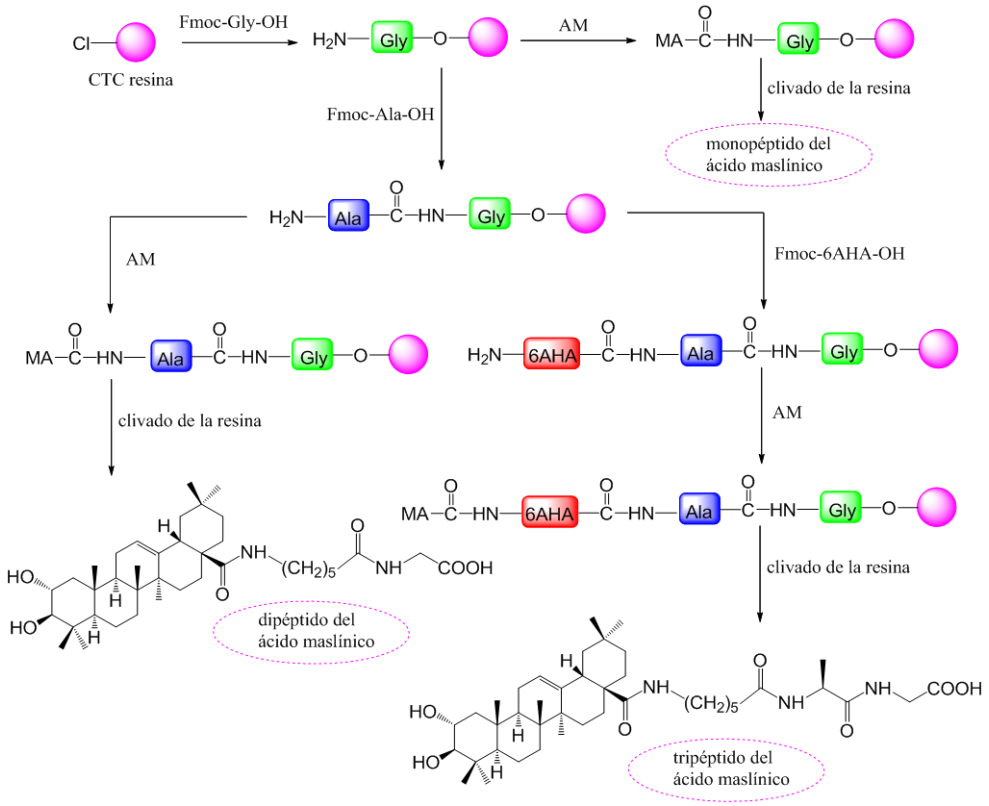

Figura 14. Obtención de derivados de ácido maslínico con uno, dos o tres aminoácidos.

[21] Parra, A. *et al.* Solution- and solid-phase synthesis and anti-HIV activity of maslinic acid derivatives containing amino acids and peptides. *Bioorg. Med. Chem.* **17,** 1139–1145 (2009).

En un segundo estudio, se obtuvo una biblioteca de derivados bifuncionalizados de los ácidos maslínico y oleanólico. Estos derivados se obtuvieron mediante Síntesis Orgánica en Fase Sólida, acoplando sobre el grupo carboxilo de C-28, 6 aminoácidos diferentes, y 10 grupos acilo distintos sobre los grupos hidroxilo de C-3 ó C-2/C-3 (Fig. 15).[22]

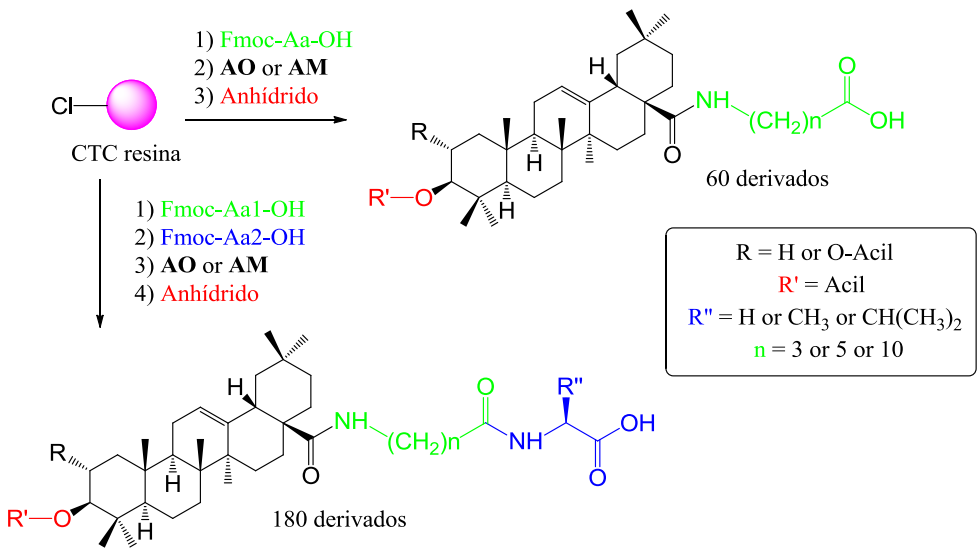

Figura 15. Obtención de diferentes derivados de los ácidos oleanólico y maslínico bifuncionalizados.

[22] Parra, A. *et al.* Solid-phase library synthesis of bi-functional derivatives of oleanolic and maslinic acids and their cytotoxicity on three cancer cell lines. *ACS Comb. Sci.* **16,** 428–447 (2014).

Para finalizar este apartado de reactividad, comentar que nuestro grupo de investigación realiza también reacciones de biotransformación con microorganismos, utilizando para ello una serie de hongos filamentosos, gracias a los cuales se ha podido estudiar un poco más la reactividad de nuestros dos productos naturales triterpénicos. Un ejemplo de ello es la biotransformación que se realizó con el hongo *Rhizomucor miehei* que fue capaz de hidroxilar el ácido oleanólico tanto en el anillo A, como en el anillo B, e incluso el carbono de C-30 (Fig. 16).[23]

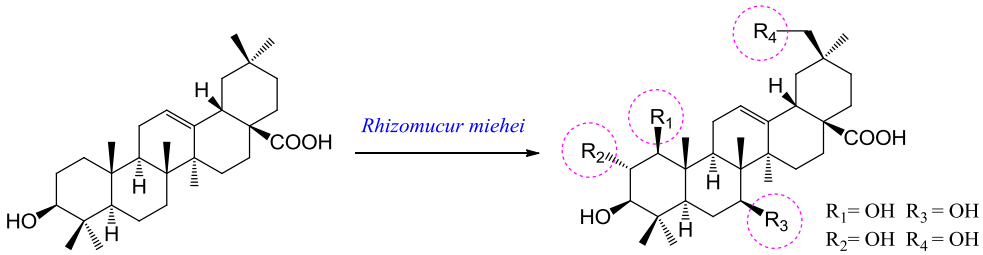

Figura 16. Biotransformación del ácido oleanólico por *Rhizomucur miehei*.

5. PROPIEDADES BIOLÓGICAS DE LOS ÁCIDOS OLEANÓLICO Y MASLÍNICO

Los ácidos oleanólico y maslínico presentan importantes actividades biológicas que demuestran su potencial terapéutico frente a ciertas enfermedades como son el cáncer y el SIDA, pero muestran una baja solubilidad en agua y por tanto una baja biodisponibilidad, impidiendo que sus actividades biológicas se manifiesten con todo su potencial. Por ello, se intentó mejorar su biodisponibilidad mediante la formación de distintos derivados que pudiesen aumentar su actividad biológica.

A continuación se realizará un resumen de las distintas actividades biológicas que presentan estos productos naturales.

[23] Martinez, A. *et al.* Phytochemistry Biotransformation of oleanolic and maslinic acids by Rhizomucor miehei. **94**, 229–237 (2013).

5.1. Propiedades biológicas de ácido oleanólico

El ácido oleanólico presenta una amplia gama de actividades farmacológicas, una de las más importantes es su acción hepatoprotectora. Recientemente se ha observado que posee efectos antidiabéticos en diversos modelos *in vitro* e *in vivo*, teniendo la capacidad de reducir la presión sanguínea, los niveles de glucosa en sangre, el colesterol total y aumentar la insulina plasmática. Las vías de señalización aún no se han dilucidado, si bien se ha podido comprobar que ejerce su acción sobre el receptor nuclear PPARδ, activándolo.[24] Las propiedades antibacterianas también se han estudiado frente a distintas bacterias como: *Streptococcus mutans*, *Streptococcus sobrinus*, *Mycobacterium tuberculosis*, *Staphylococcus aureus*, *Bacillus subtilis*, etc.[25]

En los últimos años el ácido oleanólico ha sido ensayado frente a distintos tipos de cánceres, encontrándose efectos antiproliferativos en varias líneas celulares tumorales,[26] entre las que se destacan el cáncer de mama (MCF7 y MDA-MB-231),[27] leucemia (K562, HEL y JURKAT)[28], cáncer de pulmón (A549)[29] cáncer de páncreas (Panc-28)[30], y cáncer de piel (B16-2F2).[31]

[24] Zhang, Z. *et al.* Oleanolic acid ameliorates high glucose-induced endothelial dysfunction via PPARδ activation. *Sci. Rep.* **7,** 40237 (2017).
[25] Jesus, J. A. *et al.* Antimicrobial Activity of Oleanolic and Ursolic Acids: An Update. *Evidence-Based Complement. Altern. Med.* **2015,** 1–14 (2015).
[26] Shanmugam, M. K. *et al.* Oleanolic acid and its synthetic derivatives for the prevention and therapy of cancer: Preclinical and clinical evidence. *Cancer Lett.* **346,** 206–216 (2014).
[27] Allouche, Y. *et al.* Antioxidant, antiproliferative, and pro-apoptotic capacities of pentacyclic triterpenes found in the skin of olives on MCF-7 human breast cancer cells and their effects on DNA damage. *J. Agric. Food Chem.* **59,** 121–130 (2011).
[28] Ng, Y. P., Chen, Y., Hu, Y., Ip, F. C. F. & Ip, N. Y. Olean-12-Eno[2,3-c] [1,2,5]Oxadiazol-28-Oic Acid (OEOA) Induces G1 Cell Cycle Arrest and Differentiation in Human Leukemia Cell Lines. *PLoS One* **8,** (2013).
[29] Wang, J. *et al.* Radiosensitizing effect of oleanolic acid on tumor cells through the inhibition of GSH synthesis in vitro. *Oncol. Rep.* **30,** 917–924 (2013).
[30] Wei, J. *et al.* Oleanolic acid arrests cell cycle and induces apoptosis via ROS-mediated mitochondrial depolarization and lysosomal membrane permeabilization in human pancreatic cancer cells. *J. Appl. Toxicol.* **33,** 756–765 (2013).
[31] Hata, K., Hori, K. & Takahashi, S. Differentiation- and apoptosis-inducing activities by pentacyclic triterpenes on a mouse melanoma cell line. *J. Nat. Prod.* **65,** 645–648 (2002).

En la mayoría de los casos el ácido oleanólico tiene un efecto apoptótico y en otros antiproliferativo, pero su efecto es mínimo y una posible razón podría ser la solubilidad limitada que presenta en agua y que afecta a su biodisponibilidad. Se encuentran derivados de este ácido, por modificación química o biológica de su estructura, que mejora su actividad biológica, como por ejemplo el ácido 2-ciano-3,12-dioxooleana-1,9(11)-dien-28-oico(CDDO) que aumenta considerablemente su actividad frente a células de cáncer de piel.[32]

Por último, y no menos importante, se ha visto que el ácido oleanólico presenta actividad anti-VIH, inhibiendo la proteasa del virus,[33] cuya función está relacionada con la rotura de los precursores poliproteínicos virales para dar lugar a proteínas maduras que formarán nuevos viriones.

5.2. Propiedades biológicas de ácido maslínico

El ácido maslínico es uno de los triterpenos más estudiados, presentando numerosas actividades biológicas entre las que destacamos su efecto antioxidante en ensayos *in vivo,*[34] donde se demuestra que los animales que presentan diabetes y a los que se le administra este ácido, se produce una disminución de un marcador de la peroxidación lipídica (MDA) y un aumento de la actividad de las enzimas antioxidantes (superóxido dismutasa y glutatión peroxidasa) en los tejidos hepáticos, cardiacos y renales. Otros estudios indican que este producto natural posee efectos antimaláricos, actuando sobre las enzimas metaloproteasas, inhibiendo la etapa esquizonte del ciclo de vida de *Plasmodium falciparum*.[35]

[32] Ikeda, T. Induction of redox imbalance and apoptosis in multiple myeloma cells by the novel triterpenoid 2-cyano-3, 12-dioxoolean-1, 9-dien-28-oic acid. *Mol. Cancer Ther.* **3,** 39–45 (2004).
[33] Patel, R. V & Park, S. W. Journey Describing the Discoveries of Anti-HIV Triterpene Acid Families Targeting HIV-Entry/Fusion, Protease Functioning and Maturation Stages. *Curr. Top. Med. Chem.* **14,** 1940–1966 (2014).
[34] Mkhwanazi, B. N., Serumula, M. R., Myburg, R. B., Heerden, F. R. Van & Musabayane, C. T. Antioxidant effects of maslinic acid in livers, hearts and kidneys of streptozotocin-induced diabetic rats: effects on kidney function. *Ren. Fail.* **36,** 419–431 (2014).
[35] Moneriz, C., Mestres, J., Bautista, J. M., Diez, A. & Puyet, A. Multi-targeted activity of maslinic acid as an antimalarial natural compound. *FEBS J.* **278,** 2951–2961 (2011).

La actividad antiinflamatoria también ha sido estudiada *in vitro* e *in vivo*, poniendo de manifiesto que el ácido maslínico actúa sobre la expresión de las enzimas proinflamatorias y citoquinas como COX-2, TNF-a e IL-6, dando lugar a una disminución de la inflamación.[36]

El ácido maslínico actúa también como parasitostático, comprobándose que impide la reproducción de parásitos protozoarios de la familia *Phyllum apicomplexa*. Estos estudios se han realizado en la Universidad de Granada por el Departamento de Parasitología y nuestro grupo de investigación dando como resultado una patente internacional titulada, "*Uso del ácido maslínico como agente antiparasitario frente a protozoarios del Phylum apicomplexa" (WO2006ES00500 2006090)*.

La utilización de ácido maslínico como aditivo alimentario animal, ha dado resultados destacables. Así, la adición de ácido maslínico a la dieta de truchas arco iris[37] y en doradas (*Sparus aurata*)[38] se traduce en un mayor tamaño/peso de estos animales, apreciándose un mayor contenido de proteínas tanto en hígado como en músculo.

Al igual que el ácido oleanólico, el ácido maslínico, ha sido estudiado frente a diferentes líneas celulares tumorales para ver su efecto en distintos tipos de cáncer,[39] de la que se destacan: A549 (carcinoma de pulmón humano), SK-OV-3 (cáncer de ovario), SK-MEL-2 (melanoma humano), XF-498 (cáncer del sistema nervioso central), HCT-15 (cáncer de colon), HSC-2 (carcinoma escamoso oral humano), y HSG (cáncer de las glándulas salivares). Además se ha comprobado, que ejerce también un efecto de inhibición de la proteasa del VIH.[40]

[36] Fukumitsu, S., Villareal, M. O., Fujitsuka, T., Aida, K. & Isoda, H. Anti-inflammatory and anti-arthritic effects of pentacyclic triterpenoids maslinic acid through NF-kB inactivation. *Mol. Nutr. Food Res.* ***60****,* 399–409 (2015).
[37] Fernández-Navarro, M., Peragón, J., Amores, V., De La Higuera, M. & Lupiáñez, J. A. Maslinic acid added to the diet increases growth and protein-turnover rates in the white muscle of rainbow trout (Oncorhynchus mykiss). *Comp. Biochem. Physiol. - C Toxicol. Pharmacol.* **147,** 158–167 (2008).
[38] Rufino-Palomares, E. E. *et al.* The role of maslinic acid in the pentose phosphate pathway during growth of gilthead sea bream (Sparus Aurata). *Aquac. Nutr.* **19,** 709–720 (2013).
[39] Rufino-Palomares, E. E. *et al.* Anti-cancer and anti-angiogenic properties of various natural pentacyclic triterpenoids and some of their chemical derivatives. *Curr. Org. Chem.* **19,** 919–947 (2015).
[40] Mayaux, J. F. *et al.* Triterpene derivatives that block entry of human immunodeficiency virus type 1 into cells. *Proc Natl Acad Sci U S A* **91,** 3564–3568 (1994).

6. IMPORTANCIA DE LA SOLUBILIDAD Y BIODISPONIBILIDAD DE COMPUESTOS BIOACTIVOS

La polaridad de una molécula es imprescindible para que aumente su solubilidad en agua. En este sentido, la introducción de nuevos grupos funcionales a una molécula serviría para mejorar su solubilidad en agua, así, un alqueno sin otro grupo funcional, no es soluble en agua, mientras que si le añadimos un grupo hidroxilo, y formamos metanol, etanol o propanol, se hace más soluble en agua.

La solubilidad es la capacidad de un soluto de disolverse en un disolvente para formar una solución homogénea. Es una propiedad esencial para aquellos compuestos con fines terapéuticos, porque deben disolverse para ser absorbidas a través de las membranas y llegar al sitio de acción. Por consiguiente, la solubilidad es uno de los parámetros más importantes que influyen en la biodisponibilidad del fármaco, es decir, la capacidad de un fármaco para estar disponible en una concentración apropiada en el sitio de acción, independientemente de la forma de dosificación farmacéutica y la vía de administración.[41]

La biodisponibilidad de un fármaco o principio activo es la cantidad del mismo que pasa al torrente sanguíneo para posteriormente ejercer su acción farmacológica. La poca solubilidad en el medio de un compuesto es un factor limitante para su absorción, por ello, para que su efecto sea adecuado es necesario que el principio activo esté disuelto en el sitio donde se lleve a cabo la absorción. La utilización de un producto natural con una adecuada solubilidad garantiza la acción terapéutica.[42]

[40] Mayaux, J. F. *et al.* Triterpene derivatives that block entry of human immunodeficiency virus type 1 into cells. *Proc Natl Acad Sci U S A* **91**, 3564–3568 (1994).
[41] Censi, R. & Di Martino, P. Polymorph impact on the bioavailability and stability of poorly soluble drugs. *Molecules* **20**, 18759–18776 (2015).
[42] Martín, A.; Molina, E. Polimorfismo farmacéutico. *Ámbito farmacéutico farmacocinética* **25**, 94-100 (2006).

Los ácidos oleanólico y maslínico son compuestos prácticamente insolubles en agua debido a su esqueleto carbonado de 30 átomos de carbono dispuestos en cinco anillos. Presentan varias funciones oxigenadas como un grupo carboxilo en C-28 y un grupo hidroxilo en C-3, para el ácido oleanólico, o dos grupos hidroxilo en C-2 y C-3 en el caso del ácido maslínico. Se ha podido comprobar que la presencia de un grupo carboxílico, introducido por una reacción de acilación, sobre los grupos hidroxilo en C-2 y/o C-3, mejora la solubilidad de estos productos naturales. Por lo tanto, las modificaciones en las funciones oxigenadas de estas moléculas (C-2, C-3 y C-28) parecen ser una vía para mejorar la solubilidad de nuestros productos de partida.

Teniendo en cuenta esta información, nuestro grupo de investigación, en colaboración con los Departamentos de Física Aplicada de las Universidades de Granada y Málaga, ha puesto a punto un ensayo para medir la solubilidad de algunos de estos derivados obtenidos, y también se han realizado unos primeros ensayos para el estudio de la formación de posibles nanopartículas con los mismos.

7. REACCIONES DE PEGILACIÓN

Un objetivo importante de este trabajo, como ya se ha mencionado, es mejorar la solubilidad de los compuestos naturales triterpénicos objeto de nuestro estudio. Para ello se han llevado a cabo reacciones de PEGilación con el fin de obtener derivados PEGilados con mayor solubilidad en medios acuosos.

La PEGilación es el proceso de unión covalente de polietilenglicol (PEG) a otra molécula que puede ser un fármaco, una proteína u otra molécula pequeña. El politetilenglicol (PEG) es el polieter comercialmente más importante y suele tener una masa molecular inferior a 20.000 g/mol. Los PEG son solubles en agua, metano, benceno, diclorometano, e insolubles en dietiléter y hexano, y se obtienen mediante la unión repetitiva

de unidades de etilenglicol, H-(OCH_2CH_2)$_n$-OH, formando polímeros lineales o ramificados de diferentes masas.

Existe una gran variedad de modificaciones químicas y tipos de PEG (Fig. 17) para preparar derivados activos con un grupo funcional adecuado para ser acoplado con la biomolécula objetivo. Los grupos funcionales más utilizados en proteínas, péptidos y otras moléculas objeto de la PEGilación suelen ser: amino, carboxilo, tiol, hidroxilo, etc.

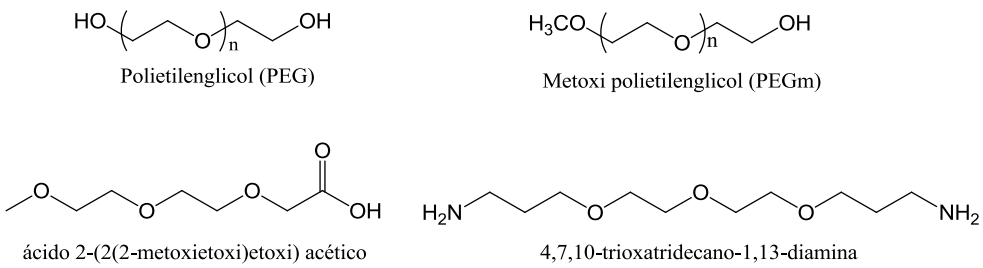

Figura 17. Tipos de PEG más utilizados.

La conjugación de biomoléculas con PEG presenta varias ventajas:

- Aumento de la solubilidad en agua.
- Estabilización de moléculas lábiles por su fácil degradación química.
- Reducción de la inmunogenicidad.
- Protección de la degradación proteolítica.
- Modificación de la biodistribuición y la biodisponibilidad.
- Penetración del fármaco por endocitosis.
- Aumento del tiempo de residencia en el cuerpo.

A finales de los años 70, al profesor Frank Davis le surgió la idea de conjugar un PEG con una proteína,[43] con el objetivo de que proteínas recombinantes fueran menos inmunogénicas para el organismo, y por tanto mejoraran su circulación y su vida útil. Pensó que si conseguía conjugar un polímero hidrofílico con la proteína, podría no ser reconocido por el sistema inmune como una molécula extraña. Realizó estudios sobre esta idea eligiendo una enzima, la catalasa de hígado bovino como proteína modelo,[44] a la que unió covalentemente metoxipolietilenglicol, descubriendo que efectivamente tenía una inmunogenicidad reducida y una vida útil más larga. Estos resultados dieron lugar a las primeras publicaciones sobre proteínas PEGiladas.

A raíz de estos acontecimientos, se siguió investigando sobre las PEGilaciones y sus posibilidades en la industria farmacéutica, teniendo en la actualidad una gran relevancia, ya que se están utilizando numerosos fármacos PEGilados para mejorar las propiedades de los mismos. Un ejemplo de ello son los interferones (INF), proteínas que son producidas por el sistema inmunitario como respuesta a agentes patógenos. Actualmente los interferones se están utilizando como terapias frente a hepatitis, virus VIH, esclerosis múltiple, leucemia, etc. Un ejemplo son los interferones INFa, fármacos para el tratamiento de la hepatitis C y B que presentan el inconveniente de que se degradan rápidamente una vez administrados. Así pues, para ser eficaces es necesario administrarlos con frecuencia para proporcionar concentraciones óptimas dentro del intervalo terapéutico, esto reduce la eficacia y conduce a un aumento de las condiciones adversas.[45]

[43] Hoffman, A. S. The early days of PEG and PEGylation. *Acta Biomater.* **40,** 1–5 (2016).
[44] Abuchowski, A., Es, T. V, Palczuk, N. C. & Davis, F. F. Alteration of immunological properties of bovine serum albumin by covalent attachment of poly(ethylene glycol). *J. Control. Rel.* **252,** 3578–3581 (1977).
[45] Thomas, T. & Foster, G. Nanomedicines in the treatment of chronic hepatitis C--focus on pegylated interferon alpha-2a. *Int. J. Nanomedicine* **2,** 19–24 (2007).

En los últimos años estos interferones han sido PEGilados como es el caso del interferón alfa-2a, donde estudios en ratas han demostrado que la PEGilación mejoró la biodisponibilidad, por un aumento de la absorción, mejoró la actividad antiviral y redujo la inmunogenicidad en comparación con el compuesto no PEGilado.[46] Hoy en día el PEG-interferón alfa-2 está siendo administrado para el tratamiento de adultos con hepatitis C crónica con enfermedad hepática.

Otro ejemplo son los estudios que actualmente se están realizando sobre fragmentos de anticuerpos (FAB anti-IL-17A) utilizados frente a enfermedades respiratorias, donde se ha demostrado *in vivo* que la PEGilación de este anticuerpo aumenta su permanencia en pulmón, mejorando su actividad terapéutica.[47]

Aunque la técnica de PEGilación se realiza principalmente en proteínas y enzimas, actualmente se está promoviendo para moléculas orgánicas pequeñas mejorando su biodisponibilidad. Destacamos la zidobudina (AZT)[48] que fue el primer fármaco aprobado por la administración de alimentos y fármacos (FDA) para el tratamiento del síndrome de inmunodeficiencia adquirida (SIDA), causado por el virus de la inmunodeficiencia humana (VIH), con el inconveniente de que su eficacia terapéutica sufre varias limitaciones clínicas, como su corta vida media, su toxicidad relacionada con la dosis y la resistencia a los medicamentos. Para superar estas limitaciones, el fármaco fue sometido a distintas reacciones de PEGilación usando para ello distintos tipos de PEG con el fin de estudiar cómo afecta dicha PEGilación al fármaco. Los resultados han sido muy prometedores (Fig. 18).

[46] Bailon, P. *et al.* Rational Design of a Potent, Long-Lasting Form of Interferon: A 40 kDa Brached Polythylene Glycol-Conjugated Interferon a-2a for the Treatment of Hepatitis C. *Bioconjug. Chem.* **12,** 195–202 (2001).
[47] Freches, D. *et al.* PEGylation prolongs the pulmonary retention of an anti-IL-17A Fab' antibody fragment after pulmonary delivery in three different species. *Int. J. Pharm.* **521,** 120–129 (2017).
[48] Li, W. *et al.* Synthesis, drug release and anti-HIV activity of a series of PEGylated zidovudine conjugates. *Int. J. Biol. Macromol.* **50,** 974–980 (2012).

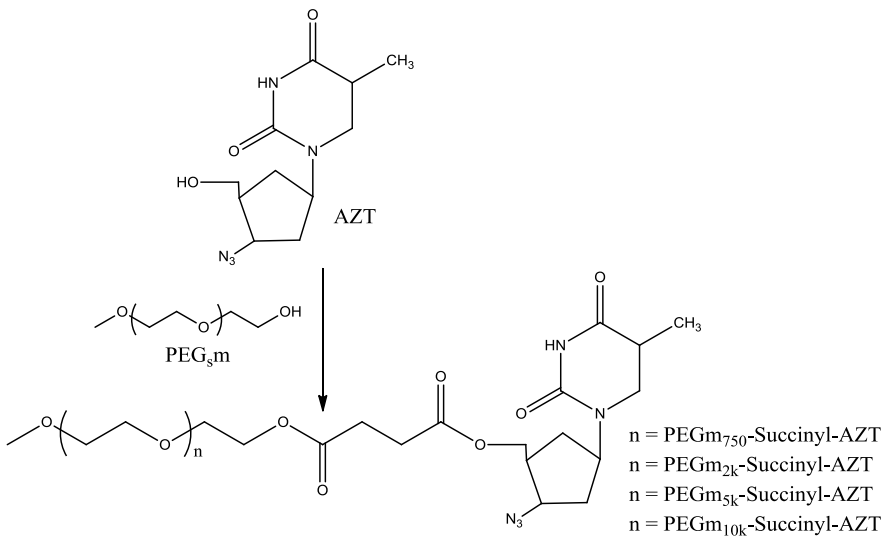

Figura 18. PEGilación del fármaco ATZ (zidobudina).

Viendo estos antecedentes, se ha realizado una serie de reacciones de PEGilación sobre compuestos triterpénicos con el objetivo de estudiar cómo afecta la PEGilación sobre la actividad biológica de estos compuestos. Una vez sintetizados todos estos derivados, se estudiarán sus actividades anti-tumorales y anti-HIV, dada la gran incidencia de estas enfermedades sobre la población mundial.

8. El CÁNCER

Según la Organización Mundial de la Salud el cáncer es la segunda causa de muerte en el mundo, ocasionando en 2015 unos 8.8 millones de muertes.

Se define el cáncer como el conjunto de enfermedades en las cuales un grupo de células normales sufren una transformación y empiezan a crecer de forma incontrolada, sin seguir las reglas del ciclo normal de las células. Esta transformación es consecuencia de la activación o mutación de genes reguladores que codifican el ciclo celular.

Para comprender mejor el origen del cáncer, es necesario entender cómo se dividen las células, es decir, cómo se produce el ciclo celular.

8.1. Ciclo celular

El ciclo celular es el mecanismo a través del cual las células crecen y se multiplican. Es un mecanismo muy complejo y bien regulado donde intervienen numerosos genes, encontrándose divido en 4 fases: Fases G1, S, G2 y M.

La fase G1 es la primera fase de crecimiento del ciclo celular, en la cual, la célula aumenta de tamaño debido a la síntesis y desarrollo de estructuras como son los microtúbulos, los microfilamentos de actina, los ribosomas, las proteínas, etc. Cuando las condiciones son desfavorables para las células que se encuentran en esta fase, pueden entrar en un periodo de reposo llamado G0, donde permanecen en este estado días, semanas o años dependiendo del organismo. Este estado de latencia se debe a la ausencia de factores de crecimiento.

La fase S es donde se produce la síntesis y duplicación del ADN. Esta fase se caracteriza por contener el doble de proteínas nucleares y de ADN.

La fase G2 es una tercera etapa de crecimiento debido a que continúa la síntesis de proteínas y síntesis de ARN. Es una etapa de preparación para la mitosis donde la cromatina se condensa para dar lugar a los cromosomas. Hay que destacar que en esta fase se reparan algunos errores que ocurren en la duplicación del ADN.

La fase M es la mitosis, donde la célula se divide para dar lugar a dos células idénticas.

La duración del ciclo celular es muy variable dependiendo del tipo de organismo, así, en *Echerichia coli* es de 30 minutos, en levaduras unas 2 horas, en fibroblastos de mamífero en cultivo unas 20 horas.

Anteriormente se mencionó que el ciclo celular es un mecanismo muy complejo donde intervienen numerosos genes que codifican proteínas, asegurando su correcto funcionamiento. Esta complejidad viene determinada por un conjunto de proteínas reguladoras como son las quinasas dependientes de ciclinas (CDk) y ciclinas que pueden formar complejos CDK-ciclinas implicadas en la progresión de cada fase del ciclo. Hay que destacar lo que se denominan puntos de control del ciclo, que se caracterizan por ser zonas donde puede ocurrir la detención del transcurso normal del ciclo (arresto), en presencia de ADN dañado para repararlo y evitar alteraciones genéticas. Se distinguen varios puntos de control siendo los más importantes, el punto de transición G1/S, el punto de transición G2/M y el punto de control en la mitosis en la transición de metafase a anafase (Fig. 19).

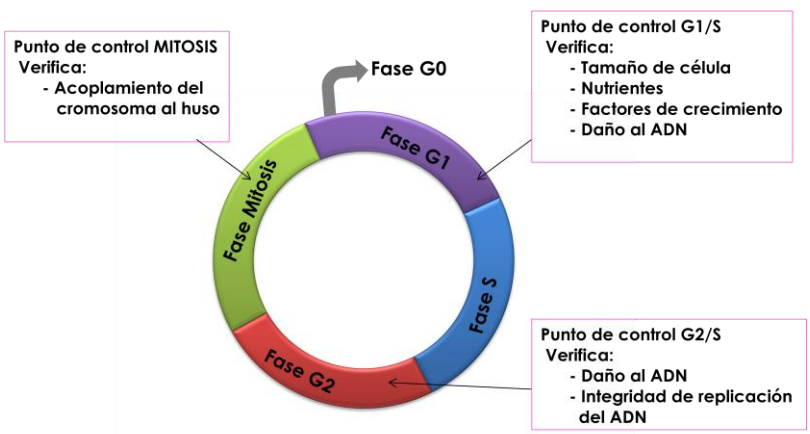

Figura 19. Ciclo celular.

Cuando hay daño en el ADN y la célula no puede repararlo en los distintos puntos de control, se activa un mecanismo de muerte celular programada (apoptosis) para eliminar dicha célula y que no pase a las

siguientes generaciones. Estos puntos de control son muy importantes proporcionando una barrera contra el cáncer y representan una buena opción para la aplicación de los agentes quimioterapéuticos.[49] Es por ello que para que se desarrolle un cáncer deben de fallar múltiples mecanismos que hagan que este tipo de células no active la señalización de la apoptosis y se divida más rápidamente evitando la muerte.

Existe una relación entre genes que intervienen en la regulación de la apoptosis, y genes que intervienen en el desarrollo del cáncer. Un ejemplo, es el gen que codifica la proteína p53, que inhibe la progresión del ciclo celular en caso de daño, aumentando sus niveles hasta detener el ciclo celular en G1/G0. El gen p53 se encuentra mutado en muchos tipos de tumores humanos, impidiendo la parada del ciclo celular ocasionando que las células continúen dividiéndose dando lugar a un cáncer.

8.2. Apoptosis

La apoptosis es un mecanismo de muerte celular programada que se produce en respuesta a señales internas (intrínsecas) y externas (extrínsecas). Se trata de un mecanismo muy importante en los organismos multicelulares, ejerciendo un papel esencial como mecanismo homeostático, con el fin de mantener las poblaciones celulares constantes en los tejidos o actuar como mecanismo de defensa cuando las células son dañadas por agentes nocivos.[50] Los fármacos usados para la quimioterapia del cáncer producen daño en el ADN, conduciendo a la muerte por apoptosis.

[49] Klermund, J., Bender, K. & Luke, B. High nutrient levels and torc1 activity reduce cell viability following prolonged telomere dysfunction and cell cycle arrest. *Cell Rep.* **9,** 324–335 (2014).
[50] Wen, B. *et al.* NIH Public Access. *October* **454**, 42–54 (2007).

La apoptosis no hay que confundirla con el proceso de necrosis (Fig. 20). La diferencia está en que la necrosis es un mecanismo desordenado en el que la célula se hincha por tomar agua del exterior de forma incontrolada provocando que la membrana se rompa y se libere todo el contenido citoplasmático al exterior, mientras que en la apoptosis se produce una condensación de la cromatina, disminución del volumen celular, la fosfatidilserina que normalmente se encuentra dentro de la membrana celular queda expuesta en su superficie, se produce fragmentación del ADN, la membrana plasmática forma unas invaginaciones sin llegar a romperse dando lugar a los cuerpos apoptóticos que serán fagocitados y degradados por los macrófagos.

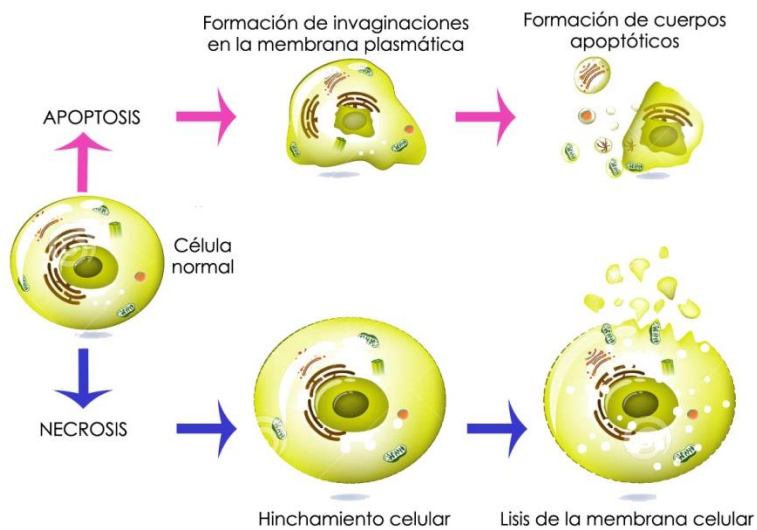

Figura 20. Diferencia entre necrosis y apoptosis (modificado de Dreamstime.com).

La iniciación de la apoptosis a nivel molecular puede desencadenarse por diferentes señales intracelulares y extracelulares activándose dos tipos de rutas, la ruta intrínseca o la ruta extrínseca de muerte celular mediada por unas enzimas de aspartato-proteasas denominadas caspasas.[51]

[51] Taylor, R. C., Cullen, S. P. & Martin, S. J. Apoptosis: controlled demolition at the cellular level. *Nat. Rev. Mol. Cell Biol.* **9**, 231–241 (2008).

Ambas rutas se diferencian en los mecanismos moleculares que las activan, así como en las caspasas iniciadoras responsables de la activación (Fig. 21).

La ruta intrínseca o mitocondrial se caracteriza por ser iniciada por diferentes estímulos, como agentes físicos o químicos, que causan daño celular, entre los que se encuentran fármacos quimioterapéuticos, neurotoxinas, radiación ultravioleta, moléculas del estrés oxidativo, etc., que desencadenan la activación de la apoptosis. Esta vía está controlada por una familia de proteínas denominadas Bcl-2, clasificándose en proteínas pro-apoptóticas como por ejemplo, BAX, Bid, Puma, etc y proteínas no apoptóticas como Bcl-2, Bcl-XL, etc.[52] Así por ejemplo, la inhibición de Bcl-2 junto con la activación de BAX da como resultado una actuación sobre la mitocondria, liberándose factores mitocondriales como el citocromo C, que conduce a la activación de la caspasa 9, que a su vez activa la caspasa 3, enzima principal de la inducción de la apoptosis. Hay que tener en cuenta que en muchos tipos de células tumorales la proteína Bcl-2 está sobreexpresada, bloqueando la apoptosis y permitiendo que dicha célula continúe dividiéndose, provocando un tumor.

La ruta extrínseca o apoptosis mediada por receptores, se induce cuando un ligando extracelular se une a un receptor de los llamados receptores de muerte celular (FAS, TNFR, TRAILR) necesarios para la transmisión de la señal de apoptosis.[53]

[52] Walensky, L. D. BCL-2 in the crosshairs: tipping the balance of life and death. *Cell Death Differ.* **13,** 1339–1350 (2006).
[53] Pérez, E. H., Alarcón-, F. J., Almanza-pérez, J. C. & López-díaz, N. E. Receptores de muerte , apoptosis y su relación con la fibrosis hepática. **11,** 54–62 (2010).

Estos receptores poseen el llamado dominio de muerte (DD) que tras la interacción de un ligando, como por ejemplo TNF (factor de necrosis tumoral) y FasL (ligando Fas), entre otros, sufren un cambio conformacional desencadenando moléculas adaptadoras (FADD) permitiendo la movilización de un conjunto de proteínas y caspasas que conduce a la activación de la caspasa 8, activando a su vez la caspasa 3 dando lugar a la apoptosis.

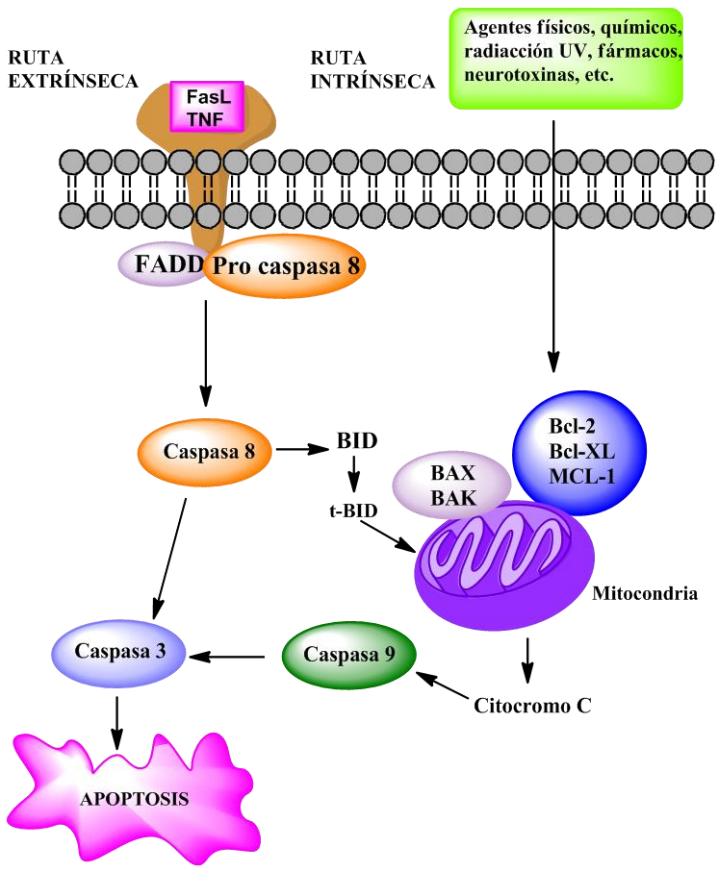

Figura 21. Esquema de las rutas intrínseca y extrínseca de la apoptosis.

El mecanismo de apoptosis es muy importante para el buen funcionamiento del desarrollo de un organismo y para evitar que daños en el ADN pasen a siguientes generaciones, por ello, una diana para enfrentarnos a células malignas, es la búsqueda de compuestos bioactivos

capaces de activar el mecanismo apoptótico con el fin de eliminar a estas células anormales.

9. VIRUS DE LA INMUNODEFICIENCIA HUMANA (VIH)

El virus del VIH es el responsable de provocar el síndrome de la inmunodeficiencia humana (SIDA) que se caracteriza por una debilidad del sistema inmunitario por el ataque del virus a las células encargadas de defender al organismo. Como consecuencia, dicho organismo se encuentra desprotegido poniéndose en riesgo de contraer graves infecciones o neoplasias.

En 1983 el virus del VIH fue aislado por primera vez en un paciente con linfadenopatía a partir de células del nódulo linfático.[54]

Se conocen dos tipos de virus, el VIH tipo 1 (VIH-1) que hace referencia a los virus genéticamente relacionados en varias regiones de África, Asia, Europa y América, y el VIH tipo 2 (VIH-2) que es endémico de África central presentando una menor mortalidad y patogenicidad que el VIH-1, considerado el responsable de la epidemia mundial. Ambos tipos dan lugar al SIDA, pero presentan diferencias en su organización genómica, ya que alrededor del 40% presentan similitud en sus secuencias.[55]

En la presente memoria se llevará a cabo un estudio del HIV-1 por su amplia distribución mundial. Según la Organización Mundial de la Salud (OMS), se estima que el número de personas infectadas con el HIV-1 es de 39.7 millones.

[54] Barré-Sinoussi, F. *et al.* Isolation of a T-Lymphotropic Retrovirus from a Patient at Risk for Acquired Immune Deficiency Syndrome (AIDS). *Mont. Source Sci. New Ser.* 220, 868–871 (1983).
[55] Vela, C. M., Bernal, C. & García, F. Diagnóstico Y Tratamiento De Las Infecciones Por El Virus De La Inmunodeficiencia Humana Tipo 2. (1985).

9.1. Estructura del virus VIH-1

El VIH-1 es un virus que pertenece a la familia *retroviridae* concretamente a la subfamilia de los *lentivirus*.

El VIH como retrovirus, se caracteriza por ser una partícula infecciosa (virión) icosaédrica de unos 80-100nn de diámetro en cuya estructura podemos distinguir tres capas (Fig. 22):

- Capa externa o envoltura lipoproteíca, constituida por dos tipos de glucoproteínas, la gp120 que es una glucoproteína de superficie y la gp41, glucoproteína transmembrana. Ambas constituyen una membrana lipídica. Debajo de esta membrana encontramos una matriz o cubierta intermedia formada por la proteína p17 en estructura icosaédrica.

- Cápside icosaédrica, compuesta por la proteína p24 en disposición helicoidal.

- Capa interna o nucleoide, formada por la proteína p9, la cual envuelve al genoma viral y donde se localizan enzimas muy importantes para el virus, como son la proteasa, la integrasa y la transcriptasa reversa.

El genoma del virus está constituido por dos copias iguales de ARN de cadena sencilla, de polaridad positiva. Los genes que codifican las proteínas virales los podemos dividir en: estructurales, reguladores y auxiliares (Fig.23).

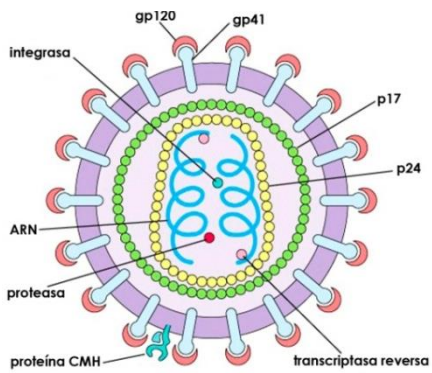

Figura 22. Estructura del virus VIH (modificado de www.emaze.com).

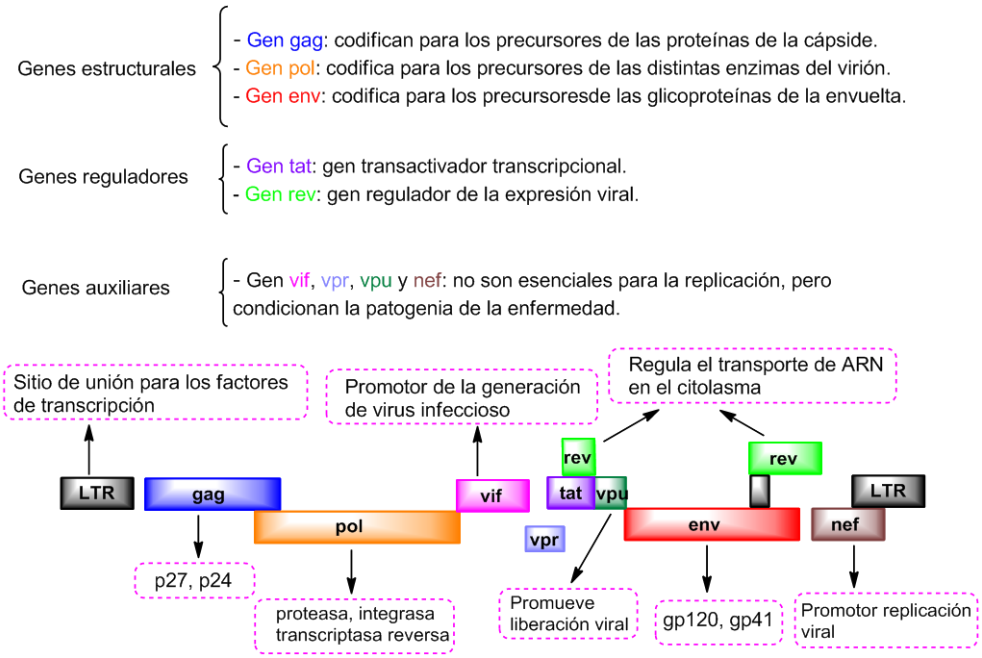

Figura 23. Esquema genoma HIV.

9.2. Ciclo biológico VIH

Para comprender mejor la actuación del virus es necesario conocer su ciclo de vida replicativo, permitiendo centrar la búsqueda de nuevas biomoléculas activas según la fase del ciclo. Se distinguen 6 fases: a) entrada del virus a la célula huésped, b) transcripción, c) integración del ADN viral, d) periodo de latencia, e) síntesis de ARN y expresión de proteínas, f) síntesis de ARN y expresión de proteína, f) ensamblaje, maduración y liberación de las partículas virales (Fig. 24).

a) Entrada del virus a la célula huésped

Antes de penetrar el virus en la célula huésped, el VIH tiene que reconocer a la célula que va a infectar, para ello, este virus se ha especializado en reconocer una inmonoglobulina, el antígeno CD4, localizado principalmente en la membrana plasmática de los linfocitos T, aunque también se encuentra expresado en otras células como son

macrófagos, monocitos, células de la microglía y células dendríticas. Otros receptores que se han descubierto recientemente y que el virus es capaz de reconocer para entrar en la célula, son los receptores CCR5 en macrófagos y CXR4 en linfocitos T.[56] Una vez reconocidos los receptores, el VIH se une a la célula por la interacción del dominio transmembrana de Env (gp120) con CD4, produciendo un cambio conformacional, generando la unión y fusión de la membrana del virus y de la célula.

El mecanismo de la fusión no se conoce en profundidad, aunque hace relativamente poco tiempo, en 2015, se determinó la estructura de una región de gp41, permitiendo la propuesta de un modelo molecular para el mecanismo de la fusión de las membranas.[57]

b) Transcripción

Tras la fusión del virus con la célula huésped, el genoma viral es liberado al citoplasma celular donde se llevará a cabo la síntesis del ADN viral a partir del ARN viral, gracias a la acción de la enzima transcriptasa inversa que produce una hebra de ADN, dando lugar a un híbrido ADN/ARN. La síntesis de la segunda cadena se produce por la acción de la ARNasa, degradando el ARN y obteniendo una hebra de ADN complementaria a la anterior.

c) Integración del ADN viral

Sintetizado el ADN viral, se produce su translocación junto a varias proteínas al núcleo para integrarse en el genoma de la célula huésped. Se produce por la acción de la enzima denominada integrasa.

[56] Chikere, K., Chou, T., Gorry, P. R. & Lee, B. Affinofile profiling: How efficiency of CD4/CCR5 usage impacts the biological and pathogenic phenotype of HIV. *Virology* **435,** 81–91 (2013).
[57] Apellániz, B. *et al.* The atomic structure of the HIV-1 gp41 transmembrane domain and its connection to the immunogenic membrane-proximal external region. *J. Biol. Chem.* **290,** 12999–13015 (2015).

d) Periodo de latencia

Una vez integrado el ADN viral, puede ocurrir que permanezca latente durante un tiempo corto o prolongado dependiendo de los casos. El paso de esta fase a la reactivación para proseguir con el ciclo, depende de factores celulares como es el caso de la proteína NF-KB (complejo de proteínas que controla la transcripción del ADN), implicada en la respuesta celular frente a estímulos como la radiación ultravioleta, el estrés, la infección por virus o las bacterias, etc.[58]

e) Síntesis de ARN y expresión de proteínas

Una vez producida la reactivación del virus, se produce la síntesis de ARN viral a partir del ADN viral del núcleo, que posteriormente será transportado al citoplasma donde se producirá la expresión de los genes virales. Distinguimos dos etapas, en la primera se produce una transcripción temprana de los genes reguladores tat, rev y nef, y en la segunda una transcripción tardía de los genes estructurales codificados por gag, pol y env y genes auxiliares vif, vpr y vpu. El gen tat es un activador de la transcripción que permite la síntesis del ARN viral. El gen Rev codifica una proteína que se encarga de transportar los ARN mensajeros del núcleo al retículo endoplasmático, donde son traducidos a proteínas por los ribosomas y que posteriormente serán transportados al citoplasma.

f) Ensamblaje, maduración y liberación de las partículas virales

Una vez sintetizadas las proteínas obtenidas tras la traducción, una enzima denominada proteasa se encarga de cortarlas para obtener pequeñas proteínas constitutivas del virus que se irán ensamblando para formar una nueva partícula del virus. La poliproteína $Pr55^{Gag}$ (Gag) es importante para el ensamblaje, se encarga de reclutar el genoma viral y dirige la formación de la càpside.[59]

[58] Perkins, N. D. Integrating cell-signalling pathways with NF-kappaB and IKK function. *Nat. Rev. Mol. Cell Biol.* **8**, 49–62 (2007).
[59] Mailler, E. *et al.* The life-cycle of the HIV-1 gagRNA complex. *Viruses* **8**, 1–19 (2016).

Finalmente, una vez hayan madurado las nuevas proteínas virales, son liberadas mediante un proceso de gemación a través de la membrana plasmática, quedando libres los viriones y preparados para infectar a otra célula huésped.

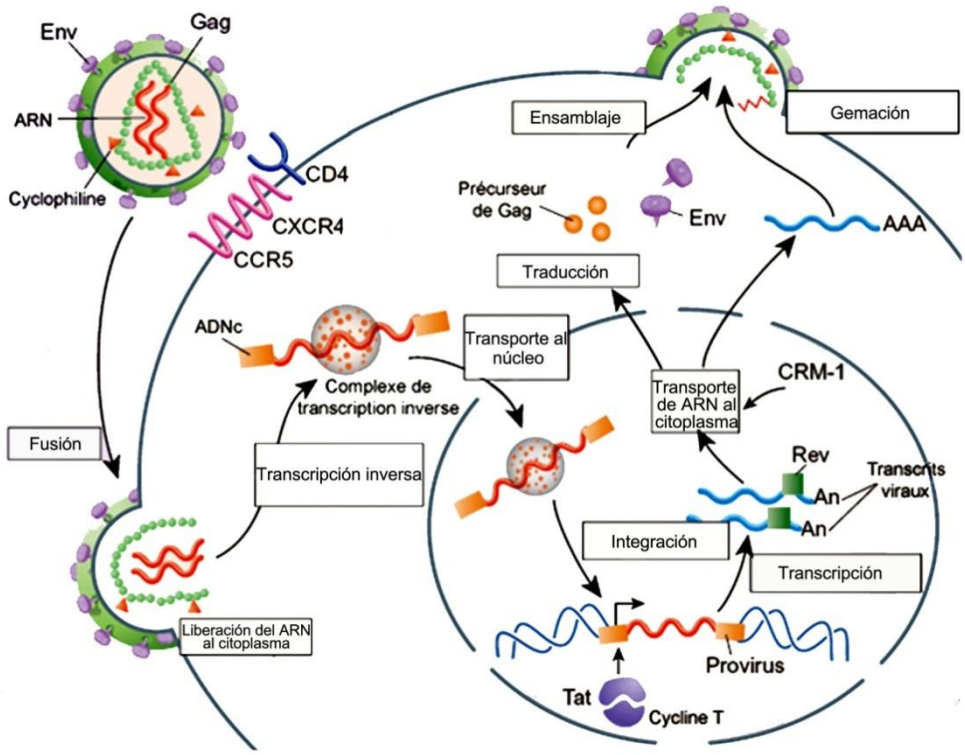

Figura 24. Ciclo biológico del VIH (modificado de http://ies.rayuela.mostoles.educa.madrid.org/deptos/dbiogeo/recursos/Apuntes/BioGeoBach1/6-Clasificacion/ActualAcelulares.htm).

II OBJETIVOS

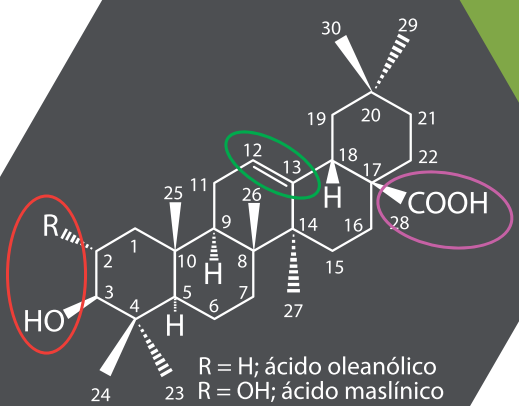

El trabajo de investigación desarrollado en esta memoria se encuadra dentro del campo de los Productos Naturales, en el área de la Química Orgánica. Como materia prima se han utilizado los productos procedentes de los desechos de la molturación de la aceituna, lo que permite el aprovechamiento de recursos naturales propios de nuestra región, que por su abundancia y contaminación suponen un problema para Andalucía. El ácido oleanólico (ácido 3β-hidroxiolean-12-en-28-óico, AO) y el ácido maslínico (ácido 2a,3β-dihidroxiolean-12-en-28-óico, AM), son los principales componentes triterpénicos de estos residuos, los cuales han manifestado numerosas y variadas propiedades biológicas. Una de las características que presentan estos ácidos es su poca solubilidad en agua, lo que influye de forma notable en su biodisponibilidad, y que conlleva que sus propiedades biológicas no se manifiesten con todo su potencial.

Por estos motivos el objetivo global del presente trabajo es "la derivatización de los productos naturales, ácido oleanólico y ácido maslínico, para la obtención de una librería de derivados, mejorando su solubilidad y sus actividades anti-cancerígenas y anti-VIH".

En este trabajo se han llevado a cabo los siguientes objetivos:

- Semisíntesis y evaluación antiproliferativa de triterpenos pentacíclicos PEGilados mediante la unión de agentes pegilantes ácido y diamino.

- Síntesis y estudio biológico del derivado 3β-succiniloxiolean-12-en-28-oato de bencilo, frente a células tumorales de melanoma (B16-F10).

- Síntesis y evaluación antiproliferativa *in vitro* de ácidos triterpénicos PEGilados mediante la unión de fragmentos de polietilénglicol de distintos tamaños.

- Síntesis y estudio de derivados conjugados de ácidos triterpénicos con diferentes diaminas como potenciales agentes anti-cancerígenos.

- Síntesis Orgánica en Fase Sólida de una biblioteca de derivados de ácido oleanólico y su estudio frente a la inhibición de la proteasa del VIH-1.

III ANTECEDENTES

Existen numerosos estudios con extractos vegetales de una gran variedad de plantas que presentan propiedades biológicas asociadas a la presencia de compuestos terpénicos. En los últimos años se han publicado numerosos artículos donde se han puesto de manifiesto un amplio espectro de actividades de estos triterpenos, destacando sobre todo los que presentan un esqueleto de lupano, oleanano o ursano.[60] A continuación, se detalla un estudio bibliográfico sobre distintos tipos de terpenos y sus derivados, que poseen actividades anti-cancerígenas y anti-VIH.

1. TERPENOS Y DERIVADOS CON ACTIVIDADES ANTI-CANCERÍGENAS

Como se comentó con anterioridad, dentro de los terpenos se pueden encontrar desde los compuestos más sencillos, como son los monoterpenos, a los más complejos como los triterpenos, presentando muchos de ellos actividad anti-cancerígena. Se describe a continuación un resumen de los distintos terpenos con actividad anti-cancerígena.

1.1. Monoterpenos, sesquiterpenos y diterpenos

Monoterpenos como el D-limoneno y el alcohol perilílico (Fig. 25) son productos naturales que inhiben el desarrollo de varios tipos de cánceres.

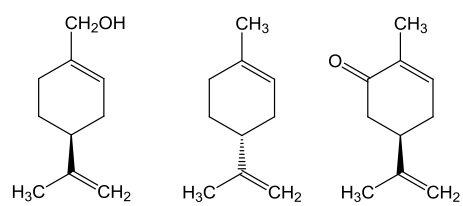

Figura 25. Monoterpenos con actividad anti-cancerígena.

[60] Sifaoui, I. *et al.* In vitro effects of triterpenic acids from olive leaf extracts on the mitochondrial membrane potential of promastigote stage of Leishmania spp. *Phytomedicine* **21,** 1689–1694 (2014).

El D-limoneno está presente en la cáscara de los cítricos y también es un componente de los aceites esenciales de la alcaravea, lavanda, anís, canela, menta, romero, salvia, etc. Estudios realizados recientemente *in vitro* en células de cáncer de colon (LS174T), ha dado como resultado una inhibición de la viabilidad de estas células, causando una muerte celular por apoptosis y observándose un aumento en la concentración de la proteína BAX y citocromo C de la mitocondria, así como una disminución de BcL-2 induciendo la apoptosis.[61] Este efecto de inducción de la apoptosis se ha visto también en células de leucemia (K562 y HL-60),[62] en células de cáncer gástrico (MGC803)[63] y en cáncer de próstata (DU-145 y PZ-HPV-7),[64] tras el tratamiento de D-limoneno.

El alcohol perilílico se puede encontrar también en la alcaravea, aceite de lavanda y la lila, así como en cerezas, arándanos, menta, hierbabuena, etc. Presenta una estructura muy similar al D-limoneno, la diferencia es que el alcohol perilílico posee un grupo hidroxilo. Al igual que el D-limoneno, el alcohol perilílico posee propiedades anticancerígenas frente al cáncer de colon (HCT 116)[65] y al cáncer de páncreas (BxPC-3).[66] El alcohol perilílico posee mejores resultados que el D-limoneno y por ello, este monoterpeno está en fase clínica 2 para el cáncer de piel[67] y el cáncer de mama.[68]

[61] Jia, S. S. *et al.* Induction of apoptosis by D-limonene is mediated by inactivation of Akt in LS174T human colon cancer cells. *Oncol. Rep.* **29,** 349–354 (2013).
[62] Ji, J. *et al.* Induction of apoptosis by d-limonene is mediated by a caspase-dependent mitochondrial death pathway in human leukemia cells. *Leuk. Lymphoma* **47,** 2617–2624 (2006).
[63] Zhang, X.-Z., Wang, L., Liu, D.-W., Tang, G.-Y. & Zhang, H.-Y. Synergistic inhibitory effect of berberine and d-limonene on human gastric carcinoma cell line MGC803. *J. Med. Food* **17,** 955–62 (2014).
[64] Rabi, T. & Bishayee, A. d -Limonene sensitizes docetaxel-induced cytotoxicity in human prostate cancer cells: Generation of reactive oxygen species and induction of apoptosis. *J. Carcinog.* **8,** 9 (2009).
[65] Bardon, S., Foussard, V., Fournel, S. & Loubat, A. Monoterpenes inhibit proliferation of human colon cancer cells by modulating cell cycle-related protein expression. *Cancer Lett* **181,** 187–194 (2002).
[66] Wiseman, D. a, Werner, S. R. & Crowell, P. L. Cell cycle arrest by the isoprenoids perillyl alcohol, geraniol, and farnesol is mediated by p21(Cip1) and p27(Kip1) in human pancreatic adenocarcinoma cells. *J. Pharmacol. Exp. Ther.* **320,** 1163–70 (2007).
[67] Stratton, S. P. *et al.* A phase 2a study of topical perillyl alcohol cream for chemoprevention of skin cancer. *Cancer Prev. Res.* **3,** 160–169 (2010).
[68] Bailey, H. H. *et al.* Phase II trial of daily oral perillyl alcohol (NSC 641066) in treatment-refractory metastatic breast cancer. *Cancer Chemother. Pharmacol.* **62,** 149–157 (2008).

Otro monoterpeno con actividad frente al cáncer es la L-carvona (Fig. 25), terpenoide que se encuentra principalmente en la menta (*Mentha spitaca*) y que posee dicho olor característico. Los estudios han demostrado que es capaz de arrestar el ciclo celular en la fase S dando como resultado la inducción de la apoptosis en el cáncer de mama.[69]

Las lactonas sesquiterpénicas (Fig. 26) son triterpenoides de gran importancia debido a sus propiedades biológicas, dentro de las cuales se encuentran la citotoxicidad frente a células cancerígenas. La artemisinina, aislada de *Artemisia annua,* es un fármaco antimalárico que recientemente ha demostrado presentar actividad anti-cancerígena frente a células ME-180 (cáncer de cuello de útero), con un efecto antiproliferativo y proapoptótico en dichas células tumorales.[70] Un derivado de la artemisinina, la dihidroartemisinina, induce apoptosis en células de carcinoma hepatocelular (HCC) por pérdida del potencial de membrana mitocondrial, observándose que la apoptosis ocurre por la ruta intrínseca.[71] Otro tipo de lactona es la partenolida que produce apoptosis frente a varios tipos de líneas celulares tumorales como Panc-1 (cáncer de páncreas),[72] HeLa (cáncer cervical)[73] y HepG2 (cáncer de hígado).[74]

[69] Patel, P. B. & Thakkar, V. R. L-Carvone Induces p53, Caspase 3 Mediated Apoptosis and Inhibits the Migration of Breast Cancer Cell Lines. *Nutr. Cancer* **66,** 453–462 (2014).
[70] Mondal, A. & Chatterji, U. Artemisinin Represses Telomerase Subunits and Induces Apoptosis in HPV-39 Infected Human Cervical Cancer Cells. *J. Cell. Biochem.* **116,** 1968–1981 (2015).
[71] Qin, G. *et al.* Dihydroartemisinin induces apoptosis preferentially via a Bim-mediated intrinsic pathway in hepatocarcinoma cells. *Apoptosis* **20,** 1072–1086 (2015).
[72] Liu, W. Parthenolide suppresses pancreatic cell growth by autophagy-mediated apoptosis. 453–461 (2017).
[73] Jeyamohan, S., Moorthy, R. K., Kannan, M. K. & Arockiam, A. J. V. Parthenolide induces apoptosis and autophagy through the suppression of PI3K/Akt signaling pathway in cervical cancer. *Biotechnol. Lett.* **38,** 1–10 (2016).
[74] Sun, J. *et al.* Parthenolide-induced apoptosis, autophagy and suppression of proliferation in HepG2 cells. *Asian Pacific J. Cancer Prev.* **15,** 4897–4902 (2014).

Determinados derivados de la partenolida se han ensayado frente a la leucemia y al glioma mostrando mejores resultados que su precursor, siendo más citotóxicos y más estables.[75] Para finalizar con este tipo de compuestos, hay que destacar que la tapsigargina, que actualmente está siendo muy estudiada por sus propiedades biológicas, ha destacado porque induce apoptosis en células HepG2, mediante la activación de las caspasas 12, 9 y 3.[76]

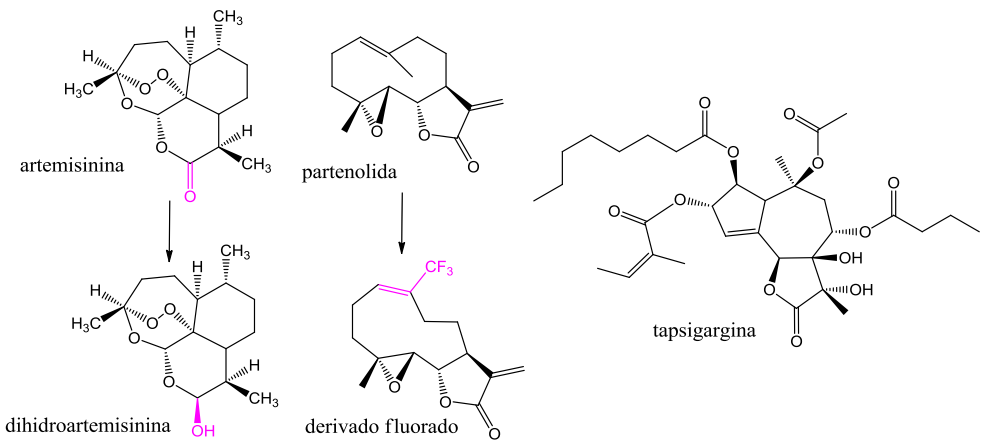

Figura 26. Lactonas sesquiterpénicas con actividad anti-tumoral.

Los taxoides son diterpenos cíclicos polioxigenados con esqueleto de taxano, que se aislan principalmente de la corteza de los árboles *Taxus spp*. Presentan actividades anti-tumorales, destacando el paclitaxel o taxol, compuesto de gran importancia en la medicina oncológica (Fig. 27). Actualmente se está utilizando como fármaco quimioterapéutico para el cáncer de mama, de ovario y pulmón bajo el nombre de taxol®.[77] Este compuesto se caracteriza por actuar a nivel del ciclo celular degradando el huso mitótico, conduciendo a la muerte celular por el arresto o parada del ciclo en la fase G2/M.

[75] Yang, Z. J. *et al.* Syntheses and Biological Evaluation of Costunolide, Parthenolide, and Their Fluorinated Analogues. *J. Med. Chem.* **58,** 7007–7020 (2015).
[76] Wang, C. *et al.* Thapsigargin induces apoptosis when autophagy is inhibited in HepG2 cells and both processes are regulated by ROS-dependent pathway. *Environ. Toxicol. Pharmacol.* **41,** 167–179 (2016).
[77] Weaver, B. A. How Taxol/paclitaxel kills cancer cells. *Mol. Biol. Cell* **25,** 2677–81 (2014).

El problema que presenta actualmente el taxol es la resistencia de muchos pacientes al mismo, lo que está causando la aparición de nuevos derivados con el objetivo de minimizar este problema.[78] Un ejemplo destacado es el derivado denominado docetaxol, el cual se está utilizando como fármaco quimiterapeútico frente al cáncer de mama, de pulmón y de próstata, encontrándose en fase clínica II para el cáncer gástrico en combinación con otros fármacos.[79]

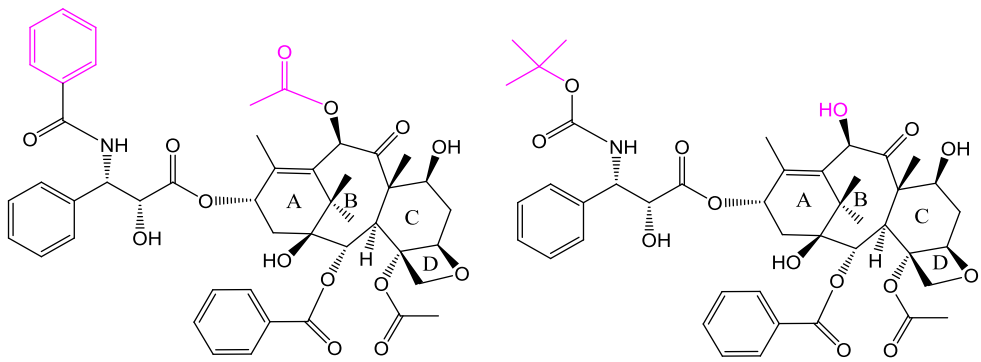

Figura 27. Estructura del paclitaxel y su derivado docetaxol.

Existen otros diterpenos con actividad antitumoral, siendo el más destacado el ácido abiético y algunos de sus derivados, que actualmente se están investigando frente al cáncer de pulmón (A549), al cáncer de próstata (PC-3) y al cáncer de ovario (SKOV-3) (Fig. 28).[80]

[78] Lai, D., Ho, K. C., Hao, Y. & Yang, X. Taxol resistance in breast cancer cells is mediated by the hippo pathway component TAZ and its downstream transcriptional targets Cyr61 and CTGF. *Cancer Res.* **71,** 2728–2738 (2011).
[79] H., C. *et al.* Phase I/II study of a combination of capecitabine, cisplatin and intraperitonealdocetaxel (XP ID) in patients with advanced gastric cancer with peritoneal metastasis. *J. Clin. Oncol.* **33,** no pagination (2015).
[80] Xu, H. *et al.* Identification of a diverse synthetic abietane diterpenoid library for anticancer activity. *Bioorg. Med. Chem. Lett.* **27,** 505–510 (2016).

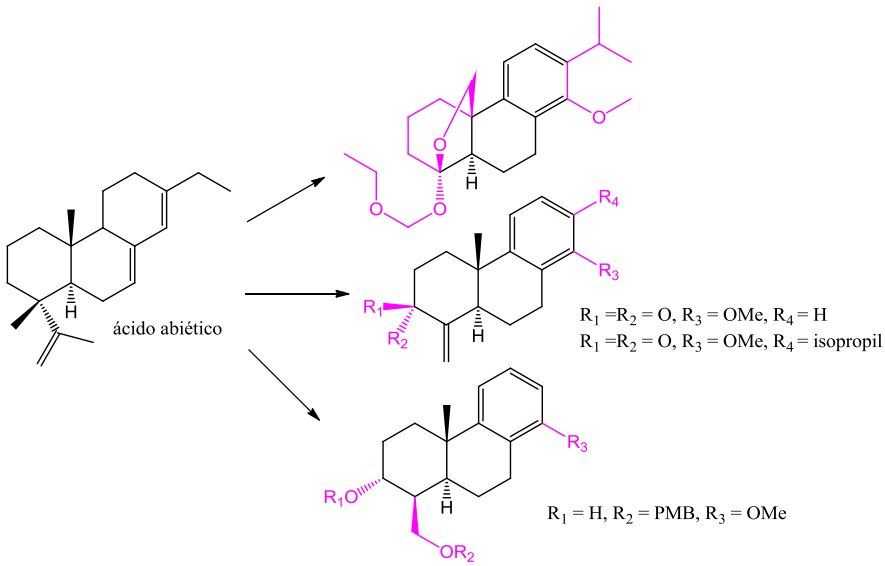

Figura 28. Ácido abiético y sus derivados con actividad anti-tumoral.

1.2. Triterpenos pentacíclicos

Como se comentó con anterioridad, los triterpenos con esqueleto de lupano, oleanano y ursano son los más estudiados, presentando un amplio número de actividades biológicas, siendo una de las más importantes su efecto antitumoral (Fig. 29). En este apartado, se describe un resumen de un estudio bibliográfico sobre los distintos compuestos con actividad anti-cancerígena en función del tipo de esqueleto que presentan.

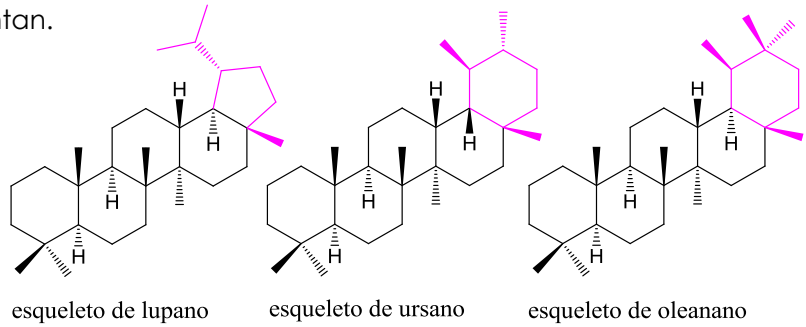

Figura 29. Esqueletos de lupano, ursano y oleanano.

Hay que destacar que los triterpenos son moléculas que están poco funcionalizadas, en donde la actividad biológica viene determinada por dos o tres funciones, constituyendo las zonas diana sobre las que actuar en caso de derivatizar dichas moléculas, con la finalidad de mejorar sus actividades biológicas.

Los compuestos triterpénicos exhiben un gran número de propiedades biológicas, sin embargo nos centraremos en una de las actividades que tiene mayor relevancia, la actividad anti-tumoral. Estos compuestos triterpénicos han sido estudiados en detalle en los últimos años, y esos trabajos nos han aportado abundante información sobre el tipo de modificaciones que se pueden llevar a cabo en sus estructuras para potenciar su efecto anti-cancerígeno.

- Los triterpenos con esqueleto de lupano han sido estudiados por varios grupos de investigación por su potencial terapéutico, siendo el lupeol, la betulina y el ácido betulínico los más estudiados.

El lupeol (3β-lup-20(29)-en-3-ol) (Fig. 30), se puede encontrar en numerosas plantas y se caracteriza por poseer un grupo hidroxilo en C-3. Se ha comprobado su actividad anti-cancerígena en varias líneas tumorales entre las que destacamos B16-F10 (melanoma de ratón), A549 (carcinoma de pulmón), A2780 (cáncer de ovario), etc.[81] Aunque sus actividades han sido moderadas, en la actualidad se sigue investigando su acción frente al cáncer, habiéndose observado un efecto significativo frente a células de carcinoma hepático (SMMC-7721) en estudios *in vitro* e *in vivo*.[82]

[81] Hap, T. & Gehring, U. Biological activities of. ***5***, 285–332 (2008).
[82] Jin, Y. *et al.* Lupeol enhances radiosensitivity of human hepatocellular carcinoma cell line SMMC-7721 in vitro and in vivo. *Int. J. Radiat. Biol.* 1–27 (2014).

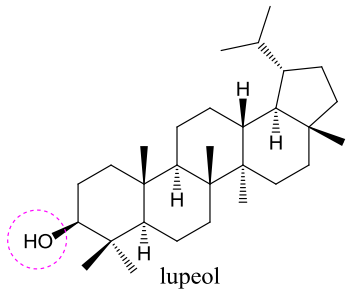

Figura 30. Triterpeno con esqueleto de lupano, lupeol.

La betulina (lup-20(29)-en-3β,28-diol) (Fig. 31), aislada de la corteza del abedul, ha mostrado efectos anti-tumorales, inhibiendo significativamente la viabilidad de las células SGC7901 (cáncer gástrico avanzado), demostrándose que la inducción de la apoptosis está mediada a través de la ruta apoptótica intrínseca.[83] Este compuesto se caracteriza por poseer un grupo hidroxilo en C-3 y otro grupo hidroxilo en C-28. Un estudio ha puesto de manifiesto que la sustitución de grupos acetilo en C-3 y C-28 da como resultado una mejoría en la actividad frente a varias líneas tumorales como el cáncer de ovario (A-2780) y el adenocarcinoma de colon (DLD-1 y HTC-116).[84]

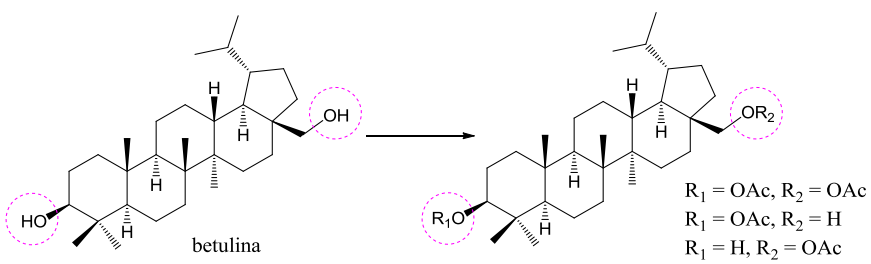

Figura 31. Betulina y derivados con efectos anti-tumorales.

[83] Li, Y. *et al.* Betulin induces reactive oxygen species-dependent apoptosis in human gastric cancer SGC7901 cells. *Arch. Pharm. Res.* **39,** 1257–1265 (2016).
[84] Kommera, H., Kaluderović, G. N., Kalbitz, J. & Paschke, R. Synthesis and anticancer activity of novel betulinic acid and betulin derivatives. *Arch. Pharm. (Weinheim).* **343,** 449–457 (2010).

El ácido betulínico (ácido 3β-hidroxi-lup-20(29)-en-28-oico) (Fig. 32), está distribuido por todo el reino vegetal y es el compuesto triterpénico más importante con esqueleto de lupano. En 1995 se descubrió que este ácido inhibía de forma selectiva a líneas celulares tumorales de melanoma (MEL-1, MEL-2, MEL-4), induciendo la apoptosis por arresto del ciclo celular en fase G0/G1.[85] Estos estudios permitieron observar su posible potencial como compuesto anti-cancerígeno. El ácido betulínico se caracteriza por ser una molécula difuncionalizada que presenta un grupo hidroxilo en C-3 y un grupo carboxilo en C-28. Se han realizado numerosos estudios que han demostrado que el grupo carboxilo en C-28 tiene una clara relevancia en su actividad biológica. Por ejemplo, al esterificar dicho ácido para la obtención de diferentes derivados, se observaba una mejora de dicha actividad. También se llevaron a cabo reacciones de acilación sobre el grupo hidroxilo de C-3, obteniéndose resultados satisfactorios. En la actualidad se siguen realizando modificaciones de su estructura para aumentar su biodisponibilidad ya que, al igual que los productos naturales de partida de la presente memoria, poseen problemas de baja solubilidad. Un estudio a destacar es la conjugación directa sobre el hidroxilo de C-3 de cuatro tipos de reactivos PEGs (moléculas derivadas del polietilénglicol), dando como resultado un aumento de la solubilidad, una disminución de la citotoxicidad *in vitro* frente a cáncer de pulmón (A549 y LLC) y una mejor supervivencia de ratones portadores de tumores tratados con estos nuevos derivados en comparación con los resultados obtenidos con el ácido betulínico.[43]

[85] Duncan, C., Dougall, H., Johnston, P. & Green, S. © 199 5 Nature Publishing Group *Nat. Med.* **1,** 546–551 (1995).

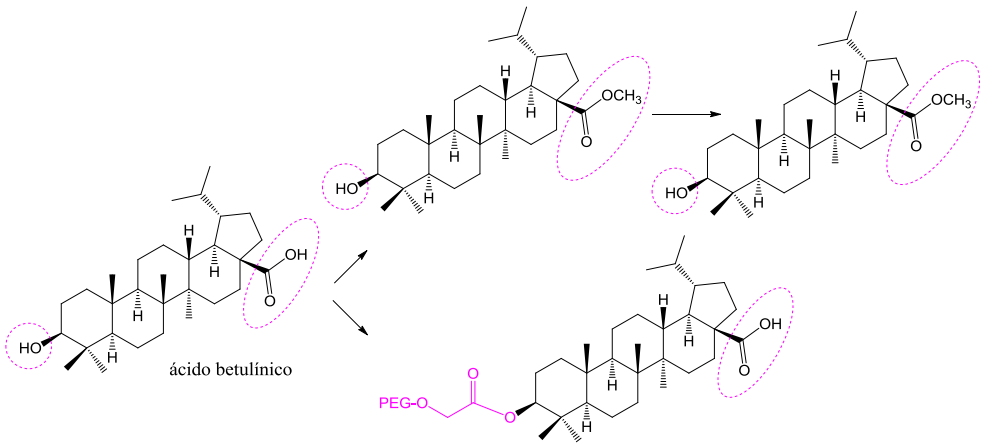

Figura 32. Derivados del ácido betulínico con actividad anti-cancerígena.

- Entre los triterpenos con esqueleto de ursano, destacamos al ácido ursólico (Fig. 33), componente principal del revestimiento de plantas y de la cera de diversas frutas como peras, manzanas, aceitunas, etc. Posee un amplio abanico de propiedades biológicas, destacando por sus propiedades como agente quimiopreventivo y quimioterapéutico en varias líneas celulares tumorales.[86] Ensayos *in vivo* e *in vitro* sugieren que puede ser un buen candidato para el tratamiento de tumores, pero presentan el mismo incoveniente que el ácido betulínico, una baja solubilidad y una limitada biodisponibilidad. Para suplir este inconveniente se están llevando a cabo modificaciones en su estructura sobre los grupos funcionales en C-3 y C-28.

[86] Shanmugam, M. K. *et al.* Ursolic acid in cancer prevention and treatment: Molecular targets, pharmacokinetics and clinical studies. *Biochem. Pharmacol.* **85,** 1579–1587 (2013).

Estas modificaciones han supuesto una mejora en su actividad biológica frente a distintos tipos de cánceres. Diversos grupos de investigación prepararon una serie de derivados con el fin de investigar que modificaciones son importantes para su actividad biológica. Un dato interesante es que la introducción de un grupo acetilo en C-3 o de un grupo amino en C-3 y un resto amino en C-28 mejoraba significativamente su actividad.[87] En un estudio reciente, la modificación en C-28 por la introducción de un grupo amino, mejoró significativamente la inhibición del crecimiento celular, así como cuando se esterificaron los grupos funcionales de C-3 y C-28 con anhídrido succínico.[88]

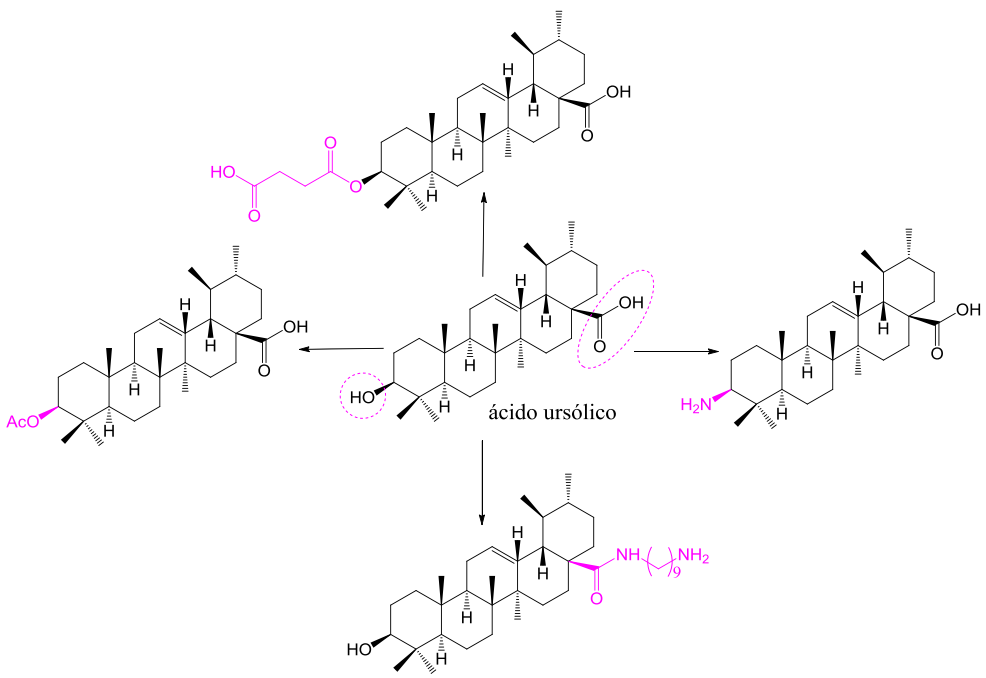

Figura 33. Distintos derivados del ácido ursólico con actividad anti-cancerígena.

[87] Chen, H. *et al.* Evolution in medicinal chemistry of ursolic acid derivatives as anticancer agents. *Eur. J. Med. Chem.* **92,** 648–655 (2015).
[88] Meng, Y.-Q. *et al.* Synthesis and antitumor activity evaluation of novel ursolic acid derivatives. *J. Asian Nat. Prod. Res.* **18,** 280–288 (2016).

- Los triterpenos con esqueleto de oleanano presentan una amplia diversidad estructural. En este grupo se encuentran numerosas moléculas con importantes actividades biológicas, pero nos centraremos en los ácidos oleanólico y maslínico, por ser los productos naturales de partida nuestro estudio.

El ácido oleanólico es uno de los triterpenos pentacíclicos más estudiados por sus múltiples propiedades biológicas. En los últimos años se han obtenido numerosos derivados modificando las zonas funcionalizadas de su estructura química, el grupo hidroxilo de C-3, el doble enlace C-12/C-13 y el grupo carboxilo de C-28. Estudios *in vitro* e *in vivo* han reportado que este compuesto induce apoptosis e inhibe el crecimiento de células tumorales.

La baja solubilidad que presenta hace necesaria su derivatización, con objeto de potenciar sus propiedades anti-tumorales y mejorar su solubilidad en medios acuosos. Un ejemplo de ello es el derivado CDDO (ácido 2-ciano-3,12-dioxooleana-1,9(11)-dien-28-oico), que presenta un grupo ciano en C-2 y dos grupos cetonas en C-3 y C-12, y que exhibe actividad anti-cancerígena por activación de la vía apoptótica extrínseca en células de leucemia. Derivados obtenidos por modificación de CDDO, como su metil éster en C-28 (CDDO-Me), poseen una mayor actividad que sus precursores en distintas líneas celulares tumorales como cáncer de pulmón, cáncer de mama, cáncer de próstata, cáncer de ovario y osteosarcoma.[89] Hay que destacar que el CDDO-Me ha completado con éxito un ensayo clínico para la fase I del tratamiento del cáncer.[90]

[89] Petronelli, A., Pannitteri, G. & Testa, U. Triterpenoids as new promising anticancer drugs. *Anticancer. Drugs* **20**, 880–892 (2009).
[90] Hong, D. S. *et al.* A phase I first-in-human trial of bardoxolone methyl in patients with advanced solid tumors and lymphomas. *Clin. Cancer Res.* **18**, 3396–3406 (2012).

La síntesis de otros derivados de CDDO, como aquellos que tienen unido un grupo imidazol en C-28 (CDDO-im), distintas amidas como CDDO-MA (metilamida), CDDO-EA (etilamida) y CDDO-TFEA (trifluoroetilamida), también han mostrado un efecto apoptótico en distintas células tumorales (Fig. 34).[91]

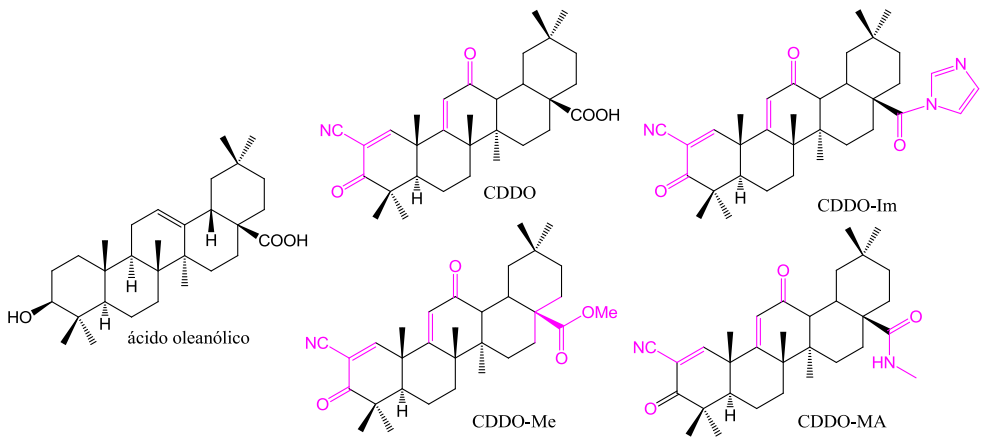

Figura 34. Derivados de ácido oleanólico con actividad apoptótica.

Otro tipo de derivados del ácido oleanólico se formaron introduciendo, en los sitios activos de la molécula, grupos imidazol carbamatos, *N*-alquilimidazoles o *N*-acilimidazoles, que presentaban una mejor actividad antiproliferativa frente a células de cáncer de páncreas (Fig. 35). Este estudio pone de manifiesto que los derivados amídicos sintetizados son más efectivos cuando no existe un grupo acetilo en C-3. Además, los derivados con un grupo carbamato eran más activos cuando presentaban un grupo imidazol en la posición C-28, y menos activos con un grupo metoxi en dicha posición.[92]

[91] Kuo, R.-Y., Qian, K., Morris-Natschke, S. L. & Lee, K.-H. Plant-derived triterpenoids and analogues as antitumor and anti-HIV agents. *Nat. Prod. Rep.* **26,** 1321–1344 (2009).
[92] Leal, A. S., Wang, R., Salvador, J. a R. & Jing, Y. Synthesis of novel heterocyclic oleanolic acid derivatives with improved antiproliferative activity in solid tumor cells. *Org. Biomol. Chem.* **11,** 1726–38 (2013).

Recientemente se han sintetizado una serie de derivados del ácido oleanólico modificando el anillo C de su estructura triterpénica. Estos compuestos se ensayaron en distintas líneas celulares tumorales resultando que el derivado con mayor actividad citotóxica frente a células de cáncer de mama (MCF-7) era el que tenía un grupo diénico en el anillo C y un grupo metilo en C-28 (Fig. 35).[93]

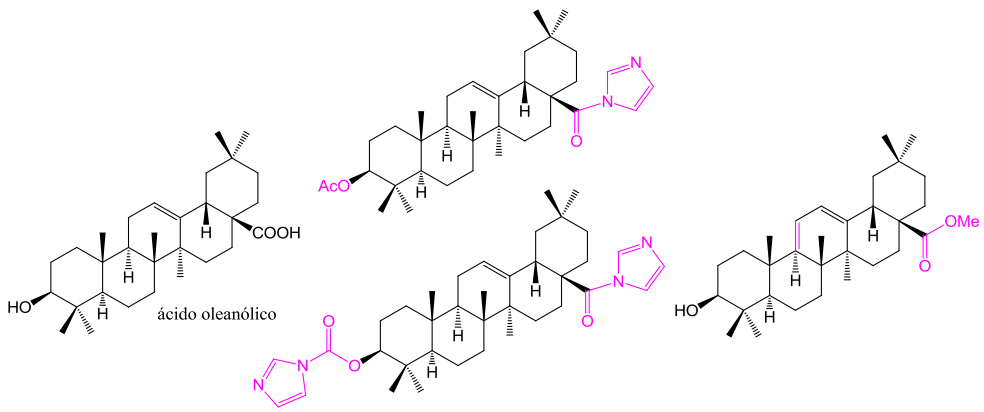

Figura 35. Derivados del ácido oleanólico con grupos imidazol y dieno derivado.

El ácido maslínico se ha estudiado menos que el ácido oleanólico, posiblemente por su menor disponibilidad, aunque en los últimos años está creciendo su interés por su potencial como agente anti-cancerígeno. Se ha visto que ésteres y amidas de este ácido en C-28 mejoran su actividad frente a varias líneas celulares como HT29 (adenocarcinoma de colon), MCF7 (cáncer de mama), A549 (carcinoma de pulmón), entre otras (Fig. 36).[94] En este estudio se sintetizaron diversos derivados, observándose que el derivado éster propílico se mostró más potente que el éster etílico. También se pudo concluir que los derivados con grupos con dobles enlaces produjeron una disminución de la actividad.

[93] Pattnaik, B., Lakshma Nayak, V., Ramakrishna, S. & Venkata Mallavadhani, U. Synthesis of ring-C modified oleanolic acid derivatives and their cytotoxic evaluation. *Bioorg. Chem.* **68,** 152–158 (2016).
[94] Siewert, B., Pianowski, E. & Csuk, R. Esters and amides of maslinic acid trigger apoptosis in human tumor cells and alter their mode of action with respect to the substitution pattern at C-28. *Eur. J. Med. Chem.* **70,** 259-272 (2013).

Las amidas que se sintetizaron en este estudio mostraron menos citotoxicidad que los ésteres pero eran más activas que el producto de partida.

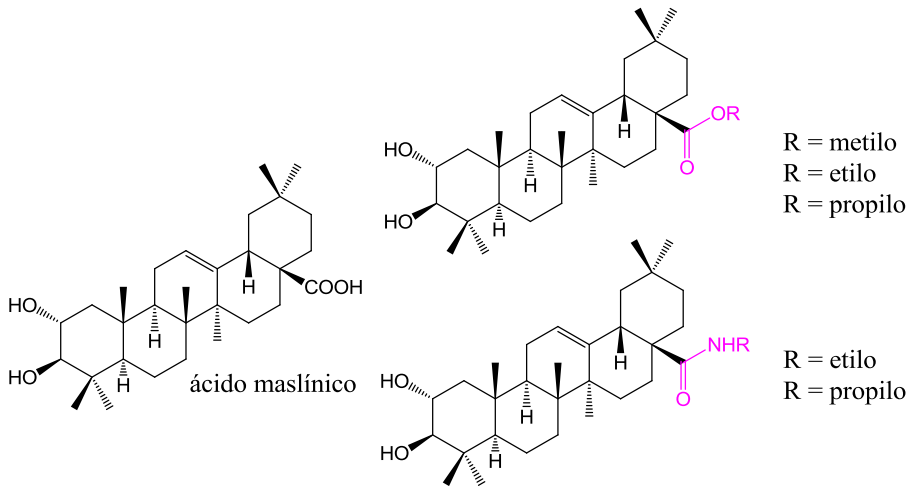

Figura 36. Amidas y ésteres del ácido maslínico con actividad anti-cancerígena.

Las derivatizaciones realizadas de los ácidos oleanólico y maslínico en los últimos años por nuestro grupo de investigación, comentados anteriormente en esta introducción (Fig. 37), han puesto de manifiesto que los derivados acilados exhiben efectos citotóxicos como inhibidores del crecimiento frente a células de melanoma de ratón (B16-F10), siendo más activos los que presentan un grupo bencilo en el grupo carboxilo de C-28 y fragmentos dicarboxílicos polares sobre los grupos hidroxilo del anillo A.[18] Por otro lado, derivados aminoacilados de estos ácidos, presentan buena actividad citotóxica frente a células de melanoma de ratón (B16-F10), adenocarcinoma de colon humano (HT29) y hepatocarcinoma de humano (HepG2), observándose que, aquellos compuestos que presentan en su estructura un ω-aminoácido de cadena larga (11AUA) en el grupo carboxílico en C-28 y un grupo acilo (acetilo o butanoilo) en el grupo hidroxilo en C-3 o en los de C-2/C-3 del anillo A, mejoraban considerablemente su actividad. [22]

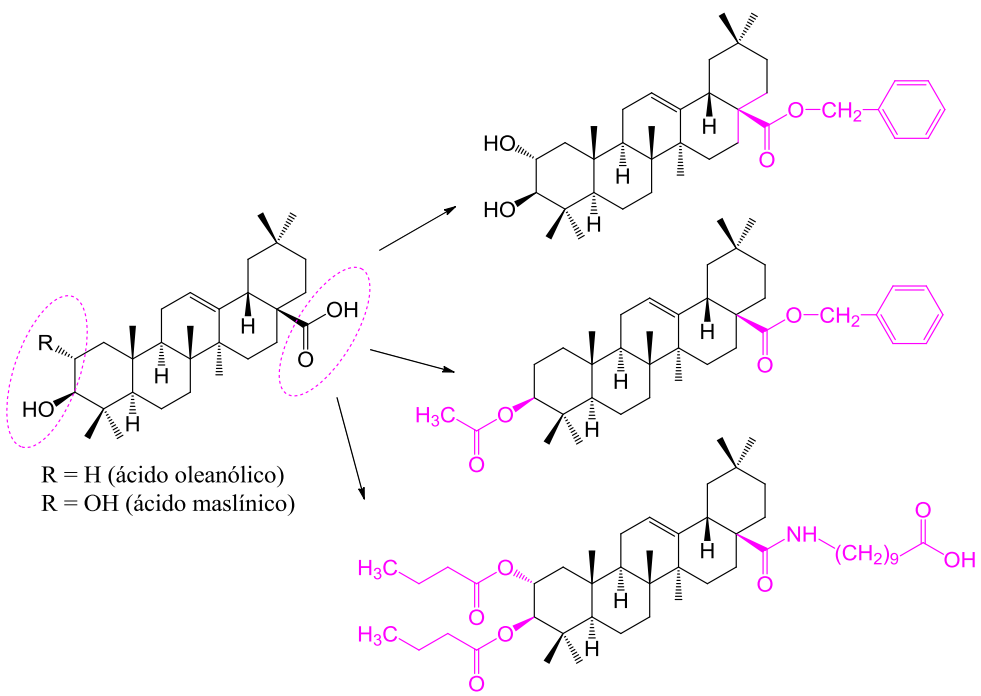

Figura 37. Derivados de los ácidos oleanólico y maslínico con actividad anti-tumoral.

2. TERPENOS Y DERIVADOS CON ACTIVIDADES ANTI-VIH

Como se vio anterieomente en esta introducción, el ciclo de vida del VIH es muy complejo, e intervienen numerosas proteínas y enzimas en las distintas fases. Los fármacos o nuevas moléculas bioactivas frente al VIH tienen su diana en una fase concreta del ciclo. Así, podemos clasificarlos según en la fase del ciclo donde actúen, en:

- Inhibidores de la entrada: evitan que el VIH penetre en las células. Su mecanismo de acción se debe a que son capaces de adherirse a las proteínas de superficie del VIH (gp120, gp41) o a los receptores CD4, CCR5 y CXR4 quedando bloqueados e impidiendo que el VIH se pueda adherir a la superficie de las células huésped.

- Inhibidores nucleósidos de la transcriptasa reversa: se caracterizan por ser capaces de evitar que el material genético del VIH se pueda unir correctamente al material genético de la célula infectada. Esta acción se debe a que presentan una estructura similar a los nucleótidos usados por esta enzima para transformar el ARN en ADN y como consecuencia el nuevo ADN no puede formarse correctamente.

- Inhibidores no nucleósidos de la transcriptasa reversa: se unen al enzima evitando que el ARN se convierta en ADN.

- Inhibidores de la integrasa: actúan bloqueando la integración evitando que el virus inserte su ADN en el material genético de la célula huésped.

- Inhibidores de la transcripción: bloquean la transcripción.

- Inhibidores de la proteasa: son capaces de evitar que las células infectadas por el virus no puedan producir nuevas copias debido a que bloquean la enzima, impidiendo que ésta corte las hebras de material genético que darán lugar a los nuevos viriones.

Entre los tipos de terpenos con actividad anti-HIV, destacamos algunos diterpenos, sesquiterpenos y sobre todo triterpenos pentacíclicos.

A continuación, se realizará un estudio bibliográfico de los tipos de terpenos que son activos frente al virus del VIH, teniendo en cuenta la fase en la que pueden actuar dichos compuestos, y destacando que algunos de estos compuestos están siendo utilizados como fármacos para mejorar la calidad de vida de los enfermos de SIDA o están en fase clínica.

2.1. Sesquiterpenos y diterpenos

Entre los sesquiterpenos cabe destacar dos productos naturales aislados de *Litsea verticillata* (familia *Lauraceae*), el oxyfillendiol B y el 1,2,3,4-tetrahidro-2,5-dimetil-8-(1-metil-etil)-1,2-naftalenediol que presentan

actividad anti-HIV, actuando en la fase de replicación del virus VHI-1(Fig. 38).[95]

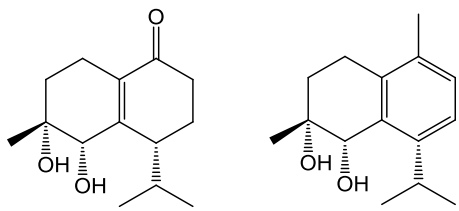

oxyfillendiol B

1,2,3,4-tetrahidro-2,5-dimetil-8-(1-metil-etil)-1,2-naftalenediol

Figura 38. Sesquiterpenos que inhiben la replicación del virus VIH-1.

Diversos estudios han podido determinar que distintos tipos de diterpenos son capaces de actuar inhibiendo la replicación del virus VIH-1. Entre ellos se destaca la henrin A, un nuevo diterpeno aislado de las hojas de *Pteris henryi* con estructura de ent-kaurano, que ha demostrado una importante inhibición de la replicación en células 293T (células de riñón embrionario humano) infectadas con el plásmido de expresión de la envuelta del virus VSV-G y un vector del VIH de replicación pNL4-3.Luc.RE) (Fig. 39).[96] El ingenol, aislado de *Euphorbia tirucalli,* y sus derivados, también han presentado inhibición de la replicación del VIH en células infectadas 293T con plásmidos pNL4.3 y pNL4.3-Luc del virus, lo que les convierte en compuestos potenciales para la terapia del VIH.[97]

[95] Zhang, H. J. *et al.* Sesquiterpenes and butenolides, natural anti-HIV constituents from Litsea verticillata. *Planta Med.* **71,** 452–457 (2005).
[96] Li, W. F. *et al.* Henrin A: A new anti-HIV Ent-kaurane diterpene from Pteris henryi. *Int. J. Mol. Sci.* **16,** 27978–27987 (2015).
[97] Abreu, C. M. *et al.* Dual role of novel ingenol derivatives from Euphorbia tirucalli in HIV replication: Inhibition of de novo infection and activation of viral LTR. *PLoS One* **9,** 1–14 (2014).

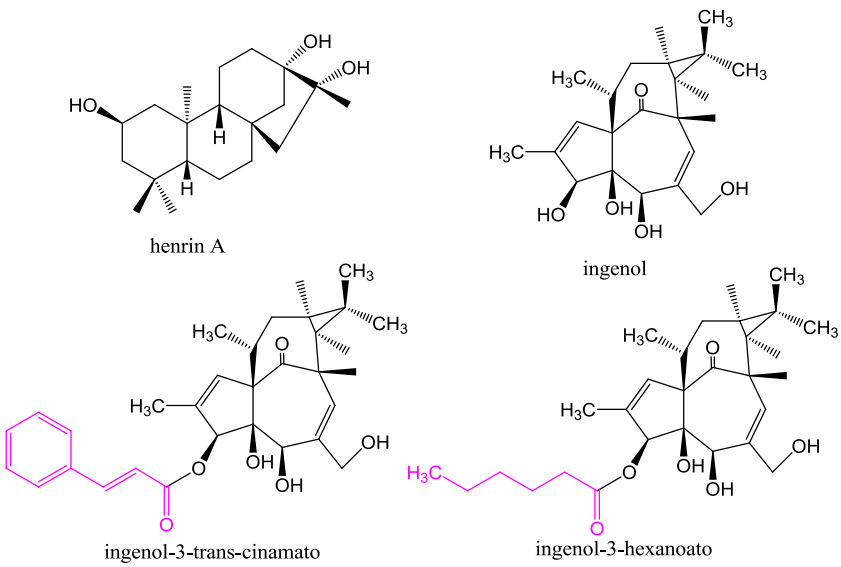

Figura 39. Diterpenos que inhiben la replicación del virus VIH-1.

Otro diterpeno con importante actividad biológica frente al VIH es la andrografolida, aislada de *Andrographis paniculata*, y que inhibe la fusión celular mediada por gp120, uniéndose a regiones de dicha proteína, impidiendo que el virus penetre en la célula huésped (Fig. 40).[98]

Por último, cabe destacar un producto natural denominado calanolida A, que actúa a nivel de la transcriptasa inversa inhibiéndola, siendo un tipo de inhibidor no nucleósido. Recientemente se están realizando estudios clínicos usando la calanolida A en combinación con otros inhibidores como lamivudina y nelfinavir, que se utilizan como fármacos frente al VIH, con objeto de comprobar su eficacia y toxicidad (Fig. 40).[99]

[98] Uttekar, M. M. *et al.* Anti-HIV activity of semisynthetic derivatives of andrographolide and computational study of HIV-1 gp120 protein binding. *Eur. J. Med. Chem.* **56,** 368–374 (2012).
[99]Xue, H. *et al.* Highly suppressing wild-type HIV-1 and Y181C mutant HIV-1 strains by 10-chloromethyl-11-demethyl-12-oxo-calanolide A with druggable profile. *J. Med. Chem.* **53,** 1397–1401 (2010).

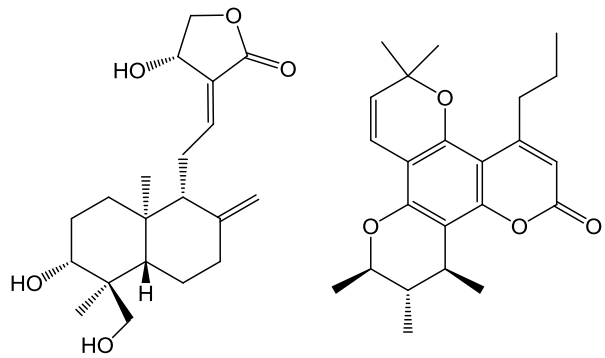

andrografolida calanolida A

Figura 40. Diterpenos con actividad frente al VIH.

2.2. Triterpenos

Dentro de los terpenos, los triterpenos son los compuestos que presentan mayores actividades anti-HIV. En la actualidad, están siendo muy estudiados tanto los compuestos naturales, como los derivados sintéticos de los mismos, con objeto de encontrar nuevas moléculas frente al VIH que no tengan resistencia al virus con el paso del tiempo.

Los triterpenos más estudiados son el ácido betulínico, ácido morónico, el ácido oleanólico y el ácido maslínico entre otros.

El ácido betulínico, con esqueleto de lupano, es capaz de inhibir la replicación del VIH. El primer estudio que se realizó fue en 1994, en el que se observó la inhibición *in vitro* del VIH en linfocitos H9. Desde entonces, éste ácido está siendo uno de los más utilizados como producto de partida para el desarrollo de nuevos derivados con mayor potencial frente al virus del VIH.[100]

[100]From, A. P. & Clavzflqrum, S. anti-hiv activity of structurally related triterpenoids. *Journal of Natural Products* **57**, 243–247 (1994).

Modificaciones en el grupo hidroxilo de C-3 del ácido betulínico, mediante reacciones de acilación con distintos tipos de anhídridos, han demostrado la importancia de la funcionalidad éster en C-3. Ejemplo de ello, es el derivado llamado bevirimat (ácido 3-*O*-(3',3'-dimetilsuccinil)-betulínico), cuya principal característica es la formación de un éster con un 3,3-dimetilsuccínico en el grupo hidroxilo de C-3. Este compuesto bloquea la replicación del VIH-1 en una etapa tardía de la maduración viral. Estudios de fase cínica I y II empezaron a realizarse, con resultados muy prometedores como fármaco frente al virus,[9] aunque otros restudios han puesto de manifiesto una alta resistencia farmacológica debido a la existencia de variantes del VIH-1.[101] Actualmente, nuevos derivados de bevirimat están siendo sintetizados con el fin de mejorar la resistencia al VIH-1. Ejemplo de ello, es la modificación del grupo carboxilo de C-28 por la introducción de ácidos ω-aminoalcanoicos y 1,ω-diaminoalcanos que están dando buenos resultados frente a la resistencia de distintas cepas del HIV-1(Fig. 41).[102]

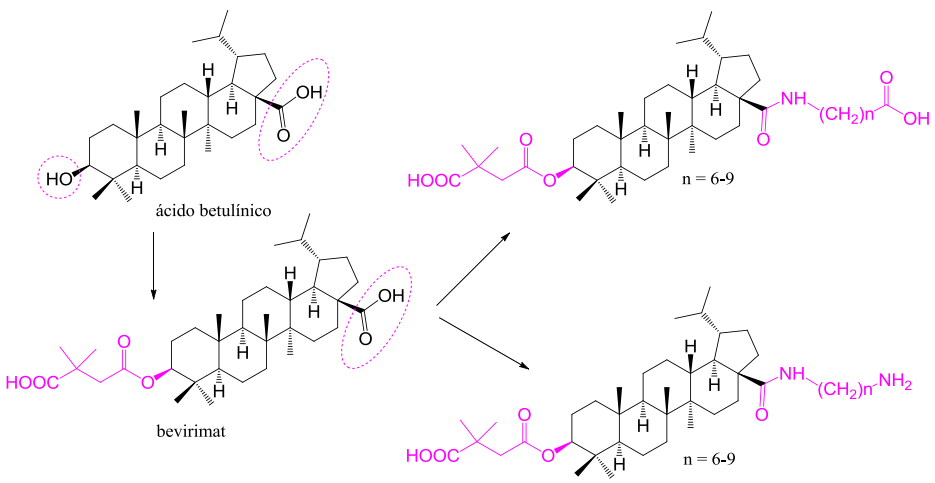

Figura 41. Ácido betulínico, bevirimat y derivados.

[101] Martin, D. E., Salzwedel, K. & Allaway, G. P. Review Bevirimat : a novel maturation inhibitor for the treatment of HIV-1 infection. Antiviral Chemistry Et Chemotherapy **19**,107–113 (2008).
[102] Dang, Z. *et al.* New Betulinic Acid Derivatives for Bevirimat-Resistant Human Immunode fi ciency Virus Type–1. *J. Med. Chem.* **56**, 2029-2037 (2013).

El ácido morónico se caracteriza por presentar una grupo carbonilo en C-3 del anillo A de la estructura triterpénica, mostrando actividad anti-VIH en linfocitos H9.[103] La síntesis de derivados de este ácido empezaron a realizarse sobre el grupo funcional en C-3 mediante el empleo de reacciones de acilación, debido a que esta sustitución es fundamental para la actividad anti-VIH. Estudios de estructura-actividad pusieron de manifiesto la necesidad de modificar también el grupo carboxilo de C-28.[104] Los derivados bifuncionalizados de este ácido dieron mejores resultados, destacando aquellos compuestos que estaban sustituidos en C-3 por un 3,3-dimetilsuccinil y en C-28 por distintas aminas de diferente tamaño de cadena (Fig. 42).[105]

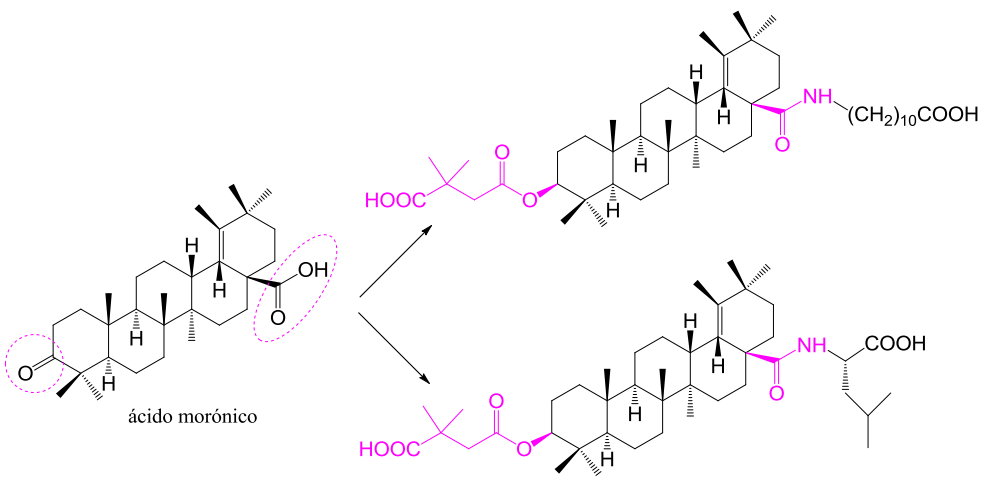

Figura 42. Ácido morónico y derivados con actividad anti-VIH.

[103] Ito, J. *et al.* Anti-AIDS Agents 48. Anti-HIV Activity of Moronic Acid Derivatives and the New Melliferone-Related Triterpenoid Isolated from Brazilian Propolis. *J. Nat. Prod.* **64**, 1278–1281 (2001).
[104] Qian, K. *et al.* Anti-AIDS Agents 81 . Design, synthesis, and Structure - Activity Relationship Study of Betulinic Acid and Moronic Acid Derivatives as Potent HIV Maturation Inhibitors. *J. Med. Chem.* **53**, 3133–3141 (2010).
[105] Yu, D. *et al.* Anti-AIDS Agents 69 . Moronic Acid and Other Triterpene Derivatives as Novel Potent Anti-HIV Agents. *J. Med. Chem.* **49**, 5462–5469 (2006).

Los ácidos oleanólico y maslínico presentan actividad anti-VIH, inhibiendo la proteasa del virus, tal y como se vio en la introducción de esta memoria, en el apartado de propiedades biológicas. A lo largo de estos años, ambos ácidos han sido estudiados para potenciar dicha actividad. Se ha llevado a cabo la síntesis de derivados de estos ácidos, modificando el grupo o los grupos hidroxilo de C-3 o C2/C3 y el grupo carboxilo de C-28. Los sustituyentes utilizados para este fin han sido diversos, como por ejemplo ésteres, aminas y aminoácidos. Como conclusión de todos estos estudios se observó que los derivados con mejores resultados frente a la inhibición de la proteasa del VIH eran aquellos que se encontraban difuncionalizados.[91]

Nuestro grupo de investigación ha llevado a cabo un estudio de derivados de ambos ácidos con distintos acilos sobre el o los grupos hidroxilo de C-3 o C-2/C-3 (Fig. 43) del anillo A. Los compuestos de partida eran los propios ácidos triterpénicos naturales o sus derivados bencilados en C-28. Se demostró que un gran número de derivados eran potentes inhibidores de la proteasa, mejorando considerablemente su actividad en comparación con los precursores. Los derivados más activos fueron los que presentaban un sustituyente dicarboxílico polar en C-2 o en C-2 y C-3 del esqueleto triterpénico.[18]

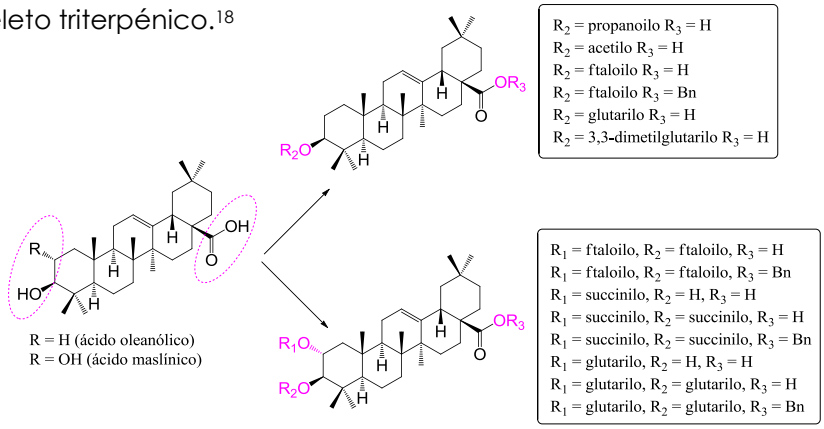

Figura 43. Derivados de los ácidos oleanólico y maslínico que inhiben la proteasa del VIH.

IV MATERIALES Y MÉTODOS

1. INSTRUMENTACIÓN Y MÉTODOS QUÍMICOS BÁSICOS

1.1. Instrumentación general básica

Los disolventes utilizados para la obtención y purificación de los productos naturales triterpénicos y sus derivados se evaporaron mediante el uso de un rotavapor de la casa Büchi, modelo 210. Para la realización de reacciones simultáneas se utilizó un Carousel 12 plus Reaction Station de la casa Radleys. Los puntos de fusión microscópicos han sido determinados en un aparato tipo Stuart de la casa Reichert.

1.2. Técnicas cromatográficas

1.2.1. Cromatografía en capa fina

Durante el seguimiento de las distintas reacciones y purificación de los derivados obtenidos, se usó la cromatografía en capa fina utilizando como fase estacionaria gel de sílice Merck 7747, en capas de 0.25 mm de espesor en vidrio o en cromatoplacas Merck TLC Sílica gel 60 de 5×10 cm. La visualización de los productos se llevó a cabo con un revelador compuesto de una mezcla de agua, ácido sulfúrico y anhídrido acético glacial en una proporción 4:1:20 respectivamente. A esta mezcla se le denomina "óleum". Como eluyentes de la fase móvil se han empleado los siguientes disolventes: diclorometano, n-hexano, acetona, acetato de etilo, metanol, como tal o en mezclas de polaridad creciente.

1.2.2. Cromatografía flash a media presión

Para la separación y purificación de los distintos derivados, se utilizó la cromatografía en columna con gel de sílice (Sharlau 60, 40-60 μm). El diámetro de las columnas de vidrio usadas, fue variable en función de la cantidad de muestra a separar. La presión de trabajo fue en torno a 0.5-1 atmósferas. Se ha utilizado un gradiente de polaridad creciente con

disolventes o mezclas de disolventes de diclorometano-acetona, diclorometano-metanol y n-hexano-acetato de etilo.

1.3. Métodos de determinación estructural

1.3.1. Espectroscopia de masas

Los espectros de masas se han llevado a cabo por ionización a presión atmosférica por electro spray (ESI) en un sistema con analizador de tiempo de vuelo (TOF) WATERS modelo LCT Premier XE, con jeringa de infusión para muestras líquidas y con UPLC AcquityBinarySolvent manager como cromatógrafo. El volumen inoculado de muestra fue de 2 µL CH_3CN/H_2O y se empleó una columna en fase reversa Acquity UPLC BECH C18 130 Å1.7 µm 2.1 mm x 50 mm. Los datos se expresan en unidades de masa (m/z).

1.3.2. Espectroscopia de resonancia magnética nuclear (RMN)

Los espectros de ^{1}H RMN y ^{13}C RMN se han realizado en un espectrómetro VARIAN Inova 400 y 500 MHz, empleando $CDCl_3$ como disolvente habitual. Las señales en ^{13}C RMN monodimensional se asignaron utilizando un ángulo de inclinación de 135º mediante la secuencia de pulsos DEPT. Los desplazamientos químicos (δ) se expresan en ppm y las constantes de acoplamiento (J) en Hz.

1.3.3. Espectroscopia de infrarrojo (IR)

Los espectros de infrarrojo fueron determinados en un espectrofotómetro modelo MATTSON SATELLITE FTIR. Los distintos compuestos fueron preparados como películas sólidas finas sobre cristales de NaCl o con pastillas de KBr. Las frecuencias de los máximos de absorción se expresan en cm^{-1}.

1.3.4. Rotaciones específicas ([a]$_D$)

Las rotaciones específicas se midieron en $CHCl_3$ o MeOH, a la temperatura del laboratorio (25ºC) en el polarímetro modelo PERKIN-ELMER 241, en una célula de 1 dm de longitud.

1.4. Aislamiento y caracterización de los ácidoss oleanólico y maslínico

Los ácidos oleanólico y maslínico se aíslan de los subproductos de la industria olivarera a partir de los desechos de la molturación de la aceituna (orujo) según el procedimiento que ha sido desarrollado por el grupo de investigación "Biotransformación y Química de productos Naturales", encontrándose perfectamente detallado en sendas patentes nacional (P96061652) e internacional (W098/04331) titularizadas por la Universidad de Granada.

El procedimiento del aislamiento de ambos ácidos (Fig. 44) es llevado a cabo por extracción en soxhlet del orujo con acetato de etilo. El disolvente es recuperado pudiendo ser usado para posteriores extracciones. De esta extracción, se obtiene una fracción líquida que tras ser concentrada aparece un residuo sólido constituido por una mezcla de ácido oleanólico y ácido maslínico, en una proporción 30:70 respectivamente. Este residuo sólido es preparado para su separación por columna de cromatografía, aislando ambos ácidos por separado. Los disolventes usados para este fin, es una mezcla de diclorometano/acetona de polaridades crecientes, empezando la separación por una polaridad de 40:1, respectivamente. El control de la separación se realiza mediante cromatografía de capa fina. Las distintas fracciones obtenidas son agrupadas por composición similar, siendo una de ellas el ácido oleanólico y la otra el ácido maslínico. Una vez concentradas dichas fracciones se procede al estudio de sus propiedades espectroscópicas. En condiciones normales, a partir de un residuo sólido de 120 g de mezcla con ambos

ácidos se obtiene un 19,7% (23.67 g) de ácido oleanólico y un 66.7% (80.04 g) de ácido maslínico.

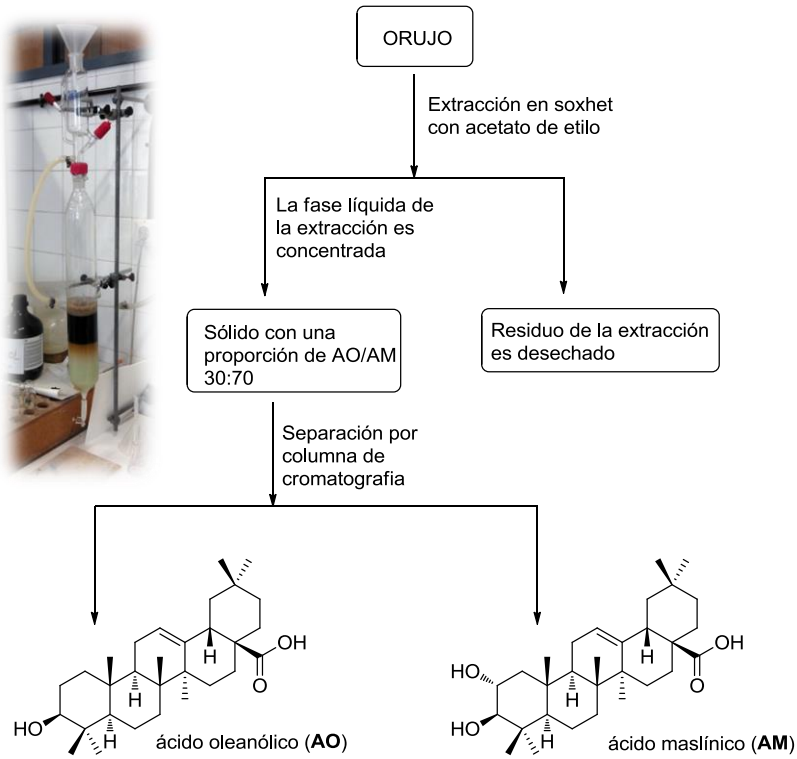

Figura 44. Esquema aislamiento de los ácidos oleanólico y maslínico. En la fotografía se aprecia una columna de cromatografía para la separación de los ácidos oleanólico y maslínico.

Ácido oleanólico (ácido 3β-hidroxiolean-12-en-28-oico): sólido blanco; p.f 306-308 ºC. $[\alpha]_D$ = + 80 (c 1, $CHCl_3$). IR (KBr)ν_{max} /cm^{-1}: 3438, 2930, 2869 y 1690; ^{1}H RMN (500 MHz, CD_3OD) δ_H 5.15 (dd, 1H, J_1= J_2 = 3.6 Hz, H-12), 3.07 (dd, 1H, J_1 = 6.9 Hz, J_2 = 9.0 Hz, H-3), 2.71 (dd, 1H, J_1 = 4.7 Hz, J_2 = 14.0 Hz, H-18), 1.01 (s, 3H, Me), 0.85 (s, 3H, Me), 0.80 (s, 3H, Me), 0.78 (s, 3H, Me), 0.78 (s, 3H, Me), 0.65 (s, 3H, Me), 0.64 (s, 3H, Me);. ^{13}C RMN (125 MHz, CD_3OD) δ_C 180.8 (C-28), 145.2 (C-13), 123.7 (C-12), 79.7 (C-3), 56.8 (C-5), 49.1 (C-9), 47.6 (C-17), 47.3 (C-19), 42.9 (C-14), 42.3 (C-18), 40.6 (C-8), 39.8 (C-1), 39,9 (C-4), 38.2 (C-10), 34.9 (C-21), 34.0 (C-22), 33.8 (C-7), 33.6 (C-29), 31.6 (C-20), 28.8 (C-23), 28.7 (C-15), 27,9 (C-2), 26.4 (C-27), 24.5 (C-11), 24.1 (C-16), 24.0 (C-

30), 19.5 (C-6), 16.3 (C-24), 15.9 (C-25), 17.7 (C-26); HR-LSIMS *(m/z)*: 479.3504, ($C_{30}H_{48}O_3Na^+$ $[M+Na]^+$ calculado 479.3501).

Ácido maslínico (2a,3β-dihidroxiolean12-en-28-oico): sólido blanco; p.f 267-269 ºC; $[\alpha]_D$ = + 54 (c 1, $CHCl_3$:MeOH, 2:1); IR (KBr)ν_{max} /cm^{-1}: 3386, 2936, 2867, 1690; ^{1}H RMN (300 MHz, CD_3OD) δ_H 5.16 (dd, 1H, J_1 = J_2 = 3.5 Hz, H-12), 3.45 (ddd, 1H, J_1 = 4.4 Hz, J_2 = 9.1 Hz, J_3 = 11.2 Hz, H-2), 2.84 (d, 1H, J = 9.1 Hz, H-3), 2.71 (dd, 1H, J_1 = 4.3 Hz, J_2 = 13.9 Hz, H-18), 0.93 (s, 3H, Me), 0.82 (s, 3H, Me), 0.77 (s, 3H, Me), 0.72 (s, 3H, Me), 0.69 (s, 3H, Me), 0.59 (s, 3H, Me), 0.58 (s, 3H, Me); ^{13}C RMN (75 MHz, CD_3OD) δ_C 181.8 (C-28), 145.3 (C-13), 123.5 (C-12), 84.4 (C-3), 69.5 (C-2), 56.7 (C-5), 49.0 (C-9), 48.1 (C-1), 47.6 (C-17), 47.2 (C-19), 42.9 (C-14), 42.7 (C-18), 40.6 (C-8), 40.5 (C-4), 39.3 (C-10), 34.9 (C-21), 33.9 (C-22), 33.8 (C-7), 31.6 (C-20), 29.3 (C-23), 28.8 (C-15), 26.4 (C-27), 24.61 (C-11), 24.0 (C-16), 24.0 (C-30), 19.6 (C-6), 17.8 (C-26), 17.5 (C-25), 17.1 (C-24); HR-LSIMS *(m/z)*: 495.3458, ($C_{30}H_{48}O_4Na^+$ $[M+Na]^+$ calculado 495.3450).

1.5. Procedimientos de síntesis generales

Las reacciones químicas indicadas mas abajo, se encuentran detalladas en las distintas publicaciones del apartado V de la presente Tesis Doctoral. Dichas reacciones son:

- Reacción de bencilación.

- Reacción de acilación.

- Reacciones de PEGilación.

- Reacciones de amidación.

2. INSTRUMENTACIÓN Y MÉTODOS BIOLÓGICOS BÁSICOS

2.1. Instrumentación general básica

- Cabina de flujo laminar
- Estufa de cultivo
- Autoclave
- Espectrofotómetro
- Citómetro
- Microscopio óptico

2.2 Técnicas de cultivo celular

2.2.1. Subcultivos celulares: preparación del medio de cultivo y mantenimiento

Las distintas líneas celulares fueron mantenidas en flascones de 75 cm^2 crecidas en medio DMEM (glucosa 25 mM, L-glutamina 2mM), suplementado con suero bovino fetal (10%), penicilina (10.000 unidades por mL) y estreptomicina (10 mg/mL), siendo incubadas a 37ºC en una atmósfera al 5% de CO_2 y 95% de humedad. Antes de suplementar el medio de cultivo con el suero bovino fetal, es calentado durante 20-30 minutos a 55ºC para inactivar el complemento y evitar que reaccione y dañe a las células.

Cuando las células se encontraron próximas a la confluencia (90%-95%), fueron despegadas del soporte de incubación con tripsina (1x) durante 5 minutos en estufa de cultivo. Posteriormente, se inactivó la tripsina añadiendo medio de cultivo. A continuación, las células fueron recogidas, centrifugadas a 1500 rpms durante 5 minutos a temperatura ambiente y sembradas para la realización de los distintos ensayos o para su mantenimiento.

2.2.2. Conservación de las líneas celulares

Las líneas celulares fueron congeladas en suero bovino fetal inactivado con un 10% de dimetilsulfóxido (DMSO). Fueron repartidas en distintos viales de congelación o crio-tubos a 1 mL por cada vial. La congelación se llevó a cabo utilizando un crio-contenedor a -80ºC.

2.2.3. Descongelación de las líneas celulares

Para una descongelación rápida de las líneas celulares, los crio-tubos se sumergieron en un baño a 37ºC, procurando que el tapón no se moje. A continuación, las células fueron diluidas en medio de cultivo, centrifugadas a 1500 rpms durante 5 minutos, sembradas en flascones de 25 cm^2 e incubadas a 37ºC en una atmósfera al 5% de CO_2 y 95% de humedad.

2.3. Métodos para la determinación de las propiedades biológicas

2.3.1. Determinación del número de células

Antes de realizar los ensayos biológicos, se estableció el número de células necesarias para cada ensayo. Para ello, se efectuó una serie de medidas para determinar el número de células a sembrar. Tras el crecimiento de las células y tras alcanzar la confluencia, se procedió a despegarlas del soporte de incubación para su medición por espectofotometría, mediante el ensayo con MTT (bromuro de 3-(4,5-dimetiltiazol-2-ilo)-2,5-difeniltetrazol). La absorbancia óptima para realizar los ensayos, está comprendida entre 1-1.5. Este rango es proporcional a la cantidad necesaria de células para le realización de los ensayos. El recuento de células se llevó a cabo mediante *Conteo* celular en cámara de Neubauer.

2.3.2. Determinación de citotoxicidad mediante el ensayo de MTT

El ensayo del MTT, se basa en la reducción metabólica del bromuro de 3-(4,5-dimetiltiazol-2-ilo)-2,5-difeniltetrazol en un compuesto coloreado de color azul denominado formazan con un máximo de absorbancia a 570 nm. El formazan puede ser cuantificado por colorimetría. La cantidad de células vivas es proporcional a la cantidad de formazan producido. Los resultados se miden por absorbancia.

2.3.3. Citometría de flujo

La citometría de flujo es una técnica que permite obtener información de diferentes parámetros de la célula ocurridos durante la muerte o proliferación celular. El método se basa en hacer pasar una suspensión de células por delante de un haz de láser de un citómetro, provocando que el impacto de cada célula con el rayo de luz, emita ciertas señales que serán recogidas y digitalizadas. Las aplicaciones de esta técnica son múltiples: muestran información sobre la morfología de la célula, fenotipo, análisis de ADN (ciclo celular), estudios de inducción de apoptosis, etc. El marcaje de las células con distintos fluoróforos permite la posibilidad de todos estos estudios.

a) Estudio de la apoptosis

Durante el proceso de la apoptosis, se producen cambios que pueden ser detectados mediante citometría de flujo. Uno de ellos es la fosfatidilserina que queda expuesta en una proporción mayor a lo habitual en la monocapa externa de la membrana plasmática de la célula apoptótica. La exposición de fosfatidilserina es utilizada para la cuantificación por citometría de flujo. El método utilizado es un doble marcaje de las células tratadas y no tratadas, con anexina V-FITC/Ioduro de propidio. La anexina V-FITC, se caracteriza por estar conjugada con isoticianato de fluoresceína capaz de interaccionar de forma específica

con la fosfatidilserina, pudiéndose cuantificar el grado de apoptosis. El marcaje con ioduro de propidio (IP) es proporcional al contenido de ADN, siendo también cuantificado por citometría. Este doble marcaje permite distinguir distintos estados de la célula (Fig. 45).

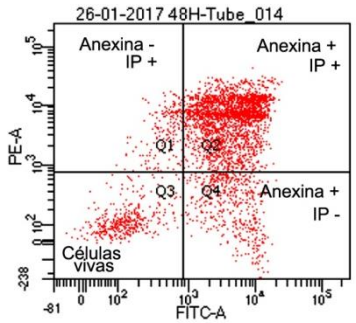

Tube: Tube_014

Population	#Events	%Parent	%Total
All Events	10,000	####	100.0
P1	3,686	36.9	36.9
Q1	190	5.2	1.9
Q2	2,619	71.1	26.2
Q3	386	10.5	3.9
Q4	491	13.3	4.9

- Células con apoptosis temprana: anexina V positiva / IP negativa (Q4).

- Células con apoptosis tardía: anexina V positiva / IP positiva (Q2)

- Necrosis: anexina V negativa / IP positiva (Q1).

Figura 45. Resultados de citometría del análisis de la apoptosis.

b) Estudio del ciclo celular

La cantidad de ADN de una célula se analiza por citometría, para determinar la presencia de células con una alteración del contenido de ADN (células aneuploides), obteniendo así, el porcentaje de células en cada fase del ciclo celular. Las células normales poseen una cantidad de ADN conocida. Así, en la fase G_0/G_1, la célula posee un contenido diploide de ADN, en la fase S, la célula duplica su material genético siendo tetraploide, en la fase G_2 y al inicio de la mitosis, la célula mantiene este doble contenido de ADN hasta que se divide en dos células hijas, presentando ambas células hijas un contenido de ADN diploide.

El método usado para cuantificar la cantidad de ADN en las distintas fases del ciclo celular mediante citometría, es el marcaje con

ioduro de propidio, capaz de integrarse en el ADN. Los resultados obtenidos se recogen en una serie de histogramas (Fig. 46) comparados con los de poblaciones celulares control (células no tratadas).

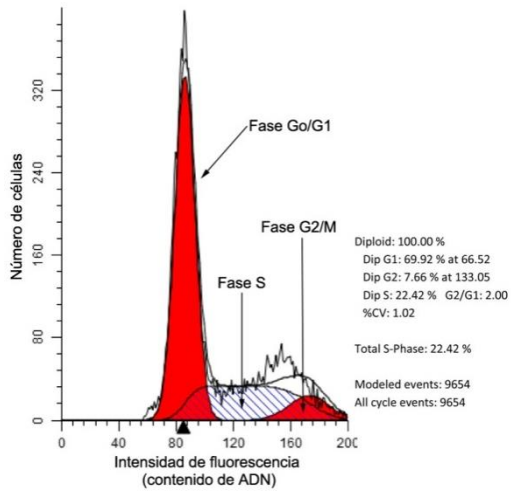

Figura 46. Histograma del ciclo celular.

c) Estudio del cambio de potencial de la membrana mitocondrial

El daño oxidativo se estudió mediante análisis citoquímico del potencial de la membrana mitocondrial, con dihidrorhodamina 123 (DHR). La DHR, es capaz de oxidarse en contacto con las células vivas, formándose un producto altamente fluorescente, denominado rodamina (Rh 123). La formación de este compuesto puede ser monitorizada por espectroscopía de fluorescencia, usando longitudes de onda de excitación y emisión de 500 y 536 nm respectivamente. Este ensayo se realiza mediante citometría de flujo, donde la intensidad de fluorescencia de Rh 123, junto con la tinción de ioduro de propidio, aporta información sobre los cambios que puedan ocurrir en el potencial de la membrana mitocondrial.

En la membrana mitocondrial existe un trasiego de electrones que mantienen el potencial de membrana. La DHR tiene especificidad por la mitocondria, capaz de captar radicales libres provocados por ese trasiego

de electrones. Cuando la DHR capta un radical libre se oxida, dando lugar a Rh 123, la cual emite fluorescencia. Si no existen radicales libres debido a una alteración en el potencial de membrana, no se produce fluorescencia. La fluorescencia puede ser captada mediante citometría de flujo. Los datos obtenidos, aportan la siguiente información (Fig. 47):

- Si hay apoptosis y la tinción con rodamina es positiva, el potencial de membrana permanece intacto. Esta consecuencia da a entender que la membrana mitocondrial está intacta y la ruta de la apoptosis puede estar determinada por la vía de apoptosis extrínseca.

- Si hay apoptosis y la tinción con rodamina es negativa, el potencial de membrana se ve alterado provocando que la mitocondria se vuelva permeable. Este resultado indica, que la apoptosis puede estar determinada por la vía de apoptosis intrínseca.

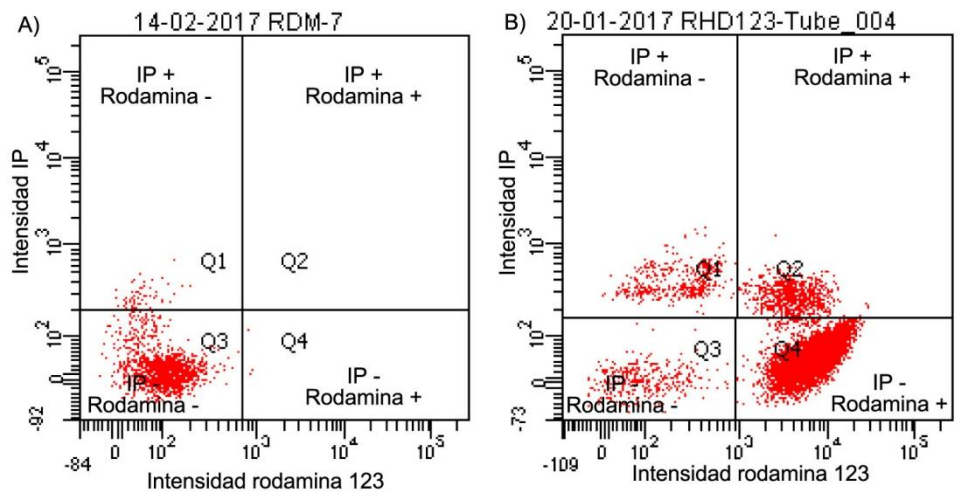

Figura 47. Análisis por citometría del cambio de potencial de membrana mitocondrial. A) Compuesto que induce apoptosis por vía intrínseca, B) Compuesto que induce apoptosis por vía extrínseca.

2.3.4. Tinción con Hoechst

Los cambios morfológicos a nivel nuclear pueden ser observados mediante microscopía de fluorescencia, utilizando la tinción de Hoeschst. Con esta técnica, se tiñe la cromatina poniendo de manifiesto la condensación de la cromatina, fragmentación del núcleo y la aparición de cuerpos apoptóticos.

2.4. Líneas celulares

Todas las líneas celulares fueron suministradas por el banco de células del CIC de la Universidad de Granada a ecepción de la línea no tumoral HPF.

- Línea tumoral B16-F10 (ATTC: CRL-6474): Originalmente aislada de ratones, derivada del melanoma de piel. Se caracteriza por presentar un potente poder metastático.
- Línea tumoral HT29 (ECACC: 91072201): Línea tumoral de adenocarcinoma de colon humano de grado II. Aislada originalmente a partir del cáncer de una mujer caucásica de 44 años de edad.

- Línea tumoral HepG2 (ECACC: 85011430): Línea tumoral de hepatocarcinoma humano. Aislada de un hombre caucasiano de 15 años de edad con un carcinoma hepatocelular bien diferenciado.

- Línea no tumoral IEC-18 (ECACC: 88011801): Línea celular aislada a partir del epitelio intestinal de rata, poseen características propias de células normales.

- Línea no tumoral WRL68 (ECACC: 89121403): Línea celular aislada de hígado de embrión humano.

- Línea no tumoral HPF (ScienCell cno. 3300): Línea celular aislada del tejido pulmonar humano.

2.5. Ensayo de inhibición frente a la proteasa del VIH-1

El ensayo de inhibición de los diferentes derivados obtenidos frente a la proteasa HIV-1, se comenta ampliamente en el apartado V, publicación 5: "Síntesis Orgánica en Fase Sólida de una biblioteca de derivados de ácido oleanólico y su estudio frente a la inhibición de la proteasa del VIH-1"

V PUBLICACIONES

PUBLICACIÓN 1

Semi-synthesis and antiproliferative evaluation of PEGylated pentacyclic triterpenos

(JCR: Medicinal Chemistry: Ind. Imp. 3.902, nº6, Q1)

European Journal of Medicinal Chemistry 118 (2016) 64–78

Contents lists available at ScienceDirect

European Journal of Medicinal Chemistry

journal homepage: http://www.elsevier.com/locate/ejmech

Research paper

Semi-synthesis and antiproliferative evaluation of PEGylated pentacyclic triterpenes

Marta Medina-O'Donnell [a], Francisco Rivas [a, **], Fernando J. Reyes-Zurita [b], Antonio Martinez [a], Samuel Martin-Fonseca [a], Andres Garcia-Granados [a], Rosa M. Ferrer-Martín [c], Jose A. Lupiañez [b, ***], Andres Parra [a, *]

[a] Departamento de Quimica Organica, Facultad de Ciencias, Universidad de Granada, E-18071 Granada, Spain
[b] Departamento de Bioquimica y Biologia Molecular I, Facultad de Ciencias, Universidad de Granada, E-18071 Granada, Spain
[c] Departamento de Biología Celular, Facultad de Ciencias, Universidad de Granada, E-18071 Granada, Spain

ARTICLE INFO

Article history:
Received 10 September 2015
Received in revised form
5 April 2016
Accepted 6 April 2016
Available online 9 April 2016

Keywords:
Triterpene
Oleanolic acid
Maslinic acid
PEGylation
Apoptosis

ABSTRACT

Several PEGylated derivatives of oleanolic and maslinic acids have been semi-synthesized, attaching one acid-PEG reagent to the hydroxyl group/s at C-2 or C-2/C-3 of the A rings of these natural triterpenes, and also to their corresponding C-28 benzyl derivatives. Several monomeric and dimeric PEGylated compounds have also been produced by linking one diamine-PEG reagent to the carboxyl group at C-28 of the same natural triterpenes and also to their corresponding C-2 or C-2/C-3 acetylated derivatives. The cytotoxic effects of 12 triterpenic PEGylated derivatives in three cancer-cell lines (B16–F10, HT29, and Hep G2) have been assayed. The best results have been achieved by the PEGylated-amine derivative of oleanolic acid, with IC_{50} concentrations between 0.22 and 3.78 μM, being between 28- and 963-fold more effective than its natural precursor. The percentages of apoptosis induction have also been determined for the five PEGylated derivatives with the lowest cytotoxicity data. All five compounds showed apoptotic effects on the treated cells, with a total apoptosis rate of 99% in the B16–F10 cells, 80% in the Hep G2 cells, and 51% in the HT29 cells. We have also studied the changes in the mitochondrial membrane potential (MMP) to elucidate the possible mechanism involved in the apoptotic responses (intrinsic or extrinsic). Finally, to verify the results found in the cytometry assays, we have used fluorescence microscopy techniques to determine changes in the cell morphology. These PEGylated derivatives of natural triterpenoids, which can induce apoptosis at very low concentrations in different tumour lines, may represent new effective therapeutic drugs against these diseases.

1. Introduction

Triterpenes, among of the most numerous and diverse groups of natural products from plants, belong to a broad family of compounds biosynthetically produced by cyclic reactions from 2,3-oxidesqualene [1]. Biologically, the most important triterpenoid structures are oleanane, ursane, lupane, and dammarane [2].

Oleanolic and maslinic acids are two oleanane triterpenoids that can be extracted in large amounts from olive-oil milling by-products [3]. These compounds have been used in conventional medicine for their anti-inflammatory, hepatoprotective, analgesic, anti-diabetic, antimicrobial, virostatic, anticancer, and anti-HIV effects [4–13]. Natural triterpenoids provide very useful scaffolds to produce derivatives with improved biological properties [14–22]. Our research group has performed a series of systematic chemical modifications of oleanolic and maslinic acids, seeking to improve their biological activities [23,24]. We have also studied the apoptotic effects of maslinic acid in several cancer-cell lines, via mitochondrial or intrinsic apoptotic pathway [25] or extrinsic apoptotic pathway [26].

Dimeric compounds have been synthesized for several biological applications [27–29]. Several studies of dimeric oleanane derivatives, linked at C-28, have investigated the possible improvement of their biological properties, such as anti-tumour,

* Corresponding author.
** Corresponding author.
*** Corresponding author.
E-mail addresses: frivas@ugr.es (F. Rivas), jlcara@ugr.es (J.A. Lupiañez), aparra@ugr.es (A. Parra).

http://dx.doi.org/10.1016/j.ejmech.2016.04.016
0223-5234/

ABSTRACT

Several PEGylated derivatives of oleanolic and maslinic acids have been semi-synthesized, attaching one acid-PEG reagent to the hydroxyl group/s at C-2 or C-2/C-3 of the A rings of these natural triterpenes, and also to their corresponding C-28 benzyl derivatives. Several monomeric and dimeric PEGylated compounds have also been produced by linking one diamine-PEG reagent to the carboxyl group at C-28 of the same natural triterpenes and also to their corresponding C-2 or C-2/C-3 acetylated derivatives. The cytotoxic effects of 12 triterpenic PEGylated derivatives in three cancer-cell lines (B16-F10, HT29, and Hep G2) have been assayed. The best results have been achieved by the PEGylated-amine derivative of oleanolic acid, with IC_{50} concentrations between 0.22 and 3.78 μM, being between 28- and 963-fold more effective than its natural precursor. The percentages of apoptosis induction have also been determined for the five PEGylated derivatives with the lowest cytotoxicity data. All five compounds showed apoptotic effects on the treated cells, with a total apoptosis rate of 99% in the B16-F10 cells, 80% in the Hep G2 cells, and 51% in the HT29 cells. We have also studied the changes in the mitochondrial-membrane potential (MMP) to elucidate the possible mechanism involved in the apoptotic responses (intrinsic or extrinsic). Finally, to verify the results found in the cytometry assays, we have used fluorescence microscopy techniques to determine changes in the cell morphology. These PEGylated derivatives of natural triterpenoids, which can induce apoptosis at very low concentrations in different tumour lines, may represent new effective therapeutic drugs against these diseases.

Keywords: Triterpene; Oleanolic acid; Maslinic acid; PEGylation; Apoptosis.

1. Introduction

Triterpenes, among of the most numerous and diverse groups of natural products from plants, belong to a broad family of compounds biosynthetically produced by cyclic reactions from 2,3-oxidesqualene [1]. Biologically, the most important triterpenoid structures are oleanane, ursane, lupane, and dammarane [2].

Oleanolic and maslinic acids are two oleanane triterpenoids that can be extracted in large amounts from olive-oil milling by-products [3]. These compounds have been used in conventional medicine for their anti-inflammatory, hepatoprotective, analgesic, anti-diabetic, antimicrobial, virostatic, anticancer, and anti-HIV effects [4–13]. Natural triterpenoids provide very useful scaffolds to produce derivatives with improved biological properties [14–22]. Our research group has performed a series of systematic chemical modifications of oleanolic and maslinic acids, seeking to improve their biological activities [23,24]. We have also studied the apoptotic effects of maslinic acid in several cancer-cell lines, via mitochondrial or intrinsic apoptotic pathway [25] or extrinsic apoptotic pathway [26].

Dimeric compounds have been synthesized for several biological applications [27–29]. Several studies of dimeric oleanane derivatives, linked at C-28, have investigated the possible improvement of their biological properties, such as anti-tumour, anti-HCV, or inhibitors of glycogen phosphorylase [30–33].

Most pentacyclic triterpenes are not sufficiently water soluble, hampering biological tests and resulting in their low bioavailability [34–37]. The poor solubility of these compounds is probably the main limitation for finding a formulation suitable for their application as biological agents in humans. Several technologies, including the use of cyclodextrins, micro- and nanoemulsions, liposomes, polymeric nanoparticles, and nanocapsules, have been developed to improve the pharmacokinetic properties of these triterpene compounds [38–40]. Another option to

improve the solubility of these triterpene compounds is to semi-synthesize derivatives, attaching diverse functional groups to the carboxyl group at C-28 and/or to the hydroxyl groups of the A ring of these molecules. Thus, polar functional groups such as quaternary ammonium salts [41], glycosides [42], acylated oximes [43], amino acids or peptides [44–46], or acyl groups [47], have been used for increasing the bioavailability of these triterpenoids in order to improve their therapeutic efficacy.

In 1977, Abuchowski et al. reported that the covalent attachment of polyethylene glycol (PEG) to albumin reduced the immunogenicity of albumin [48], and also that PEGylated biomolecules had a longer blood-circulation time than did the corresponding normal biomolecules [49]. Since then, PEGylation, a covalent attaching polyethylene glycol (PEG) polymer to biological active agents, has been widely recognized as one of the most promising techniques to improve the therapeutic effect of drugs [50–53]. PEG polymer has been considered as a versatile candidate for prodrug conjugation due to its high aqueous solubility [54]. Originally, this technology was applied mainly with macromolecules, such as proteins or enzymes [55,56]. These PEG conjugates with small molecules, such as steroids [57,58], alkaloids [59], terpenes [60], coumarins [61], medium-chain triglycerides [62], ibuprofen [63,64], ferulic acids [65], or lipoic acid derivatives [66], are water-soluble, biocompatible, nontoxic, and non-immunogenic polymeric systems.

In this study, several PEGylated derivatives of oleanolic and maslinic acids have been semi-synthesized to test for their biological properties. Thus, we have prepared four PEGylated compounds, attaching one acid-PEG reagent to the hydroxyl group/s at C-2 or C-2/C-3 of the A rings of the natural triterpenes (oleanolic and maslinic acids), and also to their corresponding C-28 benzyl derivatives. Similarly, we have semi-synthesized a new set of PEGylated monomeric and dimeric compounds by linking one diamine-PEG reagent to the carboxyl group at C-28 of the same natural triterpenes, and also to their corresponding C-2 or C-2/C-3 acetylated derivatives. We have assayed the cytotoxic effect of 12 triterpenic

PEGylated derivatives in three cancer-cell lines (B16-F10, HT29, and Hep G2). All assayed cytotoxic compounds were found active in the apoptotic process, and these results were confirmed by microscopic fluorescence with Hoechst staining. Also, we have established the percentage of cells in the different cell-cycle phases in order to identify the potential cytostatic effects induced by the triterpene derivatives tested, in terms of their cytotoxic action. Finally, we have studied the changes in the mitochondrial-membrane potential (MMP) to formulate hypotheses concerning the plausible apoptotic mechanisms activated by the different compounds assayed.

2. Results and discussion

2.1. Chemistry

Oleanolic acid (**I**, 3β-hydroxyolean-12-en-28-oic acid, **OA**) [67] and maslinic acid (**II**, 2a,3β-dihydroxyolean-12-en-28-oic acid, **MA**) [68] (Fig. 1) are natural pentacyclic triterpene compounds and widely distributed in the plant kingdom. These compounds were benzylated to protect the carboxyl group at C-28 of the triterpene skeleton, producing the corresponding 28-benzyl derivatives (**III**, **OA-Bn**, and **IV**, **MA-Bn**), respectively (Fig. 1) [23,69]. Similarly, to protect the hydroxyl group/s of the A ring, OA and MA were acetylated, yielding the corresponding 3β-acetyl or 2a,3β-diacetyl derivatives (**V**, **OA-Ac**, and **VI**, **MA-Ac**), respectively (Fig. 1) [70,71].

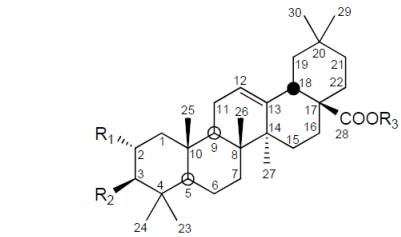

I: $R_1 = R_3 = H$, $R_2 = OH$ (oleanolic acid, **OA**)
II: $R_1 = R_2 = OH$, $R_3 = H$ (maslinic acid, **MA**)
III: $R_1 = H$, $R_2 = OH$, $R_3 = Bn$ (28-benzyl oleanolate, **OA-Bn**)
IV: $R_1 = R_2 = OH$, $R_3 = Bn$ (28-benzyl maslinate, **MA-Bn**)
V: $R_1 = R_3 = H$, $R_2 = OAc$ (3-acetyl oleanolic acid, **OA-Ac**)
VI: $R_1 = R_2 = OAc$, $R_3 = H$ (2,3-diacetyl maslinic acid, **MA-Ac**)

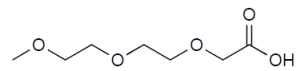

VII: 2-(2-(2-metoxyetoxy)etoxy)acetic acid, **PEG-COOH**

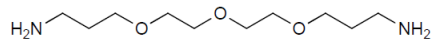

VIII: 4,7,10-trioxatridecane-1,13-diamine, **H_2N-PEG-NH_2**

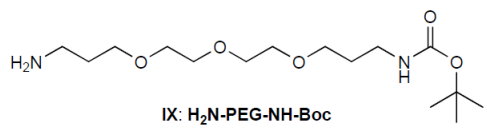

IX: **H_2N-PEG-NH-Boc**

Fig. 1. Structures of precursors (**I**-**VI**) and PEG reagents (**VII**-**IX**).

2.1.1. PEGylated-acid derivatives

The PEGylated-acid derivatives of OA and MA were semi-synthesized, linking 2-(2-(2-methoxyethoxy)ethoxy)acetic acid (**VII**, PEG-COOH) (Fig. 1) to the hydroxyl group/s of the A ring of OA (**I**), MA (**II**), OA-Bn (**III**), or MA-Bn (**IV**). Therefore, when OA (**I**) or its 28-benzyl derivative (**III**) was dissolved in DMF in the presence of DIPCDI and DMAP, and PEG-COOH (**VII**) was added, the PEGylated derivatives **1** and **2** were formed, respectively, in high yields (Scheme 1). These derivatives had similar spectroscopic properties, the main difference being the presence of a benzyl group on the carboxyl group at C-28 in derivative **2**. On the other hand, the main differences between the PEGylated derivatives (**1** and **2**) and the corresponding starting products (**I** and **III**) were the ^{1}H NMR signals of H-3,

due to the PEG group linked to the hydroxyl group at C-3. Thus, whereas H-3 signals appeared at δ_H 3.07 and 3.21 for **I** and **III**, respectively, these signals were situated at δ_H 4.59 and 4.52, respectively, for the corresponding PEGylated derivatives (**1** and **2**).

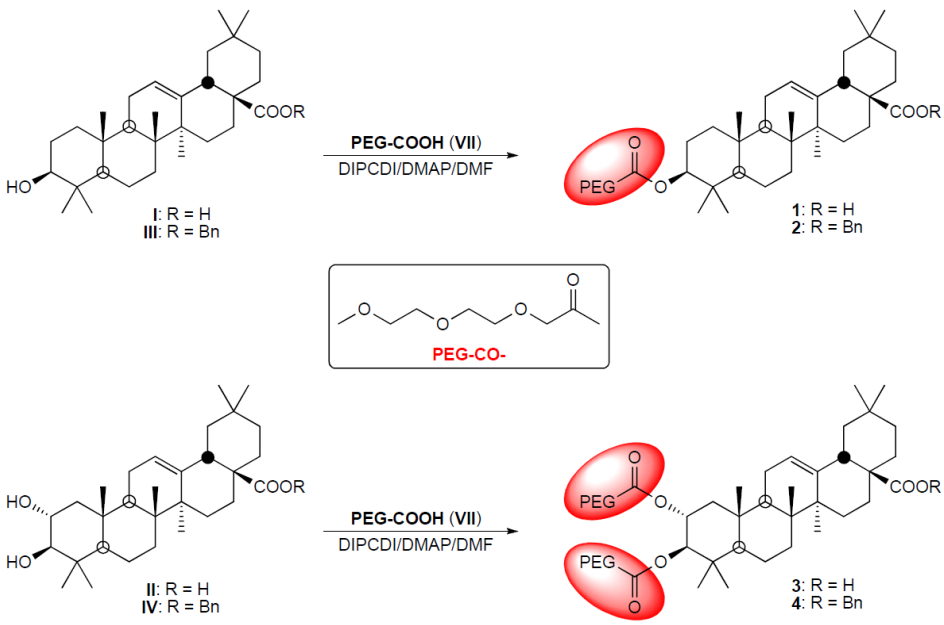

Scheme 1. PEGylation of precursors (**I**-**IV**) with PEG-COOH reagent (**VII**).

In a similar reaction process, MA (**II**) and MA-Bn (**IV**) were PEGylated to produce derivatives **3** and **4**, respectively. In these compounds (**3** and **4**), the main spectroscopic differences with the starting products (**II** and **IV**) were the ^{1}H NMR signals of H-2 and H-3. Thus, H-2 and H-3 were situated at δ_H 3.45 and 2.84, and at δ_H 3.69 and 2.97, for **II** and **IV**, respectively, but appeared at δ_H 5.14 and 4.82, and at δ_H 5.10 and 4.79 for derivatives **3** and **4**, respectively.

All these PEGylated derivatives (**1**-**4**), with one or two PEG-COOH group/s linked to the hydroxyl group/s at C-2 (**1** or **2**) or C-2/C-3 (**3** or **4**), showed in their ^{1}H NMR spectra: one or two AB-system/s between 4.15-4.00 ppm, a multiplet about 3.80-3.30 ppm (-CH_2O-), and one or two singlet

signal/s around δ_H 3.30 (CH_3O-). Also, the ^{13}C NMR spectra of these PEGylated derivatives (**1**-**4**) showed signals of one or two carboxyl group/s (about δ_C 170), several methylene groups (72-68 ppm), and one or two methyl group/s (about δ_C 59).

2.1.2. PEGylated-amine derivatives

A new set of PEGylated derivatives, from natural (**I**-**II**) or semi-synthetic triterpenes (**V**-**VI**), were produced by linking 4,7,10-trioxatridecane-1,13-diamine (**VIII**, H_2N-PEG-NH_2) (Fig. 1) to the carboxylic group at C-28 of the triterpene skeleton through an amide bond. This reagent (**VIII**), with two amino groups at the ends of the chain, could produce monomeric or dimeric PEGylated-amine derivatives, depending of the stoichiometric conditions. Firstly, using the reagent **IX** (H_2N-PEG-NH-Boc) to avoid the formation of dimeric derivatives, we semi-synthesized several monomeric PEGylated-amine derivatives (Fig. 1). This reagent (**IX**) was produced selectively by blocking one of the amino groups of the reagent **VIII** through a tert-butyloxycarbonyl protecting group (Boc). Thus, when **VIII** was treated with di-tert-butyl dicarbonate (Boc_2O), in dry DCM, the reagent **IX** was formed in good yield.

The triterpene acids OA (**I**), MA (**II**), OA-Ac (**V**), or MA-Ac (**VI**) were treated separately with the reagent **IX**, giving the PEGylated-amine derivatives **5**, **6**, **7**, and **8**, respectively (Scheme 2). The NMR spectra of these compounds (**5**-**8**) were similar to their precursors (**I**, **II**, **V**, and **VI**), the main differences being the signals of the protons of the PEG group of each compound. Thus, the ^1H NMR spectra showed the signal of the amide group at C-28 (between 6.27 and 6.17 ppm), and signals of the methylene groups (δ_H 3.75-3.05) also appeared, and finally singlet signals of the three methyls of the Boc group (about δ_H 1.40). Furthermore, the ^{13}C NMR spectra of these compounds (**5**-**8**) showed the signal of the carboxyl group at C-28 (about δ_C 178), more shielded because there was now an amide group on this carbon atom; the signal of the protecting Boc group (about δ_C 156, 79, and 29); and finally the methylene and the methyl groups of the PEG chain

(about δ_C 70, 37, and 29) (Supplementary material). From these PEGylated-amine derivatives (**5**-**8**), the Boc group was removed from end of the PEG chain by treatment with THF/HCl (37%), giving the PEGylated-amine derivatives **9**, **10**, **11**, and **12**, respectively (Scheme 2).

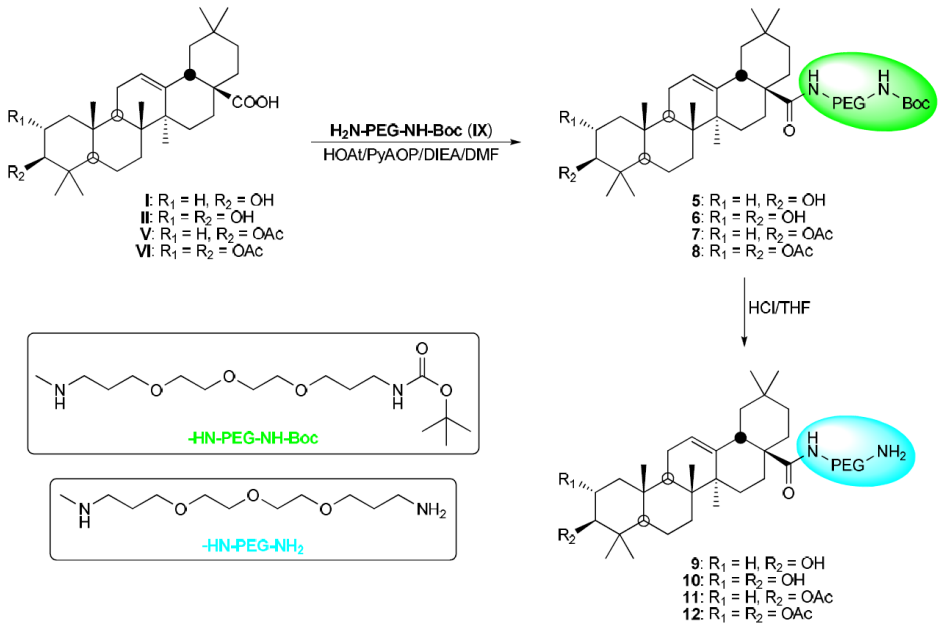

Scheme 2.PEGylation of precursors (**I**, **II**, **V**, and **VI**) with H_2N-PEG-NH-Boc reagent (**IX**), and deprotection of the Boc group.

For the semi-synthesis of the dimeric PEGylated-amine derivatives from the substrates **I**, **II**, **V**, and **VI**, the reaction conditions of the PEGylation process were modified (Scheme 3). Before coupling the H_2N-PEG-NH_2 reagent (**VIII**) with the carboxyl group at C-28 of two triterpene molecules of the substrates (**I**, **II**, **V**, and **VI**), we activated this carboxyl group with 2-(1H-Benzotriazole-1-yl)-1,1,3,3-tetramethyluronium tetrafluoroborate (TBTU). This salt (TBTU) acts as a highly efficient coupling reagent and has been widely used in carbon-nitrogen bond-forming reactions for the synthesis of peptides, including the synthesis of some pharmaceutical peptides [72,73]. The reaction to produce the TBTU derivatives of substrates **I**, **II**, **V**, and **VI** was performed by adding TBTU to a solution of these compounds in dry THF, in the presence of DIEA, at rt (Scheme 3). Under these conditions, the TBTU derivatives **13**, **14**, **15**, and **16** were formed in high yields (>90%). The ^{1}H NMR

spectra of these derivatives (**13**-**16**) showed three narrow signals between 8.0 and 7.3 ppm corresponding to the four aromatic protons of the TBTU group. Furthermore, in the ^{13}C NMR spectra of these compounds (**13**-**16**) appeared the signals of six aromatic carbon atoms (between 143 and 108 ppm) of the TBTU group.

These TBTU derivatives (**13**-**16**), with the carboxyl group at C-28 activated, were coupled with the H_2N-PEG-NH_2 reagent, in dry DCM, in the presence of K_2CO_3 (Scheme 3). Under these reaction conditions, the dimeric PEGylated-amine derivatives **17**, **18**, **19**, and **20** were synthesized at high yields (76-85%). In this reaction the previously produced monomeric PEGylated-amine derivatives (**9**-**12**) were also formed, but with low yields (7-13%). The molecular formulae of **17** ($C_{70}H_{116}N_2O_7$), **18** ($C_{70}H_{116}N_2O_9$), **19** ($C_{74}H_{120}N_2O_9$), and **20** ($C_{78}H_{124}N_2O_{13}$) confirmed that these compounds had two triterpene molecules linked to the H_2N-PEG-NH_2 reagent. The NMR spectra of these dimeric PEGylated-amine derivatives (**17**-**20**) were very similar to those of the monomeric PEGylated-amine derivatives (**9**-**12**), due to the symmetric structure of the dimeric compounds.

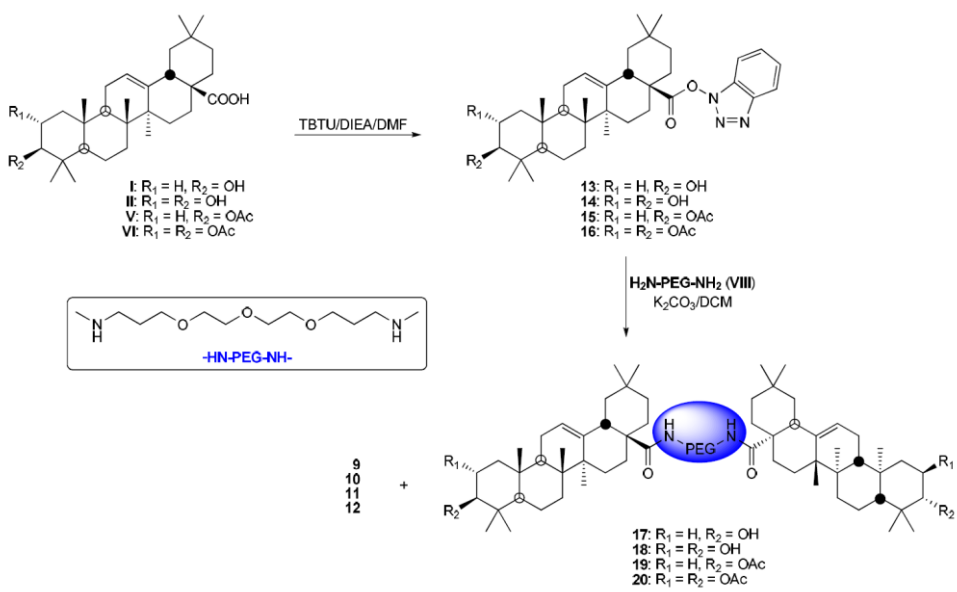

Scheme 3. PEGylation of the TBTU derivatives (**13**-**16)** with H_2N-PEG-NH_2 reagent (**VII**).

2.2. Effects of triterpene derivatives on cancer-cell proliferation

The effects of 12 oleanolic and maslinic acid derivatives (**1**-**4**, **9**-**12**, and **17**-**20**) on the proliferation of three cancer-cell lines (B16-F10, murine melanoma cells, HT29, colon-cancer cells, and Hep G2, hepatome cells) were examined. All cell lines were treated with increasing concentrations of these derivatives. The viability was determined by formazan dye uptake and expressed as percentage of untreated control cells. In these three cell lines, the concentrations of compounds required for 50% growth inhibition (IC_{50}) were determined (Table 1).

Table 1
Growth-inhibitory effects of OA and MA derivatives on B16-F10, HT29, and Hep G2 cells.

Compd #	B16-F10	* IC_{50} of precursor / IC_{50} of compd #	HT29	* IC_{50} of precursor / IC_{50} of compd #	Hep G2	* IC_{50} of precursor / IC_{50} of compd #
OA(**I**)	106.4 ± 3.7	1.0	429.9 ± 0.7	1.0	211.8 ± 0.5	1.0
1	17.24 ± 0.08	6.2	13.49 ± 0.08	31.9	17.47 ± 0.19	12.1
9	3.78 ± 0.01	28.1	3.58 ± 0.03	120.1	0.22 ± 0.05	962.7
17	123.12 ± 3.95	0.9	85.62 ± 1.19	5.0	66.73 ± 1.36	3.2
OA-Bn(**III**)	52.2 ± 0.9	2.0	67.08 ± 3.21	6.4	38.73 ± 1.65	5.5
2	174.87 ± 2.32	0.6	61.58 ± 3.87	7.0	84.07 ± 2.36	2.5
OA-Ac(**V**)	64.7 ± 2.8	1.6	148.48 ± 8.36	2.9	103.67 ± 4.12	2.0
11	201.07 ± 0.41	0.5	138.26 ± 3.49	3.1	68.69 ± 0.71	3.1
19	119.03 ± 0.76	0.9	83.21 ± 1.02	5.2	24.40 ± 0.22	8.7
MA(**II**)	36.2 ± 2.5	1.0	32.2 ± 3.8	1.0	99.2 ± 15.5	1.0
3	48.44 ± 0.61	0.7	39.70 ± 0.01	0.8	59.91 ± 0.65	1.7
10	11.41 ± 0.02	3.2	11.78 ± 0.04	2.7	7.68 ± 0.01	12.9
18	118.10 ± 1.51	0.3	82.76 ± 0.41	0.4	96.71 ± 1.33	1.0
MA-Bn(**IV**)	36.2 ± 3.8	1.0	15.29 ± 0.54	2.1	17.02 ± 0.03	5.8
4	21.08 ± 0.01	1.7	31.60 ± 0.58	1.0	12.79 ± 0.35	7.8
MA-Ac(**VI**)	44.1 ± 3.8	0.8	69.14 ± 2.95	0.5	50.16 ± 1.02	2.0
12	104.07 ± 0.02	0.3	130.49 ± 4.26	0.2	176.16 ± 2.25	0.6
20	107.16 ± 0.13	0.3	64.35 ± 1.41	0.5	113.05 ± 0.53	0.9

The IC_{50} values were calculated considering control untreated cells as 100% of viability. Cell-growth inhibition was analysed by the MTT assay, as described in Experimental section.
* Relationship between IC_{50} of OA or MA and the IC_{50} of the each compound. All assays were realized two times using three replicates. Values, means ± S.E.M.

All compounds displayed cytotoxicity in the conditions assayed (range 0–300 µg/mL), with IC_{50} data between 0.22 to 201 µM, showing four compounds (**1**, **4**, **9**, and **10**) with IC_{50} concentrations lower than 30 µM, in the three cell lines tested. According to the analysis of the different cell lines assayed, the percentage of PEGylated derivatives that improved the results of cytotoxicity compared to their precursors was variable; the lowest was that of the B16-F10 cell line (33%), and the highest those of the HT29 (66%) and Hep G2 (75%) cell lines. The best IC_{50} data (3.78, 3.58, and 0.22 µM) correspond to compound **9**, the PEGylated-amine derivative of oleanolic acid, being 28-fold more effective than its natural precursor (OA, **I**) on the proliferation of the B16-F10 cell line, 120-fold more effective on the HT29 cell line, and 963-fold more effective on the Hep G2 cell line (Chart 1). Another three PEGylated derivatives (**1**, **4**, and **10**) also showed better IC_{50} data than their precursors. The best cytotoxic results were achieved by the PEGylated-amine derivatives (**9** and **10**) of oleanolic and maslinic acids. These results could be related to the increased polarity of these PEGylated-amine derivatives.

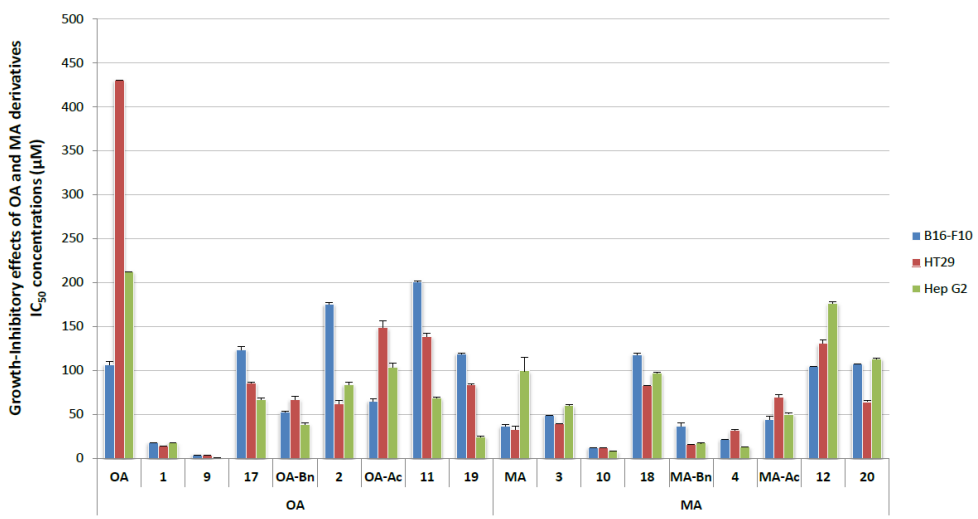

Chart 1.Growth-inhibitory effects of OA and MA derivatives, on B16-F10, HT29, and Hep G2 cells. All assays were realized two times using three replicates.

2.3. Characterization of apoptotic effects by flow cytometry

The apoptotic determination assays were conducted through double staining with annexin V (An-V), conjugated fluorescein isothiocyanate (FITC), and propidium iodide (PI). Apoptosis in the three cancer-cell lines was assessed 72 h after treatment with the five PEGylated derivatives with the lowest cytotoxicity data (**1**, **3**, **4**, **9**, and **10**). The percentages of apoptosis were determined with annexin V–FICT/PI by flow-activated cell sorter (FACS) cytometry analysis, differentiating early apoptotic cells (An-V^+ and PI^-) from late apoptotic (An-V^+ and PI^+), necrotic (An-V^- and PI^+), or normal cells (An-V^- and PI^-).

All five compounds showed apoptotic effects on the treatment cells, with a percentage of total apoptosis that reached 99% in B16-F10 cells, 80% in Hep G2 cells, and 51% in HT29 cells (Chart 2). In addition, the percentages of the necrotic population were negligible. All compounds tested in the cell line HT29 showed moderate percentages of total apoptosis, which corresponded largely to early apoptosis, and therefore the results of late apoptosis were very low. These findings may indicate that the apoptosis mechanism in HT29 cells was relatively more delayed than in the other cell lines, which can be related to the increased cell-cycle arrest observed (see Section 2.4), possibly due to the cytostatic effects induced by these compounds in this cell line.

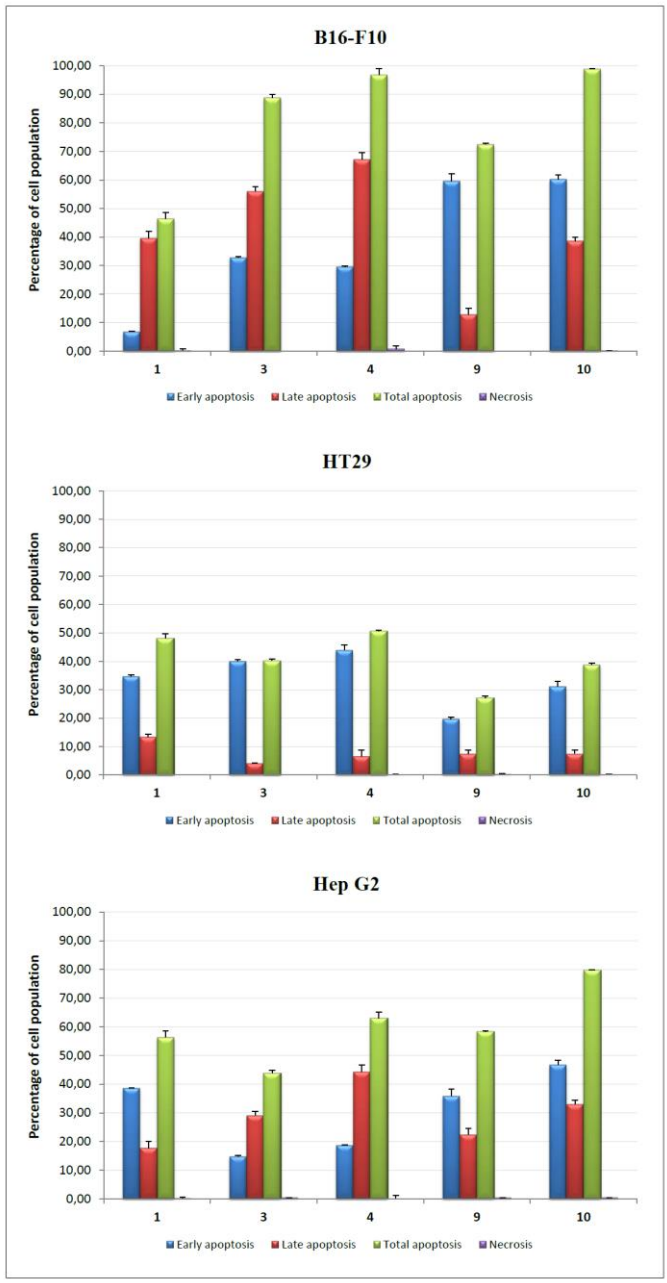

Chart 2. Flow cytometry analysis of Annexin V-FITC staining and PI accumulation after exposure of B16-F10, HT29, and Hep G2 cells, to OA and MA derivatives for 72 h. Cell lines were treated at concentrations equal to its IC_{50} values. Early apoptotic cells (blue bars) were annexin V^+ PI^-, whereas late apoptotic cells (red bars) were annexin V^+ PI^+, total apoptosis (green bars) were annexin V^+ and necrotic cells (purple bars) were annexin V^- PI^+. Values are expressed as means ± S.E.M. of at least two experiments in duplicate.

Three of the five compounds tested (**3**, **4**, and **10**) showed a total apoptosis rate of around 90% in B16-F10 cells, appreciably better than those achieved by its precursor (MA, **II**, around 60%) [47]. Furthermore, two of these compounds (**4** and **10**) displayed total apoptosis percentages of 60-80% in Hep G2 cells. The PEGylated-acid derivatives (**3** and **4**) showed higher rates of late apoptosis than of early apoptosis, while the PEGylated-amine derivative (**10**) exhibited a higher percentage of early apoptosis (Chart 2). The apoptotic effects of the PEGylated-amine derivative **9**, with the lowest IC_{50} concentration in all the three cell lines, were not the most relevant, probably because of its high cytotoxicity, thereby reducing the number of measurable apoptotic cells at 72 h.

2.4. Cell-cycle arrest and distribution

In view of the cell-growth inhibition caused by these PEGylated derivatives, we investigated their effects on their cell-cycle distribution, in order to determine a possible cytostatic effect provoked by the cytotoxic response. The percentages of cells in the different phases of the cell cycle were analysed at 72 h, by the incorporation of PI. The three cancer-cell lines, B16-F10, HT29, and Hep G2, were treated with the selected triterpene derivatives (**1**, **3**, **4**, **9**, and **10**), at their respective IC_{50} concentrations for each cell line. Flow cytometry was used to measure DNA ploidy and alterations in cell-cycle profiles. The DNA content was proportional to the PI fluorescence, allowing us to determine the percentage of cells in each cell-cycle phase, and also to visualize the cell subpopulations with different DNA content. Changes in DNA concentrations are characteristic of apoptosis or cell-cycle arrest.

The DNA-histogram analysis revealed that three of the compounds tested (**3**, **4**, and **9**), produced cell-cycle arrest in the three cell lines selected, increasing the number of cells in the G0/G1 phase. Compound **10** caused cell-cycle arrest in B16-F10 and HT29 cells, and compound **1** only in B16-F10 cells. These increases were accompanied by a decrease in the percentage of proliferating cells in the S phase. Changes in the G2/M

phase were less significant, especially with the B16-F10 and HT29 cell lines (Chart 3). The highest increases of cells in the G0/G1 phase were observed in the HT29 cancer-cell line (except for compound **1**). Also, these compounds caused more than a 40% of drop in the percentage of cells in the S phase. These results, along with the relative delay in the induction of apoptosis detected, could indicate a possible cell-differentiation effect prompted by these compounds in HT29 cells.

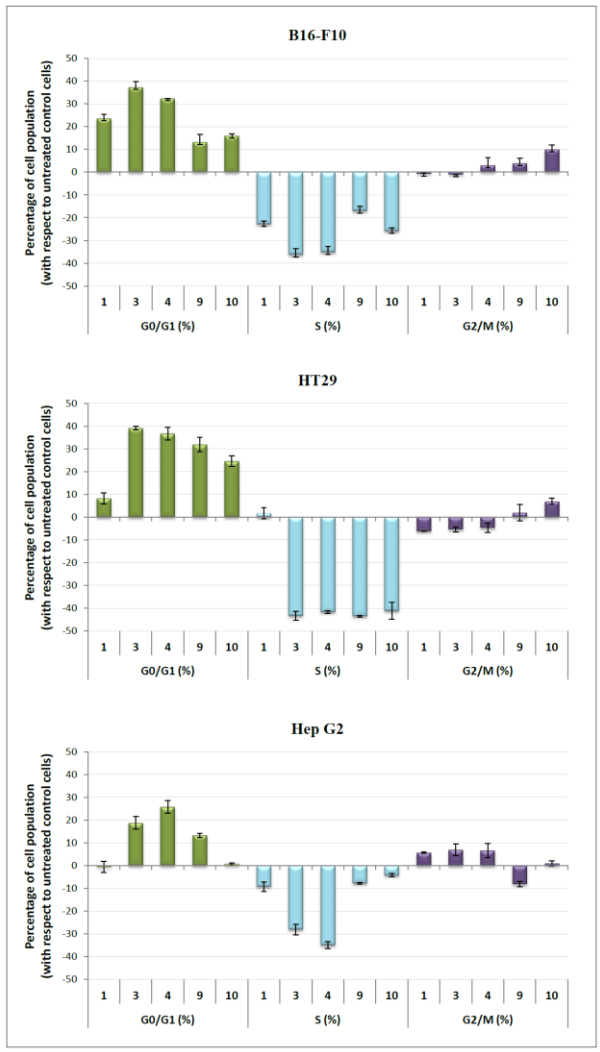

Chart 3. Changes in the percentages of cells, in each of the cell-cycle phase, have been performed with respect to untreated control cells. B16F10, HT29, and Hep G2 cells were treated with OA or MA derivatives, at its IC_{50} concentrations. Cell-cycle analysis was conducted after propidium iodide staining, G0/G1 phase (green bars), S phase (light-blue bars), and G2/M phase (purple bars). Values represent means ± S.E.M. of at least two independent experiments performed in triplicate.

2.5. Effects on changes in mitochondrial membrane potential

Loss of mitochondrial membrane potential (MMP) during a process of apoptosis has been associated with an intrinsic apoptosis-activation mechanism, while inducing apoptosis without MMP changes may suggest activation of the extrinsic apoptotic pathway. We analysed the MMP to elucidate the possible mechanism involved in the apoptotic responses, in the three cell lines (B16-F10, HT29, and Hep G2), of the PEGylated derivatives, at the same time and concentration of the cytotoxic and apoptotic responses. Changes in the mitochondrial-membrane potential were examined by monitoring the cell fluorescence after double staining with Rh123 (rhodamine 123) and PI (propidium iodide). Rh123 is a membrane-permeable fluorescent cationic dye that is selectively taken up by mitochondria directly proportional to the MMP.

In the B16-F10 cell line, only the PEGylated-amine derivative **9** clearly disrupted the mitochondrial membrane, with loss of the MMP and negative Rh123 staining. In the HT29 cell line, compounds **4** and **9** triggered the loss of MMP, while only compound **1** did in the Hep G2 cell line (Chart 4). These results suggest an activation of an intrinsic apoptotic pathway for these compounds. Moreover, in the B16-F10 cell line, with compounds **1**, **3**, and **4**, the apoptosis induction was not clearly concomitant with the MMP disturbance. This occurred also for compounds **1** and **3** in the HT29 cell line, and only for compound **9** in the Hep G2 cell line (Chart 4). These results suggest extrinsic apoptotic pathway activation for these compounds. Changes in MMP for compound **10** were also observed in the three cell lines selected, but with a similar cell population of Rh123 positive and negative, so that the apoptotic pathway activation for this compound remained unclear.

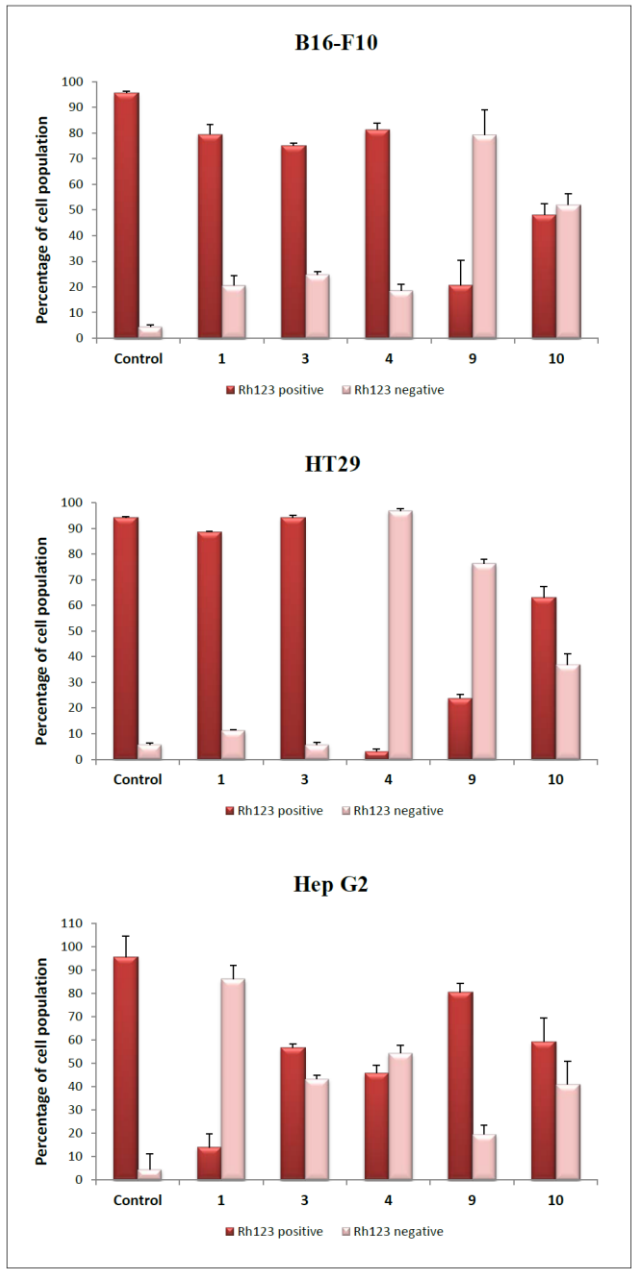

Chart 4. Flow-cytometry analysis of rhodamine 123 and PI staining after exposure of B16-F10, HT29, and Hep G2 cells to OA and MA derivatives, for 72 h with respect to the control untreated cells. Cell lines were treated at concentrations equal to its IC_{50} values. Rh123 positive cells (dark-red bars) were rhodamine 123^+ with PI^+ or PI^-. Rh123 negative cells (light-red bars) were rhodamine 123^- with PI^- or PI^+. Values are expressed as means ± S.E.M. of at least two experiments in duplicate.

2.6. Apoptotic morphological changes in cells (Hoechst-stained)

Fluorescence microscopy can determine changes in the cell morphology, and can be useful to verify the results of cytometry assays. Fluorescence microscopy revealed that a significant number of cells treated with the selected compounds acquired apoptotic features (Fig. 2). We selected compounds **3** and **10**, because their images were the most explanatory and representative. Compound **9**, with the highest cytotoxicity, was not selected due to the low density in the number of cells within the field of view.

The morphological analysis of Hoechst-stained cells, i.e. the B16-F10, HT29, and Hep G2 cells, indicated remarkable morphological changes (Fig. 2), as stains in nuclei containing nicked DNA, a characteristic exhibited by cells in apoptotic cell death. The treated cells showed typical apoptotic features, such as diminished cell size, spherical cell shapes, and bubble-shaped regions within the cell surface. The apoptotic morphological changes observed also included cell shrinkage, chromatin condensation, loss of normal nuclear architecture, and disruption of cell-membrane integrity.

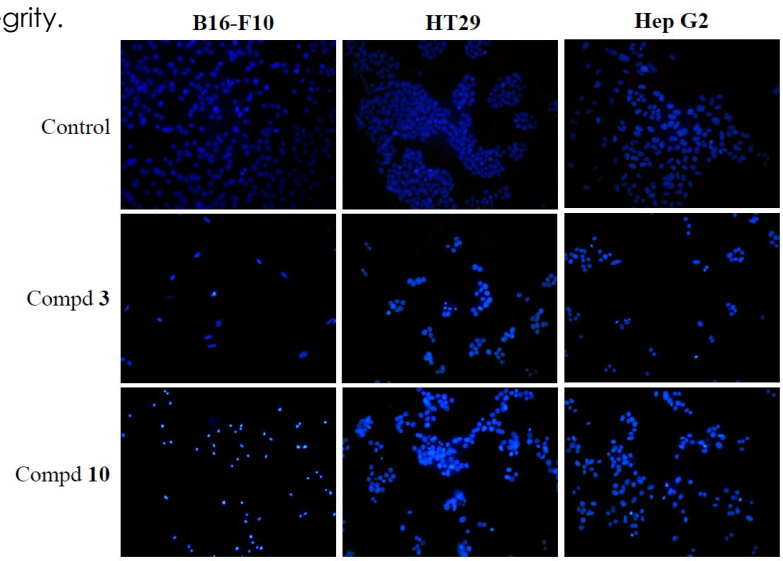

Fig. 2. Morphology changes in B16-F10, HT29, and Hep G2 cells. The cells were analysed after exposure 72 h to OA or MA derivatives, at its IC_{50} concentrations values. Morphology of cells was examined using fluorescence microscopy after Hoechst-stained.

3. Conclusions

Twelve PEGylated derivatives of oleanolic and maslinic acids were semi-synthesized to evaluate their antiproliferative effects. These triterpenic derivatives were tested for cytotoxicity in three cancer-cell lines (B16-F10, Hep G2, and HT29), and in many cases proved more cytotoxic than natural triterpenes. The best results were achieved by the PEGylated-amine derivative (**9**) of oleanolic acid, with IC_{50} concentrations between 0.22 and 3.78 μM, being between 28- and 963-fold more effective than its natural precursor (OA).

The percentages of apoptosis induction were determined for the five PEGylated derivatives (**1**, **3**, **4**, **9**, and **10**) with the lowest cytotoxicity data. Compound **10** registered a total apoptosis rate of 99% in B16-F10 cells and 80% in Hep G2 cells. Compounds **3**, **4**, and **9** displayed percentages of total apoptosis of 89%, 97%, and 72% in B16-F10 cells, respectively. The moderate percentages of apoptosis that induced all the compounds tested in the cell line HT29, and the increase in cell-cycle arrest observed, may be due to the cytostatic effects of these compounds in this cell line. In the other two cell lines (B16-F10 and Hep G2), the PEGylated-acid derivatives **1**, **3**, and **4**, showed higher rates of late apoptosis than of early apoptosis, while the PEGylated-amine derivatives **9** and **10**, exhibited a higher percentage of early apoptosis.

In the B16-F10 and HT29 cell lines, most of the compounds assayed produced cell-cycle arrest in the G0/G1 phase. This cycle arrest, together with a higher percentage of early apoptosis showed by some compounds, may be related to the delay in the apoptotic process and probably to induced cell differentiation. The MMP results suggest the activation of the apoptotic pathways, either intrinsic or extrinsic, for the different compounds for the various cell lines. The morphological analysis of Hoechst-stained cells, in the three cell lines, with the selected compounds **3** and **10**, indicated that they had undergone remarkable morphological changes.

The induction of apoptosis at very low concentrations showed by some of these triterpenic PEGylated derivatives, in different tumour lines, suggest that they could be used in the future as new, safe, and effective anticancer drugs.

4. Experimental

4.1. General experimental chemical procedures.

Measurements of NMR spectra were made in a VARIAN Inova unity (300 MHz ^{1}H NMR), and VARIAN direct drive (400 and 500 MHz ^{1}H NMR) spectrometers. The ^{13}C chemical shifts were assigned with the aid of distortionless enhancement by polarization transfer (DEPT) using a flip angle of 135º. IR spectra were recorded on a MATTSON SATELLITE FTIR spectrometer. Optical rotations were measured with a Perkin-Elmer 241 polarimeter at 25 ºC. Purity of new compounds was determined by a WATERS ACQUITY UPLC system (ultra-performance liquid chromatography) coupled with a WATERS SYNAPT G2 HRMS spectrometer (high-resolution mass spectra) with ESI (electrospray ionization). The purities of all compounds were confirmed to be ≥ 95%. Melting points (mp) were determined using a Kofler (Reichter) apparatus and were uncorrected. All reaction solvents and chromatography solvents were distilled prior to use. Commercially available reagents were used without further purification. Merck silica-gel 60 aluminium sheets (ref. 1.16835) were used for TLC, and spots were rendered visible by spraying with H_2SO_4–AcOH, followed by heating to 120 ºC, and also visualized under UV at 254 nm. Merck silica-gel 60 (0.040–0.063 mm, ref. 1.09385) was used for flash chromatography. CH_2Cl_2 (Fisher, ref. D/1852/17), $CHCl_3$ (Fisher, ref. C/4960/17), or n-hexane (Merck, ref. 1.04374), with increasing amounts of Me_2CO (Fisher, ref. A/0600/17), MeOH (Fisher, ref. M/4000/17), or AcOEt (Fisher, ref. E/0900/17), were used as eluents (all the solvents had an analytical reagent-grade purity). The PEG reagents 2-(2-(2-methoxyethoxy)ethoxy)acetic acid (VII, PEG-COOH, CAS Number 16024-58-1) and 4,7,10-trioxatridecane-1,13-diamine (VIII, H_2N-PEG-NH_2, CAS Number 4246-51-9) were purchased from

Sigma-Aldrich. Other specific reagents, as Boc_2O (CAS Number 24424-99-5) and TBTU (CAS Number 125700-67-6), were also purchased from Sigma-Aldrich.

*4.2. Isolation of OA (**I**) andMA (**II**).*

OA (**I**) and MA (**II**) were isolated from solid olive-oil-production wastes, which were extracted successively in a Soxhlet with hexane and EtOAc. Hexane extracts were a mixture of OA and MA (80:20), whereas this relationship was (20:80) for the EtOAc extracts. Both products were purified from these mixtures by column chromatography over silica gel, eluting with a $CHCl_3$/MeOH or CH_2Cl_2/acetone mixtures of increasing polarity [74].

4.3. Synthesis of OA and MA derivatives.

*4.3.1. Benzyl oleanolate (**III**).*

BnCl (418 µL) was added in a relationship of 2:1 to a solution of OA (**I**, 912 mg, 2 mmol) in DMF (8 mL) with K_2CO_3 (0.61 g). The reaction was stirred for 4 h at 55 °C. The mixture was diluted with water and extracted with DCM, and the organic layer dried with anhydrous Na_2SO_4. The solvent was removed under reduced pressure, and the residue was purified by column chromatography using DCM/Acetone (10:1) to give OA-Bn (**III**) as a white solid (710 mg, 83%) [69].

*4.3.2. Benzyl maslinate (**IV**).*

BnCl (418 µL) was added in a relationship of 2:1 to a solution of MA (**II**, 944 mg, 2 mmol) in DMF (8 mL) with K_2CO_3 (0.61 g). The reaction was stirred for 4 h at 55 °C. The mixture was diluted with water and extracted with DCM, and the organic layer dried with anhydrous Na_2SO_4. The solvent was removed under reduced pressure, and the residue was purified by column chromatography using DCM/acetone (10:1) to give MA-Bn (**IV**) as a white solid (690 mg, 81%) [23].

*4.3.3. 3β-Acetyl oleanolic acid (**V**).*

Ac_2O (1 mL) was added slowly to a solution of OA (**I**, 1368 mg, 3 mmol) in pyridine (10 mL). The reaction was performed with stirring at reflux for 1 h. Cold water was added to the reaction mixture, and afterwards this was extracted with DCM, and the organic layer was dried with anhydrous Na_2SO_4. The solvent was removed under reduced pressure and the residue was purified by column chromatography using DCM/acetone (10:1) to give OA-Ac (**V**) as a white solid (95%) [70].

*4.3.4. 2β,3β-Diacetyl maslinic acid (**VI**).*

Ac_2O (2 mL) was added slowly to a solution of MA (**II**, 1416 mg, 3 mmol) in pyridine (10 mL). The reaction was performed with at reflux for 1 h. Cold water was added to the reaction mixture, and afterwards this was extracted with DCM, and the organic layer was dried with anhydrous Na_2SO_4. The solvent was removed under reduced pressure and the residue was purified by column chromatography using DCM/acetone (10:1) to give MA-Ac (**VI**) as a white solid (90%) [71].

*4.4. PEGylation of OA (**I**) and OA-Bn (**III**).*

Oleanolic acid (**I**) or 28-benzyl oleanolic acid (**III**) (0.44 mmol), were separately dissolved in DMF (2 mL). Then, DIPCDI (4 mmol), DMAP (0.12 mmol) and 2-(2-(2-methoxyethoxy)ethoxy)acetic acid (**VII**, 4 mmol), were added. The reaction mixture was maintained at reflux for 4 h, and then was diluted with water and extracted three times with DCM. The organic layer was dried with anhydrous Na_2SO_4 and the solvent was removed under reduced pressure. Finally, the residue was purified by column chromatography using hexane/ethyl acetate as solvents, yielding compound **1** (95%) and **2** (94%), respectively.

*4.4.1. Compound **1***

White solid, mp 120–122 °C; $[\alpha]^{25}_D$ + 58 (c 1 in MeOH); IR ν_{max}(KBr)/cm^{-1} 2938, 1749, 1728, 1691, 1205, 1107, 1010 and 969; δ_H ($CDCl_3$, 300 MHz): 5.26 (dd, 1H, $J_1 = J_2$ = 3.5 Hz, H-12), 4.59 (dd, 1H, $J_1 = J_2$ = 7.8 Hz, H-

3), 4.13 (collapsed AB system, 2H, CH_2CO PEG group), 3.76-3.56 (m, 8H, CH_2O PEG group), 3.39 (s, 3H, CH_3O PEG group), 2.81 (dd, 1H, J_1 = 3.2, J_2 = 13.4 Hz, H-18), 1.12, 0.92, 0.92, 0.89, 0.85, 0.83, 0.74 (s, 3H each, methyl groups); δ_C ($CDCl_3$, 75 MHz) see Table S1 (Supplementary material); ESI-HRMS m/z calcd for $C_{37}H_{60}O_7Na$ $[M+Na]^+$ 639.4237, found 639.4238.

4.4.2. Compound ***2***

Syrup; $[\alpha]^{25}_D$ + 38 (c 1 in MeOH); IR ν_{max}(film)/cm^{-1} 2943, 1748, 1724, 1455, 1254, 1198, 1120, 1010 and 749; δ_H ($CDCl_3$, 500 MHz): 7.25 (m, 5H, benzyl group), 5.20 (dd, 1H, J_1 = J_2 = 3.5 Hz, H-12), 5.01 and 4.96 (AB system, 1H each, J = 12.5 Hz, benzyl group), 4.52 (dd, 1H, J_1 = 7.5, J_2 = 9.0 Hz, H-3), 4.08 and 4.04 (AB system, 1H each, J = 16.5 Hz, CH_2CO PEG group), 3.68-3.47 (m, 8H, CH_2O PEG group), 3.29 (s, 3H, CH_3O PEG group), 2.83 (dd, 1H, J_1 = 3.9, J_2 = 13.7 Hz, H-18), 1.04, 0.84, 0.82, 0.82, 0.78, 0.77, 0.52 (s, 3H each, methyl groups); δ_C ($CDCl_3$, 125 MHz) see Table S1 (Supplementary material); ESI-HRMS m/z calcd for $C_{44}H_{66}O_7Na$ $[M+Na]^+$ 729.4706, found 729.4724.

*4.5. PEGylation of MA (**II**) and MA-Bn (**IV**).*

Maslinic acid (**II**) or 28-benzyl maslinic acid (**IV**) (0.44 mmol), were separately dissolved in DMF (2 mL). Then DIPCDI (8 mmol), DMAP (0.12 mmol) and 2-(2-(2-methoxyethoxy)ethoxy)acetic acid (**VII**, 8 mmol), were added. The reaction mixture was processed as described above for the PEGylation reactions of OA (**I**) and OA-Bn (**III**). Finally, the residue was purified by column chromatography using hexane/ethyl acetate as solvents, yielding compound **3** (90%) and **4** (92%), respectively.

4.5.1. Compound ***3***

Syrup; $[\alpha]^{25}_D$ + 9 (c 1 in MeOH); IR ν_{max}(film)/cm^{-1} 2941, 1755, 1731, 1694, 1198, 1105, 1026 and 991; δ_H ($CDCl_3$, 500 MHz): 5.25 (dd, 1H, J_1 = J_2 = 3.5 Hz, H-12), 5.14 (ddd, 1H, J_1 = 5.0, J_2 = 10.5, J_3 = 15.5 Hz, H-2), 4.82 (d, 1H, J = 10.5 Hz, H-3), 4.14 and 4.09 (AB system, 1H each, J = 16.5 Hz, CH_2CO PEG group), 4.05 and 4.00 (AB system, 1H each, J = 16.5 Hz, CH_2CO PEG group), 3.71-3.53 (m, 16H, CH_2O PEG groups), 3.37 and 3.36 (s, 3H each, CH_3O PEG

groups), 2.81 (dd, 1H, J_1 = 4.5 Hz, J_2 = 14.0 Hz, H-18), 1.11, 1.04, 0.91, 0.89, 0.89, 0.87, 0.72 (s, 3H each, methyl groups); δ_C ($CDCl_3$, 125 MHz) see Table S1 (Supplementary material); ESI-HRMS m/z calcd for $C_{44}H_{73}O_{12}$ $[M+1]^+$ 793.5102, found 793.5097.

4.5.2. Compound ***4***

White solid, mp 100–102 °C; $[a]^{25}_D$ + 4 (*c* 1 in MeOH); IR ν_{max}(KBr)/cm^{-1} 2941, 1755, 1728, 1455, 1257, 1199, 1107, 1027 and 734; δ_H ($CDCl_3$, 500 MHz): 7.30 (m, 5H, benzyl group), 5.23 (dd, 1H, J_1 = J_2 = 3.5 Hz, H-12), 5.10 (ddd, 1H, J_1 = 4.7, J_2 = 10.0, J_3 = 15.2 Hz, H-2), 5.06 and 5.00 (AB system, 1H each, *J* = 12.5 Hz, benzyl group), 4.79 (d, 1H, *J* = 10.0 Hz, H-3), 4.11 and 4.06 (AB system, 1H each, *J* = 16.5 Hz, CH_2CO PEG group), 4.02 and 3.97 (AB system, 12H each, *J* = 16.7 Hz, CH_2CO PEG group), 3.69-3.60 (m, 16H, CH_2O PEG groups), 3.35 and 3.34 (s, 3H each, CH_3O PEG groups), 2.87 (dd, 1H, J_1 = 4.5, J_2 = 14.0 Hz, H-18), 1.12, 1.10, 1.07, 0.98, 0.88, 0.86, 0.54 (s, 3H each, methyl groups); δ_C ($CDCl_3$, 125 MHz) see Table S1 (Supplementary material); ESI-HRMS m/z calcd for $C_{51}H_{79}O_{12}$ $[M+1]^+$ 883.5572, found 883.5592.

*4.6. Selective Protection of the reagent H_2N-PEG-NH_2 (**VIII**) with Boc_2O.*

A solution of di-tert-butyl dicarbonate (Boc_2O, 2.75 mmol) in dried DCM (2 mL) was added slowly, drop to drop, to a solution of 4,7,10-trioxatridecane-1,13-diamine (**VIII**, 6.8 mmol) in DCM (20 mL). The reaction mixture was maintained at rt for 12 h, and then was diluted with water and extracted three times with DCM. The organic layer was dried with anhydrous Na_2SO_4 and the solvent was removed under reduced pressure and thus the mono-blocked derivative H_2N-PEG-NH-Boc (**IX**, 85%) was produced.

4.6.1. Compound ***IX***

Syrup; δ_H ($CDCl_3$, 400 MHz): 5.13 (m, 1H, NH PEG-Boc group), 3.64-3.49 (m, 12H, 6 CH_2 PEG group), 3.20 (m, 2H, 1 CH_2 PEG group), 2.80 (m, 2H, 1 CH_2 PEG group), 1.76-1.69 (m, 4H, 2 CH_2 PEG group), 1.41 (s, 9H, 3 CH_3 Boc group); δ_C ($CDCl_3$, 100 MHz): 156.2 (CO-Boc), 79.0 (CO-Boc), 70.6, 70.3, 70.2,

69.6 (6C, CH_2 PEG group), 39.7, 38.5, 32.9, 29.7 (4C, CH_2 PEG group), 28.6 (3 CH_3 Boc group).

*4.7. PEGylation of compounds **I**, **II**, **III**, or **IV** with reagent **IX**.*

In four flasks (20 mL), compound **IX** (0.45 mmol in each) was dissolved in DMF (5 mL in each) and afterwards, compounds **I**, **II**, **V**, or **VI** (2 mmol), HOAt (3 mmol), PyAOP (2 mmol) and DIPEA (8 mmol), were added to each flask. The reaction mixture of each flask was heated at 100 °C for 12 h, diluted with water and extracted three times with DCM. Each organic layer was dried with anhydrous Na_2SO_4 and the solvent was removed under reduced pressure. Finally, each residue was purified by column chromatography using hexane/ethyl acetate as the solvent and thus compounds **5** (94%), **6** (91%), **7** (86%), or **8** (90%) were yielded, respectively.

*4.7.1. Compound **5***

Syrup; $[\alpha]^{25}_D$ + 26 (c 1 in MeOH); IR ν_{max}(film)/cm^{-1} 3394, 2938, 1691, 1521, 1454, 1365, 1250, 1169, 1095 and 840; δ_H ($CDCl_3$, 500 MHz): 6.22 (dd, 1H, J_1 = J_2 = 5.3 Hz, NH PEG group), 5.35 (dd, 1H, J_1 = J_2 = 3.3 Hz, H-12), 4.95 (bs, 1H, NH-Boc PEG group), 3.65-3.09 (m, 16H, CH_2O PEG group), 3.20 (dd, 1H, J_1 = 4.3, J_2 = 7.3 Hz, H-3), 2.53 (dd, 1H, J_1 = 12.8, J_2 = 13.0 Hz, H-18), 1.43 (s, 9H, CH_3 Boc group), 1.15, 0.98, 0.90, 0.90, 0.90, 0.78, 0.75 (s, 3H each, methyl groups); δ_C ($CDCl_3$, 125 MHz) see Table S2 (Supplementary material); ESI-HRMS m/z calcd for $C_{45}H_{79}N_2O_7$ $[M+1]^+$ 759.5887, found 759.5864.

*4.7.2. Compound **6***

Syrup; $[\alpha]^{25}_D$ + 31 (c 1 in MeOH); IR ν_{max}(film)/cm^{-1} 3712, 3682, 2939, 1691, 1517, 1363, 1052, 1033, 1013 and 845; δ_H ($CDCl_3$, 500 MHz): 6.24 (dd, 1H, J_1 = J_2 = 5.0 Hz, NH PEG group), 5.36 (dd, 1H, J_1 = J_2 = 3.3 Hz, H-12), 4.93 (bs, 1H, NH-Boc PEG group), 3.67-3.10 (m, 16H, CH_2O PEG group), 3.50 (ddd, 1H, J_1 = 2.0, J_2 = 5.5, J_3 = 7.5 Hz, H-2), 3.00 (d, 1H, J = 5.5 Hz, H-3), 2.50 (dd, 1H, J_1 = 3.8, J_2 = 13.3 Hz, H-18), 1.43 (s, 9H, CH_3 Boc group), 1.15, 1.04, 0.98, 0.90, 0.90, 0.83, 0.80 (s, 3H each, methyl groups); δ_C ($CDCl_3$, 125 MHz) see Table S2

(Supplementary material); ESI-HRMS m/z calcd for $C_{45}H_{79}N_2O_8$ $[M+1]^+$ 775.5836, found 775.5815.

*4.7.3. Compound **7***

White solid, mp 102–104 °C; $[a]^{25}_D$ + 23 (c 1 in MeOH); IR ν_{max}(KBr)/cm^{-1} 2941, 2871, 1692, 1518, 1365, 1246, 1169, 1098, 1032 and 838; δ_H ($CDCl_3$, 500 MHz): 6.27 (dd, 1H, $J_1 = J_2$ = 5.8 Hz, NH PEG group), 5.34 (dd, 1H, $J_1 = J_2$ = 3.3 Hz, H-12), 4.97 (bs, 1H, NH-Boc PEG group), 4.45 (dd, 1H, $J_1 = J_2$ = 8.0 Hz, H-3), 3.74-3.06 (m, 16H, CH_2O PEG group), 2.50 (dd, 1H, J_1 = 3.5, J_2 = 13.0 Hz, H-18), 2.01 (s, 3H, acetyl group), 1.40 (s, 9H, CH_3 Boc group), 1.12, 0.90, 0.90, 0.90, 0.83, 0.82, 0.72 (s, 3H each, methyl groups); δ_C ($CDCl_3$, 125 MHz) see Table S2 (Supplementary material); ESI-HRMS m/z calcd for $C_{47}H_{81}N_2O_8$ $[M+1]^+$ 801.5993, found 801.6015.

*4.7.4. Compound **8***

Syrup; $[a]^{25}_D$ + 2 (c 1 in MeOH); IR ν_{max}(film)/cm^{-1} 2939, 1739, 1643, 1518, 1364, 1247, 1170, 1051, 1033 and 851; δ_H ($CDCl_3$, 500 MHz): 6.17 (dd, 1H, $J_1 = J_2$ = 4.8 Hz, NH PEG group), 5.33 (dd, 1H, $J_1 = J_2$ = 5.0 Hz, H-12), 5.10 (ddd, 1H, J_1 = 5.0, J_2 = 10.0, J_3 = 15.5 Hz, H-2), 4.98 (bs, 1H, NH-Boc PEG group), 4.74 (d, 1H, J = 10.0 Hz, H-3), 3.60-3.10 (m, 16H, CH_2O PEG group), 2.54 (dd, 1H, J_1 = 5.0, J_2 = 10.0 Hz, H-18), 2.05 and 1.97 (s, 3H each, acetyl groups), 1.43 (s, 9H, CH_3 Boc group), 1.14, 1.05, 0.90, 0.90, 0.90, 0.89, 0.75 (s, 3H each, methyl groups); δ_C ($CDCl_3$, 125 MHz) see Table S2 (Supplementary material); ESI-HRMS m/z calcd for $C_{49}H_{83}N_2O_{10}$ $[M+1]^+$ 859.6048, found 859.6050.

*4.8. Boc-Deprotection reaction of compounds **5**, **6**, **7**, and **8**.*

Compounds **5**, **6**, **7**, or **8** (0.3 mmol of each) were separately dissolved in THF (20 mL each), and then concentrated HCl (37%, 2 mL) was added to each solution. The reaction mixture was maintained at rt for 24 h, and then was diluted with water and extracted three times with DCM. The organic layer was dried with anhydrous Na_2SO_4 and the solvent was removed under reduced pressure. Finally, each residue was purified by column chromatography using hexane/ethyl acetate as solvents and thus

compound **9** (95%), **10** (93%), **11** (92%), or **12** (94%) were yielded, respectively.

*4.8.1. Compound **9***

Syrup; $[\alpha]^{25}_D$ + 35 (c 1 in MeOH); IR ν_{max}(film)/cm^{-1} 3372, 2925, 2866, 1631, 1529, 1385, 1094, 1031 and 996; δ_H ($CDCl_3$, 500 MHz): 6.26 (dd, 1H, J_1 = J_2 = 5.5 Hz, NH PEG group), 5.31 (dd, 1H, J_1 = J_2 = 3.3 Hz, H-12), 3.64-3.06 (m, 16H, CH_2O PEG group), 2.83 (dd, 1H, J_1 = J_2 = 6.7 Hz, H-3), 2.50 (dd, 1H, J_1 = 7.0, J_2 = 13.5 Hz, H-18), 1.12, 0.95, 0.87, 0.87, 0.87, 0.74, 0.71 (s, 3H each, methyl groups); δ_C ($CDCl_3$, 125 MHz) see Table S2 (Supplementary material); ESI-HRMS m/z calcd for $C_{40}H_{70}N_2O_5Na$ $[M+Na]^+$ 681.5182, found 681.5159.

*4.8.2. Compound **10***

White solid, mp 105–107 °C; $[\alpha]^{25}_D$ + 31 (c 1 in MeOH); IR ν_{max}(KBr)/cm^{-1} 3709, 3682, 2938, 2863, 1625, 1346, 1053, 1033 and 753; δ_H ($CDCl_3$, 500 MHz): 6.37 (dd, 1H, J_1 = J_2 = 5.5 Hz, NH PEG group), 5.37 (dd, 1H, J_1 = J_2 = 3.3 Hz, H-12), 3.73-3.10 (m, 16H, CH_2O PEG group), 3.39 (ddd, 1H, J_1 = 6.5, J_2 = 9.5, J_3 = 13.5 Hz, H-2), 3.01 (d, 1H, J = 9.5 Hz, H-3), 2.51 (dd, 1H, J_1 = 3.0, J_2 = 12.5 Hz, H-18), 1.14, 1.02, 0.96, 0.95, 0.89, 0.81, 0.74 (s, 3H each, methyl groups); δ_C ($CDCl_3$, 125 MHz) see Table S2 (Supplementary material); ESI-HRMS m/z calcd for $C_{40}H_{70}N_2O_6Na$ $[M+Na]^+$ 697.5132, found 697.5098.

*4.8.3. Compound **11***

White solid, mp 102–104 °C; $[\alpha]^{25}_D$ + 36 (c 1 in MeOH); IR ν_{max}(KBr)/cm^{-1} 2972, 2940, 2922, 2867, 1773, 1245, 1054, 1033 and 1011; δ_H ($CDCl_3$, 500 MHz): 6.17 (dd, 1H, J_1 = J_2 = 6.0 Hz, NH PEG group), 5.34 (dd, 1H, J_1 = J_2 = 3.5 Hz, H-12), 4.48 (dd, 1H, J_1 = 8.5, J_2 = 11.0 Hz, H-3), 3.67-3.08 (m, 16H, CH_2O PEG group), 2.54 (dd, 1H, J_1 = 4.0, J_2 = 16.0 Hz, H-18), 2.04 (s, 3H, acetyl group), 1.14, 0.93, 0.90, 0.90, 0.86, 0.85, 0.76 (s, 3H each, methyl groups); δ_C ($CDCl_3$, 125 MHz) see Table S2 (Supplementary material); ESI-HRMS m/z calcd for $C_{42}H_{73}N_2O_6$ $[M+1]^+$ 701.5469, found 701.5474.

*4.8.4. Compound **12***

White solid, mp 108–110 °C; [a]$^{25}_{D}$ + 3 (c 1 in MeOH); IR ν_{max}(KBr)/cm^{-1} 2973, 2921, 2864, 1740, 1246, 1231, 1054, 1033 and 1013; δ_H ($CDCl_3$, 500 MHz): 6.17 (dd, 1H, $J_1 = J_2$ = 5.5 Hz, NH PEG group), 5.32 (dd, 1H, $J_1 = J_2$ = 3.5 Hz, H-12), 5.08 (ddd, 1H, J_1 = 4.5, J_2 = 10.5, J_3 = 15.0 Hz, H-2), 4.74 (d, 1H, J = 10.5 Hz, H-3), 3.65-3.09 (m, 16H, CH_2O PEG group), 2.54 (dd, 1H, J_1 = 3.5, J_2 = 13.0 Hz, H-18), 2.05 and 1.97 (s, 3H each, acetyl groups), 1.13, 1.04, 0.90, 0.90, 0.90, 0.89, 0.75 (s, 3H each, methyl groups); δ_H ($CDCl_3$, 125 MHz) see Table S2 (Supplementary material); ESI-HRMS m/z calcd for $C_{44}H_{75}N_2O_8$ $[M+1]^+$ 759.5523, found 759.5495.

*4.9. Formation of the TBTU-derivatives of **I**, **II**, **III**, or **IV**.*

DIEA (0.3 mmol) and TBTU (0.66 mmol) were added to four solutions of compounds **I**, **II**, **III**, or **IV** (0.44 mmol of each) in THF (20 mL each). The reactions mixtures were maintained art for 12 h and then diluted with water and extracted three times with DCM. The organic layers were dried with anhydrous Na_2SO_4 and the solvent was removed under reduced pressure. Finally, each residue was purified by column chromatography using hexane/ethyl acetate as solvents and, thus, compounds **13** (90%), **14** (92%), **15** (91%), or **16** (90%) were yielded, respectively.

*4.9.1. Compound **13***

White solid, mp 140–142 °C; [a]$^{25}_{D}$ + 4 (c 1 in MeOH); IR ν_{max}(KBr)/cm^{-1} 3379, 2939, 1809, 1464, 1385, 1140, 1050, 1032, 1000 and 749; δ_H ($CDCl_3$, 500 MHz): 8.03 (m, 1H, TBTU group), 7.50 (m, 1H, TBTU group), 7.37 (m, 2H, TBTU group), 5.36 (dd, 1H, $J_1 = J_2$ = 3.5 Hz, H-12), 3.20 (dd, 1H, J_1 = 4.0, J_2 = 11.0 Hz, H-3), 2.97 (dd, 1H, J_1 = 4.5, J_2 = 14.0 Hz, H-18), 1.21, 0.99, 0.98, 0.96, 0.89, 0.84, 0.78 (s, 3H each, methyl groups); δ_C ($CDCl_3$, 125 MHz) see Table S3 (Supplementary material); ESI-HRMS m/z calcd for $C_{36}H_{52}N_3O_3$ $[M+1]^+$ 574.4009, found 574.4020.

*4.9.2. Compound **14***

White solid, mp 153–155 °C; $[a]^{25}_D$ + 6 (*c* 1 in MeOH); IR ν_{max}(KBr)/cm^{-1} 3704, 3678, 2941, 1807, 1457, 1374, 1052, 1033, 1016 and 738; δ_H ($CDCl_3$ 400 MHz): 8.05 (m, 1H, TBTU group), 7.52 (m, 1H, TBTU group), 7.38 (m, 2H, TBTU group), 5.38 (dd, 1H, $J_1 = J_2$ = 3.6 Hz, H-12), 3.69 (ddd, 1H, J_1 = 4.4, J_2 = 10.0, J_3 = 14.4 Hz, H-2), 3.01 (d, 1H, *J* = 10.0 Hz, H-3), 2.98 (dd, 1H, J_1 = 4.0, J_2 = 13.5 Hz, H-18), 1.22, 1.05, 1.00, 0.98, 0.97, 0.85, 0.84 (s, 3H each, methyl groups); δ_C ($CDCl_3$, 100 MHz) see Table S3 (Supplementary material); ESI-HRMS m/z calcd for $C_{36}H_{52}N_3O_4$ $[M+1]^+$ 590.3958, found 590.3954.

*4.9.3. Compound **15***

White solid, mp 120–122 °C; $[a]^{25}_D$ + 15 (*c* 1 in MeOH); IR ν_{max}(KBr)/cm^{-1} 2942, 1808, 1459, 1367, 1230, 1153, 1084, 1033, 1002 and 743; δ_H ($CDCl_3$, 500 MHz): 8.04 (m, 1H, TBTU group), 7.51 (m, 1H, TBTU group), 7.38 (m, 2H, TBTU group), 5.37 (dd, 1H, $J_1 = J_2$ = 3.5 Hz, H-12), 4.50 (dd, 1H, J_1 = 7.0, J_2 = 8.0 Hz, H-3), 2.98 (dd, 1H, J_1 = 4.5, J_2 = 13.5 Hz, H-18), 2.04 (s, 3H, acetyl group), 1.21, 1.00, 0.97, 0.93, 0.88, 0.86, 0.85 (s, 3H each, methyl groups); δ_C ($CDCl_3$, 125 MHz) see Table S3 (Supplementary material); ESI-HRMS m/z calcd for $C_{38}H_{54}N_3O_4$ $[M+1]^+$ 616.4114 found 616.4099.

*4.9.4. Compound **16***

White solid, mp 155–157 °C; $[a]^{25}_D$ + 8 (*c* 1 in MeOH); IR ν_{max}(KBr)/cm^{-1} 2972, 1806, 1457, 1367, 1249, 1227, 1052, 1032, 1015 and 742; δ_H ($CDCl_3$, 400 MHz): 8.05 (m, 1H, TBTU group), 7.52 (m, 1H, TBTU group), 7.38 (m, 2H, TBTU group), 5.37 (dd, 1H, $J_1 = J_2$ = 3.5 Hz, H-12), 5.10 (ddd, 1H, J_1 = 5.0, J_2 = 10.5, J_3 = 15.5 Hz, H-2), 4.75 (d, 1H, *J* = 10.0 Hz, H-3), 2.98 (dd, 1H, J_1 = 4.0, J_2 = 13.5 Hz, H-18), 2.06 and 1.97 (s, 3H each, acetyl groups), 1.21, 1.06, 1.00, 0.98, 0.92, 0.91, 0.85 (s, 3H each, methyl groups); δ_C ($CDCl_3$, 100 MHz) see Table S3 (Supplementary material); ESI-HRMS m/z calcd for $C_{40}H_{56}N_3O_6$ [M+1]+ 674.6169, found 674.4187.

*4.10. PEGylation of compounds **13**, **14**, **15**, or **16** with reagent **VIII**.*

K_2CO_3 (1.0 mmol) and 4,7,10-trioxatridecane-1,13-diamine (**VIII**, 0.175 mmol) were added to four solutions of compounds **13**, **14**, **15**, or **16** (0.35 mmol of each) in DCM (20 mL each). Each reaction mixture was stirred at rt for 4 h and then diluted with water and extracted three times with DCM. The organic layer was dried with anhydrous Na_2SO_4 and the solvent was removed under reduced pressure. Finally, each residue was purified by column chromatography, using hexane/ethyl acetate as solvents and thus the dimeric compounds **17** (76%), **18** (81%), **19** (79%), or **20** (85%) were yielded, respectively. Small percentages of the monomeric compounds (**9**, 13%; **10**, 10%; **11**, 11%; or **12**, 7%) were also yielded, respectively.

*4.10.1. Compound **17***

White solid, mp 139–141 °C; $[\alpha]^{25}_D$ + 26 (*c* 1 in MeOH); IR ν_{max}(KBr)/cm^{-1} 3672, 2922, 2863, 2844, 1628, 1054, 1033, 1012 and 839; δ_H (CD_3OD, 400 MHz): 7.28 (dd, 1H, $J_1 = J_2$ = 5.2 Hz, NH PEG group), 5.42 (dd, 1H, $J_1 = J_2$ = 3.2 Hz, H-12), 3.74-3.18 (m, 16H, CH_2O PEG group), 3.22 (dd, 1H, $J_1 = J_2$ = 6.8 Hz, H-3), 2.83 (dd, 1H, J_1 = 3.6, J_2 = 13.2 Hz, H-18), 1.24, 1.04, 1.01, 1.01, 0.97, 0.85, 0.84 (s, 3H each, methyl groups); δ_C (CD_3OD, 100 MHz) see Table S3 (Supplementary material); ESI-HRMS m/z calcd for $C_{70}H_{117}N_2O_7$ $[M+1]^+$ 1097.8861, found 1097.8876.

*4.10.2. Compound **18***

White solid, mp 150–152 °C; $[\alpha]^{25}_D$ + 34 (*c* 1 in MeOH); IR ν_{max}(KBr)/cm^{-1} 3709, 3679, 2967, 2863, 1633, 1054, 1033, 1012 and 845; δ_H (CD_3OD, 400 MHz): 7.29 (dd, 1H, $J_1 = J_2$ = 5.6 Hz, NH PEG group), 5.41 (dd, 1H, $J_1 = J_2$ = 3.2 Hz, H-12), 3.72-3.18 (m, 16H, CH_2O PEG group), 3.57 (ddd, 1H, J_1 = 6.5, J_2 = 9.6, J_3 = 13.0 Hz, H-2), 2.95 (d, 1H, J = 9.6 Hz, H-3), 2.82 (dd, 1H, J_1 = 3.6, J_2 = 13.2 Hz, H-18), 1.22, 1.06, 1.05, 0.99, 0.96, 0.85, 0.83 (s, 3H each, methyl groups); δ_C (CD_3OD, 100 MHz) see Table S3 (Supplementary material); ESI-HRMS m/z calcd for $C_{70}H_{117}N_2O_9$ $[M+1]^+$ 1129.8759, found 1129.8749.

*4.10.3. Compound **19***

White solid, mp 103–105 °C; $[a]^{25}_D$ + 23 (c 1 in MeOH); IR ν_{max}(KBr)/cm^{-1} 2972, 2940, 2865, 1733, 1243, 1054, 1033, 1011 and 730; δ_H ($CDCl_3$, 400 MHz): 6.17 (dd, 1H, $J_1 = J_2$ = 5.2 Hz, NH PEG group), 5.33 (dd, 1H, $J_1 = J_2$ = 3.2 Hz, H-12), 4.48 (dd, 1H, J_1 = 6.4, J_2 = 9.6 Hz, H-3), 3.65-3.07 (m, 16H, CH_2O PEG group), 2.53 (dd, 1H, J_1 = 3.2, J_2 = 12.8 Hz, H-18), 2.03 (s, 3H, acetyl group), 1.13, 0.92, 0.89, 0.89, 0.85, 0.84, 0.75 (s, 3H each, methyl groups); δ_C ($CDCl_3$, 100 MHz) see Table S3 (Supplementary material); ESI-HRMS m/z calcd for $C_{74}H_{121}N_2O_9$ $[M+1]^+$ 1181.9072, found 1181.9044.

*4.10.4. Compound **20***

White solid, mp 132–134 °C; $[a]^{25}_D$ +13 (c 1 in MeOH); IR ν_{max}(KBr)/cm^{-1} 2941, 2867, 1738, 1643, 1367, 1247, 1045, 1032 and 751; δ_H ($CDCl_3$, 400 MHz): 6.16 (dd, 1H, $J_1 = J_2$ = 5.2 Hz, NH PEG group), 5.30 (dd, 1H, $J_1 = J_2$ = 3.2 Hz, H-12), 5.06 (ddd, 1H, J_1 = 4.8, J_2 = 10.4, J_3 = 15.2 Hz, H-2), 4.71 (d, 1H J = 10.4 Hz, H-3), 3.63-3.05 (m, 16H, CH_2O PEG group), 2.52 (dd, 1H, J_1 = 3.6, J_2 = 12.8 Hz, H-18), 2.02 and 1.94 (s, 3H each, acetyl groups), 1.11, 1.02, 0.87, 0.87, 0.87, 0.86, 0.72 (s, 3H each, methyl groups); δ_C ($CDCl_3$, 100 MHz) see Table S3 (Supplementary material); ESI-HRMS m/z calcd for $C_{78}H_{125}N_2O_{13}$ $[M+1]^+$ 1297.9182, found 1297.9202.

4.11. Biological experimental procedures

4.11.1. Drugs

The different compounds used in cell treatment were dissolved before use at 5 mg/mL in DMSO. A stock solution was frozen and stored at –20 °C. Prior to the experiments, this solution was diluted in cell-culture medium. Apoptosis, cell cycle, mitochondrial-membrane potential, and Hoescht stained were measured at the IC_{50} concentration (concentration causing 50% reduction in growth). All the experiments were measured and compared to the control after 72 h of treatment.

4.11.2. Cell culture

Mouse melanoma cells B16-F10 (ATCC no. CRL-6475), human colorectal adenocarcinoma cell line HT29 (ECACC no. 9172201; ATCC no. HTB-38), and human hepatocarcinoma cell line Hep G2 (ECACC no. 85011430), were cultured in DMEM supplemented with 2 mM glutamine, 10% heat-inactivated FCS, 10.000 units/mL of penicillin and 10 mg/mL of streptomycin, being incubated at 37 ºC in an atmosphere of 5% CO_2 and 95% humidity. Subconfluent monolayer cells were used in all experiments. All cell lines used were provided by the cell bank of the University of Granada, Spain.

4.11.3. Cell-proliferation activity assay

The effect of treating each product upon proliferation in B16-F10 murine melanoma cells, HT29 colon carcinoma cells, and Hep G2 hepatocarcinoma cells was measured using the MTT assay (Sigma, MO, USA), which is based on the ability of live cells to cleave the tetrazolium ring, thus producing formazan, which absorbs at 570 nm.

Cell viability was determined by measuring the absorbance of MTT dye staining of living cells. For this assay, $5 \cdot 10^3$ B16-F10 cells, $6 \cdot 10^3$ HT29 cells, $15 \cdot 10^3$ Hep G2 cells, were grown on a 96-well plate and incubated with the different products (0–300 µg/ml). After 72 h, 100 µL of MTT solution (0.5 mg/mL) was added to each well. After 1.5 h of incubation the cells were washed twice with PBS, and the formazan was resuspended in 100 µL DMSO. Relative cell viability, with respect to untreated control cells, was measured by absorbance at 550 nm on an ELISA plate reader (Tecan Sunrise MR20-301, TECAN, Austria). Derivatives that showed high cytotoxicity were used to perform studies of apoptosis, cell cycle, mitochondrial-membrane potential, and morphological changes with Hoescht staining.

4.11.4. Annexin V–FICT/propidium iodide flow-cytometric analysis.

The extension apoptosis was analysed with flow-cytometry by using a FACScan flow-cytometer (fluorescence-activated cell sorter) (Coulter

Corporation, Hialeah, FL, USA). In brief, $5 \cdot 10^4$ B16-F10 cells, $11 \cdot 10^4$ HT29 cells, $15 \cdot 10^4$ Hep G2 cells, were plated in 24-well plates with 1.5 mL of medium following treatment with the compounds for 72 h, at the IC_{50} concentrations calculated previously. The cells were collected and resuspended in binding buffer (10 mM HEPES/NaOH, pH 7.4, 140 mM NaCl, 2.5 mM $CaCl_2$). Annexin V-FITC conjugate (1 µg/mL) was added and incubated for 30 min at rt in darkness. Just before FACS analysis, cells were stained with 20 µL of 1 mg/mL PI solution. In each experiment, approximately $10 \cdot 10^3$ cells were analysed and the experiment was duplicated twice.

4.11.5. Cell cycle

The cell cycle was analysed with flow cytometry by using a fluorescence-activated cell sorter (FACS) at 488 nm in an Epics XL flow cytometer (Coulter Corporation, Hialeah, FL, USA). For this assay $5 \cdot 10^4$ B16-F10 cells, $11 \cdot 10^4$ HT29 cells, and $15 \cdot 10^4$ Hep G2 cells were plated in 24-well plates with 1.5 mL of medium, following treatment with the compounds for 72 h, at the IC_{50} concentration. After treatment, the cells were washed twice with PBS, harvested by tripsinization, and then resuspended in TBS 1X (10 mMTris, 150 mM NaCl); subsequently Vindelov Buffer (100 mMTris, 100 mM NaCl, 10 mg/mL Rnasa, 1 mg/mL PI, pH 8) was added. The samples were allowed to stand for 15 min on ice. Just before FACS analysis, cells were stained with 20 µL of 1 mg/mL PI solution. The data were analysed to determine the percentage of cells at each phase of the cell cycle (G0/G1, S and G2/M). In each experiment, approximately $10 \cdot 10^3$ cells were analysed and the experiment was duplicated twice.

4.11.6. Flow-cytometry analysis of the mitochondrial-membrane potential

Oxidative damage was studied by flow-cytometry analysis of the ROS levels, using dihydrorhodamine (DHR) oxidized to the highly fluorescent product rhodamine (Rh123). The formation of rhodamine can be monitored by fluorescence spectroscopy using excitation and emission wavelengths of 500 and 536 nm, respectively. The intracellular measurement of the reactive oxygen species was made by cytometry determination of Rh123. In the

same way as in the apoptosis assays, $5 \cdot 10^4$ B16-F10 cells, $11 \cdot 10^4$ HT29 cells, and $15 \cdot 10^4$ Hep G2 cells, were plated in 24-well plates, and treated with the compounds that exhibited high cytotoxic activity for 72 h, at the IC_{50} concentration. After treatment, the medium was removed and a fresh medium with DHR, at a final concentration of 5 µg/mL, was added. After 30 min of incubation, the medium was removed and the cells were washed and resuspended in PBS with 5 µg/mL of PI. The intensity of fluorescence from Rh123 and PI was determined using a FACScan flow cytometer (fluorescence-activated cell sorter) (Coulter Corporation, Hialeah, FL, USA).

4.11.7. Fluorescence microscopy Hoechst-stained.

The morphological changes were analysed by fluorescent microscopy using Hoechst-stained. For this, $5 \cdot 10^4$ B16-F10 cells, $11 \cdot 10^4$ HT29 cells, and $15 \cdot 10^4$ Hep G2 cells were plated in coverslip on 24-well plates. After 24 h the compounds were added and the cells were incubated for 72 h at their respective IC_{50} values. Then the cells were washed twice with PBS, treated in cold MeOH for 3 min, and afterwards, washed in PBS and incubated in 500 µL of Hoechst solution (50 ng/mL) in PBS for 15 min in darkness. The samples were visualized by fluorescent microscopy (DMRB, Leica Microsystems, Wetzlar, Germany) with a DAPI filter.

Acknowledgments

This work was financially supported by grants from the "Consejería de Innovación, Ciencia y Empresa" of the "Junta de Andalucía" (FQM–7372), and the "Plan Propio" of the University of Granada. We thank David Nesbitt for reviewing the English of the manuscript.

5. References

[1] R. Thimmappa, K. Geisler, T. Louveau, P. O'Maille, A. Osbourn, Triterpene Biosynthesis in Plants, Annu. Rev. Plant Biol. 65 (2014) 225–257.

[2] R.A. Hill, J.D. Connolly, Triterpenoids, Nat. Prod. Rep. 32 (2015) 273–327 (and references therein).

[3] A. Garcia-Granados, Process for the industrial recovery of oleanolic and maslinic acids contained in the olive milling byproducts, PCT. Int. Appl. WO 9804331, 1998.

[4] J.A. Jesus, J.H.G. Lago, M.D. Laurenti, E.S. Yamamoto, L.F.D. Passero,Antimicrobial activity of oleanolic and ursolic acids: an update, Evidence-based Complementary and alternative medicine, eCAM (2015) 620472.

[5] J.A.R. Salvador, A.S. Leal, D.P.S. Alho, B.M.F. Goncalves, A.S. Valdeira, V.I. S. Mendes, Y. Jing, Highlights of pentacyclic triterpenoids in the cancer settings, Stud. Nat. Prod. Chem. 41 (2014) 33–73.

[6] G. Lozano-Mena, M. Sanchez-Gonzalez, M.E. Juan, J.M. Planas, Maslinic acid, a natural phytoalexin-type triterpene from olives - a promising nutraceutical?, Molecules 19 (2014) 11538–11559.

[7] N.R. Parikh, A. Mandal, D. Bhatia, K.S. Siveen, G. Sethi, A. Bishayee, Oleanane triterpenoids in the prevention and therapy of breast cancer: current evidence and future perspectives, Phytochem. Rev. 13 (2014) 793–810.

[8] C. Sanchez-Quesada, A. Lopez-Biedma, F. Warleta, M. Campos, G. Beltran, J.J. Gaforio, Bioactive properties of the main triterpenes found in olives, virgin olive oil, and leaves of Oleaeuropaea, J. Agric. Food Chem. 61 (2013) 12173–12182.

[9] J.M. Castellano, A. Guinda, T. Delgado, M. Rada, J.A. Cayuela, Biochemical basis of the antidiabetic activity of oleanolic acid and related pentacyclic triterpenes, Diabetes 62 (2013) 1791–1799.

[10] K.I. Wolska, A.M. Grudniak, B. Fiecek, A. Kraczkiewicz-Dowjat, A. Kurek, Antibacterial activity of oleanolic and ursolic acids and their derivatives, Central Eur. J. Biol. 5 (2010) 543–553.

[11] V.R. Preedy, R.R. Watson, Olives and Olive Oil in Health and Disease Prevention, Elsevier, London, 2010.

[12] J.A.R. Salvador, Pentacyclic Triterpenes as Promising Agents in Cancer, Nova Science Publishers, New York, 2010.

[13] N. Sultana, A. Ata, Oleanolic acid and related derivatives as medicinally important compounds, J. Enzym. Inhib. Med. Chem. 23 (2008) 739–756.

[14] J. Wiemann, L. Heller, R.Csuk, Targeting cancer cells with oleanolic and ursolic acid derived hydroxamates, Bioorg. Med. Chem. Lett. 26 (2016) 907–909.

[15] D. Rodriguez-Hernandez, A.J. Demuner, L.C.A. Barbosa, R.Csuk, L. Heller, Hederagenin as a triterpene template for the development of new antitumor compounds, Eur. J. Med. Chem. 105, (2015) 57–62.

[16] L.F. Rocha e Silva, C.Ramalhete, K.L.Nogueira, S.Mulhovo, M.J.U. Ferreira, A.M.Pohlit, In vivo evaluation of isolated triterpenes and semi-synthetic derivatives as antimalarial agents, E. J. Med. Chem. 102 (2015) 398–402.

[17] L. Huang, H. Luo, Q. Li, D. Wang, J. Zhang, X.Hao, X. Yang, Pentacyclic triterpene derivatives possessing polyhydroxyl ring A inhibit Gram-positive bacteria growth by regulating metabolism and virulence genes expression, Eur. J. Med. Chem. 95 (2015) 64–75.

[18] J.Wiemann, L. Heller, V. Perl, R. Kluge, D.Ströhl, R.Csuk, Betulinic acid derived hydroxamates and betulin derived carbamates are interesting scaffolds for the synthesis of novel cytotoxic, Eur. J. Med. Chem. 106 (2015) 194–210.

[19] J.A.R. Salvador, A.S. Leal, D.P.S. Alho, B.M.F. Goncalves, A.S. Valdeira, V.I.S. Mendes, Y. Jing, Highlights of pentacyclic triterpenoids in the cancer settings, Stud. Nat. Prod. Chem. 41 (2014) 33–73.

[20] M.K. Shanmugam, X. Dai, A.P. Kumar, B.K.H. Tan, G. Sethi, A. Bishayee, Oleanolic acid and its synthetic derivatives for the prevention and therapy of cancer: Preclinical and clinical evidence, Cancer Lett. 346 (2014) 206–216.

[21] K.T. Liby, M.B. Sporn, Synthetic oleanane triterpenoids: multifunctional drugs with a broad range of applications for prevention and treatment of chronic disease, Pharmacol. Rev. 64 (2012) 972–1003.

[22] M.B. Sporn, K.T. Liby, M.M. Yore, L. Fu, J.M. Lopchuk, G.W. Gribble, New synthetic triterpenoids: Potent agents for prevention and treatment of tissue injury caused by inflammatory and oxidative stress, J. Nat. Prod. 74 (2011) 537–545.

[23] A. Parra, F. Rivas, S. Martin-Fonseca, A. Garcia-Granados, A. Martinez, Maslinic acid derivatives induce significant apoptosis in b16f10 murine melanoma cells, Eur. J. Med. Chem. 46 (2011) 5991–6001.

[24] A. Parra, F. Rivas, P.E. Lopez, A. Garcia-Granados, A. Martinez, F. Albericio, N. Marquez, E. Munoz, Solution- and solid-phase synthesis and anti-HIV activity of maslinic acid derivatives containing amino acids and peptides, Bioorg. Med. Chem. 17 (2009) 1139–1145.

[25] F.J. Reyes-Zurita, E.E. Rufino-Palomares, J.A. Lupiañez, M. Cascante, Maslinic acid, a natural triterpene from Oleaeuropaea L., induces apoptosis in HT29 human colon-cancer cells via the mitochondrial apoptotic pathway, Cancer let. 273 (2009) 44–54.

[26] F.J. Reyes-Zurita, E.E. Rufino-Palomares, P.P. Medina, E.L. Garcia-Salguero, J. Peragon, M. Cascante, J.A. Lupiañez, Antitumour activity on extrinsic apoptotic targets of the triterpenoid maslinic acid in p53-deficient Caco-2 adenocarcinoma cells, Biochimie 95 (2013) 2157–2167.

[27] J. Kim, M. Movassaghi, Biogenetically-inspired total synthesis of epidithiodiketopiperazines and related alkaloids, Acc. Chem. Res. 48 (2015) 1159–1171.

[28] S. Tadano, H. Ishikawa, Synthesis of tryptophan-based dimeric diketopiperazine alkaloids using bioinspired reactions, Synlett 25 (2014) 157–162.

[29] S.K. Chauthe, S.B. Bharate, G. Periyasamy, A. Khanna, K.K. Bhutani, P.D. Mishra, I.P. Singh, One pot synthesis and anticancer activity of dimeric phloroglucinols, Bioorg. Med. Chem. Lett. 22 (2012) 2251–2256.

[30] K.G. Cheng, C.H. Su, L.D. Yang, J. Liu, Z.F. Chen, Synthesis of oleanolic acid dimers linked at C-28 and evaluation of anti-tumor activity, Eur. J. Med. Chem. 89 (2015) 480–489.

[31] F. Yu, Y. Peng, Q. Wang, Y. Shi, L. Si, H. Wang, Y. Zheng, E. Lee, S. Xiao, M. Yu, Y. Li, C. Zhang, H. Tang, C. Wang, L. Zhang, D. Zhou, Development of bivalent oleanane-type triterpenes as potent HCV entry inhibitors, Eur. J. Med. Chem. 77 (2014) 258–268.

[32] F. Yu, Q. Wang, Z. Zhang, Y. Peng, Y. Qiu, Y. Shi, Y. Zheng, S. Xiao, H. Wang, X. Huang, L. Zhu, K. Chen, C. Zhao, C. Zhang, M. Yu, D. Sun, L. Zhang, D. Zhou, Development of Oleanane-Type Triterpenes as a New Class of HCV Entry Inhibitors, J. Med. Chem. 56 (2013) 4300–4319.

[33] K. Cheng, J. Liu, H. Sun, J. Xie, Synthesis of oleanolic acid dimers as inhibitors of glycogen phosphorylase, Chem. Biodivers. 7 (2010) 690–697.

[34] R. Rodriguez-Rodriguez, Oleanolic acid and related triterpenoids from olives on vascular function: molecular mechanisms and therapeutic perspectives, Curr. Med. Chem. 22 (2015) 1414–1425.

[35] H. Chen, Y. Gao, A. Wang, X. Zhou, Y. Zheng, J. Zhou, Evolution in medicinal chemistry of ursolic acid derivatives as anticancer agents, Eur. J. Med. Chem. 92 (2015) 648–655.

[36] Z. Du, Z. Liu, Z. Ning, Y. Liu, Z. Song, C. Wang, A. Lu, Prospects of boswellic acids as potential pharmaceutics, Planta Med. 81 (2015) 259–271.

[37] R. Csuk, Betulinic acid and its derivatives: a patent review (2008 - 2013), Expert Opin. Ther. Pat. 24 (2014) 913–923.

[38] C. Soica, C. Trandafirescu, C. Danciu, D. Muntean, C. Dehelean, G. Simu, New improved drug delivery technologies for pentacyclic triterpenes: A review, Protein Pept. Lett. 21 (2014) 1137–1145.

[39] H.L. Alvarado, G. Abrego, M.L. Garduno-Ramirez, B. Clares, A.C. Calpena, M.L. Garcia, Design and optimization of oleanolic/ursolic acid-loaded nanoplatforms for ocular anti-inflammatory applications, Nanomedicine 11 (2015) 521–530.

[40] D.K.W. Man, L. Casettari, M. Cespi, G. Bonacucina, G.F. Palmieri, S.C.W. Sze, G.P.H. Leung, J.K.W. Lam, P.C.L. Kwok, Oleanolic acid loaded PEGylated PLA and PLGA nanoparticles with enhanced cytotoxic activity against cancer cells, Mol. Pharmaceutics 12 (2015) 2112–2125.

[41] D. Biedermann, B. Eigenrova, M. Hajduch, J. Sarek, Synthesis and evaluation of biological activity of the quaternary ammonium salts of lupane-, oleanane-, and ursane-type acids, Synthesis (2010) 3839–3848.

[42] K. Xu, F. Chu, G. Li, X. Xu, P. Wang, J. Song, S. Zhou, H. Lei, Oleanolic acid synthetic oligoglycosides: a review on recent progress in biological activities, Pharmazie 69 (2014) 483–495.

[43] B. Bednarczyk-Cwynar, L. Zaprutko, Recent advances in synthesis and biological activity of triterpenic acylated oximes, Phytochem. Rev. 14 (2015) 203–231.

[44] A.I. Govdi, N.V. Sokolova, I.V. Sorokina, D.S. Baev, T.G. Tolstikova, V.I. Mamatyuk, D.S. Fadeev, S.F. Vasilevsky, V.G. Nenajdenko, Synthesis of new betulinic acid-peptide conjugates and in vivo and in silico studies of the influence of peptide moieties on the triterpenoid core activity, MedChemComm 6 (2015) 230–238.

[45] A. Parra, S. Martin-Fonseca, F. Rivas, F.J. Reyes-Zurita, M. Medina-O'Donnell, E.E. Rufino-Palomares, A. Martinez, A. Garcia-Granados, J.A. Lupiañez, F. Albericio, Solid-phase library synthesis of bi-

functional derivatives of oleanolic and maslinic acids and their cytotoxicity on three cancer cell lines, ACS Comb. Sci. 16 (2014) 428–447.

[46] E.O. Onyango, L. Fu, M. Cao, K.T. Liby, M.B. Sporn, G.W. Gribble, Synthesis and biological evaluation of amino acid methyl ester conjugates of 2-cyano-3,12-dioxooleana-1,9(11)-dien-28-oic acid against the production of nitric oxide (NO), Bioorg. Med. Chem. Lett. 24 (2014) 532–534.

[47] A. Parra, S. Martin-Fonseca, F. Rivas, F.J. Reyes-Zurita, M. Medina-O'Donnell, A. Martinez, A. Garcia-Granados, J.A. Lupiañez, F. Albericio, Semi-synthesis of acylated triterpenes from olive-oil industry wastes for the development of anticancer and anti-HIV agents, Eur. J. Med. Chem. 74 (2014) 278–301.

[48] A. Abuchowski, T. Van Es, N.C. Palczuk, F.F. Davis, Alteration of immunological properties of bovine serum albumin by covalent attachment of polyethylene glycol, J. Biol. Chem. 252 (1977) 3578–3581.

[49] A. Abuchowski, J.R. McCoy, N.C. Palczuk, T. Van Es, F.F. Davis, Effect of covalent attachment of polyethylene glycol on immunogenicity and circulating life of bovine liver catalase, J. Biol. Chem. 252 (1977) 3582–3586.

[50] A. Kolate, D. Baradia, S. Patil, I. Vhora, G. Kore, A. Misra, PEG - A versatile conjugating ligand for drugs and drug delivery systems, J. Controlled Release 192 (2014) 67–81.

[51] G. Pasut, F.M. Veronese, State of the art in PEGylation: The great versatility achieved after forty years of research, J. Controlled Release 161 (2012) 461–472.

[52] P. Bailon, C.Y. Won, PEG-modified biopharmaceuticals, Expert Opin. Drug Delivery 6 (2009) 1–16.

[53] F.M. Veronese, A. Mero, The impact of PEGylation on biological therapies, BioDrugs 22 (2008) 315–329.

[54] W. Li, P. Zhan, E. De Clercq, H. Lou, X. Liu, Current drug research on PEGylation with small molecular agents, Prog. Polym. Sci. 38 (2013) 421–444.

[55] I.W. Hamley, PEG-peptide conjugates, Biomacromolecules 15 (2014) 1543–1559.

[56] E.M. Pelegri-O'Day, E.W. Lin, H.D. Maynard, Therapeutic protein-polymer conjugates: Advancing beyond PEGylation, J. Am. Chem. Soc. 136 (2014) 14323–14332.

[57] E. Doganci, M. Gorur, C. Uyanik, F. Yilmaz, Synthesis of AB3-type miktoarm star polymers with steroid core via a combination of "Click" chemistry and ring opening polymerization techniques, J. Polym. Sci., Part A: Polym. Chem. 52 (2014) 3390–3399.

[58] F. Le Devedec, D. Fuentealba, S. Strandman, C. Bohne, X.X. Zhu, Aggregation behavior of pegylated bile acid derivatives, Langmuir 28 (2012) 13431–13440.

[59] P.M. Castillo, M. De la Mata, M.F. Casula, J.A. Sanchez-Alcazar, A.P. Zaderenko, PEGylated versus non-PEGylated magnetic nanoparticles as camptothecin delivery system, Beilstein J. Nanotechnol. 5 (2014) 1312–1319.

[60] M. Zacchigna, F. Cateni, S. Drioli, G. Procida, T. Altieri, PEG-ursolic acid conjugate: synthesis and in vitro release studies, Sci. Pharm. 82 (2014) 411–421.

[61] M.K. Pandey, S. Balwani, P.K. Sharma, V.S. Parmar, B. Ghosh, A.C. Watterson, Design, synthesis and anti-inflammatory evaluation of PEGylated 4-methyl and 4,8-dimethylcoumarins, Eur. J. Pharm. Sci. 39 (2010) 134–140.

[62] O.M. Feeney, H.D. Williams, C.W. Pouton, C.J.H. Porter, 'Stealth' lipid-based formulations: Poly(ethylene glycol)-mediated digestion inhibition improves oral bioavailability of a model poorly water soluble drug, J. Controlled Release 192 (2014) 219–227.

[63] M. Mumuni A., F.C. Kenechukwu, S.A. Chime, J.D. Ogbonna, A.T. Mora, Anti-inflammatory and pharmacokinetics evaluation of

PEGylated ibuprofen tablet formulation, Drug Delivery 21 (2014) 315–319.

[64] G. Mattheolabakis, C.C. Wong, Y. Sun, C.A. Amella, R. Richards, P.P. Constantinides, B. Rigas, Pegylation improves the pharmacokinetics and bioavailability of small-molecule drugs hydrolyzable by esterases: A study of phospho-ibuprofens, J. Pharmacol. Exp. Ther. 351 (2014) 61–66.

[65] F. Nicks, A. Richel, G. Richard, P. Laurent, B. Wathelet, J.P. Wathelet, M. Paquot, Green synthesis and antioxidant activity of new PEGylated ferulic acids, Tet. Lett. 53 (2012) 2402–2405.

[66] C. Lu, B.M. Kim, K.Y. Chai, Design, synthesis and evaluation of PEGylated lipoic acid derivatives with functionality as potent anti-melanogenic agents, Eur. J. Med. Chem. 46 (2011) 5184–5188.

[67] A. Garcia-Granados, A. Martinez, J.N. Moliz, A. Parra, F. Rivas, 3β-hydroxyolean-12-en-28-oic acid (oleanolic acid), Molecules 3 (1998) M87.

[68] A. Garcia-Granados, A. Martinez, J.N. Moliz, A. Parra, F. Rivas, 2a,3β-dihydroxyolean-12-en-28-oic acid (maslinic acid), Molecules 3 (1998) M88.

[69] R. Weis, W. Seebacher, Complete assignment of 1H and 13C NMR spectra of new pentacyclic triterpene acid benzyl esters, Magn. Reson. Chem. 40 (2002) 455–457.

[70] A. Garcia-Granados, J. Dueñas, J.N. Moliz, A. Parra, F.L. Perez, J.A. Dobado, J. Molina, Semi-synthesis of triterpene A-ring derivatives from oleanolic and maslinic acids. Theoretical and experimental ^{13}C chemical shifts, J. Chem. Res. (M) (2000) 326–339.

[71] A. Garcia-Granados, J. Dueñas, E. Melguizo, J.N. Moliz, A. Parra, F.L. Perez, J.A. Dobado, J. Molina, Semi-synthesis of triterpene A-ring derivatives from oleanolic and maslinic acids. Part II. Theoretical and experimental ^{13}C chemical shifts, J. Chem. Res. (M) (2000) 653–670.

[72] C.A.G.N. Montalbetti, V.Falque, Amide bond formation and peptide coupling, Tetrahedron 61 (2005)10827–10852.

[73] S. Balalaie, M. Mahdidoust, R. Eshaghi-Najafabadi, 2-(1H-Benzotriazole-1-yl)-1,1,3,3-tetramethyluronium tetrafluoroborate as an efficient coupling reagent for the amidation and phenylhydrazation of carboxylicacids at room temperature, J. Iran. Chem. Soc. 4 (2007) 364–369.

[74] A. Martinez, F. Rivas, A. Perojil, A. Parra, A. Garcia-Granados, A. Fernandez-Vivas, Biotransformation of oleanolic and maslinic acids by Rhizomucor miehei. Phytochem. 94 (2013) 229–237.

6. Supporting Information

Table S1.^{13}C NMR spectroscopic data (δ_C) for compounds **1**–**4**.

No. (type)	**1**	**2**	**3**	**4**
1 (CH_2)	38.3	38.1	43.9	44.0
2 (CH_2)	23.8	23.6		
2 (CH)			70.6	70.6
3 (CH)	82.1	81.6	80.9	80.9
4 (C)	38.0	37.9	38.6	39.6
5 (CH)	55.5	55.3	54.9	55.0
6 (CH_2)	18.4	18.2	18.3	18.2
7 (CH_2)	32.8	32.7	32.5	32.5
8 (C)	39.5	39.3	39.4	39.4
9 (CH)	47.8	47.5	47.6	47.5
10 (C)	37.2	36.9	39.4	38.2
11 (CH)	23.6	23.4	23.6	23.4
12 (CH)	122.8	122.4	122.2	122.0
13 (C)	143.8	143.7	143.8	143.8
14 (C)	41.8	41.7	41.7	41.7
15 (CH_2)	27.9	27.6	27.7	27.6
16 (CH_2)	23.1	23.1	22.9	23.0
17 (C)	46.8	46.7	46.6	46.7
18 (CH)	41.2	41.4	41.0	41.4
19 (CH_2)	46.0	45.9	45.9	45.9
20 (C)	30.9	30.7	30.8	30.7
21 (CH_2)	34.0	33.9	33.9	33.9
22 (CH_2)	32.7	32.3	32.5	32.4
23 (CH_3)	28.3	28.1	28.6	28.5
24 (CH_3)	16.9	16.7	16.5	16.8
25 (CH_3)	15.6	15.4	17.2	16.4
26 (CH_3)	17.3	16.9	17.7	17.7
27 (CH_3)	26.1	25.9	26.0	25.9
28 (COO)	184.6	177.4	183.9	177.4
29 (CH_3)	33.3	33.1	33.2	33.1
30 (CH_3)	23.8	23.7	23.7	23.7
Bn (C)		136.4		136.4
Bn (CH)		128.4[a]		128.4[a]
Bn (CH)		128.0[a]		128.0[a]
Bn (CH)		127.9		127.9
Bn (CH_2)		65.9		65.9
PEG (COO)	170.8	170.3	170.3	170.3
PEG (COO)			170.2	170.1
PEG (CH_2)	72.0	72.0	72.0[a]	72.0[a]
PEG (CH_2)	71.0	70.9	71.1[a]	71.0[a]
PEG (CH_2)	70.7	70.7	70.7[a]	70.9[a]
PEG (CH_2)	70.6	70.6	70.6[a]	70.6[a]
PEG (CH_2)	68.9	68.8	68.5[a]	68.5[a]
PEG (CH_3)	59.1	59.0	59.1[a]	59.1[a]

[a] two carbon atoms in this chemical shift.

Table S2. ^{13}C NMR spectroscopic data (δ_C) for compounds **5**–**12**.

No. (type)	**5**	**6**	**7**	**8**	**9**	**10**	**11**	**12**
1 (CH_2)	38.6	46.8	38.1	44.0	38.6	46.9	38.3	44.0
2 (CH_2)	27.3		23.5		27.3		23.5	
2 (CH)		68.9		70.4		68.9		70.1
3 (CH)	79.1	83.9	80.8	80.7	79.1	83.7	81.0	80.7
4 (C)	37.1	38.3	38.1	39.5	37.1	38.4	37.8	39.5
5 (CH)	55.3	55.3	55.8	55.0	55.2	55.3	55.4	54.9
6 (CH_2)	18.4	18.4	18.1	18.3	18.4	18.4	18.4	18.3
7 (CH_2)	32.9	32.8	32.6	33.0	32.8	32.8	32.9	32.9
8 (C)	39.5	39.6	39.4	39.6	39.5	39.6	39.6	39.6
9 (CH)	47.7	47.7	47.4	47.6	47.7	47.7	47.7	47.6
10 (C)	38.9	39.3	36.8	38.2	38.9	39.3	37.1	38.2
11 (CH)	23.8	23.7	23.6	23.7	23.7	23.7	23.7	23.7
12 (CH)	122.9	122.6	122.8	122.3	122.8	122.6	122.7	122.3
13 (C)	144.9	144.9	144.5	145.0	144.9	145.0	145.0	145.0
14 (C)	42.2	42.1	42.0	42.2	42.1	42.2	42.2	42.2
15 (CH_2)	27.4	27.4	27.2	27.4	27.5	27.4	27.5	27.4
16 (CH_2)	23.7	23.7	23.5	23.7	23.7	23.8	23.5	23.7
17 (C)	46.3	46.3	46.2	46.3	46.3	46.3	46.3	46.3
18 (CH)	42.2	42.2	42.0	42.2	42.2	42.3	42.3	42.2
19 (CH_2)	46.9	46.5	46.7	46.8	46.9	46.6	46.9	46.8
20 (C)	30.9	30.8	30.7	30.9	30.9	30.9	30.9	30.9
21 (CH_2)	34.3	34.2	34.1	34.3	34.3	34.3	34.3	34.3
22 (CH_2)	32.5	32.4	32.3	32.4	32.5	32.5	32.5	32.4
23 (CH_3)	28.2	28.7	28.0	28.6	28.2	28.8	28.2	28.5
24 (CH_3)	15.5	16.6	15.4	16.6	15.5	16.8	15.6	16.6
25 (CH_3)	15.7	16.9	16.6	17.1	15.7	17.0	16.8	17.1
26 (CH_3)	17.1	17.1	16.9	17.8	17.1	17.2	17.1	17.8
27 (CH_3)	25.9	25.9	27.7	26.0	25.9	26.0	25.9	25.9
28 (COO)	178.5	178.3	178.7	178.0	178.5	178.2	178.1	178.0
29 (CH_3)	33.2	33.1	33.0	33.2	33.2	33.2	33.2	33.2
30 (CH_3)	23.8	23.8	23.6	23.8	23.8	23.8	23.8	23.8
Ac (COO)			171.0	171.0			171.1	171.0
Ac (COO)				170.9				170.7
Ac (CH_3)			21.3	21.3			21.4	21.3
Ac (CH_3)				21.1				21.1
PEG (CH_2)	70.5[a]	70.7	70.2	70.7[a]	70.7[a]	70.7[a]	70.7[a]	70.7[a]
PEG (CH_2)	70.1	70.6[a]	70.1	70.5	70.4[a]	70.5[a]	70.4[a]	70.4[a]
PEG (CH_2)	70.2	70.4	69.9	70.4	70.1[a]	70.1[a]	70.1[a]	70.1[a]
PEG (CH_2)	69.7	70.3	69.8[a]	70.1				
PEG (CH_2)	69.7	70.0	69.1	70.0				
PEG (CH_2)	37.3[a]	37.7[a]	37.7[a]	37.7[a]	37.7[a]	37.8[a]	37.7[a]	37.7[a]
PEG (CH_2)	29.8	29.8	29.7	29.8	29.4[a]	29.4[a]	29.5[a]	29.5[a]
PEG (CH_2)	29.5	29.3	29.6	29.4				
Boc (COO)	156.3	156.2	156.4	156.2				
Boc (C)	79.1	79.0	79.2	79.1				
Boc (CH_3)	28.6[b]	28.6[b]	28.4[b]	28.6[b]				

[a] two carbon atoms in this chemical shift.

[b] three carbon atoms in this chemical shift.

Table S3.[13]C NMR spectroscopic data (δ_C) for compounds**13**–**20**.

No. (type)	**13**	**14**	**15**	**16**	**17**	**18**	**19**	**20**
1 (CH_2)	38.7	46.6	38.3	44.1	38.7	38.7	38.3	37.7
2 (CH_2)	27.3		23.7		27.9		23.6	
2 (CH)		69.0		70.1		69.4		70.0
3 (CH)	79.0	84.1	81.0	80.8	79.7	84.4	80.9	80.6
4 (C)	37.1	38.4	37.1	38.3	38.2	39.3	37.0	39.4
5 (CH)	55.3	55.5	55.5	55.1	56.7	56.6	55.3	54.8
6 (CH_2)	18.4	18.5	18.3	18.4	19.5	19.6	18.3	18.3
7 (CH_2)	32.9	32.9	32.9	32.8	34.4	34.4	32.8	34.2
8 (C)	39.6	39.7	39.6	39.7	40.7	40.8	39.5	39.5
9 (CH)	47.7	47.7	47.6	47.6	49.0	49.0	47.6	47.5
10 (C)	38.9	39.3	37.8	39.5	38.5	40.5	37.8	38.2
11 (CH)	23.6	23.7	23.6	23.7	24.6	24.7	23.7	23.7
12 (CH)	124.0	123.9	124.0	123.6	124.0	123.8	122.6	122.2
13 (C)	142.2	142.3	142.5	142.4	145.3	145.4	144.9	144.9
14 (C)	42.0	42.1	42.0	42.1	42.9	43.0	42.1	42.1
15 (CH_2)	28.2	28.2	28.2	28.1	28.7	28.5	27.4	27.3
16 (CH_2)	23.2	23.3	23.3	23.3	24.0	24.0	23.6	23.7
17 (C)	47.7	47.8	47.8	47.7	47.5	47.5	46.3	46.2
18 (CH)	41.7	41.7	41.7	41.7	42.7	42.7	42.2	42.1
19 (CH_2)	45.6	45.6	45.6	45.6	47.7	47.7	46.8	46.7
20 (C)	30.7	30.8	30.8	30.8	31.6	31.6	30.9	30.8
21 (CH_2)	33.8	33.8	33.8	33.8	35.1	35.1	34.3	32.8
22 (CH_2)	32.5	32.6	32.6	32.6	33.9	33.8	32.5	32.3
23 (CH_3)	28.2	28.8	28.2	28.6	28.7	29.3	28.1	29.4
24 (CH_3)	15.5	16.8	15.6	16.6	16.0	17.2	15.5	16.5
25 (CH_3)	15.7	16.9	16.8	17.4	16.4	17.5	16.8	17.0
26 (CH_3)	17.4	17.5	17.4	17.8	18.0	18.0	17.1	17.7
27 (CH_3)	25.8	25.9	25.8	25.9	26.5	26.5	25.9	25.8
28 (COO)	173.7	173.7	173.8	173.7	180.2	180.1	178.1	177.9
29 (CH_3)	33.0	33.1	33.0	33.1	33.6	33.6	33.1	33.1
30 (CH_3)	23.6	23.7	23.7	23.7	24.1	24.1	23.8	23.7
Ac (COO)			171.1	171.0			171.1	170.9
Ac (COO)				170.6				170.6
Ac (CH_3)			21.5	21.3			21.4	21.2
Ac (CH_3)				21.1				21.0
TBTU (C)	143.6	143.7	143.7	143.7				
TBTU (C)	128.9	128.9	128.9	128.9				
TBTU (CH)	128.6	128.6	128.7	128.6				
TBTU (CH)	124.7	124.8	124.7	124.8				
TBTU (CH)	120.6	120.7	120.7	120.7				
TBTU (CH)	108.3	108.3	108.3	108.3				
PEG (CH_2)					71.5[a]	71.6[a]	70.7[a]	70.6[a]
PEG (CH_2)					71.3[a]	71.4[a]	70.4[a]	70.3[a]
PEG (CH_2)					70.6[a]	70.7[a]	70.0[a]	70.0[a]
PEG (CH_2)					39.8[a]	38.7[a]	37.7[a]	37.7[a]
PEG (CH_2)					30.3[a]	30.4[a]	29.4[a]	29.4[a]

[a] two carbon atoms in this chemical shift.

Table S4. Flow-cytometry analysis of Annexin V–FITC staining and PI accumulation after exposure of B16-F10, HT29, and Hep G2 cells to PEGylated derivatives **1**, **3**, **4**, **9**, and **10**.

Cell Line	Compd	Population (%)				
		Normal	Early apoptosis	Late apoptosis	Total apoptosis	Necrosis
B16-F10	Control	97.55 ± 0.50	0.75 ± 0.07	0.75 ± 0.21	1.50 ± 0.28	0.75 ± 0.07
	1	52.75 ± 2.48	6.80 ± 0.14	39.60 ± 2.40	46.40 ± 2.26	0.35 ± 0.50
	3	11.10 ± 0.99	32.80 ± 0.42	56.05 ± 1.49	88.85 ± 1.06	0.00 ± 0.00
	4	2.70 ± 1.56	29.60 ± 0.14	67.25 ± 2.33	96.85 ± 2.19	0.80 ± 1.13
	9	27.55 ± 0.21	59.65 ± 2.48	12.85 ± 2.19	72.50 ± 0.28	0.00 ± 0.00
	10	0.90 ± 0.14	60.25 ± 1.49	38.65 ± 1.34	98.90 ± 0.14	0.20 ± 0.01
HT29	Control	96.65 ± 0.78	1.65 ± 0.07	0.65 ± 0.35	2.30± 0.42	1.05 ± 0.35
	1	51.85 ± 1.49	34.70 ± 0.57	13.45 ± 0.92	48.15 ± 1.49	0.00 ± 0.00
	3	59.75 ± 0.50	40.10 ± 0.57	0.15 ± 0.07	40.25 ± 0.50	0.00 ± 0.00
	4	48.95 ± 0.07	43.95 ± 1.91	6.70 ± 2.12	50.65 ± 0.21	0.15 ± 0.21
	9	72.45 ± 0.64	19.70 ± 0.71	7.45 ± 1.34	27.15 ± 0.64	0.25 ± 0.21
	10	61.00 ± 0.57	31.25 ± 1.63	7.60 ± 1.13	38.85 ± 0.50	0.20 ± 0.14
Hep G2	Control	99.55 ± 0.07	0.30 ± 0.01	0.00 ± 0.00	0.30 ± 0.01	0.10 ± 0.01
	1	43.50 ± 4.67	38.65 ± 0.78	17.70 ± 5.09	56.35 ± 4.31	0.20 ± 0.28
	3	55.70 ± 5.52	14.75 ± 4.74	29.10 ± 1.27	43.85 ± 6.01	0.40 ± 0.42
	4	37.00 ± 1.27	18.65 ± 1.06	44.35 ± 0.21	63.00 ± 1.27	0.00 ± 0.00
	9	41.35 ± 1.77	35.90 ± 0.42	22.45 ± 1.34	58.35 ± 1.77	0.35 ± 0.07
	10	19.75 ± 0.78	46.75 ± 0.21	33.05 ± 0.92	79.80 ± 0.71	0.40 ± 0.01

Cell lines were treated at concentrations equal to its IC_{50} values. Values are expressed as means ± S.E.M. of three experiments in duplicate. Normal cells were annexin V^- PI^-, early apoptotic cells were annexin V^+ PI^-, whereas late apoptotic cells were annexin V^+ PI^+, total apoptosis (early apoptosis plus late apoptosis) were annexin V^+, and necrotic cells were annexin V^- PI^+.

Table S5. Percentages of cell population, in each phase of the cell cycle, in B16-F10, HT29, and Hep G2 cell lines incubated with the selected PEGylated OA or MA derivatives for 72 h.

Cell Line	Compd	Population (%)		
		Phase G0/G1	Phase S	Phase G2/M
B16-F10	Control	50.69 ± 0.61	48.31 ± 0.74	1.01 ± 0.13
	1	74.28 ± 1.82	25.44 ± 1.42	0.28 ± 0.39
	3	87.93 ± 2.59	12.07 ± 2.59	0.00 ± 0.00
	4	83.03 ± 0.04	13.13 ± 2.47	3.85 ± 3.44
	9	63.89 ± 3.36	31.33 ± 1.91	4.78 ± 2.27
	10	66.66 ± 0.84	22.44 ± 1.23	10.91 ± 2.07
HT29	Control	55.18 ± 0.22	48.31 ± 1.49	6.23 ± 1.70
	1	63.47 ± 2.43	49.98 ± 2.43	0.00 ± 0.00
	3	94.28 ± 0.83	4.97 ± 1.90	0.76 ± 1.07
	4	91.87± 2.72	6.63 ± 0.59	1.51 ± 2.14
	9	87.11 ± 3.22	4.78 ± 0.40	8.12 ± 3.62
	10	79.78 ± 2.40	7.12 ± 3.75	13.10 ± 1.34
Hep G2	Control	39.41 ± 1.56	54.71 ± 2.37	8.47 ± 2.55
	1	38.88 ± 0.23	45.44 ± 0.64	14.18 ± 1.70
	3	58.19 ± 0.87	26.70 ± 1.83	15.45 ± 2.70
	4	65.20 ± 3.73	19.76 ± 1.45	15.04 ± 3.17
	9	52.70 ± 2.99	46.97 ± 2.47	0.34 ± 0.48
	10	40.22 ± 0.47	50.45 ± 0.70	9.34 ± 1.17

Cell-cycle analysis was conducted after PI staining. Values represent means ± S.E.M. of at least two independent experiments performed in triplicate.

Table S6: Flow-cytometry analysis of rhodamine 123 and PI staining after exposure of B16-F10, HT29, and Hep G2 cells to the selected PEGylated OA and MA derivatives.

	B16-F10 (%)		HT29 (%)		Hep G2 (%)	
Compd	$Rh123^+$	$Rh123^-$	$Rh123^+$	$Rh123^-$	$Rh123^+$	$Rh123^-$
Control	95.60 ± 0.57	4.45 ± 0.64	94.25 ± 0.35	5.80 ± 0.42	88.30 ± 8.87	11.70 ± 6.80
1	79.45 ± 3.89	20.65 ± 3.75	88.65 ± 0.35	11.35 ± 0.21	13.95 ± 5.73	86.05 ± 5.73
3	75.05 ± 2.47	24.90 ± 1.13	94.30 ± 0.85	5.70 ± 0.85	56.70 ± 1.56	43.20 ± 1.56
4	81.35 ± 2.47	18.60 ± 2.55	3.15 ± 0.78	96.90 ± 0.71	45.70 ± 3.40	54.25 ± 3.46
9	20.75± 19.73	79.30± 19.80	23.75 ± 1.63	76.30 ± 1.56	80.45 ± 3.60	19.60 ± 3.68
10	48.05 ± 4.45	51.95 ± 4.45	63.10 ± 4.24	36.95 ± 4.17	59.20 ± 10.0	40.85 ± 9.97

Flow-cytometry analyses were performed for 72 h. Cell lines were treated at concentrations equal to its IC_{50} values. Rh123 positive cells were rhodamine 123^+ with PI^+ or PI^-. Rh123 negative cells were rhodamine 123^- with PI^- or PI^+. Values are expressed as means ± S.E.M. of at least two experiments in duplicate.

PUBLICACIÓN 2

The oleanolic acid derivative, 3-O-succinyl-28 Obenzyl oleanolate, induces apoptosis in B16–F10 melanoma cells via the mitochondrial apoptotic pathway

(JCR: Multidisciplinary Chemistry: Ind.Imp. 3.289, nº49, Q2)

RSC Advances

PAPER

View Article Online
View Journal | View Issue

Cite this: *RSC Adv.*, 2016, **6**, 93590

The oleanolic acid derivative, 3-*O*-succinyl-28-*O*-benzyl oleanolate, induces apoptosis in B16–F10 melanoma cells *via* the mitochondrial apoptotic pathway

Fernando J. Reyes-Zurita,*[a] Marta Medina-O'Donnell,[b] Rosa M. Ferrer-Martin,[c] Eva E. Rufino-Palomares,[a] Samuel Martin-Fonseca,[b] Francisco Rivas,[b] Antonio Martínez,[b] Andrés García-Granados,[b] Amalia Pérez-Jiménez,[a] Leticia García-Salguero,[a] Juan Peragón,[d] Khalida Mokhtari,[ae] Pedro P. Medina,[af] Andrés Parra*[b] and José A. Lupiáñez*[a]

Oleanolic acid (**1**) is a pentacyclic triterpene present in olive pomace, which is known to induce apoptosis and to have anti-tumor properties; however, high concentrations of this product are necessary to produce cytotoxic effects. The 3-*O*-succinyl-28-*O*-benzyl oleanolate derivative (**4**) presents greater cytotoxicity and apoptosis effects than its natural precursor, oleanolic acid, or its benzyl derivative (**2**). This study examines the response of B16–F10 melanoma cells to treatment with compound **4**, in comparison to **1** and **3**. Our studies show that treatment with **4** results in a significant inhibition of cell proliferation in a dose-dependent manner and causes apoptotic cell death. At concentrations inhibiting cell growth by 50% and 80%, compound **4** induces strong G_0/G_1 cell-cycle arrest, around 72–95% apoptosis, and mitochondrial disturbances confirmed by FACS analysis, which probably involve the activation of the intrinsic apoptotic route. Morphological changes including cell shrinkage, chromatin condensation, and loss of nuclear architecture were also observed. In this report, we demonstrated for the first time that in melanoma cancer cells, compound **4** exerts a significant anti-proliferation effect by inducing the apoptotic process with mitochondrial depolarization. These findings support the role of compound **4** as a new, potential therapeutic tool against aberrant cell proliferation in melanoma.

Received 25th July 2016
Accepted 17th September 2016

DOI: 10.1039/c6ra18879f

www.rsc.org/advances

1. Introduction

Triterpenoid compounds are present in a wide range of plants that are used in traditional medicine, and are known to have anti-tumor properties.[1–8] They are also involved in metabolic regulation,[5,9–14] metabolic syndrome treatment[15] and growth processes.[16–22] All these compounds belong to a broad family of compounds obtained by cyclic reactions of 2,3-oxidosqualene.[23] Triterpenoids in plants, are secondary metabolites that are not essential for growth or development, but might contribute to their survival (*e.g.* phytoalexin), and are involved in the protection of plants against pathogens or pests.[24] Currently, about one-fourth of all medications contain an active ingredient derived from plants. The most important triterpenoid structures are oleanane, ursane, lupane and dammarane.[25]

Oleanolic acid (**1**), an oleanane-type triterpenoid, is a natural compound that belongs to the pentacyclic triterpene family and is widely distributed in the plant kingdom. Oleanolic compounds for the current study were isolated in high amounts from the olive-pressing residues. Oleanolic acid (**1**) possesses many biological properties, including anti-inflammatory, anti-HIV and cytotoxic activities.[26] This compound (**1**) has also been described as an inhibitor of skin tumor progression.[26] This natural compound (**1**) provides a very useful scaffold for obtaining derivatives with improved biological properties.[27–29] Our research group has performed a series of systematic chemical modifications of **1** to improve its biological activities.[30,31]

Most pentacyclic triterpenes are not sufficiently water soluble, which hampers biological tests, and results in their low

[a]*Department of Biochemistry and Molecular Biology I, Faculty of Science, University of Granada, 18071 Granada, Spain. E-mail: ferjes@ugr.es; jlcara@ugr.es; Fax: +34 958 249945; Tel: +34 958 243252; +34 958 243089*
[b]*Department of Organic Chemistry, Faculty of Science, University of Granada, 18071 Granada, Spain. E-mail: aparra@ugr.es; Fax: +34 958 240480; Tel: +34 958 240480*
[c]*Department of Cellular Biology, Faculty of Science, University of Granada, 18071 Granada, Spain*
[d]*Department of Experimental Biology, Biochemistry and Molecular Biology Section, University of Jaen, 23071 Jaen, Spain*
[e]*Department of Biology, Faculty of Sciences, Mohammed I University, BP 717 60000 Oujda, Morocco*
[f]*Centre of Genomic and Oncologic Investigation (GENyO), Pfizer Pharmaceutical-University of Granada-Government of Andalusia, Technological Park of Health Sciences, 18016 Granada, Spain*

Abstract

Oleanolic acid (**1**) pentacyclic triterpene present in olive pomace, which is known to induce apoptosis and to have anti-tumor properties; however, high concentrations of this product are necessary to produce cytotoxic effects. The 3-*O*-succinyl-28-*O*-benzyl oleanolate derivative (**4**) presents greater cytotoxicity and apoptosis effects than its natural precursor, oleanolic acid, or its benzyl derivative (**2**). This study examines the response of B16-F10 melanoma cells to treatment with compound **4**, in comparison to **1** and **3**. Our studies show that treatment with **4** results in a significant inhibition of cell proliferation in a dose-dependent manner and causes apoptotic cell death. At concentrations inhibiting cell growth by 50% and 80%, compound **4** induce strong G_0/G_1 cell-cycle arrest, around 72-95% of apoptosis, and mitochondrial disturbances confirmed by FACS analysis, which probably involve the activation of the intrinsic apoptotic route. Morphological changes including cell shrinkage, chromatin condensation, and loss of nuclear architecture were also observed. In this report, we demonstrated for the first time that in melanoma cancer cells, compound **4** exerts a significant anti-proliferation effect by inducing apoptotic process with mitochondrial depolarization. These findings support the role of compound **4** as a new, potential therapeutic tool against aberrant cell proliferation in melanoma.

***Key words**: 3-O-succinyl-28-O-benzyl oleanolate, Triterpene derivatives, Cytotoxicity activity, Cell cycle, Apoptosis, Anti-cancer, Green chemistry.*

1. Introduction

Triterpenoid compounds are present in a wide range of plants that are used in traditional medicine, and known to have anti-tumor properties.[1-8] They are also involved in metabolic regulation[5, 9-14], metabolic syndrome treatment[15] and growth processes.[16-22] All these compounds belong to a broad family of compounds obtained by cyclic reactions of 2,3-oxidesqualene.[23] Triterpenoids in plants, are secondary metabolites that are not essential for growth or development, but might contribute to their survival (e.g. phytoalexin), and are involved in the protection of plants against pathogens or pests.[24] Currently, about one-fourth of all medications contain an active ingredient derived from plants. The most important triterpenoid structures are oleanane, ursane, lupane and dammarane.[25]

Oleanolic acid (**1**), an oleanane-type triterpenoid, is a natural compound that belongs to the pentacyclic triterpene family and is widely distributed in the plant kingdom. Oleanolic compounds for the current study were isolated in high amounts from the olive-pressing residues. Oleanolic acid (**1**) possesses many biological properties, including anti-inflammatory, anti-HIV and cytotoxic activities.[26] This compound (**1**) has also been described as an inhibitor of skin tumor progression.[26] This natural compound (**1**) provides a very useful scaffold for obtaining derivatives with improved biological properties.[27-29] Our research group has performed a series of systematic chemical modifications of **1** to improve its biological activities.[30,31]

Most pentacyclic triterpenes are not sufficiently water soluble, which hampers biological tests, and results in their low bioavailability.[32-34] One option to improve the solubility of these triterpene compounds is to semi-synthesize derivatives by attaching diverse functional groups to the hydroxyl groups of the A ring and/or to the carboxyl group at C-28. Our group has demonstrated that acyl oleanolic acid derivatives with a polar dicarboxylic fragment as the acyl group on C-3 present major cytotoxic and apoptotic effects, compared to their natural precursor (**1**).[30,31,35] Chemical modifications of natural triterpenoid compounds have resulted in products

that have improved biological activities, compared to their natural precursors. Our group has shown that several triterpene derivatives, with mono- or di-peptidyl groups at C-28, and acyl groups at C-2 or C-2/C-3 of the triterpene skeleton, exhibit cytotoxic properties on B16−F10, HT29, or Hep G2 cancer cell lines.[30]

Apoptosis, or programmed cell death, is defined as an active physiological process of cell self-destruction. Agents that suppress the proliferation of malignant cells by inducing apoptosis may be useful in both the chemoprevention and chemotherapy of cancer. Two major pathways have been described during apoptotic activation: the mitochondrial or intrinsic pathway, and the death-receptor or extrinsic pathway.

The intrinsic pathway involves the mitochondrial disruption and a decrease in the mitochondrial membrane potential.[35,36] This apoptotic route involves the mitochondria-dependent activation of initiator caspases, which in turn activate downstream executive caspases, such as caspase-3. Our research group has demonstrated that the oleanane-type triterpenoid, maslinic acid selectively induces anti-tumor and pro-apoptotic effects in HT29 colon cancer cells.[1] The activation of the intrinsic apoptotic pathway is mediated by mitochondrial Bax activation and Bcl-2 inhibition, resulting in the mitochondrial membrane disruption, increase of ROS, activation of caspase-9, caspase-3 and caspase-7.[2,3] Maslinic acid induced differentiation in this cell line before the activation of the apoptotic process.[1, 2]

The extrinsic death-receptor pathway is triggered by the death ligand through the formation of the death-inducing signaling complex that results in caspase-8 and caspase-10 activation, which initiates the downstream apoptotic signaling.[32, 37, 38] Maslinic acid also produces the direct activation of apoptosis through an extrinsic apoptotic pathway in Caco-2 colon cancer cells, involving caspase-8 activation, bid cleavage, caspase-9 and caspase-3 activation, with a lower cell-cycle arrest;[5] caspase-9 and ROS generation were not observed.[8]

The evaluation of mitochondrial potential at the cytotoxic and apoptotic concentrations can help to determine the possible molecular mechanism involved in the apoptotic response.[31] We describe here the anti-cancer effects of three oleanolic acid derivatives. In order to increase the apoptotic activity of these products, compound **1** was benzylated to obtain 28-benzyl derivative (**2**) and the 3-succinyl-28-benzyl derivative (**4**) (Fig.1).

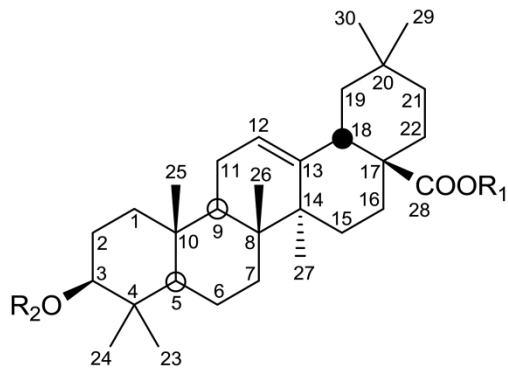

1: $R_1 = R_2 = H$
2: $R_1 = Bn$, $R_2 = H$
3: $R_1 = H$, $R_2 = Succinyl$
4: $R_1 = Bn$, $R_2 = Succinyl$

Figure 1. Structure of the triterpene skeleton of oleanolic acid (**1**), and its derivatives: 28-*O*-benzyl oleanolate (**2**), 3-*O*-succinyl oleanolic acid (**3**), and 3-*O*-succinyl-28-*O*-benzyl oleanolic acid (**4**).

Following treatment with **4**, a potent apoptotic and anti-proliferation effect in melanoma B16-F10 cancer cells, including cell-cycle arrest in the G_0 phase with the disappearance of S phase, was observed. The compound **4** also produced over 90% of apoptosis induction through mitochondrial disturbances, with clear morphological changes in the nucleus and the cytoplasm. On the other hand, compound **2** produced 40% of apoptosis induction, similar to the natural triterpene, without affecting the mitochondrial membrane potential.

Agents that suppress the proliferation of malignant cells by inducing apoptosis could be useful in cancer therapy. Consequently, compound **4** may provide a useful new therapeutic strategy for skin melanoma.

2. Experimental section

2.1. Apparatus and Materials

The purity of compounds was determined by a Waters Acquity UPLC system (ultra-performance liquid chromatography) coupled with a Waters Synapt G2 HRMS spectrometer (high-resolution mass spectra) with ESI (electrospray ionization). The purities of all compounds were confirmed to be ≥ 95%. Measurements of NMR spectra (300.13 MHz ^{1}H and 75.47 MHz ^{13}C) were made in $CDCl_3$ (which also provided the lock signal) using a VARIAN Inova unity (300 MHz ^{1}H NMR). The ^{13}C chemical shifts were assigned with the aid of distortionless enhancement by polarization transfer (DEPT) using a flip angle of 135°. IR spectra were recorded on a MATTSON SATELLITE FTIR spectrometer. Optical rotations were measured on a Perkin-Elmer 241 polarimeter at 25 °C. Melting points (mp) were determined using a Kofler (Reichter) apparatus and were uncorrected.

All reaction solvents and chromatography solvents were distilled prior to use. Commercially available reagents were used without further purification. Merck silica-gel 60 aluminum sheets (ref. 1.16835) were used for TLC, and spots were rendered visible by spraying with H_2SO_4–AcOH, followed by heating to 120 °C, and were also visualized under UV at 254 nm. Merck silica-gel 60 (0.040–0.063 mm, ref. 1.09385) was used for flash chromatography. CH_2Cl_2 (Fisher, ref. D/1852/17), $CHCl_3$ (Fisher, ref. C/4960/17), or *n*-hexane (Merck, ref. 1.04374), with increasing amounts of acetone (Fisher, ref. A/0600/17), MeOH (Fisher, ref. M/4000/17), or EtOAc (Fisher, ref. E/0900/17), were used as eluents (all the solvents had an analytical reagent-grade purity).

The plant Material, a specimen of the plant of *Olea europaea* (order Lamiales, family Oleaceae) was collected in Almegíjar, Granada, Spain in May 2001. This plant was identified by Laura Baena from the herbarium of the University of Granada. A voucher specimen (53489-1-1) was deposited at the University of Granada Herbarium, Granada, Spain.

2.2. Synthesis and Characterization of 3-O-Succinyl-28-O-Benzyl Oleanolate and its intermediates (1-4)

2.2.1 Oleanolic Acid (1). This compound (**1**) was isolated from solid olive-oil-production wastes, which were extracted with hexane, using a Soxhlet extractor. Hexane extracts were concentrated and **1** was purified from these residues by column chromatography over silica gel, eluting with a $CHCl_3$/MeOH or CH_2Cl_2/acetone mixtures of increasing polarity;[39, 40] a white solid, mp 306-308 °C; $[a]_D$= +80 (c 1, $CHCl_3$); IR (KBr) ν_{max}: 3438, 2930, 2869, 1690 cm^{-1} was obtained. The compound (**1**) presents a mass spectrum that corresponds to a molecular formula of $C_{30}H_{48}O_3$ and therefore, has a molecular weight of 456 amu. In its ^1H NMR spectrum, the more deshielded signals appeared at 5.25 ppm (1H, dd, J_1=J_2= 3.6 Hz) for the olefinic proton of C-12, 3.16 ppm (1H, dd, J_1=4.8 Hz, J_2=11.2 Hz) for the equatorial proton of C-3 geminal to the hydroxyl at this position and 2.84 ppm (1H, dd, J_1 = 3.7 Hz, J_2 = 13.6 Hz) for the allylic hydrogen of C-18. Finally, the signals of the seven angular methyl groups were observed at δ_H 1.15 (s, 3H C-27), 0.97 (s, 3H C-23), 0.93 (s, 3H C-25 and 3H C-30), 0.90 (s, 3H C-29), 0.80 (s, 3H C-26) and 0.77 (s, 3H, C-24). This structure was confirmed by studying the ^{13}C NMR, COSY, HMBC and HMQC mono- and bi-dimensional spectra exhaustively and is completely concordant with those in the literature.

2.2.2 28-O-Benzyl Oleanolate (2). BnCl (418 µL) was added in a 2:1 ratio to a solution of **1** (912 mg, 2 mmol) in DMF (8 mL) with K_2CO_3 (0.61 g). The reaction was stirred for 4 h at 55 °C. The mixture was diluted with water and extracted with CH_2Cl_2, and the organic layer was dried with anhydrous Na_2SO_4. The solvent was removed under reduced pressure, and the residue was purified by column chromatography using CH_2Cl_2/acetone (10:1) to give **2** as a white solid (710 mg, 83%) (Scheme 1),[41] with mp 221-223 °C; $[a]_D$ +64 (c 1, $CHCl_3$: MeOH, 2:1); IR ν_{max} (KBr)/cm^{-1}: 3371, 2940, 2891, 1668. This compound has a molecular mass of 561 amu and in its ^1H NMR spectrum, in addition to the above mentioned signals, at 7.48 ppm (m, 5H) it presents the signal of the aromatic protons and at 5,00 ppm (2H, AB system, J = 12.0 Hz) it presents the signal of the methylene benzyl group. Moreover, the more

significant signals of compound **2** in its ^{13}C NMR spectrum are shown at 177.6 ppm (C-28, this signal is shielded from 184.5 ppm for OA as a consequence of the benzyl ester formation), 136.7 ppm (a quaternary carbon of the benzyl group), around 128.0 ppm (five methane carbons of the benzyl group) and 66.1 ppm (methylene group of the benzyl group).

2.2.3 3-O-Succinyl Oleanolic Acid (3). Succinic anhydride (236 mg, 2 mmol) was slowly added to a solution of **1** (456 mg, 1 mmol) in pyridine (5 mL). The reaction was maintained at room temperature while stirring for 24 h. Cold water was added to the reaction mixture, followed by an extraction with CH_2Cl_2, and the organic layer was dried with anhydrous Na_2SO_4. The solvent was removed under reduced pressure and the residue was purified by column chromatography using CH_2Cl_2/acetone (10:1) to give **3** as a white solid (90%) (Scheme 1),[42] with mp 190–192 °C; $[a]_D$ + 49 (*c* 1 in $CHCl_3$: MeOH, 2:1); IR ν_{max} (KBr)/cm^{-1}: 3394, 3018, 2854 and 1712. This compound has a molecular mass of 565 amu. The main spectroscopic difference between the succinylated compound (**3**) and the corresponding substrate (**1**) was the deshielding of the signal of the H-3 geminal proton because of the presence of succinyl group on C-3, in this sense, this signal was situated at δ_H 3.19 for (**1**) and δ_H 4.51 for (**3**). Moreover, in the ^{13}C NMR spectrum of **3,** the four signals of the four carbons of the succinyl group appear at δ_H 178.6 and 171.8, due to free carboxylic group and carboxylate group, and δ_H 29.6 and 29.4, corresponding to the two methylene groups. The other signals in this spectrum of this compound remain practically unaltered.

2.2.4 3-O-Succinyl-28-O-Benzyl Oleanolate (4). BnCl (210 µL) was added in 2:1 ratio to a solution of *3-O-succinyl oleanolic acid* (**3**, 556 mg, 1 mmol) in DMF (4 mL) with K_2CO_3 (0.30 g). The reaction was stirred for 4 h at 55 °C. The mixture was diluted with water and extracted with CH_2Cl_2, and the organic layer was dried with anhydrous Na_2SO_4. The solvent was removed under reduced pressure, and the residue was purified by column chromatography, using CH_2Cl_2/acetone (10:1) to give **4** (Scheme 1) as a colourless oil, $[a]_D$ + 38 (*c* 1 in $CHCl_3$: MeOH, 2:1); IR ν_{max}(film)/cm^{-1}: 3377, 3020, 2859 and 1720. This compound (**4**) has a molecular mass of 670 amu

and presented the above mentioned NMR spectroscopic characteristics when both functional groups of the molecule were modified as a succinyl derivative at C-3 (deshielding of H-3 from 3.19 ppm to 4.48 ppm, due to the esterification the hydroxyl group at this position) and as a benzyl ester at C-28 (appearance of the methylene group signal at 5.05 ppm and a multiplet signal at 7.31 ppm). On the other hand, all the carbons of the two new functional groups at C-3 and C-28 appear adequately in its ^{13}C NMR spectrum. This bifunctional compound (**4**) was also obtained by succinylation of 28-benzyl oleanolate (**2**). Succinic anhydride (73 mg, 0.732 mmol) was slowly added to a solution of **2** (100 mg, 0.183 mmol) in pyridine (2 mL). The mixture was treated as described above for the succinylation of **1** and thus, compound **4** was again formed.[31]

2.3. Anti-cancer test on colon cancer cells

The different compounds used in cell treatment (**1**, **2**, **3**, and **4**) (Fig.1) were dissolved before use at 10 mg mL^{-1} in 50% DMSO and 50% PBS. The stock solution was frozen and stored at -20 °C. Prior to the experiments, this solution was diluted with cell-culture medium. Apoptosis, cell-cycle, mitochondrial-membrane potential and Hoescht-stained were measured at the IC_{50} and IC_{80} concentrations (concentrations causing 50% and 80% reduction in growth). All the experiments were compared to the controls after 72 h of treatment.

2.3.1. Cell-proliferation Activity Assay.

Murine melanoma cell line B16-F10 (ECACC CRL-6475) was cultured in DMEM supplemented with 2 mM glutamine, 10% heat-inactivated FCS, 10.000 units per mL of penicillin and 10 mg mL^{-1} of streptomycin, and incubated at 37 °C in an atmosphere of 5% CO_2, and 95% humidity. Sub-confluent monolayer cells were used in all experiments.

The cell line was provided by the cell bank of the University of Granada, Spain. B16-F10 cells were derived from a melanoma from the skin of a C57BL/6 strain mouse, and are adherent cells with fibroblast-like

appearance, capable of producing melanin, and forming metastatic tumor nodules in the lung upon injecting mice.[43] The clone F10 of B16 cells are susceptible to lysis mediated by syngeneic lymphocytes.[44]

The effect of the treatment with products **1**, **2**, **3**, and **4** on the proliferation of B16-F10 melanoma cells was measured using the MTT assay (Sigma, MO, USA), which is based on the ability of live cells to cleave the tetrazolium ring, thus producing formazan, which absorbs at 570 nm. Cell viability was determined by measuring the absorbance of MTT dye staining of living cells. For this assay, $11x10^3$ B16-F10 cells were grown in a 96-well plate and incubated with the different derivatives (0-80 μg mL^{-1}). After 72 h, 100 mL of MTT solution (0.5 mg mL^{-1}) were added to each well. After 2 h of incubation, the cells were washed twice with PBS, and formazan was resuspended in 100 μL DMSO.

Relative cell viability, with respect to untreated control cells, was measured based on the absorbance at 550 nm on an ELISA plate reader (Tecan Sunrise MR20-301, TECAN, Austria). Derivatives that showed high cytotoxicity were used to perform apoptosis, cell-cycle, mitochondrial-membrane potential analysis and studies on morphological changes with Hoescht-staining.

2.3.2. Cell-cycle Analysis.

The cell-cycle was analyzed with flow cytometry by using a fluorescence-activated cell sorter (FACS) at 488 nm in an Epics XL flow cytometer (Coulter Corporation, Hialeah, FL, USA), as described previously[34]. For this assay $11x10^4$ B16-F10 cells per well were plated in 12 well plates with 2 mL of medium. After 24 h, the different compounds (**1**, **2**, and **4**) were added and the cells were incubated for 72 h. The doses used for each compound were their respective IC_{50} and IC_{80} values as determined by the cell proliferation activity assay.

Cells were washed twice with PBS and harvested by trypsinization, resuspended in TBS 1X (10 mM Tris, 150 mM NaCl) and subsequently, Vindelov buffer (100 mM Tris, 100 mM NaCl, 10 mg mL^{-1} RNase, 1 mg mL^{-1}

Propidium iodide [PI], pH 8) was added. Just before measurements, the total DNA content was stained with 1 mg mL^{-1} PI. The cell-cycle was analyzed using Multicycle software. The data were analyzed to determine the percentage of cells at each phase of the cell-cycle (G_0/G_1, S and G_2/M). Approximately $10x10^3$ cells were analyzed in each experiment. All experiments were performed three times with two replicates per experiment.

2.3.3. Annexin VeFICT/PI Flow-cytometric Analysis.

The extent of apoptosis was analyzed with flow-cytometry by using a FACScan flow-cytometer (fluorescence-activated cell sorter, Coulter Corporation, Hialeah, FL, USA). Briefly, $11x10^4$ B16-F10 cells were plated in 12 well plates with 2 mL of medium, following treatment with the different compounds (**1**, **2**, and **4**), for 72 h at the IC_{50} and IC_{80} concentrations calculated previously. The cells were collected and resuspended in binding buffer (10 mM HEPES/NaOH, pH 7.4, 140 mM NaCl, 2.5 mM $CaCl_2$). Annexin VeFITC conjugate (1 µg mL^{-1}) was added, followed by incubation for 30 min at RT in the dark. Just before FACS analysis, the cells were stained with 20 µL of 1 mg mL^{-1} PI solution. In each experiment, approximately $20x10^3$ cells were analyzed and the experiment was performed twice in triplicate.

2.3.4. Flow-cytometry Analysis of the Mitochondrial-membrane Potential.

Oxidative damage was studied by flow-cytometry analysis of the mitochondrial membrane potential using dihydrorhodamine 123 (DHR) which is oxidized to the highly fluorescent product, rhodamine (Rh123). The formation of Rh123 can be monitored by fluorescence spectroscopy, using excitation and emission wavelengths of 500 and 536 nm, respectively. The intracellular measurement of the mitochondrial membrane potential was made by the cytometric determination of Rh123. The intensity of fluorescence from Rh123 and PI was determined using a FACScan flow-cytometer (fluorescence-activated cell sorter, Coulter Corporation, Hialeah, FL, USA).

Similar to the apoptosis assays, $11x10^4$ B16-F10 cells were plated in 12-well plates and treated with the different compounds (**1**, **2**, and **4**) at their IC_{50} and IC_{80} concentrations. Following the treatment, the medium was removed and fresh medium with DHR at a final concentration of 5 µg mL^{-1} was added. After 30 min of incubation, the medium was removed and the cells were washed and resuspended in PBS with 5 µg mL^{-1} of PI.

2.3.5. Hoechst-staining.

The morphological changes were analyzed by fluorescent microscopy, using Hoechst staining. For this, $11x10^4$ B16-F10 cells were plated onto a coverslip in 12-well plates. After 24 h, different compounds (**1**, **2**, and **4**) were added and the cells were incubated for a further 72 h at their respective IC_{50} and IC_{80} values. The cells were washed twice with PBS and treated with cold 100% MeOH for 3 min. Subsequently, the cells were washed in PBS and incubated in 500 µL of Hoechst solution (50 ng mL^{-1}) in PBS for 15 min in the dark. The samples were prepared with mounting medium, Mowiol, and visualized by fluorescent microscopy (DMRB, Leica Microsystems, Wetzlar, Germany) with a DAPI filter.

2.4. Statistical analysis

Statistical analyses were performed with the GraphPad Prism 5.0 software. All quantitative data are summarized as the mean ± standard deviation (SD) or mean standard error (SEM). For each assay, Student's t test was used for statistical comparison with the untreated control cells. A limit of $p \leq 0.05$ was considered to be statistically significant. Key: $p < 0.05$ (*), $p \leq 0.01$ (**) and $p \leq 0.001$ (***). All data shown here are representative of at least three independent experiments performed in duplicate.

3. Results and Discussion

3.1 Chemistry synthesis

3.1.1 Synthetic route to 3-*O*-Succinyl-28-O-Benzyl Oleanolate.

The synthetic route to the target 3-*O*-succinyl-28-O-benzyl oleanolate is depicted in Scheme 1. The starting compound **1**, oleanolic acid (3β-hydroxyolean-12-en-28-oic acid) is a natural compound present in different plants. For the current study, this compound was isolated from the olive-pressing residues by extraction processes with different solvents. The benzylation of **1** by treatment with benzyl chloride in DMF to achieve 28-*O*-benzyl oleanolate (**2**, was carried to protect the carboxylic group at C-28 of the oleanane skeleton and to obtain a derivative that has an aromatic group attached at this position. Subsequently, the succinylation process was performed by treating (**1**) with succinyl anhydride (2:1 ratio) in pyridine for 24 h at RT; 3-*O*-succinyl oleanolic acid (**3**) was obtained in high yield. Finally, 28-*O*-benzyl oleanolate (**2**) was succinylated following similar conditions to those indicated above for **1** and thus, the bifunctional derivative 3-*O*-succinyl-28-O-benzyloleanolate (**4**) was obtained in high yield. This bifunctional derivative (**4**) of **1** was also obtained by succinylation of 28-benzyloleanolate (**2**) in similar conditions, as previously indicated. After the target compound was successfully prepared, the structural characteristics of the compound were examined on UV, MS and NMR spectroscopy.

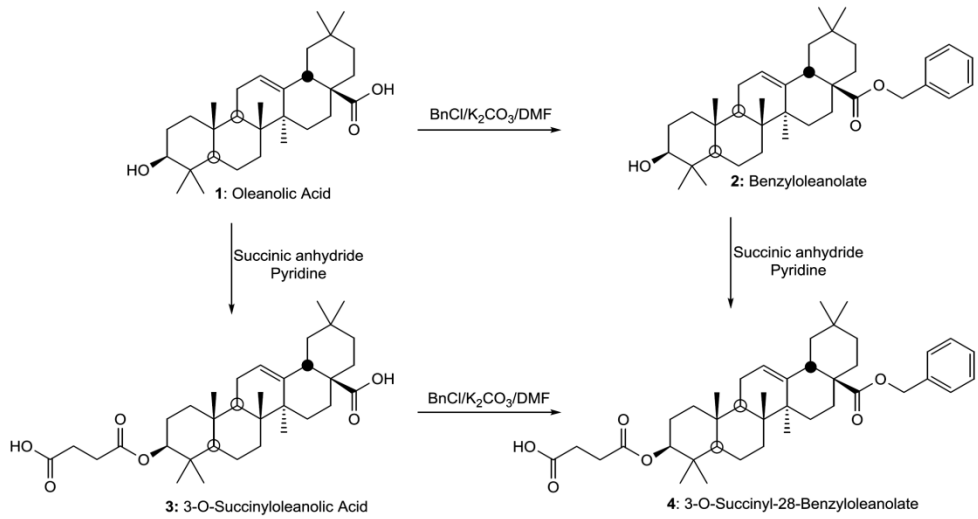

Scheme 1. Synthetic route of 3-*O*-Succinyl-28-*O*-Benzyl Oleanolate. Oleanolic acid (**1**) is treatment with benzyl chloride to achieve 28-*O*-benzyl oleanolate (**2**), or it can be succinylated with succinyl anhydride to achieve 3-*O*-succinyl oleanolic acid (**3**). Compound **2** is then succinylated, and **3** is benzylated, following similar conditions as described for **1**, obtained the 3-*O*-succinyl-28-O-benzyl oleanolate (**4**).

3.2 Anti-cancer activities

3.2.1 Inhibition of B16-F10 skin-melanoma cell proliferation.

In this work, the potential cytotoxic effect of these semi-synthesized derivatives (**2**, **3**, **4**) was examined via the proliferation of B16-F10 murine melanoma cell line, compared to its natural precursor (**1**), using the MTT assay. B16-F10 cells were treated with increasing doses of each compound. Their viability was determined by formazan dye uptake and expressed as a percentage of untreated control cell proliferation. Compounds **1**, **2** and **4** induced a dose-dependent decrease in viable formazan accumulating cells after 72 h of treatment, ranging from 0 to 80 μg mL^{-1}.

The concentration (expressed in μg mL^{-1}) of products required for 50% and for 80% growth inhibition (IC_{50} and IC_{80}) were determined for all products (Fig. 2). The treatment with **1** showed quite high values of IC_{50} and IC_{80} (IC_{50} = 46.2 ± 1.4 and IC_{80} = 50.2 ± 2.0). For treatment with **2**, the IC_{50} value was reduced almost to half (IC_{50} = 29.0 ± 1.7 and IC_{80} = 47.4 ± 2.4). The

treatment with **3** had no effect on cancer cell proliferation, not reaching the IC_{50} value.

The treatment with **4** had the lowest IC_{50} value (IC_{50} = 15.3 ± 0.6 and IC_{80} = 44.3 ± 3.1), being three times lower than that of its natural precursor (**1**), and was half that of **2**. These effects could to be related to the increase polarity of the whole molecule, without a significant increase in molecular weight or volume. The compounds **1**, **2** and **4** that showed cytotoxic effects in the range of concentrations assayed were selected for the rest of the assays: cell-cycle analysis, characterization of apoptosis, changes in mitochondrial membrane potential and Hoechst-staining.

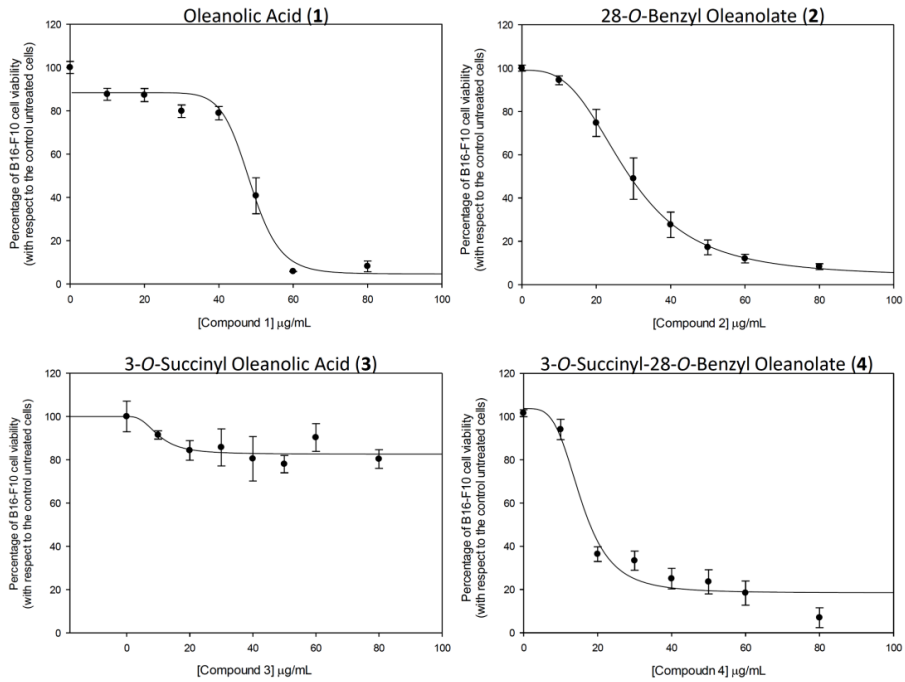

Comp. #	R_1	R_2	IC_{50} (µg/mL)	IC_{80} (µg/mL)	IC_{50} OA/ IC_{50} compound #
1	H	H	46,20 ± 1,47	50,17 ± 1,97	1,0
2	H	Benzyl	29,01 ± 1,66	47,41 ± 2,42	1,6
3	Succinyl	H	N/A	N/A	---
4	Succinyl	Benzyl	15,33 ± 0,59	44,43 ± 3,15	3,0

Fig. 2 The effects of oleanolic acid (**1**), 28-*O*-benzyl oleanolate (**2**), 3-*O*-succinyl oleanolic acid (**3**), and 3-*O*-succinyl-28-*O*-benzyl oleanolate (**4**), on the viability of B16-F10 murine skin-melanoma cells. After treatment with the compounds for 72 h in the range of 0 to 80 µg mL^{-1}, each point represents the mean value ± S.D. of at least two independent experiments performed in triplicate. IC_{50} and IC_{80} are the concentrations required for 50% and 80% of growth inhibition, respectively.

The effects of the selected products, **1**, **2** and **4** on cell-cycle distribution were investigated to determine a possible cytostatic effect attached to the cytotoxic response. The distribution of cells in different cell-cycle phases was analyzed after 72 h of treatment, by the incorporation of propidium iodide (PI). B16-F10 melanoma cells were treated with the products at IC_{50} and IC_{80} concentrations, determined previously.

3.2.2. Cell-cycle arrest and distribution.

Flow cytometry was used to measure DNA ploidy, as well as alterations in cell-cycle profiles. In this way, cell subpopulations with differing DNA content allow the determination of the percentage of cells in each cell-cycle phase. Changes in DNA concentration are characteristic of apoptosis or cell-cycle arrest. DNA histogram analysis revealed that the two derivatives, **2** and **4**, produced a significant cell-cycle arrest (Fig. 3), increasing the number of cells in the G_0/G_1 phase. Compound **2** increased this population up to 68% at IC_{50}, and 75% at IC_{80} concentration. Compound **4** produced a major effect with an increase up to 79% at IC_{50}, and 84% at IC_{80} concentration. These increases were accompanied by a decrease in the percentage of proliferating cells in S phase (up to 25% for **2** and 16% for **4** at IC_{80} concentrations). Changes in the G_2/M phase were less significant. The cell-cycle arrest observed could also be related to the induction of differentiation by **4** in this cell type.

A wide range of studies in recent years have shown that triterpenoids hinder carcinogenesis by intervening in pathways such as carcinogen activation, DNA repair, cell-cycle arrest, cell differentiation and the induction of apoptosis in cancer cells.[1,45,46] The identification of new cytotoxic agents that enhance or restore the capability of malignant tumor cells to undergo apoptosis may be crucial for more effective anticancer therapies. [1,39,40]

Apoptosis is one of the body's most potent defenses against cancer; the pathogenesis of many forms of this degenerative disease is closely connected with aberrantly regulated apoptotic cell death. Different

mechanisms that regulate apoptosis associated with mediators that trigger or inhibit cell death have led to the development of therapeutic strategies against cancer.

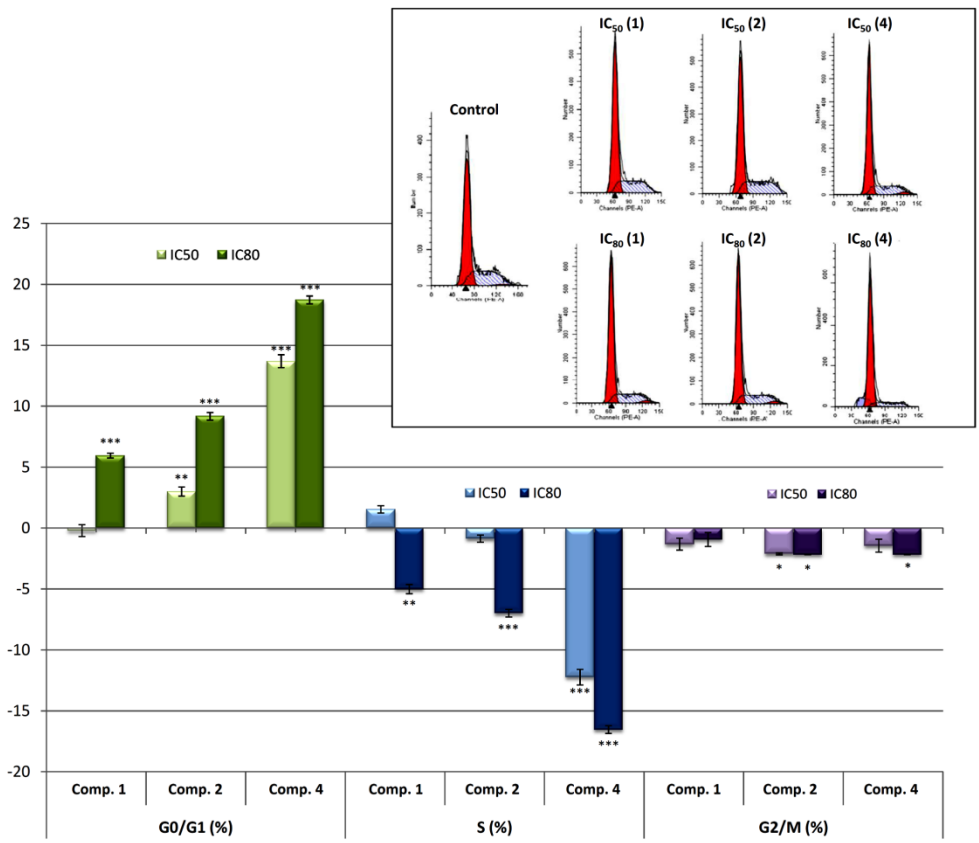

Fig.3 Top: Histograms of cell-cycle of B16-F10 skin-melanoma cells 72 h after treatment with compounds **1**, **2** and **4**, at IC_{50} and IC_{80} concentrations. Bottom: Increase in the percentage of cells in each cell-cycle phase with respect to untreated control cells. Cell-cycle was conducted after propidium iodide (PI) staining, as described in the Experimental section. Values represent means ± S.E.M of at least three independent experiments performed in duplicate. Key: $p < 0.05$ (*), $p \leq 0.01$ (**), and $p \leq 0.001$ (***), respect to untreated control cells.

In most of the pentacyclic triterpenoids, the cytotoxic effects are often accompanied by cytostatic effect. These cytostatic effects are frequently associated with apoptosis induction or differentiation cell process activation. The cell-cycle machinery is an alternative target for the identification of novel biomarkers for cancer detection and prognosis, providing target validation for cell-cycle-directed therapies. As the products

(**1**, **2** and **4**) inhibited cell growth, we investigated their effect on cell-cycle distribution in B16-F10 skin-melanoma cells after 72 h of treatment. In this respect, two derivatives, **2** and **4**, produced cell-cycle arrest in the G_0/G_1 phase.

Compound **4** induces greater cell-cycle arrest in G_0/G_1 phase, which is approximately 15% at IC_{50} concentration and 20% at IC_{80} concentration, coinciding with apoptotic cell death and thus, contributing to the inhibition of cell growth. This could indicate a likely induction of cell differentiation in response to the anti-cancer properties of product **4**. Further studies, such as the determination of the expression of the differentiation marker enzymes, would be necessary to assert this point.

3.2.3. Apoptosis induction in B16-F10 murine melanoma cells.

Annexin V-FITC staining and PI accumulation were used to determine the percentage of apoptotic cells. Early events in the apoptotic process are loss of plasma membrane asymmetry, accompanied by translocation of phosphatidyl-serine (PS) from the inner to the outer membrane leaflet, thereby exposing PS to the external environment.[47] The phospholipid-binding protein annexin V has a high affinity for PS and binds to cells fluorescently labelled with FITC (fluorescein isothiocyanate). The percentages of apoptosis, as determined with annexin V-FITC/PI flow cytometry analysis are shown in Fig.4.

Assessment of apoptosis in B16-F10 cells was performed 72 h after treatment with the compounds **1**, **2** and **4** at IC_{50} and IC_{80} concentrations. FACS analysis using Annexin V-FITC staining and PI accumulation was used to differentiate normal cells (Annexin-V^- and PI^-), early apoptotic cells (Annexin-V^+ and PI^-), late apoptotic cells (Annexin-V^+ and PI^+) and necrotic cells (Annexin-V^- and PI^+).

The three compounds demonstrated apoptotic effects on the treated cells, with high percentage of total apoptosis (early apoptotic together with late apoptotic cells), reaching an IC_{50} concentration of 42% (28.1% early apoptosis and 16.4% late apoptosis) in response to compound

1, 28% (12.2% early apoptosis and 29.1% late apoptosis) for compound **2**, and 69% (48.8% early apoptosis and 20.5% late apoptosis) for compound **4**.

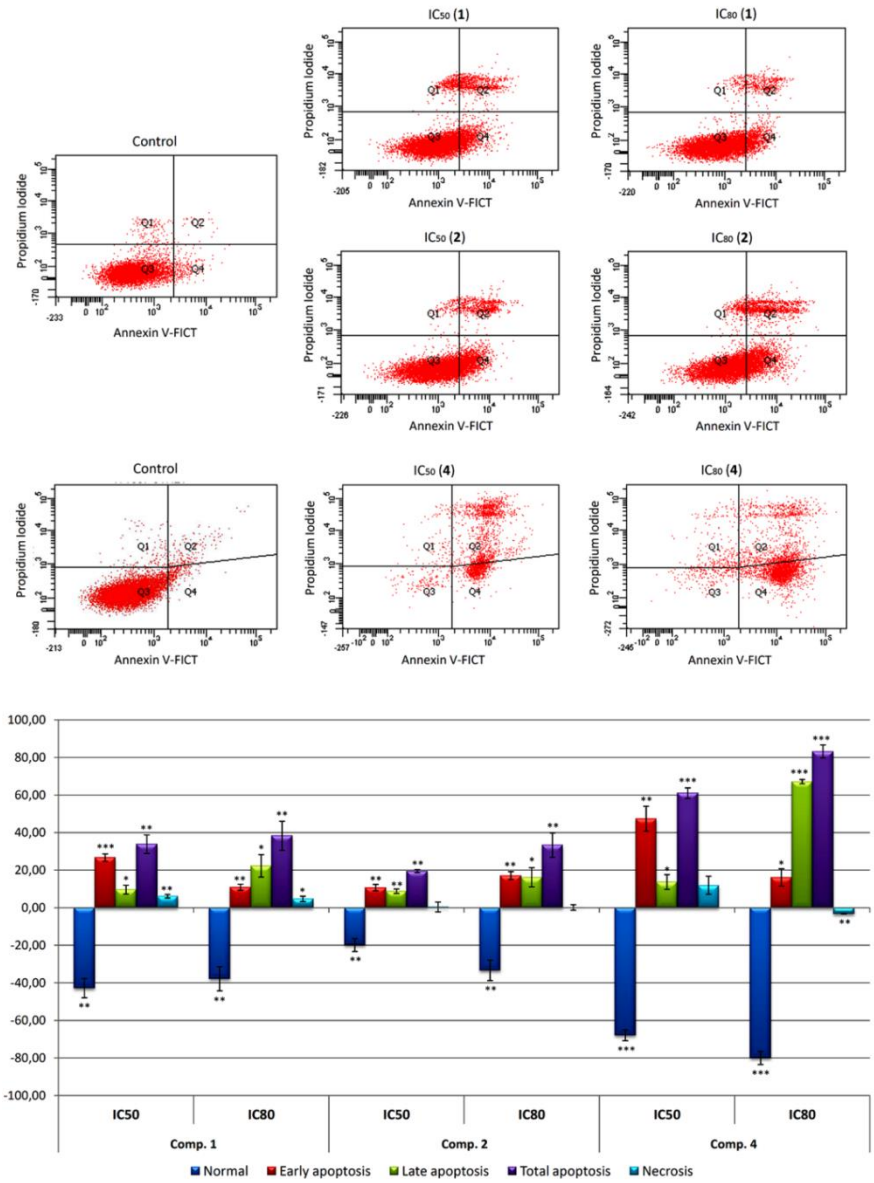

Fig.4 Effects of compounds **1**, **2**, and **4** on apoptosis in B16-F10 skin-melanoma cells, after 72 h treatment, at IC_{50} and IC_{80} concentrations. Top: Diagrams of annexin V/propidium iodide (IP) flow cytometry. B16-F10 cells were labeled with annexin V-FICT/PI as described in Experimental section. The right quadrants of each diagram represent apoptotic cells (Q2, late apoptosis; Q4, early apoptosis). Early apoptotic cells were annexin V^+ PI^-, whereas late apoptotic cells were annexin V^+, PI^+. Bottom: Flow cytometry analysis of Annexin V-FITC staining and PI accumulation, values represent means ± S.E.M of three experiments in duplicate. Key: $p < 0.05$ (*), $p \leq 0.01$ (**), and $p \leq 0.001$ (***), respect to untreated control cells.

At IC_{80} concentration, these percentages were 47% (12.4% early and 29.1% late apoptosis) for **1**, 42% (18.6% early apoptosis and 23% late apoptosis) for **2**, and 92% (16.6% early apoptosis and 73.9% late apoptosis) in the treatment with **4**. In addition, the percentages of the necrotic population were not noteworthy. The apoptotic effect in response to **4**, with the lowest IC_{50} concentration was the most significant.

In most cases, the highest percentage of apoptosis was achieved at IC_{80} concentrations. In all cases, the number of apoptotic cells increased concomitantly with dose concentration. The low values of IC_{50} concentrations and good percentages of apoptosis attained by these derivatives, especially by **4**, show that they could be used as promising anti-cancer drugs; further studies will be necessary to strengthen this point.

The apoptotic process frequently does not function in tumor cells. The intrinsic and extrinsic apoptotic activation routes have been described in the apoptotic effect of numerous triterpenoids, such as maslínico acid, ursolic acid, betulinic acid, OA and its derivatives.[1-3, 5] With alterations to the Bcl-2 protein family balance, loss of mitochondrial membrane potential, and the release of mitochondrial cytochrome-c occur.[48,49]

3.2.4. Mitochondrial membrane potential disturbances.

Mitochondria constitute a key target in synthetic and natural triterpenoids.[50] Pentacyclic triterpene compounds have proved to be able to activate the intrinsic apoptotic pathway, mediated by mitochondrial disruption.[2,3,51] In a first approximation of molecular mechanism, we analyzed the mitochondrial-membrane potential (MMP). Changes in this membrane potential can be associated with the intrinsic mechanism of apoptosis activation, while apoptosis induction without MMP changes may suggest activation of the extrinsic apoptotic pathway.

We investigated the MMP to determine the possible mechanism involved in the apoptotic responses. The changes in MMP were analyzed by monitoring the cell fluorescence following double staining with Rh123 and

PI. Rh123 is a membrane-permeable fluorescent cationic dye that is selectively taken up by mitochondria, and directly proportional to MMP.[52]

Changes in MMP were analyzed by flow-cytometry staining with Rh123/IP after treatment with the compounds **1**, **2**, and **4** for 72 h, at IC_{50} and IC_{80} concentrations. The apoptosis induction by **2** did not produce any changes in MMP, suggesting that the apoptosis was triggered by the extrinsic apoptotic pathway activation. Compounds **1** and **4** clearly produced MMP disturbances with loss of MMP and negative Rh123 staining.

The treatment with these products showed a decrease in the Rh123 positive cells stained, 63.8% at IC_{50} and 80.1% at IC_{80} concentrations for **1**, and 78.1% at IC_{50} and 69.8% at IC_{80} concentration in response to **4**, with a concomitant increase in Rh123 negative cells stained (Fig. 5). Therefore, the mitochondrial disruption, together with apoptosis, could indicate the activation of the intrinsic apoptotic route in B16-F10 cell line in response to **1** and **4**. Nevertheless, no changes in mitochondrial potential were observed following treatment with **2**.

These results clearly show mitochondrial disturbances following treatment with **1** and **4** in B16-F10 murine melanoma cells, which could be related to the activation of the mitochondrial or intrinsic apoptotic pathway by these products. Further molecular studies will be necessary to confirm this assertion.

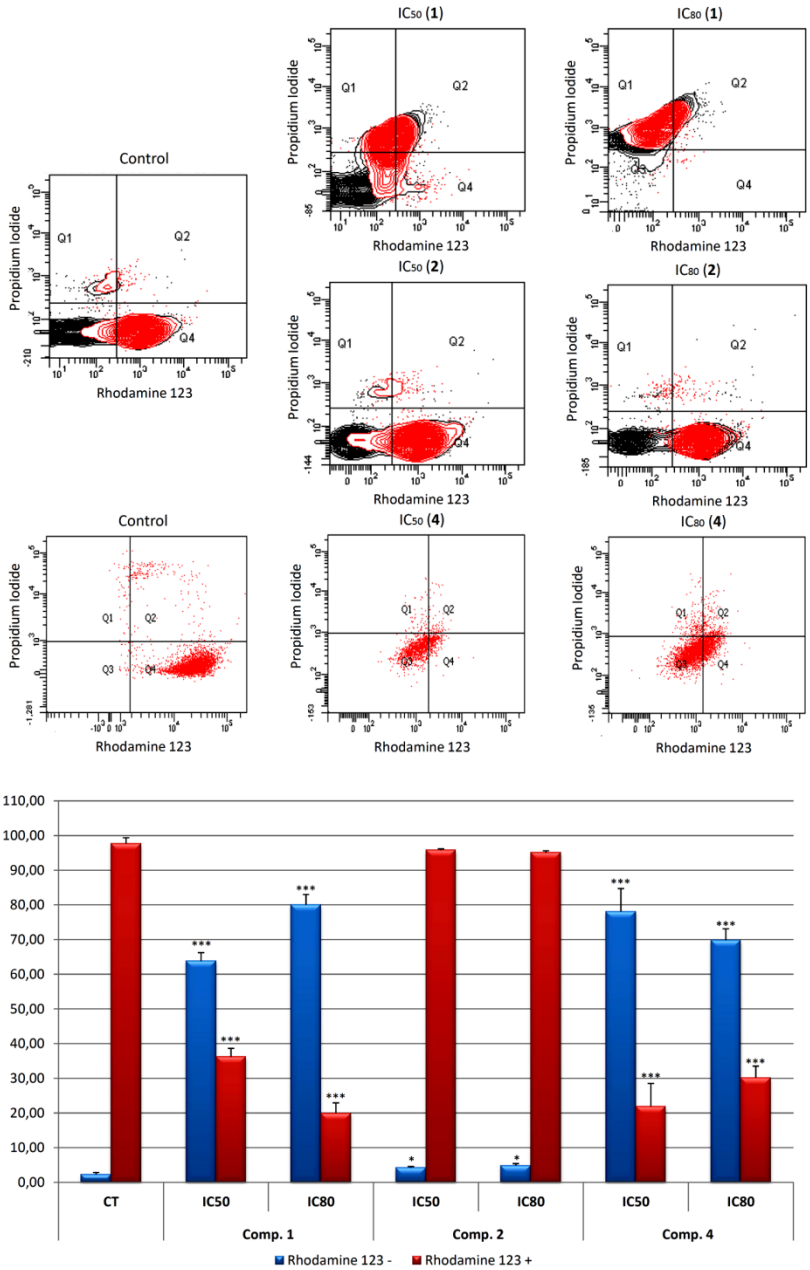

Fig. 5 Effects of compounds **1**, **2**, and **4** on mitochondrial membrane potential in B16-F10 skin-melanoma cells, after 72 h treatment, at IC_{50} and IC_{80} concentrations. Top: Diagram of rhodamine 123/propidium iodide flow-cytometry. B16-F10 cells were labeled with Rh123/IP as described in Experimental section. The right quadrants of each diagram (Q2 and Q4) represent positive cells stained with Rh123. Bottom: Percentage of Rh123 positive and negative B16-F10 cell population, in comparison with untreated control cells (CT). Values are expressed as means ± S.E.M of three experiments in duplicate. Key: $p < 0.05$ (*), $p \leq 0.01$ (**), and $p \leq 0.001$ (***), respect to untreated control cells.

3.2.5. Morphological apoptotic changes.

The Hoechst procedure stains nuclei that contain nicked DNA, a characteristic exhibited by cells in apoptotic cell death. Fluorescence microscopy can determine changes in the cell morphology. The fluorescence microscopic observations showed that a significant number of cells treated with the selected compounds acquired apoptotic features (Fig. 6).

The morphological analysis of Hoechst-stained cells in B16-F10 cells indicated that they had undergone remarkable morphological changes. After 72 h exposure to compounds **1**, **2**, and **4** (at IC_{50} and IC_{80} concentrations), the cells showed typical apoptotic changes, including cell shrinkage, chromatin condensation, and the loss of normal nuclear architecture. Fluorescence microscopic observation after Hoechst staining showed that a significant number of cells treated with compound **4** acquired apoptotic features, as evident from nuclear fragmentation, and the prominent disruption of the cell-membrane integrity.

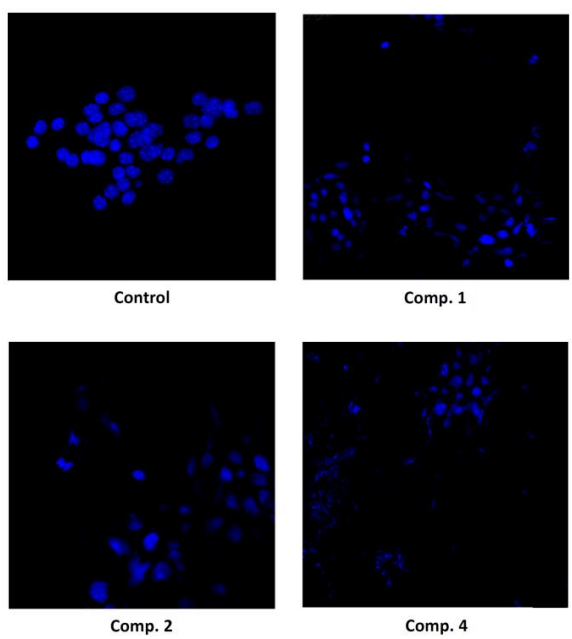

Fig. 6 Morphology changes in B16-F10 skin-melanoma cells after exposure to compounds **1**, **2** and **4** for 72 h, at IC_{50} concentrations. The samples were prepared with mounting medium, Mowiol, and the cells were examined using fluorescence microscopy following Hoechst-staining as described in Experimental section.

4. Conclusions

This study is the first to investigate the apoptotic effects of the oleanolic acid derivatives, **2**, **3** and **4**, in comparison to their natural precursor. Our data provide evidence that these products exert anti-proliferative and pro-apoptotic effects on B16-F10 skin-melanoma cells, a model for malignant melanoma cells. Moreover, they induce morphological changes that are characteristic of apoptosis, such as chromatin condensation and fragmentation, as well as cell shrinkage and loss of cell-membrane asymmetry, as demonstrated by fluorescence microscopy. These effects are greater in response to **4**, compared to its precursor, with smaller IC_{50} and IC_{80} values and a greater percentage of apoptosis induction. In conclusion, the 3-*O*-succinyl-28-*O*-benzyl oleanolate (**4**), a novel oleanolic acid derivative, is able to induce apoptosis in murine skin-melanoma cells, probably via the intrinsic mitochondrial pathway. The precise molecular signaling pathway by which this compound induces apoptosis needs to be investigated. Nevertheless, our data could contribute to the development this compound and related compounds for use as cancer chemotherapeutics or chemopreventive agents. The apoptotic potency of **4** suggests that it may be an effective compound in the prevention or treatment of the skin-melanoma.

Authors' Contribution

Fernando J. Reyes-Zurita, Andrés Parra and José A. Lupiáñez conceived and designed the study protocol. Fernando J. Reyes-Zurita, Marta Medina-O'Donnell, Rosa M. Ferrer-Martín, Eva E. Rufino-Palomares, Amalia Pérez-Jiménez, Leticia García-Salguero, Khalida Mokhtari, Juan Peragón, Pedro P. Medina and José A. Lupiáñez performed all cell culture (*in vitro*) and other biological experiments. Samuel Martín-Fonseca, Francisco Rivas, Antonio Martínez, Andrés García-Granados and Andrés Parra performed all the synthesis and purification experiments of SBOA and OA. Fernando J. Reyes-Zurita, Marta Medina-O'Donnell, Rosa M. Ferrer-Martín, Eva E. Rufino-Palomares, Amalia Pérez-Jiménez, Khalida Mokhtari, Leticia García-

Salguero and Pedro P. Medina contributed to reagents, materials, and analysis tools. Fernando J. Reyes-Zurita, Eva E. Rufino-Palomares, Leticia García-Salguero, Juan Peragón, Pedro P. Medina, Andrés Parra and José A. Lupiáñez conducted the data analysis. Fernando J. Reyes-Zurita, Andrés Parra and José A. Lupiáñez contributed to the paper preparation.

Acknowledgements

This study was supported by grants Group BIO 157 from the Technology and Innovation Council of the Andalucian regional government and AGL2006-12210-C03-02/ALI, SAF2005-01627, ISCIII-RTICC (RD06/0020/0046) from the Spanish government and European Union FEDER funds.

5. REFERENCES

1. F. J. Reyes, J. J. Centelles, J. A. Lupiáñez and M. Cascante, *FEBS Lett*, 2006, **580**, 6302-6310.
2. F. J. Reyes-Zurita, E. E. Rufino-Palomares, J. A. Lupiáñez and M. Cascante, *Cancer Lett*, 2009, **273**, 44-54.
3. F. J. Reyes-Zurita, G. Pachon-Pena, D. Lizarraga, E. E. Rufino-Palomares, M. Cascante and J. A. Lupiáñez, *BMC Cancer*, 2011, **11**, 154.
4. S. Sanchez-Tena, F. J. Reyes-Zurita, S. Diaz-Moralli, M. P. Vinardell, M. Reed, F. Garcia-Garcia, J. Dopazo, J. A. Lupiáñez, U. Gunther and M. Cascante, *PLoS One*, 2013, **8**, e59392.
5. F. J. Reyes-Zurita, E. E. Rufino-Palomares, P. P. Medina, E. Leticia Garcia-Salguero, J. Peragon, M. Cascante and J. A. Lupiáñez, *Biochimie*, 2013, **95**, 2157-2167.
6. E. E. Rufino-Palomares, A. Pérez-Jiménez, F. J. Reyes-Zurita, L. García-Salguero, K. Mokhtari, A. Herrera-Merchán, P. P. Medina, J. Peragón and J. A. Lupiáñez, *Cur Org Chem*, 2015, **19**, 919-947.
7. J. Peragón, E. E. Rufino-Palomares, I. Muñoz-Espada, F. J. Reyes-Zurita and J. A. Lupiáñez, *Int J Mol Sci*, 2015, **16**, 21681-21694.

8. F. J. Reyes-Zurita, E. E. Rufino-Palomares, L. García-Salguero, J. Peragón, P. P. Medina, A. Parra, M. Cascante and J. A. Lupiáñez, *PLoS One*, 2016, **11**.
9. E. Rufino-Palomares, F. J. Reyes-Zurita, C. A. Fuentes-Almagro, M. de la Higuera, J. A. Lupiáñez and J. Peragón, *Proteomics*, 2011, **11**, 3312-3325.
10. E. E. Rufino-Palomares, F. J. Reyes-Zurita, L. García-Salguero, K. Mokhtari, P. P. Medina, J. A. Lupiáñez and J. Peragón, *J Proteomics*, 2013, **83**, 15-25.
11. S. Schwarz, A. Loesche, S. D. Lucas, S. Sommerwerk, I. Serbian, B. Siewert, E. Pianowski and R. Csuk, *Eur J Med Chem*, 2015, **103**, 438-445.
12. K. Mokhtari, E. E. Rufino-Palomares, A. Pérez-Jiménez, F. J. Reyes-Zurita, C. Figuera, L. García-Salguero, P. P. Medina, J. Peragón and J. A. Lupiáñez, *Evid.-Based Compl. Alt.*, 2015, **2015**.
13. M. Cascante, S. Sanchez-Tena, D. Lizarraga, M. A. Reed, J. B. Carrigan, S. Diaz-Moralli, G. Alcarraz-Vizan, F. J. Reyes-Zurita, J. J. Centelles, M. P. Vinardell, J. A. Lupiáñez, V. Noe, C. J. Ciudad, J. L. Torres and U. Gunther, *Febs J*, 2013, **280**, 628-629.
14. A. Pérez-Jiménez, E. E. Rufino-Palomares, N. Fernández-Gallego, M. C. Ortuño-Costela, F. J. Reyes-Zurita, J. Peragón, L. García-Salguero, K. Mokhtari, P. P. Medina and J. A. Lupiáñez, *Phytomedicine*, 2016, **23**, 1301-1311.
15. E. E Rufino-Palomares, F. J Reyes-Zurita, L. García-Salguero, J. Peragón, M. de la Higuera and J. A Lupiáñez, *Comp. Biochem. Phys. C*, 2016, **187**, 32-42.
16. M. Fernandez-Navarro, J. Peragon, F. J. Esteban, M. de la Higuera and J. A. Lupiáñez, *Comp Biochem Physiol C Toxicol Pharmacol*, 2006, **144**, 130-140.
17. M. Fernandez-Navarro, J. Peragon, V. Amores, M. de la Higuera and J. A. Lupiáñez, *Comp Biochem Physiol C Toxicol Pharmacol*, 2008, **147**, 158-167.

18. M. Fernández-Navarro, J. Peragón, F.J. Esteban, V. Amores, M. de la Higuera, J.A. Lupiáñez. In *Olives and olive oil in health and disease prevention*, ed. V. R. Perry and R. R. Watson, Elsevier Inc., London, England., 2009, ch. 157, pp. 1415-1421.
19. E. E. Rufino-Palomares, F. J. Reyes-Zurita, L. García-Salguero, J. Peragón, M. de la Higuera and J. A. Lupiáñez, *Aquacul Nutr*, 2012, **18**, 138-151.
20. E. E. Rufino-Palomares, F. J. Reyes-Zurita, L. García-Salguero, J. Peragón, M. de la Higuera and J. A. Lupiáñez, *Aquacul Nutr*, 2012, **18**, 568-580.
21. E. E. Rufino-Palomares, F. J. Reyes-Zurita, L. Garcia-Salguero, J. Peragon, M. de la Higuera and J. A. Lupiáñez, *Aquacul Nutr*, 2013, **19**, 709-720.
22. E. E. Rufino-Palomares, J. Peragón, F. J. Reyes-Zurita, L. García-Salguero and J. A. Lupiáñez, *FEBS J*, 2012, **279**, 229-230.
23. R. Thimmappa, K. Geisler, T. Louveau, P. O'Maille and A. Osbourn, *Annu Rev Plant Biol*, 2014, **65**, 225-257.
24. W. S. Kombargi, S. E. Michelakis and C. A. Petrakis, *J Econ Entomol*, 1998, **91**, 993-998.
25. R. A. Hill and J. D. Connolly, *Nat Prod Rep*, 2015, **32**, 273-327.
26. H. Tokuda, H. Ohigashi, K. Koshimizu and Y. Ito, *Cancer Lett*, 1986, **33**, 279-285.
27. M. K. Shanmugam, X. Dai, A. P. Kumar, B. K. Tan, G. Sethi and A. Bishayee, *Cancer Lett*, 2014, **346**, 206-216.
28. K. T. Liby and M. B. Sporn, *Pharmacol Rev*, 2012, **64**, 972-1003.
29. M. Medina-O'Donnell, F. Rivas, F. J. Reyes-Zurita, A. Martinez, S. Martin-Fonseca, A. Garcia-Granados, R. M. Ferrer-Martin, J. A. Lupiáñez and A. Parra, *Eur J Med Chem*, 2016, **118**, 64-78.
30. A. Parra, S. Martín-Fonseca, F. Rivas, F. J. Reyes-Zurita, M. Medina-O'Donnell, E. E. Rufino-Palomares, A. Martínez, A. García-Granados, J. A. Lupiáñez and F. Albericio, *ACS Comb Sci*, 2014.

31. A. Parra, S. Martin-Fonseca, F. Rivas, F. J. Reyes-Zurita, M. Medina-O'Donnell, A. Martinez, A. Garcia-Granados, J. A. Lupiáñez and F. Albericio, *Eur J Med Chem*, 2014, **74**, 278-301.
32. R. Rodriguez-Rodriguez, *Curr Med Chem*, 2015, **22**, 1414-1425.
33. Z. Du, Z. Liu, Z. Ning, Y. Liu, Z. Song, C. Wang and A. Lu, *Planta Med*, 2015, **81**, 259-271.
34. R. Csuk, *Expert Opin Ther Pat*, 2014, **24**, 913-923.
35. X. Wang, *Genes Dev*, 2001, **15**, 2922-2933.
36. S. Y. Sun, N. Hail, Jr. and R. Lotan, *J Natl Cancer Inst*, 2004, **96**, 662-672.
37. A. Ashkenazi, *Cytokine Growth Factor Rev*, 2008, **19**, 325-331.
38. O. Micheau and J. Tschopp, *Cell*, 2003, **114**, 181-190.
39. A. Garcia-Granados, *P.C.T. Int. Appl, WO 9804331 Chem. Abstr. 128: 179706*, 1998.
40. A. Garcia-Granados, A. Martinez, J. N. Moliz, A. Parra and F. Rivas, *Molecules*, 1998, **3**, M88-M88.
41. R. Weis and W. Seebacher, *Magn Reson Chem*, 2002, **40**, 455-457.
42. J. Yang, J. W. Quail and Z. C. Jia, *Acta Crystallogr C*, 1997, **53**, 349-351.
43. I. J. Fidler, *Cancer Res*, 1975, **35**, 218-224.
44. I. J. Fidler and C. Bucana, *Cancer Res*, 1977, **37**, 3945-3956.
45. P. Dzubak, M. Hajduch, D. Vydra, A. Hustova, M. Kvasnica, D. Biedermann, L. Markova, M. Urban and J. Sarek, *Nat Prod Rep*, 2006, **23**, 394-411.
46. T. Ikeda, M. Sporn, T. Honda, G. W. Gribble and D. Kufe, *Cancer Res*, 2003, **63**, 5551-5558.
47. K. Takano, Y. Nakamura and Y. Yoneda, *Neuroscience*, 2003, **120**, 961-967.
48. P. O. Harmand, R. Duval, C. Delage and A. Simon, *Int J Cancer*, 2005, **114**, 1-11.
49. V. Zuco, R. Supino, S. C. Righetti, L. Cleris, E. Marchesi, C. Gambacorti-Passerini and F. Formelli, *Cancer Lett*, 2002, **175**, 17-25.

50. A. Petronelli, G. Pannitteri and U. Testa, *Anticancer Drugs*, 2009, **20**, 880-892.

51. R. Martin, J. Carvalho-Tavares, E. Ibeas, M. Hernandez, V. Ruiz-Gutierrez and M. L. Nieto, *Cancer Res*, 2007, **67**, 3741-3751.

52. R. K. Emaus, R. Grunwald and J. J. Lemasters, *Biochim Biophys Acta*, 1986, **850**, 436-448.

PUBLICACIÓN 3

Synthesis and *in vitro* antiproliferative evaluation of PEGylated triterpene acids

(JCR: Pharmacology & Pharmacy: Ind.Imp. 2.408, nº124, Q2)

Fitoterapia 120 (2017) 25–40

Contents lists available at ScienceDirect

Fitoterapia

journal homepage: www.elsevier.com/locate/fitote

Synthesis and *in vitro* antiproliferative evaluation of PEGylated triterpene acids

Marta Medina-O'Donnell[a], Francisco Rivas[a,*], Fernando J. Reyes-Zurita[b,*], Antonio Martinez[a], Francisco Galisteo-González[c], Jose A. Lupiañez[b], Andres Parra[a,*]

[a] Departamento de Química Orgánica, Facultad de Ciencias, Universidad de Granada, E-18071 Granada, Spain
[b] Departamento de Bioquímica y Biología Molecular I, Facultad de Ciencias, Universidad de Granada, E-18071 Granada, Spain
[c] Departamento de Física Aplicada, Facultad de Ciencias, Universidad de Granada, E-18071 Granada, Spain

ARTICLE INFO

Keywords:
Triterpene
Oleanolic acid
Maslinic acid
PEGylation
Cytotoxicity
Apoptosis

ABSTRACT

A set of PEGylated derivatives of oleanolic and maslinic acids has been semi-synthesised, attaching ethylene glycol, diethylene glycol, triethylene glycol or tetraethylene glycol to the C-28 carboxyl group of these natural triterpenes and some derivatives. Another set of PEGylated derivatives has been semi-synthesised by connecting the same four ethylene glycols to the hydroxyl groups of the A ring of these triterpenic acids, through a carbonate linker, by reaction with trichloromethyl chloroformate. The aqueous solubility of some of these PEGylated derivatives has been compared with that of maslinic acid. The cytotoxic effects of 28 triterpenic PEGylated derivatives in three cancer-cell lines (B16-F10, HT29, and Hep G2) have been assayed. The best results have been achieved with the HT29 cell line, and specifically with the oleanolic acid derivatives having ethylene glycol or tetraethylene glycol attached to the C-28 carboxyl group, which are approximately 27-fold more effective than their natural precursor. Eight PEGylated derivatives have been selected to compare the cytotoxicity results in the HT29 cancer-cell line with those of a non-tumour cell line of the same tissue (IEC-18), four of which were less cytotoxic in the non-tumour cell line. These compounds showed apoptotic effects on treated cells, with percentages of total apoptosis between 20% and 53%, relative to control, at 72 h and IC_{50} concentration, and between 29% to 62%, relative to control, for the same time and IC_{80} concentration. We have also found that with the treatment of these compounds in HT29 cancer cells, cell-cycle arrest occurred in the G0/G1 phase. Finally, we have also studied changes in mitochondrial membrane potential during apoptosis of HT29 cancer cells, and the results suggest an activation of the extrinsic apoptotic pathway for these compounds.

1. Introduction

Natural products have been central to traditional medicine for many years [1,2]. Nature has been a source of drugs since the beginning of history in many cultures, and about half of the drugs available today are related to natural compounds [3,4]. On the other hand, the traditional Mediterranean diet is characterized by the intake of vegetal foods such as grapes and olives, and their corresponding liquid extracts, wine and oil. Consumption of this type of food has often been associated with a low incidence of the different types of cancer [5–8]. The olive-oil industry produces a large amount of waste, solids, and liquids, which represent a serious environmental problem in many producing regions [9,10]. However, these wastes contain a set of remarkable chemical substrates and therefore constitute a potentially valuable resource [11,12].

Pentacyclic triterpene acids, such as oleanolic acid (3β-hydroxyolean-12-en-28-oic acid, OA, **I**) [13] and maslinic acid (2α,3β-dihydroxyolean-12-en-28-oic acid, MA, **II**) [14] are two natural products present in abundance in industrial olive-oil waste [15]. These triterpene acids have some promising biological properties as anti-tumour [16–25], antioxidant [26,27], antimicrobial [28,29], antimalarial [30], anti-inflammatory [31] agents. Certain structural modifications of these triterpenoids can have a strong impact on their biological activities [32–34]. Some of these structural modifications involve the formation of simple derivatives at several functional positions of their skeleton. In recent years, our research group has reported the semi-syntheses of various triterpene derivatives from the corresponding natural products and has evaluated its cytotoxicity and apoptotic capacity in several cancer-cell lines, showing a significant enhancement of these activities [35,36].

Polyethylene glycol (PEG) is a synthetic polymer which, for its non-toxic, non-immunogenic, non-antigenic, and non-amphiphilic proper-

* Corresponding authors.
E-mail addresses: frivas@ugr.es (F. Rivas), ferjes@ugr.es (F.J. Reyes-Zurita), aparra@ugr.es (A. Parra).

http://dx.doi.org/10.1016/j.fitote.2017.05.006
Received 19 April 2017; Received in revised form 12 May 2017; Accepted 16 May 2017
Available online 25 May 2017
0367-326X/

Abstract

A set of PEGylated derivatives of oleanolic and maslinic acids has been semi-synthesised, attaching ethylene glycol, diethylene glycol, triethylene glycol or tetraethylene glycol to the C-28 carboxyl group of these natural triterpenes and some derivatives. Another set of PEGylated derivatives has been semi-synthesised by connecting the same four ethylene glycols to the hydroxyl groups of the A ring of these triterpenic acids, through a carbonate linker, by reaction with trichloromethyl chloroformate. The aqueous solubility of some of these PEGylated derivatives has been compared with that of maslinic acid. The cytotoxic effects of 28 triterpenic PEGylated derivatives in three cancer-cell lines (B16-F10, HT29, and Hep G2) have been assayed. The best results have been achieved with the HT29 cell line, and specifically with the oleanolic acid derivatives having ethylene glycol or tetraethylene glycol attached to the C-28 carboxyl group, which are approximately 27-fold more effective than their natural precursor. Eight PEGylated derivatives have been selected to compare the cytotoxicity results in the HT29 cancer-cell line with those of a non-tumour cell line of the same tissue (IEC-18), four of which were less cytotoxic in the non-tumour cell line. These compounds showed apoptotic effects on treated cells, with percentages of total apoptosis between 20% and 53%, relative to control, at 72 h and IC_{50} concentration, and between 29% to 62%, relative to control, for the same time and IC_{80} concentration. We have also found that with the treatment of these compounds in HT29 cancer cells, cell-cycle arrest occurred in the G0/G1 phase. Finally, we have also studied changes in mitochondrial membrane potential during apoptosis of HT29 cancer cells, and the results suggest an activation of the extrinsic apoptotic pathway for these compounds.

Keywords: Triterpene; oleanolic acid; maslinic acid; PEGylation; cytotoxicity; apoptosis.

1. Introduction

Natural products have been central to traditional medicine for many years [1,2]. Nature has been a source of drugs since the beginning of history in many cultures, and about half of the drugs available today are related to natural compounds [3,4]. On the other hand, the traditional Mediterranean diet is characterized by the intake of vegetal foods such as grapes and olives, and their corresponding liquid extracts, wine and oil. Consumption of this type of food has often been associated with a low incidence of the different types of cancer [5–8]. The olive-oil industry produces a large amount of waste, solids, and liquids, which represent a serious environmental problem in many producing regions [9,10]. However, these wastes contain a set of remarkable chemical substrates and therefore constitute a potentially valuable resource [11,12].

Pentacyclic triterpene acids, such as oleanolic acid (3β-hydroxyolean-12-en-28-oic acid, OA, **I**) [13] and maslinic acid (2α,3β-dihydroxyolean-12-en-28-oic acid, MA, **II**) [14] are two natural products present in abundance in industrial olive-oil waste [15]. These triterpene acids have some promising biological properties as anti-tumour [16–25], antioxidant [26,27], antimicrobial [28,29], antimalarial [30], anti-inflammatory [31] agents. Certain structural modifications of these triterpenoids can have a strong impact on their biological activities [32–34]. Some of these structural modifications involve the formation of simple derivatives at several functional positions of their skeleton. In recent years, our research group has reported the semi-syntheses of various triterpene derivatives from the corresponding natural products and has evaluated its cytotoxicity and apoptotic capacity in several cancer-cell lines, showing a significant enhancement of these activities [35,36].

Polyethylene glycol (PEG) is a synthetic polymer which, for its non-toxic, non-immunogenic, non-antigenic, and non-amphiphilic properties, has a key function in drug delivery [37,38]. The strategy called PEGylation is the incorporation of polyethylene glycol reagents of different chain lengths into proteins, peptides or small molecules. Currently, PEGylation

technologies are widely used in the preparation of drugs and there are a large number of commercially available PEGylation reagents [39,40]. Recently, our research group has reported the semi-synthesis and antiproliferative evaluation of several PEGylated derivatives of oleanolic and maslinic acids [41].

In this study, other PEGylated derivatives of oleanolic and maslinic acids have been semi-synthesised to test for their biological activities. Firstly, we prepared a set of PEGylated derivatives, attaching ethylene glycol, diethylene glycol, triethylene glycol or tetraethylene glycol to the C-28 carboxyl group of the natural triterpenes (OA and MA) and some derivatives. Secondly, another set of PEGylated derivatives was semi-synthesised by connecting the same four ethylene glycols to the hydroxyl groups of the A ring of the triterpenic acids (OA and MA), through a carbonate linker, by reaction with trichloromethyl chloroformate. We have also compared the aqueous solubility of some PEGylated derivatives of MA with that of MA. Finally, we also tested the cytotoxic effects of these 28 PEGylated derivatives on three cancer-cell lines (B16-F10, HT29 and Hep G2). We have selected eight of these derivatives to compare the cytotoxicity results in the HT29 cancer-cell line with those of a non-tumour cell line from the same tissue (IEC-18). Four of these compounds were then chosen to perform various cytometric assays. All of the cytotoxic compounds tested were active in the apoptotic process. In addition, we established the percentage of cells in the different cell-cycle phases. Finally, we studied the changes in the mitochondrial membrane potential (MMP) to formulate hypotheses on the plausible apoptotic mechanisms activated by the different compounds tested.

2. Results and Discussion

2.1. Semi-synthesis of PEGylated derivatives on the C-28 carboxylic group

Oleanolic acid (**I**, 3β-hydroxyolean-12-en-28-oic acid, OA) and maslinic acid (**II**, 2a,3β-dihydroxyolean-12-en-28-oic acid, MA) are natural pentacyclic triterpenes with an oleanane skeleton (Fig. 1). These

compounds (OA and MA), widely present in the plant kingdom, were obtained from wastes from the olive-oil industry [42]. These triterpene acids were acetylated to protect the hydroxyl group/s of the A ring, yielding the corresponding 3β-acetylated (**III**, OA-Ac) or 2α,3β-diacetylated (**IV**, MA-Ac) derivatives [43,44]. Similarly, to protect the C-28 carboxyl group, these triterpene acids (OA and MA) were benzylated, producing the corresponding benzyl derivatives (**V**, OA-Bn, and **VI**, MA-Bn) [45,46].

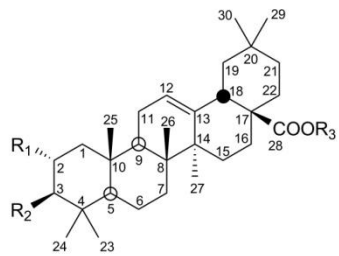

I: $R_1 = R_3 = H$, $R_2 = OH$ (oleanolic acid, **OA**)
II: $R_1 = R_2 = OH$, $R_3 = H$ (maslinic acid, **MA**)
III: $R_1 = R_3 = H$, $R_2 = OAc$ (3β-acetyl oleanolic acid, **OA-Ac**)
IV: $R_1 = R_2 = OAc$, $R_3 = H$ (2α,3β-diacetyl maslinic acid, **MA-Ac**)
V: $R_1 = H$, $R_2 = OH$, $R_3 = Bn$ (28-benzyl oleanolate, **OA-Bn**)
VI: $R_1 = R_2 = OH$, $R_3 = Bn$ (28-benzyl maslinate, **MA-Bn**)

Fig. 1. Structures of precursors (**I**-**VI**).

The starting compounds **I-IV** were used to get a set of PEGylated triterpene derivatives by forming an ester bond between the C-28 carboxylic group and several polyethylene glycol reagents with different chain lengths. Four PEG reagents (mono-, di-, tri-, or tetra-ethylene glycol) were chosen to analyse how much influence the length of this glycol chain has on the chemical and biological properties of these PEGylated derivatives. The semi-syntheses of these PEGylated derivatives were performed in two consecutive reactions. The first consisted of activating the C-28 carboxyl group of each triterpene acid by forming the corresponding TBTU-derivative. Thus, each starting product (**I-IV**) was treated with *O*-(benzotriazol-1-yl)-*N*,*N*,*N'*,*N'*-tetramethyluronium tetrafluoroborate (TBTU), in the presence of *N*,*N*-diisopropylethylamine (DIEA), in DMF [41]. In the second step, each of these four activated C-28 intermediates were now treated with the corresponding PEG reagent (mono-, di-, tri-, or tetra-

ethylene glycol), in the presence of K_2CO_3, in dioxane, yielding 16 PEGylated derivatives (**1-16**) (Scheme 1).

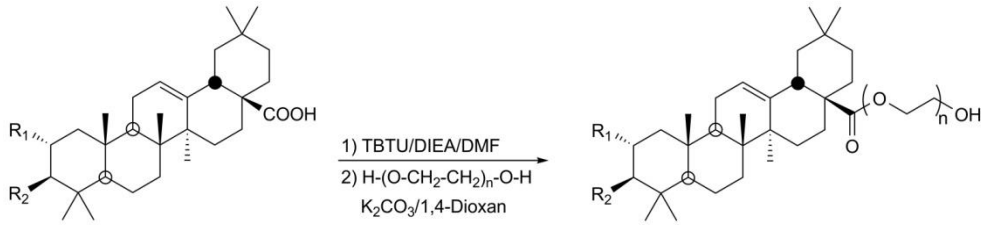

I: R_1 = H, R_2 = OH
II: R_1 = R_2 = OH
III: R_1 = H, R_2 = OAc
IV: R_1 = R_2 = OAc

1-4: R_1 = H, R_2 = OH, n = 1, 2, 3, or 4
5-8: R_1 = R_2 = OH, n = 1, 2, 3, or 4
9-12: R_1 = H, R_2 = OAc, n = 1, 2, 3, or 4
13-16: R_1 = R_2 = OAc, n = 1, 2, 3, or 4

Scheme 1. PEGylation reaction of precursors (**I-IV**) with several ethylene glycol reagents.

The NMR spectra of these compounds (**1**-**16**) were similar to their corresponding precursors (**I-IV**), the main differences being the proton signals of the PEG group of each compound. Thus, the ^{1}H NMR spectra showed a signal at about δ_H 4.20 due to the methylene group attached directly to the C-28 carboxyl group of the corresponding triterpene, and between δ_H 3.80-3.50, other signals due to the other methylene groups of the corresponding PEG group. The ^{13}C NMR spectra of these compounds (**1**-**16**) differed from those of their corresponding precursors (**I-IV**), in the number of signals due to the PEG group of these derivatives (2, 4, 6, or 8 signals, respectively), which were situated between 60 and 70 ppm.

2.2. Semi-synthesis of PEGylated derivatives on the hydroxyl groups of the A-ring

Starting compounds **V** and **VI** (OA-Bn and MA-Bn) were used to obtain new PEGylated triterpene derivatives at the hydroxyl group/s of the A-ring of these compounds. The semi-synthesis of these derivatives required the use of a carbonate linker to attach the corresponding PEG reagent to the respective triterpenic compound. Treatment of the starting compound **V** (OA-Bn) with trichloromethyl chloroformate (diphosgene) in the presence

of *N*,*N*-dimethylaniline (DMA) in THF, yielded a chloroformate derivative, an unstable intermediate which was not isolated. Subsequently, the reaction of this intermediate with several mono-, di-, tri- or tetra-ethylene glycol reactants in the presence of *N*,*N*-diisopropylmethylamine (DIEA) and 4-dimethylaminopyridine (DMAP), in toluene, gave the PEGylated derivatives **17**-**20** (Scheme 2).

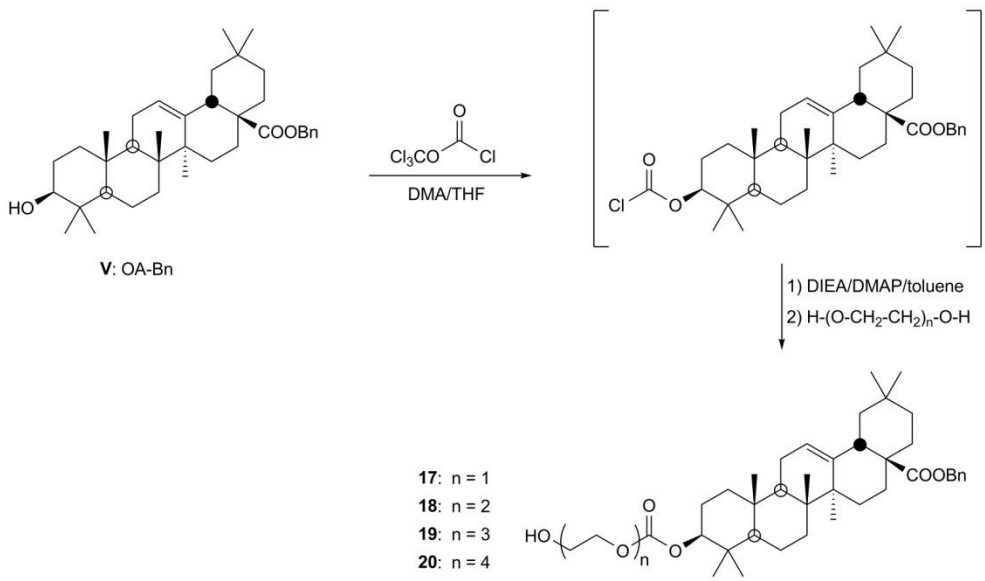

Scheme 2. PEGylation reaction of precursor **V** with several ethylene glycol reagents.

The main differences of the ^{1}H NMR spectra of compounds **17-20** and that of their precursor (**V**), were the signal of H-3 (δ_H 4.30), deshielded by the presence of a carbonate group at C-3, and the proton signals of the PEG group of each compound. In addition, the ^{13}C NMR spectra of derivatives **17-20** showed a signal situated around δ_C 155, due to the carbonate group at C-3, and a variable number of methylene carbon signals (between 72 and 62 ppm) corresponding to the different PEG groups present in these derivatives.

A similar treatment with diphosgene of the starting compound **VI** (MA-Bn) led to a very stable compound (**21**) (Scheme 3). This product (**21**) was formed through successive reactions of the diphosgene reagent with the two hydroxyl groups of the A ring, giving a cyclic carbonate between

C-2 and C-3. NMR spectra of **21** confirmed this structure. Thus, in their ^{1}H NMR spectrum the H-2 and H-3 signals were deshielded due to the presence of the cyclic carbonate, now being at δ_H 4.43 and 3.80, respectively, and in their ^{13}C NMR spectrum appeared a signal of a carbonate group at δ_C 155.5.

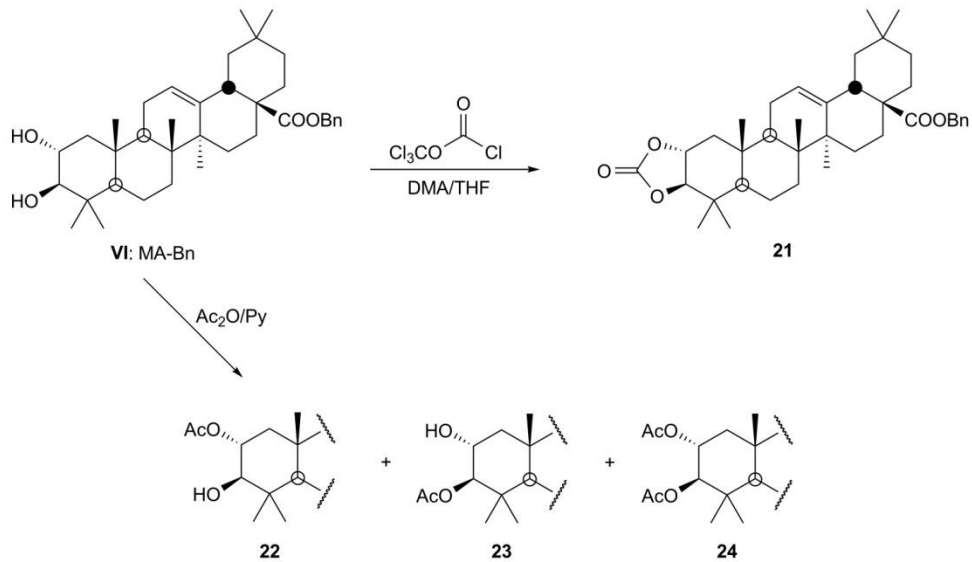

Scheme 3. Reaction of **VI** with diphosgene.Controlled acetylation reaction of **VI**.

In the process of obtaining PEGylated derivatives of MA-Bn (**VI**), it was necessary to protect one of the hydroxyl groups of the A ring of this compound (**VI**) in order to avoid the formation of the cyclic carbonate. This protection was achieved by selective controlled acetylation of the C-2 or C-3 hydroxyl groups by treatment with acetic anhydride (Ac_2O) in pyridine (Py) (Scheme 3). Therefore, treatment with Ac_2O/Py of the starting compound MA-Bn (**VI**) gave the acetylated derivatives **22** (46%), **23** (30%), and **24** (14%) [35]. The monoacetylated compounds (**22** and **23**) were respectively treated with diphosgene, in the presence of DMA, in THF, resulting in the corresponding unstable chloroformate derivatives. Reaction of these intermediates with mono-, di, tri- or tetra-ethylene glycol, in the

presence of DIEA and DMAP, in toluene, respectively, yielded the PEGylated derivatives (**25**-**28** and **29**-**32**) (Scheme 4).

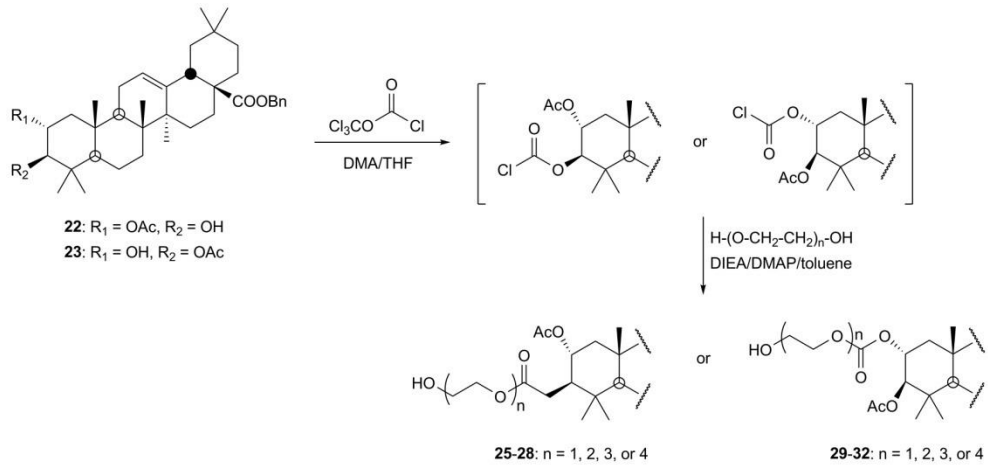

Scheme 4. PEGylation reactions of compounds **22** and **23**.

The ^{1}H NMR spectra of the PEGylated derivatives **25-28** were similar to those of compounds **17**-**20**, except for the presence in the former of a geminal proton signal (H-2) to an acetoxyl group at C-2 (around δ_H 5.00). Moreover, the ^{1}H NMR spectra of the PEGylated derivatives **29**-**32** were also similar to those of compounds **25**-**28**, the acetoxyl group now being located at C-3 and its geminal proton signal (H-3) appearing around 4.75 ppm. The ^{13}C NMR of these compounds (**25**-**28** and **29**-**32**) confirmed the presence of a carboxyl group (around δ_C 170), a carbonate group (around δ_C 155), and various oxygenated methylene carbons (between δ_C 72 and 62) corresponding to the PEG group present in these derivatives.

Some of these 28 PEGylated derivatives (**1**-**20** and **25**-**32**) were tested for their aqueous solubility and also for some of their potential biological activities.

2.3. Aqueous solubility of some PEGylated derivatives

It is assumed, taking into account the lipophilic molecular structure that the concentration of the pentacyclic triterpenic acids in water is rather low, making it difficult to perform biological tests in the cell medium [47]. We determined the aqueous solubility values of some PEGylated derivatives (**5**-**8**) and compared them with that of the corresponding starting compound (MA, **II**). These solubilities were measured using a new method specifically developed for this purpose, as detailed in the Experimental Section, and the aqueous solubility results are shown in Table 1.

Table 1
Water solubility values of the PEGylated derivatives **5**-**8** and MA (**II**). Solubility ratio between these PEGylated derivatives (**5**-**8**) and MA (**II**).

Compd #	Solubility (μg/L)	PEG Solubility / MA Solubility
5	160 ± 20	44
6	240 ± 30	66
7	480 ± 70	133
8	1720 ± 90	477
MA (**II**)*	3.6 ± 0.4	---
MA (**II**)**	3.96	---

* Experimental solubility in water for MA (**II**), at 20 °C.
** Estimated solubility in water for MA (**II**) from a Log Kow (Octanol-water partition coefficient) of 6.82, at 25°C [48].

As expected, the aqueous solubility of MA (**II**) had a very low experimental value (3.6 μg/L), which was corroborated with its theoretical value (3.96 μg/L; Table 1) [48]. This very low aqueous solubility of MA (**II**) represents a major problem in conducting biological tests, because this compound partially precipitates in the cell media. The water solubility of the PEGylated derivatives **5**-**8** was higher than that of their starting compound (MA, **II**), increasing with the chain length of the PEG reagent. Thus, the aqueous solubilities of derivatives **5**-**8** were 44-, 66-, 133-, or 477-fold higher than that of MA (**II**) (Table 1). As a result of the increased solubility, these compounds no longer precipitated in the cell media.

2.4. Effects of triterpene derivatives on cancer-cell proliferation

The cytotoxic effects of the 28 PEGylated derivatives (**1**-**20** and **25**-**32**) on the proliferation of three cancer-cell lines (B16-F10, murine melanoma cells, HT29, colon-cancer cells, and Hep G2, hepatome cells) were studied. All these cell lines were treated with increasing concentrations of these PEGylated derivatives and viability was determined by formazan dye uptake, expressed as a percentage of untreated control cells. The IC_{50} values for each derivative, in the three cell lines, are given in Table 2.

All compounds were cytotoxic in the conditions assayed (range 0–250 μg/mL), showing IC_{50} values between 10 to 130 μM. Except for compounds **10**, **12**, **17**, and **18** on B16-F10 cell line, and **18** on Hep G2 cell line, most of the compounds tested showed better IC_{50} data (Table 2) than did the corresponding precursors (**I**-**V**, **22**, and **23**). According to the analysis of the three cell lines tested, the percentage of PEGylated derivatives that improved the cytotoxicity results compared to their precursors was variable, being 62% for B16-F10, 80% for HT29, and 74% for Hep G2. Therefore, the formation of PEGylated derivatives in these pentacyclic triterpenes improved their cytotoxicity effects on these three cancer-cell lines. However, the influence of the chain length of the PEG reagent on the cytotoxicity of these PEGylated derivatives was not clear, so SAR analysis of these derivatives was not easy. The cytotoxicity results of these PEGylated derivatives of oleanolic and maslinic acids, conjugated with one to four ethylene glycol units, show that these compounds are less active than certain PEGylated-amine derivatives of these triterpene compounds, while showing similar results to those of the PEGylated derivatives with a PEG-acid group [41].

Table 2
Growth-inhibitory effects of PEGylated derivatives on B16-F10, HT29, and Hep G2 cells.

Compd #	B16-F10	*IC_{50} of precursor / IC_{50} of compd #	HT29	* IC_{50} of precursor / IC_{50} of compd #	Hep G2	* IC_{50} of precursor / IC_{50} of compd #
OA (**I**)	106.40 ± 3.70	1.0	429.9 ± 0.70	1.0	211.80 ± 0.50	1.0
1	20.43 ± 0.31	5.2	16.16 ± 0.92	27.0	23.83 ± 1.20	8.9
2	80.99 ± 1.53	1.3	35.22 ± 0.09	12.2	63.08 ± 2.36	3.4
3	74.07 ± 1.48	1.4	55.38 ± 0.26	7.8	59.97 ± 0.52	3.5
4	20.60 ± 1.57	5.2	16.76 ± 0.01	26.0	18.68 ± 0.78	11.3
MA (**II**)	36.20 ± 2.50	1.0	32.20 ± 3.80	1.0	99.20 ± 15.50	1.0
5	29.74 ± 3.75	1.2	10.98 ± 0.23	2.9	52.13 ± 1.54	1.9
6	16.60 ± 0.02	2.2	10.00 ± 0.53	3.2	14.91 ± 0.62	6.7
7	18.55 ± 0.23	2.0	15.06 ± 0.10	2.1	17.23 ± 0.20	5.8
8	14.56 ± 0.06	2.5	11.06 ± 0.08	2.9	14.75 ± 0.06	6.7
OA-Ac (**III**)	64.70 ± 2.80	1.0	148.48 ± 8.36	1.0	103.67 ± 4.12	1.0
9	12.93 ± 0.05	5.0	89.34 ± 5.25	1.7	31.99 ± 0.91	3.2
10	114.26 ± 1.96	0.6	133.48 ± 2.25	1.1	98.86 ± 3.62	1.0
11	12.52 ± 0.31	5.0	24.48 ± 0.12	6.1	18.09 ± 0.80	5.7
12	87.61 ± 3.51	0.7	66.64 ± 0.55	2.2	61.24 ± 2.75	1.7
MA-Ac (**IV**)	44.10 ± 3.80	1.0	69.14 ± 2.95	1.0	50.16 ± 1.02	1.0
13	22.33 ± 2.59	2.0	17.66 ± 0.05	3.9	25.32 ± 0.29	2.0
14	47.63 ± 0.41	0.9	45.15 ± 0.08	1.5	45.49 ± 0.14	1.1
15	17.67 ± 0.15	2.5	15.94 ± 0.29	4.3	18.76 ± 0.39	2.7
16	12.03 ± 0.38	3.7	10.72 ± 0.51	6.5	10.05 ± 0.07	5.0
OA-Bn (**V**)	52.20 ± 0.90	1.0	67.08 ± 3.21	1.0	38.73 ± 1.65	1.0
17	112.05 ± 0.63	0.5	48.90 ± 0.57	1.4	35.58 ± 1.51	1.1
18	113.24 ± 9.17	0.5	60.42 ± 2.12	1.1	50.43 ± 0.48	0.8
19	46.73 ± 2.00	1.1	29. 71 ± 0.59	2.3	18.63 ± 0.54	2.1
20	51.80 ± 1.01	1.0	39.22 ± 0.56	1.7	30.55 ± 0.31	1.3
22	38.15 ± 0.09	1.0	41.68 ± 0.83	1.0	47.34 ± 4.03	1.0
25	22.76 ± 2.43	1.7	17.96 ± 0.42	2.3	18.52 ± 0.06	2.6
26	17.54 ± 0.23	2.2	14.95 ± 0.08	2.8	16.66 ± 0.04	2.8
27	36.28 ± 0.14	1.1	20.00.± 0.51	2.1	19.54 ± 0.39	2.4
28	23.98 ± 1.31	1.6	22.13 ± 1.61	1.9	16.41 ± 0.01	2.9
23	113.48 ± 3.47	1.0	85.86 ± 2.35	1.0	84.00 ± 4.71	1.0
29	21.73 ± 1.95	5.2	16.91 ± 0.78	5.1	19.55 ± 0.06	4.3
30	17.18 ± 0.15	6.6	15.92 ± 0.06	5.4	17.85 ± 0.24	4.7
31	16.11 ± 0.24	7.0	16.34 ± 0.23	5.3	18.13 ± 0.01	4.6
32	14.85 ± 0.04	7.6	23.78 ± 4.18	3.6	22.45 ± 0.78	3.7

The IC_{50} values (μM) were calculated considering control untreated cells as 100% of viability. Cell-growth inhibition was analysed by the MTT assay, as described in Experimental section.
* Relationship between IC_{50} of the corresponding precursor and the IC_{50} of the each compound. All assays were realized two times using three replicates. Values, means ± S.E.M.

In general, the best cytotoxicity results were achieved with the HT29 cell line. For this reason, several PEGylated derivatives (**1**, **4**, **5**, **8**, **25**, **26**, **29** and **30**) were chosen to perform various biological assays with this cell line.Compounds **1** and **4** are derivatives of OA (**I**) having ethylene glycol or

tetraethylene glycol attached to the C-28 carboxylic group of the triterpene, which had very good cytotoxic behaviour in the HT29 cell line, being around 27-fold more effective than their precursor (OA, **I**) (Table 2). Compounds **5** and **8** are derivatives of MA (**II**), which were chosen for their similarity to **1** and **4**. Compounds **25** and **26** are derivatives of 2-acetyl MA-Bn (**22**), and compounds **29** and **30** of 3-acetyl MA-Bn (**23**); having ethylene glycol or diethylene glycol attached through a carbonate linker to the hydroxyl groups of C-2 or C-3. In addition, the cytotoxicity results of these derivatives with the HT29 cancer-cell line were compared to those of a non-tumour cell line from the same tissue (IEC-18, intestinal epithelium rat cell) (Table 3). Four compounds (**4**, **5**, **8** and **26**) were chosen to perform the following cytometric assays because they were less cytotoxic in the non-tumour cell line IEC-18 than in the HT29 cancer-cell line. Compounds **4** and **8** showed the most significant differences in their cytotoxic effects on these two cell lines (Table 3).

Table 3
Growth-inhibitory effects of several PEGylated derivatives on HT29 cancer cells and IEC-18 non-tumour cells.

Compd #	HT29	IEC-18
1	16.16 ± 0.92	10.21 ± 0.15
4	16.76 ± 0.01	30.48 ± 2.78
5	10.98 ± 0.23	11.07 ± 0.11
8	11.06 ± 0.08	16.21 ± 0.13
25	17.96 ± 0.42	15.01 ± 0.79
26	14.95 ± 0.08	17.84 ± 1.83
29	16.91 ± 0.78	13.99 ± 0.10
30	15.92 ± 0.06	13.43 ± 0.11

The IC_{50} values (μM) were calculated considering control untreated cells as 100% of viability.

2.5. Characterization of apoptotic effects

Apoptosis is one of the body's most potent defences against cancer. The pathogenesis of many forms of this degenerative disease is closely related to the aberrantly regulated death of apoptotic cells [49]. The level of apoptosis in cancer cells has been considered a leading indicator of the anti-tumour activity of potentially therapeutic substances.

Early events in the apoptotic process include the loss of asymmetry of the plasma membrane, accompanied by translocation of phosphatidylserine (PS) from the leaflet of the inner to the outer membrane, thus exposing PS to the external environment [50]. The phospholipid-binding protein annexin V (An-V) has a high affinity for PS and binds to fluorescently labelled cells with fluorescein isothiocyanate (FITC). The process of determining the degree of apoptosis was performed by double staining with annexin V, conjugated FITC and propidium iodide (PI). Percentages of apoptosis were determined at IC_{50} and IC_{80} concentrations by Annexin V-FITC/PI flow-cytometric analysis on the HT29 cancer-cell line at 24, 48, and 72 h after the addition of the four PEGylated derivatives selected (**4**, **5**, **8**, and **26**; Fig. 2). Prior to the studies of apoptosis, the cytotoxicity of these PEGylated derivatives on the HT29 cell line at 24, 48, and 72 h was analysed (Table 4). The lower IC_{50} values for compounds **4** and **26** were reached at 48 h, with noteworthy differences compared to those registered at 24 h. However, the lower IC_{50} values for compounds **5** and **8** were reached at 72 h, with less pronounced differences than at 24 and 48 h.

Table 4
Growth-inhibitory effects of four PEGylated derivatives on HT29 cancer cells at three different times.

Compd #	HT29 (24 h)	HT29 (48 h)	HT29 (72 h)
4	39.95 ± 0.28	16.41 ± 0.03	16.76 ± 0.01
5	17.81 ± 3,03	12.67 ± 0.17	10.98 ± 0.23
8	14.67 ± 0.25	14.37 ± 0.02	11.06 ± 0.08
26	20.88 ± 1.34	14.24 ± 0.02	14.95 ± 0.08

The IC_{50} values (μM) were calculated considering control untreated cells as 100% of viability.

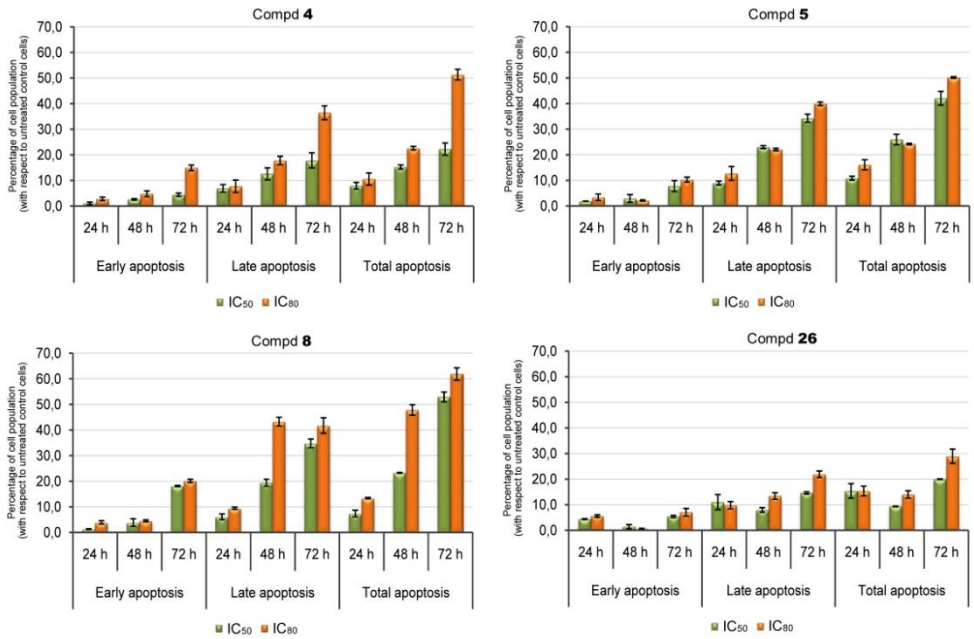

Fig. 2. Flow cytometry analysis of Annexin V-FITC staining and PI accumulation after exposure of HT29 cells to **4**, **5**, **8**, and **26** derivatives for 24, 48, and 72 h. Cell lines were treated at concentrations equal to their IC_{50} and IC_{80} values. Values are expressed as means ± S.E.M. of at least two experiments in duplicate.

The four compounds tested (**4**, **5**, **8**, and **26**) showed apoptotic effects on treated cells, with percentages of total apoptosis (early and late apoptosis) ranging from 20% to 53% relative to control, at 72 h and IC_{50} concentration. While at IC_{80} concentration and for the same time, these percentage results ranged from 29% to 62% relative to control (Fig. 2). Compound **8** achieved the best total apoptosis value (61.9% relative to control) at the IC_{80} concentration. The microscopic optical photographs of Figure 3 shows the apoptotic morphological changes triggered by the selected PEGylated derivatives (**4**, **5**, **8**, and **26**) on HT29 cancer cells at their respective IC_{50} concentrations and at 72 h.

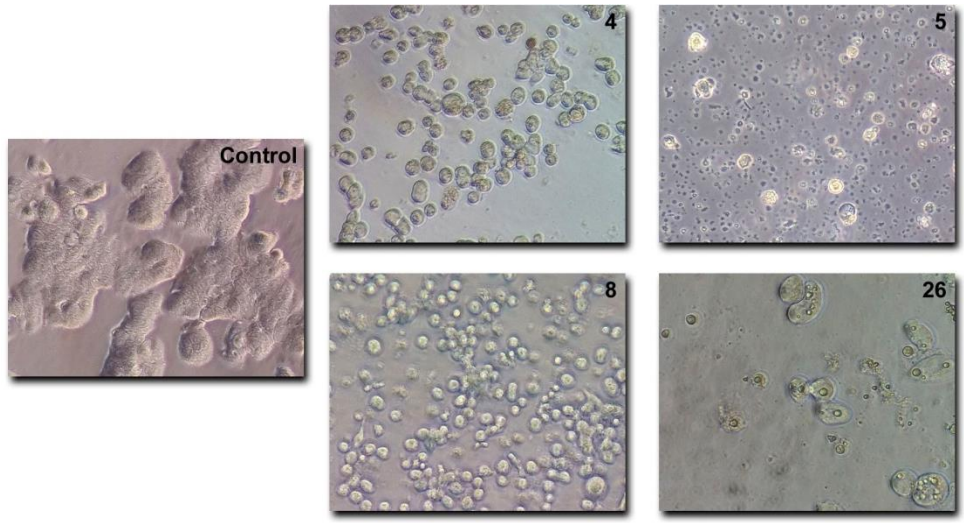

Fig. 3. Morphology changes in HT29 cells. The cells were analysed after exposure 72 h to **4**, **5**, **8**, and **26** derivatives, at its IC_{50} concentrations values. Morphology of cells was examined using optical microscopy.

All assays performed with these compounds showed that the percentages of late apoptosis were higher than those of early apoptosis. Furthermore, in general, the percentages of apoptosis were higher at the IC_{80} concentration than at the IC_{50} concentration, and the percentages of the necrotic population were negligible. The relationship between the percentage of apoptosis and the different times used (24, 48, and 72 h) was clear for compounds **4**, **5**, and **8**, increasing as time progressed. However, this variation in the percentage of apoptosis is not as clear for compound **26**, since a higher percentage was noted at 24 h than at 48 h, although the highest values were reached at 72 h.

The identification of new cytotoxic agents to restore the ability of cancer cells to undergo apoptosis may be a key strategy in new cancer therapies.

2.6. Cell-cycle arrest and distribution

Cell-cycle machinery represents an alternative target for the identification of new biomarkers in the detection and prognosis of cancer [51]. Changes in DNA concentration are characteristic of apoptosis or cell-cycle arrest. The cell cycle was analysed to determine whether the

compounds tested had any effect on cell-cycle progression. Cell percentages were studied in the different phases of the cell cycle, incorporating propidium iodide (PI), to determine a possible cytostatic effect provoked by the cytotoxic response. Thus, HT29 cells were treated with the PEGylated derivatives **4**, **5**, **8**, and **26** at their respective IC_{50} and IC_{80} concentrations, for 24, 48, and 72 h (Fig. 4).

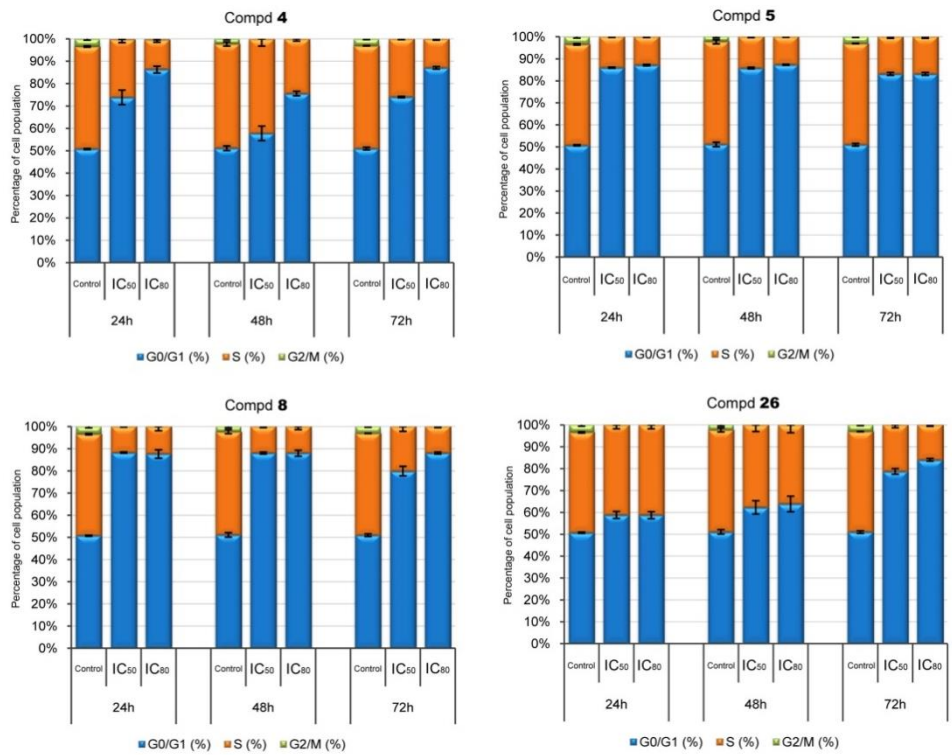

Fig. 4. Percentage of the cell population in each phase of the cell cycle. HT29 cells were treated with **4**, **5**, **8**, and **26** derivatives at their respective IC_{50} and IC_{80} concentrations for 24, 48, and 72 h. Values represent means ± S.E.M. of at least two independent experiments performed in duplicate.

The DNA-histogram analysis revealed that the compounds tested boosted the number of cells in the G0/G1 phase, while concomitantly lowering the number of cells in the phase S, especially in the G2/M phase, with practically 0% of the population. Only compound **4** showed concentration dependence in its response and only compound **26** showed an increase of cells in the G0/G1 phase as time progressed. Larger

differences with respect to control cells were found after 72 h of treatment at their respective IC_{80} concentrations. In this case, control cells showed 51% of the cells in the G0/G1 phase, whereas the PEGylated derivatives tested (**4**, **5**, **8**, and **26**) resulted in 83-88% cells being in the same phase (G0/G1). In addition, these compounds significantly decreased to 12-16% the percentage of cells in the S phase compared to the control (46%). In particular, compound **8** increased the HT29 cell population in the G0/G1 phase to 88% and decreased in the S phase to 12%. These results show that the treatment with these compounds in HT29 cancer cells resulted in cell-cycle arrest in the G0/G1 phase, which could indicate a possible cell-differentiation effect prompted by these compounds.

2.7. Effects on changes in mitochondrial membrane potential

Apoptosis can occur through two essential pathways, one being the intrinsic one, which causes mitochondrial disruption and leads to loss of mitochondrial membrane potential (MMP); by contrast, the induction of apoptosis without MMP changes may suggest the activation of the extrinsic apoptotic pathway.

We analysed the MMP to elucidate the possible mechanism involved in the apoptotic responses of the selected PEGylated derivatives (**4**, **5**, **8**, and **26**) in HT29 cell line at their respective IC_{50} and IC_{80} concentrations, for 24, 48, and 72 h. Changes in MMP were examined by monitoring cell fluorescence after double staining with rhodamine 123 (Rh123) and PI. A negative Rh123 staining suggests an intrinsic apoptotic activation pathway, whereas a positive Rh123 staining an extrinsic apoptotic pathway. All of the compounds assayed (**4**, **5**, **8**, and **26**) showed to a greater extent positive staining of Rh123, for all times and concentrations tested, and therefore neither disrupted the mitochondrial membrane no triggered the loss of MMP. These results suggest an activation of the extrinsic apoptotic pathway for these compounds. Additional molecular studies will be needed to confirm the possible activation of extrinsic apoptosis in response to these PEGylated compounds. The

percentages of the cell population, after 72 h of incubation and at their respective IC_{80} concentrations, are shown in Fig. 5.

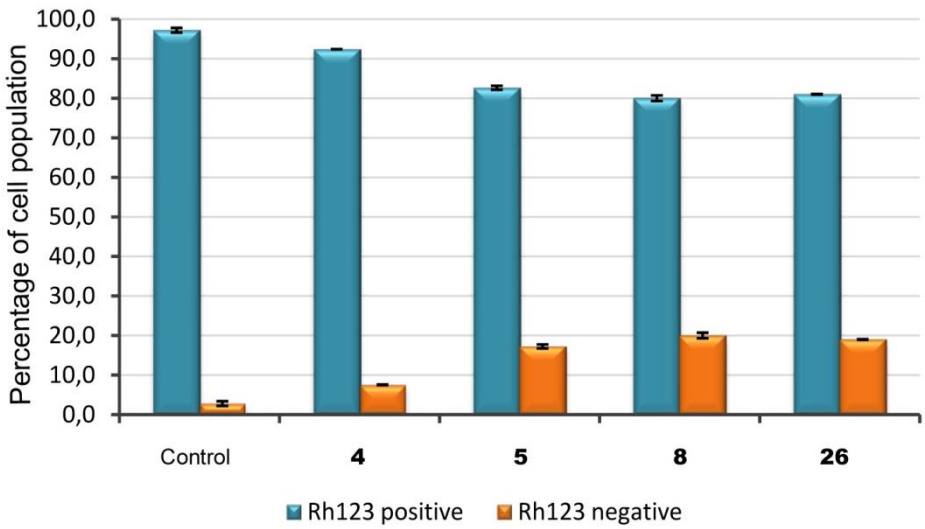

Fig. 5. Flow-cytometry analysis of Rh123 and PI staining after exposure of HT29 cells to **4**, **5**, **8**, and **26** derivatives at their IC_{80} concentrations for 72 h. Rh123 positive cells (blue bars) were rhodamine 123^+ with PI^+ or PI^-. Rh123 negative cells (orange bars) were rhodamine 123^- with PI^- or PI^+. Values are expressed as means ± S.E.M. of at least two experiments in duplicate.

3. Conclusions

A total of 28 PEGylated derivatives of oleanolic and maslinic acids were semi-synthesised to evaluate their antiproliferative effects on three cancer-cell lines (B16-F10, Hep G2, and HT29). A relatively high percentage of these PEGylated derivatives improved the cytotoxicity results of their precursors, registering 62% for B16-F10, 80% for HT29, and 74% for Hep G2. The best results were achieved with the OA derivatives having ethylene glycol or tetra ethylene glycol attached to the C-28 carboxyl group, which were approximately 27-fold more effective than their natural precursor (OA) in the HT29 cell line. Eight of these PEGylated derivatives were selected to compare their cytotoxicity results in the HT29 cancer-cell line with those from a non-tumour cell line from the same tissue (IEC-18), four of which were less cytotoxic in the non-tumour cell line. These four compounds (**4**, **5**, **8**, and **26**) showed apoptotic effects on the HT29 cell line, with total apoptosis percentages with respect to control ranging from 20% to 53%, at 72 h and

IC_{50} concentration, and from 29% to 62%, for the same time and IC_{80} concentration. Compound **8** registered a total apoptosis rate of 61.9%, relative to the control, at the IC_{80} concentration.

All compounds tested (**4**, **5**, **8**, and **26**) in the HT29 cell line resulted in cell-cycle arrest in the G0/G1 phase. The MMP results suggested the activation of the extrinsic pathway during apoptosis of HT29 cancer cells caused by these compounds.

4. Experimental

4.1. General Chemistry

Measurements of NMR spectra were made in VARIAN direct drive (400 and 500 MHz ^{1}H NMR) spectrometers. The ^{13}C chemical shifts were assigned with the aid of distortion less enhancement by polarization transfer (DEPT) using a flip angle of 135°. IR spectra were recorded on a MATTSON SATELLITE FTIR spectrometer. Optical rotations were measured with a Perkin-Elmer 241 polarimeter at 25 °C. The purity of new compounds was determined by a WATERS ACQUITY UPLC system (ultra-performance liquid chromatography), coupled with a WATERS SYNAPT G2 HRMS spectrometer (high-resolution mass spectra), with ESI (electrospray ionization). The purities of all compounds were confirmed to be ≥ 95%. Melting points (mp) were determined using a Kofler (Reichter) apparatus and are uncorrected. All reaction solvents and chromatography solvents were distilled prior to use. Commercially available reagents were used without further purification. Merck silica-gel 60 aluminium sheets (ref. 1.16835) were used for TLC, and spots were rendered visible by spraying with H_2SO_4–AcOH, followed by heating to 120 °C, and also visualized under UV at 254 nm. Merck silica-gel 60 (0.040–0.063 mm, ref. 1.09385) was used for flash chromatography. CH_2Cl_2 (Fisher, ref. D/1852/17), $CHCl_3$ (Fisher, ref. C/4960/17), or n-hexane (Merck, ref. 1.04374), with increasing amounts of Me_2CO (Fisher, ref. A/0600/17), MeOH (Fisher, ref. M/4000/17), or EtOAc (Fisher, ref. E/0900/17), were used as eluents (all the solvents had an analytical reagent-grade purity). The PEG reagents ethylene glycol (CAS Number 107-21-1),

diethylene glycol (CAS Number 111-46-6), triethylene glycol (CAS Number 112-27-6), and tetraethylene glycol (CAS Number 112-60-7) were purchased from Sigma-Aldrich.

4.2. Plant Material

A specimen of the plant of *Olea europaea* (order Lamiales, family Oleaceae) was collected in Almegíjar, Granada, Spain in May 2001. This plant was identified by Laura Baena from the herbarium of the University of Granada. A voucher specimen (53489-1-1) was deposited at the University of Granada Herbarium (GDA), Granada, Spain.

4.3. Isolation of OA (I) and MA (II)

OA (**I**) and MA (**II**) were isolated from solid olive-oil-production wastes, which were extracted successively in a Soxhlet with hexane and EtOAc. Hexane extracts were a mixture of OA and MA (80:20), whereas this relationship was (20:80) for the EtOAc extracts. Both products were purified from these mixtures by column chromatography over silica gel, eluting with a $CHCl_3$–MeOH or CH_2Cl_2–Me_2CO mixtures of increasing polarity [52]. These natural compounds can also be extracted more efficiently using an alternative method such as microwave-assisted extraction [42].

4.4. Synthesis of OA and MA derivatives

4.4.1. 3β-Acetoxyolean-12-en-28-oic acid (OA-Ac, III)

Ac_2O (1 mL) was slowly added to a solution of OA (**I**, 1368 mg, 3 mmol) in pyridine (10 mL). The reaction was stirred at reflux for 1 h, and then cold water was added. This reaction mixture was extracted with CH_2Cl_2 and the organic layer was dried with dry Na_2SO_4. The solvent was removed under reduced pressure and the residue was purified by column chromatography using CH_2Cl_2–Me_2CO (10:1) to give OA-Ac (**III**) as a white solid (95%) [43].

4.4.2. 2α,3β-Diacetoxyolean-12-en-28-oic acid (MA-Ac, IV)

Ac_2O (2 mL) was slowly added to a solution of MA (**II**, 1416 mg, 3 mmol) in pyridine (10 mL). The reaction was stirred at reflux for 1 h, and then cold water was added. This reaction mixture was extracted with CH_2Cl_2 and the organic layer was dried with dry Na_2SO_4. The solvent was removed under reduced pressure and the residue was purified by column chromatography using CH_2Cl_2–Me_2CO (10:1) to give MA-Ac (**IV**) as a white solid (90%) [44].

4.4.3. Benzyl oleanolate (OA-Bn, V)

BnCl (418 µL) was added in a relationship of 2:1 to a solution of OA (**I**, 912 mg, 2 mmol) in DMF (8 mL) with K_2CO_3 (0.61 g). The reaction was stirred for 4 h at 55 °C. The mixture was diluted with water and extracted with CH_2Cl_2, and the organic layer dried with dry Na_2SO_4. The solvent was removed under reduced pressure, and the residue was purified by column chromatography using CH_2Cl_2–Me_2CO (10:1) to give OA-Bn (**V**) as a white solid (710 mg, 83%)[45].

4.4.4. Benzyl maslinate (MA-Bn, VI)

BnCl (418 µL) was added in a relationship of 2:1 to a solution of MA (**II**, 944 mg, 2 mmol) in DMF (8 mL) with K_2CO_3 (0.61 g). The reaction was stirred for 4 h at 55 °C. The mixture was diluted with water and extracted with CH_2Cl_2, and the organic layer dried with dry Na_2SO_4. The solvent was removed under reduced pressure, and the residue was purified by column chromatography using CH_2Cl_2–Me_2CO (10:1) to give MA-Bn (**VI**) as a white solid (690 mg, 81%)[46].

4.5. PEGylation reactions on the C-28 carboxylic group of compounds I-IV

DIEA (0.3 mmol) and TBTU (0.66 mmol) were added to four solutions of compounds **I**, **II**, **III**, or **IV** (0.44 mmol of each) in THF (20 mL each). The reaction mixtures were maintained at room temperature for 12 h and then diluted with water and extracted three times with CH_2Cl_2. The organic layers

were dried with dry Na_2SO_4 and the solvent was removed under reduced pressure. Finally, each residue was purified by column chromatography using hexane/EtOAc as eluents, yielding the corresponding TBTU derivatives [41]. K_2CO_3 (1.0 mmol) and the corresponding ethylene glycol reagent (3.5 mmol of mono-, di-, tri, or tetraethylene glycol) were then added to 4 solutions of the TBTU derivatives (0.35 mmol of each) in 1,4-dioxane (15 mL each). Each reaction mixture was stirred at reflux for 12 h, and CH_2Cl_2 was then added to each mixture reaction and washed several times with water. The organic layer was dried with dry Na_2SO_4 and the solvent was removed under reduced pressure. Finally, each residue was purified by column chromatography, using hexane–EtOAc as eluents and, therefore, the PEGylated derivatives **1**-**16** were obtained, respectively, with percentages of between 79% and 83%.

4.5.1. 2-Hydroxyethyl oleanolate (1)

White solid, yield 82%, mp 131–133 °C; $[a]_D$ +39 (c 1 in $CHCl_3$); IR (KBr) ν_{max} 3431, 2950, 1737, 1455, 1365, 1228, 1029 cm^{-1}; δ_H ($CDCl_3$, 500 MHz): 5.30 (dd, 1H, J_1 = J_2 = 3.5 Hz, H-12), 4.22–4.11 (m, 2H, CH_2 PEG group), 3.81–3.78 (m, 2H, CH_2 PEG group), 3.21 (dd, 1H, J_1 = 4.5 Hz, J_2 = 11.5 Hz, H-3), 2.87 (dd, 1H, J_1 = 4.5 Hz, J_2 = 14.0 Hz, H-18), 1.14, 0.98, 0.93, 0.90, 0.89, 0.77, 0.74 (s, 3H each, methyl groups); δ_C ($CDCl_3$, 125 MHz): 178.3 (C-28), 144.3 (C-13), 122.5 (C-12), 79.2 (C-3), 66.2, 61.6 (CH_2 PEG group), 55.4 (C-5), 47.7 (C-9), 47.1 (C-17), 45.9 (C-19), 42.0 (C-14), 41.6 (C-18), 39.5 (C-8), 38.9 (C-4), 38.6 (C-1), 38.6 (C-10), 34.0 (C-21), 33.2 (Me), 32.9 (C-7), 32.6 (C-22), 30.9 (C-20), 28.3 (Me), 27.8 (C-15), 27.3 (C-2), 26.0 (Me), 23.8 (C-11), 23.8 (Me), 23.2 (C-16), 18.5 (C-6), 17.2 (Me), 15.7 (Me), 15.5 (Me); ESI-HRMS *m/z* calcd for $C_{32}H_{53}O_4$ $[M+1]^+$ 501.3944, found 501.3956.

4.5.2. 5-Hydroxy-3-oxapentyl oleanolate (2)

White solid, yield 81%, mp 134–136 °C; $[a]_D$ +28 (c 1 in $CHCl_3$); IR (KBr) ν_{max} 3391, 2930, 1738, 1441, 1366, 1216, 1027 cm^{-1}; δ_H ($CDCl_3$, 500 MHz): 5.30 (dd, 1H, J_1 = J_2 = 3.6 Hz, H-12), 4.24–4.16 (m, 2H, CH_2 PEG group), 3.73–3.57 (m, 6H, CH_2 PEG group), 3.20 (dd, 1H, J_1 = 4.8 Hz, J_2 = 11.2 Hz, H-3), 2.87 (dd, 1H, J_1 =

4.2 Hz, J_2 = 13.8 Hz, H-18), 1.13, 0.98, 0.91, 0.90, 0.89, 0.78, 0.73 (s, 3H each, methyl groups); δ_C ($CDCl_3$, 125 MHz): 177.5 (C-28), 144.0 (C-13), 122.3 (C-12), 79.1 (C-3), 72.0, 69.0, 63.1, 61.6 (CH_2 PEG group), 55.1 (C-5), 47.4 (C-9), 46.6 (C-17), 45.7 (C-19), 41.5 (C-14), 41.1 (C-18), 39.2 (C-8), 38.6 (C-4), 38.3 (C-1), 36.9 (C-10), 33.7 (C-21), 32.9 (C-7), 32.6 (Me), 32.3 (C-22), 30.5 (C-20), 27.9 (Me), 27.5 (C-15), 27.0 (C-2), 25.7 (Me), 23.4 (C-11), 23.4 (Me), 23.0 (C-16), 18.2 (C-6), 16.8 (Me), 15.4 (Me), 15.1 (Me); ESI-HRMS *m/z* calcd for $C_{34}H_{57}O_5$ $[M+1]^+$ 545.4206, found 545.4212.

4.5.3. 8-Hydroxy-3,6-dioxaoctyl oleanolate (3)

Transparent syrup, yield 80%; $[a]_D$ +38 (*c* 1 in $CHCl_3$); IR (film) ν_{max} 3432, 2927,1723, 1461, 1385, 1235, 1045 cm^{-1}; δ_H ($CDCl_3$, 500 MHz): 5.23 (dd, 1H, $J_1 = J_2$ = 3.5 Hz, H-12), 4.17–4.12 (m, 2H, CH_2 PEG group), 3.69–3.55 (m, 10H, CH_2 PEG group), 3.16 (dd, 1H, J_1 = 4.8 Hz, J_2 = 11.3 Hz, H-3), 2.82 (dd, 1H, J_1 = 4.3 Hz, J_2 = 13.8 Hz, H-18), 1.10, 0.93, 0.87, 0.85, 0.84, 0.73, 0.68 (s, 3H each, methyl groups); δ_C ($CDCl_3$, 125 MHz): 177.7 (C-28), 143.7 (C-13), 122.4 (C-12), 78.9 (C-3), 72.6, 70.6, 70.4, 69.2, 63.3, 61,7 (CH_2 PEG group), 55.3 (C-5), 47.6 (C-9), 46.7 (C-17), 45.9 (C-19), 41.3 (C-14), 41.3 (C-18), 39.4 (C-8), 38.8 (C-4), 38.5 (C-1), 37.0 (C-10), 33.9 (C-21), 33.1 (Me), 32.8 (C-7), 32.4 (C-22), 30.7 (C-20), 28.2 (Me), 27.7 (C-15), 27.2 (C-2), 25.9 (Me), 23.6 (Me), 23.4 (C-11), 23.0 (C-16), 18.4 (C-6), 17.7 (Me), 15.7 (Me), 15.4 (Me); ESI-HRMS *m/z* calcd for $C_{36}H_{61}O_6$ $[M+1]^+$ 589.4468, found 589.4439.

4.5.4. 11-hydroxy-3,6,9-trioxaundecyl oleanolate (4)

Transparent syrup, yield 80%; $[a]_D$ +41 (*c* 1 in $CHCl_3$); IR (film) ν_{max} 3455, 2926, 1725, 1455, 1365, 1202, 1046 cm^{-1}; δ_H ($CDCl_3$, 400 MHz): 5.30 (dd, 1H, $J_1 = J_2$ = 3.4 Hz, H-12), 4.19–4.14 (m, 2H, CH_2 PEG group), 3.72–3.58 (m, 14 H, CH_2 PEG group), 3.20 (dd, 1H, J_1 = 5.0 Hz, J_2 = 11.0 Hz, H-3), 2.86 (dd, 1H, J_1 = 4.2 Hz, J_2 = 13.9 Hz, H-18), 1.11, 0.97, 0.90, 0.88, 0.87, 0.76, 0.71 (s, 3H each, methyl groups); δ_C ($CDCl_3$, 100 MHz): 177.7 (C-28), 143.8 (C-13), 122.5 (C-12), 79.1 (C-3), 72.6, 70.8, 70.7, 70.7, 70.5, 69.3, 63.4, 61.8 (CH_2 PEG group), 55.3 (C-5), 47.7 (C-9), 46.8 (C-17), 46.0 (C-19), 41.8 (C-14), 41.4 (C-18), 39.4 (C-8), 38.9

(C-4), 38.6 (C-1), 37.1 (C-10), 34.0 (C-21), 33.2 (Me), 32.9 (C-7), 32.5 (C-22), 30.8 (C-20), 28.2 (Me), 27.8 (C-15), 27.3 (C-2), 26.0 (Me), 23.7 (Me), 23.5 (C-11), 23.1 (C-16), 18.4 (C-6), 17.1 (Me), 15.7 (Me), 15.4 (Me); ESI-HRMS *m/z* calcd for $C_{38}H_{65}O_7$ [M+1]$^+$ 633.4730, found 633.4737.

4.5.5. 2-Hydroxyethyl maslinate (5)

White solid, yield 83%,mp 170–172 °C; $[a]_D$ +42 (*c* 1 in $CHCl_3$); IR (KBr) ν_{max} 3281, 2944, 1724, 1453, 1385, 1228, 1034 cm^{-1}; δ_H ($CDCl_3$, 400 MHz): 5.30 (dd, 1H, $J_1 = J_2 = 5.2$ Hz, H-12), 4.21–4.13 (m, 2H, CH_2 PEG group), 3.79–3.76 (m, 2H, CH_2 PEG group), 3.67 (ddd, 1H, $J_1 = 4.0$ Hz, $J_2 = 9.2$ Hz, $J_3 = 14.4$ Hz, H-2), 2.98 (dd, 1H, $J_1 = 9.2$ Hz, H-3), 2.86 (dd, 1H, $J_1 = 4.2$ Hz, $J_2 = 13.8$ Hz, H-18), 1.13, 1.00, 0.96, 0.92, 0.90, 0.80, 0.73 (s, 3H each, methyl groups); δ_C ($CDCl_3$, 100 MHz): 178.3 (C-28), 144.2 (C-13), 122.3 (C-12), 84.0 (C-3), 69.0 (C-2), 66.1, 61.5 (CH_2 PEG group), 55.4 (C-5), 47.7 (C-9), 47.0 (C-17), 46.5 (C-1), 45.9 (C-19), 41.9 (C-14), 41.6 (C-18), 39.5 (C-8), 39.3 (C-4), 38.4 (C-10), 33.9 (C-21), 33.2 (Me), 32.7 (C-7), 32.6 (C-22), 30.8 (C-20), 28.8 (Me), 27.7 (C-15), 26.0 (Me), 23.8 (Me), 23.6 (C-11), 23.1 (C-16), 18.5 (C-6), 17.2 (Me), 16.9 (Me), 16.7 (Me); ESI-HRMS *m/z* calcd for $C_{32}H_{53}O_5$ [M+1]$^+$ 517.3893, found 517.3887.

4.5.6. 5-Hydroxy-3-oxapentyl maslinate (6)

White solid, yield 81%, mp 78–80 °C; $[a]_D$ +40 (*c* 1 in $CHCl_3$); IR (KBr) ν_{max} 3372, 2940, 1723, 1455, 1363, 1259, 1048 cm^{-1}; δ_H ($CDCl_3$, 400 MHz): 5.27 (dd, 1H, $J_1 = J_2 = 3.5$ Hz, H-12), 4.22–4.15 (m, 2H, CH_2 PEG group), 3.72–3.57 (m, 6H, CH_2 PEG group), 3.67 (m, 1H, H-2), 2.98 (dd, 1H, $J_1 = 9.5$ Hz, H-3), 2.85 (dd, 1H, $J_1 = 4.0$ Hz, $J_2 = 14.0$ Hz, H-18), 1.12, 1.00, 0.96, 0.91, 0.89, 0.80, 0.72 (s, 3H each, methyl groups); δ_C ($CDCl_3$, 100 MHz): 177.8 (C-28), 143.4 (C-13), 122.4 (C-12), 83.9 (C-3), 72.3, 69.0, 63.4, 61.9 (CH_2 PEG group), 69.3 (C-2), 55.4 (C-5), 47.7 (C-9), 46.8 (C-17), 46.5 (C-1), 45.9 (C-19), 41.9 (C-14), 41.4 (C-18), 39.5 (C-8), 39.3 (C-4), 38.4 (C-10), 34.0 (C-21), 33.2 (Me), 32.7 (C-7), 32.5 (C-22), 30.8 (C-20), 28.7 (Me), 27.7 (C-15), 26.0 (Me), 23.7 (Me), 23.6 (C-11), 23.1 (C-16), 18.5 (C-6), 17.2 (Me), 16.9 (Me), 16.7 (Me); ESI-HRMS *m/z* calcd for $C_{34}H_{57}O_6$ [M+1]$^+$ 561.4155, found 561.4155.

4.5.7. 8-Hydroxy-3,6-dioxaoctyl maslinate (7)

White solid, yield 81%, mp 97–99 °C; $[a]_D$ +31 (*c* 1 in $CHCl_3$); IR (KBr) ν_{max} 3280, 2942, 1729, 1466, 1258, 1056, 1033 cm^{-1}; δ_H ($CDCl_3$, 500 MHz): 5.30 (dd, 1H, $J_1 = J_2 = 3.5$ Hz, H-12), 4.22–4.14 (m, 2H, CH_2 PEG group), 3.72–3.58 (m, 10H, CH_2 PEG group), 3.66 (m, 1H, H-2), 2.97 (dd, 1H, $J_1 = 9.5$ Hz, H-3), 2.85 (dd, 1H, $J_1 = 3.8$ Hz, $J_2 = 14.0$ Hz, H-18), 1.11, 1,00, 0.96, 0.91, 0.89, 0.80, 0.71 (s, 3H each, methyl groups); δ_C ($CDCl_3$,125 MHz): 177.7 (C-28), 143.8 (C-13), 122.3 (C-12), 83.9 (C-3), 72.7, 70.7, 70.5, 69.0, 63.3, 61.8, (CH_2 PEG group), 69.3 (C-2), 55.4 (C-5), 47.7 (C-9), 46.8 (C-17), 46.5 (C-1), 45.9 (C-19), 41.8 (C-14), 41.4 (C-18), 39.5 (C-8), 39.3 (C-4), 38.4 (C-10), 34.0 (C-21), 33.2 (Me), 32.7 (C-7), 32.5 (C-22), 30.8 (C-20), 28.7 (Me), 27.7 (C-15), 26.0 (Me), 23.7 (Me), 23.6 (C-11), 23.1 (C-16), 18.5 (C-6), 17.1 (Me), 16.9 (Me), 16.7 (Me); ESI-HRMS *m/z* calcd for $C_{36}H_{61}O_7$ $[M+1]^+$ 605.4417, found 605.4437.

4.5.8. 11-Hydroxy-3,6,9-trioxaundecyl maslinate (8)

White solid, yield 80%,mp 75–77 °C; $[a]_D$ +38 (*c* 1 in $CHCl_3$); IR (KBr) ν_{max} 3275, 2969, 1737, 1725, 1453, 1365, 1203 cm^{-1}; δ_H ($CDCl_3$, 500 MHz): 5.26 (dd, 1H, $J_1 = J_2 = 3.0$ Hz, H-12), 4.21–4.14 (m, 2H, CH_2 PEG group), 3.72–3.60 (m, 14 H, CH_2 PEG group), 3.63 (m, 1H, H-2), 2.96 (dd, 1H, $J_1 = 9.5$ Hz, H-3), 2.86 (dd, 1H, $J_1 = 2.5$ Hz, $J_2 = 13.0$ Hz, H-18), 1.11, 1.00, 0.95, 0.90, 0.88, 0.80, 0.71 (s, 3H each, methyl groups); δ_C ($CDCl_3$, 125 MHz): 177.7 (C-28), 143.8 (C-13), 122.3 (C-12), 83.9 (C-3), 72.7, 70.7, 70.6, 70.6, 70.4, 69.2, 63.4, 61.8 (CH_2 PEG group), 69.0 (C-2), 55.4 (C-5), 47.7 (C-9), 46.8 (C-17), 46.4 (C-1), 45.9 (C-19), 41.8 (C-14), 41.4 (C-18), 39.5 (C-8), 39.3 (C-4), 38.4 (C-10), 34.0 (C-21), 33.2 (Me), 32.7 (C-7), 32.5 (C-22), 30.8 (C-20), 28.8 (Me), 27.7 (C-15), 26.0 (Me), 23.7 (Me), 23.6 (C-11), 23.0 (C-16), 18.5 (C-6), 17.1 (Me), 16.9 (Me), 16.7 (Me); ESI-HRMS *m/z* calcd for $C_{38}H_{65}O_8$ $[M+1]^+$ 649.4679, found 649.4673.

4.5.9. 2-Hydroxyethyl 3β-acetoxyolean-12-en-28-oate (9)

White solid, yield 81%,mp 143–145 °C; $[a]_D$ +44 (*c* 1 in $CHCl_3$); IR (KBr) ν_{max} 2970, 2927, 1738, 1441, 1365, 1217, 1229 cm^{-1}; δ_H ($CDCl_3$, 500 MHz): 5.30 (dd, 1H, $J_1 = J_2 = 3.5$ Hz, H-12), 4.48 (dd, 1H, $J_1 = 7.0$ Hz, $J_2 = 8.5$ Hz, H-3), 4.21–

4.13 (m, 2H, CH_2 PEG group), 3.82–3.77 (m, 2H, CH_2 PEG group), 2.86 (dd, 1H, J_1 = 4.3 Hz, J_2 = 13.7 Hz, H-18), 2.03 (s, 3H, acetyl group), 1.13, 0.91, 0.91, 0.90, 0.86, 0.84, 0.74 (s, 3H each, methyl groups); δ_C ($CDCl_3$, 125 MHz): 178.3 (C-28), 171.2 (CO acetyl group), 144.2 (C-13), 122.4 (C-12), 81.0 (C-3), 66.2, 61.6 (CH_2 PEG group), 55.4 (C-5), 47.7 (C-9), 47.1 (C-17), 45.9 (C-19), 41.9 (C-14), 41.6 (C-18), 39.5 (C-8), 38.3 (C-1), 37.8 (C-4), 37.0 (C-10), 33.9 (C-21), 33.2 (Me), 32.8 (C-7), 32.6 (C-22), 30.8 (C-20), 28.2 (Me), 27.8 (C-15), 26.0 (Me), 23.8 (Me), 23.6 (C-2), 23.5 (C-11), 23.2 (C-16), 21.4 (CH_3 acetyl group), 18.3 (C-6), 17.2 (Me), 16.8 (Me), 15.5 (Me); ESI-HRMS *m*/z calcd for $C_{34}H_{54}O_5Na$ $[M+Na]^+$ 565.3869, found 565.3854.

4.5.10. 5-Hydroxy-3-oxapentyl 3β-acetoxyolean-12-en-28-oate (10)

White solid, yield 81%, mp 144–146 °C; $[a]_D$ +43 (*c* 1 in $CHCl_3$); IR (KBr) ν_{max} 2929, 1725, 1440, 1468, 1362, 1239, 1022 cm^{-1}; δ_H ($CDCl_3$, 400 MHz): 5.27 (dd, 1H, J_1 = J_2 = 3.4 Hz, H-12), 4.48 (dd, 1H, J_1 = 6.4 Hz, J_2 = 12.4 Hz, H-3), 4.24–4.13 (m, 2H, CH_2 PEG group), 3.72–3.57 (m, 6H, CH_2 PEG group), 2.85 (dd, 1H, J_1 = 4.2 Hz, J_2 = 13.8 Hz, H-18), 2.02 (s, 3H, acetyl group), 1.11, 0.91, 0.90, 0.88, 0.85, 0.84, 0.72 (s, 3H each, methyl groups); δ_C ($CDCl_3$, 100 MHz): 177.8 (C-28), 171.1 (CO acetyl group), 143.8 (C-13), 122.5 (C-12), 81.0 (C-3), 72.3, 69.3, 63.4, 61.9 (CH_2 PEG group), 55.4 (C-5), 47.6 (C-9), 46.9 (C-17), 45.9 (C-19), 41.8 (C-14), 41.4 (C-18), 39.5 (C-8), 38.2 (C-1), 37.8 (C-4), 37.0 (C-10), 34.0 (C-21), 33.2 (Me), 32.8 (C-7), 32.5 (C-22), 30.8 (C-20), 28.1 (Me), 27.7 (C-15), 26.0 (Me), 23.7 (Me), 23.6 (C-2), 23.5 (C-11), 23.1 (C-16), 21.4 (CH_3 acetyl group), 18.3 (C-6), 17.1 (Me), 16.8 (Me), 15.5 (Me); ESI-HRMS *m*/z calcd for $C_{36}H_{58}O_6Na$ $[M+Na]^+$ 609.4131, found 609.4128.

4.5.11. 8-Hydroxy-3,6-dioxaoctyl 3β-acetoxyolean-12-en-28-oate (11)

White solid, yield 80%, mp 73–75 °C; $[a]_D$ +40 (*c* 1 in $CHCl_3$); IR (KBr) ν_{max} 2941, 2970, 1738, 1440, 1365, 1229, 1216 cm^{-1}; δ_H ($CDCl_3$, 400 MHz): 5.26 (dd, 1H, J_1 = J_2 = 3.4 Hz, H-12), 4.46 (dd, 1H, J_1 = 8.0 Hz, J_2 = 16.0 Hz, H-3), 4.20–4.14 (m, 2H, CH_2 PEG group), 3.72–3.57 (m, 10H, CH_2 PEG group), 2.84 (dd, 1H, J_1 = 3.2 Hz, J_2 = 10.8 Hz, H-18), 2.02 (s, 3H, acetyl group), 1.10, 0.90, 0.89, 0.87,

0.84, 0.83, 0.71 (s, 3H each, methyl groups); δ_C ($CDCl_3$, 100 MHz): 177.7 (C-28), 171.1 (CO acetyl group), 143.8 (C-13), 122.4 (C-12), 81.0 (C-3), 72.6, 70.7, 70.5, 69.3, 63.3, 61.9 (CH_2 PEG group), 55.4 (C-5), 47.6 (C-9), 46.8 (C-17), 45.9 (C-19), 41.8 (C-14), 41.4 (C-18), 39.4 (C-8), 38.2 (C-1), 37.8 (C-4), 37.0 (C-10), 33.9 (C-21), 33.2 (Me), 32.8 (C-7), 32.4 (C-22), 30.8 (C-20), 28.1 (Me), 27.7 (C-15), 25.9 (Me), 23.7 (Me), 23.6 (C-2), 23.5 (C-11), 23.1 (C-16), 21.4 (CH_3 acetyl group), 18.3 (C-6), 17.1 (Me), 16.8 (Me), 15.5 (Me); ESI-HRMS *m/z* calcd for $C_{38}H_{62}O_7Na$ $[M+Na]^+$ 653.4393, found 653.4399.

4.5.12. 11-Hydroxy-3,6,9-trioxaundecyl 3β-acetoxyolean-12-en-28-oate(12)

Transparent syrup, yield 79%; $[a]_D$ +32 (*c* 1 in $CHCl_3$); IR (film) ν_{max} 3281, 2944, 1724, 1453, 1385, 1228, 1034 cm^{-1}; δ_H ($CDCl_3$, 400 MHz): 5.27 (dd, 1H, $J_1 = J_2$ = 3.4 Hz, H-12), 4.48 (dd, 1H, J_1 = 8.4 Hz, J_2 = 16.0 Hz, H-3), 4.20–4.10 (m, 2H, CH_2 PEG group), 3.73–3.60 (m, 14H, CH_2 PEG group), 2.85 (dd, 1H, J_1 = 4.2 Hz, J_2 = 13.8 Hz, H-18), 2.03 (s, 3H, acetyl group), 1.12, 0.92, 0.91, 0.89, 0.85, 0.84, 0.72 (s, 3H each, methyl groups); δ_C ($CDCl_3$, 100 MHz): 177.7 (C-28), 171.1 (CO acetyl group), 143.8 (C-13), 122.5 (C-12), 81.0 (C-3), 72.6, 70.8, 70.8, 70.7, 70.5, 69.3, 63.4, 61.9 (CH_2 PEG group), 55.4 (C-5), 47.7 (C-9), 46.8 (C-17), 46.0 (C-19), 41.8 (C-14), 41.4 (C-18),39.5 (C-8), 38.3 (C-1), 37.8 (C-4), 37.1 (C-10), 34.0 (C-21), 33.2 (Me), 32.8 (C-7), 32.5 (C-22), 30.8 (C-20), 28.2 (Me), 27.8 (C-15), 26.0 (Me), 23.8 (Me), 23.7 (C-2), 23.6 (C-11), 23.1 (C-16), 21.4 (CH_3 acetyl group), 18.4 (C-6), 17.1 (Me), 16.8 (Me), 15.5 (Me); ESI-HRMS *m/z* calcd for $C_{40}H_{67}O_8$ $[M+1]^+$ 675.4836, found 675.4835.

4.5.13. 2-Hydroxyethyl 2a,3β-diacetoxyolean-12-en-28-oate (13)

White solid, yield 82%, mp 100–102 °C; $[a]_D$ +13 (*c* 1 in $CHCl_3$); IR (KBr) ν_{max} 2949, 1744, 1451, 1366, 1230,1257, 1030 cm^{-1}; δ_H ($CDCl_3$, 500 MHz): 5.29 (dd, 1H, $J_1 = J_2$ = 3.5 Hz, H-12), 5.08 (1H, ddd, J_1 = 4.5 Hz, J_2 = 10.0 Hz, J_3 = 15.0 Hz, H-2), 4.73 (d, 1H, J = 10.0 Hz, H-3), 4.21–4.10 (m, 2H, CH_2 PEG group), 3.82–3.76 (m, 2H, CH_2 PEG group), 2.90 (dd, 1H, J_1 = 4.3 Hz, J_2 = 13.8 Hz, H-18), 2.04 and 2.0 (s, 3H each, acetyl group), 1.12, 1.04, 0.92, 0.90, 0.90, 0.89, 0.74 (s, 3H each, methyl groups); δ_C ($CDCl_3$, 125 MHz): 178.2 (C-28), 171.0, 170.6 (CO

acetyl groups), 144.3 (C-13), 122.1 (C-12), 80.8 (C-3), 70.1 (C-2), 66.2, 61.6 (CH_2 PEG group), 55.5 (C-5), 47.6 (C-9), 47.0 (C-17), 46.0 (C-19), 44.0 (C-1), 41.9 (C-14), 41.6 (C-18), 39.5 (C-4), 39.5 (C-10), 38.3 (C-8), 34.0 (C-21), 33.2 (Me), 32.6 (C-7), 32.6 (C-22), 30.8 (C-20), 28.6 (Me), 27.7 (C-15), 26.0 (Me), 23.7 (Me), 23.6 (C-11), 23.1 (C-16), 21.3, 21.0 (CH_3 acetyl groups), 18.3 (C-6), 17.8 (Me), 17.1 (Me), 16.6 (Me); ESI-HRMS *m/z* calcd for $C_{36}H_{56}O_7Na$ $[M+Na]^+$ 623.3924, found 623.3918.

4.5.14. 5-Hydroxy-3-oxapentyl 2a,3β-diacetoxyolean-12-en-28-oate (14)

White solid, yield 82%,mp 60–62 °C; $[a]_D$ +6 (c 1 in $CHCl_3$); IR (KBr) ν_{max} 2970,1738, 1435, 1365, 1229, 1217 cm^{-1}; δ_H ($CDCl_3$, 400 MHz): 5.28 (dd, 1H, J_1 = J_2 = 3.8 Hz, H-12), 5.09 (ddd, 1H, J_1 = 4.8 Hz, J_2 = 10.4 Hz, J_3 = 15.2 Hz , H-2), 4.74 (d, 1H, *J* = 10.4 Hz, H-3), 4.26–4.13 (m, 2H, CH_2 PEG group), 3.74–3.56 (m, 6H, CH_2 PEG group), 2.87 (dd, 1H, J_1 = 3.6 Hz, J_2 = 14.0 Hz, H-18), 2.05 and 1.98 (s, 3H each, acetyl group), 1.12, 1.05, 0.98, 0.91, 0.90, 0.89, 0.73 (s, 3H each, methyl groups); δ_C ($CDCl_3$, 100 MHz): 177.8 (C-28), 171.0, 170.7 (CO acetyl groups), 143.9 (C-13), 122.2 (C-12), 80.8 (C-3), 72.3, 69.3, 63.4, 62.0 (CH_2 PEG group), 70.2 (C-2), 55.0 (C-5), 47.7 (C-9), 46.9 (C-17), 46.0 (C-19), 44.0 (C-1), 41.9 (C-14), 41.4 (C-18), 39.5 (C-4), 39.5 (C-10), 38.3 (C-8), 34.0 (C-21), 33.2 (Me), 32.6 (C-7), 32.5 (C-22), 30.8 (C-20), 28.6 (Me), 27.7 (C-15), 26.0 (Me), 23.7 (Me), 23.6 (C-11), 23.1 (C-16), 21.3, 21.1 (CH_3 acetyl groups), 18.4 (C-6), 17.8 (Me), 17.1 (Me), 16.6 (Me); ESI-HRMS *m/z* calcd for $C_{38}H_{60}O_8Na$ $[M+Na]^+$ 667.4186, found 667.4178.

4.5.15. 8-Hydroxy-3,6-dioxaoctyl 2a,3β-diacetoxyolean-12-en-28-oate (15)

Transparent syrup, yield 80%; $[a]_D$ +5 (c 1 in $CHCl_3$); IR (film)ν_{max} 2970, 1738, 1454, 1366, 1230, 1121, 1031 cm^{-1}; δ_H ($CDCl_3$, 500 MHz): 5.27 (dd, 1H, J_1 = J_2 = 3.8 Hz, H-12), 5.08 (ddd, 1H, J_1 = 5.0 Hz, J_2 = 10.5 Hz, J_3 = 15.5 Hz , H-2), 4.73 (d, 1H, *J*= 10.5 Hz, H-3), 4.24–4.14 (m, 2H, CH_2 PEG group), 3.75–3.59 (m, 10H, CH_2 PEG group), 2.86 (dd, 1H, J_1 = 4.2 Hz, J_2 = 14.2 Hz, H-18), 2.04 and 1.97 (s, 3H each, acetyl group), 1.11, 1.04, 0.91, 0.90, 0.89, 0.88, 0.72 (s, 3H, each, methyl groups); δ_C ($CDCl_3$, 125 MHz): 177.7 (C-28), 171.0, 170.7 (CO acetyl groups),

143.9 (C-13), 122.1 (C-12), 80.8 (C-3), 72.6, 70.7, 70.6, 69.3, 63.4, 61.9 (CH_2 PEG group), 70.1 (C-2), 55.0 (C-5), 47.7 (C-9), 46.8 (C-17), 45.9 (C-19), 44.0 (C-1), 41.9 (C-14), 41.4 (C-18), 39.5 (C-4), 39.5 (C-10), 38.3 (C-8), 34.0 (C-21), 33.2 (Me), 32.6 (C-7), 32.5 (C-22), 30.8 (C-20), 28.6 (Me), 27.7 (C-15), 25.9 (Me), 23.7 (Me), 23.6 (C-11), 23.1 (C-16), 21.3, 21.0 (CH_3 acetyl groups), 18.4 (C-6), 17.8 (Me), 17.1 (Me), 16.6 (Me); ESI-HRMS *m/z* calcd for $C_{40}H_{64}O_9Na$ $[M+Na]^+$ 711.4448, found 771.4454.

4.5.16. 11-Hydroxy-3,6,9-trioxaundecyl 2α,3β-diacetoxyolean-12-en-28-oate (16)

Transparent syrup, yield 79%; $[\alpha]_D$ +7 (c 1 in $CHCl_3$); IR (film) ν_{max} 2969, 1738, 1455, 1366, 1230, 1120, 1063, 1031 cm^{-1}; δ_H ($CDCl_3$, 500 MHz): 5.26 (dd, 1H, $J_1 = J_2 = 3.2$ Hz, H-12), 5.08 (1H, ddd, $J_1 = 4.5$ Hz, $J_2 = 10.5$ Hz, $J_3 = 15.5$ Hz , H-2), 4.73 (d, 1H, $J = 10.5$ Hz, H-3), 4.21–4.10 (m, 2H, CH_2 PEG group), 3.76–3.59 (m, 14H, CH_2 PEG group), 2.90 (dd, 1H, $J_1 = 3.72$ Hz, $J_2 = 13.7$ Hz, H-18), 2.04 and 1.96 (s, 3H each, acetyl groups), 1.11, 1.04, 0.91, 0.90, 0.89, 0.88, 0.72 (s, 3H, each, methyl groups); δ_C ($CDCl_3$, 125 MHz): 177.7 (C-28), 171.0, 170.7 (CO acetyl groups), 143.9 (C-13), 122.1 (C-12), 80.7 (C-3), 72.6, 70.8, 70.7, 70.7, 70.5, 69.3, 63.5, 61.9, (CH_2 PEG group), 70.2 (C-2), 55.0 (C-5), 47.6 (C-9), 46.8 (C-17), 45.9 (C-19), 44.0 (C-1), 41.8 (C-14), 41.4 (C-18), 39.5 (C-4), 39.5 (C-10), 38.3 (C-8), 34.0 (C-21), 33.2 (Me), 32.6 (C-22), 32.5 (C-7), 30.8 (C-20), 28.5 (Me), 27.7 (C-15), 25.9 (Me), 23.7 (Me), 23.6 (C-11), 23.0 (C-16), 21.3, 21.0 (CH_3 acetyl groups), 18.3 (C-6), 17.8 (Me), 17.1 (Me), 16.6 (Me); ESI-HRMS *m/z* calcd for $C_{42}H_{68}O_{10}Na$ $[M+Na]^+$ 755.4710, found 755.4725.

4.6. PEGylation reactions on the C-3 hydroxyl group of OA-Bn (V)

Trichloromethyl Chloroformate (diphosgene, 1 mmol) and *N*,*N*-dimethylaniline (DMA, 1 mmol) were added to a solution of OA-Bn (**V**, 1 mmol) in THF (5 mL), at 0 °C in an argon atmosphere. This reaction mixture was stirred under these conditions for 15 min and at room temperature for an additional 12 h. When the reaction was complete, Et_2O was added and the mixture reaction was filtered. The liquid residue was washed successively with HCl (0.2 M), NaOH (0.2 M) and H_2O. The organic layer was dried with

dry Na_2SO_4 and the solvent was removed under reduced pressure to give a syrup residue corresponding to the OA-Bnchloroformate derivative.

DIEA (1.5 mmol) and DMAP (0.5 mmol) were added to 4 identical solutions of this chloroformate intermediate (1 mmol each) in toluene (5 mL each), at 0 °C in an argon atmosphere. After that, a solution of the corresponding PEG reagent (1 mmol of mono-, di, tri- or tetraethylene glycol) in toluene (1 mL) was added to each reaction mixture. The four reactions were stirred under these conditions for 15 min and at room temperature for an additional 12 h. When the reactions finished, the solvent was evaporated under reduced pressure and the residues were purified on a silica-gel chromatography column using CH_2Cl_2–Me_2CO as eluents, obtaining the PEGylated derivatives **17**-**20**, with percentages of between 88% and 94%.

4.6.1. Benzyl 3β-(4-hydroxy-2-oxabutanoyloxy)olean-12-en-28-oate (17)

White solid, yield 94%, mp 63–65 °C; $[a]_D$ +44 (c 1 in $CHCl_3$); IR (KBr) ν_{max} 2970, 1738, 1366, 1229, 1216, 1092, 965, 695 cm^{-1}; δ_H ($CDCl_3$, 500 MHz): 7.37–7.28 (m, 5H, benzyl group), 5.28 (dd, 1H, $J_1 = J_2 = 3.5$ Hz, H-12), 5.09 and 5.04 (AB system, 2H, J = 12.5 Hz, benzyl group), 4.35 (dd, 1H, $J_1 = 5.5$ Hz, $J_2 = 11.0$ Hz, H-3), 4.28–4.22 (m, 2H, CH_2 PEG group), 3.86–3.84 (m, 2H, CH_2 PEG group), 2.90 (dd, 1H, $J_1 = 4.3$ Hz, $J_2 = 15.2$ Hz, H-18), 1.12, 0.93, 0.92, 0.90, 0.90, 0.87, 0.61 (s, 3H each, methyl groups); δ_C ($CDCl_3$, 125 MHz): 177.6 (C-28), 155.6 (CO carbonate group), 143.9 (C-13), 136.6 (C benzyl group), 128.5, 128.5, 128.1, 128.1, 128.0 (CH benzyl group), 122.5 (C-12), 86.0 (C-3), 69.2, 61.3 (CH_2 PEG group), 66.1 (CH_2 benzyl group), 55.5 (C-5), 47.7 (C-9), 46.9 (C-17), 46.0 (C-19), 41.8 (C-14), 41.5 (C-18), 39.4 (C-8), 38.2 (C-1), 38.1 (C-4), 37.0 (C-10), 34.0 (C-21), 33.2 (Me), 32.8 (C-7), 32.5 (C-22), 30.8 (C-20), 28.1 (Me), 27.8 (C-15), 26.0 (Me), 23.8 (Me), 23.6 (C-2), 23.5 (C-11), 23.2 (C-16), 18.3 (C-6), 17.0 (Me), 16.8 (Me), 15.5 (Me); ESI-HRMS *m*/z calcd for $C_{40}H_{59}O_6$ $[M+1]^+$ 635.4312, found 635.4304.

4.6.2. Benzyl 3β-(7-hydroxy-2,5-dioxaheptanoyloxy)olean-12-en-28-oate (18)

White solid,yield 92%, mp 40–42 °C; $[a]_D$ +47 (*c* 1 in $CHCl_3$); IR (KBr) ν_{max} 2945, 1738, 1455, 1365, 1253, 1011, 965, 696 cm^{-1}; δ_H ($CDCl_3$, 500 MHz): 7.36–7.28 (m, 5H, benzyl group), 5.28 (dd, 1H, $J_1 = J_2 = 3.5$ Hz, H-12), 5.09 and 5.04 (AB system, 2H, $J = 12.4$ Hz, benzyl group), 4.34 (dd, 1H, $J_1 = 6.0$ Hz, $J_2 = 10.5$ Hz, H-3), 4.30–4.28 (m, 2H, CH_2 PEG group), 3.74–3.60 (m, 6H, CH_2 PEG group), 2.90 (dd, 1H, $J_1 = 4.0$ Hz, $J_2 = 13.5$ Hz, H-18), 1.12, 0.93, 0.92, 0.90, 0.90, 0.87, 0.60 (s, 3H each, methyl groups); δ_C ($CDCl_3$, 125 MHz): 177.6 (C-28), 155.5 (CO carbonate group), 143.9 (C-13), 136.6 (C benzyl group), 128.5, 128.5, 128.1, 128.1, 128.0 (CH benzyl group), 122.5 (C-12), 85.8 (C-3), 72.5, 69.2, 66.6, 61.9 (CH_2 PEG group), 66.1 (CH_2 benzyl group), 55.5 (C-5), 47.7 (C-9), 46.9 (C-17), 46.0 (C-19), 41.8 (C-14), 41.5 (C-18), 39.4 (C-8), 38.2 (C-1), 38.1 (C-4), 37.0 (C-10), 34.0 (C-21), 33.2 (Me), 32.8 (C-7), 32.5 (C-22), 30.8 (C-20), 28.1 (Me), 27.8 (C-15), 26.0 (Me), 23.8 (Me), 23.6 (C-2), 23.5 (C-11), 23.2 (C-16), 18.3 (C-6), 17.0 (Me), 16.8 (Me), 15.5 (Me); ESI-HRMS *m/z* calcd for $C_{42}H_{63}O_7$ $[M+1]^+$ 679.4574, found 679.4573.

4.6.3. Benzyl 3β-(10-hydroxy-2,5,8-trioxadecanoyloxy)olean-12-en-28-oate (19)

Transparent syrup, yield 91%; $[a]_D$ +38 (*c* 1 in $CHCl_3$); IR (film) ν_{max} 2945, 1737, 1455, 1253, 1121, 966, 734, 696 cm^{-1}; δ_H ($CDCl_3$, 500 MHz): 7.36–7.29 (m, 5H, benzyl group), 5.28 (dd, 1H, $J_1 = J_2 = 3.5$ Hz, H-12), 5.09 and 5.04 (AB system, 2H, $J = 12.8$ Hz, benzyl group), 4.33 (dd, 1H, $J_1 = 5.8$ Hz, $J_2 = 10.8$ Hz, H-3), 4.29–4.27 (m, 2H, CH_2 PEG group), 3.74–3.60 (m, 10H, CH_2 PEG group), 2.90 (dd, 1H, $J_1 = 4.0$ Hz, $J_2 = 13.5$ Hz, H-18), 1.12, 0.92, 0.92, 0.90, 0.90, 0.86, 0.60 (s, 3H each, methyl groups); δ_C ($CDCl_3$, 125 MHz): 177.6 (C-28), 155.4 (CO carbonate group), 143.9 (C-13), 136.6 (C benzyl group), 128.5, 128.5, 128.1, 128.1, 128.0 (CH benzyl group), 122.5 (C-12), 85.7 (C-3), 72.6, 70.8, 70.5, 69.2, 66.7, 62.0 (CH_2 PEG group), 66.1 (CH_2 benzyl group), 55.5 (C-5), 47.7 (C-9), 46.9 (C-17), 46.0 (C-19), 41.8 (C-14), 41.5 (C-18), 39.4 (C-8), 38.2 (C-1), 38.1 (C-4), 37.0 (C-10), 34.0 (C-21), 33.2 (Me), 32.8 (C-7), 32.5 (C-22), 30.8 (C-20),

28.1 (Me), 27.8 (C-15), 26.0 (Me), 23.8 (Me), 23.6 (C-2), 23.5 (C-11), 23.2 (C-16), 18.3 (C-6), 17.0 (Me), 16.8 (Me), 15.5 (Me); ESI-HRMS *m/z* calcd for $C_{44}H_{67}O_8$ $[M+1]^+$ 723.4836, found 723.4809.

4.6.4. Benzyl 3β-(13-hydroxy-2,5,8,11-tetraoxatridecanoyloxy)olean-12-en-28-oate (20)

Transparent syrup, yield 88%; $[a]_D$ +36 (c 1 in $CHCl_3$); IR (film) ν_{max} 2944, 1737, 1455, 1365, 1254, 1120, 966, 697 cm^{-1}; δ_H ($CDCl_3$, 500 MHz): 7.38–7.26 (m, 5H, benzyl group), 5.28 (dd, 1H, $J_1 = J_2 = 3.5$ Hz, H-12), 5.09 and 5.04 (AB system, 2H, $J = 12.5$ Hz, benzyl group), 4.32 (dd, 1H, $J_1 = 5.8$ Hz, $J_2 = 10.8$ Hz, H-3), 4.30–4.26 (m, 2H, CH_2 PEG group), 3.78–3.60 (m, 14H, CH_2 PEG group), 2.90 (dd, 1H, $J_1 = 4.3$ Hz, $J_2 = 13.8$ Hz, H-18), 1.12, 0.92, 0.92, 0.90, 0.90, 0.86, 0.60 (s, 3H each, methyl groups); δ_C ($CDCl_3$, 125 MHz): 177.6 (C-28), 155.4 (CO carbonate group), 143.9 (C-13), 136.6 (C benzyl group), 128.6, 128.6, 128.1, 128.1, 128.0 (CH benzyl group), 122.5 (C-12), 85.7 (C-3), 72.6, 70.8, 70.7, 70.5, 70.2, 69.2, 66.8, 61.9 (CH_2 PEG group), 66.1 (CH_2 benzyl group), 55.5 (C-5), 47.7 (C-9), 46.9 (C-17), 46.0 (C-19), 41.8 (C-14), 41.5 (C-18), 39.5 (C-8), 38.2 (C-1), 38.1 (C-4), 37.0 (C-10), 34.0 (C-21), 33.2 (Me), 32.8 (C-7), 32.5 (C-22), 30.9 (C-20), 28.1 (Me), 27.8 (C-15), 26.0 (Me), 23.8 (Me), 23.6 (C-2), 23.5 (C-11), 23.2 (C-16), 18.3 (C-6), 17.0 (Me), 16.8 (Me), 15.5 (Me); ESI-HRMS *m/z* calcd for $C_{46}H_{71}O_9$ $[M+1]^+$ 767.5098, found 767.5098.

4.7. Treatment of MA-Bn (VI) with trichloromethylchloroformate

Trichloromethyl chloroformate (diphosgene, 1 mmol) and *N*,*N*-dimethylaniline (DMA, 1 mmol) were added to a solution of OA-Bn (**V**, 1 mmol) in THF (5 mL), at 0 °C in an argon atmosphere. This reaction mixture was treated as described in the PEGylation reaction of OA-Bn (**V**) to give **21**.

4.7.1. Benzyl 2α,3β-(oxomethylidenedioxy)olean-12-en-28-oate (21)

White solid, yield 80%, mp 95–97 °C; $[a]_D$ +54 (c 1 in $CHCl_3$); IR (KBr) ν_{max} 2970, 1805, 1727, 1365, 1216, 1177, 730, 692 cm^{-1}; δ_H ($CDCl_3$, 500 MHz): 7.34–7.30 (m, 5H, benzyl group), 5.28 (dd, 1H, $J_1 = J_2 = 3.7$ Hz, H-12), 5.08 and

5.06 (AB system, 2H, J = 12.5 Hz, benzyl group), 4.43 (ddd, 1H, J_1 = 4.0 Hz, J_2 = 11.5 Hz, J_3 = 16.0 Hz , H-2), 3.80 (d, 1H, J = 11.5 Hz, H-3), 2.90 (dd, 1H, J_1 = 4.5 Hz, J_2 = 14.0 Hz, H-18), 1.14, 1.12, 1.03, 0.95, 0.93, 0.91, 0.60 (s, 3H each, methyl groups); δ_C ($CDCl_3$, 125 MHz): 177.4 (C-28), 155.5 (CO carbonate group), 144.2 (C-13), 136.5 (C benzyl group), 128.5, 128.5, 128.1, 128.1, 128.0 (CH benzyl group), 121.7 (C-12), 91.8 (C-3), 77.5 (C-2), 66.1 (CH_2 benzyl group), 56.0 (C-5), 47.9 (C-9), 46.7 (C-17), 45.9 (C-19), 41.9 (C-14), 41.4 (C-18), 41.1 (C-1), 40.5 (C-8), 39.8 (C-4), 37.8 (C-10), 33.9 (C-21), 33.2 (Me), 32.7 (C-7), 32.4 (C-22), 30.8 (C-20), 28.0 (Me), 27.6 (C-15), 26.1 (Me), 23.8 (C-11), 23.7 (Me), 23.0 (C-16), 17.7 (C-6), 17.3 (Me), 17.2 (Me), 16.1 (Me); ESI-HRMS m/z calcd for $C_{38}H_{53}O_5$ $[M+1]^+$ 589.3893, found 589.3885.

4.8. Controlled acetylation of MA-Bn (VI)

Ac_2O (2 mL) was slowly added to a solution of MA-Bn (**VI**, 1416 mg, 3 mmol) in pyridine (10 mL). The reaction was stirred at 0 ºC for 24 h, and then cold water was added. This reaction mixture was extracted with CH_2Cl_2 and the organic layer was dried with dry Na_2SO_4. The solvent was removed under reduced pressure and the residue was purified by column chromatography using CH_2Cl_2–Me_2CO (10:1) to give the acetylated derivatives: Benzyl 2a-acetoxy-3β-hydroxyolean-12-en-28-oate (**22**, 46%), benzyl 3β-acetoxy-2a-hydroxyolean-12-en-28-oate (**23**, 30%), and benzyl 2a,3β-diacetoxyolean-12-en-28-oate (**24**, 14%) [35].

4.9. PEGylation reactions on the C-2 or C-3 hydroxyl groups of 22 and 23

Trichloromethyl chloroformate (diphosgene, 1 mmol) and *N*,*N*-dimethylaniline (DMA, 1 mmol) were added to two solutions of **22** (1 mmol) and **23** (1 mmol) in THF (5 mL each), at 0 ºC in an argon atmosphere. These reaction mixtures were treated as described in the PEGylation reaction of OA-Bn (**V**) to give the corresponding chloroformate derivatives of **22** and **23**.

DIEA (1.5 mmol) and DMAP (0.5 mmol) were added to four identical solutions of each of these chloroformate intermediates (1 mmol each) in toluene (5 mL each) at 0 ºC in an argon atmosphere. Thereafter, a solution

of the corresponding PEG reagent (1 mmol of mono-, di-, tri- or tetra-ethylene glycol) in toluene (1 mL) was added to each reaction mixture. The eight PEGylation reactions were treated as described in the PEGylation reaction of OA-Bn (**V**), giving derivatives **25**-**32**, with percentages of between 81% and 85%.

4.9.1. Benzyl 2a-acetoxy-3β-(4-hydroxy-2-oxabutanoyloxy)olean-12-en-28-oate (25)

White solid, yield 85%, mp 72–74 °C; $[\alpha]_D$ +11 (c 1 in $CHCl_3$); IR (KBr) ν_{max} 2945, 1739, 1366, 1230, 1217, 1012, 967, 696 cm^{-1}; δ_H ($CDCl_3$, 500 MHz): 7.33–7.30 (m, 5H, benzyl group), 5.26 (dd, 1H, $J_1 = J_2 = 3.3$ Hz, H-12), 5.09 and 5.04 (AB system, 2H, $J = 12.5$ Hz, benzyl group), 5.08 (ddd, 1H, $J_1 = 4.5$ Hz, $J_2 = 10.5$ Hz, $J_3 = 15.5$ Hz , H-2), 4.52 (d, 1H, $J = 10.5$ Hz, H-3), 4.33–4.18 (m, 4H, CH_2 PEG group), 2.90 (dd, 1H, $J_1 = 4.5$ Hz, $J_2 = 13.5$ Hz, H-18), 2.00 (s, 3H, acetyl group) 1.11, 1.01, 0.97, 0.91, 0.91, 0.89, 0.51 (s, 3H each, methyl groups); δ_C ($CDCl_3$, 125 MHz): 177.5 (C-28), 170.7 (CO acetyl group), 155.9 (CO carbonate group), 143.9 (C-13), 136.6 (C benzyl group), 128.5, 128.5, 128.1, 128.1, 128.0 (CH benzyl group), 122.2 (C-12), 85.7 (C-3), 70.3 (C-2), 69.5, 61.2 (CH_2 PEG group), 66.1 (CH_2 benzyl group), 55.1 (C-5), 47.6 (C-9), 46.8 (C-17), 45.9 (C-19), 44.0 (C-1), 41.8 (C-14), 41.5 (C-18), 39.5 (C-8), 39.4 (C-4), 38.2 (C-10), 34.0 (C-21), 33.2 (Me), 32.6 (C-7), 32.5 (C-22), 30.8 (C-20), 28.4 (Me), 27.7 (C-15), 26.0 (Me), 23.7 (Me), 23.6 (C-11), 23.1 (C-16), 21.2 (CH_3 acetyl group), 18.3 (C-6), 17.6 (Me), 16.9 (Me), 16.5 (Me); ESI-HRMS *m/z* calcd for $C_{42}H_{61}O_8$ $[M+1]^+$ 693.4366, found 693.4354.

4.9.2. Benzyl 2a-acetoxy-3β-(7-hydroxy-2,5-dioxaheptanoyloxy)olean-12-en-28-oate(26)

Transparent syrup, yield 83%; $[\delta]_D$ +9 (c 1 in $CHCl_3$); IR (film) ν_{max} 2945, 1739, 1455, 1261, 1232, 1031, 967, 696 cm^{-1}; δ_H ($CDCl_3$, 500 MHz): 7.32–7.27 (m, 5H, benzyl group), 5.25 (dd, 1H, $J_1 = J_2 = 3.3$ Hz, H-12), 5.09 and 5.04 (AB system, 2H, $J = 10.5$ Hz, benzyl group), 5.08 (ddd, 1H, $J_1 = 4.5$ Hz, $J_2 = 9.0$ Hz, $J_3 = 15.5$ Hz , H-2), 4.52 (d, 1H, $J = 9.0$ Hz, H-3), 4.34–4.24 (m, 2H, CH_2 PEG group),

3.72–3.57 (m, 6H, CH_2 PEG group), 2.90 (dd, 1H, J_1 = 3.7 Hz, J_2 = 14.0 Hz, H-18), 1.92 (s, 3H, acetyl group) 1.11, 1.01, 0.96, 0.91, 0.90, 0.89, 0.57 (s, 3H each, methyl groups); δ_C ($CDCl_3$, 125 MHz): 177.5 (C-28), 170.6 (CO acetyl group), 155.7 (CO carbonate group), 143.9 (C-13), 136.5 (C benzyl group), 128.5, 128.5, 128.1, 128.1, 128.0 (CH benzyl group), 122.2 (C-12), 85.5 (C-3), 72.6, 69.0, 66.9, 61.8 (CH_2 PEG group), 70.2 (C-2), 66.1 (CH_2 benzyl group), 55.0 (C-5), 47.6 (C-9), 46.8 (C-17), 45.9 (C-19), 43.9 (C-1), 41.8 (C-14), 41.4 (C-18), 39.6 (C-8), 39.4 (C-4), 38.2 (C-10), 33.9 (C-21), 33.2 (Me), 32.5 (C-7), 32.4 (C-22), 30.8 (C-20), 28.4 (Me), 27.6 (C-15), 25.9 (Me), 23.7 (Me), 23.6 (C-11), 23.1 (C-16), 21.2 (CH_3 acetyl group), 18.2 (C-6), 17.6 (Me), 16.9 (Me), 16.5 (Me); ESI-HRMS *m*/z calcd for $C_{44}H_{65}O_9$ $[M+1]^+$ 737.4629, found 737.4622.

4.9.3. Benzyl 2a-acetoxy-3β-(10-hydroxy-2,5,8-trioxadecanoyloxy)olean-12-en-28-oate (27)

Transparent syrup, yield 82%; $[a]_D$ +8 (c 1 in $CHCl_3$); IR (film) ν_{max} 2944, 1740, 1366, 1261, 1232, 1121, 1031, 696 cm^{-1}; δ_H ($CDCl_3$, 500 MHz): 7.34–7.29 (m, 5H, benzyl group), 5.26 (dd, 1H, $J_1 = J_2$ = 3.5 Hz, H-12), 5.09 and 5.04 (AB system, 2H, *J* = 10.5 Hz, benzyl group), 5.07 (ddd, 1H, J_1 = 4.5 Hz, J_2 = 11.5 Hz, J_3 = 17.5 Hz , H-2), 4.53 (d, 1H, *J* = 11.5 Hz, H-3), 4.33–4.23 (m, 2H, CH_2 PEG group), 3.73–3.58 (m, 10H, CH_2 PEG group), 2.90 (dd, 1H, J_1 = 4.0 Hz, J_2 = 13.5 Hz, H-18), 1.99 (s, 3H, acetyl group) 1.12, 1.02, 0.97, 0.92, 0.92, 0.90, 0.58 (s, 3H each, methyl groups); δ_C ($CDCl_3$, 125 MHz): 177.5 (C-28), 170.6 (CO acetyl group), 155.6 (CO carbonate group), 143.9 (C-13), 136.5 (C benzyl group), 128.5, 128.5, 128.1, 128.1, 128.0 (CH benzyl group), 122.2 (C-12), 85.4 (C-3), 72.7, 70.8, 70.5, 69.1, 67.0, 61.9 (CH_2 PEG group), 70.2 (C-2), 66.1 (CH_2 benzyl group), 55.1 (C-5), 47.6 (C-9), 46.8 (C-17), 45.9 (C-19), 43.9 (C-1), 41.8 (C-14), 41.5 (C-18), 39.6 (C-8), 39.4 (C-4), 38.2 (C-10), 34.0 (C-21), 33.2 (Me), 32.6 (C-7), 32.5 (C-22), 30.8 (C-20), 28.4 (Me), 27.7 (C-15), 26.0 (Me), 23.8 (Me), 23.6 (C-11), 23.1 (C-16), 21.2 (CH_3 acetyl group), 18.3 (C-6), 17.6 (Me), 16.9 (Me), 16.5 (Me); ESI-HRMS *m*/zcalcd for $C_{46}H_{69}O_{10}$ $[M+1]^+$ 781.4891, found 781.4897.

4.9.4. Benzyl 2a-acetoxy-3β-(13-hydroxy-2,5,8,11-tetraoxatridecanoyloxy) olean-12-en-28-oate (28)

Transparent syrup, yield 82%; $[a]_D$ +10 (c 1 in $CHCl_3$); IR (film) ν_{max} 2945, 1741, 1367, 1262, 1234, 1121, 1121, 697 cm^{-1}; δ_H ($CDCl_3$, 500 MHz): 7.35–7.27 (m, 5H, benzyl group), 5.26 (dd, 1H, $J_1 = J_2 = 3.0$ Hz, H-12), 5.09 and 5.04 (AB system, 2H, $J = 12.5$ Hz, benzyl group), 5.06 (ddd, 1H, $J_1 = 5.5$ Hz, $J_2 = 12.5$ Hz, $J_3 = 16.5$ Hz , H-2), 4.40 (d, 1H, $J = 10.5$ Hz, H-3), 4.32–4.22 (m, 2H, CH_2 PEG group), 3.72–3.59 (m, 14H, CH_2 PEG group), 2.90 (dd, 1H, $J_1 = 3.8$ Hz, $J_2 = 13.8$ Hz, H-18), 2.03 (s, 3H, acetyl group), 1.11, 1.00, 1.00, 0.90, 0.90, 0.89, 0.57 (s, 3H each, methyl groups); δ_C ($CDCl_3$, 125 MHz): 177.5 (C-28), 170.6 (CO acetyl group), 155.7 (CO carbonate group), 143.9 (C-13), 136.5 (C benzyl group), 128.5, 128.5, 128.1, 128.1, 128.0 (CH benzyl group), 122.2 (C-12), 85.3 (C-3), 72.6, 70.8, 70.8, 70.7, 70.5, 69.1, 67.1, 61.9 (CH_2 PEG group), 70.3 (C-2), 66.1 (CH_2 benzyl group), 55.1 (C-5), 47.6 (C-9), 46.8 (C-17), 45.9 (C-19), 43.9 (C-1), 41.8 (C-14), 41.5 (C-18), 39.6 (C-8), 39.5 (C-4), 38.2 (C-10), 34.0 (C-21), 33.2 (Me), 32.6 (C-7), 32.5 (C-22), 30.8 (C-20), 28.4 (Me), 27.7 (C-15), 26.0 (Me), 23.8 (Me), 23.6 (C-11), 23.1 (C-16), 21.2 (CH_3 acetyl group), 18.3 (C-6), 17.6 (Me), 16.9 (Me), 16.5 (Me); ESI-HRMS *m/z* calcd for $C_{48}H_{73}O_{11}$ $[M+1]^+$ 825.5153, found 825.5148.

4.9.5. Benzyl 3β-acetoxy-2a-(4-hydroxy-2-oxabutanoyloxy)olean-12-en-28-oate (29)

Transparent syrup, yield 83%; $[a]_D$ +8 (c 1 in $CHCl_3$); IR (film) ν_{max} 2970, 1740, 1366, 1230, 1217, 1029, 956, 696 cm^{-1}; δ_H ($CDCl_3$, 500 MHz): 7.36–7.28 (m, 5H, benzyl group), 5.27 (dd, 1H, $J_1 = J_2 = 3.5$ Hz, H-12), 5.09 and 5.04 (AB system, 2H, $J = 12.5$ Hz, benzyl group), 4.91 (ddd, 1H, $J_1 = 4.5$ Hz, $J_2 = 10.5$ Hz, $J_3 = 15.0$ Hz , H-2), 4.80 (d, 1H, J =10.5 Hz, H-3), 4.27–4. 17 (m, 2H, CH_2 PEG group), 3.86–3.78 (m, 2H, CH_2 PEG group), 2.90 (dd, 1H, $J_1 = 4.5$ Hz, $J_2 = 13.8$ Hz, H-18), 2.08 (s, 3H, acetyl group), 1.12, 1.02, 0.92, 0.91, 0.90, 0.90, 0.59 (s, 3H each, methyl groups); δ_C ($CDCl_3$, 125 MHz): 177.5 (C-28), 171.1 (CO acetyl group), 155.1 (CO carbonate group), 143.9 (C-13), 136.5 (C benzyl group), 128.5, 128.5, 128.1, 128.1, 128.0 (CH benzyl group), 122.1 (C-12), 80.6 (C-3), 74.8 (C-

2), 69.5, 61.1 (CH_2 PEG group), 66.1 (CH_2 benzyl group), 54.9 (C-5), 47.6 (C-9), 46.8 (C-17), 45.9 (C-19), 43.9 (C-1), 41.8 (C-14), 41.5 (C-18), 39.6 (C-8), 39.5 (C-4), 38.3 (C-10), 34.0 (C-21), 33.2 (Me), 32.6 (C-7), 32.5 (C-22), 30.8 (C-20), 28.5 (Me), 27.7 (C-15), 26.0 (Me), 23.8 (Me), 23.6 (C-11), 23.1 (C-16), 21.0 (CH_3 acetyl group), 18.3 (C-6), 17.8 (Me), 16.9 (Me), 16.5 (Me); ESI-HRMS *m/z* calcd for $C_{42}H_{61}O_8$ $[M+1]^+$ 693.4366, found 693.4371.

4.9.6. Benzyl 3β-acetoxy-2a-(7-hydroxy-2,5-dioxaheptanoyloxy)olean-12-en-28-oate (30)

Transparent syrup, yield 82%; $[a]_D$ +12 (c 1 in $CHCl_3$); IR (film) ν_{max} 2944, 1740, 1370, 1263, 1232, 1231, 1157, 1030, 697 cm^{-1}; δ_H ($CDCl_3$, 400 MHz): 7.35–7.27 (m, 5H, benzyl group), 5.26 (dd, 1H, $J_1 = J_2 = 3.4$ Hz, H-12), 5.08 and 5.03 (AB system, 2H, $J = 12.4$ Hz, benzyl group), 4.90 (ddd, 1H, $J_1 = 4.8$ Hz, $J_2 = 10.0$ Hz, $J_3 = 15.2$ Hz , H-2), 4.75 (d, 1H, $J = 10.0$ Hz, H-3), 4.31–4.18 (m, 2H, CH_2 PEG group), 3.74–3.56 (m, 6H, CH_2 PEG group), 2.90 (dd, 1H, $J_1 = 3.8$ Hz, $J_2 = 13.8$ Hz, H-18), 2.04 (s, 3H, acetyl group), 1.08, 0.99, 0.89, 0.89, 0.87, 0.86, 0.55 (s, 3H each, methyl groups); δ_C ($CDCl_3$, 100 MHz): 177.5 (C-28), 171.0 (CO acetyl group), 155.0 (CO carbonate group), 143.9 (C-13), 136.5 (C benzyl group), 128.5, 128.5, 128.1, 128.1, 128.0 (CH benzyl group), 122.1 (C-12), 80.5 (C-3), 74.6 (C-2), 72.6, 68.9, 66.9, 61.8 (CH_2 PEG group), 66.1 (CH_2 benzyl group), 54.9 (C-5), 47.6 (C-9), 46.8 (C-17), 45.9 (C-19), 43.9 (C-1), 41.8 (C-14), 41.4 (C-18), 39.6 (C-8), 39.4 (C-4), 38.3 (C-10), 33.9 (C-21), 33.2 (Me), 32.5 (C-7), 32.4 (C-22), 30.8 (C-20), 28.5 (Me), 27.6 (C-15), 25.9 (Me), 23.7 (Me), 23.6 (C-11), 23.1 (C-16), 21.0 (CH_3 acetyl group), 18.3 (C-6), 17.7 (Me), 16.9 (Me), 16.5 (Me); ESI-HRMS *m/z* calcd for $C_{44}H_{65}O_9$ $[M+1]^+$ 737.4629, found 737.4622.

4.9.7. Benzyl 3β-acetoxy-2a-(10-hydroxy-2,5,8-trioxadecanoyloxy)olean-12-en-28-oate (31)

Transparent syrup, yield 82%; $[a]_D$ +6 (c 1 in $CHCl_3$); IR (film) ν_{max} 2944, 1740, 1455, 1367, 1263, 1231, 1122, 1029, 734 cm^{-1}; δ_H ($CDCl_3$, 500 MHz): 7.35–7.27 (m, 5H, benzyl group), 5.26 (dd, 1H, $J_1 = J_2 = 3.5$ Hz, H-12), 5.08 and 5.03 (AB system, 2H, $J = 12.7$ Hz, benzyl group), 4.90 (ddd, 1H, $J_1 = 4.5$ Hz, $J_2 = 10.5$

Hz, J_3 = 15.0 Hz , H-2), 4.75 (d, 1H, J = 10.5 Hz, H-3), 4.29–4.12 (m, 2H, CH_2 PEG group), 3.73–3.58 (m, 10H, CH_2 PEG group), 2.90 (dd, 1H, J_1 = 4.5 Hz, J_2 = 13.7 Hz, H-18), 2.06 (s, 3H, acetyl group), 1.11, 1.01, 0.92, 0.90, 0.89, 0.89, 0.58 (s, 3H each, methyl groups); δ_C ($CDCl_3$, 125 MHz): 177.5 (C-28), 170.9 (CO acetyl group), 154.9 (CO carbonate group), 143.9 (C-13), 136.5 (C benzyl group), 128.5, 128.5, 128.1, 128.1, 128.0 (CH benzyl group), 122.1 (C-12), 80.5 (C-3), 74.5 (C-2), 72.6, 70.8, 70.5, 69.0, 67.0, 61.9, (CH_2 PEG group), 66.0 (CH_2 benzyl group), 54.9 (C-5), 47.6 (C-9), 46.8 (C-17), 45.9 (C-19), 43.9 (C-1), 41.8 (C-14), 41.4 (C-18), 39.6 (C-8), 39.4 (C-4), 38.3 (C-10), 34.0 (C-21), 33.2 (Me), 32.5 (C-7), 32.4 (C-22), 30.8 (C-20), 28.5 (Me), 27.6 (C-15), 25.9 (Me), 23.7 (Me), 23.6 (C-11), 23.1 (C-16), 21.0 (CH_3 acetyl group), 18.3 (C-6), 17.7 (Me), 16.9 (Me), 16.5 (Me); ESI-HRMS *m*/zcalcd for $C_{46}H_{69}O_{10}$ $[M+1]^+$ 781.4891, found 781.4869.

4.9.8. Benzyl 3β-acetoxy-2a-(13-hydroxy-2,5,8,11-tetraoxatridecanoyloxy) olean-12-en-28-oate (32)

Transparent syrup, yield 81%; $[a]_D$ +7 (c 1 in $CHCl_3$); IR (film) ν_{max} 2943, 1741, 1455, 1369, 1263, 1232, 1121, 1030, 697 cm^{-1}; δ_H ($CDCl_3$, 500 MHz): 7.35–7.27 (m, 5H, benzyl group), 5.26 (dd, 1H, J_1 = J_2 = 3.5 Hz, H-12), 5.08 and 5.03 (AB system, 2H, J = 12.5 Hz, benzyl group), 4.90 (ddd, 1H, J_1 = 4.5 Hz, J_2 = 10.0 Hz, J_3 = 15.0 Hz , H-2), 4.75 (d, 1H, J = 10.0 Hz, H-3), 4.31–4.21 (m, 2H, CH_2 PEG group), 3.79–3.59 (m, 14H, CH_2 PEG group), 2.90 (dd, 1H, J_1 = 3.8 Hz, J_2 = 13.7 Hz, H-18), 2.06 (s, 3H, acetyl group), 1.11, 1.01, 0.92, 0.90, 0.89, 0.89, 0.58 (s, 3H each, methyl groups); δ_C ($CDCl_3$, 125 MHz): 177.5 (C-28), 170.8 (CO acetyl group), 154.9 (CO carbonate group), 143.9 (C-13), 136.5 (C benzyl group), 128.5, 128.5, 128.1, 128.1, 128.0 (CH benzyl group), 122.1 (C-12), 80.4 (C-3), 74.5 (C-2), 72.6, 70.8, 70.8, 70.6, 70.5, 69.0, 67.1, 61.9 (CH_2 PEG group), 66.0 (CH_2 benzyl group), 54.9 (C-5), 47.6 (C-9), 46.8 (C-17), 45.9 (C-19), 43.9 (C-1), 41.8 (C-14), 41.4 (C-18), 39.6 (C-8), 39.4 (C-4), 38.3 (C-10), 34.0 (C-21), 33.2 (Me), 32.5 (C-7), 32.4 (C-22), 30.8 (C-20), 28.5 (Me), 27.6 (C-15), 25.9 (Me), 23.7 (Me), 23.6 (C-11), 23.1 (C-16), 21.0 (CH_3 acetyl group), 18.3 (C-6), 17.7 (Me), 16.9 (Me), 16.5 (Me); ESI-HRMS *m*/z calcd for $C_{48}H_{73}O_{11}$ $[M+1]^+$ 825.5153, found 825.5163.

4.10. Solubility of MA and its pegylated derivatives 5-8

Solubility was measured according to a new method specifically developed for this purpose. Thus, an excess of each solute was added to 200 mL of ultra-pure water in a 250 mL glass bottle. The different samples were magnetically stirred in a thermostatic water bath at 20.0ºC (± 0.1 °C) for 48 h to ensure equilibrium. The stirring was then stopped and the samples left in the bath for another 24 h to allow the solids to settle. From the upper part of the liquid, 150 mL were carefully extracted to minimize the presence of solids. The liquid was then filtered through an Amicon Ultra centrifugal filter (Millipore, Madrid, Spain) with a molecular weight cut-off (MWCO) of 10 kDa. The first 20 ml of filtrate was discarded, and the manipulation and centrifugation was performed at temperature above 20 ºC to avoid crystallization.

The volume of the filtered samples was determined and then transferred to a round-bottom flask. The water was completely removed under reduced pressure at 40ºC, and the residue was dissolved in HPLC-grade methanol (the volume depends on an initial approximate determination of water solubility).

Concentrations of solute were measured using HPLC (Alliance 2690, Waters, Milford, USA). The system consisted of a vacuum degasser, a quaternary pump, an automatic sampler, and a diode-array detector. The detection wavelength was set at 205 nm and the separation column was a Novapak C-18 (3.9 x 250 mm, 4 µm) manufactured by Waters (Milford, USA) with a mobile phase composed of acetonitrile and water with 0.1% fluoroacetic acid. Each experiment was repeated three times to check the reproducibility of the measurement.

4.11. Drugs

The different compounds used in cell treatment were dissolved before use at 5 mg/mL in DMSO. A stock solution was frozen and stored at -20 ºC. Prior to the experiments, this solution was diluted in cell-culture medium. Apoptosis, cell cycle and mitochondrial-membrane potential

were measured at IC_{50} and IC_{80} (concentration causing 50% and 80% reduction in growth compared to control), for 24, 48, and 72 h.

4.12. Cell culture

B16-F10 mouse melanoma cells (ATCC No. CRL-6475), HT29 human colorectal adenocarcinoma cell line (ECACC No. 9172201; ATCC No. HTB-38), Hep G2 human hepatocarcinome cell line (ECACC No. 85011430), and the non-tumour cell line of rat epithelium IEC-18 (ECACC No. 88011801), were obtained from the cell bank of the University of Granada, Spain. All cells were cultured in Dulbecco's modified eagle's medium (DMEM) supplemented with 2 mM glutamine, 10% heat-inactivated foetal calf serum (FCS), 10.000 units/mL of penicillin and 10 mg/mL of streptomycin, being incubated at 37°C in an atmosphere of 5% CO_2 and 95% humidity. Subconfluent monolayer cells were used in all experiments.

4.13. Cell-proliferation activity assay

The MTT assay (Sigma, MO, USA) was used to measure the cell viability of all derivatives, based on the ability of living cells to reduce 3-(4,5-dimethylthiazol-2-yl)-2,5-diphenyltetrazolium bromide to formazan, which has an absorbance at 570 nm.

For this assay, $5 \cdot 10^3$ B16-F10 cells, $6 \cdot 10^3$ HT29 cells, $15 \cdot 10^3$ Hep G2 cells, and $15 \cdot 10^3$ IEC-18 cells, were grown on a 96-well plate and incubated for 24 h. The cells were treated with the different compounds in triplicate to various concentrations (0–250 µg/mL) and incubated for 72 h. After 72 h, 100 µL of MTT solution (0.5 mg/mL) was added to each well. After 2 h of incubation, the cells were washed twice with phosphate buffered saline (PBS), and the formazan was resuspended in 100 µL DMSO. Relative cell viability, with respect to untreated control cells, was measured by absorbance at 550 nm on an ELISA plate reader (Tecan Sunrise MR20-301, TECAN, Austria).

4.14. Annexin V-FICT/PI flow-cytometric analysis

The extension apoptosis was analysed with flow cytometry by using a FACScan flow cytometer (fluorescence-activated cell sorter) (Coulter Corporation, Hialeah, FL, USA). For this assay, $11 \cdot 10^4$ HT29 cells were plated in 24-well plates with 1.5 mL of medium and incubated for 24 h. After this time the cells were treated with the selected derivatives (**4**, **5**, **8**, and **26**) in triplicate for 24, 48, and 72 h at IC_{50} and IC_{80} concentrations. The cells were collected and resuspended in binding buffer (10 mM HEPES / NaOH, pH 7.4, 140 mM NaCl, 2.5 mM $CaCl_2$). Annexin V-FITC conjugate (1 µg/mL) was then added and incubated for 15 min at room temperature in darkness. Just before analysis by flow cytometry, cells were stained with 5 µL of 1 mg/mL PI solution. In each experiment, approximately $10 \cdot 10^3$ cells were analysed and the experiment was duplicated twice.

4.15. Cell cycle

The cell cycle was analysed with flow cytometry by using a fluorescence-activated cell sorter (FACS) at 488 nm in an Epics XL flow cytometer (Coulter Corporation, Hialeah, FL, USA). For this assay, $11 \cdot 10^4$ HT29 cells were plated in 24-well plates with 1.5 mL of medium and incubated for 24 h. Cells were treated with the derivatives **4**, **5**, **8**, and **26** in triplicate for 24, 48, and 72 h, at their respective IC_{50} and IC_{80} concentration. After treatment, the cells were washed twice with PBS, trypsinized and resuspended in 1 x TBS (10 mMTris, 150 mM NaCl), and thereafter Vindelov buffer (100 mMTris, 100 mM NaCl, 10 mg/mL Rnase, 1 mg/mL PI, pH 8) was added. Cells were stored on ice and just before measurement were stained with 10 µL of 1 mg/mL PI solution. The data were analysed to determine the percentage of cells at each phase of the cell cycle (G0/G1, S and G2/M). In each experiment, approximately $10 \cdot 10^3$ cells were analysed and the experiment was duplicated twice.

4.16. Flow-cytometry analysis of the mitochondrial membrane potential

Analysis of the mitochondrial membrane potential was studied by flow cytometry using dihydrorhodamine (DHR), which is oxidised to a fluorescent product, rhodamine (Rh123). The fluorescence emitted can be monitored by fluorescence spectroscopy using excitation and emission wavelengths of 500 and 536 nm, respectively. In the same manner as in the above assays, $11 \cdot 10^4$ HT29 cells were plated in 24-well plates with 1.5 mL of fresh medium and subsequently treated in triplicate with derivatives **4**, **5**, **8**, and **26** for 24, 48, and 72 h, at their respective IC_{50} and IC_{80} concentrations. After treatment, the culture medium was renewed with fresh medium adding 0.5 µL DHR, obtaining a final concentration of 5 µg/mL. Cells were incubated for 1 h at 37 °C in an atmosphere of 5% CO2, and 95% humidity, and subsequently washed and resuspended in PBS with 5 µg/mL PI. The fluorescence intensity was measured using a FACScan flow cytometer (fluorescence-activated cell sorter).

Associated Content

Supporting information available: ^1H and ^{13}C NMR spectra of all new compounds and a table of the percentage of apoptosis of four compounds tested.

Abbreviations Used

An-V, annexin V; DIEA, *N*,*N*-diisopropylethylamine; DHR, dihydrorhodamine; DMA, *N*,*N*-dimethylaniline; DMAP, 4-dimethylaminopyridine; DMEM, Dulbecco's modified eagle's medium; FCS, foetal calf serum; FITC, fluorescein isothiocyanate; MA, maslinic acid; MA-Ac, 2α,3β-diacetoxyolean-12-en-28-oic acid; MA-Bn, benzyl maslinate; MMP, mitochondrial membrane potential; MTT, 3-(4,5-dimethylthiazol-2-yl)-2,5-diphenyltetrazolium bromide; MWCO, molecular weight cut-off; OA, oleanolic acid; OA-Ac, 3β-acetoxyolean-12-en-28-oic acid; OA-Bn, benzyl oleanolate; PBS, phosphate buffered saline; PEG, polyethylene glycol; PI,

propidium iodide; PS, phosphatidylserine; Rh123, rhodamine 123; TBTU, *O*-(benzotriazol-1-yl)-*N*,*N*,*N'*,*N'*-tetramethyluroniumtetrafluoroborate.

Acknowledgments

This work was financially supported by grants from the "Consejería de Innovación, Ciencia y Empresa" of the "Junta de Andalucía" (P11-FQM-7372), and the "Plan Propio" of the University of Granada. We thank David Nesbitt for reviewing the English of the manuscript.

References

[1] H. Yuan, Q. Ma, L. Ye, G. Piao, The traditional medicine and modern medicine from natural products, Molecules 21 (2016) 559–577.

[2] G.A. Cordell, M.D. Colvard, Natural products and traditional medicine: Turning on a paradigm, J. Nat. Prod. 75 (2012) 514–525.

[3] D.J. Newman, G.M. Cragg, Natural products as sources of new drugs from 1981 to 2014, J. Nat. Prod. 79 (2016) 629–661.

[4] D.A. Dias, S. Urban, U. Roessner, Historical overview of natural products in drug discovery, Metabolites 2 (2012) 303–336.

[5] M. Gerber, The Mediterranean diet: How much protection against cancers?,Phytotherapie 13 (2015) 82–90.

[6] G. Buckland, N. Travier, A. Agudo, A. Fonseca-Nunes, C. Navarro, P. Lagiou, C. Demetriou, P. Amiano, M. Dorronsoro, M.D. Chirlaque, et al., Olive oil intake and breast cancer risk in the Mediterranean countries of the European prospective investigation into cancer and nutrition study, Int. J. Cancer 131 (2012) 2465–2469.

[7] C. Pelucchi, C. Bosetti, E. Negri, L. Lipworth, C. La Vecchia, Olive oil and cancer risk: An update of epidemiological findings through 2010, Curr. Pharm. Des. 17 (2011) 805–812.

[8] L. Verberne, A. Bach-Faig, G. Buckland, L. Serra-Majem, Association between the Mediterranean diet and cancer risk: a review of observational studies, Nutr. Cancer 62 (2010) 860–870.

[9] I.S. Arvanitoyannis, A.Kassaveti, S. Stefanatos, Olive oil waste

treatment: a comparative and critical presentation of methods, advantages & disadvantages, Crit. Rev. Food Sci.Nutr. 47 (2007) 187–229.

[10] N. Azbar, A. Bayram, A. Filibeli, A. Muezzinoglu, F. Sengul, A. Ozer, A review of waste management options in olive oil production, Crit. Rev. Env. Sci. Technol. 34 (2004) 209–247.

[11] J. Fernandez-Bolanos, G. Rodriguez, R. Rodriguez, R. Guillen, A. Jimenez, Extraction of interesting organic compounds from olive oil waste, Grasas y Aceites 57 (2006) 95–106.

[12] J. Fernandez-Bolanos, G. Rodriguez, E. Gomez, R. Guillen, A. Jimenez, A. Heredia, R. Rodriguez, Total recovery of the waste of two-phase olive oil processing: Isolation of added-value compounds, J. Agr. Food Chem. 52 (2004) 5849–5855.

[13] A. Garcia-Granados, A. Martinez, J.N. Moliz, A. Parra, F. Rivas, 3□-hydroxyolean-12-en-28-oic acid (oleanolic acid), Molecules 3 (1998) M87.

[14] A. Garcia-Granados, A. Martinez, J.N. Moliz, A. Parra, F. Rivas, 2□,3□-dihydroxyolean-12-en-28-oic acid (maslinic acid), Molecules 3 (1998) M88.

[15] A. Fernandez-Hernandez, A. Martinez, F. Rivas, J. A. Garcia-Mesa, A. Parra, Effect of the solvent and the sample preparation on the determination of triterpene compounds in two-phase olive-mill-waste samples, J. Agric. Food Chem. 63 (2015) 4269–4275.

[16] S. Sommerwerk, L. Heller, C. Kerzig, A.E. Kramell, R. Csuk, Rhodamine B conjugates of triterpenoic acids are cytotoxic mitocans even at nanomolar concentrations, Eur. J. Med. Chem. 127 (2017) 1–9.

[17] S. Sommerwerk, L. Heller, J. Kuhfs, R. Csuk, Urea derivates of ursolic, oleanolic and maslinic acid induce apoptosis and are selective cytotoxic for several human tumor cell lines, Eur. J. Med. Chem. 119 (2016) 1–16.

[18] S. Sommerwerk, L. Heller, J. Kuhfs, R. Csuk, Selective killing of cancer cells with triterpenoic acid amides – The substantial role of an

aromatic moiety alignment, Eur. J. Med. Chem. 122 (2016) 452–464.

[19] F.J. Reyes-Zurita, E.E. Rufino-Palomares, L. Garcia-Salguero, J. Peragon, P.P. Medina, A. Parra, M. Cascante, J.A. Lupiañez, Maslinic acid, a natural triterpene, induces a death receptor-mediated apoptotic mechanism in Caco-2 p53-deficient colon adenocarcinoma cells, PLoS One 11 (2016) e0146178 (1–16).

[20] F.J. Reyes-Zurita, M. Medina-O'Donnell, R.M. Ferrer-Martin, E.E. Rufino-Palomares, S. Martin-Fonseca, F. Rivas, A. Martinez, A. Garcia-Granados, A. Perez-Jimenez, L. Garcia-Salguero, J. Peragon, K. Mokhtari, P.P. Medina, A. Parra, J.A. Lupiañez, The oleanolic acid derivative, 3-O-succinyl-28-O-benzyl oleanolate, induces apoptosis in B16–F10 melanoma cells via the mitochondrial apoptotic pathway, RSC Adv. 6 (2016) 93590–93601.

[21] L. Heller, A. Knorrscheidt, F. Flemming, J. Wiemann, S. Sommerwerk, I.Z. Pavel, A. Al-Harrasi, R. Csuk, Synthesis and proapoptotic activity of oleanolic acid derived amides, Bioorg. Chem. 68 (2016) 137–151.

[22] K.G. Cheng, C.H. Su, J.Y. Huang, J. Liu, Y.T. Zheng, Z.F. Chen, Conjugation of uridine with oleanolic acid derivatives as potential antitumor agents,Chem. Biol. Drug.Des. 88 (2016) 329–340.

[23] K.G. Cheng, C.H. Su, J.Y. Huang, H.S. Wang, J. Liu,Y.T. Zheng, Z.F. Chen, Synthesis and cytotoxic evaluation of several oleanolic acid-uracil/thymine conjugates, Med. Chem. Commun. 7 (2016) 972–981.

[24] J. Wiemann, L. Heller, R. Csuk, Targeting cancer cells with oleanolic and ursolic acid derived hydroxamates, Bioorg. Med. Chem. Lett. 26 (2016) 907–909.

[25] J.M. Patlolla, C.V. Rao, Triterpenoids for cancer prevention and treatment: Current status and future prospects, Curr. Pharm. Biotechnol. 13 (2012) 147–155.

[26] B.N. Mkhwanazi, M.R. Serumula, R.B. Myburg, F.R. Van Heerden, C.T. Musabayane, Antioxidant effects of maslinic acid in livers, hearts and kidneys of streptozotocin-induced diabetic rats: Effects on kidney function, Ren. Fail. 36 (2014) 419–431.

[27] M.C. Yin, M.C. Lin, M.C. Mong, C.Y. Lin, Bioavailability, distribution, and antioxidative effects of selected triterpenes in mice, J. Agric. Food Chem. 60 (2012) 7697–7701.

[28] J.A. Jesus,J.H.G. Lago, M.D.Laurenti,E.S. Yamamoto, L.F.D.Passero, Antimicrobial activity of oleanolic and ursolic acids: an update. eCAM (2015) 620472.

[29] F. Yu, Q. Wang, Z. Zhang, Y. Peng, Y. Qiu, Y. Shi, Y. Zheng, S. Xiao, H. Wang, X. Huang, L. Zhu, K. Chen, C. Zhao, C. Zhang, M. Yu, D. Sun, L. Zhang, D. Zhou, Development of oleanane-type triterpenes as a new class of HCV entry inhibitors, J. Med. Chem. 56 (2013) 4300–4319.

[30] C. Moneriz, J. Mestres, J.M. Bautista, A. Diez, A. Puyet, Multi-targeted activity of maslinic acid as an antimalarial natural compound, FEBS J. 278 (2011) 2951–2961.

[31] S. Fukumitsu, M.O. Villareal, T. Fujitsuka, K. Aida, H. Isoda, Anti-inflammatory and anti-arthritic effects of pentacyclic triterpenoids maslinic acid through NF-κB inactivation, Mol.Nutr. Food Res. 60 (2016) 399–409.

[32] E.E. Rufino-Palomares, A. Perez-Jimenez, F.J. Reyes-Zurita, L. Garcia-Salguero, K. Mokhtari, A. Herrera-Merchan, P.P. Medina, J. Peragon, J.A. Lupiañez, Anti-cancer and anti-angiogenic properties of various natural pentacyclic tri-terpenoids and some of their chemical derivatives, Curr. Org. Chem. 19 (2015) 919–947.

[33] J.A.R. Salvador, A.S.Leal, D.P.S. Alho, B.M.F. Goncalves, A.S. Valdeira, V.I.S. Mendes, Y. Jing, Highlights of pentacyclic triterpenoids in the cancer settings, Stud. Nat. Prod. Chem. 41 (2014) 33–73.

[34] M.K. Shanmugam, X. Dai, A.P. Kumar, B.K.H. Tan, G.Sethi, A. Bishayee, Oleanolic acid and its synthetic derivatives for the prevention and therapy of cancer: Preclinical and clinical evidence, Cancer Lett. 346 (2014) 206–216.

[35] A. Parra, S. Martin-Fonseca, F. Rivas, F.J. Reyes-Zurita,M. Medina-O'Donnell, A. Martinez, A. Garcia-Granados, J.A. Lupiañez, F. Albericio, Semi-synthesis of acylated triterpenes from olive-oil industry

wastes for the development of anticancer and anti-HIV agents, Eur. J. Med. Chem.74 (2014) 278–301.

[36] A. Parra, S. Martin-Fonseca, F. Rivas, F.J. Reyes-Zurita, M. Medina-O'Donnell, E.E. Rufino-Palomares, A. Martinez, A. Garcia-Granados, J.A. Lupiañez, F. Albericio, Solid-phase library synthesis of bi-functional derivatives of oleanolic and maslinic acids and their cytotoxicity on three cancer cell lines, ACS Comb. Sci. 16 (2014) 428–447.

[37] A. Kolate, D. Baradia, S. Patil, I. Vhora, G. Kore, A. Misra, PEG - A versatile conjugating ligand for drugs and drug delivery systems, J. Controlled Release, 192 (2014) 67–81.

[38] W. Li, P. Zhan, E. De Clercq, H. Lou, X. Liu, Current drug research on PEGylation with small molecular agents, Prog. Polym. Sci. 38 (2013) 421–444.

[39] P.L. Turecek, M.J. Bossard, F.Schoetens, I.A. Ivens, PEGylation of biopharmaceuticals: A review of chemistry and nonclinical safety information of approved drugs, J. Pharm. Sci. 105 (2016) 460–475.

[40] G. Pasut, F.M. Veronese, State of the art in PEGylation: the great versatility achieved after forty years of research, J. Controlled Release 161 (2012) 461–472.

[41] M. Medina-O'Donnell, F. Rivas, F.J. Reyes-Zurita, A. Martinez, S. Martin-Fonseca, A. Garcia-Granados, R.M. Ferrer-Martin, J.A. Lupianez, A. Parra, Semi-synthesis and antiproliferative evaluation of PEGylated pentacyclic triterpenos, Eur. J. Med. Chem. 118 (2016) 64–78.

[42] I. Fernandez-Pastor, A. Fernandez-Hernandez, S. Perez-Criado, F. Rivas, A. Martinez, A. Garcia-Granados, A. Parra, Microwave-assisted extraction versus Soxhlet extraction to determine triterpene acids in olive skins, J. Sep. Sci. 40 (2017) 1209–1217.

[43] A. Garcia-Granados, J. Dueñas, J.N. Moliz, A. Parra, F.L. Perez, J.A. Dobado, J. Molina, Semi-synthesis of triterpene A-ring derivatives from oleanolic and maslinic acids. Theoretical and experimental ^{13}C chemical shifts. J. Chem. Res. (M) (2000) 326–339.

[44] A. Garcia-Granados, J. Dueñas, E. Melguizo, J.N. Moliz, A. Parra, F.L.

Perez, J.A. Dobado, J. Molina, Semi-synthesis of triterpene A-ring derivatives from oleanolic and maslinic acids. Part II. Theoretical and experimental ^{13}C chemical shifts, J. Chem. Res. (M) (2000) 653–670.

[45] R. Weis, W. Seebacher, Complete assignment of 1H and 13C NMR spectra of new pentacyclic triterpene acid benzyl esters, Magn. Reson. Chem. 40 (2002) 455–457.

[46] A. Parra, F. Rivas, S. Martin-Fonseca, A. Garcia-Granados, A. Martinez, Maslinic acid derivatives induce significant apoptosis in b16f10 murine melanoma cells, Eur. J. Med. Chem. 46 (2011) 5991–6001.

[47] S. Jaeger, K. Winkler, U. Pfueller, A. Scheffler, Solubility studies of oleanolic acid and betulinic acid in aqueous solutions and plant extracts of Viscum album L. Planta Medica 73 (2007) 157–162.

[48] The Good Scents Company, Estimation Program Interface (EPI) system summary of maslinic acid. http://www.thegoodscentscompany.com/episys/ep1683981.html, (accessed March 2017), (accessed March 2017).

[49] A. Ashkenazi,W.J. Fairbrother,J.D. Leverson, A.J. Souers, From basic apoptosis discoveries to advanced selective BCL-2 family inhibitors, Nat. Rev. Drug Discov. 16 (2017) 273–284.

[50] S.W.G. Tait, D.R. Green, Mitochondria and cell death: outer membrane permeabilization and beyond, Nat. Rev. Mol. Cell Biol. 11 (2010) 621–632.

[51] M. Malumbres, M.Barbacid, Cell cycle, CDKs and cancer: a changing paradigm, Nat. Rev. Cancer 9 (2009) 153–166.

[52] A. Martinez, F. Rivas, A. Perojil, A. Parra, A. Garcia-Granados, A. Fernandez-Vivas, Biotransformation of oleanolic and maslinic acids by Rhizomucor miehei.Phytochem. 94 (2013) 229–237.

6. Supporting Information

Table S1. Flow-cytometry analysis of Annexin V-FITC staining and PI accumulation after exposure of HT29 cells to PEGylated derivatives **4**, **5**, **8**, and **26**.

Compd. **4**	Time	IC_{50}	IC_{80}
Early apoptosis	24 h	1.05 ± 0.49	2.80 ± 0.70
	48 h	2.60 ± 0.28	4.80 ± 1.13
	72 h	4.40 ± 0.65	14.90 ± 1.08
Late apoptosis	24 h	6.90 ± 1.48	7.75 ± 2.40
	48 h	12.60 ± 2.32	17.80 ± 1.63
	72 h	17.85 ± 2.96	36.45 ± 2.68
Total apoptosis	24 h	7.95 ± 1.27	10.55 ± 2.38
	48 h	15.20 ± 0.85	22.60 ± 0.71
	72 h	22.25 ± 2.35	51.35 ± 2.06

Compd. **5**	Time	IC_{50}	IC_{80}
Early apoptosis	24 h	1.90 ± 0.01	3.40 ± 1.27
	48 h	2.95 ± 1.48	2.15 ± 0.21
	72 h	7.80 ± 2.11	10.30 ± 0.99
Late apoptosis	24 h	8.95 ± 0.78	12.70 ± 2.69
	48 h	23.00 ± 0.57	22.05 ± 0.49
	72 h	34.30 ± 1.56	39.90 ± 0.71
Total apoptosis	24 h	10.85 ± 0.78	16.10 ± 1.96
	48 h	25.95 ± 2.05	24.20 ± 0.28
	72 h	42.10 ± 2.67	50.20 ± 0.28

Compd. **8**	Time	IC_{50}	IC_{80}
Early apoptosis	24 h	1.30 ± 0.14	3.95 ± 0.64
	48 h	3.85 ± 1.48	4.55 ± 0.35
	72 h	18.15 ± 0.21	20.15 ± 0.64
Late apoptosis	24 h	6.10 ± 1.13	9.50 ± 0.42
	48 h	19.45 ± 1.34	43.30± 1.70
	72 h	34.80 ± 1.70	41.75 ± 3.04
Total apoptosis	24 h	7.40 ± 1.27	13.45 ± 0.21
	48 h	23.30 ± 0.14	47.85 ± 2.05
	72 h	52.95 ± 1.91	61.90 ± 0.40

Compd. **26**	Time	IC_{50}	IC_{80}
Early apoptosis	24 h	4.40 ± 0.14	5.55 ± 0.49
	48 h	1.40 ± 0.85	0.60 ± 0.14
	72 h	5.40 ± 0.42	7.05 ± 1.48
Late apoptosis	24 h	11.00 ± 2.97	9.80 ± 1.41
	48 h	7.95 ± 0.92	13.40 ± 1.27
	72 h	14.60 ± 0.42	21.90 ± 1.27
Total apoptosis	24 h	15.40 ± 2.83	15.35 ± 1.91
	48 h	9.35 ± 0.07	14.00 ± 1.41
	72 h	20.00 ± 0.07	28.95 ± 2.76

Cell lines were treated at concentrations equal to their corresponding IC_{50} and IC_{80} values. Values are expressed as means ± S.E.M. of three experiments in duplicate. Early apoptotic cells were annexin V^+ PI^-, whereas late apoptotic cells were annexin V^+ PI^+, total apoptosis (early apoptosis plus late apoptosis) were annexin V^+.

PUBLICACIÓN 4

Diamine and PEGylated-diamine conjugates of triterpenic acids as potential anticancer agents

Enviado "European Journal of Medicinal Chemistry"
(JCR: Medicinal Chemistry: Ind.Imp. 3.902, nº6, Q1)

Marta Medina-O'Donnell[a], Francisco Rivas [a,**], Fernando J. Reyes-Zurita [b,***], Antonio Martinez[a], Jose A. Lupiañez[b], Andres Parra [a,*]

[a] Departamento de Química Orgánica. Facultad de Ciencias, Universidad de Granada, E-18071 Granada, Spain

[b] Departamento de Bioquímica y Biología Molecular I. Facultad de Ciencias, Universidad de Granada, E-18071 Granada, Spain

* Corresponding author. Tel.: +34-958-240480

** Corresponding author. Tel./Fax: +34-958-240479

*** Corresponding author. Tel.: +34-958-243252

*E-mail addresses:*aparra@ugr.es (A. Parra), frivas@ugr.es (F. Rivas), ferjes@ugr.es (F.J. Reyes-Zurita)

ABSTRACT

A set of 18 amide derivatives of oleanolic or maslinic acid has been semi-synthesised. Twelve of these derivatives were formed, attaching three 1,ω-diamino alkanes of different chain length to one or two units of oleanolic or maslinic acid, through the carboxyl group of C-28 of these natural triterpenes. The other six derivatives were semi-synthesised by connecting each of the six C-28 amide derivatives of OA or MA, with a free amino group, to a PEG-acid reagent (3,6,9-trioxadecanoic acid). The cytotoxic effects of these 18 triterpenic derivatives in three cancer-cell lines (B16-F10, HT29, and Hep G2) have been assayed, and have been compared to three non-tumour cell lines of the same or a similar tissue (HPF, IEC-18, and WRL68). The percentages of these non-tumour cells living at the IC_{50} values of the triterpene compounds in the corresponding cancer cells have been calculated, with cell viability values for the non-tumour HPF line ranging from 81% and 94%, for almost all diamine conjugates of the triterpenic acids tested. The best cytotoxic results were achieved with the diamine conjugates of oleanolic or maslinic acid with the shortest and the longest diamine chain (IC_{50} values from 0.76 mM to 1.76 mM), on the B16-F10 cell line, being between 140- and 20-fold more effective than their corresponding precursors. Four diamine conjugates of these triterpenic acids showed apoptotic effects on treated cells of the B16-F10 line, with total apoptosis rates, relative to control, between 73% and 90%.The DNA-histogram analysis revealed that all compounds tested produced cell-cycle arrest in B16-F10 cells, increasing the number of these cells in the S phase. Most of the compounds analysed, except one, did not produce changes in mitochondrial membrane potential during apoptosis of B16-F10 cancer cells, suggesting an activation of the extrinsic apoptotic pathway for these compounds.

Keywords: Triterpene; oleanolic acid; maslinic acid; diamine conjugate; cytotoxicity; apoptosis.

1. Introduction

Cancer is a universal disease, which shows great complexity and, in many cases, has lethal results. Chemotherapy is one of several treatments used against cancer, although it usually causes significant side effects [1,2].

A number of new anti-cancer drugs have been achieved from natural sources or by structural modification of natural products [3,4]. The search for better cytotoxic agents remains a relevant key in the discovery of drugs with anticancer activity. The semi-synthesis of new products through the structural modification of the functional groups of natural compounds can produce derivatives with greater biological activity and with lesser side effects [5,6].

Triterpenoids are natural compounds present in many plants of nature that have been used as anti-cancer, anti-inflammatory, anti-oxidant, antiviral, anti-bacterial, antifungal and anti-diabetic agents and which exhibit hepato-, cardio-, and neuroprotective properties [7]. Particular attention has been paid to the study of the anticancer ability of these triterpenic compounds because they show relevant cytotoxic properties against tumour cells while maintaining low activity against normal cells [8–12].

Oleanolic acid (3β-hydroxyolean-12-en-28-oic acid, OA, **I**) [13] and maslinic acid (2α,3β-dihydroxyolean-12-en-28-oic acid, MA, **II**) [14] are two naturally occurring pentacyclic triterpenic compounds present in abundance in the industrial olive-oil waste [15]. These triterpenic acids have promising pharmacological properties [16,17]. Certain structural modifications of these triterpenoids, which in many cases suppose the formation of simple derivatives in the functional groups of the molecules, can have a strong impact on their biological properties [18,19]. In recent years, our research group has reported the semi-synthesis of a large number of derivatives of these natural triterpenic acids, which inhibited proliferation and induced apoptosis in several cancer-cell lines [20–24].

A relatively high percentage of drugs have an amide group in their structure. Furthermore, several studies have recently been published on the

increase in the biological activities of the C-28 amino conjugates of various pentacyclic triterpenic acids with respect to their natural precursors [25–30]. Also, several diamine conjugate dimers of oleanolic acid have been designed and synthesised for various biological applications [31,32]. These researches support that the synthesis of triterpene amide derivatives can be a very effective way of finding novel cytotoxic agents for the treatment of cancer.

In this study, several C-28 amide derivatives of oleanolic or maslinic acids have been semi-synthesised to test for their biological properties. Firstly, a set of 12 derivatives was prepared, attaching propane-1,3-diamine, hexane-1,6-diamine, or decane-1,10-diamine to one or two units of oleanolic or maslinic acid, through the carboxyl group of C-28 of these natural triterpenes. Secondly, another set of six PEGylated derivatives was semi-synthesised by connecting each of the six C-28 amide derivatives of OA or MA, with a free amino group, to a PEG-acid reagent (3,6,9-trioxadecanoic acid). Finally, the cytotoxic effects of these 18 amide derivatives on three cancer-cell lines (B16-F10, HT29, and Hep G2) were tested, and the results of 12 of them, the most active, were compared to three non-tumour cell lines of the same or a similar tissue (HPF, IEC-18, and WRL68). Percentages of live non-tumour cells were calculated using the IC_{50} values of the triterpenic compounds on the corresponding cancer cells. Eight of these compounds were selected to perform various cytometric assays. All tested cytotoxic compounds were active in the apoptotic process. In addition, we established the percentage of cells in the different cell-cycle phases, and we also studied the changes in the mitochondrial membrane potential (MMP) to formulate hypotheses on the plausible apoptotic mechanisms activated by the different compounds tested.

2. Results and discussion

2.1. Chemistry

Oleanolic acid (**I**, 3β-hydroxyolean-12-en-28-oic acid, OA) and maslinic acid (**II**, 2a,3β-dihydroxyolean-12-en-28-oic acid, MA) (Fig. 1) are natural occurring pentacyclic triterpenes present in high proportions in olive-oil wastes. These compounds can be isolated by different extraction methods, using solvents of different polarity, such as methanol, ethyl acetate and/or n-hexane [33,34]. These triterpene acids (OA or MA) have been used as substrates for the amidation and PEGylation reactions described below.

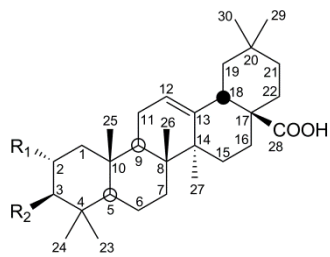

I: R_1 = H, R_2 = OH (oleanolic acid, **OA**)
II: R_1 = R_2 = OH, (maslinic acid, **MA**)

Fig. 1. Structures of oleanolic and maslinic acid.

Several C-28 amide derivatives of oleanolic or maslinic acid were semi-synthesised to evaluate their biological properties. These OA- or MA-diamine conjugates (**1**-**12**) were prepared attaching propane-1,3-diamine, hexane-1,6-diamine, or decane-1,10-diamine to one or two units of oleanolic or maslinic acid, through the carboxyl group of C-28 of these natural triterpenes (Scheme 1). The diamine reagents were selected with different chain lengths to evaluate their influence on the biological activities of the triterpenic derivatives formed (**1**-**12**). In order to improve the effectiveness of this amidation reaction between the different diamine reagents and the C-28 carboxyl group of the triterpenic compounds (OA or MA), this carboxyl group was activated with *O*-(Benzotriazol-1-yl)-*N*,*N*,*N*',*N*'-tetramethyluroniumtetrafluoroborate (TBTU). The reaction to produce the TBTU derivatives of OA or MA was performed by adding TBTU to each of the

solutions of these compounds in dry THF, in the presence of DIEA, at rt [22]. Then, each TBTU derivative (OA or MA) was dissolved in CH_2Cl_2 and each solution was split in three parts. The corresponding diamine reagent (propane-1,3-diamine, hexane-1,6-diamine, or decane-1,10-diamine) was then added in presence of K_2CO_3 to each of the six new solutions, yielding the derivatives **1**-**12** (Scheme 1). From each reaction two compounds were achieved: **1** (65%) and **2** (28%), **3** (63%) and **4** (27%), **5** (62%) and **6** (29%), **7** (64%) and **8** (28%), **9** (63%) and **10** (29%), and **11** (62%) and **12** (30%).

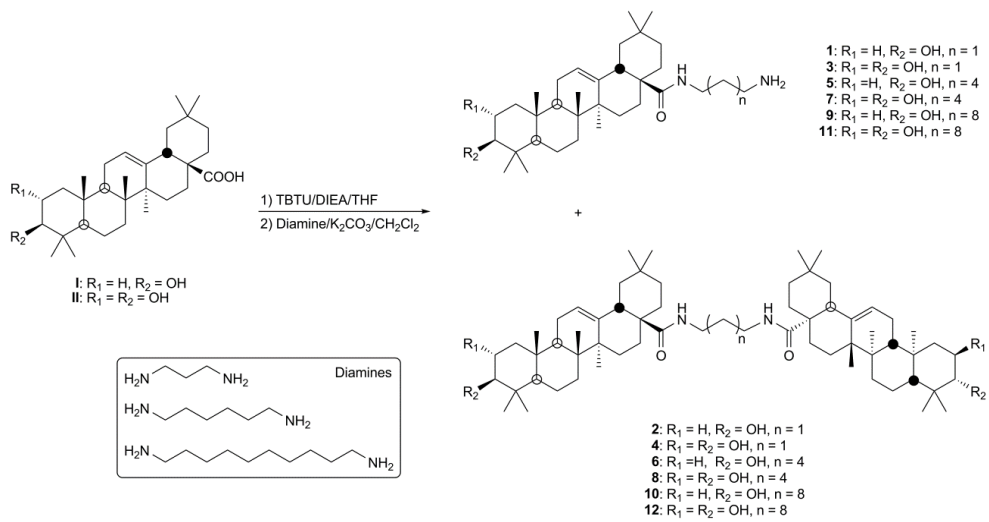

Scheme 1. Synthesis of the diamine conjugates of OA or MA and their corresponding dimeric analogues.

The difference in the atomic mass between an amide derivative of OA and its dimeric analogue (**1** and **2**, **5** and **6**, or **9** and **10**) was always 438 Da, whereas this difference between the pairs of amide derivatives of MA (**3** and **4**, **7** and **8**, or **11** and **12**) was 454 Da. These atomic mass differences confirmed that compounds **2**, **4**, **6**, **8**, **10**, and **12** were the corresponding dimeric analogues of compounds **1**, **3**, **5**, **7**, **19**, and **11**, in which a second molecule of the corresponding triterpene had coupled to the free amino group (Scheme 1). The ^{1}H NMR spectra of these diamine conjugates (**1**-**12**) were similar to that of their corresponding precursor (OA or MA). The main observed differences of the ^{1}H NMR spectra of derivatives **1**, **3**, **5**, **7**, **9**, and **11** (one unit of a triterpene compound) were two multiplet signals of the

protons of the carbon atom (C-1') attached to the amide group, at δ_H 3.50-3.30 and at δ_H 3.15-2.95, and another triplet signal at approximately δ_H 2.75, corresponding to the protons of the last carbon atom (C-3', C-6', or C-10') attached to the free amino group. However, for the dimeric analogues (**2**, **4**, **6**, **8**, **10**, and **12**), the main observed differences were only two multiplet signals of the protons of the carbon atoms attached to the amide groups, at δ_H 3.40-3.25 and at δ_H 3.15-2.95, since these compounds are symmetrical. In the ^{13}C NMR spectra of these diamine conjugates, the main differences observed were also in the chemical shifts of the terminal carbon atoms of the diamine chain. Thus, in the ^{13}C NMR spectra of derivatives **1**, **3**, **5**, **7**, **9**, and **11** (one unit of a triterpene compound), the signal of the last carbon atom of the diamine chain (C-3', C-6', or C-10') was situated at δ_C 40-42, while the signal of the carbon atom (C-1') attached to the amide group always appeared between 38-40 ppm. However, for the dimeric analogues (**2**, **4**, **6**, **8**, **10**, and **12**), the signals of both terminal carbons were situated at δ_C 36 for the propane-1,3-diamine conjugates (**2** and **4**), and at δ_C 39 for the hexane-1,6-diamine and the decane-1,10-diamine conjugates (**6**, **8**, **10**, and **12**).

Several PEGylated derivatives (**13**-**18**) were synthesised from the OA- or MA-diamine conjugates with a free amino group (**1**, **3**, **5**, **7**, **9**, and **11**) (Scheme 2). Thus, a new amide bond was formed by coupling each of these diamine conjugates with the commercial PEG-acid reagent (3,6,9-trioxadecanoic acid, PEG-COOH), yielding the corresponding PEGylated-diamine conjugates of OA or MA: **13** (91%), **14** (88%), **15** (89%), **16** (91%), **17** (94%), and **18** (89%).

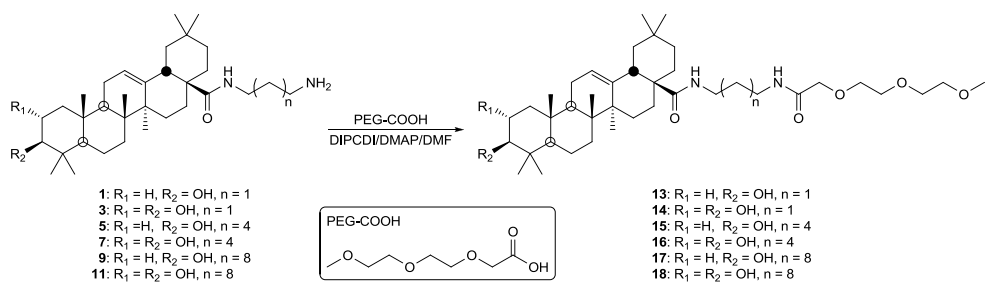

Scheme 2. Synthesis of the PEGylated-diamine conjugates of OA or MA.

The main differences observed between the ^{1}H NMR spectra of these PEGylated derivatives (**13-18**) and those of their corresponding precursors (**1**, **3**, **5**, **7**, **9**, and **11**) were the signal of a new amide NH proton, between 7.35 and 7.00 ppm, the signals of five methylene protons of the PEG group, between 4.00 and 3.50 ppm, and that of the methyl protons of the same PEG group at δ_H 3.35. In the ^{13}C NMR spectra, the same type of differences were observed between these PEGylated derivatives (**13**-**18**) and their corresponding precursors (**1**, **3**, **5**, **7**, **9**, and **11**). Thus, the signals of a new carboxamide carbon atom (δ_C 171.0-170.0), five methylene carbon atoms (δ_C 72.0-70.0) and a methyl carbon atom (δ 59) of the PEG group, were present in the ^{13}C NMR spectra of these PEGylated derivatives (**13**-**18**).

2.2. Effects of diamine and PEGylated-diamine conjugates on cancer-cell proliferation

The effects of 12 OA- or MA-diamine conjugates (**1**-**12**) and 6 PEGylated-diamine conjugates (**13**-**18**), compared with those of their precursors (OA or MA), on the proliferation of three cancer-cell lines (B16-F10, murine melanoma cells, HT29, colon-cancer cells, and Hep G2, hepatome cells) were investigatedby an MTT assay. Cell viability was determined by uptake of formazan dye and expressed as a percentage of untreated control cells. In these three cell lines, the concentration of those compounds at which the response (or binding) was reduced by half (IC_{50}) was determined (Table 1).

Table 1
Growth-inhibitory effects of the diamine conjugates and its dimer analogues of OA or MA (**1**-**12**), and the PEGylated-diamine conjugates of OA or MA (**13**-**18**), on B16-F10, HT29, and Hep G2 cells.

Type of compound	Compd #	B16-F10	* IC_{50} of precursor / IC_{50} of compd #	HT29	* IC_{50} of precursor / IC_{50} of compd #	Hep G2	* IC_{50} of precursor / IC_{50} of compd #
Precursor	OA (**I**)	106.4 ± 3.7	1.0	429.9 ± 0.7	1.0	211.8 ± 0.5	1.0
Diamine conjugate	**1**	0.76 ± 0.03	140.0	3.97 ± 0.19	108.3	4.75 ± 0.01	44.6
	5	2.15 ± 0.15	49.5	4.66 ± 0.01	92.3	4.56 ± 0.01	46.5
	9	1.75 ± 0.08	60.8	4.72 ± 0.36	91.1	5.85 ± 0.10	36.2
Diamine conjugate dimer	**2**	66.22 ± 0.97	1.6	72.95 ± 2.06	5.9	53.13 ± 3.53	4.0
	6	80.73 ± 0.09	1.3	73.74 ± 1.91	5.8	105.34 ± 0.28	2.0
	10	104.78 ± 0.73	1.0	109.24 ± 1.25	3.9	128.59 ± 2.86	1.6
PEGylated diamine conjugate	**13**	9.14 ± 1.38	11.6	125.15 ± 1.21	3.4	120.09 ± 2.87	1.8
	15	11.34 ± 0.66	9.4	11.74 ± 0.33	36.6	19.32 ± 0.12	11.0
	17	9.41 ± 0.04	11.3	11.90 ± 0.27	36.1	12.99 ± 0.01	16.3
Precursor	MA (**II**)	36.2 ± 2.5	1.0	32.2 ± 3.8	1.0	99.2 ± 15.5	1.0
Diamine conjugate	**3**	1.56 ± 0.04	23.2	5.80 ± 0.03	5.6	4.85 ± 0.17	20.5
	7	6.25 ± 0.21	5.8	7.84 ± 0.27	4.1	8.64 ± 0.03	11.5
	11	1.76 ± 0.02	20.6	4.48 ± 0.03	7.2	4.13 ± 0.01	24.0
Diamine conjugate dimer	**4**	43.48 ± 5.34	0.8	77.23 ± 1.84	0.4	73.48 ± 1.16	1.4
	8	72.73 ± 1.53	0.5	53.82 ± 0.81	0.6	105.90 ± 2.72	0.9
	12	92.19 ± 1.43	0.4	70.88 ± 2.19	0.5	96.37 ± 6.54	1.0
PEGylated diamine conjugate	**14**	17.65 ± 0.27	2.1	37.31 ± 0.65	0.9	31.57 ± 0.41	3.1
	16	20.27 ± 0.01	1.8	20.34 ± 0.27	1.6	19.04 ± 0.04	5.2
	18	12.26 ± 0.39	3.0	13.25 ± 0.13	2.4	13.68 ± 0.17	7.3

The IC_{50} values (mM) were calculated considering control untreated cells as 100% of viability. Cell-growth inhibition was analysed by the MTT assay, as described in Experimental section.
* Relationship between IC_{50} of OA or MA and the IC_{50} of each compound. All assays were realized two times using three replicates. Values, means ± S.E.M.

All compounds tested induced a dose-dependent decrease in the viability of cells after 72 h of treatment, ranging from 0 to 200 mg/mL. According to the analysis of the different type of compounds tested, the best results were achieved by the OA- or MA-diamine conjugates (**1**, **3**, **5**, **7**, **9**, and **11**), with IC_{50} concentrations lower than 10 mM in the three cancer-cell lines. The PEGylated-diamine conjugates of OA or MA (**13**-**18**) also showed low cytotoxicity data with IC_{50} concentrations, which in most cases did not exceed 20 mM. Since the OA- or MA-diamine conjugate dimers (**2**, **4**, **6**, **8**, **10**, and **12**) showed IC_{50} values higher than those of the other types

of derivatives, these compounds were discarded for the following cytometric studies. In general, the best cytotoxic results were produced by the OA- or MA-diamine conjugates (**1**, **3**, **9**, and **11**), with the shortest and the longest diamine chain (3 or 10 carbon atoms), on the B16-F10 cell line (0.76 mM, 1.56 mM, 1.75 mM, and 1.76 mM, respectively), being between 140- and 20-fold more effective than their corresponding precursors (OA or MA). The IC_{50} values of these derivatives (**1**, **3**, **9**, and **11**) are slightly higher with the other two cancer-cell lines (HT29 and Hep G2), around 5 mM, being between 108- and 6-fold more effective than OA or MA (Table 1, Fig. 2).

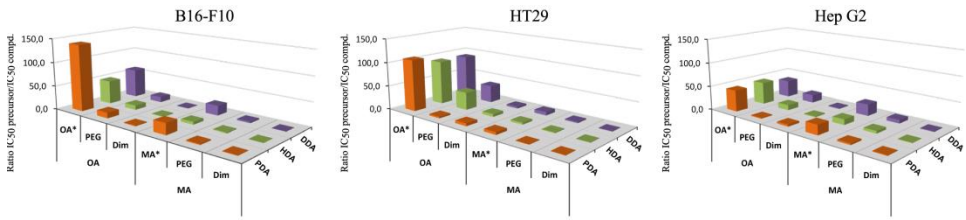

Fig. 2. Relationship between IC_{50} of OA or MA and the IC_{50} of each triterpenic derivative. OA* or MA* = Oleanolic or Maslinic acid derivatives, PEG = PEGylated derivatives(**13**-**18**), Dim = dimer derivatives (**2**, **4**, **6**, **8**, **10**, and **12**), PDA = propane-1,3-diamine, HAD = hexane-1,3-diamine, DDA = decane-1,10-diamine.

Only the diamine conjugates (**1**, **3**, **5**, **7**, **9**, and **11**) and the PEGylated-diamine conjugates (**13**-**18**) of OA or MA were selected to compare the growth-inhibitory effects of these compounds on murine melanoma cells (B16-F10) with those of a non-tumour cell line from a similar tissue, such as lung fibroblasts (HPF). In the same way, we compare the growth-inhibitory effects of these compounds on colon-cancer cells (HT29) and hepatome cells (Hep G2) with those of non-tumour cell lines of the same tissue, such as intestinal epithelial cells (IEC-18) and hepatic cells (WRL68), respectively.

In order to compare the cytotoxic effects of these compounds on the non-tumour cells (HPF, IEC-18, and WRL68) versus the cancer cells (B16-F10, HT29, and Hep G2), the percentage of viability of the non-tumour cells was calculated using the corresponding IC_{50} concentrations of the triterpenic derivatives for thecancer cells, i.e. the percentage of non-

tumour cells living at the IC_{50} values of the triterpene compounds in the corresponding cancer cells (Table 2). Almost all OA- or MA-diamine conjugates (**1**, **3**, **7**, **9**, and **11**), except **5**, and the PEGylated diamine conjugate of MA(**18**), showed cell viability values between 81% and 94% for the non-tumour HPF cell line, at the corresponding IC_{50} concentrations of the B16-F10 cancer-cell line. Only the MA-diamine conjugate (**7**) and the PEGylated diamine conjugate of OA (**17**) exceeded 80% of cell viability for the non-tumour IEC-18 cell line, at the corresponding IC_{50} concentrations of the HT29 cancer-cell line. Finally, only the OA-diamine conjugate (**9**) and the PEGylated diamine conjugates of MA (**14** and **16**) have a percentage of cell viability equal or greater than 80% for the non-tumour WRL68 cell line, at the corresponding IC_{50} concentrations of the Hep G2 cancer-cell line (Table 2).

Table 2
The percentage of viability of the non-tumour cells at the corresponding IC_{50} concentrations for the cancer cells of the diamine conjugates (**1**, **3**, **5**, **7**, **9**, and **11**) and the PEGylated-diamine conjugates (**13**-**18**)of OA or MA.

Type of compound	Compd #	Conc.*	% viability of HPF cells	Conc.**	% viability of IEC-18 cells	Conc.***	% viability of WRL68 cells
Diamine conjugate (OA)	**1**	0.76	91.87 ± 0.84	3.97	40.03 ± 1.77	4.75	54.25 ± 1.64
	5	2.15	48.32 ± 0.69	4.66	32.92 ± 0.34	4.56	43.66 ± 3.30
	9	1.75	93.89 ± 0.76	4.72	60.56 ±1.38	5.85	88.52 ± 0.62
PEGylated diamine conjugate (OA)	**13**	9.14	65.95 ± 1.12	125.15	39.04 ± 0.16	120.09	38.85 ± 0.23
	15	11.34	50.28 ± 1.44	11.74	78.14 ± 0.73	19.32	33.46 ± 0.76
	17	9.41	70.66 ± 0.64	11.90	81.46 ± 1.36	12.99	51.44 ± 0.13
Diamine conjugate (MA)	**3**	1.56	83.29 ± 1.09	5.80	72.97 ± 1.20	4.85	55.13 ± 1.17
	7	6.25	92.94 ± 1.31	7.84	87.63 ± 0.67	8.64	64.03 ± 2.40
	11	1.76	81.26 ± 0.76	4.48	51.51 ± 1.16	4.13	42.31 ± 1.49
PEGylated diamine conjugate (MA)	**14**	17.65	74.00 ± 1.56	37.31	76.38 ± 0.98	31.57	92.74 ± 0.77
	16	20.27	49.64 ± 0.34	20.34	60.18 ± 0.91	19.04	85.77 ± 3.84
	18	12.26	82.12 ± 0.94	13.25	72.54 ± 1.18	13.68	75.77 ± 1.36

* IC_{50} concentration(mM) of the triterpene derivatives in the B16-F10 cell line.
** IC_{50} concentration (mM)of the triterpene derivatives in the HT29 cell line.
*** IC_{50} concentration (mM)of the triterpene derivatives in the Hep G2 cell line.

2.3. Characterization of apoptotic effects by flow cytometry

Taking into account the cytotoxic results of these triterpenic derivatives with both cancer cells and non-tumour cells, 4 diamine conjugates (**1**, **3**, **9**, and **11**) and 4 PEGylated-diamine conjugates (**13**, **14**, **17**, and **18**) of OA or MA, were selected for the following cytometric studies on the B16-F10 cell line. Thus, the apoptotic determination assays were conducted through double staining with annexin V (An-V), conjugated fluorescein isothiocyanate (FITC), and propidium iodide (PI). These assays on the B16-F10 cell line were measured at 24, 48, and 72 h after treatment with the selected 8 triterpene derivatives at their corresponding IC_{50} concentration. The percentages of apoptosis were determined with annexin V–FICT/PI by flow-activated cell sorter (FACS) cytometry analysis (Fig. 3).

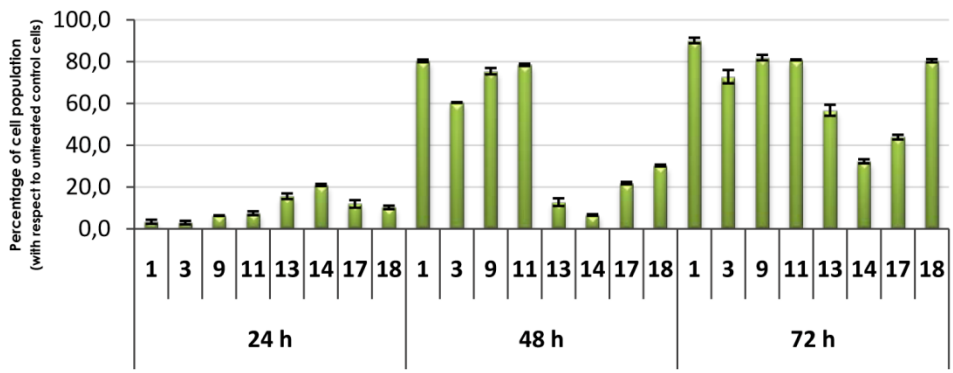

Fig. 3. Flow cytometry analysis of Annexin V-FITC staining and PI accumulation (total apoptosis) after exposure of B16-F10 to OA or MA derivatives for 24, 48, and 72 h. Cell lines were treated at concentrations equal to their corresponding IC_{50} values. Values are expressed as means ± S.E.M. of at least two experiments in duplicate.

The fourOA- or MA-diamine conjugates (**1**, **3**, **9**, and **11**) showed apoptotic effects on treated cells, with total apoptosis rates at 72 h, ranging from 73% to 90% relative to control. These percentages of total apoptosis were lower for the four PEGylated-diamine conjugates of OA or MA (**13**, **14**, **17**, and **18**), under the same conditions, ranging from 32% to 80% relative to control. In addition, the analysis of these apoptosis results at the different times tested (24, 48 and 72 h), revealed that at 24 h the percentages of

total apoptosis were very low for both types of derivatives (between 3% and 21%), although slightly higher for the PEGylated-diamine conjugates (Fig. 3). These percentages of total apoptosis underwent a major change at 48 h of the assay. While the diamine conjugates (**1**, **3**, **9**, and **11**) had percentages between 60% and 80%, the PEGylated-diamine conjugates (**13**, **14**, **17**, and **18**) did not exceed 30%. All compounds reached the highest percentage of apoptosis at 72 h. Compound **1**, the propane-1,3-diamine conjugate of OA, achieved the best total apoptosis value (>90% over control), although compounds **9** and **11**, the decane-1,10-diamine conjugates of OA or MA, and compound **18**, the PEGylated decane-1,10-diamine conjugate of MA, had total apoptosis values greater than 80% (Fig. 3). The length of the diamine chain of these derivatives does not seem to have a clear influence on the apoptosis results. Obtaining new cytotoxic compounds to restore the ability of cancer cells to undergo apoptosis may be a key strategy in new cancer therapies.

2.4. Cell-cycle arrest and distribution

Since inhibition of cell proliferation can be related to cytotoxic and cytostatic effects in response to treatment with these triterpenic derivatives, we analysed cell cycle distribution and cell cycle arrest. Flow cytometry by stained propidium iodide (PI) was used to measure DNA ploidy as well as alteration in cell cycle profiles. The percentages of cells in the different phases of the cell cycle were analysed at 48 h. These tests were not performed at 72 h because under these conditions there were not enough live cells for the results to be reliable. The cancer-cell line B16-F10 was treated with the selected diamine (**1**, **3**, **9**, and **11**) and PEGylated-diamine conjugates (**13**, **14**, **17**, and**18**) of OA or MA at their respective IC_{50} concentrations.

The DNA-histogram analyses revealed that all compounds tested produced cell-cycle arrest in B16-F10 cells, increasing the number of these cells in the S phase. These increases were accompanied by a decrease in the percentage of proliferating cells in the G0/G1 phase, being changes in

the G2/M phase less significant (Fig. 4). The S phase is the stage when DNA replication occurs.

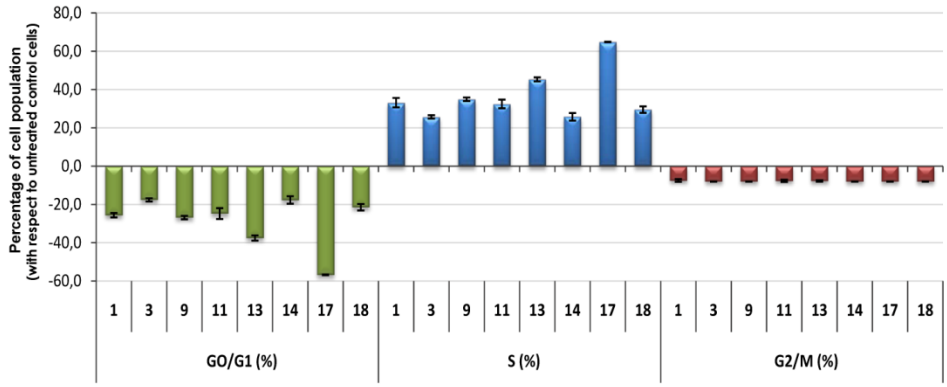

Fig. 4. Changes in the percentages of cells, in each of the cell-cycle phase, have been performed with respect to untreated control cells. B16-F10 was treated with OA or MA derivatives, at their corresponding IC_{50} concentrations. Cell-cycle analysis was conducted after propidium iodide staining, G0/G1 phase (green bars), S phase (blue bars), and G2/M phase (red bars). Values represent means ± S.E.M. of at least two independent experiments performed in triplicate.

Fig.5 shows the cell-cycle histograms of B16-F10 cancer cells, after 48 h of treatment with compounds **1**, **3**, **9** and **11**, at their corresponding IC_{50} concentration. These diamine conjugates of OA or MA were the most apoptotic compounds at 48 h. Cell-cycle arrest in this S phase had absolute populations values of 52.84%,45.43%, 45.36%, and 52.11%, respectivelyfor compounds**1**, **3**, **9**, and **11**, while the Control showed a 19.70% of population in this S phase (Fig. 5).

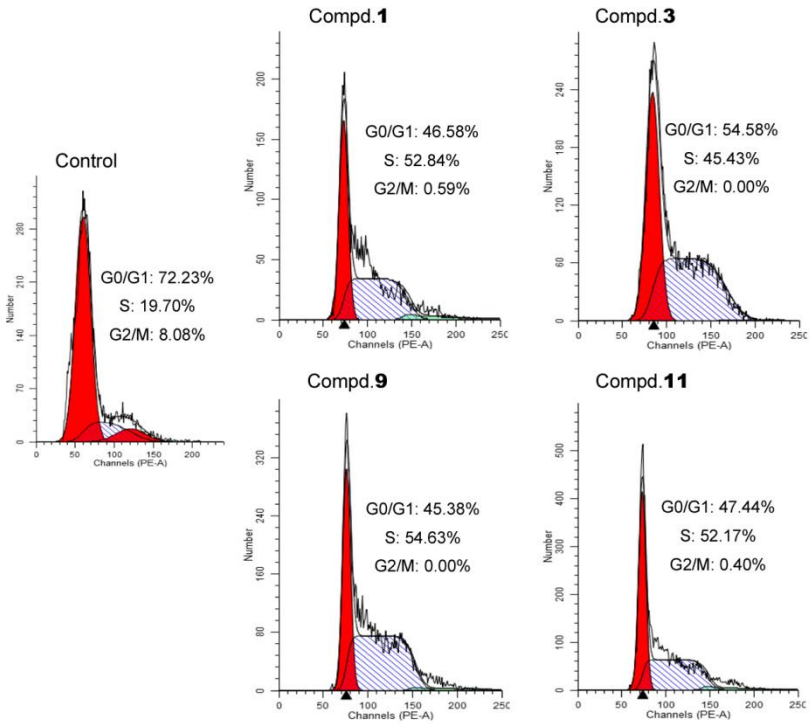

Fig. 5. Cell-cycle histograms of B16-F10 cancer cells, after 48 h of treatment with compounds **1**, **3**, **9** and **11**, at their corresponding IC_{50} concentration.

2.5. Effects on changes in mitochondrial membrane potential

Apoptosis can occur through two essential pathways, one causes mitochondrial disruption (the intrinsic pathway) and leads to loss of mitochondrial membrane potential (MMP), and the other (the extrinsic pathway) induce apoptosis without MMP changes. We analysed the MMP to elucidate the possible mechanism involved in the apoptotic responses of the selected diamine (**1**, **3**, **9**, and **11**) and PEGylated-diamine conjugates (**13**, **14**, **17**, and **18**) of OA or MA in the B16-F10 cell line, at their respective IC_{50} concentration, for 48 h. Changes in the mitochondrial membrane potential were analysed by monitoring the cell fluorescence after a double staining with rhodamine 123 (Rh123) and propidium iodide (PI). Only compound **1** clearly showed a negative Rh123 staining, causing disruption of the mitochondrial membrane with loss of MMP. This result suggests the activation of an intrinsic apoptotic pathway triggered by this propane-1,3-diamine conjugate of OA (**1**). However, the other derivatives tested (**1**, **3**, **9**,

11, **13**, **14**, **17**, and **18**) showed positive Rh123 staining, and the mitochondrial membrane was not affected, suggesting that the apoptosis caused by these OA or MA derivatives could occur through the activation ofan extrinsic pathway (Fig. 6).

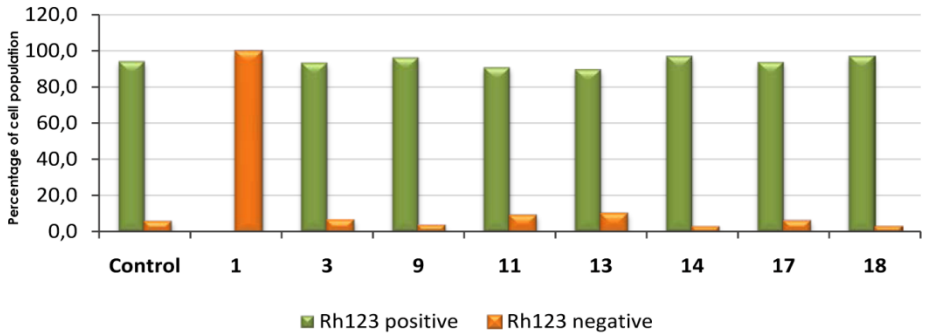

Fig. 6. Flow-cytometry analysis of rhodamine 123 and PI staining after exposure of B16-F10 cells to the selected diamine or PEGylated-diamine conjugates of OA or MA, for 48 h with respect to the control untreated cells. Cell lines were treated at concentrations equal to their corresponding IC_{50} values. Rh123 positive cells (green bars) were rhodamine 123^{+} with PI^{+} or PI^{-}. Rh123 negative cells (orange bars) were rhodamine 123^{-} with PI^{-} or PI^{+}. Values are expressed as means ± S.E.M. of at least two experiments in duplicate.

Fig. 7 shows the flow-cytometry diagrams of rhodamine 123 / propidium iodide of B16-F10 cancer cells, after 48 h of treatment with compounds **1** and **9**, at their corresponding IC_{50} concentration. These diagrams clearly showed a negative Rh123 staining for compound **1** (Quadrant 3), and a positive Rh123 staining for compound **9** (Quadrant 4) (Fig. 7).

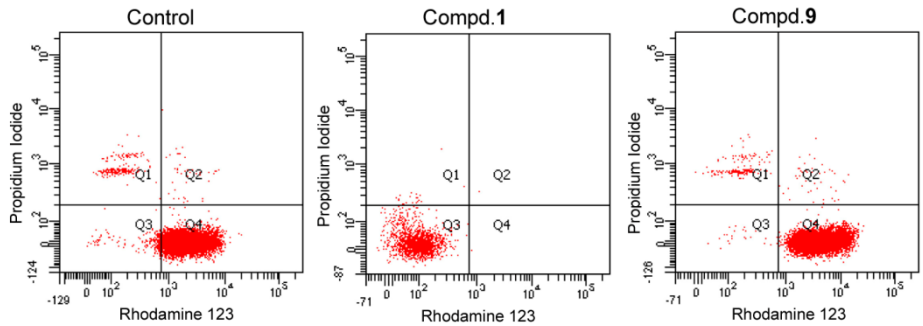

Fig. 7. Flow-cytometry diagram of rhodamine 123 / propidium iodide for compounds **1** and **9**. B16-F10 cells were labelled with Rh123 / IP as described in the Experimental Section. The right quadrants of each diagram (Q2 and Q4) represent positive Rh123 staining of cells.

3. Conclusions

Eighteen diamine or PEGylated-diamine conjugates of oleanolic or maslinic acid were semi-synthesized to evaluate their antiproliferative effects. These triterpenic derivatives were tested for cytotoxicity in three cancer-cell lines (B16-F10, HT29, and Hep G2), and except for the dimer compounds they were more cytotoxic than natural triterpenes. These results were compared to three non-tumour cell lines of the same or a similar tissue (HPF, IEC-18, and WRL68). Percentages of live non-tumour cells were calculated using the IC_{50} values of the triterpenic compounds in the corresponding cancer cells, highlighting the cell viability values (between 81% and 94%) for the non-tumour HPF line, for almost all diamine conjugates tested. The best cytotoxic results were achieved by the diamine conjugates of OA or MA with the shortest and the longest diamine chain (IC_{50} values from 0.76 mM to 1.76 mM), on the B16-F10 cell line, being between 140- and 20-fold more effective than their corresponding precursors (OA or MA).

Four diamine conjugates and four PEGylated-diamine conjugates of OA or MA were selected for several cytometric studies on the B16-F10 cell line. The four OA- or MA-diamine conjugates (**1**, **3**, **9**, and **11**) showed the best apoptotic effects on treated cells at 72 h, with total apoptosis rates between 73% and 90%. These percentages of total apoptosis were lower for the four PEGylated-diamine conjugates of OA or MA (**13**, **14**, **17**, and **18**),

under the same conditions, ranging from 32% to 80%. In addition, the percentages of total apoptosis at 24 h were very low for both types of derivatives (between 3% and 21%), although slightly higher for the PEGylated-diamine conjugates. These percentages increased to 60%-80% at 48 h for the diamine conjugates (**1**, **3**, **9**, and **11**), and did not exceed 30% for the PEGylated-diamine conjugates (**13**, **14**, **17**, and **18**). Compound **1** registered the best total apoptosis value (> 90% over control), and compounds **9**, **11**, and **18** had total apoptosis values greater than 80%. The length of the diamine chain of these derivatives did not seem to have a clear influence on these apoptosis results.

In the B16-F10 cell line, all the compounds tested produced cell-cycle arrest in the S phase. The MMP results suggested the activation of the extrinsic pathway during the apoptosis of B16-F10 cancer cells, for almost all the compounds tested, except for **1**, the most cytotoxic and apoptotic compound on this cancer-cell line, suggesting to activate the intrinsic pathway.

The induction of apoptosis at very low concentrations exhibited by some of these diamine conjugates of OA or MA in several tumour lines, and the high percent viability of the corresponding non-tumour cells at these concentrations, suggest that these compounds could be used in the future as safe and effective anticancer agents.

4. Experimental

4.1. General experimental chemical procedures.

Measurements of NMR spectra were made in VARIAN direct drive (400 and 500 MHz ^{1}H NMR) spectrometers. The ^{13}C chemical shifts were assigned with the aid of distortion less enhancement by polarization transfer (DEPT) using a flip angle of 135º. IR spectra were recorded on a MATTSON SATELLITE FTIR spectrometer. Optical rotations were measured with a Perkin-Elmer 241 polarimeter at 25 ºC. The purity of new compounds was determined by a WATERS ACQUITY UPLC system (ultra-performance liquid chromatography), coupled with a WATERS SYNAPT G2 HRMS spectrometer

(high-resolution mass spectra), with ESI (electrospray ionization). The purities of all compounds were confirmed to be ≥ 95%. Melting points (mp) were determined using a Kofler (Reichter) apparatus and are uncorrected. All reaction solvents and chromatography solvents were distilled prior to use. Commercially available reagents were used without further purification. Merck silica-gel 60 aluminium sheets (ref. 1.16835) were used for TLC, and spots were rendered visible by spraying with H_2SO_4–AcOH, followed by heating to 120 °C, and also visualized under UV at 254 nm. Merck silica-gel 60 (0.040–0.063 mm, ref. 1.09385) was used for flash chromatography. CH_2Cl_2 (Fisher, ref. D/1852/17), $CHCl_3$ (Fisher, ref. C/4960/17), or n-hexane (Merck, ref. 1.04374), with increasing amounts of Me_2CO (Fisher, ref. A/0600/17), MeOH (Fisher, ref. M/4000/17), or EtOAc (Fisher, ref. E/0900/17), were used as eluents (all the solvents had an analytical reagent-grade purity). The PEG reagent 3,6,9-trioxadecanoic acid (PEG-COOH, CAS Number 16024-58-1) and TBTU (CAS Number 125700-67-6) were purchased from Sigma-Aldrich.

*4.2. Isolation of OA (**I**) andMA (**II**).*

OA (**I**) and MA (**II**) were isolated from solid olive-oil-production wastes, which were extracted successively in a Soxhlet with hexane and EtOAc. Hexane extracts were a mixture of OA and MA (80:20), whereas this relationship was (20:80) for the EtOAc extracts. Both products were purified from these mixtures by column chromatography over silica gel, eluting with a $CHCl_3$-MeOH or CH_2Cl_2-Me_2CO mixtures of increasing polarity [34]. These natural compounds can also be extracted more efficiently using an alternative method such as microwave-assisted extraction [33].

*4.3. Amidation reactions on the C-28 carboxylic group of OA (**I**) orMA (**II**).*

DIEA (0.3 mmol each) and TBTU (0.66 mmol each) were added to a solution of OA (**I**) and to a solution of MA (**II**) (0.44 mmol of each) in THF (20 mL each). The reaction mixtures were maintained at rt for 12 h, and then diluted with water and extracted three times with CH_2Cl_2. The organic layers were dried with dry Na_2SO_4 and the solvent was removed under reduced pressure. Finally, each residue was purified by column chromatography using hexane/EtOAc as eluents, yielding the corresponding TBTU derivatives [22]. These two TBTU derivatives (0.35 mmol of each) were respectively dissolved in CH_2Cl_2 (15 mL each), and each of these two solutions were split into three new solutions, and K_2CO_3 (1 mmol each) and the corresponding diamine reagent (3 mmol of propane-1,3-diamine or hexane-1,6-diamine or decane-1,10-diamine each) were added. These reaction mixtures were maintained at rt for 5 h. Thereafter, CH_2Cl_2 was added to each reaction mixture, and then were washed several times with water. Each organic layer was treated with dry Na_2SO_4 and the solvent was removed under reduced pressure. Finally, each residue was purified in a chromatography column using CH_2Cl_2/acetone as eluent, yielding the following pairs of derivatives: **1** (65%) and **2** (28%), **3** (63%) and **4** (27%), **5** (62%) and **6** (29%), **7** (64%) and **8** (28%), **9** (63%) and **10** (29%), and **11** (62%) and **12** (30%).

*Compound **1**:* White solid, mp 97–99°C; $[\alpha]^{25}_D$ + 55 (*c* 1 in $CHCl_3$); IR ν_{max}(KBr)/cm^{-1} 3356, 2922, 1633, 1524, 1463, 1386, 1030 and 997; δ_H ($CDCl_3$, 400 MHz): 6.41 (dd, 1H, $J_1 = J_2 = 5.0$ Hz, NHCO group), 5.35 (dd, 1H, $J_1 = J_2 = 3.2$ Hz, H-12), 3.49–3.44 (m, 1H, H-1'), 3.21 (dd, 1H, $J_1 = 4.6$, $J_2 = 8.8$ Hz, H-3), 3.13–3.10 (m, 1H, H-1'), 2.77 (t, 2H, $J = 6.0$ Hz, H-3'), 2.52 (dd, 1H, $J_1 = 3.4$, $J_2 = 13.0$ Hz, H-18), 1.25, 1.15, 0.98, 0.90, 0.90, 0.78, 0.76 (s, 3H each, methyl groups); δ_C ($CDCl_3$, 100 MHz): 178.7 (C-28), 145.0 (C-13), 122.9 (C-12), 79.1 (C-3), 55.3 (C-5), 47.7 (C-9), 47.0 (C-19), 46.4 (C-17), 42.3 (C-18), 42.2 (C-14), 40.0 (C-3'), 39.5 (C-8), 38.9 (C-4), 38.7 (C-1), 37.6 (C-1'), 37.1 (C-10), 34.3 (C-21), 33.2 (Me), 32.9 (C-7), 32.6 (C-22), 32.3 (C-2'), 30.9 (C-20), 28.3 (Me), 27.5 (C-2), 27.3 (C-15), 26.0 (Me), 23.9 (C-16), 23.8 (Me), 23.7 (C-11), 18.5 (C-6), 17.1

(Me), 15.7 (Me), 15.5 (Me); ESI-HRMS m/z calcd for $C_{33}H_{57}N_2O_2$ $[M+1]^+$ 513.4420, found 513.4426.

Compound **2**: White solid, mp 118–120ºC; $[a]^{25}_D$ + 49 (c 1 in $CHCl_3$); IR ν_{max}(KBr)/cm^{-1} 3354, 2942, 1634, 1520, 1455, 1386, 1030 and 997; δ_H ($CDCl_3$, 400 MHz): 6.41 (dd, 1H, $J_1 = J_2 = 6.0$ Hz, NHCO group), 5.40 (dd, 1H, $J_1 = J_2 = 3.2$ Hz, H-12), 3.28–3.24 (m, 1H, H-1'), 3.21 (dd, 1H, $J_1 = 4.8$, $J_2 = 11.21$ Hz, H-3), 3.14–3.10 (m, 1H, H-1'), 2.64 (dd, 1H, $J_1 = 3.2$, $J_2 = 14.4$ Hz, H-18), 1.25, 1.15, 0.98, 0.91, 0.90, 0.77, 0.74 (s, 3H each, methyl groups); δ_C ($CDCl_3$, 100 MHz): 178.5 (C-28), 144.7 (C-13), 122.9 (C-12), 79.1 (C-3), 55.3 (C-5), 47.7 (C-9), 46.9 (C-19), 46.4 (C-17), 42.1 (C-14), 42.0 (C-18), 39.5 (C-8), 38.9 (C-4), 38.6 (C-1), 37.1 (C-10), 36.2 (C-1' and C-3'), 34.4 (C-21), 33.2 (Me), 33.1 (C-7), 32.6 (C-22), 30.9 (C-20), 29.8 (C-2'), 28.2 (Me), 27.5 (C-2), 27.3 (C-15), 25.9 (Me), 23.9 (C-16), 23.8 (Me), 23.7 (C-11), 18.5 (C-6), 17.1 (Me), 15.7 (Me), 15.5 (Me); ESI-HRMS m/z calcd for $C_{63}H_{101}N_2O_4$ $[M-1]^-$ 949.7761, found 949.7772.

Compound **3**: White solid, mp 110–112ºC; $[a]^{25}_D$ + 41 (c 1 in $CHCl_3$); IR ν_{max}(KBr)/cm^{-1} 3354, 2942, 1634, 1525, 1462, 1365, 1049 and 749; δ_H ($CDCl_3$, 400 MHz): 6.43 (dd, 1H, $J_1 = J_2 = 5.4$ Hz, NHCO group), 5.35 (dd, 1H, $J_1 = J_2 = 3.2$ Hz, H-12), 3.70 (ddd, 1H, $J_1 = 4.8$, $J_2 = 9.6$, $J_3 = 14.0$ Hz, H-2), 3.50–3.41 (m, 1H, H-1'), 3.13–3.10 (m, 1H, H-1'), 2.98 (d, 1H, $J = 9.6$ Hz, H-3), 2.75 (t, 1H, $J = 6.4$ Hz, H-3'), 2.52 (dd, 1H, $J_1 = 3.6$, $J_2 = 12.8$ Hz, H-18), 1.15, 1.02, 0.97, 0.90, 0.90, 0.81, 0.75 (s, 3H each, methyl groups); δ_C ($CDCl_3$, 100 MHz): 178.5 (C-28), 145.0 (C-13), 122.7 (C-12), 84.0 (C-3), 68.9 (C-2), 55.4 (C-5), 47.7 (C-9), 46.9 (C-19), 46.5 (C-1), 46.4 (C-17), 42.2 (C-14), 42.3 (C-18), 40.2 (C-3'), 39.6 (C-8), 39.3 (C-10), 38.3 (C-4), 37.8 (C-1'), 34.3 (C-21), 33.2 (Me), 32.9 (C-7), 32.6 (C-22), 32.5 (C-2'), 30.9 (C-20), 28.8 (Me), 27.5 (C-15), 26.0 (Me), 23.8 (C-16), 23.9 (Me), 23.8 (C-11), 18.5 (C-6), 17.2 (Me), 17.0 (Me), 16.8 (Me); ESI-HRMS m/z calcd for $C_{33}H_{57}N_2O_3$ $[M+1]^+$ 529.4369, found 529.4336.

Compound ***4***: White solid, mp 78–79°C; $[\alpha]^{25}_{D}$ + 45 (*c* 1 in $CHCl_3$); IR ν_{max}(KBr)/cm^{-1} 3356, 1634, 1525, 1462, 1365, 1050 and 751; δ_H ($CDCl_3$, 400 MHz): 6.43 (dd, 1H, $J_1 = J_2$ = 6.0 Hz, NHCO group), 5.35 (dd, 1H, $J_1 = J_2$ = 3.2 Hz, H-12), 3.70 (ddd, 1H, J_1 = 4.0, J_2 = 9.2, J_3 = 14.0 Hz, H-2), 3.28–3.23 (m, 1H, H-1'), 3.15–3.10 (m, 1H, H-1'), 3.01 (d, 1H, *J* = 9.2 Hz, H-3), 2.65 (dd, 1H, J_1 = 3.6, J_2 = 13.2 Hz, H-18), 1.16, 1.03, 0.98, 0.92, 0.91, 0.83, 0.74 (s, 3H each, methyl groups); δ_C ($CDCl_3$, 100 MHz): 178.6 (C-28), 144.8 (C-13), 122.7 (C-12), 84.1 (C-3), 69.0 (C-2), 55.3 (C-5), 47.7 (C-9), 46.8 (C-19), 46.5 (C-1), 46.4 (C-17), 42.2 (C-14), 42.0 (C-18), 39.6 (C-8), 39.3 (C-10), 38.4 (C-4), 36.1 (C-1' and C-3'), 34.4 (C-21), 33.2 (Me), 33.1 (C-7), 32.5 (C-22), 30.9 (C-20), 29.9 (C-2'), 28.7 (Me), 27.5 (C-15), 26.0 (Me), 23.7 (C-16), 23.8 (Me), 23.8 (C-11), 18.5 (C-6), 17.1 (Me), 16.9 (Me), 16.8 (Me); ESI-HRMS m/z calcd for $C_{63}H_{103}N_2O_6$ $[M+1]^+$ 983.7816, found 983.7781.

Compound ***5***: White solid, mp 80–82°C; $[\alpha]^{25}_{D}$ + 35 (*c* 1 in $CHCl_3$); IR ν_{max}(KBr)/cm^{-1} 3343, 2939, 1634, 1526, 1462, 1386, 1030 and 751; δ_H ($CDCl_3$, 400 MHz): 5.96 (dd, 1H, $J_1 = J_2$ = 6.0 Hz, NHCO group), 5.37 (dd, 1H, $J_1 = J_2$ = 2.8 Hz, H-12), 3.37–3.32 (m, 1H, H-1'), 3.21 (dd, 1H, J_1 = 4.4, J_2 = 10.8 Hz, H-3), 2.98–2.94 (m, 1H, H-1'), 2.78 (t, 2H, *J* = 6.0 Hz, H-6'), 2.50 (dd, 1H, J_1 = 2.8, J_2 = 13.2 Hz, H-18), 1.15, 0.98, 0.91, 0.90, 0.90, 0.78, 0.75 (s, 3H each, methyl groups); δ_C ($CDCl_3$, 100 MHz): 178.4 (C-28), 145.2 (C-13), 122.9 (C-12), 79.1 (C-3), 55.3 (C-5), 47.7 (C-9), 47.0 (C-19), 46.4 (C-17), 42.2 (C-14), 42.5 (C-18), 40.3 (C-6'), 39.5 (C-8), 39.4 (C-1'), 38.9 (C-4), 38.6 (C-1), 37.1 (C-10), 34.3 (C-21), 33.2 (Me), 32.7 (C-7), 32.6 (C-22), 30.9 (C-20), 30.0 (C-5'), 29.5 (C-2'), 28.3 (Me), 27.5 (C-2), 27.3 (C-15), 26.4 (C-3'), 25.9 (Me), 25.9 (C-4') 23.8 (C-16), 23.8 (Me), 23.7 (C-11), 18.5 (C-6), 17.1 (Me), 15.8 (Me), 15.6 (Me); ESI-HRMS m/z calcd for $C_{36}H_{63}N_2O_2$ $[M+1]^+$ 555.4890, found 555.4874.

Compound **6**: White solid, mp 84–86°C; $[\alpha]^{25}_{D}$ + 41 (*c* 1 in $CHCl_3$); IR ν_{max}(KBr)/ m^{-1} 2941, 1738, 1637, 1440, 1366, 1216 and 527; δ_H ($CDCl_3$, 400 MHz): 5.95 (dd, 1H, $J_1 = J_2$ = 5.2 Hz, NHCO group), 5.36 (dd, 1H, $J_1 = J_2$ = 3.0 Hz, H-12), 3.35–3.30 (m, 1H, H-1'), 3.20 (dd, 1H, J_1 = 4.2, J_2 = 11.0 Hz, H-3), 3.00–2.93 (m, 1H, H-1'), 2.48 (dd, 1H, J_1 = 3.2, J_2 = 13.2 Hz, H-18), 1.14, 0.97, 0.89, 0.89, 0.88, 0.77, 0.74 (s, 3H each, methyl groups); δ_C ($CDCl_3$, 100 MHz): 178.3 (C-28), 145.2 (C-13), 122.8 (C-12), 79.0 (C-3), 55.2 (C-5), 47.7 (C-9), 46.9 (C-19), 46.4 (C-17), 42.2 (C-14), 42.5 (C-18), 39.5 (C-8), 39.4 (C-1' and C-6'), 38.6 (C-4), 38.6 (C-1), 37.1 (C-10), 34.3 (C-21), 33.1 (Me), 32.6 (C-7), 32.5 (C-22), 30.8 (C-20), 29.5 (C-2' and C-5'), 28.2 (Me), 27.4 (C-2), 27.4 (C-15), 26.8 (C-3' and C-4'), 25.9 (Me), 23.9 (C-16), 23.7 (Me), 23.7 (C-11), 18.4 (C-6), 17.1 (Me), 15.7 (Me), 15.5 (Me); ESI-HRMS m/z calcd for $C_{66}H_{107}N_2O_4$ $[M-1]^-$ 991.8231, found 991.8235.

Compound **7**: White solid, mp 100–102°C; $[\alpha]^{25}_{D}$ + 38 (*c* 1 in $CHCl_3$); IR ν_{max}(KBr)/cm^{-1} 2927, 1738, 1526, 1634, 1455, 1365, 1217, 1050 and 733; δ_H ($CDCl_3$, 400 MHz): 5.90 (dd, 1H, $J_1 = J_2$ = 5.4 Hz, NHCO group), 5.36 (dd, 1H, $J_1 = J_2$ = 3.2 Hz, H-12), 3.68 (ddd, 1H, J_1= 4.8, J_2 = 9.2, J_3 = 14.0 Hz, H-2), 3.35–3.32 (m, 1H, H-1'), 3.19–3.15 (m, 1H, H-1'), 2.98 (d, 1H, *J* = 9.2 Hz, H-3), 2.69 (t, 2H, *J* = 6.4 Hz, H-6'), 2.49 (dd, 1H, J_1 = 3.6, J_2 = 12.8 Hz, H-18), 1.15, 1.02, 0.98, 0.90, 0.90, 0.82, 0.75 (s, 3H each, methyl groups); δ_C ($CDCl_3$, 100MHz): 178.2 (C-28), 145.3 (C-13), 122.6 (C-12), 83.9 (C-3), 68.9 (C-2), 55.3 (C-5), 47.7 (C-9), 46.9 (C-19), 46.5 (C-1), 46.4 (C-17), 42.5 (C-18), 42.3 (C-14), 39.6 (C-8), 39.5 (C-1'), 39.5 (C-6'), 39.3 (C-10), 38.3 (C-4), 34.3 (C-21), 33.1 (Me), 32.7 (C-7), 32.4 (C-22), 30.9 (C-20), 29.5 (C-2'), 29.5 (C-5'), 28.8 (Me), 27.4 (C-15), 26.8 (C-3'), 26.8 (C-4'), 25.9 (Me), 23.9 (C-16), 23.9 (Me), 23.9 (C-11), 18.5 (C-6), 17.1 (Me), 16.9 (Me), 16.9 (Me); ESI-HRMS m/z calcd for $C_{36}H_{63}N_2O_3$ $[M+1]^+$ 571.4839, found 571.4842.

Compound ***8***: White solid, mp 81–83ºC; $[\alpha]^{25}_{D}$ + 41 (*c* 1 in $CHCl_3$); IR ν_{max}(KBr)/cm^{-1} 2970, 1738, 1639, 1365, 1216, 1049 and 528; δ_H ($CDCl_3$, 400 MHz): 5.94 (dd, 1H, $J_1 = J_2$ = 5.4 Hz, NHCO group), 5.38 (dd, 1H, $J_1 = J_2$ = 3.2 Hz, H-12), 3.70 (ddd, 1H, J_1 = 4.4, J_2 = 9.2, J_3 = 13.6 Hz, H-2), 3.38–3.30 (m, 1H, H-1'), 3.01–2.94 (m, 1H, H-1'), 3.00 (d, 1H, *J* = 9.2 Hz, H-3), 2.50 (dd, 1H, J_1 = 3.2, J_2 = 12.8 Hz, H-18), 1.25, 1.16, 1.03, 0.99, 0.90, 0.83, 0.76 (s, 3H each, methyl groups); δ_C ($CDCl_3$, 100 MHz): 178.3 (C-28), 145.4 (C-13), 122.6 (C-12), 84.0 (C-3), 69.0 (C-2), 55.3 (C-5), 47.7 (C-9), 46.9 (C-19), 46.5 (C-1), 46.4 (C-17), 42.3 (C-14), 42.5 (C-18), 39.5 (C-1' and C-6'), 39.4 (C-8), 39.3 (C-10), 38.3 (C-4), 34.3 (C-21), 33.1 (Me), 32.7 (C-7), 32.4 (C-22), 30.9 (C-20), 29.5 (C-2' and C-5'), 28.8 (Me), 27.4 (C-15), 26.8 (C-3' and C-4'), 25.9 (Me), 23.9 (C-16), 23.9 (Me), 23.9 (C-11), 18.5 (C-6), 17.1 (Me), 16.9 (Me), 16.9 (Me); ESI-HRMS m/z calcd for $C_{66}H_{109}N_2O_6$ $[M+1]^+$ 1025.8286, found, 1025.8268.

Compound ***9***: White solid, mp 62–64ºC; $[\alpha]^{25}_{D}$ + 42 (*c* 1 in $CHCl_3$); IR ν_{max}(KBr)/cm^{-1} 3351, 2924, 1738, 1641, 1530, 1455, 1365, 1216 and 528; δ_H ($CDCl_3$, 400 MHz): 6.41 (dd, 1H, $J_1 = J_2$ = 5.2 Hz, NHCO group), 5.35 (dd, 1H, $J_1 = J_2$ = 3.2 Hz, H-12), 3.49–3.39 (m, 1H, H-1'), 3.21 (dd, 1H, J_1 = 4.6, J_2 = 11.1 Hz, H-3), 3.14–3.07 (m, 1H, H-1'), 2.77 (t, 2H, *J* = 6.0 Hz, H-10'), 2.52 (dd, 1H, J_1 = 3.6, J_2 = 13.2 Hz, H-18), 1.25, 1.15, 0.98, 0.91, 0.90, 0.78, 0.76 (s, 3H each, methyl groups); δ_C ($CDCl_3$, 100 MHz): 178.2 (C-28), 145.3 (C-13), 122.8 (C-12), 79.1 (C-3), 55.3 (C-5), 47.7 (C-9), 47.0 (C-19), 46.4 (C-17), 42.4 (C-10'), 42.3 (C-14), 42.6 (C-18), 39.6 (C-1'), 39.5 (C-8), 38.9 (C-4), 38.7 (C-1), 37.1 (C-10), 34.3 (C-21), 33.9 (C-9'), 33.2 (Me), 32.7 (C-7), 32.6 (C-22), 31.1 (C-2'), 30.9 (C-20), 29.8 (C-4'), 29.7 (C-5'), 29.6 (C-6'), 29.4 (C-7'), 28.3 (Me), 27.5 (C-2), 27.5 (C-15), 27.3 (C-3'), 27.1 (C-8'), 25.9 (Me), 24.0 (C-16), 23.8 (Me), 23.7 (C-11), 18.5 (C-6), 17.1 (Me), 15.7 (Me), 15.5 (Me); ESI-HRMS m/z calcd for $C_{40}H_{71}N_2O_2$ $[M+1]^+$ 611.5516, found 611.5534.

Compound ***10***: White solid, mp 60–62ºC; $[\alpha]^{25}_D$ + 51 (*c* 1 in $CHCl_3$); IR ν_{max}(KBr)/cm^{-1} 3415, 2920, 1737, 1636, 1528, 1450, 1365, 1216 and 519; δ_H ($CDCl_3$, 400 MHz): 5.90 (dd, 1H, $J_1 = J_2$ = 4.8 Hz, NHCO group), 5.36 (dd, 1H, $J_1 = J_2$ = 2.8 Hz, H-12), 3.37–3.32 (m, 1H, H-1'), 3.21 (dd, 1H, J_1 = 4.4, J_2 = 10.8 Hz, H-3), 3.00–2.96 (m, 1H, H-1'), 2.49 (dd, 1H, J_1 = 2.6, J_2 = 12.6 Hz, H-18), 1.25, 1.15, 0.98, 0.91, 0.90, 0.78, 0.76 (s, 3H each, methyl groups); δ_C ($CDCl_3$, 100 MHz): 178.2 (C-28), 145.3 (C-13), 122.8 (C-12), 79.1 (C-3), 55.3 (C-5), 47.7 (C-9), 47.0 (C-19), 46.4 (C-17), 42.6 (C-18), 42.3 (C-14), 39.6 (C-1' and C-10'), 39.5 (C-8), 38.7 (C-1), 38.6 (C-4), 37.1 (C-10), 34.3 (C-21), 33.1 (Me), 32.7 (C-7), 32.5 (C-22), 30.9 (C-20), 29.7 (C-2' and C-9'), 29.5 (C-3' and C-8'), 29.4 (C-4' and C-7'), 28.3 (Me), 27.5 (C-2), 27.5 (C-15), 27.3 (C-5' and C-6'), 25.9 (Me), 24.0 (C-16), 23.8 (Me), 23.7 (C-11), 18.5 (C-6), 17.1 (Me), 15.7 (Me), 15.5 (Me); ESI-HRMS m/z calcd for $C_{70}H_{117}N_2O_4$ $[M+1]^+$ 1049.9013, found 1049.8990.

Compound ***11***: White solid, mp 75–77ºC; $[\alpha]^{25}_D$ + 36 (*c* 1 in $CHCl_3$); IR ν_{max}(KBr)/cm^{-1} 2925, 1737, 1635, 1527, 1455, 1365, 1216 and 528; δ_H ($CDCl_3$, 400 MHz): 5.91 (dd, 1H, $J_1 = J_2$ = 4.8 Hz, NHCO group), 5.36 (dd, 1H, $J_1 = J_2$ = 2.8 Hz, H-12), 3.68 (ddd, 1H, J_1 = 4.0, J_2 = 9.6, J_3 = 14.0 Hz, H-2), 3.36–3.28 (m, 1H, H-1'), 3.06–2.99 (m, 1H, H-1'), 3.00 (d, 1H, J = 9.6 Hz, H-3), 2.68 (t, 2H, J = 6.4 Hz, H-10'), 2.50 (dd, 1H, J_1 = 2.4, J_2 = 12.4 Hz, H-18), 1.28, 1.16, 1.03, 0.99, 0.90, 0.82, 0.76 (s, 3H each, methyl groups); δ_C ($CDCl_3$, 100 MHz): 178.2 (C-28), 145.5 (C-13), 122.6 (C-12), 83.8 (C-3), 68.7 (C-2), 55.3 (C-5), 47.6 (C-9), 46.9 (C-19), 46.7 (C-1), 46.4 (C-17), 42.7 (C-18), 42.3 (C-14), 42.3 (C-10'), 39.6 (C-8), 39.6 (C-1'), 39.3 (C-10), 38.4 (C-4), 34.3 (C-21), 33.7 (C-9'), 33.2 (Me), 32.7 (C-7), 32.4 (C-22), 30.9 (C-20), 29.9 (C-2'), 29.8 (C-5'), 29.8 (C-4'), 29.5 (C-6'), 29.3 (C-7'), 28.8 (Me), 27.5 (C-15), 27.5 (C-3'), 27.2 (C-8'), 25.9 (Me), 23.9 (C-11), 23.8 (C-16), 23.8 (Me), 18.5 (C-6), 17.2 (Me), 17.0 (Me), 16.9 (Me); ESI-HRMS m/z calcd for $C_{70}H_{71}N_2O_3$ $[M+1]^+$ 627.5465, found 627.5478.

Compound ***12***: White solid, mp 69–71°C; $[\alpha]^{25}_{D}$ + 27 (*c* 1 in $CHCl_3$); IR ν_{max}(KBr)/cm^{-1} 2928, 1738, 1634, 1535, 1449, 1366, 1217 and 528; δ_H ($CDCl_3$, 400 MHz): 5.94 (dd, 1H, $J_1 = J_2 = 5.2$ Hz, NHCO group), 5.37 (dd, 1H, $J_1 = J_2 = 3.2$ Hz, H-12), 3.69 (ddd, 1H, $J_1 = 4.4$, $J_2 = 9.6$, $J_3 = 14.0$ Hz, H-2), 3.35–3.29 (m, 1H, H-1'), 3.02–2.96 (m, 1H, H-1'), 3.51 (d, 1H, $J = 9.6$ Hz, H-3), 2.47 (dd, 1H, $J_1 = 3.2$, $J_2 = 12.4$ Hz, H-18), 1.25, 1.16, 1.03, 0.98, 0.90, 0.83, 0.76 (s, 3H each, methyl groups); δ_C ($CDCl_3$, 100 MHz): 178.4 (C-28), 145.4 (C-13), 122.6 (C-12), 83.7 (C-3), 68.8 (C-2), 55.2 (C-5), 47.6 (C-9), 46.8 (C-19), 46.6 (C-1), 46.4 (C-17), 42.6 (C-18), 42.3 (C-14), 39.7 (C-8), 39.6 (C-1' and C-10'), 39.3 (C-10), 38.4 (C-4), 34.2 (C-21), 33.1 (Me), 32.6 (C-7), 32.4 (C-22), 30.9 (C-20), 29.8 (C-2' and C-9'), 29.6 (C-3' and C-8'), 29.3 (C-4' and C-7'), 28.7 (Me), 27.4 (C-15), 27.4 (C-5' and C-6'), 25.8 (Me), 23.8 (C-11), 23.7 (C-16), 23.7 (Me), 18.4 (C-6), 17.1 (Me), 16.9 (Me), 16.8 (Me); ESI-HRMS m/z calcd for $C_{70}H_{71}N_2O_3$ $[M+1]^+$ 1081.8912, found 1081.8900.

4.4. PEGylation reaction on the free amino group of the OA- or MA-diamine conjugates.

DIPCDI (4 mmol each) and 3,6,9-trioxadecanoic acid (PEG-COOH, 4 mmol each) were added to six solutions of compounds**1**, **3**, **5**, **7**, **9**, or **11** (1 mmol of each) in THF (20 mL each). The reaction mixtures were stirred at rt for 4 h, and then filtered and diluted with CH_2Cl_2. These organic layers were separately washed several times with water, treated with dry Na_2SO_4, and the solvent removed under reduced pressure. Finally, each residue was purified on a chromatography column using CH_2Cl_2/acetone as eluent, isolating the following PEGylated-diamine conjugates of OA or MA:**13** (91%), **14** (88%), **15** (89%), **16** (91%), **17** (94%), and **18** (89%).

Compound ***13***: Transparent syrup; $[\alpha]^{25}_{D}$ + 48 (*c* 1 in $CHCl_3$); IR ν_{max}(film)/cm^{-1} 2926, 1738, 1639, 1530, 1365, 1216, 1106 and 528; δ_H ($CDCl_3$, 500 MHz): 7.32 (dd, 1H, $J_1 = J_2$ = 6.5 Hz, NHCO group), 6.54 (dd, 1H, $J_1 = J_2$ = 6.0 Hz, NHCO group), 5.38 (dd, 1H, $J_1 = J_2$ = 3.5 Hz, H-12), 4.00 (s, 2H, CH_2 PEG group), 3.74–3.53 (m, 8H, CH_2 PEG group), 3.35 (s, 3H, CH_3 PEG group), 3.34–3.17 (m, 4H, H-3, H-1', and H-3'), 3.08–3.03 (m, 1H, H-1'), 2.64 (dd, 1H, J_1 = 3.2, J_2 = 12.8 Hz, H-18), 1.13, 0.96, 0.90, 0.88, 0.87, 0.76, 0.72 (s, 3H each, methyl groups); δ_C ($CDCl_3$, 125 MHz): 178.3 (C-28), 170.8 (C-1''), 144.6 (C-13), 122.8 (C-12), 79.0 (C-3), 71.9 (C-2''), 71.2 (C-3''), 70.5 (C-4''), 70.4 (C-5''), 70.2 (C-6''), 59.0 (C-7''), 55.2 (C-5), 47.7 (C-9), 46.7 (C-19), 46.4 (C-17), 42.0 (C-14), 41.9 (C-18), 39.5 (C-8), 38.9 (C-4), 38.5 (C-1), 37.1 (C-10), 35.9 (C-1'), 35.8 (C-3'), 34.3 (C-21), 33.1 (C-7), 32.6 (C-22), 32.6 (Me), 30.8 (C-20), 29.7 (C-2'), 28.2 (Me), 27.5 (C-2), 27.2 (C-15), 25.9 (Me), 23.6 (C-16), 23.7 (Me), 23.6 (C-11), 18.4 (C-6), 17.1 (Me), 15.7 (Me), 15.4 (Me); ESI-HRMS m/z calcd for $C_{40}H_{69}N_2O_6$ $[M+1]^+$ 673.5156, found 673.5144.

Compound ***14***: Transparent syrup; $[\alpha]^{25}_{D}$ + 23 (*c* 1 in $CHCl_3$); IR ν_{max}(film)/cm^{-1} 3343, 2923, 1737, 1645, 1532, 1365, 1104 and 558; δ_H ($CDCl_3$, 500 MHz): 7.34 (dd, 1H, $J_1 = J_2$ = 6.5 Hz, NHCO group), 6.58 (dd, 1H, $J_1 = J_2$ = 5.5 Hz, NHCO group), 5.40 (dd, 1H, $J_1 = J_2$ = 3.5 Hz, H-12), 4.00 (s, 2H, CH_2 PEG group), 3.77–3.54 (m, 9H, H-2 and 4 CH_2 PEG group), 3.37 (s, 3H, CH_3 PEG group), 3.35–3.24 (m, 3H, H-3' and H-1'), 3.08–3.04 (m, 1H, H-1'), 3.0 (d, 1H, J_1 = 9.5 Hz, H-3), 2.67 (dd, 1H, J_1 = 3.5, J_2 = 13.0 Hz, H-18), 1.14, 1.02, 0.97, 0.92, 0.89, 0.81, 0.73 (s, 3H each, methyl groups); δ_C ($CDCl_3$, 125 MHz): 178.3 (C-28), 170.9 (C-1''), 144.6 (C-13), 122.7 (C-12), 84.0 (C-3), 72.0 (C-2''), 71.3 (C-3''), 70.6 (C-4''), 70.5 (C-5''), 70.3 (C-6''), 69.1 (C-2), 59.1 (C-7''), 55.4 (C-5), 47.7 (C-9), 46.7 (C-1), 46.5 (C-19), 46.4 (C-17), 42.1 (C-14), 42.0 (C-18), 39.5 (C-8), 39.3 (C-10), 38.3 (C-4), 35.9 (C-1'), 35.9 (C-3'), 34.4 (C-21), 33.2 (C-7), 32.6 (C-22), 33.2 (Me), 30.8 (C-20), 29.8 (C-2'), 28.8 (Me), 27.5 (C-15), 26.0 (Me), 23.8 (Me), 23.7 (C-16), 23.7 (C-11), 18.5 (C-6), 17.2 (Me), 16.9 (Me), 16.8 (Me); ESI-HRMS m/z calcd for $C_{40}H_{69}N_2O_7$ $[M+1]^+$ 689.5105, found 689.5112.

Compound ***15***: Transparentsyrup; $[\alpha]^{25}_{D}$ + 35 (c 1 in $CHCl_3$); IR ν_{max}(film)/cm^{-1} 3349, 2926, 1655, 1531, 1454, 1364, 1104 and 558; δ_H ($CDCl_3$, 500 MHz): 7.02 (dd, 1H, $J_1 = J_2$ = 5.5 Hz, NHCO group), 5.93 (dd, 1H, $J_1 = J_2$ = 6.0 Hz, NHCO group), 5.35 (dd, 1H, $J_1 = J_2$ = 3.5 Hz, H-12), 3.96 (s, 2H, CH_2 PEG group), 3.74–3.52 (m, 8H, CH_2 PEG group), 3.35 (s, 3H, CH_3 PEG group), 3.34–3.17 (m, 4H, H-3, H-6', and H-1'), 2.98–2.93 (m, 2H, H-1'), 2.50 (dd, 1H, J_1 = 3.5, J_2 = 13.0 Hz, H-18), 1.13, 0.96, 0.90, 0.88, 0.88, 0.76, 0.73 (s, 3H each, methyl groups); δ_C ($CDCl_3$, 125 MHz): 178.3 (C-28), 170.0 (C-1''), 145.2 (C-13), 122.8 (C-12), 79.0 (C-3), 72.0 (C-2''), 71.1 (C-3''), 70.6 (C-4''), 70.5 (C-5''), 70.3 (C-6''), 59.1 (C-7''), 55.2 (C-5), 47.6 (C-9), 46.9 (C-19), 46.3 (C-17), 42.2 (C-14), 42.4 (C-18), 39.5 (C-1'), 39.4 (C-8), 38.8 (C-4), 38.6 (C-1), 38.9 (C-6'), 37.1 (C-10), 34.3 (C-21), 32.6 (C-7), 32.5 (C-22), 33.1 (Me), 30.8 (C-20), 29.7 (C-2'), 29.4 (C-5'), 28.2 (Me), 27.4 (C-2), 27.2 (C-15), 26.9 (C-3'), 26.7 (C-4'), 25.8 (Me), 23.9 (C-11), 23.7 (C-16), 23.7 (Me), 18.4 (C-6), 17.0 (Me), 15.7 (Me), 15.5 (Me); ESI-HRMS m/z calcd for $C_{43}H_{75}N_2O_6$ $[M+1]^+$ 715.5625, found 715.5634.

Compound ***16***: Transparent syrup; $[\alpha]^{25}_{D}$ + 29 (c 1 in $CHCl_3$); IR ν_{max}(film)/cm^{-1} 3352, 2926, 1736, 1635, 1530, 1365, 1106 and 528; δ_H ($CDCl_3$, 400 MHz): 7.00 (dd, 1H, $J_1 = J_2$ = 6.2 Hz, NHCO group), 5.91 (dd, 1H, $J_1 = J_2$ = 5.2 Hz, NHCO group), 5.37 (dd, 1H, $J_1 = J_2$ = 3.2 Hz, H-12), 4.00 (s, 2H, CH_2 PEG group), 3.71–3.54 (m, 8H, CH_2 PEG group), 3.71–3.54 (m, 1H, H-2), 3.37 (s, 3H, CH_3 PEG group), 3.34–3.24 (m, 3H, H-1' and H-6'), 3.00 (d, 1H, J_1 = 9.6 Hz, H-3), 2.96–2.93 (m, 1H, H-1'), 2.50 (dd, 1H, J_1 = 3.4, J_2 = 13.4 Hz, H-18), 1.15, 1.03, 0.98, 0.90, 0.90, 0.82, 0.75 (s, 3H each, methyl groups); δ_C ($CDCl_3$, 100 MHz): 178.2 (C-28), 170.0 (C-1''), 145.3 (C-13), 122.6 (C-12), 84.0 (C-3), 72.0 (C-2''), 71.1 (C-3''), 70.7 (C-4''), 70.6 (C-5''), 70.3 (C-6''), 69.0 (C-2), 59.1 (C-7''), 55.3 (C-5), 47.7 (C-9), 46.9 (C-1), 46.5 (C-19), 46.4 (C-17), 42.4 (C-18), 42.3 (C-14), 39.6 (C-8), 39.5 (C-1'), 39.3 (C-10), 38.9 (C-6'), 38.3 (C-4), 34.3 (C-21), 32.7 (C-7), 32.4 (C-22), 33.1 (Me), 30.9 (C-20), 29.8 (C-2'), 28.7 (C-5'), 28.7 (Me), 27.4 (C-15), 25.9 (C-3'), 25.9 (C-4'), 25.9 (Me), 23.9 (C-11), 23.7 (C-16), 23.7 (Me), 18.4 (C-6), 17.1 (Me), 16.9 (Me), 16.8 (Me); ESI-HRMS m/z calcd for $C_{43}H_{75}N_2O_7$ $[M+1]^+$ 731.5574, found 731.5560.

Compound ***17***: Transparent syrup; $[a]^{25}_{D}$ + 38 (*c* 1 in $CHCl_3$); IR ν_{max}(film)/cm^{-1} 3354, 2924, 1659, 1531, 1463, 1385, 1105 and 571; δ_H ($CDCl_3$, 500 MHz): 7.00 (dd, 1H, $J_1 = J_2$ = 5.0 Hz, NHCO group), 6.00 (dd, 1H, $J_1 = J_2$ = 5.5 Hz, NHCO group), 5.36 (dd, 1H, $J_1 = J_2$ = 3.3 Hz, H-12), 4.00 (s, 2H, CH_2 PEG group), 3.75–3.54 (m, 8H, CH_2 PEG group), 3.37 (s, 3H, CH_3 PEG group), 3.35–3.18 (m, 4H, H-3, H-1', and H-10'), 3.00–2.96 (m, 2H, H-1'), 2.50 (dd, 1H, J_1 = 3.5, J_2 = 13.0 Hz, H-18), 1.15, 0.97, 0.90, 0.90, 0.90, 0.77, 0.75 (s, 3H each, methyl groups); δ_C ($CDCl_3$, 125 MHz): 178.2 (C-28), 169.9 (C-1''), 145.3 (C-13), 122.8 (C-12), 79.0 (C-3), 72.0 (C-2''), 71.1 (C-3''), 70.7 (C-4''), 70.6 (C-5''), 70.3 (C-6''), 59.2 (C-7''), 55.3 (C-5), 47.7 (C-9), 47.0 (C-19), 46.4 (C-17), 42.2 (C-14), 42.5 (C-18), 39.6 (C-1'), 39.5 (C-8), 39.1 (C-10'), 39.0 (C-4), 38.6 (C-1), 37.1 (C-10), 34.3 (C-21), 32.7 (C-7), 32.5 (C-22), 33.1 (Me), 30.9 (C-20), 29.8 (C-2'), 29.8 (C-9'), 29.7 (C-3'), 29.6 (C-8'), 29.5 (C-4'), 29.5 (C-7'), 28.3 (Me), 27.5 (C-2), 27.3 (C-15), 27.1 (C-5'), 27.1 (C-6'), 25.9 (Me), 23.7 (C-16), 23.7 (Me), 23.9 (C-11), 18.4 (C-6), 17.1 (Me), 15.7 (Me), 15.5 (Me); ESI-HRMS m/z calcd for $C_{47}H_{83}N_2O_6$ $[M+1]^+$ 771.6251, found 711.6266.

Compound ***18***: Transparent syrup; $[a]^{25}_{D}$ + 21 (*c* 1 in $CHCl_3$); IR ν_{max}(film)/cm^{-1} 3349, 2924, 1658, 1532, 1455, 1365, 1104 and 560; δ_H ($CDCl_3$, 500 MHz): 7.03 (dd, 1H, $J_1 = J_2$ = 5.5 Hz, NHCO group), 5.90 (dd, 1H, $J_1 = J_2$ = 5.5 Hz, NHCO group), 5.33 (dd, 1H, $J_1 = J_2$ = 3.5 Hz, H-12), 3.93 (s, 2H, CH_2 PEG group), 3.66–3.51 (m, 9H, H-2 and 4 CH_2 PEG group), 3.34 (s, 3H, CH_3 PEG group), 3.31–3.20 (m, 3H, H-1' and H-10'), 2.95 (d, 1H, J_1 = 9.5 Hz, H-3), 2.98–2.94 (m, 1H, H-1'), 2.45 (dd, 1H, J_1 = 3.5, J_2 = 12.5 Hz, H-18), 1.24, 1.12, 1.00, 0.94, 0.86, 0.78, 0.72 (s, 3H each, methyl groups); δ_C ($CDCl_3$, 125 MHz): 178.1 (C-28), 170.0 (C-1''), 145.2 (C-13), 122.6 (C-12), 83.6 (C-3), 71.9 (C-2''), 71.0 (C-3''), 70.6 (C-4''), 70.5 (C-5''), 70.3 (C-6''), 68.7 (C-2), 59.1 (C-7''), 55.3 (C-5), 47.6 (C-9), 46.8 (C-1), 46.5 (C-19), 46.2 (C-17), 42.5 (C-18), 42.1 (C-14), 39.5 (C-1'), 39.4 (C-8), 39.1 (C-10), 39.1 (C-10'), 38.9 (C-4), 34.2 (C-21), 32.6 (C-7), 32.4 (C-22), 33.1 (Me), 30.7 (C-20), 29.8 (C-2'), 29.7 (C-9'), 29.6 (C-3'),29.6 (C-8'), 29.5 (C-4'), 29.4 (C-7'), 28.8 (Me), 27.3 (C-15), 27.1 (C-5'), 27.0 (C-6'), 25.8 (Me), 23.8 (C-11),

23.7 (C-16), 23.7 (Me), 18.4 (C-6), 17.1 (Me), 16.9 (Me), 16.8 (Me); ESI-HRMS m/z calcd for $C_{47}H_{83}N_2O_7$ $[M+1]^+$ 787.6200, found 787.6211.

4.11. Biological experimental procedures

4.11.1. Drugs.

The OA or MA derivatives employed in cell treatment were dissolved before use at a concentration of 5 mg/mL in DMSO. They were stored at -20 ºC, constituting the stock solution from which solutions were made for the different tests. Prior to the experiments, this solution was diluted in cell-culture medium.

4.11.2. Cell cultures.

Mouse melanoma cells B16-F10 (ATTC no. CRL-6475), human colorectal adenocarcinoma cells HT29 (ECACC no. 9172201; ATTC no. HTB-38), human hepatocarcinoma cells HepG2 (ECACC no. 85011430), non-tumour human lung fibroblasts cells HPF (ScienCellcno. 3300), non-tumour rat epithelium cells IEC-18 (ECACC no. 88011801), and non-tumour human embryo livercells WRL68 (ECACC no. 89121403), were cultured in DMEM medium supplemented with 2 mM glutamine, 10% heat-inactivated foetal calf serum (FCS), 10.000 units/mL of penicillin and 10 mg/mL of streptomycin, being incubated at 37 ºC in an atmosphere of 5% CO_2 and 95% humidity. The culture media were changed every 48 h and the confluent cultures were separated with a trypsin solution (0.25%-EDTA). Subconfluent monolayer cells were used in all experiments. All cell lines used were provided by the cell bank of the University of Granada (Spain), except for the HPF cell line that was purchased from ScienCell Research Laboratories.

4.11.3. Cell-proliferation activity assay.

The effect of the synthesised compounds on the viability of tumour and non-tumour cells was performed using the MTT assay, based on the ability of living cells to cleave the tetrazolium ring, thus producing formazan, which absorbs at 570 nm. All these compounds were assayed against the

selected cancer-cell lines, and only the diamine and PEGylated-diamine conjugates were also tested against the selected non-tumour cell lines. To examine the cytotoxic effects of these compounds, the cells were seeded in 96-well plates at an initial cell density of $5 \cdot 10^3$ B16-F10 cells, $6 \cdot 10^3$ HT29 cells, $15 \cdot 10^3$ HepG2 cells, $8 \cdot 10^3$ HPF, $15 \cdot 10^3$ IEC-18 cells, and $11 \cdot 10^3$ WRL68 cells, per well. For their growth, they were incubated for 24 h and subsequently treated with different compounds in triplicate, at different concentrations (0–200 µg/mL), and incubated for 72 h. Thereafter, 100 µL of MTT solution (0.5 mg/mL) were added to each well. After 2 h of incubation, the cells were washed twice with phosphate buffered saline (PBS), and the formazan was resuspended in 100 µL of DMSO. Relative cell viability, with respect to untreated control cells, was measured by absorbance at 550 nm on an ELISA plate reader (Tecan Sunrise MR20-301, TECAN, Austria). Compounds with low IC_{50} values (**1**, **3**, **9**, **11**, **13**, **14**, **17**, and **18**) were selected for several cytometry assays, as apoptosis, cell cycle and mitochondrial membrane potential. These experiments were measured and compared to the control after 24, 48 or 72 h of treatment.

4.11.4. Annexin V-FICT/propidium iodide flow-cytometry analysis.

Apoptosis was assessed by flow cytometry using a FACScan (fluorescence-activated cell sorter) flow cytometer (Coulter Corporation, Hialeah, FL, USA). For this assay, $5 \cdot 10^4$ B16-F10 cells were plated in 24-well plates with 1.5 mL of medium and incubated for 24 h. Subsequently, the cells were treated with the selected compounds in triplicate for 24, 48, and 72 h at their corresponding IC_{50} concentration. The cells were collected and resuspended in binding buffer (10 mM HEPES / NaOH, pH 7.4, 140 mM NaCl, 2.5 mM $CaCl_2$). Annexin V-FITC conjugate (1µg/mL) was then added and incubated for 15 min at rt in darkness. Just before the analysis by flow cytometry, cells were stained with 5 µL of 1 mg/mL PI solution. In each experiment, approximately $10 \cdot 10^3$ cells were analysed and the experiment was duplicated twice.

4.11.5. Cell Cycle.

The method used to quantify the amount of DNA in the different phases of the cell cycle (G0/G1, S, and G2/M) was performed by flow cytometry, using a fluorescence-activated cell sorter (FACS) at 488 nm in an Epics XL flow cytometer (Coulter Corporation, Hialeah, FL, USA). For this assay, $5 \cdot 10^4$ B16-F10 cells were plated in 24-well plates with 1.5 mL of medium and incubated for 24 h. After this time, the cells were treated with the different compounds selected for 48 h at their corresponding IC_{50} concentration. After treatment, the cells were washed twice with PBS, trypsinized and resuspended in 1 x TBS (10 mM Tris and 150 mM NaCl), and there after Vindelov buffer (100 mM Tris, 100 mM NaCl, 10 mg/mL Rnase, and 1 mg/mL PI, at pH 8) was added. Cells were stored on ice, and just before measurement, were stained with 10 mL of 1 mg/mL PI solution. Approximately, $10 \cdot 10^3$ cells were analysed in each experiment. The experiments were performed three times with two replicates per assay.

4.11.6. Flow-cytometry analysis of the mitochondrial-membrane potential.

The electrochemical gradient across the mitochondrial membrane was studied by analytical flow cytometry, using dihydrorhodamine (DHR). DHR is oxidized in contact with living cells, forming a highly fluorescent product called rhodamine (Rh 123). The fluorescence emitted can be monitored by fluorescence spectroscopy using excitation and emission wavelengths of 500 and 536 nm, respectively $5 \cdot 10^4$ B16-F10 cells were plated in 24-well plates, incubated for 24 h and treated with the compounds selected for 48 h at their corresponding IC_{50} concentration. After treatment, the culture medium was renewed with fresh medium adding 0.5 mL of DHR, obtaining a final concentration of 5mg/mL. Cells were incubated for 1 h at 37 ºC in an atmosphere of 5% CO_2 and 95% humidity, and subsequently washed and resuspended in PBS with 5 mg/mL of PI. The fluorescence intensity was measured using a FACScan flow cytometer (fluorescence-activated cell sorter). The experiments were performed three times with two replicates per assay.

Acknowledgments

This work was financially supported by grants from the "Consejería de Innovación, Ciencia y Empresa "of the "Junta de Andalucía" (FQM–7372). We thank David Nesbitt for reviewing the English of the manuscript.

References

[1] J.J. Monsuez, J.C. Charniot, N. Vignat, J.Y. Artigou, Cardiac side-effects of cancer chemotherapy, Int. J. Cardiol. 144 (2010) 3–15.

[2] B. Guillot, D. Bessis, O. Dereure, Mucocutaneous side effects of antineoplastic chemotherapy, Expert Opin. Drug Saf. 3 (2004) 579–587.

[3] A.D. Kinghorn, Anticancer Agents from Natural Products, second ed., CRC Press/Taylor & Francis Group, Boca Raton, FL, 2012.

[4] G.M. Cragg, P.G. Grothaus, D.J. Newman, Impact of natural products on developing new anti-cancer agents, Chem. Rev. 109 (2009) 3012–3043.

[5] M. Trendowski, Recent advances in the development of antineoplastic agentsderived from natural products, Drugs 75 (2015) 1993–2016.

[6] K.H. Lee, Discovery and development of natural product-derived chemotherapeutic agents based on a medicinal chemistry approach, J. Nat. Prod. 73 (2010) 500–516.

[7] E.E. Rufino-Palomares, A. Pérez-Jiménez, F.J. Reyes-Zurita, L. García-Salguero, K. Mokhtari, A. Herrera-Merchán, P.P. Medina, J. Peragón, J.A. Lupiáñez, Anti-cancer and anti-angiogenic properties of various natural pentacyclic triterpenoids and some of their chemical derivatives, Curr. Org. Chem. 19 (2015) 919–947.

[8] M. Chudzik, I. Korzonek-Szlacheta, W. Król, Triterpenes as potentiallycytotoxic compounds, Molecules 20 (2015) 1610–1625.

[9] J.A.R. Salvador, A.S. Leal, D.P.S. Alho, B.M.F. Goncalves, A.S. Valdeira, V.I. S. Mendes, Y. Jing, Highlights of pentacyclic

triterpenoids in the cancer settings, Stud. Nat. Prod. Chem. 41 (2014) 33–73.

[10] S.M. Kamble, S.N. Goyal, C.R. Patil, Multifunctional pentacyclic triterpenoids as adjuvants in cancer chemotherapy: a review, RSC Adv. 4 (2014) 33370–33382.

[11] M.K. Shanmugam, A.H. Nguyen, A.P. Kumar, B.K.H. Tan, G. Sethi, Targeted inhibition of tumor proliferation, survival, and metastasis by pentacyclic triterpenoids: Potential role in prevention and therapy of cancer, Cancer Lett. 320 (2012) 158–170.

[12] J.M.R. Patlolla, C.V. Rao, Triterpenoids for cancer prevention and treatment: Current status and future prospects, Current Pharm. Biotechnol. 13 (2012) 147–155.

[13] A. Garcia-Granados, A. Martinez, J.N. Moliz, A. Parra, F. Rivas, 3β-hydroxyolean-12-en-28-oic acid (oleanolicacid), Molecules 3 (1998) M87.

[14] A. Garcia-Granados, A. Martinez, J.N. Moliz, A. Parra, F. Rivas, 2a,3β-dihydroxyolean-12-en-28-oic acid (maslinicacid), Molecules 3 (1998) M88.

[15] A. Fernandez-Hernandez, A. Martinez, F. Rivas, J. A. Garcia-Mesa, A. Parra, Effect of the solvent and the sample preparation on the determination of triterpene compounds in two-phase olive-mill-waste samples, J. Agric. Food Chem. 63 (2015) 4269–4275.

[16] N.R. Parikh, A. Mandal, D. Bhatia, K.S. Siveen, G. Sethi, A. Bishayee, Oleanane triterpenoids in the prevention and therapy of breast cancer: Current evidence and future perspectives, Phytochem. Rev. 13 (2014) 793–810.

[17] G. Lozano-Mena, M. Sánchez-González, M.E. Juan, J.M. Planas, Maslinic acid, a natural phytoalexin-type triterpene from olives a promising nutraceutical?, Molecules 19 (2014) 11538–11559.

[18] M. Masullo, C. Pizza, S. Piacente, Oleanane derivatives for pharmaceutical use: a patent review (2000-2016), Expert Opin.Ther. Pat. 27 (2017) 237–255.

[19] K.T. Liby, M.B. Sporn, Synthetic oleanane triterpenoids: multifunctional drugs with a broad range of applications for prevention and treatment of chronic disease, Pharmacol. Rev. 64 (2012) 972–1003.

[20] A. Parra, S. Martin-Fonseca, F. Rivas, F.J. Reyes-Zurita, M. Medina-O'Donnell, A. Martinez, A. Garcia-Granados, J.A. Lupiañez, F. Albericio, Semi-synthesis of acylated triterpenes from olive-oil industry wastes for the development of anticancer and anti-HIV agents, Eur. J. Med. Chem. 74 (2014) 278–301.

[21] A. Parra, S. Martin-Fonseca, F. Rivas, F.J. Reyes-Zurita, M. Medina-O'Donnell, E.E. Rufino-Palomares, A. Martinez, A. Garcia-Granados, J.A. Lupiañez, F. Albericio, Solid-phase library synthesis of bi-functional derivatives of oleanolic and maslinic acids and their cytotoxicity on three cancer cell lines, ACS Comb. Sci. 16 (2014) 428–447.

[22] M. Medina-O'Donnell, F. Rivas, F.J. Reyes-Zurita, A. Martinez, S. Martin-Fonseca, A. Garcia-Granados, R.M. Ferrer-Martin, J.A. Lupianez, A. Parra, Semi-synthesis and antiproliferative evaluation of PEGylated pentacyclic triterpenos, Eur. J. Med. Chem. 118 (2016) 64–78.

[23] F.J. Reyes-Zurita, M. Medina-O'Donnell, R.M. Ferrer-Martin, E.E. Rufino-Palomares, S. Martin-Fonseca, F. Rivas, A. Martinez, A. Garcia-Granados, A. Perez-Jimenez, L. Garcia-Salguero, J. Peragon, K. Mokhtari, P.P. Medina, A. Parra, J.A. Lupiañez, The oleanolic acid derivative, 3-O-succinyl-28-O-benzyl oleanolate, induces apoptosis in B16-F10 melanoma cells via the mitochondrial apoptotic pathway, RSC Adv. 6 (2016) 93590–93601.

[24] M. Medina-O'Donnell, F. Rivas, F.J. Reyes-Zurita, A. Martinez, F. Galisteo-González, J.A. Lupiañez, A. Parra, Synthesis and in vitro antiproliferative evaluation of PEGylated triterpene acids, Fitoterapia 120 (2017) 25–40.

[25] T. Tian, X. Liu, E.S. Lee, J. Sun, Z. Feng, L. Zhao, C. Zhao, Synthesis of

novel oleanolic acid and ursolic acid in C-28 position derivatives as potential anticancer agents, Arch. Pharm. Res. 40 (2017) 458–468.

[26] S. Sommerwerk, L. Heller, C. Kerzig, A.E. Kramell, R. Csuk, Rhodamine B conjugates of triterpenoic acids are cytotoxic mitocans even at nanomolar concentrations, Eur. J. Med. Chem. 127 (2017) 1–9.

[27] L. Heller, A. Knorrscheidt, F. Flemming, J. Wiemann, S. Sommerwerk, I.Z. Pavel, A. Al-Harrasi, R. Csuk, Synthesis and proapoptotic activity of oleanolic acid derived amides, Bioorg. Chem. 68 (2016) 137–151.

[28] J.J. Swidorski, Z. Liu, S.Y. Sit, J. Chen, Y. Chen, N. Sin, B.L. Venables,D.D. Parker, B.Nowicka-Sans, B.J. Terry, T.Protack, S.Rahematpura,U.Hanumegowda, S. Jenkins, M. Krystal, I.B. Dicker, N.A. Meanwell,A.Regueiro-Ren, Inhibitors of HIV-1 maturation: Development of structure-activity relationship for C-28 amides based on C-3 benzoic acid-modified triterpenoids, Bioorg. Med. Chem. Lett. 26 (2016) 1925–1930.

[29] B. Siewert, E. Pianowski, A. Obernauer, R. Csuk, Towards cytotoxic and selective derivatives of maslinic acid, Bioorg. Med. Chem. 22 (2014) 594–615.

[30] B. Siewert, E. Pianowski, R. Csuk, Esters and amides of maslinic acid trigger apoptosis in human tumor cells and alter their mode of action with respect to the substitution pattern at C-28, Eur. J. Med. Chem. 70 (2013) 259–272.

[31] K.G. Cheng, C.H. Su, L.D. Yang, J. Liu, Z.F. Chen, Synthesis of oleanolic acid dimers linked at C-28 and evaluation of anti-tumor activity, Eur. J. Med. Chem. 89 (2015) 480–489.

[32] K. Cheng, J. Liu, H. Sun, J. Xie, Synthesis of oleanolic acid dimers as inhibitors of glycogen phosphorylase, Chem. Biodivers. 7 (2010) 690–697.

[33] I. Fernandez-Pastor, A. Fernandez-Hernandez, S. Perez-Criado, F. Rivas, A. Martinez, A. Garcia-Granados, A. Parra, Microwave-assisted extraction versus Soxhletextraction to determine triterpene acids in olive skins, J. Sep. Sci. 40 (2017) 1209–1217.

[34] A. Martinez, F. Rivas, A. Perojil, A. Parra, A. Garcia-Granados, A. Fernandez-Vivas, Biotransformation of oleanolic and maslinic acids by Rhizomucor miehei. Phytochemistry 94 (2013) 229–237.

PUBLICACIÓN 5

Síntesis Orgánica en Fase Sólida de una biblioteca de derivados de ácido oleanólico y su estudio frente a la inhibición de la proteasa del VIH-1

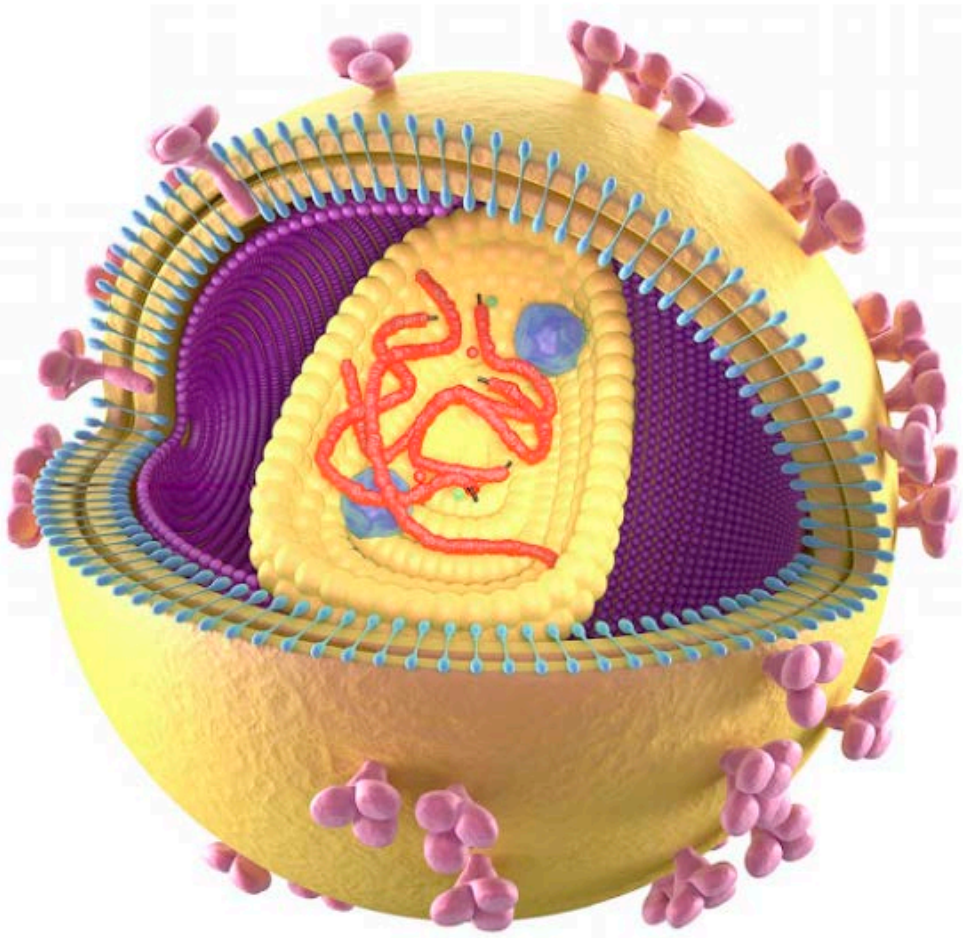

RESUMEN

Se han obtenido, mediante la técnica de Síntesis Orgánica en Fase Sólida, 120 derivados bifuncionales del ácido oleanólico. Estos derivados incorporan una o dos moléculas de aminoácido (α- y ω-aminoácidos) que se unen al grupo carboxilo C-28 del triterpeno, además de un grupo acilo (10 tipos de grupos acilo) que esterifica al grupo hidroxilo de C-3 de dicho ácido oleanólico. Se ha investigado la capacidad de inhibir la proteasa del virus VIH-1 de estos derivados de ácido oleanólico, analizando el efecto que ejercen los distintos sustituyentes presentes en el grupo carboxilo C-28 y en el grupo hidroxilo de C-3. La proteasa del VIH-1, es la responsable de la escisión de cadenas peptídicas sintetizadas al traducir a proteínas el código genético, que darán lugar a los componentes proteicos activos del virus maduro. La inhibición de la proteasa del VIH-1 representa por tanto, una vía importante para la terapia viral, impidiendo que el virus infecte nuevas células. Los ensayos llevados a cabo, pusieron de manifiesto que la mayoría de los derivados de ácido oleanólico presentaban valores de IC_{50} más bajos que los de su precursor, destacando los valores de los 3-ftaloil-28-monopeptidil y 3-ftaloil-28-dipeptidil derivados de ácido oleanólico (**1g-12g**) que alcanzaron valores de IC_{50} de concentración nanomolar. Estos resultados de IC_{50} para los diferentes derivados de ácido oleanólico, indican que estos compuestos puedan ser potenciales candidatos para futuros ensayos clínicos como inhibidores de la proteasa del VIH-1.

1. INTRODUCCIÓN

Los productos naturales juegan un papel muy importante en el desarrollo de fármacos.[1-3] De hecho, casi la mitad de los nuevos fármacos introducidos en el mercado en las últimas tres décadas han sido productos naturales o sus derivados.[4,5] El uso de métodos combinatorios como la técnica de Síntesis Orgánica en Fase Sólida, posibilita obtener bibliotecas de productos que pueden ofrecer actividades potencialmente valiosas.[6-8]

La química combinatoria, es el conjunto de procedimientos que permiten sintetizar de forma rápida, eficiente y simultánea, una gran cantidad de compuestos orgánicos, constituyendo lo que se denomina biblioteca de compuestos.[9,10] Esta forma de hacer química, fue desarrollada en 1963 por el premio Nobel Robert Bruce Merrifield, sintetizando una serie de polipéptidos, a partir de distintos aminoácidos, mediante el empleo de una fase polimérica sólida, naciendo así la Síntesis Orgánica en Fase Sólida (SOFS).[11] Tradicionalmente, la Química Orgánica estudia las reacciones entre sustancias disueltas en un medio líquido, en cambio, en química combinatoria lo más frecuente es que las sustancias que participan en la formación del compuesto final estén acopladas químicamente a un soporte sólido insoluble como son las resinas o polímeros.

La Síntesis Orgánica en Fase Sólida presenta una serie de ventajas como: el empleo de exceso de reactivos, siendo eliminados por simple filtración y lavado, la reducción de los procedimientos de aislamiento y purificación que son realizados por lavado y filtración, la utilización de disolventes difíciles, la posibilidad de automatización, etc. Cabe destacar que la SOFS también presenta algunas desventajas, pues no siempre es aplicable, siendo problemático adaptar algunas reacciones en disolución al proceso de fase sólida. Para llevar a cabo la Síntesis Orgánica en Fase Sólida es necesario en primer lugar, el hallazgo de un compuesto líder, que es la sustancia que está dotada de la actividad/es biológica/s deseadas. En la presente memoria estos compuestos líder serían los ácidos triterpénicos naturales. El paso siguiente es la utilización de estos

compuestos líder, realizando modificaciones en su estructura química con el fin de obtener de forma simultánea una librería de derivados que puedan ser utilizados para llevar a cabo ensayos biológicos.

En el apartado de antecedentes de esta memoria, se realizó un resumen bibliográfico de la actividad de los triterpenos frente al VIH, destacando los ácidos oleanólico y maslínico como inhibidores de la proteasa del VIH-1.[12] Esta proteasa actúa durante la replicación del virus, cuando las nuevas partículas del virus (viriones) están saliendo de la célula huésped. En los años noventa, se empezaron a incorporar fármacos del tipo inhibidor de la proteasa (IP), generando un descenso de la mortalidad por SIDA y aumentando la calidad de vida del paciente.[13] Fármacos como el saquinavir, ritonavir, indinavir y nelfinavir son inhibidores de la proteasa. La resistencia del virus a estos fármacos ha hecho que sea necesaria la búsqueda de nuevos compuestos bioactivos frente al VIH-1.

En este trabajo, se ha utilizado como compuesto líder al ácido oleanólico, un triterpeno pentacíclico que ha demostrado poseer interesantes propiedades biológicas como hepatoprotector, antioxidante, anti-cancerígeno e inhibidor de la proteasa del HIV.[14,15] Se han obtenido 120 derivados bifuncionales, empleando la metodología de Síntesis Orgánica en Fase Sólida para el acoplamiento de uno o dos moléculas de aminoácido (a- y ω-aminoácidos) al grupo carboxilo de C-28 y la unión de un grupo acilo (10 tipos de grupos acilo) esterificando el grupo hidroxilo de C-3. Cada uno de estos derivados obtenidos se ha ensayado frente a la proteasa del VIH-1.

2. RESULTADOS Y DISCUSIÓN

2.1 SECCIÓN QUÍMICA

El ácido oleanólico (**I**, ácido 3β-hidroxiolean-12-en-28-óico, AO) (Fig. 1) es un triterpeno pentacíclico ampliamente distribuido en el reino vegetal.[16] Este compuesto, aunque se encuentra en distintas fuentes naturales, se ha aislado de los residuos del prensado de la aceituna mediante procesos de extracción con diferentes disolventes.[17-19]

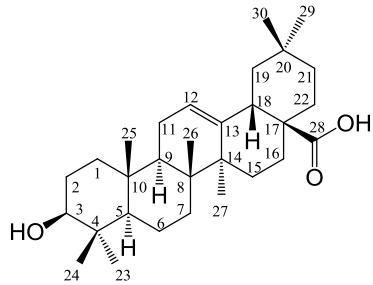

Figura 1. Estructura del ácido oleanólico.

El inconveniente que presenta este compuesto por su baja solubilidad en agua, y en general todos los ácidos triterpénicos, ha sido expuesto a lo largo de esta memoria. Para tratar de mejorar dicha solubilidad, se han utilizado diversos compuestos más polares tales como grupos acilo, aminoácidos o grupos PEG, para formar derivados de estos compuestos triterpénicos tratando de aumentar su biodisponibilidad y así optimizar su eficacia biológica.[20-23] En un trabajo anterior, se sintetizaron una serie de derivados monofuncionales mediante reacciones de acilación utilizando distintos tipos de grupos acilo (acetilo, butanoilo, ftaloilo, glutarilo, 3,3-dimetilglutarilo, hexanoilo y succinilo) que se hicieron reaccionar con el grupo hidroxilo de C-3 del ácido oleanólico.[22] A estos derivados obtenidos, se les realizó un estudio de la inhibición de la proteasa del VIH-1, donde se observó que muchos de ellos mejoraban su actividad con respecto al ácido oleanólico. También con anterioridad, se llevó a cabo, la síntesis de una serie de conjugados monofuncionales del ácido maslínico, acoplando α- y ω-aminoácidos al grupo carboxilo de C-28 del triterpeno.[23] Los ensayos de estos derivados del ácido maslínico frente al VIH, pusieron de manifiesto su acción apoptótica frente a células MT-2 (linfocitos) infectadas con el virus VIH. Teniendo en cuenta estos resultados previos, se han sintetizado nuevos derivados bifuncionales de AO. Estos derivados bifuncionales, incorporan uno o dos aminoácidos unidos al grupo carboxilo del triterpeno y un grupo acilo esterificando el grupo hidroxilo del anillo A. De entre los aminoácidos elegidos para llevar a cabo esta síntesis, se escogieron tres α-aminoácidos y tres ω-aminoácidos de

distinta cadena (Fig. 2). De los α-aminoácidos se eligieron dos aminoácidos no esenciales, glicina (GLY) y alanina (ALA), y otro esencial, la valina (VAL). Los ω-aminoácidos utilizados varían principalmente en el tamaño de su cadena, el ácido γ-aminobutírico (GABA) con una cadena de cuatro carbonos, el ácido 6-aminohexanoico (6AHA) de seis carbonos y el ácido 11-aminoundecanoico (11AUA) de once carbonos.

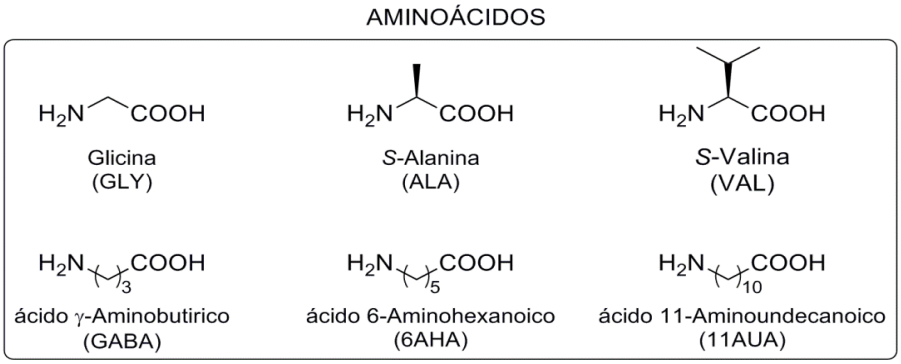

Figura 2. Aminoácidos empleados para la Síntesis Orgánica en Fase Sólida.

Los agentes acilantes empleados para la formación de los distintos derivados de AO, han sido seleccionados por sus propiedades físico-químicas y porque algunos de ellos han demostrado mejorar las actividades biológicas en los ácidos betulínico y ursólico. En la Figura 3, se presentan los 10 agentes acilantes empleados a partir del correspondiente anhídrido de ácido.

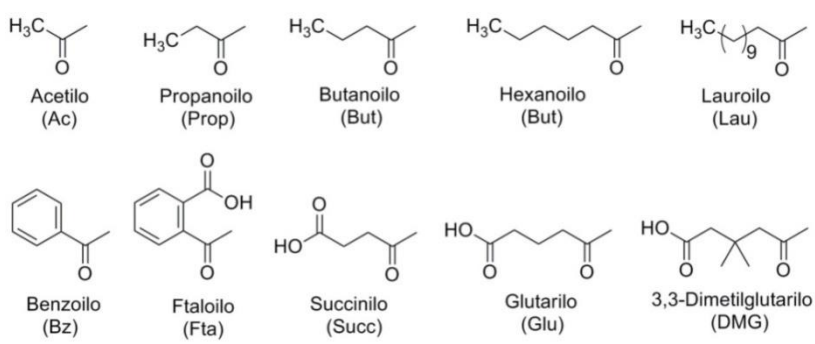

Figura 3. Grupos acilo empleados para la Síntesis Orgánica en Fase Sólida.

Para la Síntesis Orgánica en Fase Sólida, se ha empleado como resina o soporte polimérico, la resina 2-clorotritilo (CTC-PS), también llamada resina de Barlos. Esta resina, permite la liberación de los compuestos por tratamiento bajo condiciones ácidas suaves que no afectan al triterpeno.

Tal y como se indica en el Esquema 1, los monopeptidil derivados de AO, se prepararon por acoplamiento de los ω-aminoácidos (GABA, 6AHA, 11AUA) con el grupo carboxilo de C-28, usando la técnica de SOFS. Para ello, se tomaron 3 jeringas equipadas con un disco de polietileno, con una cantidad apropiada de resina de Barlos. A cada jeringa se le añadió una solución que contenía los correspondientes ω-aminoácidos. Posteriormente, se procedió al acoplamiento con el ácido oleanólico, obteniéndose los monopeptidil derivados de AO monofuncionales (**1**-**3**). A continuación, también utilizando la técnica SOFS, cada jeringa se dividió en otras 10 jeringas y se llevaron a cabo las reacciones de acilación en el hidroxilo de C-3, uniendo los distintos grupos acilo por tratamiento con los correspondientes anhídridos de ácido. Así, a partir de los compuestos intermedios (**1**-**3**) y las posibles combinaciones de los aminoácidos, se obtuvieron 30 3-acil-28-monopeptidil derivados de AO (**1a**-**3j**), que fueron ensayados frente a la proteasa del VIH-1.

La preparación de los 28-dipeptidil derivados de AO mediante la técnica SOFS, se puede observar en el Esquema 2. En este caso, el primer acoplamiento a la resina contenida en tres jeringas, se realizó con los a-aminoácidos (GLY, ALA, VAL). A continuación, se realizó un segundo acoplamiento para unir un segundo aminoácido (ω-aminoácidos). Para ello, cada jeringa se dividió en tres nuevas jeringas, añadiendo una solución con el ω-aminoácido correspondiente (GABA, 6AHA, 11AUA). De esta manera, y uniéndole a cada dipéptido el ácido oleanólico, se obtuvieron los 28-dipeptidil derivados de AO monofuncionalizados (**4**-**12**). Al igual que en la síntesis anterior, se llevaron a cabo reacciones de acilación a partir de los compuestos intermedios (**4**-**12**) con los distintos grupos acilo,

obteniéndose 90 3-acil-28-dipeptidilderivados de AO (**4a**-**12j**), que también fueron ensayados frente a la proteasa del VIH-1.

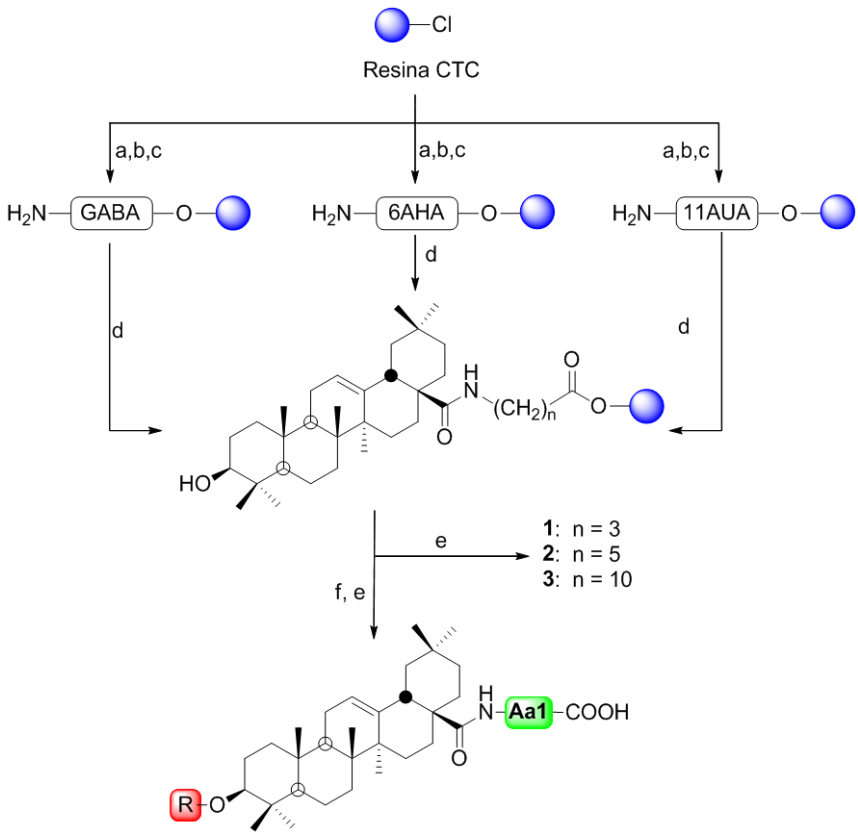

Grupo acilo acoplado	Aminoácido acoplado		
	GABA	6AHA	11AUA
Ac	**1a**	**2a**	**3a**
Prop	**1b**	**2b**	**3b**
But	**1c**	**2c**	**3c**
Hex	**1d**	**2d**	**3d**
Lau	**1e**	**2e**	**3e**
Bz	**1f**	**2f**	**3f**
Fta	**1g**	**2g**	**3g**
Succ	**1h**	**2h**	**3h**
Glu	**1i**	**2i**	**3i**
DMG	**1j**	**2j**	**3j**

Esquema 1. Semisíntesis de los derivados de ácido oleanólico monopeptidilacilados (**1a**-**3j**). Reactivos y condiciones: (a) Fmoc-GABA-OH o Fmoc-6AHA-OH o Fmoc-11AUA-OH, DIEA, DCM; (b) MeOH; (c) Piperidina-DMF (1:4); (d) AO,PyAOP, HOAt, DIEA, DMF; (e) TFA-DCM (1:99); (f) Anhídrido de ácido, Et_3N, DMAP, DMF, DCM.

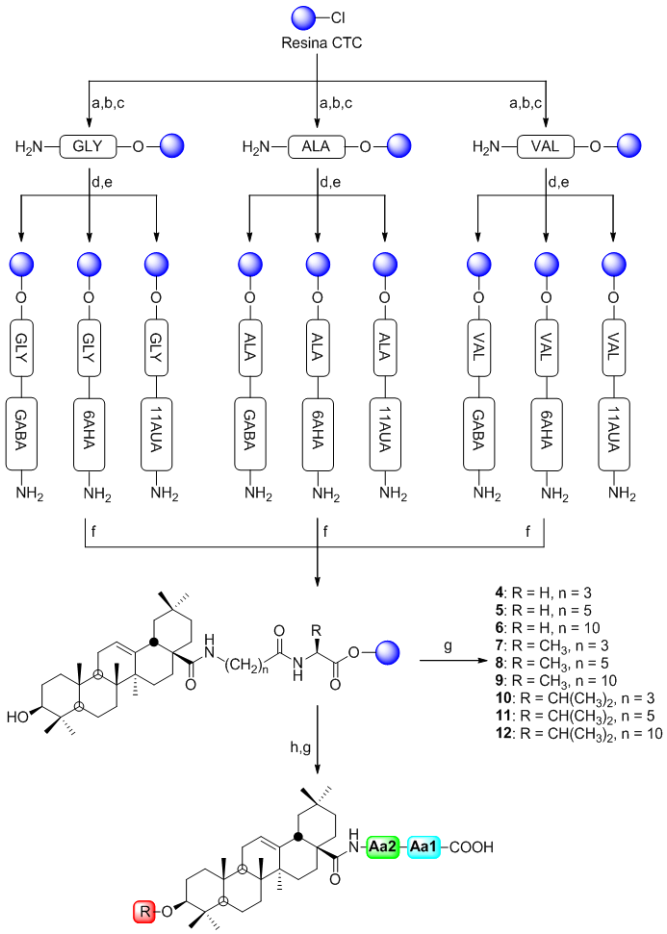

Grupo acilo acoplado	Aminoácidos acoplados								
	GLY GABA	GLY 6AHA	GLY 11AUA	ALA GABA	ALA 6AHA	ALA 11AUA	VAL GABA	VAL 6AHA	VAL 11AUA
Ac	**4a**	**5a**	**6a**	**7a**	**8a**	**9a**	**10a**	**11a**	**12a**
Prop	**4b**	**5b**	**6b**	**7b**	**8b**	**9b**	**10b**	**11b**	**12b**
But	**4c**	**5c**	**6c**	**7c**	**8c**	**9c**	**10c**	**11c**	**12c**
Hex	**4d**	**5d**	**6d**	**7d**	**8d**	**9d**	**10d**	**11d**	**12d**
Lau	**4e**	**5e**	**6e**	**7e**	**8e**	**9e**	**10e**	**11e**	**12e**
Bz	**4f**	**5f**	**6f**	**7f**	**8f**	**9f**	**10f**	**11f**	**12f**
Fta	**4g**	**5g**	**6g**	**7g**	**8g**	**9g**	**10g**	**11g**	**12g**
Succ	**4h**	**5h**	**6h**	**7h**	**8h**	**9h**	**10h**	**11h**	**12h**
Glu	**4i**	**5i**	**6i**	**7i**	**8i**	**9i**	**10h**	**11i**	**12i**
DMG	**4j**	**5j**	**6j**	**7j**	**8j**	**9j**	**10j**	**11j**	**12j**

Esquema 2. Semisíntesis de los derivados de ácido oleanólico dipeptidilacilados (**4a-12j**). Reactivos y condiciones: (a) Fmoc-GLY-OH o Fmoc-ALA-OH o Fmoc-VAL-OH, DIEA, DCM; (b) MeOH; (c) Piperidina-DMF (1:4); (d)Fmoc-GABA-OH o Fmoc-6AHA-OH o Fmoc-11AUA-OH, HOAt, DIPCDI, DMF; (e) Piperidina-DMF (1:4);(f) **OA**, PyAOP, HOAt, DIEA, DMF; (g) TFA-DCM (1:99); (h) Anhídrido de ácido, Et_3N, DMAP, DMF, DCM.

La información completa y detallada de los mono- y dipeptidil derivados de AO, así como también los 3-acil-28-monopeptidil y 3-acil-28-dipeptidil derivados de AO se describe en la Sección Experimental, mientras que sus características químicas y espectroscópicas se referencian.[23]

2.2 SECCIÓN BIOLÓGICA

En un trabajo anterior de nuestro grupo de investigación se determinó que el ácido oleanólico inhibía la proteasa del VIH-1, con un valor de IC_{50} de 57.7 μM.[22] En esa misma publicación, se formaron diversos derivados de ácido triterpénico mediante reacciones de acilación, determinándose también el grado de inhibición que ejercían estos compuestos sobre la proteasa del virus del SIDA. Las concentraciones IC_{50} de derivados como el 3-acetil-AO, el 3-ftaloil-AO, el 3-glutaril-AO o el 3-ftaloil-28-benzoil-AO disminuyeron significativamente, con valores de 3.4, 0.31, 0.56 y 0.40 μM, respectivamente, siendo entre 20 y 200 veces más potentes como agentes antivirales que su precursor (AO).[22]

Como se ha comentado en la parte química de este trabajo, se obtuvieron derivados de AO que incorporan uno o dos aminoácidos acoplados al grupo carboxilo C-28 del triterpeno y/o un grupo acilo que esterifica el grupo hidroxilo del anillo A, mediante la técnica de Síntesis Orgánica en Fase Sólida. Todos estos derivados se ensayaron frente a la proteasa del virus VIH-1.

Los valores de IC_{50} de los monopeptidil derivados de AO (**1**-**3**), se muestran en la Tabla 1. A partir de estos datos, se establece que el acoplamiento de ω-aminoácidos como el ácido γ-aminobutírico (GABA) y el ácido 6-aminohexanoico (6AHA) disminuyeron el valor de la IC_{50} del precursor (AO, 57.7μM) hasta 18.72 y 8.96 μM, respectivamente. Sin embargo, cuando se acopló un aminoácido de cadena más larga, como el ácido 11-aminoundecanoico (11AUA), el valor de su IC_{50} aumentó considerablemente, por encima de 250 μM.

Tabla 1. Valores de IC_{50} de los mono- y dipeptidil derivados de AO (**1**-**12**).

Compuesto	Aminoácido acoplado		IC_{50} (μM)
	Aa1	Aa2	
AO	-	-	57.7 ± 3.90
1	GABA	-	8,72 ± 0.86
2	6AHA	-	8,96 ± 0.04
3	11AUA	-	> 250
4	GLY	GABA	305.32 ± 16.91
5	GLY	6AHA	106.46 ± 2.40
6	GLY	11AUA	> 250
7	ALA	GABA	26.57 ± 1.48
8	ALA	6AHA	> 250
9	ALA	11AUA	> 250
10	VAL	GABA	> 250
11	VAL	6AHA	120.80 ± 1.06
12	VAL	11AUA	> 250

En esta misma Tabla 1, también se indican los valores de IC_{50} de los dipeptidil derivados de AO (**4**-**12**), obtenidos por la unión de un primer a-aminoácido de cadena corta (GLY, ALA, VAL) y posterior acoplamiento de un segundo ω-aminoácido (GABA, 6AHA, 11AUA). El derivado AO-ALA-GABA (**7**) disminuyó su IC_{50} (26.57 μM) comparado con AO. Los otros 11 dipeptidil derivados de AO presentaron IC_{50} superiores al precursor.

En la Tabla 2 se muestran valores de IC_{50} de los 30 3-acil-28-monopeptidil derivados de AO (**1a**-**3j**). Prácticamente todos los derivados acilados (**1a**-**1j)** tienen valores más altos de IC_{50} que su precursor (AO-GABA, **1**), excepto el derivado ftálico (**1g**), que presenta una concentración de IC_{50} considerablemente menor (2.21 μM). En el caso del compuesto AO-6AHA (**2**), tres de sus derivados exhibían valores significativamente menores de IC_{50}, el 3-ftaloilo (**2g**, 0.79 μM), el 3-succinilo (**2h**, 3.49 μM) y el 3-glutarilo (**2i**, 1.03 μM). Además, entre los derivados de AO-11AUA (**3**), sólo el derivado 3-ftaloilo (**3g**) presenta una IC_{50} muy baja (0.88 μM). Por lo tanto, se puede concluir que los derivados con un grupo

ftaloilo en C-3 (**1g**, **2g** y **3g**) presentan una mejor inhibición de la proteasa del VIH-1.

Tabla 2. Valores de IC_{50} de los 3-acil-28-monopeptidilderivados de AO (**1a**-**3j**).

Grupo acilo acoplado	Aminoácido acoplado					
	GABA		6AHA		11AUA	
	Comp.	IC_{50} (μM)	Comp.	IC_{50} (μM)	Comp.	IC_{50} (μM)
Ac	**1a**	32.56 ± 0.98	**2a**	66.46 ± 2.63	**3a**	199.21 ± 4.85
Prop	**1b**	111.80 ± 0.31	**2b**	155.18 ± 1.14	**3b**	168.25 ± 3.24
But	**1c**	61.48 ± 1.07	**2c**	183.56 ± 3.95	**3c**	> 250
Hex	**1d**	> 250	**2d**	> 250	**3d**	585.03 ± 15.91
Lau	**1e**	> 250	**2e**	> 250	**3e**	> 250
Bz	**1f**	55.08 ± 1.88	**2f**	> 250	**3f**	139.68 ± 1.52
Fta	**1g**	2.21 ± 0.05	**2g**	0.79 ± 0.01	**3g**	0.88 ± 0.00
Succ	**1h**	17.7 ± 0.79	**2h**	3.46 ± 0.11	**3h**	> 250
Glu	**1i**	20.38 ± 0.04	**2i**	1.03 ± 0.02	**3i**	245.25 ± 9.47
DMG	**1j**	33.34 ± 0.72	**2j**	12.35 ± 0.24	**3j**	> 250

Los valores de IC_{50} de los 3-acil-28-dipeptidil derivados de AO (**4a**-**12j**) se muestran en las Tablas 3,4 y 5. Estos valores indican que, los mejores resultados los presentan los 3-ftaloil derivados de AO (**4g**-**12g**), destacando el 3-ftaloil-28-VAL-6AHA derivado de AO (**11g**), con una concentración de IC_{50} de 0.59 μM.

Tabla 3. Valores de IC_{50} de los 3-acil-28-dipeptidil derivados de AO (**4a**-**6j**).

Grupo acilo acoplado	Aminoácidos acoplados					
	GLY-GABA		GLY-6AHA		GLY-11AUA	
	Comp.	IC_{50} (μM)	Comp.	IC_{50} (μM)	Comp.	IC_{50} (μM)
Ac	**4a**	121.79 ± 3.97	**5a**	102.06 ± 0.22	**5a**	> 250
But	**4c**	145.72 ± 6.47	**5c**	> 250	**6c**	102.31 ± 0.79
Hex	**4d**	> 250	**5d**	> 250	**6d**	> 250
Lau	**4e**	> 250	**5e**	> 250	**6e**	> 250
Bz	**4f**	180.54 ± 5.11	**5f**	> 250	**6f**	141.44 ± 0.02
Fta	**4g**	2.2 ± 0.01	**5g**	3.05 ± 0.08	**6g**	2.29 ± 0.01
Succ	**4h**	> 250	**5h**	> 250	**6h**	176.74 ± 3.23
Glu	**4i**	187.68 ± 5.57	**5i**	> 250	**6i**	> 250
DMG	**4j**	> 250	**5j**	38.81 ± 0.43	**6j**	> 250

Tabla 4. Valores de IC_{50} de los 3-acil-28-dipeptidil derivados de AO (**7a**-**9j**).

Grupo acilo acoplado	Aminoácidos acoplados					
	ALA-GABA		ALA-6AHA		ALA-11AUA	
	Comp.	IC_{50} (μM)	Comp.	IC_{50} (μM)	Comp.	IC_{50} (μM)
Ac	**7a**	> 250	**8a**	47.06 ± 1.32	**9a**	> 250
Prop	**7b**	88.09 ± 0.50	**8b**	31.04 ± 0.22	**9b**	> 250
But	**7c**	> 250	**8c**	39.96 ± 0.30	**9c**	> 250
Hex	**7d**	> 250	**8d**	> 250	**9d**	> 250
Lau	**7e**	> 250	**8e**	> 250	**9e**	> 250
Bz	**7f**	47.1 ± 0.2	**8f**	> 250	**9f**	> 250
Fta	**7g**	1.59 ± 0.04	**8g**	3.23 ± 0.11	**9g**	1.11 ± 0.02
Succ	**7h**	> 250	**8h**	40.22 ± 0.99	**9h**	80.74 ± 0.43
Glu	**7i**	6.56 ± 0.05	**8i**	38.84 ± 0.27	**9i**	> 250
DMG	**7j**	> 250	**8j**	24.07 ± 0.94	**9j**	> 250

Tabla 5. Valores de IC_{50} de los 3-acil-28-dipeptidil derivados de AO (**10a**-**12j**).

Grupo acilo acoplado	Aminoácido acoplado					
	VAL-GABA		VAL-6AHA		VAL-11AUA	
	Comp.	IC_{50} (μM)	Comp.	IC_{50} (μM)	Comp.	IC_{50} (μM)
Ac	**10a**	134.92 ± 0.42	**11a**	30.29 ± 0.98	**12a**	> 250
Prop	**10b**	> 250	**11b**	101.38 ± 0.45	**12b**	> 250
But	**10c**	> 250	**11c**	658.56 ± 13.27	**12c**	> 250
Hex	**10d**	> 250	**11d**	> 250	**12d**	> 250
Lau	**10e**	> 250	**11e**	> 250	**12e**	> 250
Bz	**10f**	125.82 ± 0.92	**11f**	> 250	**12f**	> 250
Fta	**10g**	4.58 ± 0.02	**11g**	0.59 ± 0.01	**12g**	1.16 ± 0.08
Succ	**10h**	41.48 ± 0.75	**11h**	9.63 ± 0.31	**12h**	216.42 ± 4.70
Glu	**10i**	19.84 ± 0.46	**11i**	17.87 ± 0.82	**12i**	> 250
DMG	**10j**	46.27 ± 0.61	**11j**	23.17 ± 0.73	**12j**	> 250

3. CONCLUSIONES

Se han sintetizado 12 derivados de AO acoplando uno dos moléculas de aminoácido en el grupo carbonilo de C-28 (**1**-**12**). Además, se han sintetizado 120 derivados bifuncionalizados de AO en los que, además de las moléculas de aminoácido, se les ha añadido uno de los 10 grupos acilo que se han utilizado. De estos 120 compuestos, 30 son 3-acil-28-monopeptidil derivados de AO (**1a**-**3j**) y 90 son 3-acil-28-dipeptidil derivados (**4a**-**12j**). Ambos tipos de reacciones se han llevado a cabo aplicando la filosofía de la química combinatoria, utilizando la técnica de Síntesis Orgánica en Fase Sólida, con objeto de evaluarlos como inhibidores de la proteasa del VIH.

Estos ensayos biológicos frente a la inhibición de la proteasa del VIH-1, nos han permitido estudiar la relación estructura-actividad de estos compuestos. La unión al grupo carboxilo de C-28 del ácido oleanólico de los aminoácidos más pequeños utilizados (GABA y 6AHA), mejoró apreciablemente la inhibición de la proteasa del VIH-1, mientras que el acoplamiento de un aminoácido de cadena más larga (11AUA) disminuyó este efecto. Además, la unión de dos aminoácidos a dicho grupo

carboxilo, sólo mejoró la inhibición de la proteasa del VIH-1 en una de las nueve posibles variantes, concretamente cuando los aminoácidos acoplados eran GLY y GABA (**7**). Los procesos de acilación de estos derivados de AO, mejoran en algunos casos los resultados de inhibición, particularmente cuando se utiliza el anhídrido ftálico como agente acilante, en algunos casos con valores IC_{50} de concentración nanomolar.

Los resultados obtenidos en este estudio, sugieren que los 3-ftaloil-28-monopeptidil y los 3-ftaloil-28-dipeptidil derivados del ácido oleanólico pueden ser prometedores agentes antivirales frente a la proteasa del VIH-1.

4. EXPERIMENTAL

4.1. Sección Química

4.1.1. Aislamiento de AO a partir de los residuos de la industria del aceite de oliva

El ácido oleanólico se aisló a partir de los residuos sólidos resultantes de la producción del aceite de oliva, que se extrajeron sucesivamente en un Soxhlet con hexano y AcOEt.[19] Los extractos de hexano contenían una mezcla de dos ácidos triterpénicos, los ácidos oleanólico y maslínico, en una relación (80:20) respectivamente, mientras que esta relación era inversa (20:80) para los extractos de AcOEt. Se purificaron ambas mezclas mediante cromatografía en columna sobre gel de sílice, eluyendo con mezclas de cloroformo/metanol o diclorometano/acetona de polaridad creciente.[17]

4.1.2. Procedimiento para la Síntesis Orgánica en Fase Sólida de mono- y dipeptidil derivados de AO (1-12)

El acoplamiento de los ω-aminoácidos (Aa1) a la resina de Barlos fue el primer paso para formar los monopeptidil derivados de AO (**1**-**3**). Se colocó una cantidad apropiada de resina CTC (1.30 mmol/g) en tres jeringuillas de polipropileno de 10 mL, equipadas con discos de filtro de polietileno. La resina de cada jeringa se lavó con DMF (2 mL x 3) y DCM (2 mL x 3) y se hinchó con DCM (1mL) durante 30 minutos. Pasado este

tiempo, el disolvente se filtró bajo presión reducida y se añadió a cada jeringa una solución que contenía 2 equivalentes del correspondiente aminoácido protegido Fmoc-Aa1-OH (Fmoc-GABA-OH, Fmoc-6AHA-OH o Fmoc-11AUA-OH), DIEA (10 equivalentes) y DCM (1.5 mL). Se agitó mediante un agitador orbital durante 1.5 horas. A continuación, se realizó un tratamiento con MeOH (0.75 mL bajo agitación orbital, durante 15 minutos) para ocupar todos los centros activos de la resina que no hubiesen sido sustituidos por el correspondiente aminoácido. Posteriormente, la mezcla se filtró y el acoplado Fmoc-Aa1-resina correspondiente se lavó con DCM (2 mL x 3) y DMF (2 mL x 3). La desprotección del grupo Fmoc se realizó por tratamiento con piperidina/DMF (1:4) (3 x 10 min). Finalmente, la resina se lavó de nuevo con DCM (2 mL x 3) yDMF (2 mL x 3), filtrando a presión reducida. El segundo paso para formar los 28-monopeptidil derivados de AO, fue el acoplamiento del correspondiente acoplado Aa1-resina, con ácido oleanólico mediante la formación de un enlace peptídico entre el grupo amino libre del aminoácido y el grupo carboxilo del triterpeno. Para ello, se añadió una solución de AO (3 equivalentes), PyAOP (3 equivalentes), HOAT (9 equivalentes) y DIEA (9 equivalentes) en DMF/DCM. Esta mezcla se agitó durante 24 horas y, a continuación, se llevó a cabo un proceso de seguimiento de la reacción mediante la utilización del test de Kaiser, que permite determinar la presencia o ausencia de grupos aminos libres, de forma que, si resulta negativo, se da la reacción por terminada, pudiendo proseguir con el proceso. Resultando negativa la prueba del test de Kaiser, el acoplado AO-Aa1-resina se filtró, se lavó con DMF (2 mL x 3) y DCM (2 mL x 3) y se procedió a liberar la resina del acoplado tomando una pequeña muestra de cada jeringa que es tratada con DCM:TFA (99:1) (2 mL x 3 x 30 s). A continuación, el producto correspondiente se filtró, se evaporó a presión reducida, se liofilizó y se analizó por TLC y HPLC. De este modo se obtuvieron los monopeptidil derivados de AO (**1**, **2** y **3**). Las propiedades físicas, químicas y espectroscópicas de estos compuestos están descritas en un anterior trabajo de nuestro grupo de investigación.[23]

De manera similar, se obtuvieron los 28-dipeptidil derivados de AO (**4**-**12**), acoplando en primer lugar un a-aminoácido (Aa1) (Fmoc-GLY-OH, Fmoc-ALA-OH o Fmoc-VAL-OH) a la resina. Así, tomando tres jeringas y procediendo como se ha descrito en el párrafo anterior, se formaron los correspondientes acoplados Aa1-resina. A continuación, para unir el segundo aminoácido (ω-aminoácido, Aa2), cada jeringa se dividió en tres nuevas jeringas añadiendo una solución con 4 equivalentes de Fmoc-Aa2-OH (Fmoc-GABA-OH, Fmoc-6AHA-OH o Fmoc-11AUA-OH), HOAT (4 equivalentes), DIPCDI (4 equivalentes) en DMF, al correspondiente acoplado de Aa1-resina contenida en una jeringa. La mezcla se agitó durante 1.5 horas, siendo negativo el test de Kaiser. A continuación, el acoplado Fmoc-Aa2-Aa1-resina se sometió a los lavados y desprotección descritos anteriormente. Después se filtró a presión reducida. La unión de ácido oleanólico a este acoplado Aa2-Aa-1-resina se llevó en condiciones idénticas a las anteriormente descritas. La liberación de la resina de una pequeña cantidad del acoplado AO-Aa2-Aa1-resina, la evaporación y liofilización, dieron lugar a los 28-dipeptidil derivados de AO (**4**-**12**) cuyas propiedades químicas y espectroscópicas están descritas.[25]

4.1.3. Procedimiento de acilación mediante Síntesis Orgánica en Fase Sólida de los mono- y dipeptidil derivados de AO (1a-12j)

Las doce jeringas que contenían los acoplados AO-Aa1-resina (**1**-**3**) y AO-Aa2-Aa1-resina (**4-12**) se sometieron a una reacción de acilación, dividiendo cada jeringa en 10 nuevas jeringas, añadiendo cada uno de los 10 reactivos acilantes seleccionados (anhídridos acético, propanoico, butanoico, hexanoico, dodecanoico, benzoico, ftálico, succínico, glutárico y 3,3-dimetilglutárico). Estas jeringas se trataron con los anhídridos mencionados (10 equivalentes) en presencia de DMAP (0.5 equivalentes) y Et_3N (0.5 equivalentes), en DCM/DMF (1 mL/1mL) como disolvente y se dejaron en agitación orbital durante 24 horas. La resina se filtró y se lavó con DMF (2 mL x 3) y DCM (2 mL x 3). La liberación de la resina se llevó a cabo mediante la adición a cada jeringa de una solución de DCM con

TFA (1%) (2 min x 3). De esta forma, y de acuerdo con las posibles combinaciones de uno o dos aminoácidos unidos al grupo carboxilo C-28 de AO y diez grupos acilo acoplados al grupo hidroxilo de C-3 del anillo A, se obtuvieron 120 derivados bifuncionales de AO. Los primeros 30 eran 3-acil-28-monopeptidil derivados (**1a**-**3j**) y los otros 90 eran 3-acil-28-dipeptidil de AO derivados (**4a**-**12j**). Las propiedades químicas y espectroscópicas están descritas.[25] En la figura 4, se muestra parte de la instrumentación utilizada en la Síntesis Orgánica en Fase Sólida.

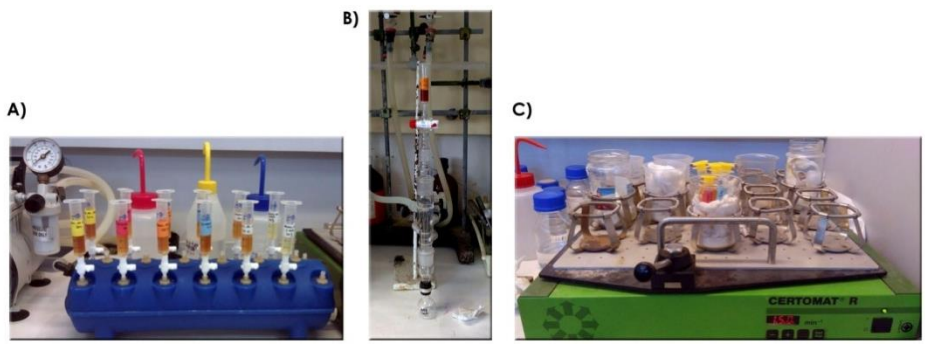

Figura 4. Equipamiento básico para la Síntesis Orgánica en Fase Sólida. A) Equipo para la preparación manual de los distintos derivados.

B) Equipo para la liberación de la resina y C) Agitador orbital.

4.2. Sección Biológica

4.2.1. Actividad antiviral frente a la proteasa del VIH-1

La actividad antiviral frente al HIV se determinó, usando la proteasa recombinante procedente de *E. coli* (PQITLWQRPL VTIKIGGQLK EALLDTGADDTVLEEMNLPG RWKPKMIGGI GGFIKVRQYD QILIEICGHK AIGTVLVGPT PVNIIGRNLL TQIGCTLNF) suministrada por BioVendorGmbH (Heidelberg, Alemania). Como sustrato, se utilizó el péptido sintético (Abz-Ala-Arg-Val-Nle-Tyr(NO_2)-Glu-Ala-Nle-NH_2) de Sigma (St. Louis, MO, USA) correspondiente al sitio de escisión p-24-p17. Su actividad, se midió utilizando la técnica de transferencia de energía de resonancia de fluorescencia (FRET). Cuando el péptido se escindió, la fluorescencia fue

monotorizada mediante un espectrofotómetro de fluorescencia (LS 50B) a una excitación/emisión de 320/4520 nm. La disminución en el porcentaje de la actividad de fluorescencia se usó para determinar el porcentaje de inhibición de la actividad, y se calculó de acuerdo con la siguiente fórmula: %inhibición: $[1-(V_{inh}/V_0)] \times 100$, donde V_{inh}= actividad enzimática en presencia de inhibidor y V_0 = actividad enzimática de control.

Como paso previo, antes de realizar los ensayos con los distintos derivados, se determinó la Km del sustrato, así como la concentración óptima del enzima (10 nM) y del sustrato (10 µM) a utilizar. Los derivados se disolvieron en DMSO a una concentración de 5 mg/mL. El tampón del ensayo fue preparado al momento (50 mM de acetato de sodio, 1 mM EDTA, 0.5 Mm DTT, 1 M NaCl, 2.5% de glicerol) añadiendo el DTT justo antes de medir, para evitar su degradación. Las concentraciones elegidas para ensayar los productos fueron: 500 µg/mL, 50 µg/mL, 5 µg/mL y 0.5 µg/mL. Cada derivado se ensayó por triplicado, y en cada ensayo se utilizó un control por triplicado con DMSO. Las mediciones en el fluorímetro para cada ensayo, se realizan durante 30 minutos, recogiendo los datos cada minuto.

El tratamiento estadístico de los resultados obtenidos, se realizó mediante el programa informático Sigmaplot, obteniendo los valores de IC_{50} para cada derivado.

5. BIBLIOGRAFÍA

[1] Cragg, G. M.; Newman, D. J. Natural Products: A Continuing Source of Novel Drug Leads. *Biochim. Biophys. Acta* **2013**, *1830*, 3670–3695.

[2] Dias, D. A.; Urban, S.; Roessner, U. A Historical Overview of Natural Products in Drug Discovery. *Metabolites* **2012**, *2*, 303–336.

[3] Ganesan, A. The Impact of Natural Products upon Modern Drug Discovery. *Curr. Opin. Chem. Biol.* **2008**, *12*, 306–317.

[4] Newman, D. J.; Cragg, G. M. Natural Products as Sources of New Drugs over the 30 Years from 1981 to 2014. *J. Nat. Prod.* **2016**, *79*, 629–661.

[5] Ngo, L. T.; Okogun, J. I.; Folk, W. R. 21st Century Natural Product Research and Drug Development and Traditional Medicines. *Nat. Prod. Rep.* **2013**, *30*, 584–592.

[6] Grabowski, K.; Baringhaus, K.-H.; Schneider, G. Scaffold Diversity of Natural Products: Inspiration for Combinatorial Library Design. *Nat. Prod. Rep.* **2008**, *25*, 892–904.

[7] Welsch, M. E.; Snyder, S. A.; Stockwell, B. R. Privileged Scaffolds for Library Design and Drug Discovery. *Curr. Opin. Chem. Biol.* **2010**, *14*, 347–361.

[8] Boldi, A. M. Libraries from Natural Product-Like Scaffolds. *Curr. Opin. Chem. Biol.* **2004**, *8*, 281–286.

[9] Hughes, I. In *Drug Discovery and Development, Volume 1*; Chorghade, M. S., Ed.; John Wiley & Sons, Inc.: Hoboken, NJ, USA, **2006**.

[10] Schnur, D. M.; Beno, B. R.; Tebben, A. J.; Cavallaro, C. Methods for combinatorial and parallel library desing.*Methods Mol. Biol.* **2011**, *672*, 387–434.

[11] Merrifield, R. B. Solid Phase Peptide Synthesis. *J. Am. Chem. Soc.* **1963**, *85*, 2149-2154.

[12] Kuo, R.; Qian, K.; Morris-natschke, S. L. & Lee, K. Plant-derived triterpenoids and analogues as antitumor and anti-HIV agents †. *Nat. Prod. Rep.* **2009**, *26*, 1321–1344.

[13] López Galera, M.R.; Gómez Domingo, M.R.; Pou Clavé, L.; Ruiz Csmps, I.; Ribera Pascuet, E.; Monteverde Junyent, J. Inhibidores de la proteasa del VIH: monitorización terapéutica de las concentraciones plasmáticas en el tratamiento antirretroviral. *Farmacia hospitalaria* **2001**, *25*, 55-66.

[14] Pollier, J.; Coossens, A. Oleanolic acid. *Phytochemistry* **2012**, *77*, 10-15.

[15] Han, B.; Peng, Z. Anti-HIV triterpenoids components. *J.Chem.Pharm.Res.* **2014**, *6*, 438-443.

[16] Jäger, S.; Trojan, H.; Kopp, T.; Laszczyk, M. N. & Scheffler, A. Pentacyclic triterpene distribution in various plants-rich sources for a new group of multi-potent plant extracts. *Molecules* **2009**,14**,** 2016–2031.

[17] A. García-Granados, A. Martinez, J.N. Moliz, A. Parra, F. Rivas, 3β-hydroxyolean-12-en-28-oic acid (oleanolicacid),*Molecules 3*, **1998**, M87.

[18] A. García-Granados, A. Martinez, J.N. Moliz, A. Parra, F. Rivas, 2a,3β-dihydroxyolean-12-en-28-oic acid (maslinicacid), Molecules *3*, **1998**, M88.

[19] Garcia-Granados, [A.]Process for the industrial recovery of oleanolic and maslinic acids contained in the olive milling byproducts, PCT. Int. Appl. **1998,** WO 9804331.

[20] Parra, A.; Rivas, F.; Martin-Fonseca, S.; Garcia-Granados, A.; Martinez, A. Maslinic acid derivatives induce significant apoptosis in b16f10 murine melanoma cells. *Eur. J. Med. Chem.* **2011**, *46*, 5991–6001.

[21] Parra, A.; Rivas, F.; Lopez, P. E.; Garcia-Granados, A.; Martinez, A.; Albericio, F.; Marquez, N.; Munoz, E. Solution- and solid-phase synthesis and anti-HIV activity of maslinic acid derivatives containing amino acids and peptides. Bioorg. Med. Chem. **2009**, *17*, 1139–1145.

[22] Parra, A.; Martin-Fonseca, S.; Rivas, F.; Reyes-Zurita, F. J.; Medina-O'Donnell, M.; Martinez, A.; Garcia-Granados, A.; Lupiañez, J. A.; Albericio, F. Semi-synthesis of acylated triterpenes from olive-oil industry wastes for the development of anticancer and anti-HIV agents. Eur. J. Med. Chem. **2014**, *74*, 278–301.

[23] Parra, A.; Martin-Fonseca, S.; Rivas, F.; Reyes-Zurita, F. J.; Medina-O'Donnell, M.; Rufino-Palomares, E. E.; Martinez, A.; Garcia-Granados, A.; Lupiañez, J. A.; Albericio, F. Solid-phase library synthesis of bi-functional derivatives of oleanolic and maslinic acids and their cytotoxicity on three cancer cell lines. ACS Comb. Sci. **2014**, *16*, 428–447.

VI OTRAS COLABORACIONES

Durante el transcurso de la presente Tesis Doctoral, se presentó la oportunidad de realizar una colaboración, entre nuestro Grupo de Investigación y el Departamento de Física Aplicada II de la Universidad de Granada y el Departamento de Física Aplicada de la Universidad de Málaga. Ambos Departamentos de Física interesados por los productos naturales triterpénicos y los derivados obtenidos con propiedades biológicas frente al cáncer y a la proteasa del VIH, propusieron la realización de nanopartículas con dichos productos.

El inconveniente de la baja solubilidad de estos compuestos naturales y algunos de sus derivados, hizo que esta propuesta se considerara muy interesante. Se tenía así, alternativa para mejorar la biodisponibilidad de aquellos compuestos con buena actividad biológica pero baja solubilidad.

Los primeros trabajos que se han llevado a cabo a lo largo de estos años, han dado lugar a cuatro publicaciones:

- Molina-Bolívar, J.A.; Galisteo-González, F.; Carnero Ruiz, C.; Medina-O'Donnell, M.; Parra, A. Spectroscopy investigation on the interaction of maslinic acid with bovine serum albumin. *JournalLuminescence*. **2014**, *156*, 141-149.


Journal of Luminescence

Volume 156, December 2014, Pages 141–149

ELSEVIER

Spectroscopic investigation on the interaction of maslinic acid with bovine serum albumin

J.A. Molina-Bolívar[a], F. Galisteo-González[b], C. Carnero Ruiz[a], M. Medina-O´Donnell[c], A. Parra[c]

- Molina-Bolívar, J.A.; Carnero Ruiz, C.; Galisteo-González, F.; Medina-O'Donnell, M.; Parra, A. Energetics of albumin-disuccinylmaslinic acid binding determined by fluorescence spectroscopy. *Fluid Phase Equilibria.* **2015**, 400, 43-52.

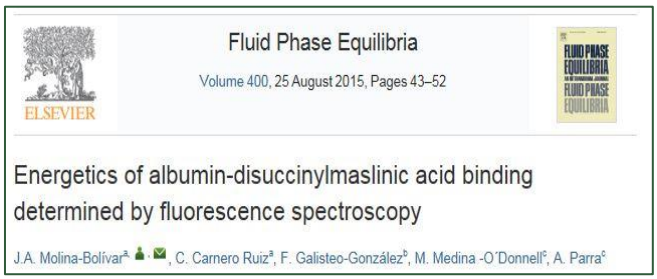
Fluid Phase Equilibria
Volume 400, 25 August 2015, Pages 43–52
ELSEVIER
Energetics of albumin-disuccinylmaslinic acid binding determined by fluorescence spectroscopy
J.A. Molina-Bolívar[a], C. Carnero Ruiz[a], F. Galisteo-González[b], M. Medina -O'Donnell[c], A. Parra[c]

- Molina-Bolívar, J.A.; Galisteo-González, F.; Carnero Ruiz, C.; Medina-O'Donnell, M.; Parra, A. Interaction between the anti-cancer drug diacetyl maslinic acid and bovine serum albumin: A biophysical study. *Journal of Molecular Liquids*. **2015**, 208, 304-313.

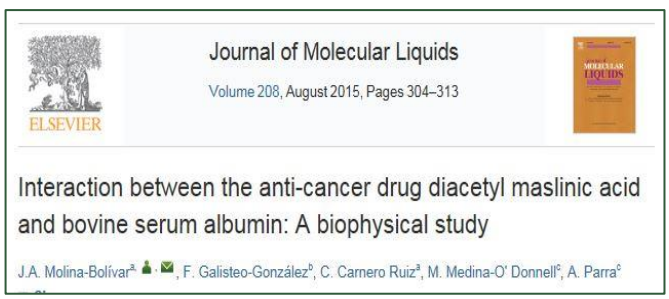
Journal of Molecular Liquids
Volume 208, August 2015, Pages 304–313
ELSEVIER
Interaction between the anti-cancer drug diacetyl maslinic acid and bovine serum albumin: A biophysical study
J.A. Molina-Bolívar[a], F. Galisteo-González[b], C. Carnero Ruiz[a], M. Medina-O' Donnell[c], A. Parra[c]

- Molina-Bolívar, J.A.; Carnero Ruiz, C.; Galisteo-González, F.; Medina-O'Donnell, M.; Parra, A. Simultaneous presence of dynamic and sphere action component in the fluorescence quenching of human serum albumin by diphthaloylmaslinic acid. *Journal of luminescence*. **2016**, 178, 259-266.


Journal of Luminescence
Volume 178, October 2016, Pages 259–266
ELSEVIER
Full Length Article
Simultaneous presence of dynamic and sphere action component in the fluorescence quenching of human serum albumin by diphthaloylmaslinic acid
J.A. Molina-Bolívar[a], C. Carnero Ruiz[a], F. Galisteo-González[b], M. Medina-O´ Donnell[c], A. Parra[c]

En estos trabajos, se estudian las interacciones entre el triterpeno y las proteínas (albúmina sérica bovina, BSA y albúmina sérica humana, HSA) mediante diferentes técnicas espectroscópicas para analizar el tipo de fuerzas que predominan, la fortaleza de esa unión y si se afecta o no la estructura de la proteína. El objetivo final, es conocer las interacciones fármaco-proteína dado que el AM y sus derivados han manifestado poseer propiedades anticancerígenas y BSA y HSA son consideradas proteínas transportadoras capaces de penetrar en los tumores malignos.

Nuestra labor en estas colaboraciones consistió, en la preparación, purificación e identificación de los distintos derivados de ácido maslínico que fueron suministrados a los citados investigadores para sus oportunos estudios químico-físicos.

VII ESPECTROS RMN

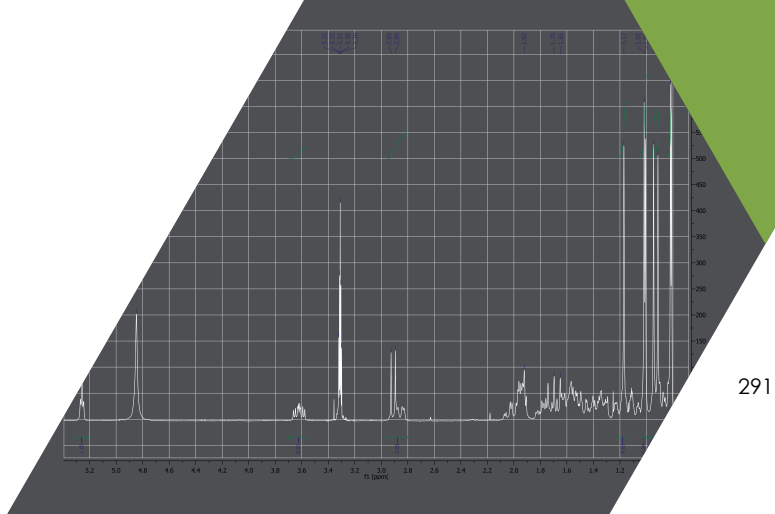

1. ESPECTROS RMN PUBLICACIÓN 1

Espectro de ^{1}H RMN del compuesto I

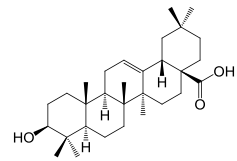

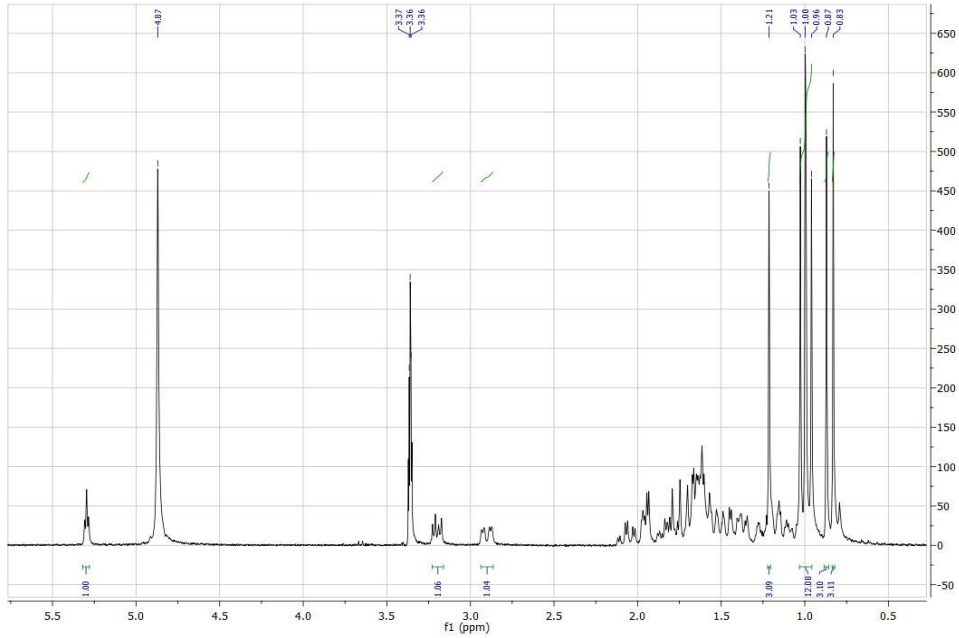

Espectro de ^{13}C RMN del compuesto I

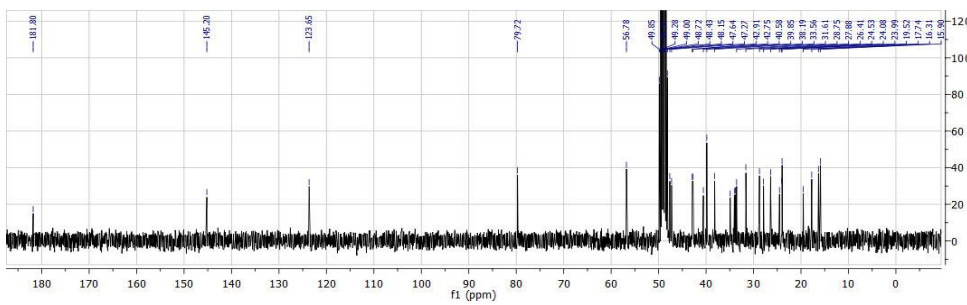

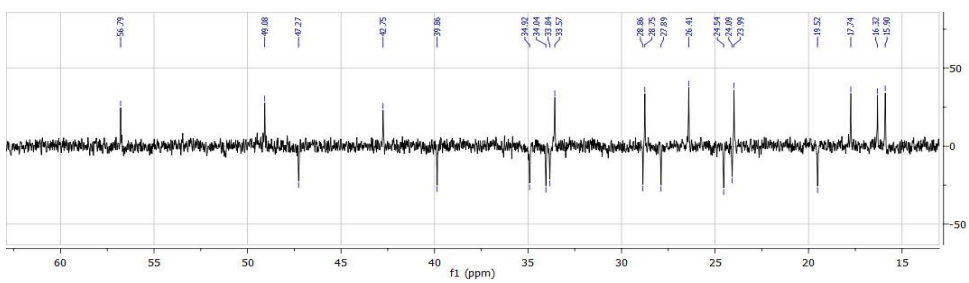

Espectro de ^{1}H RMN del compuesto II

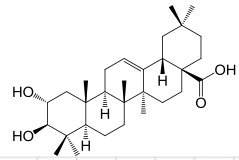

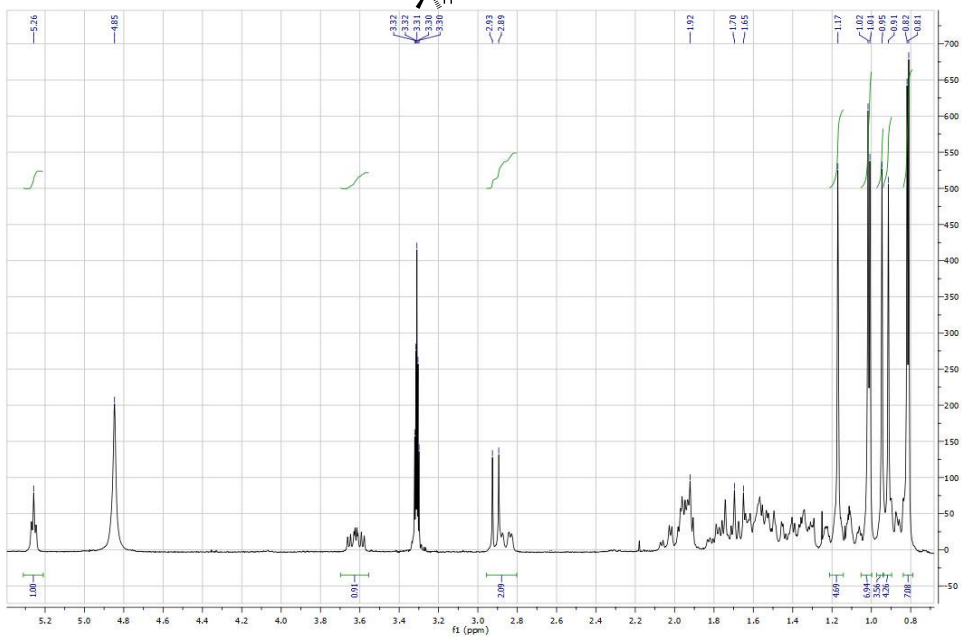

Espectro de ^{13}C RMN del compuesto II

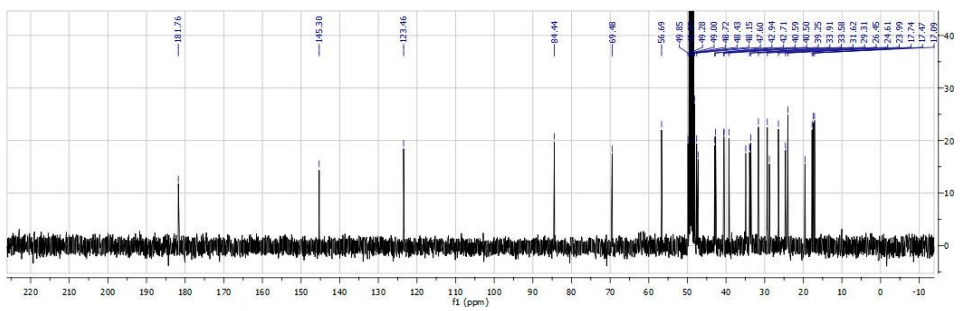

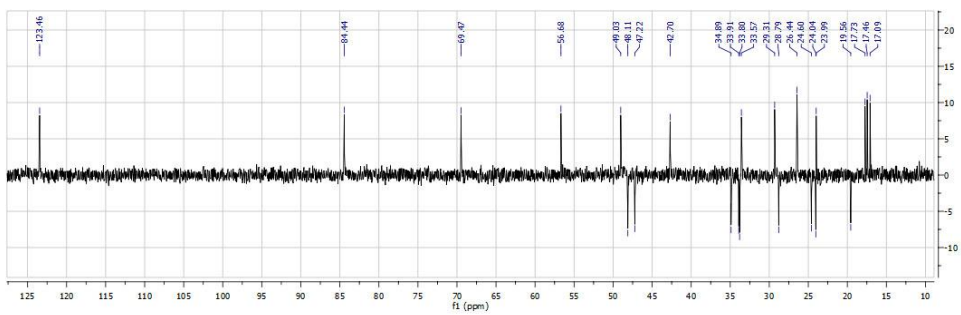

Espectro de ^{1}H RMN del compuesto III

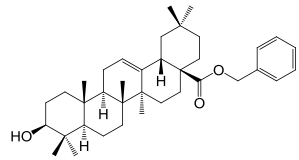

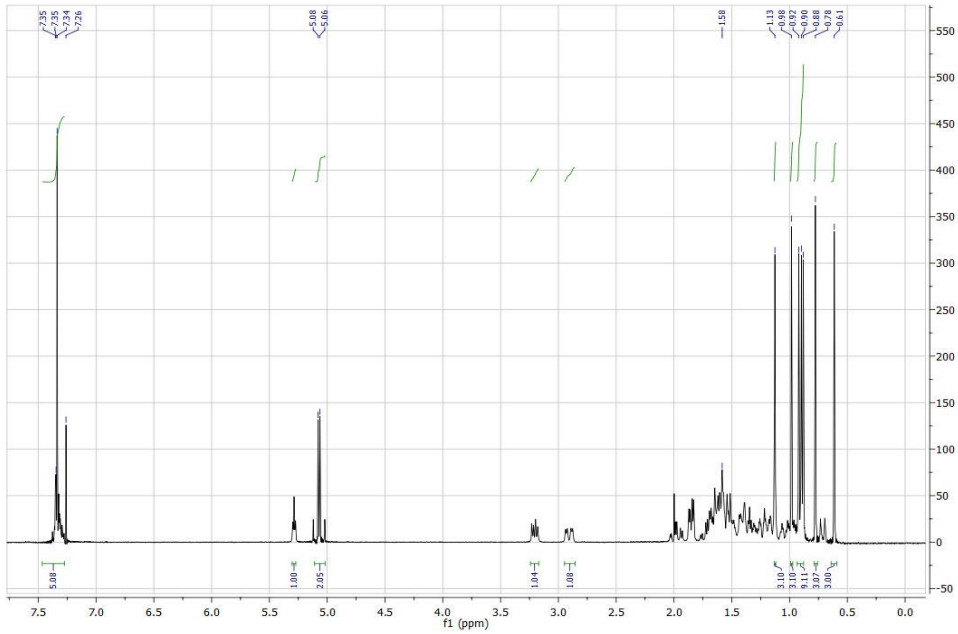

Espectro de ^{13}C RMN del compuesto III

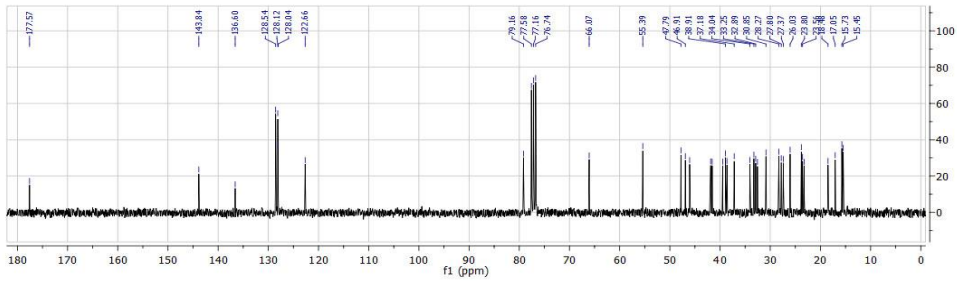

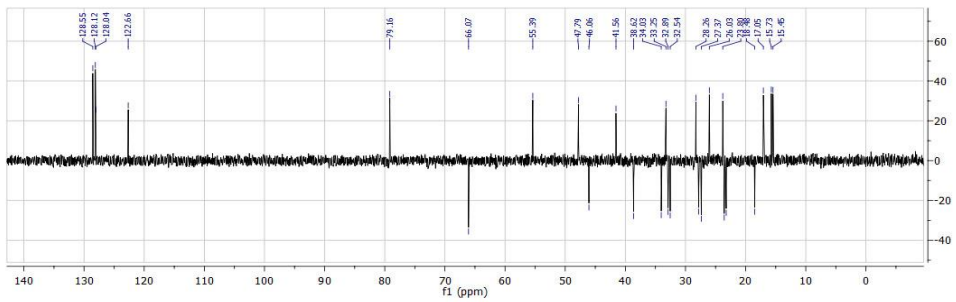

Espectro de ^{1}H RMN del compuesto IV

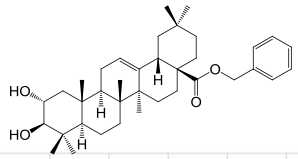

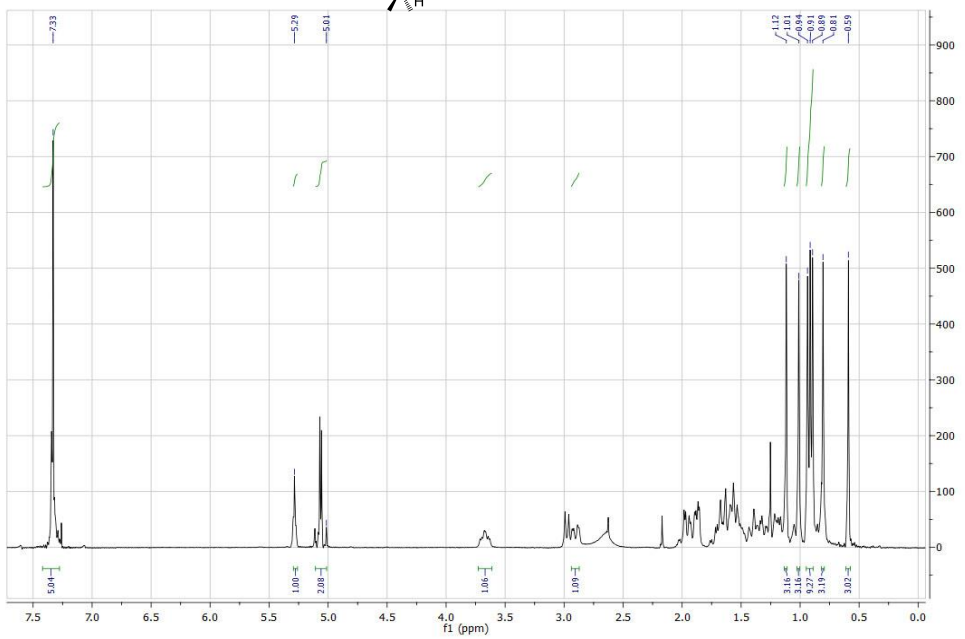

Espectro de ^{13}C RMN del compuesto IV

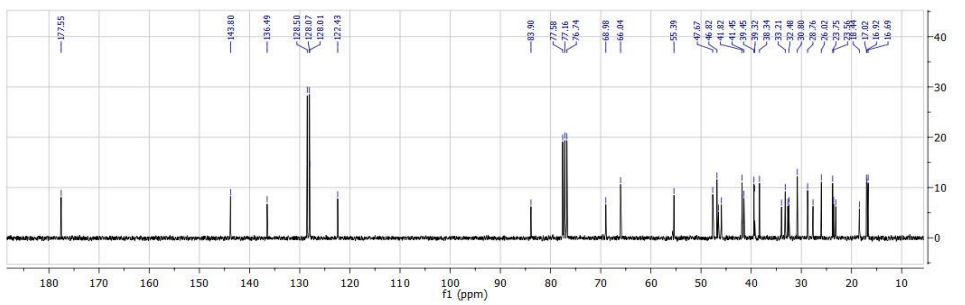

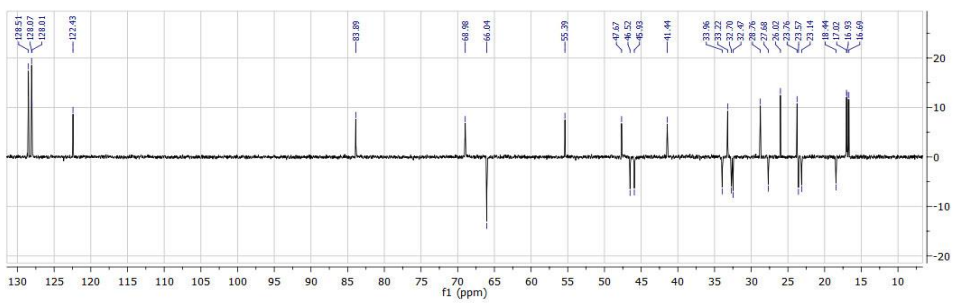

Espectro de ^{1}H RMN del compuesto V

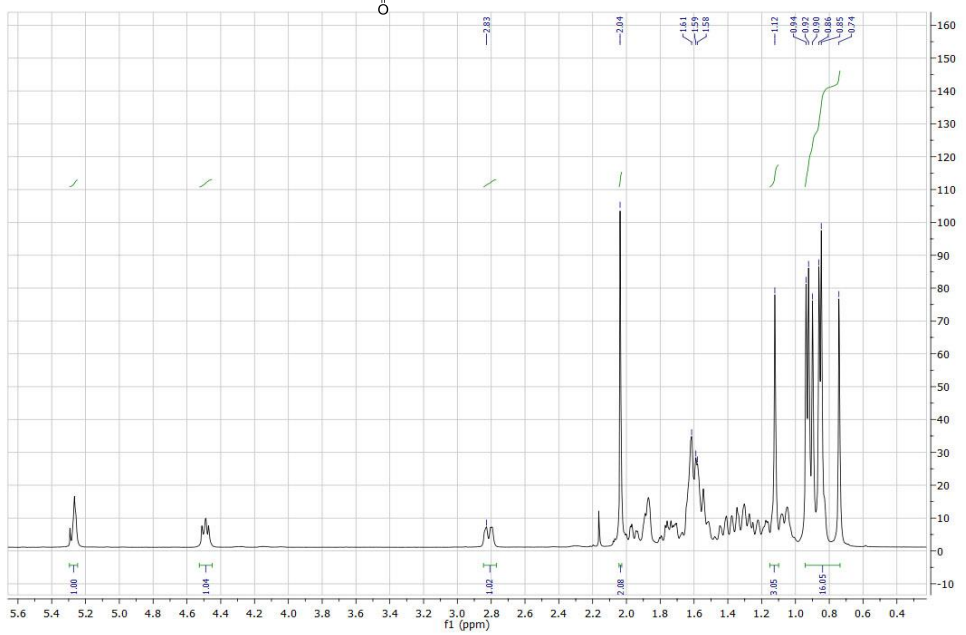

Espectro de ^{13}C RMN del compuesto V

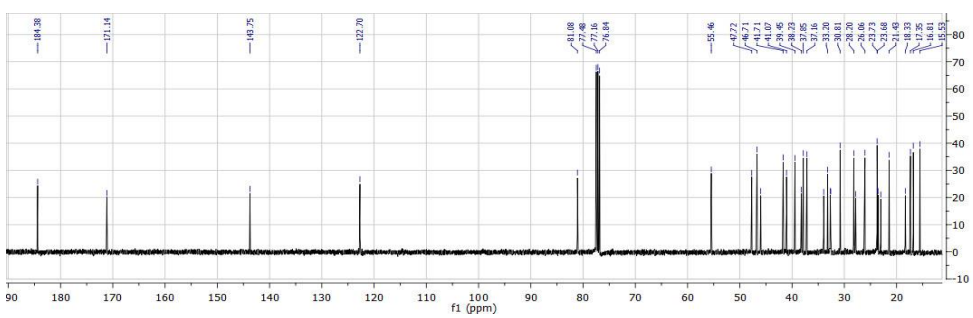

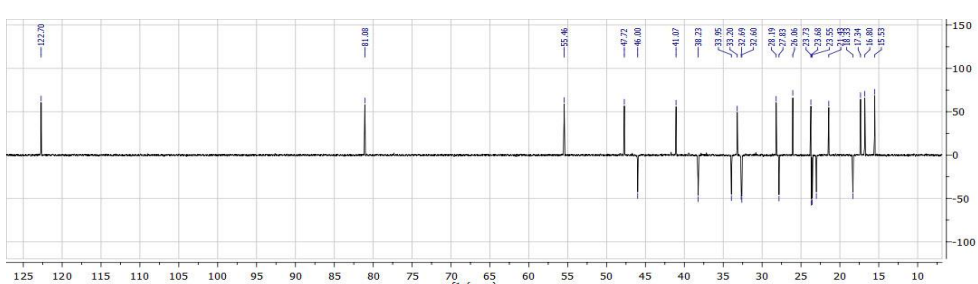

Espectro de ^{1}H RMN del compuesto VI

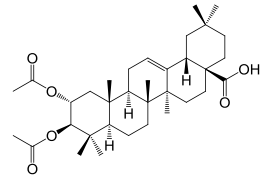

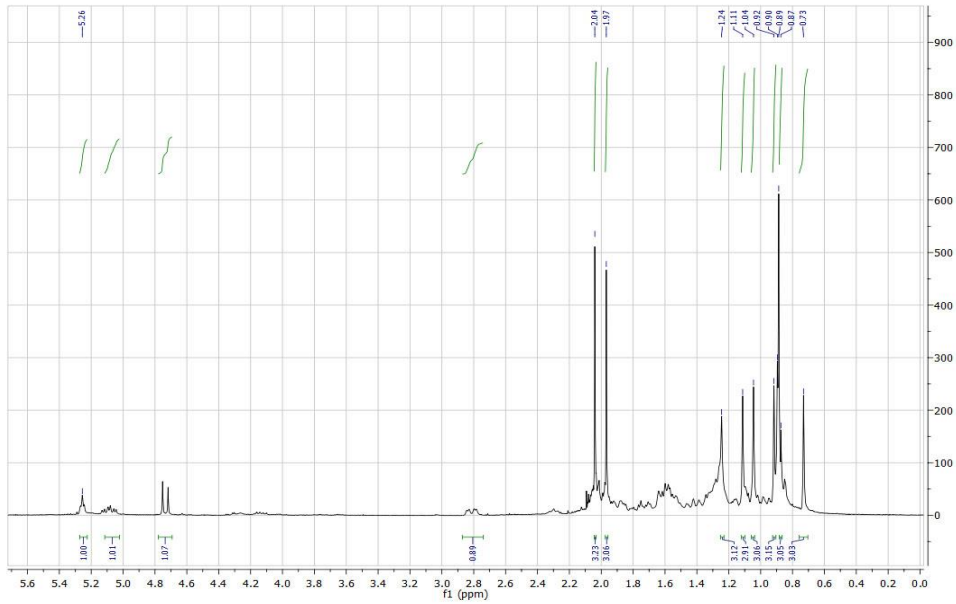

Espectro de ^{13}C RMN del compuesto VI

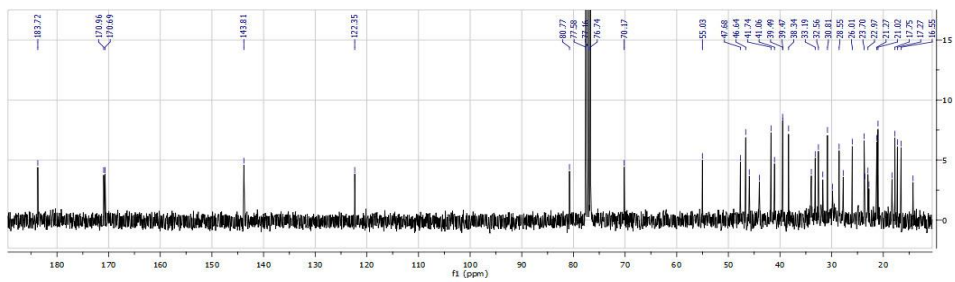

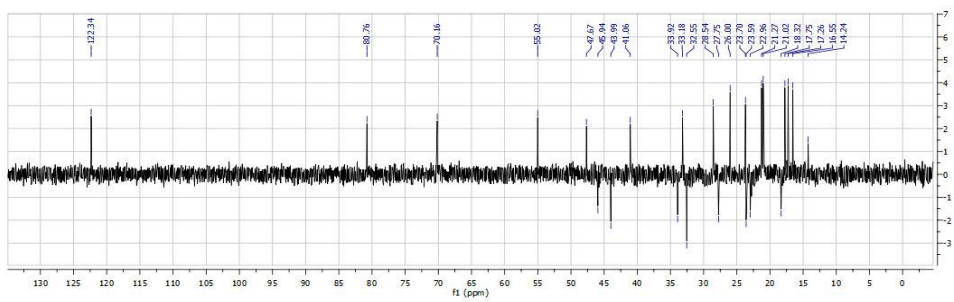

Espectro de ^{1}H RMN del compuesto 1

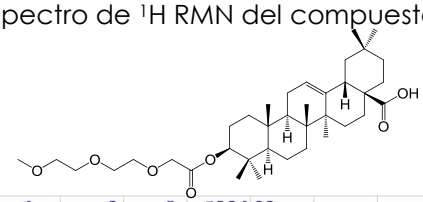

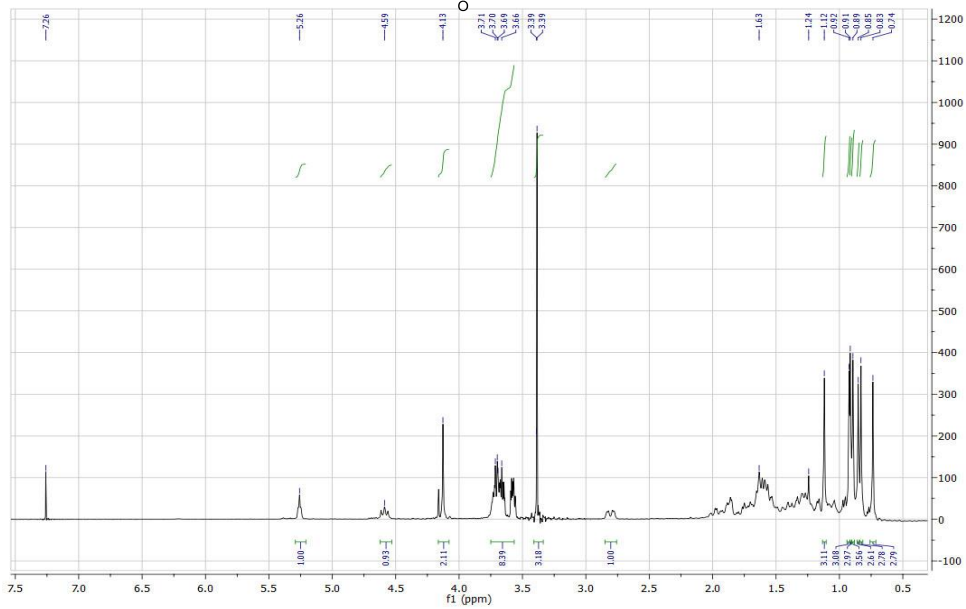

Espectro de ^{13}C RMN del compuesto 1

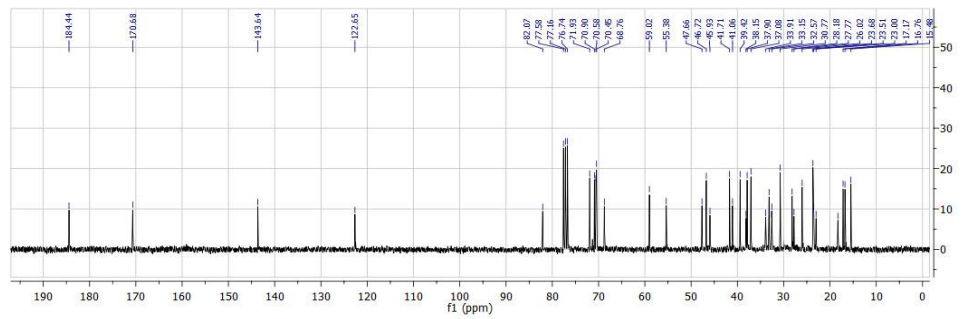

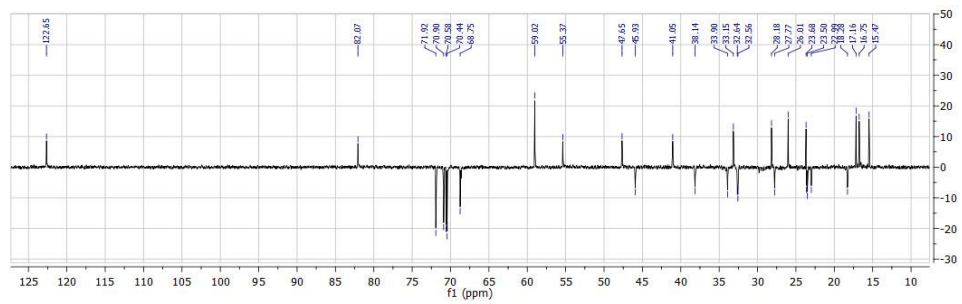

Espectro de ^{1}H RMN del compuesto 2

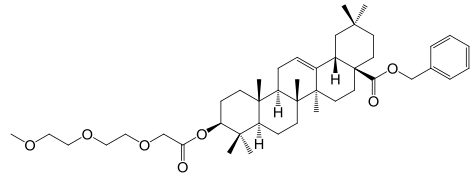

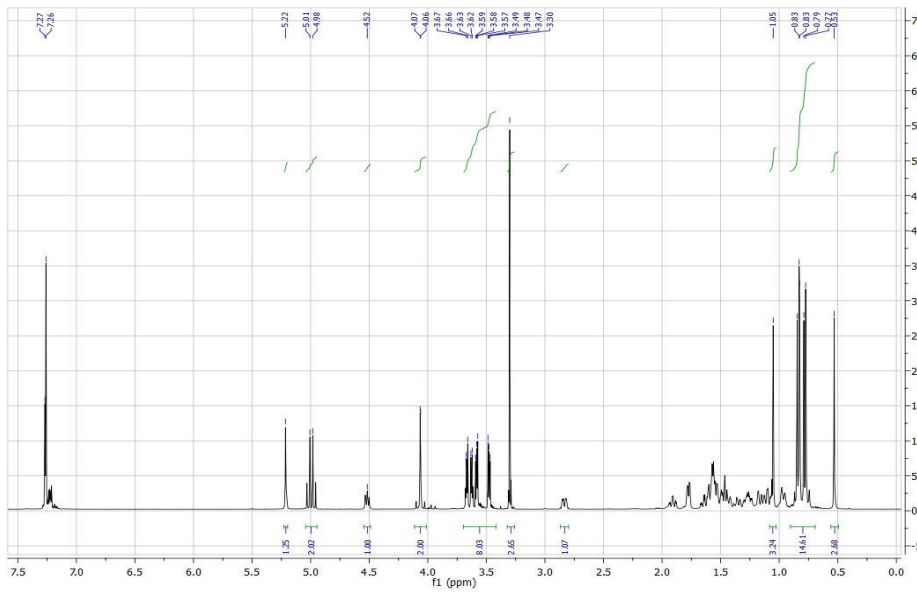

Espectro de ^{13}C RMN del compuesto 2

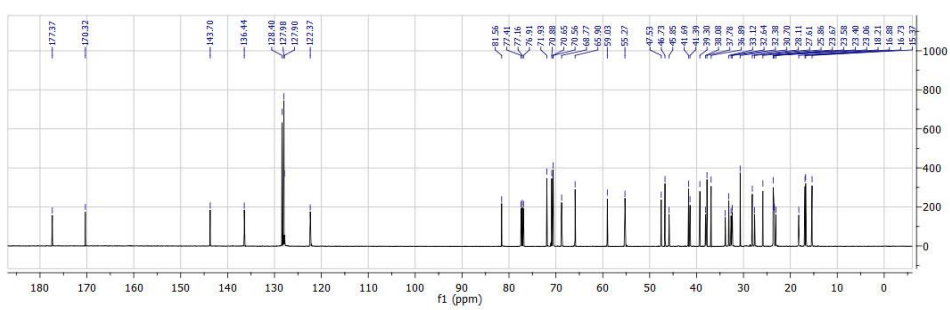

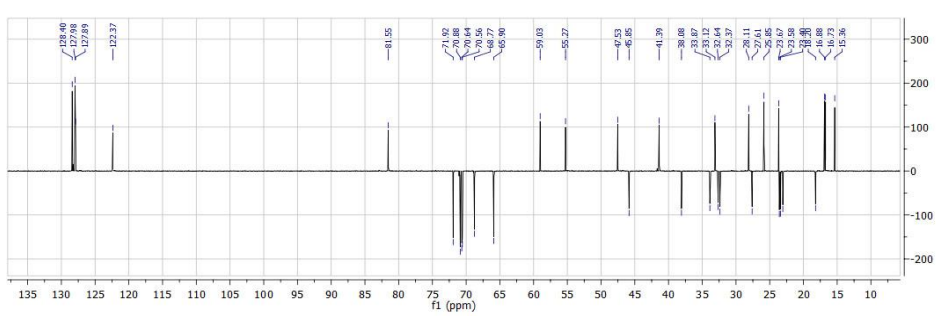

Espectro de ^{1}H RMN del compuesto 3

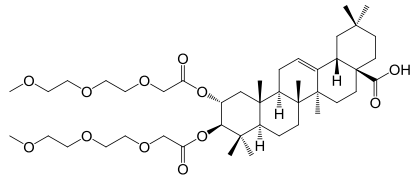

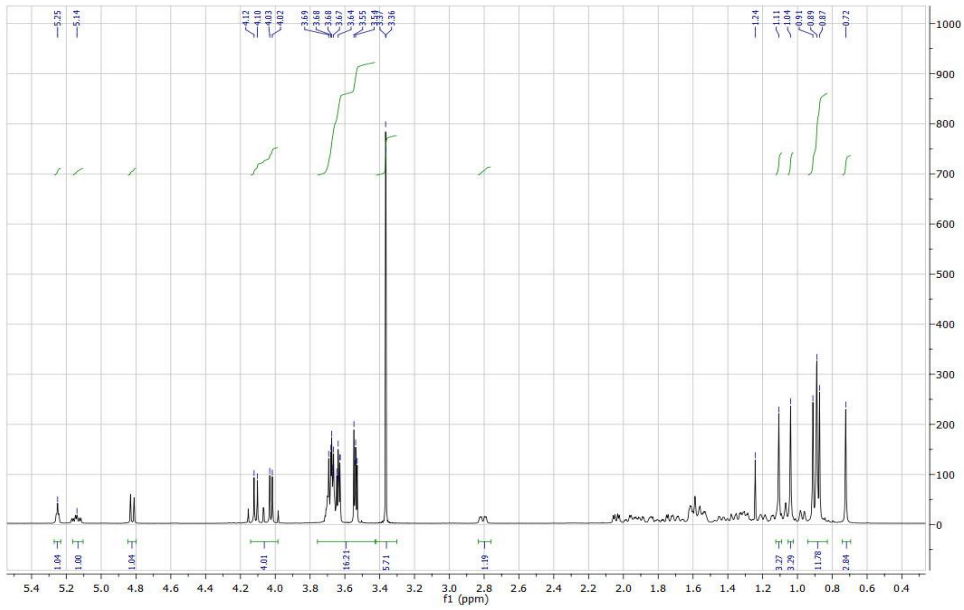

Espectro de ^{13}C RMN del compuesto 3

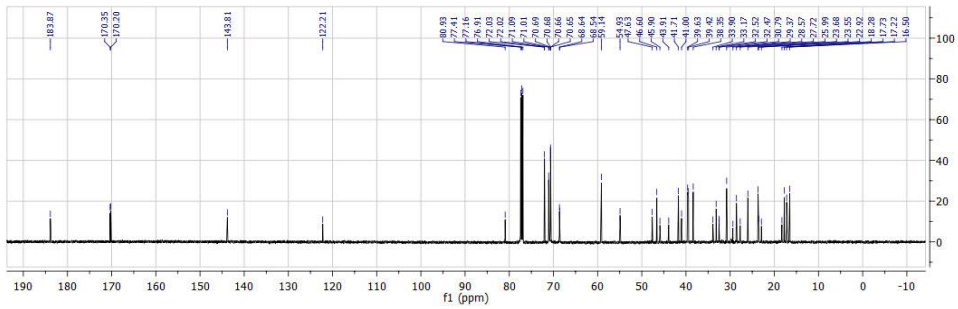

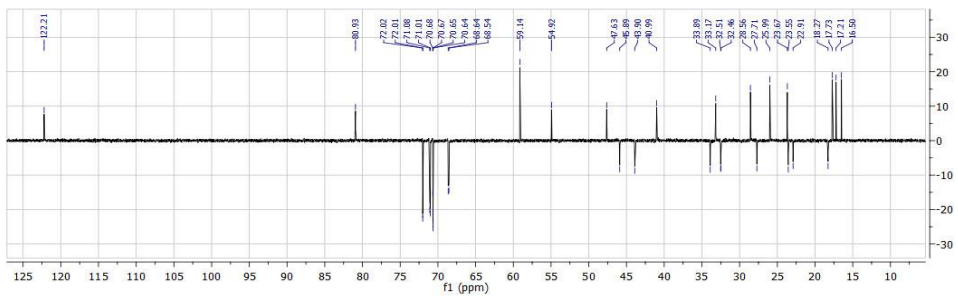

Espectro de ^{1}H RMN del compuesto 4

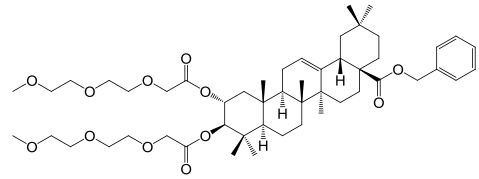

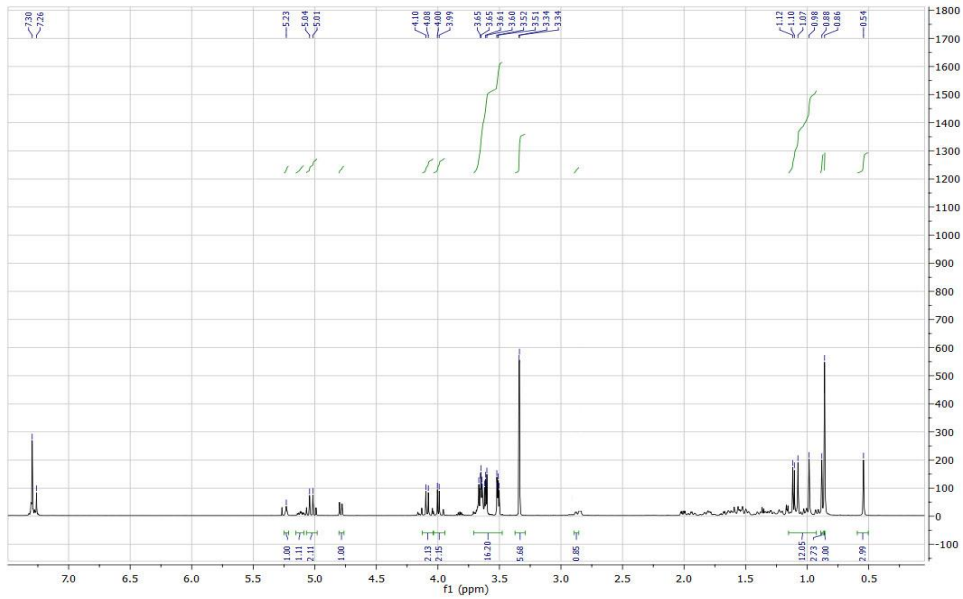

Espectro de ^{13}C RMN del compuesto 4

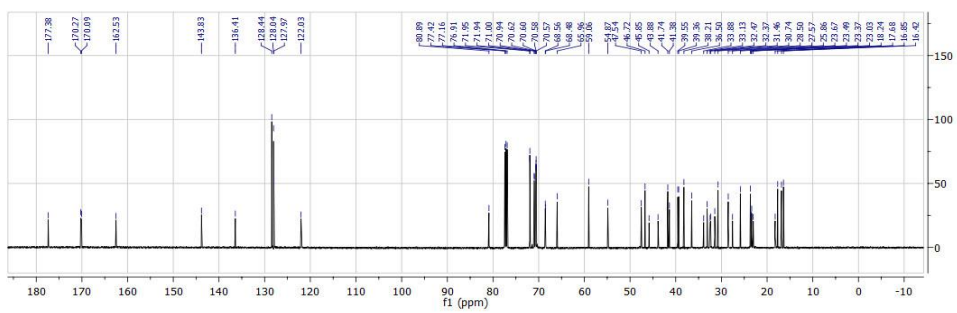

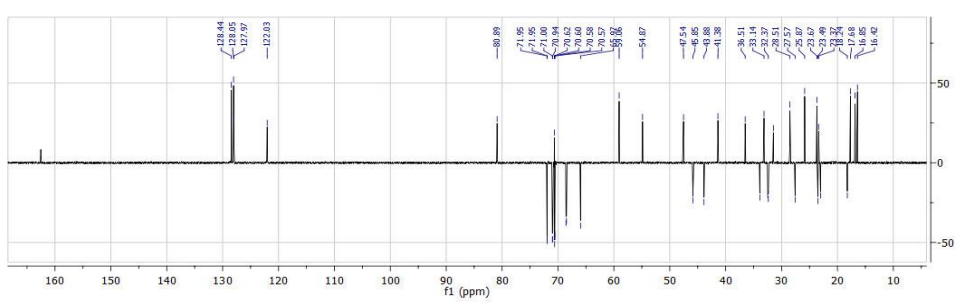

Espectro de ^{1}H RMN del compuesto 5

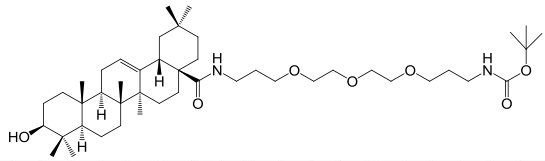

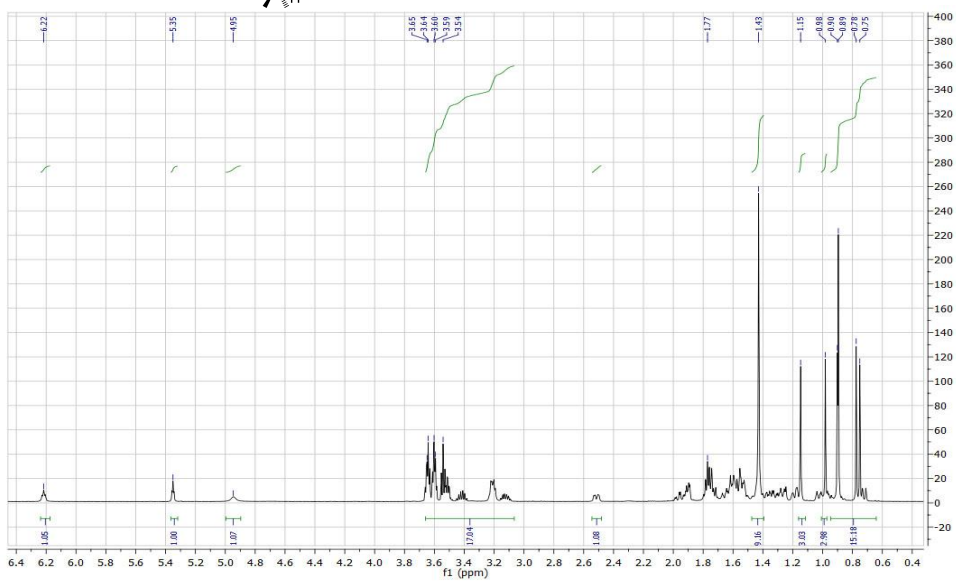

Espectro de ^{13}C RMN del compuesto 5

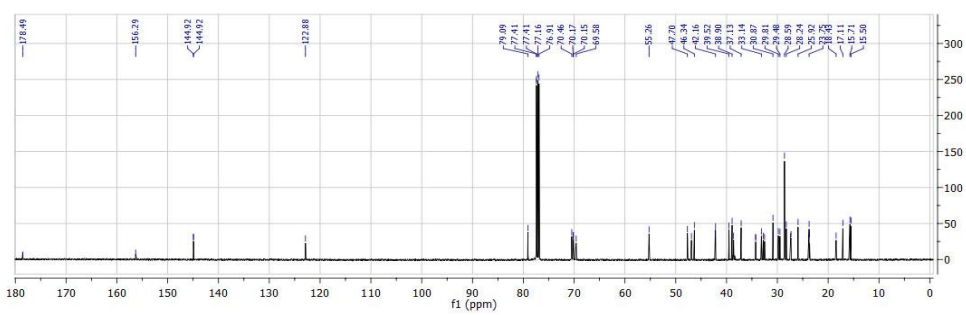

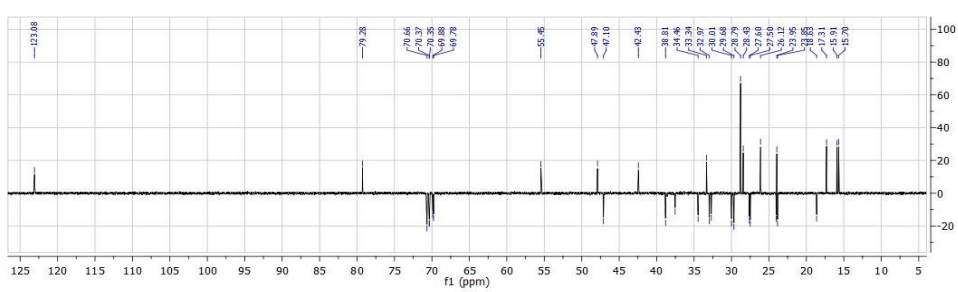

Espectro de ^{1}H RMN del compuesto 6

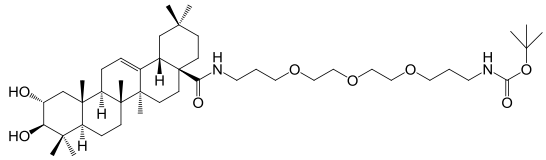

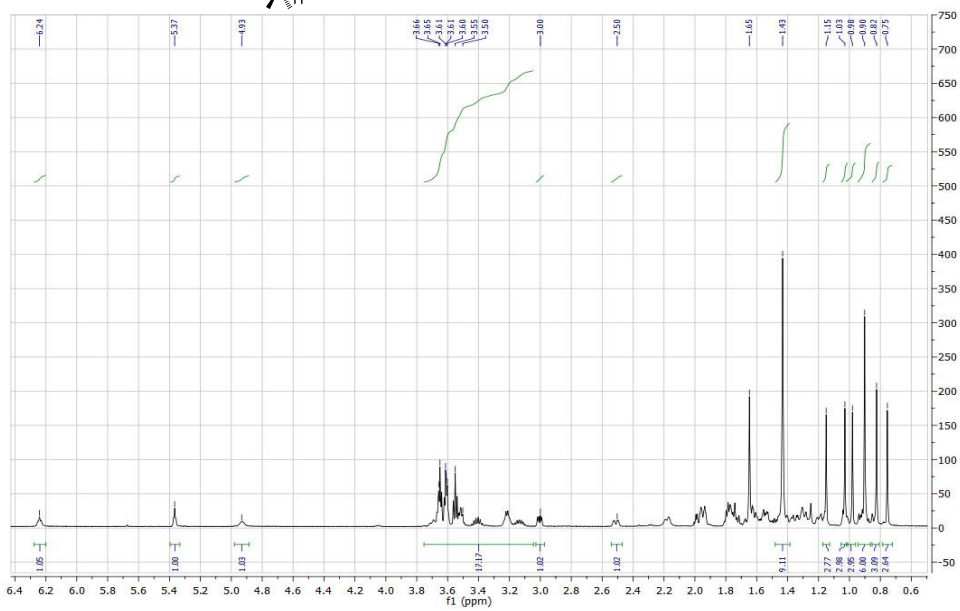

Espectro de ^{13}C RMN del compuesto 6

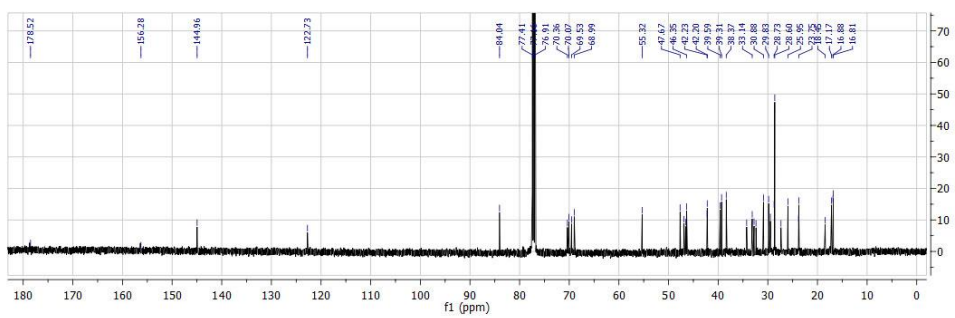

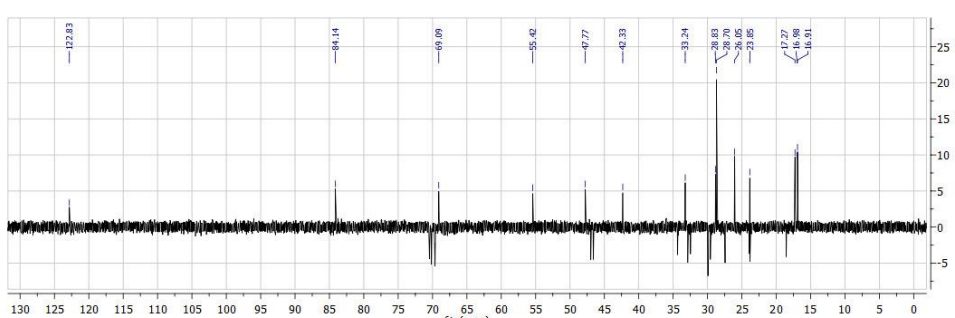

Espectro de ^{1}H RMN del compuesto 7

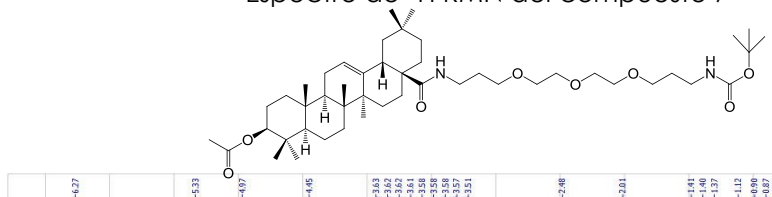

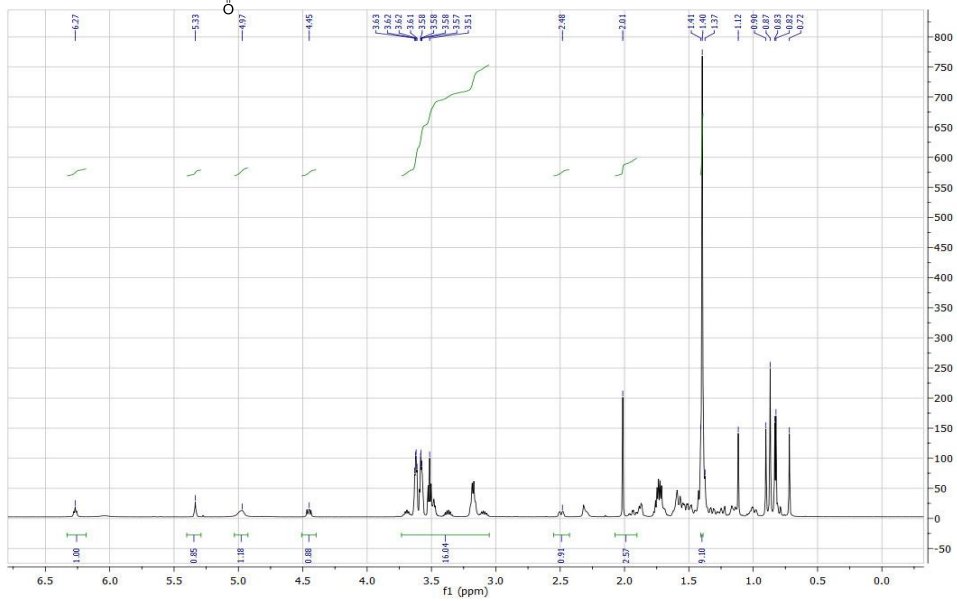

Espectro de ^{13}C RMN del compuesto 7

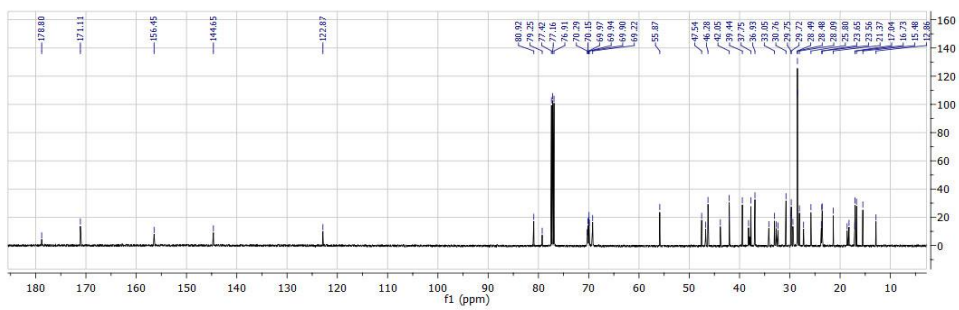

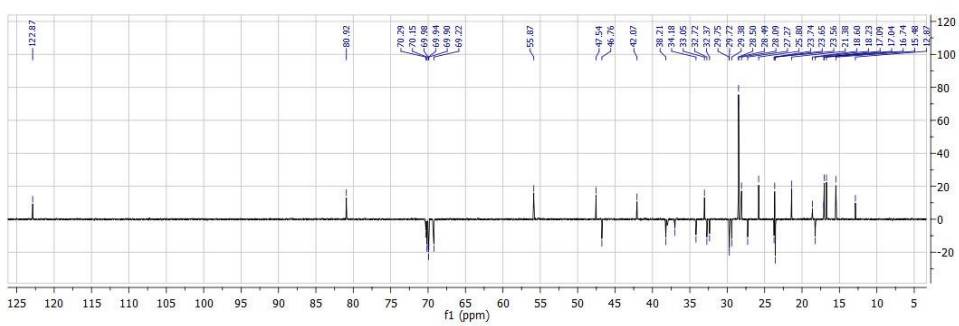

Espectro de ^{1}H RMN del compuesto 8

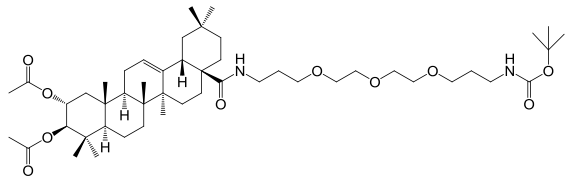

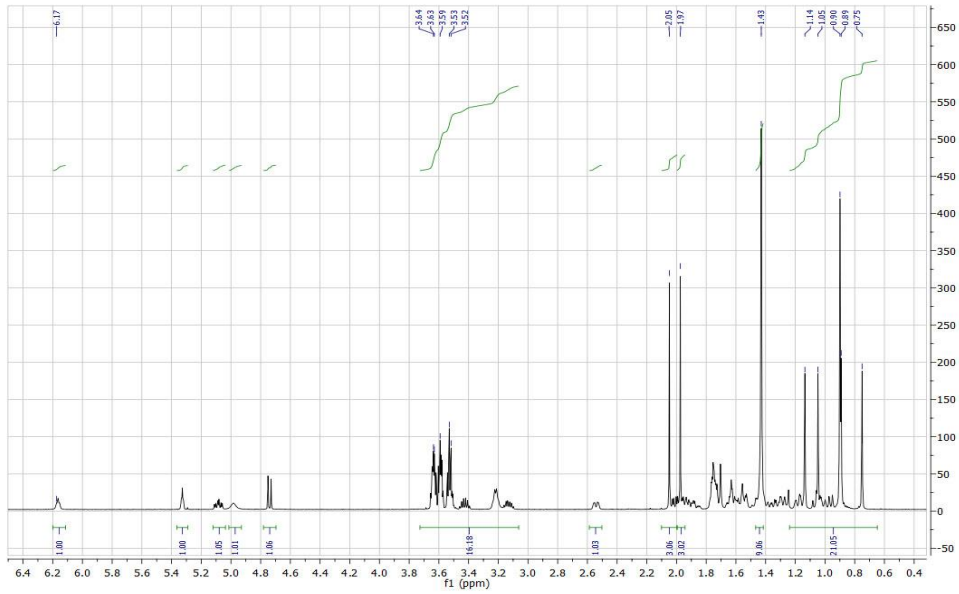

Espectro de ^{13}C RMN del compuesto 8

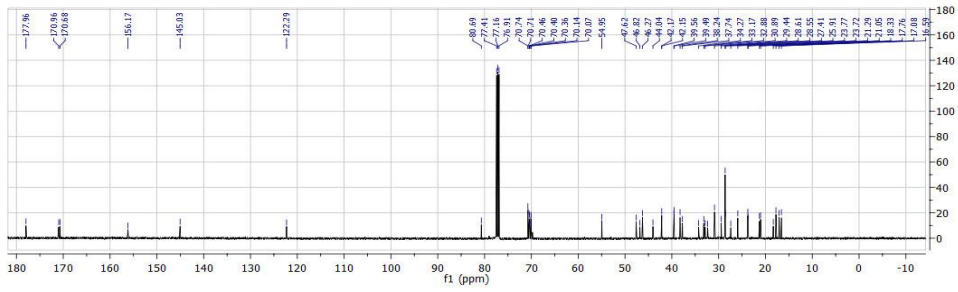

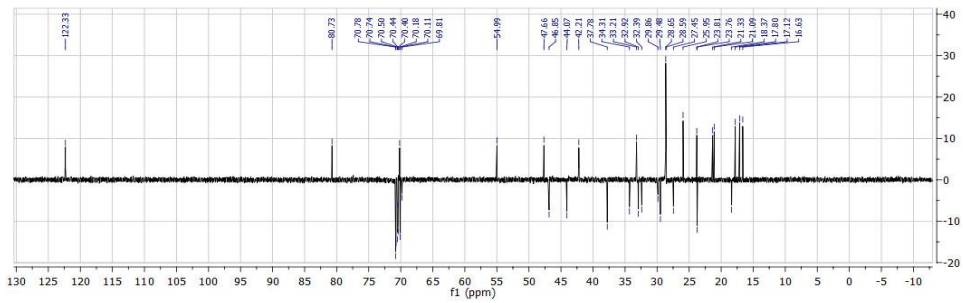

Espectro de ^{1}H RMN del compuesto 9

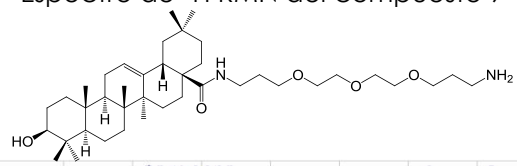

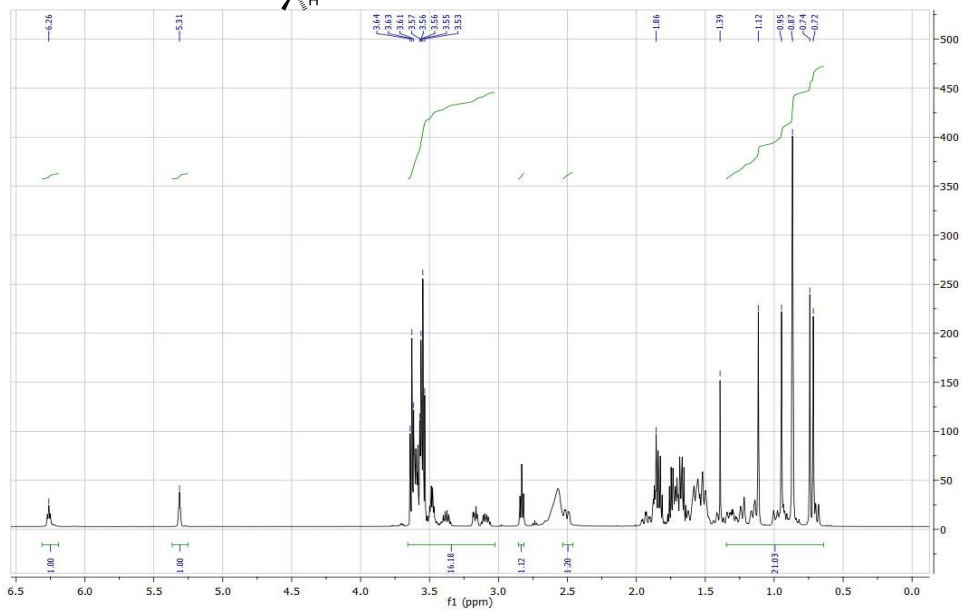

Espectro de ^{13}C RMN del compuesto 9

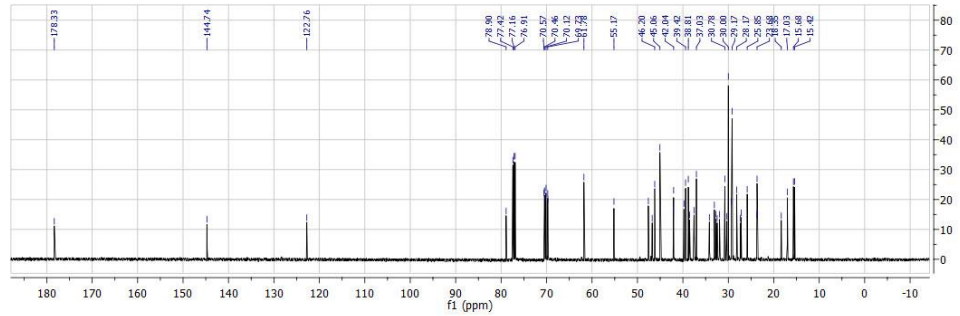

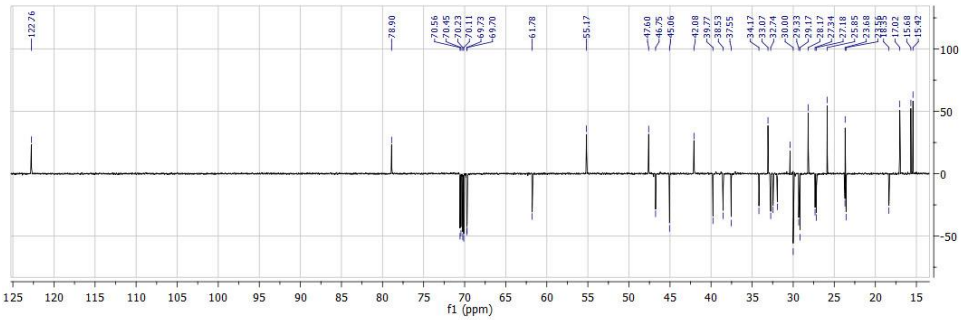

Espectro de ^{1}H RMN del compuesto 10

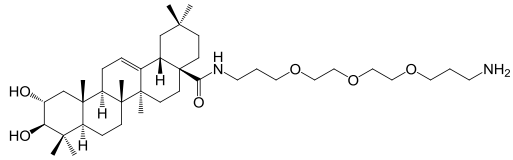

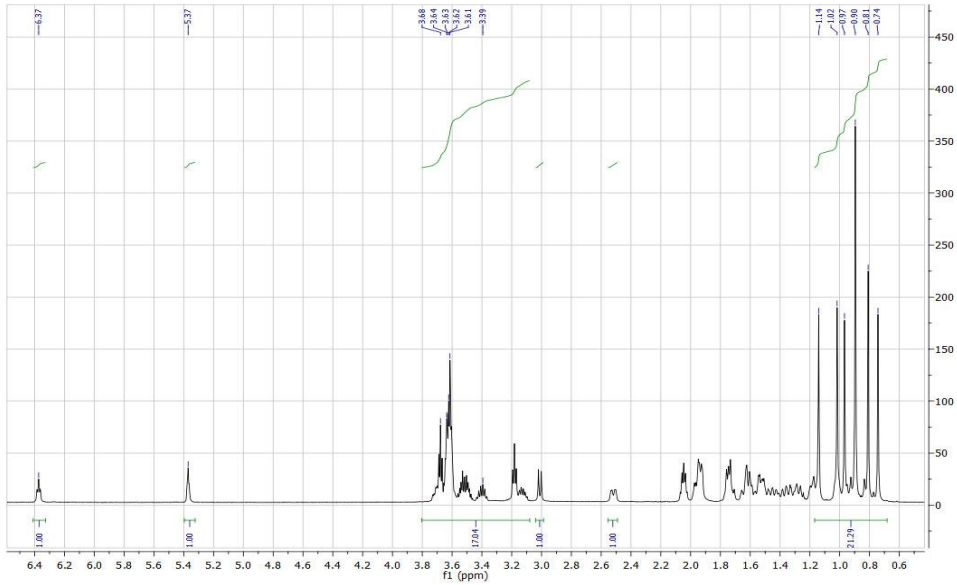

Espectro de ^{13}C RMN del compuesto 10

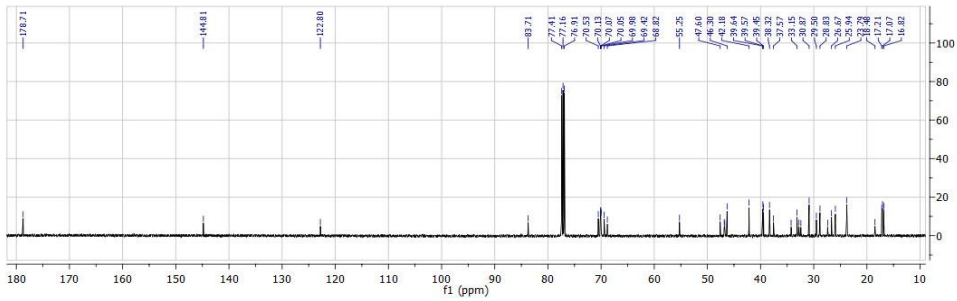

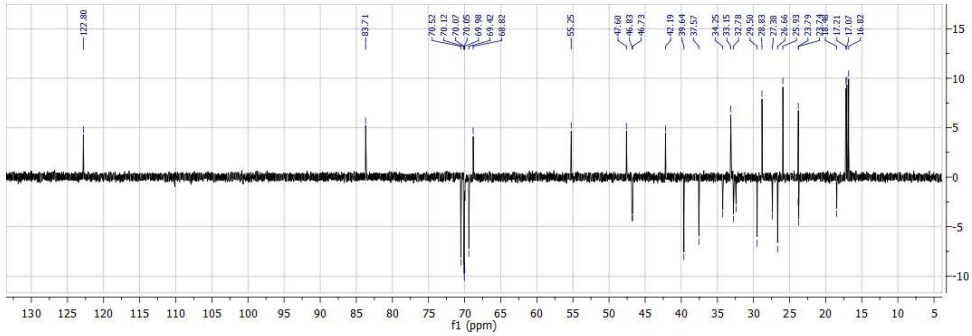

Espectro de ^{1}H RMN del compuesto 11

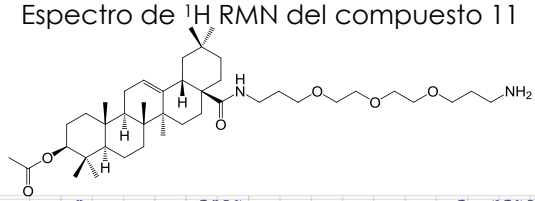

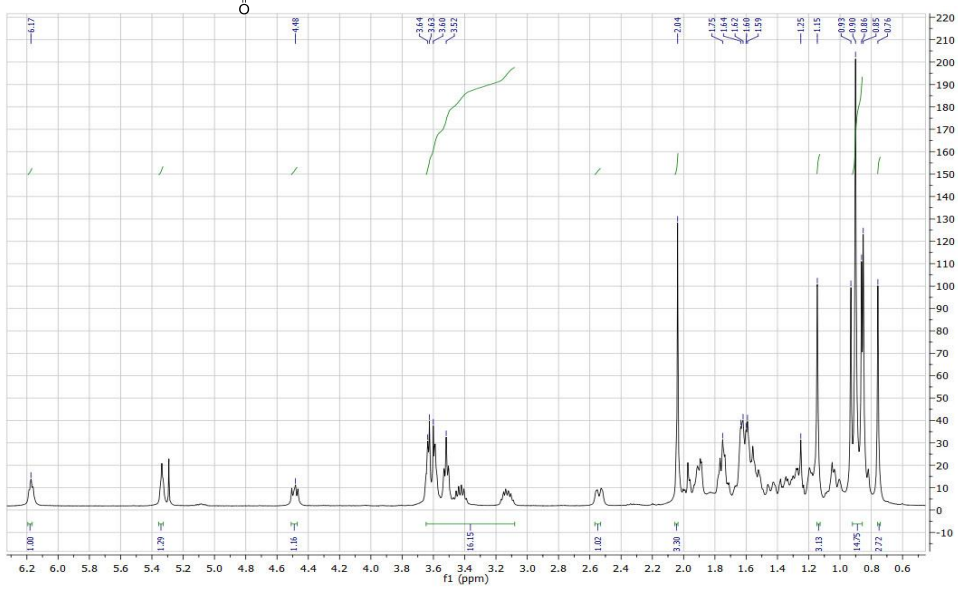

Espectro de ^{13}C RMN del compuesto 11

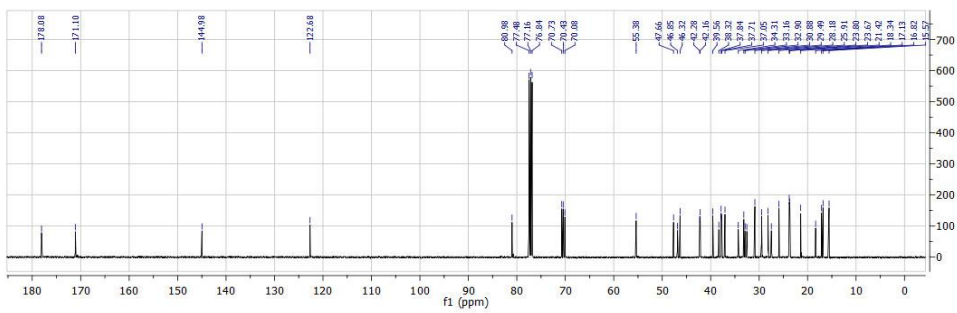

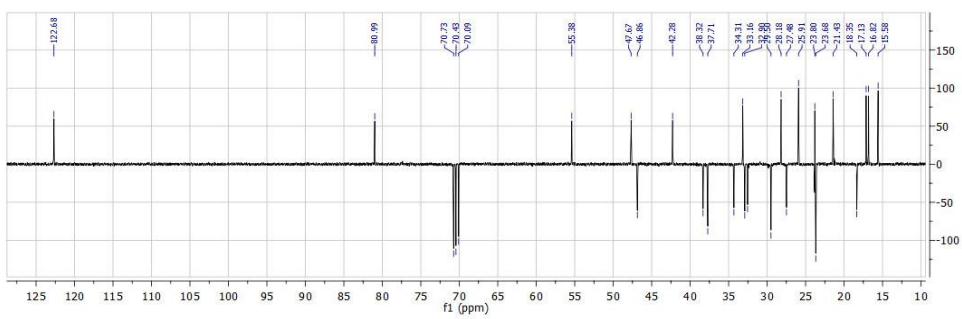

Espectro de ^{1}H RMN del compuesto 12

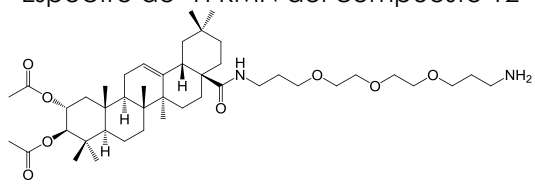

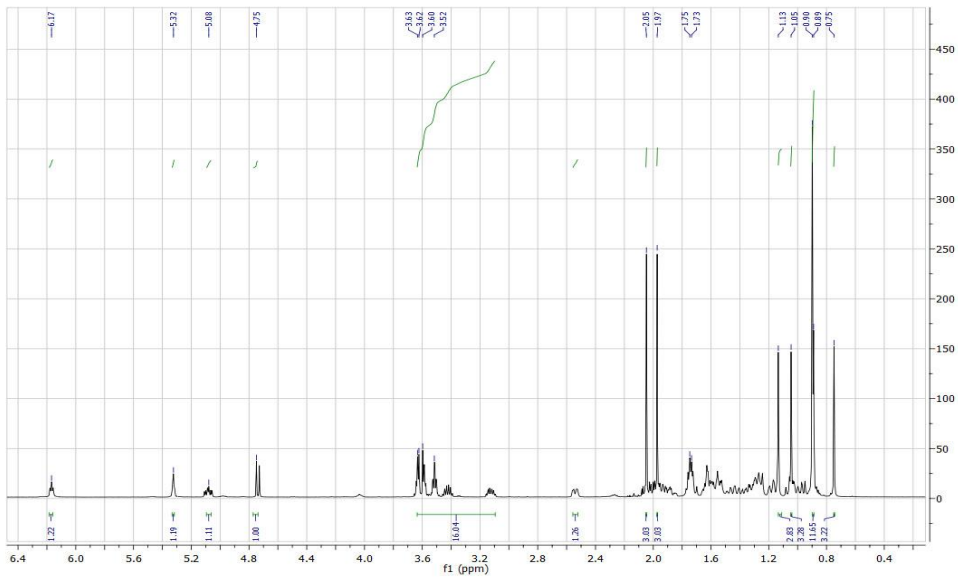

Espectro de ^{13}C RMN del compuesto 12

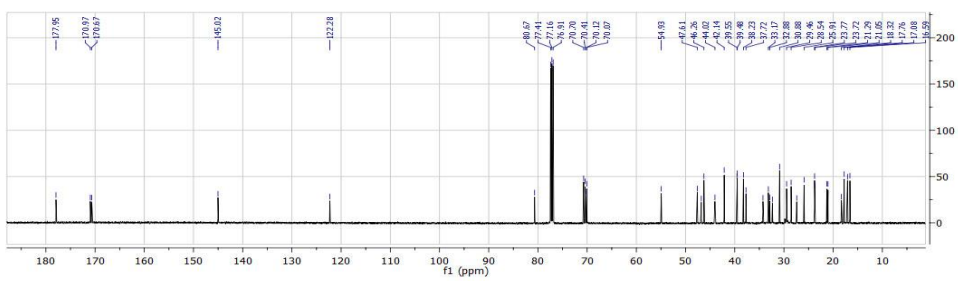

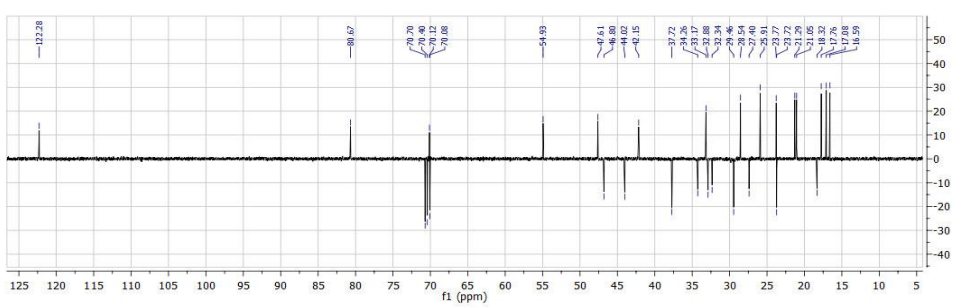

Espectro de ^{1}H RMN del compuesto 13

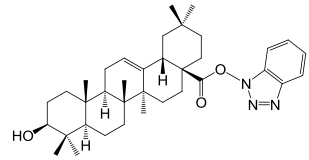

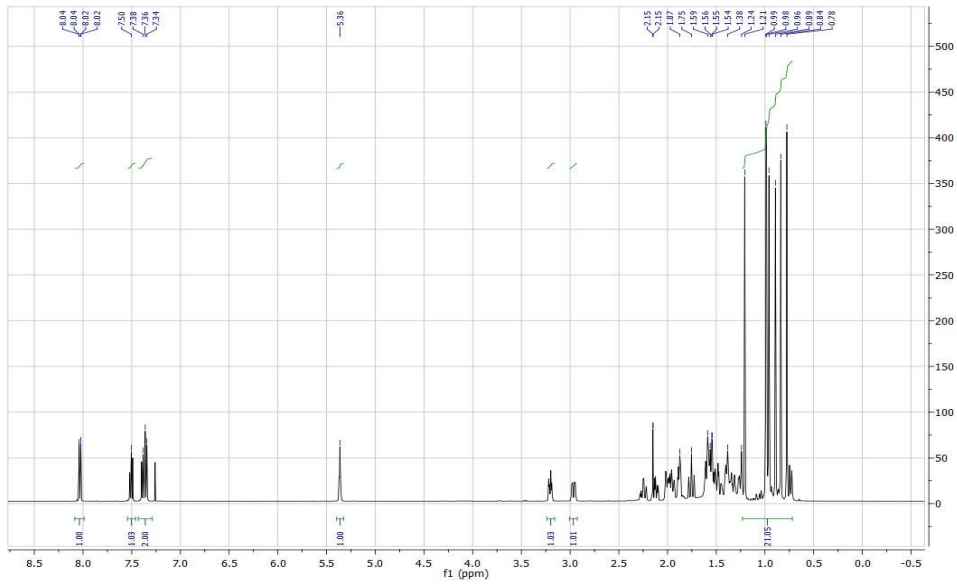

Espectro de ^{13}C RMN del compuesto 13

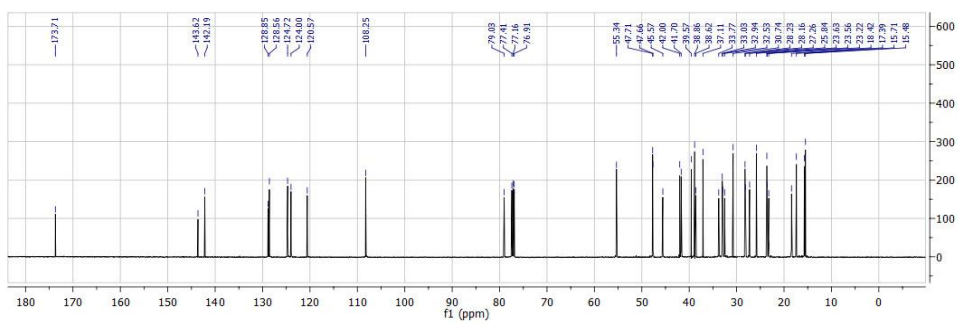

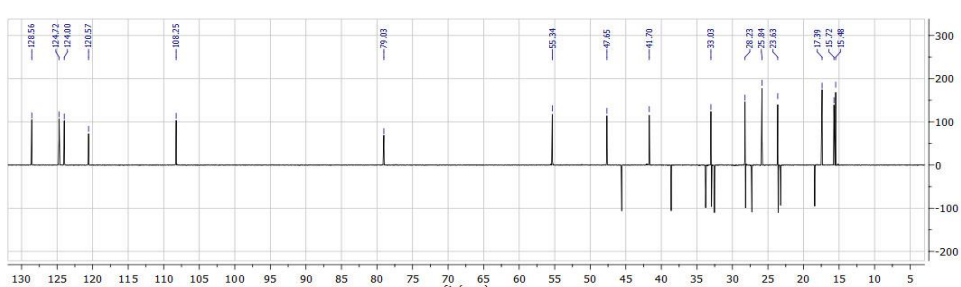

Espectro de ^{1}H RMN del compuesto 14

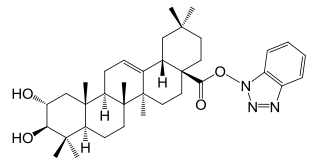

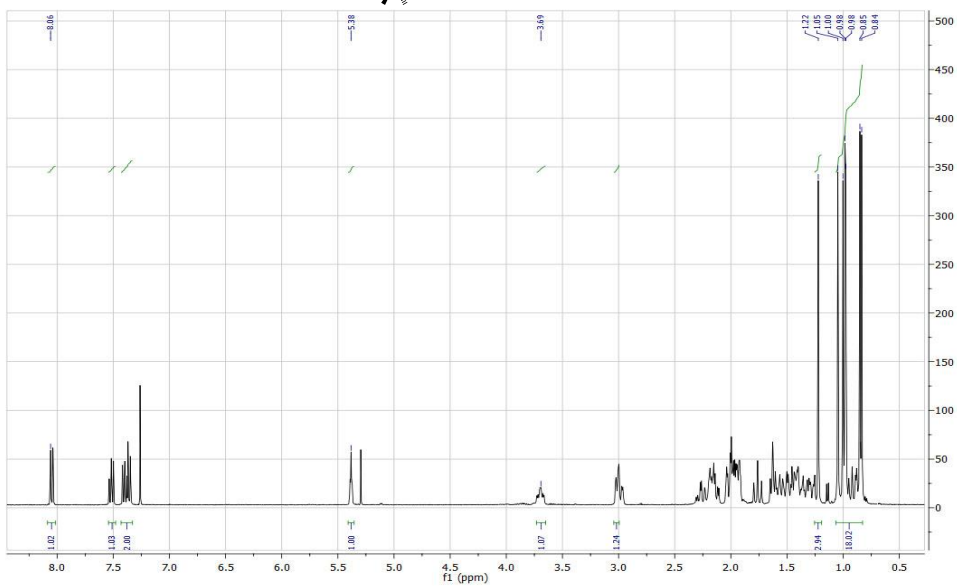

Espectro de ^{13}C RMN del compuesto 14

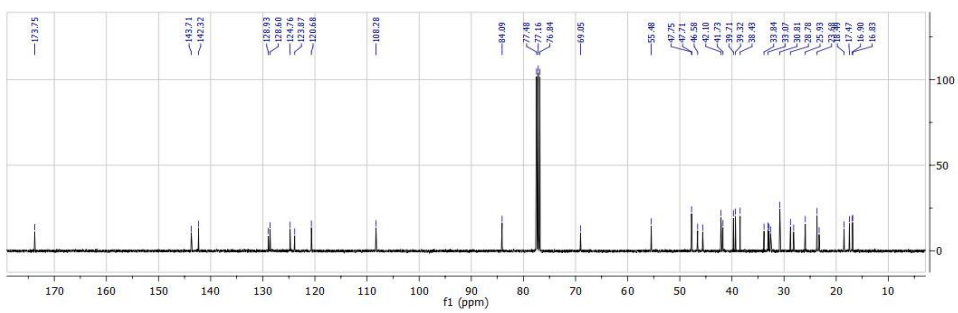

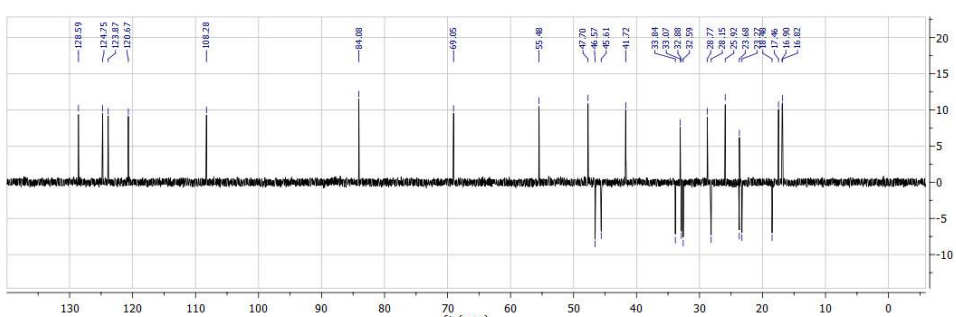

Espectro de ^{1}H RMN del compuesto 15

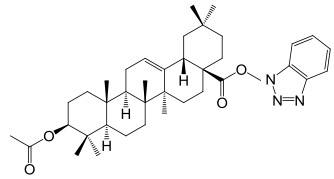

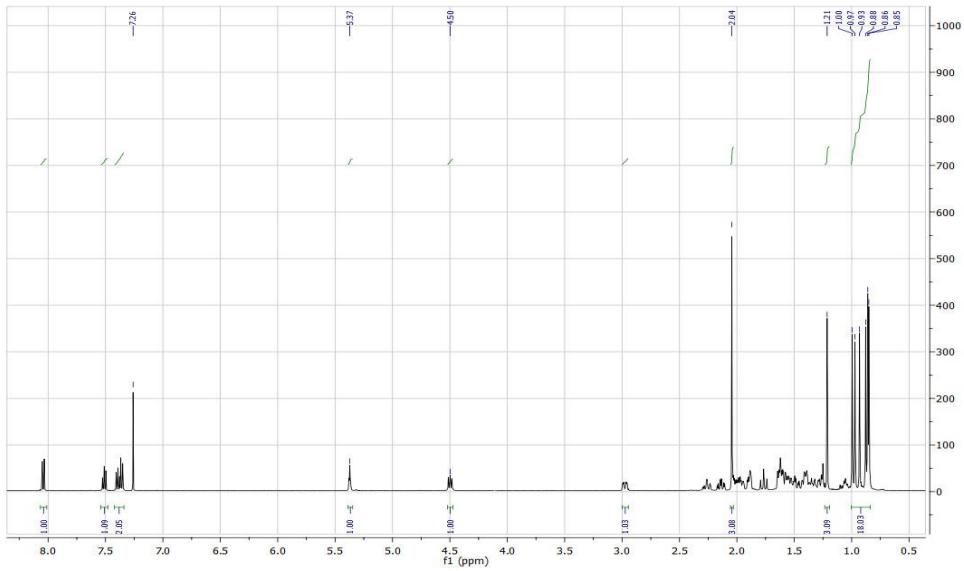

Espectro de ^{13}C RMN del compuesto 15

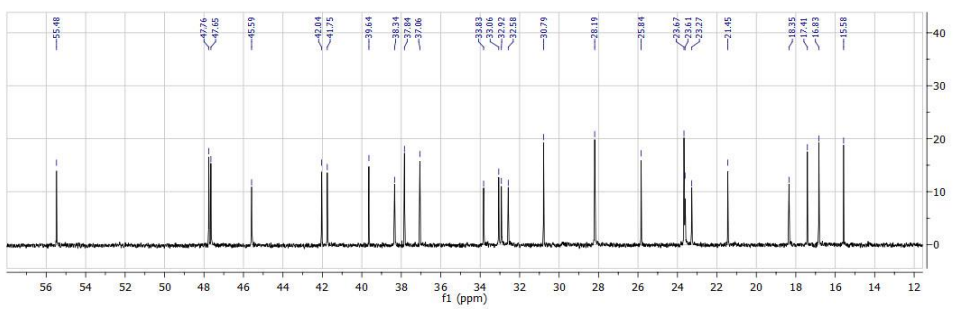

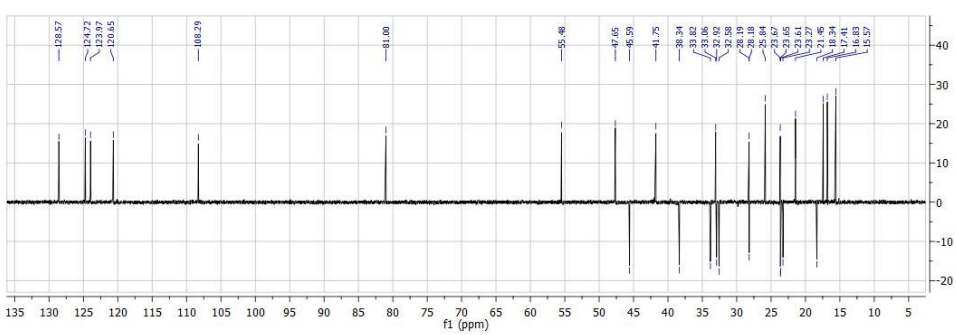

Espectro de ^{1}H RMN del compuesto 16

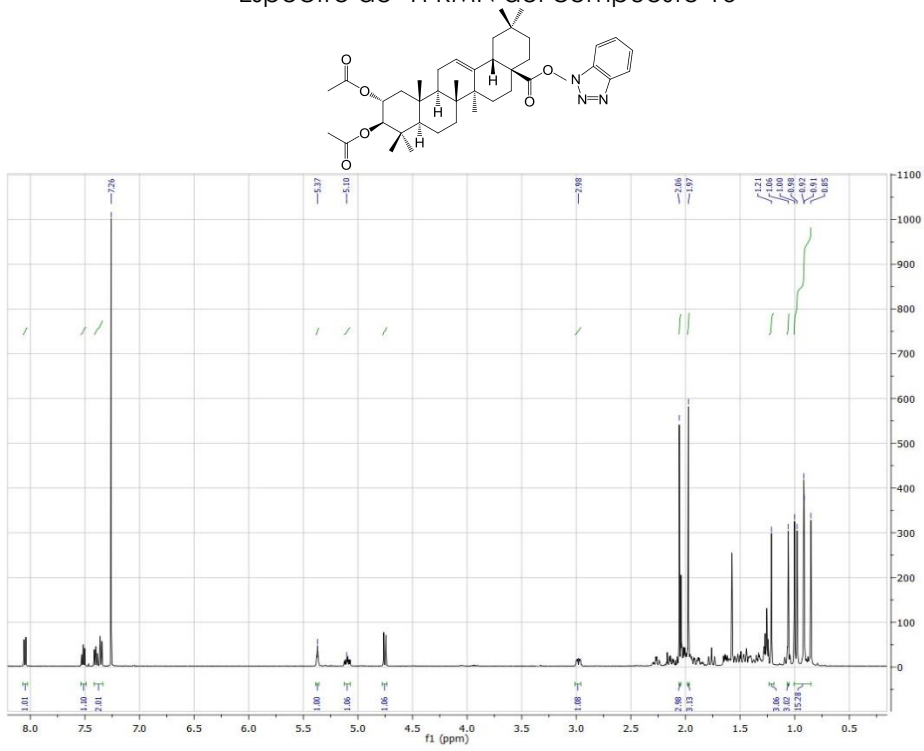

Espectro de ^{13}C RMN del compuesto 16

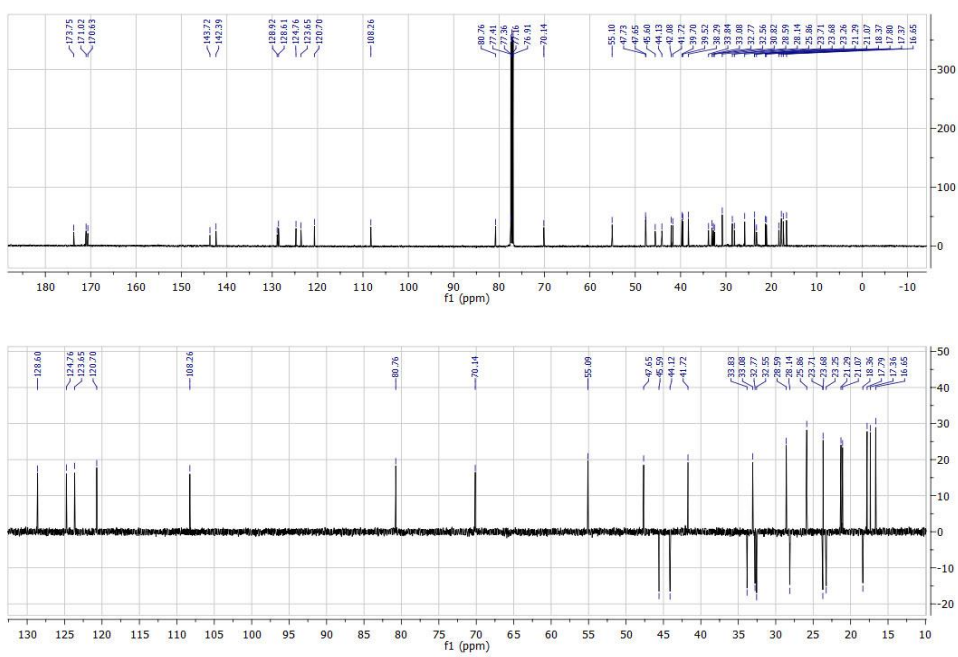

Espectro de ^{1}H RMN del compuesto 17

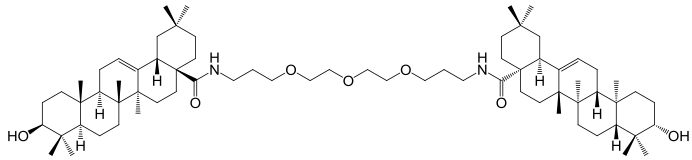

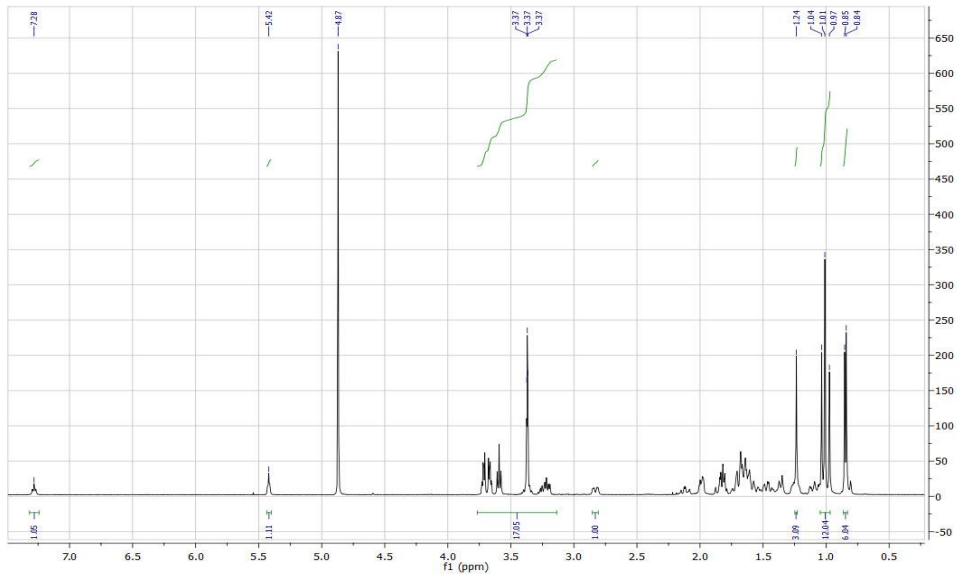

Espectro de ^{13}C RMN del compuesto 17

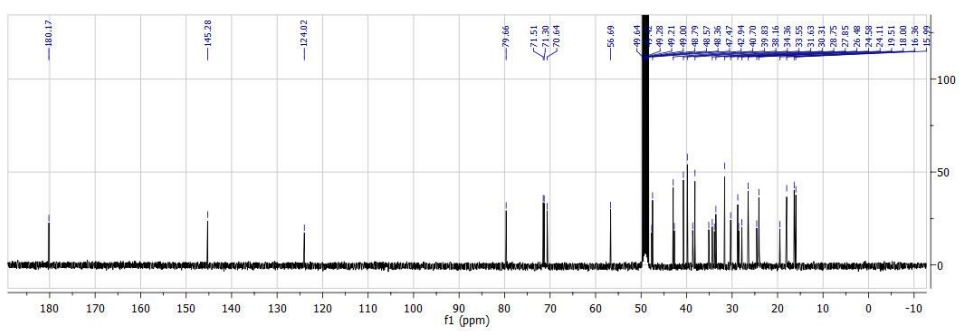

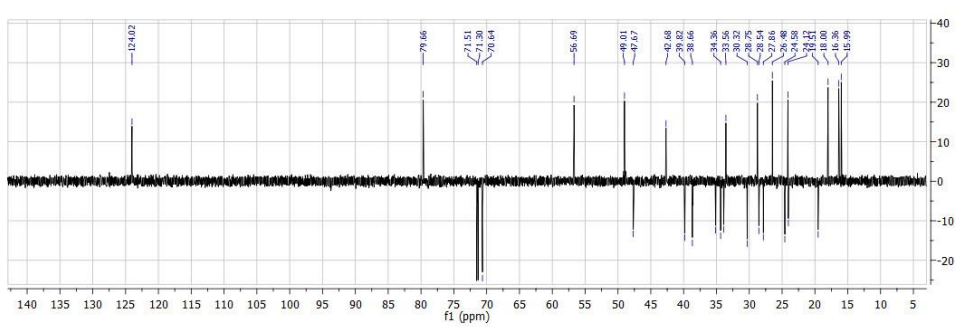

Espectro de ^{1}H RMN del compuesto 18

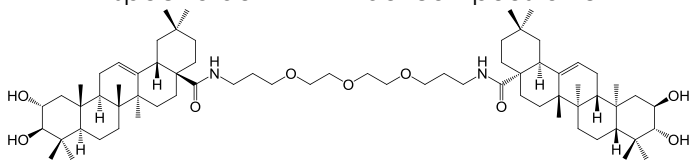

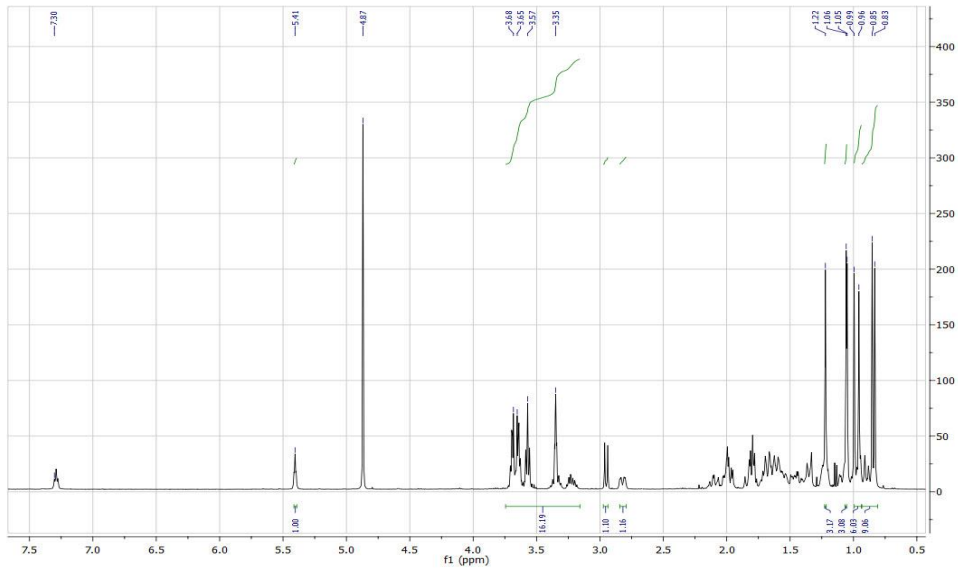

Espectro de ^{13}C RMN del compuesto 18

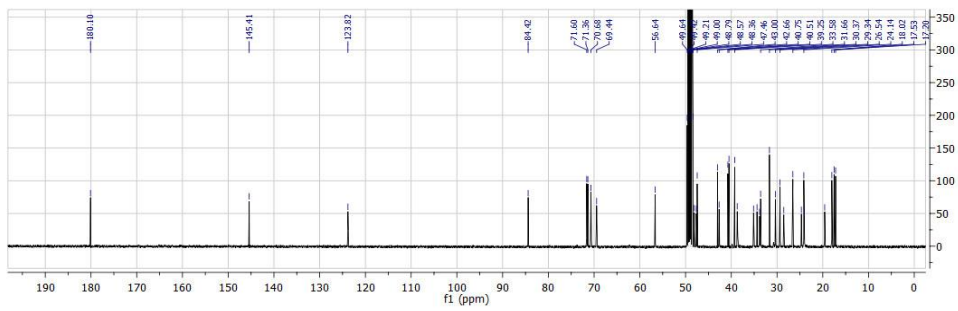

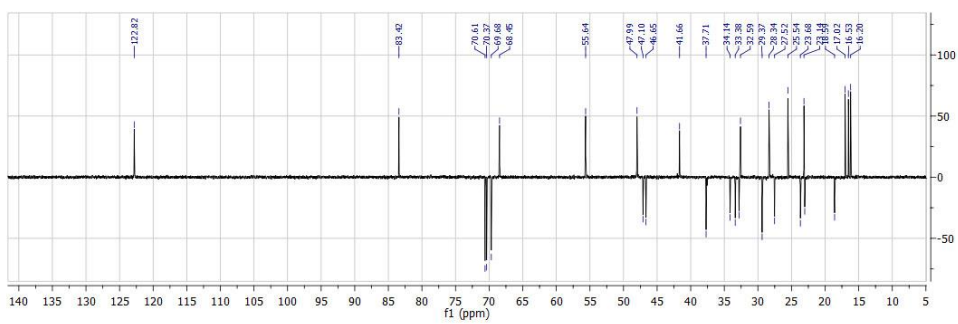

Espectro de ^{1}H RMN del compuesto 19

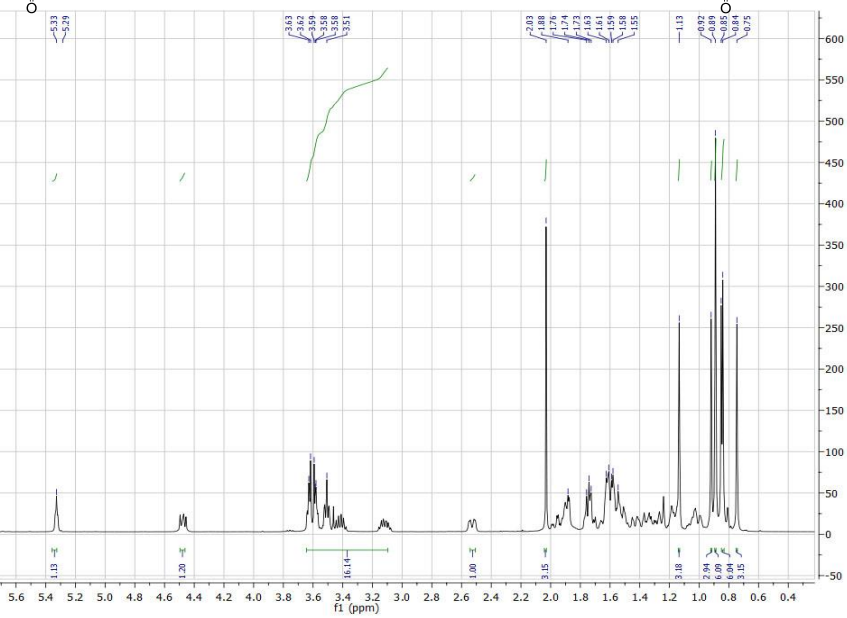

Espectro de ^{13}C RMN del compuesto 19

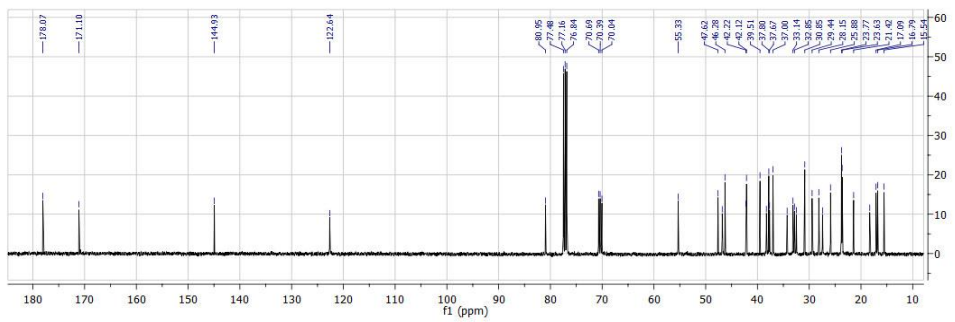

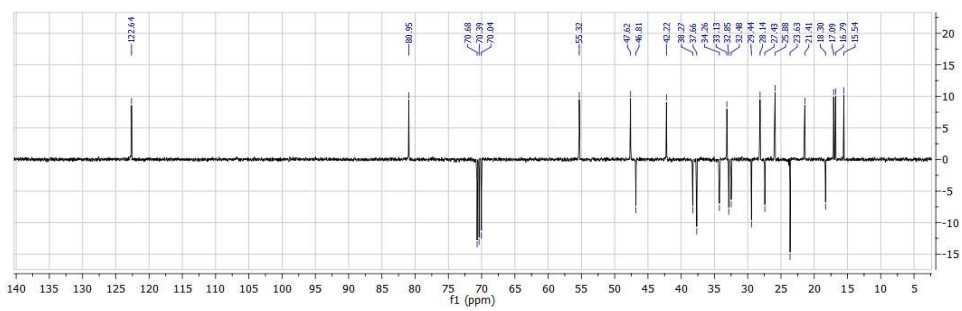

Espectro de ^{1}H RMN del compuesto 20

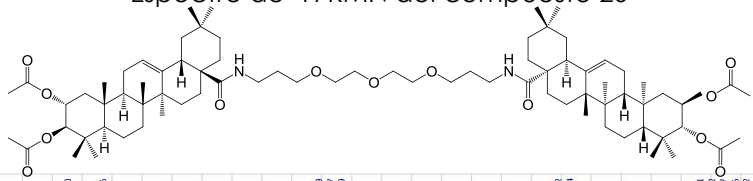

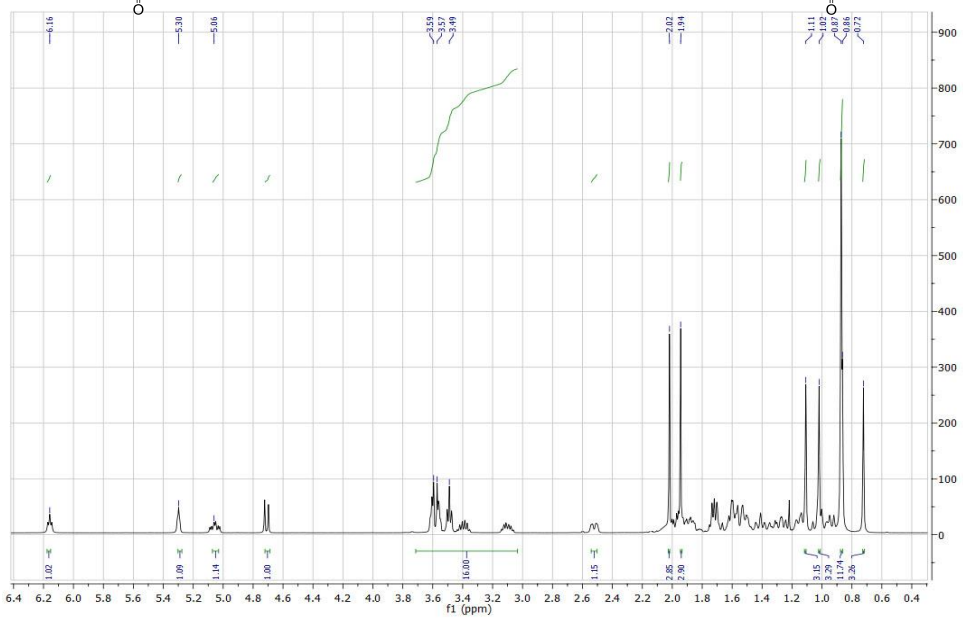

Espectro de ^{13}C RMN del compuesto 20

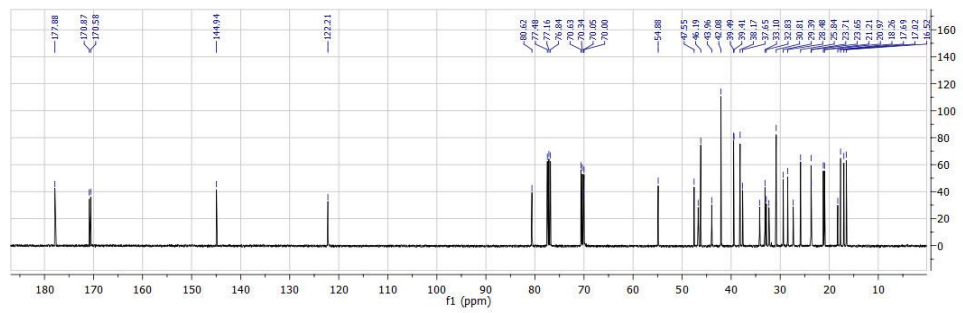

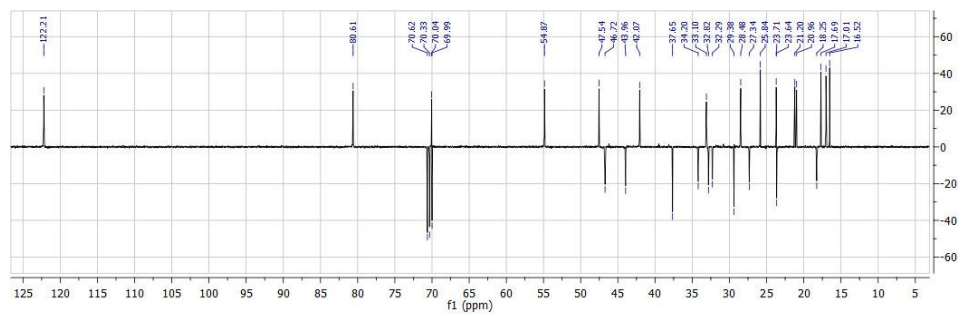

2. ESPECTROS RMN PUBLICACIÓN 2

Espectro de ^{1}H RMN del compuesto 3

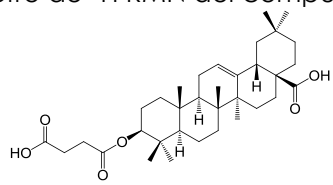

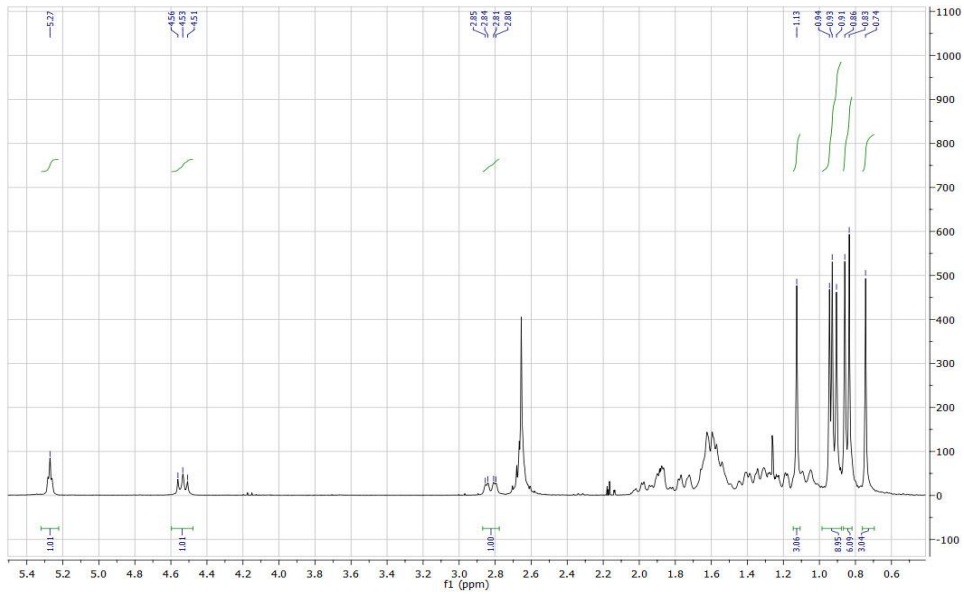

Espectro de ^{13}C RMN del compuesto 3

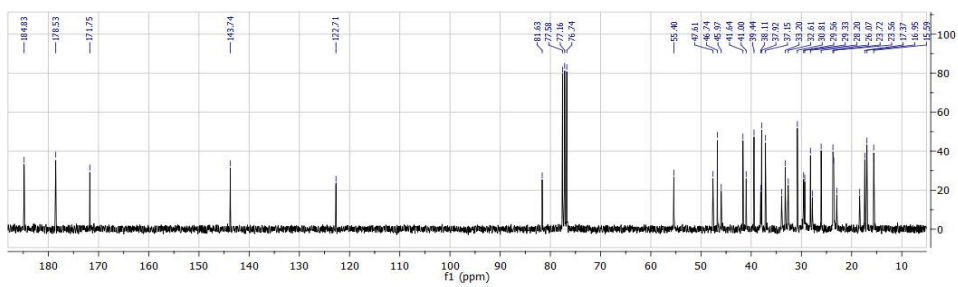

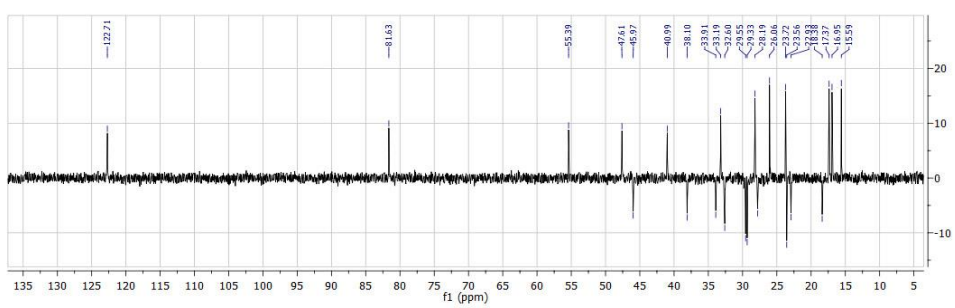

Espectro de ^{1}H RMN del compuesto 4

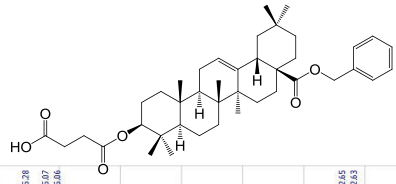

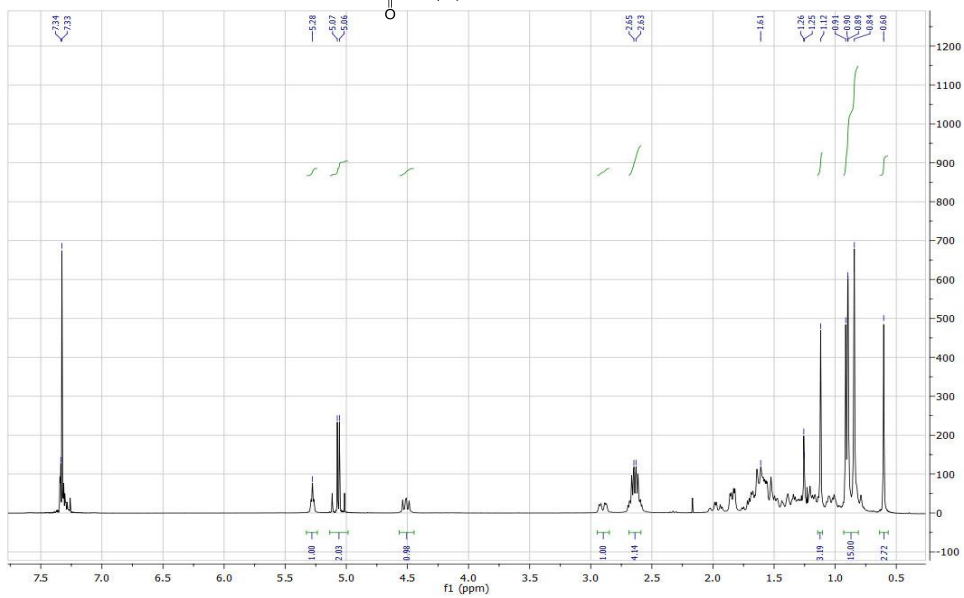

Espectro de ^{13}C RMN del compuesto 4

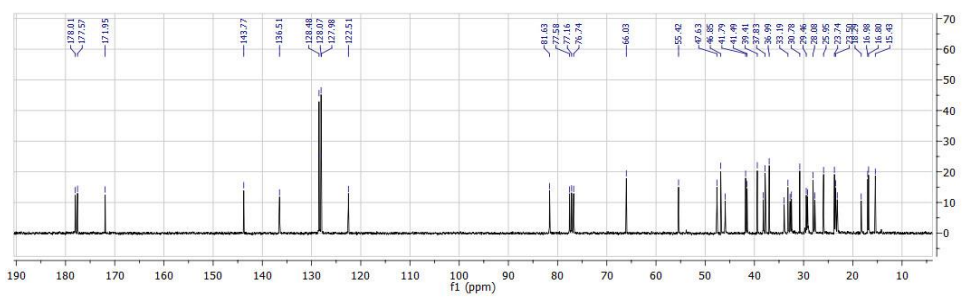

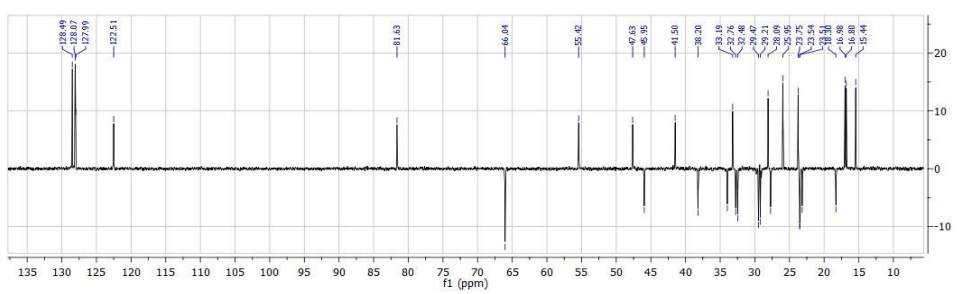

3. ESPECTROS RMN PUBLICACIÓN 3

Espectro de ^{1}H RMN del compuesto 1

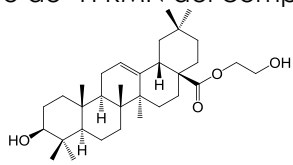

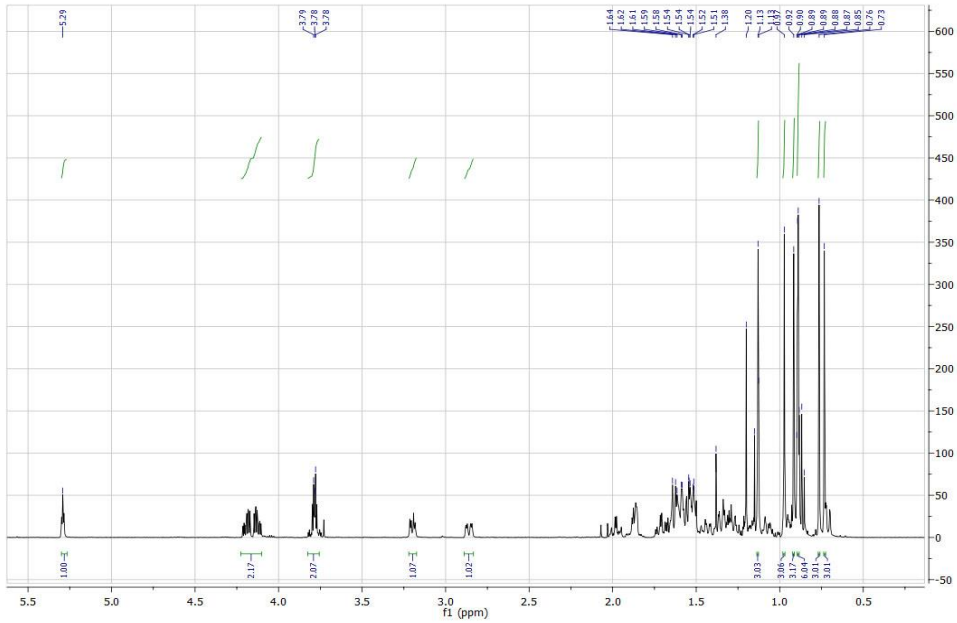

Espectro de ^{13}C RMN del compuesto 1

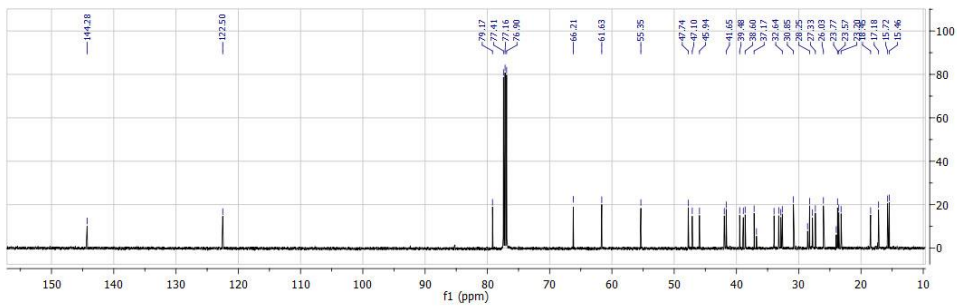

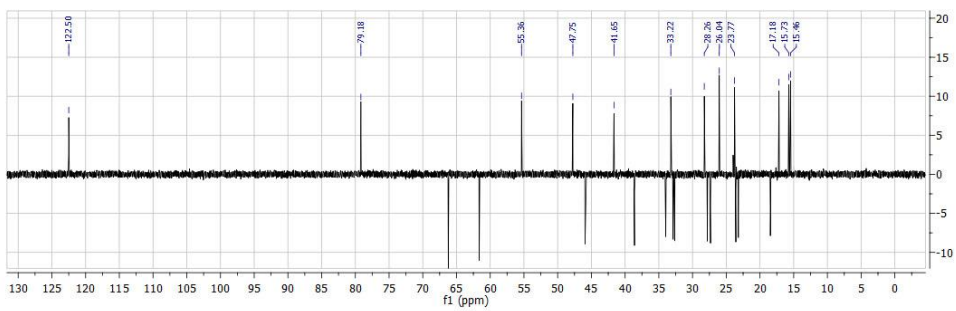

Espectro de ^{1}H RMN del compuesto 2

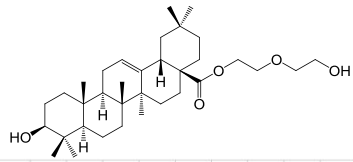

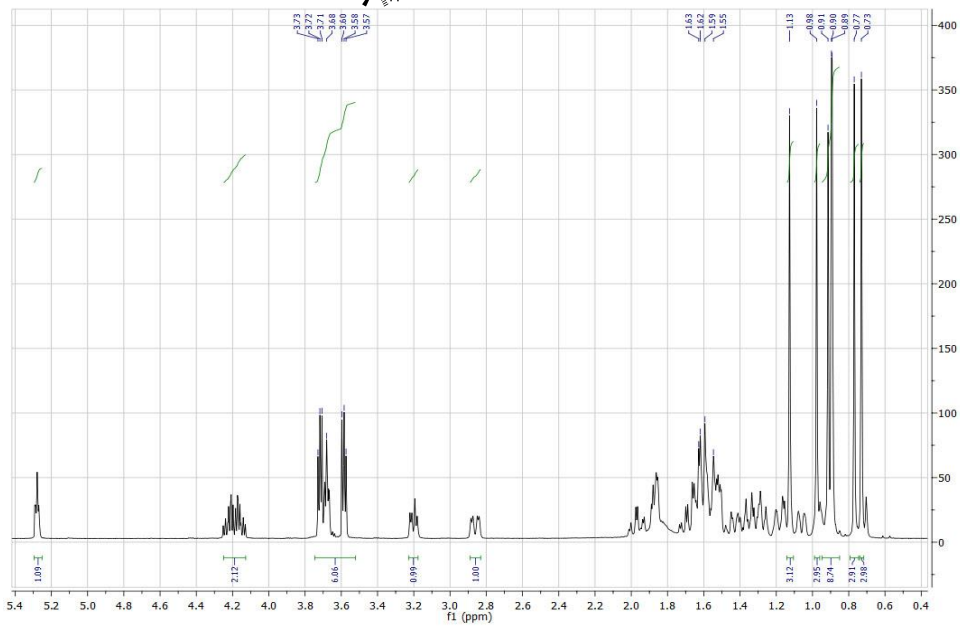

Espectro de ^{13}C RMN del compuesto 2

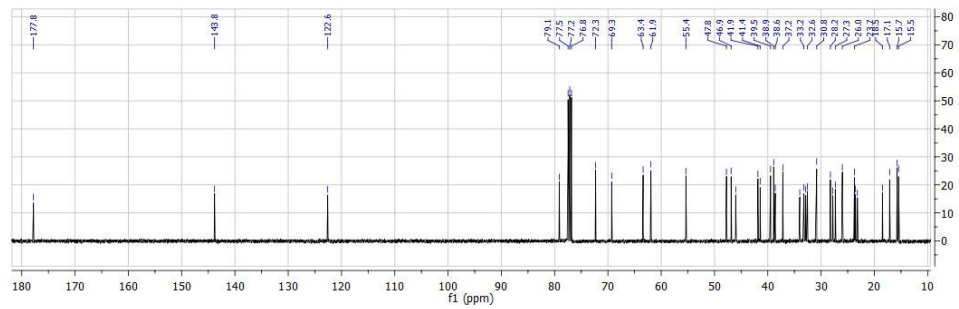

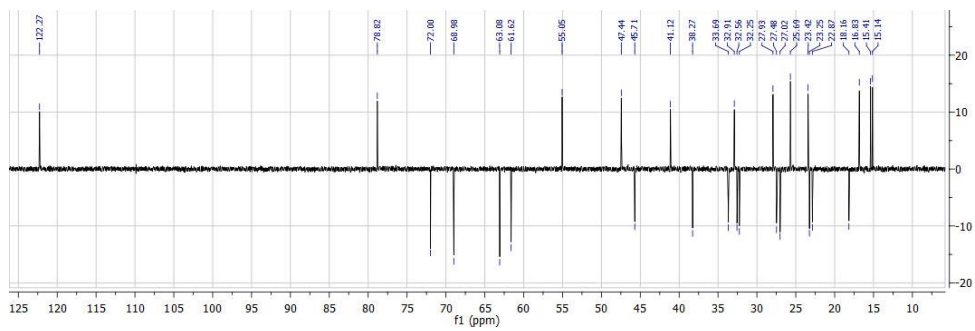

Espectro de ^{1}H RMN del compuesto 3

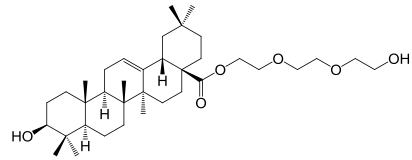

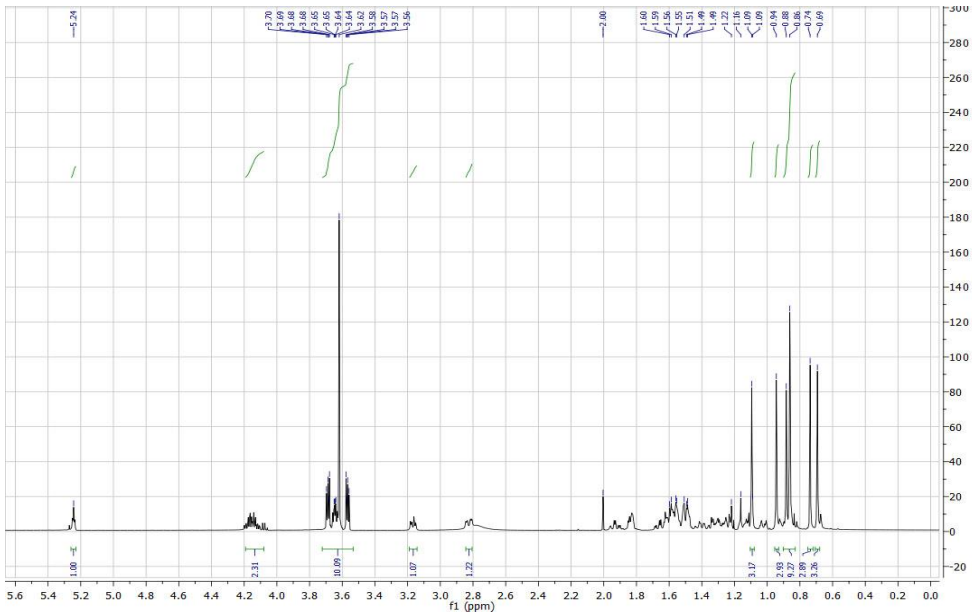

Espectro de ^{13}C RMN del compuesto 3

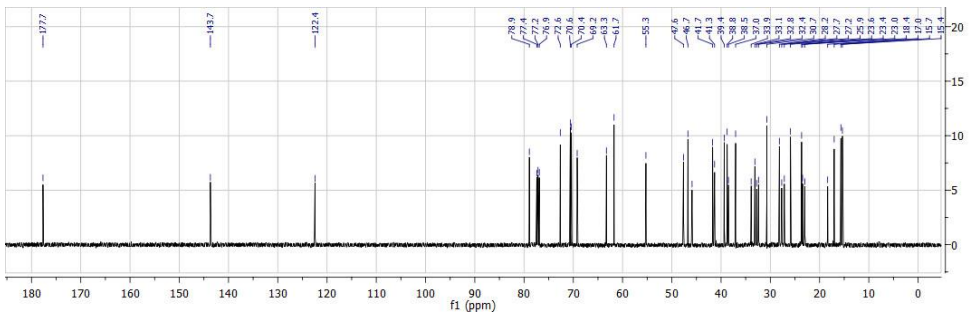

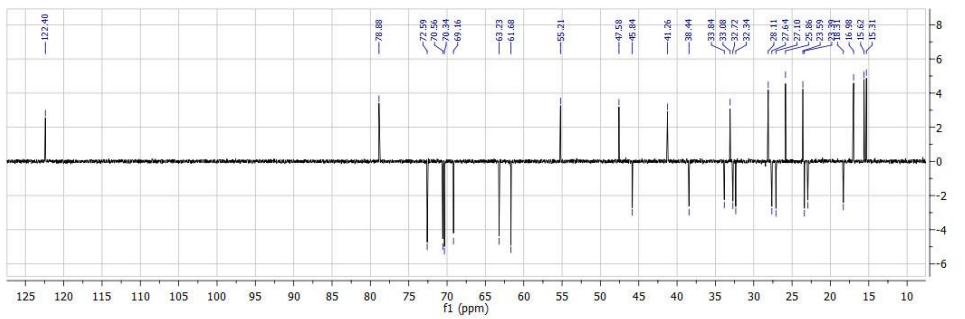

Espectro de ^{1}H RMN del compuesto 4

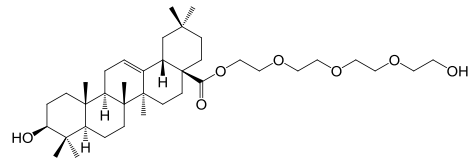

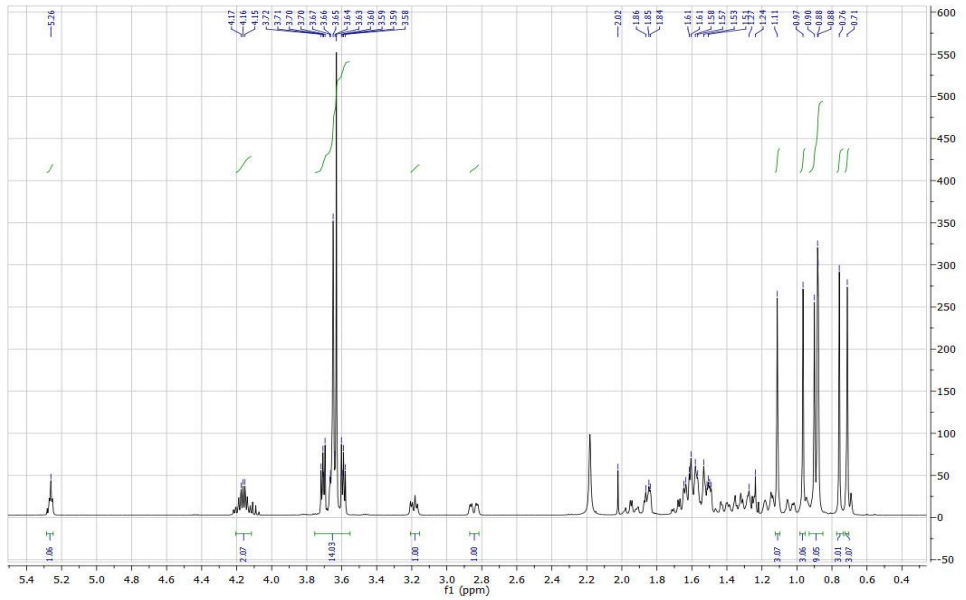

Espectro de ^{13}C RMN del compuesto 4

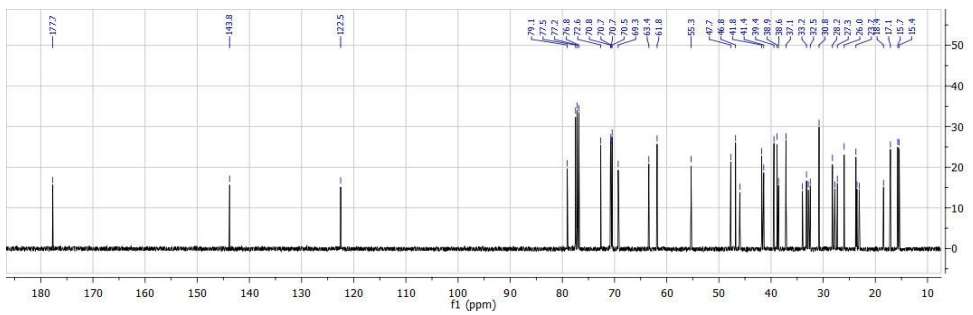

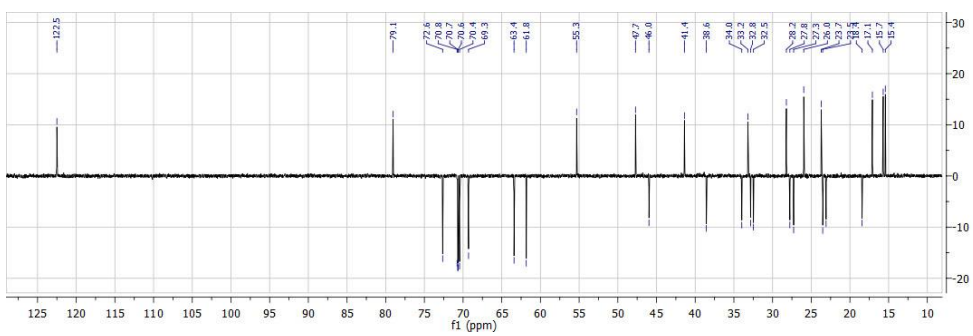

Espectro de ^{1}H RMN del compuesto 5

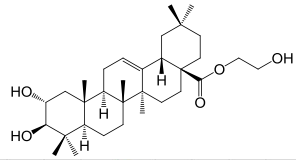

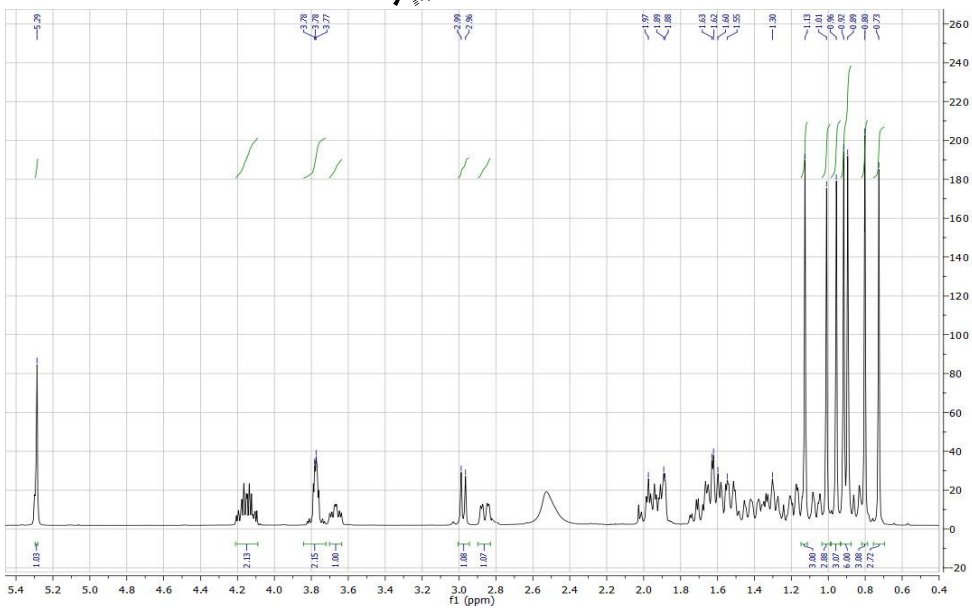

Espectro de ^{13}C RMN del compuesto 5

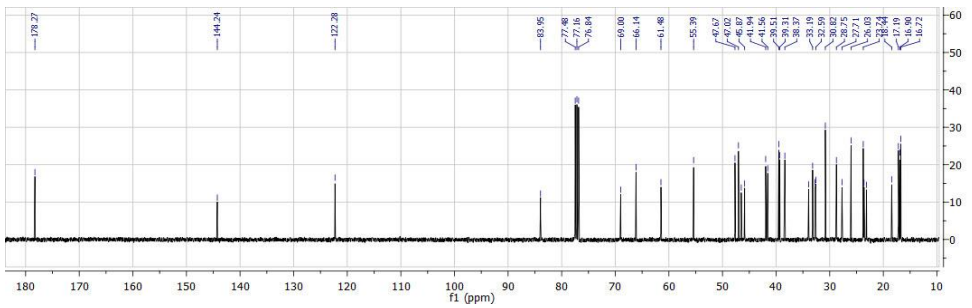

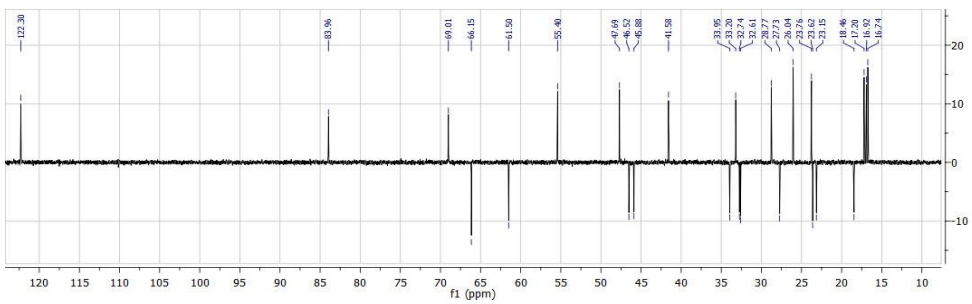

Espectro de ^{1}H RMN del compuesto 6

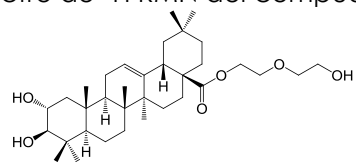

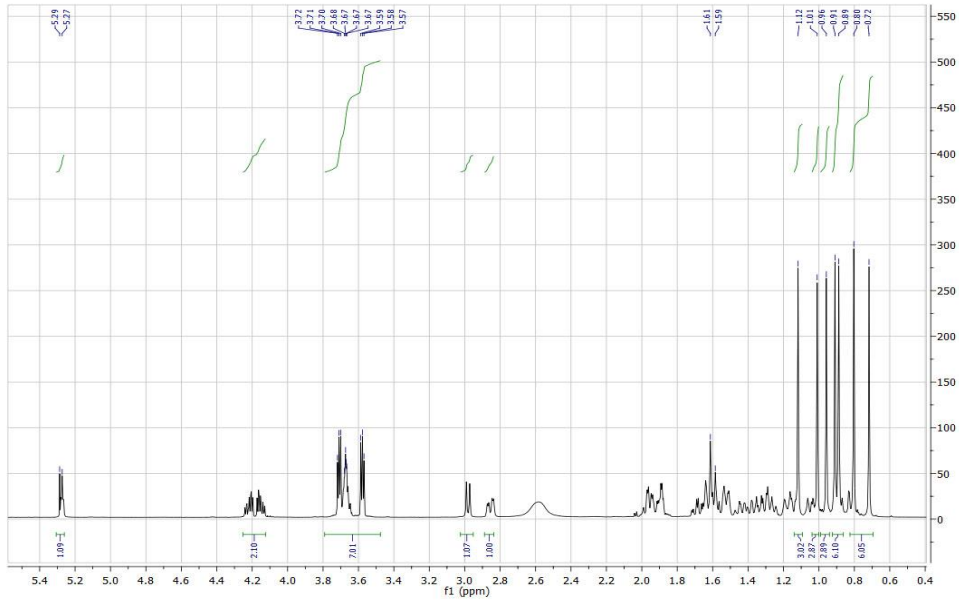

Espectro de ^{13}C RMN del compuesto 6

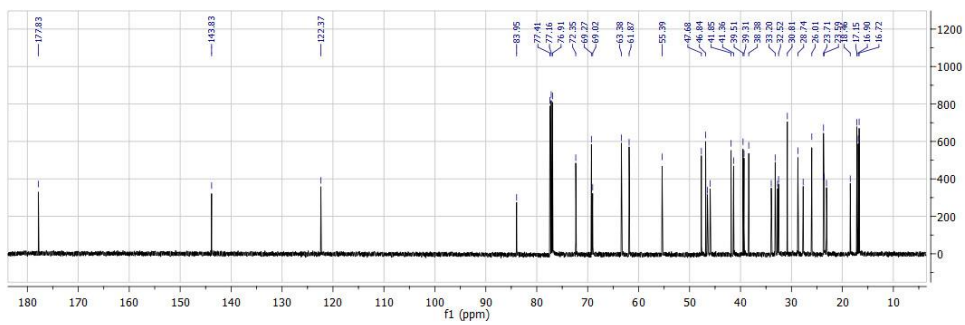

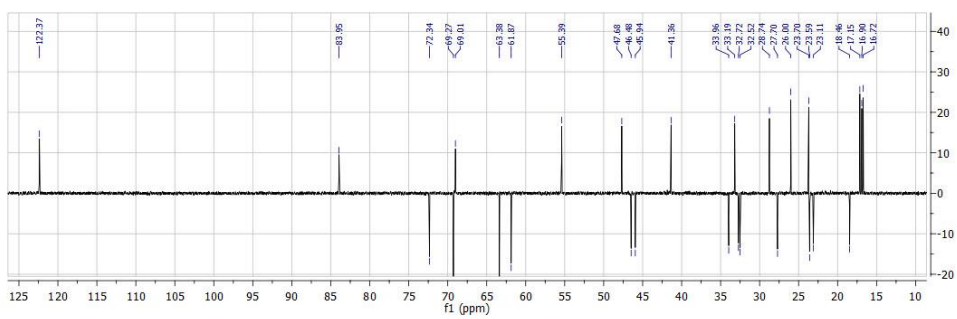

Espectro de ^{1}H RMN del compuesto 7

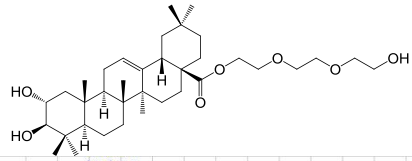

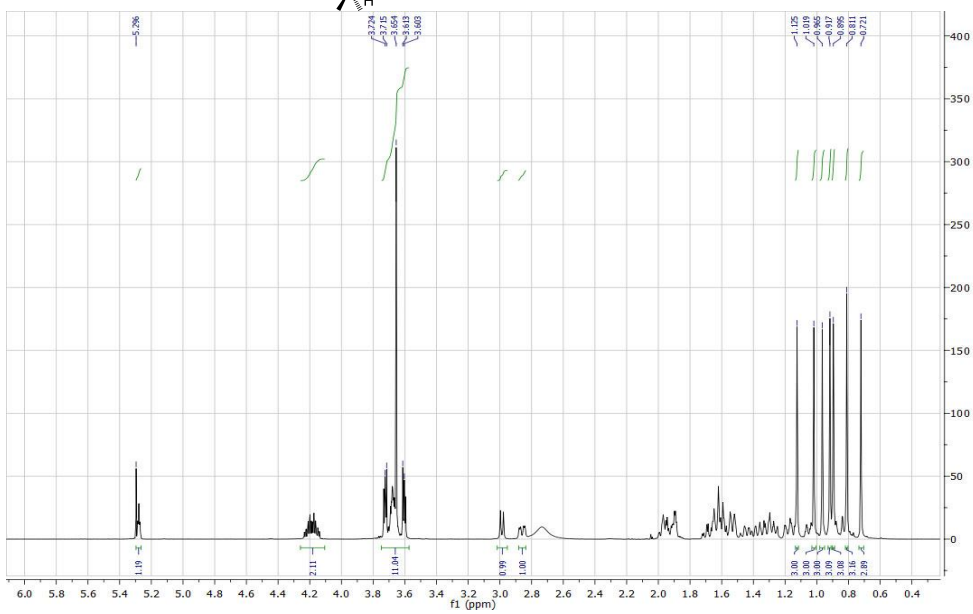

Espectro de ^{13}C RMN del compuesto 7

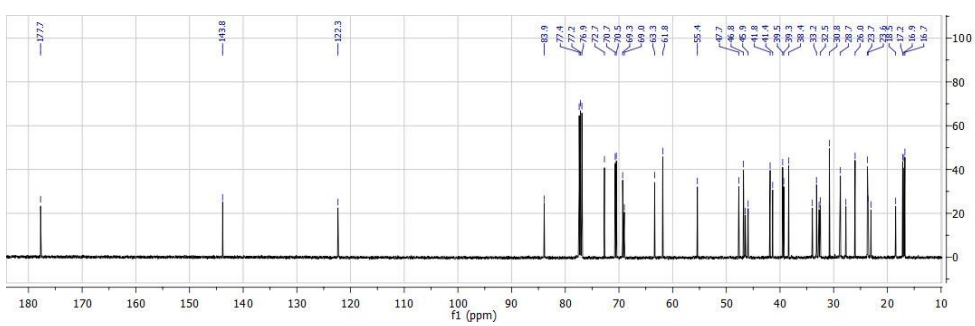

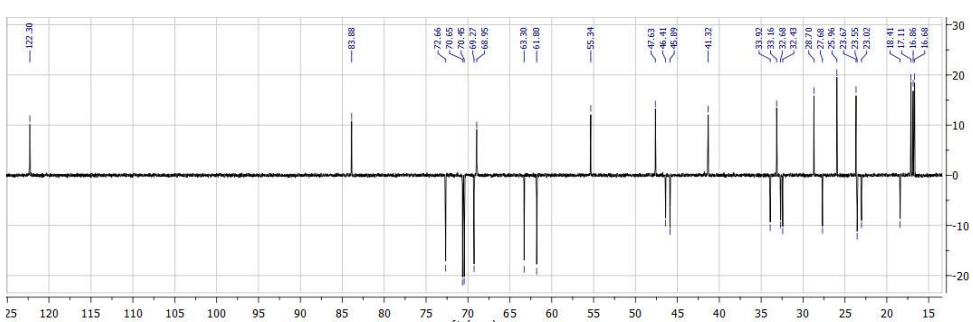

Espectro de ^{1}H RMN del compuesto 8

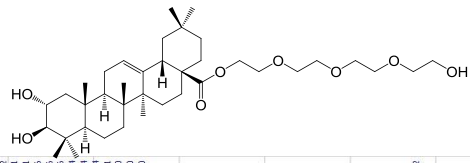

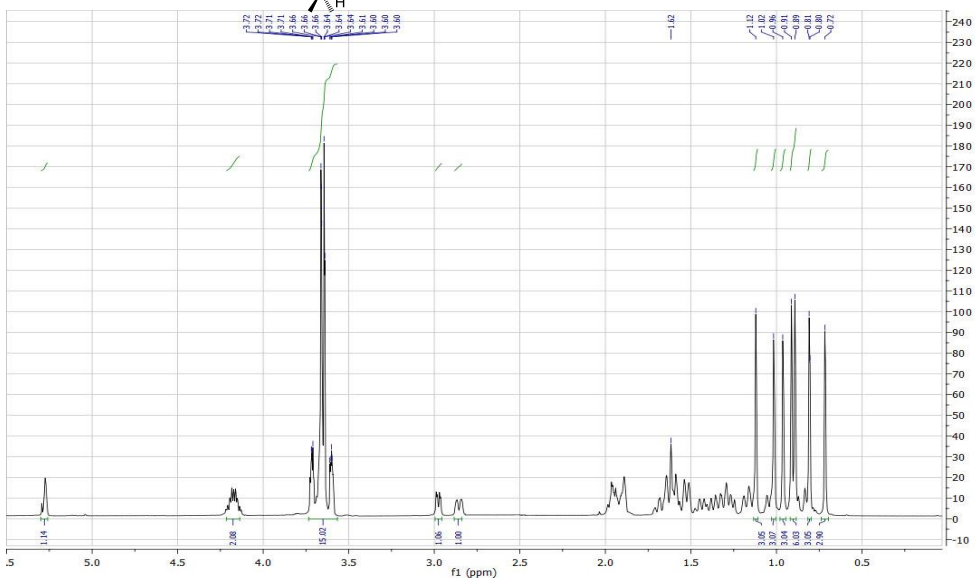

Espectro de ^{13}C RMN del compuesto 8

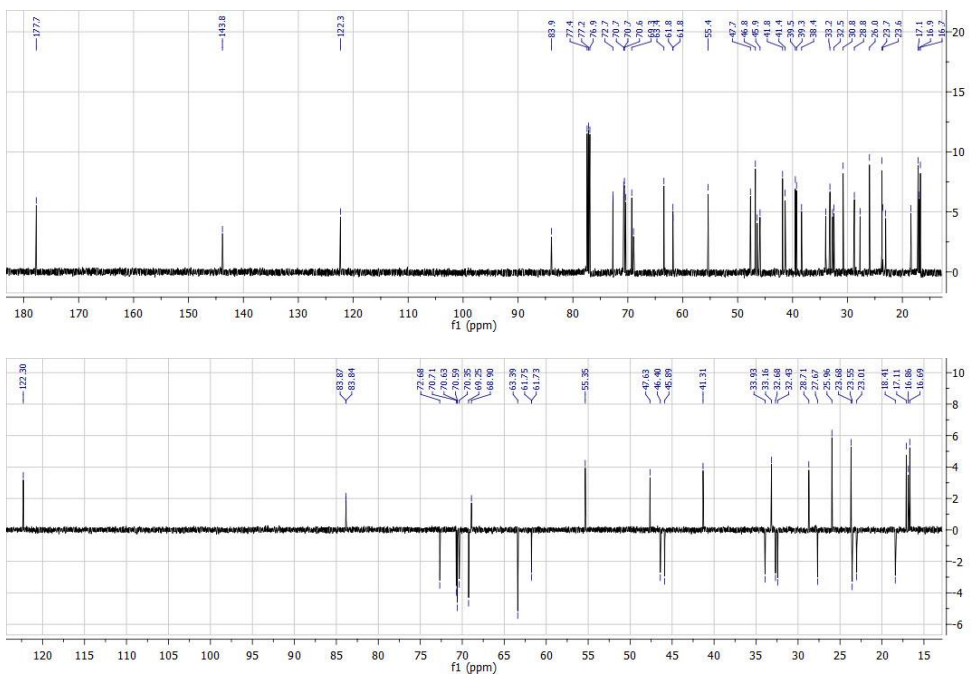

Espectro de ^{1}H RMN del compuesto 9

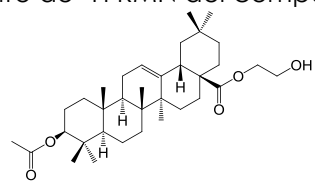

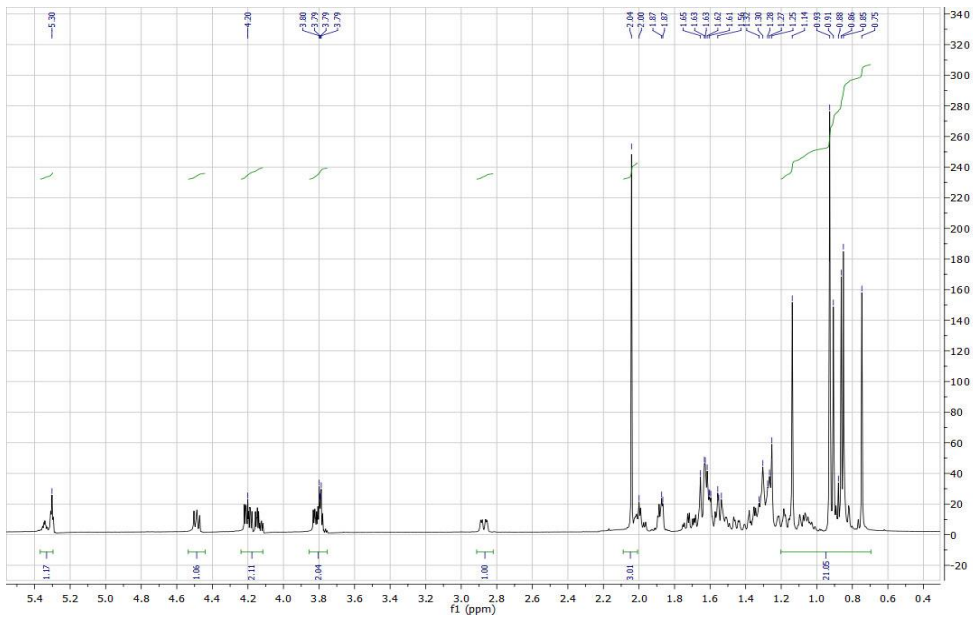

Espectro de ^{13}C RMN del compuesto 9

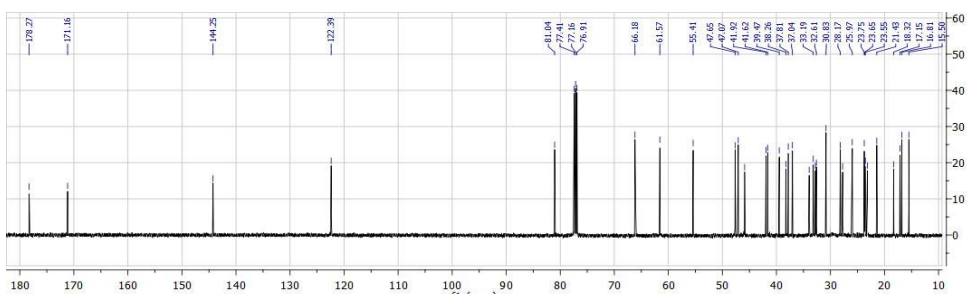

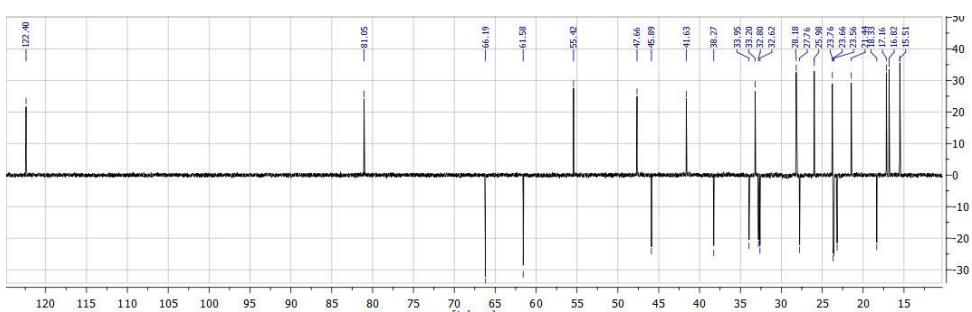

Espectro de ^{1}H RMN del compuesto 10

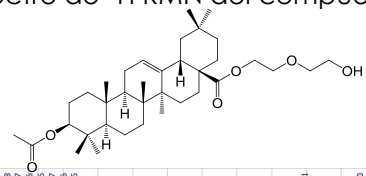

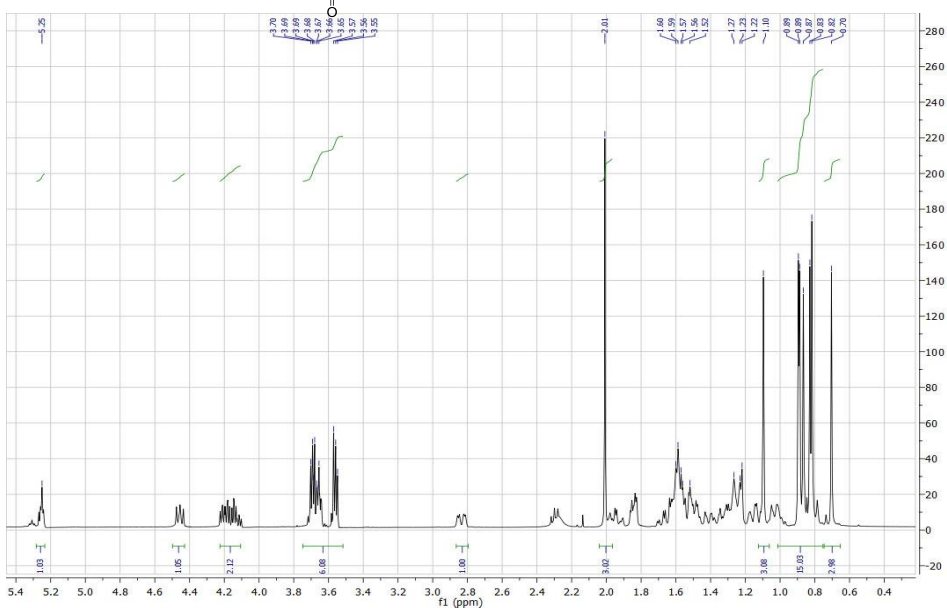

Espectro de ^{13}C RMN del compuesto 10

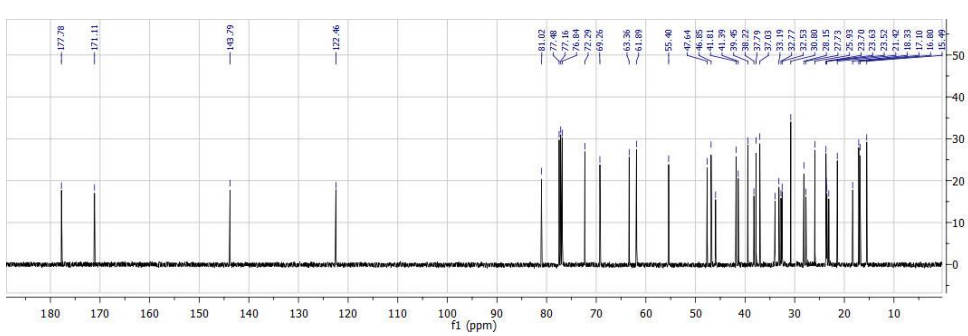

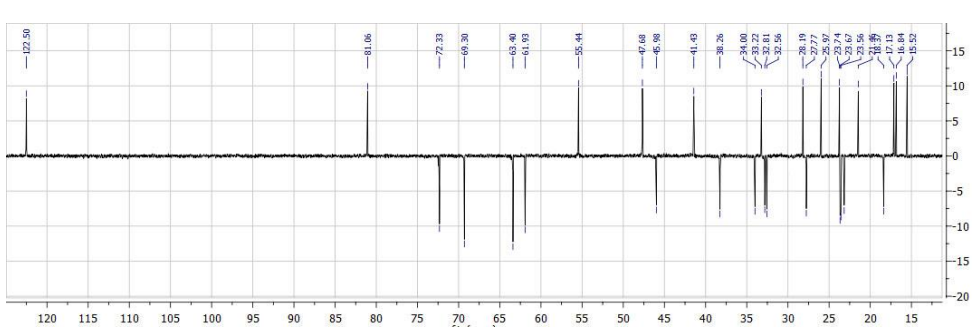

Espectro de ^{1}H RMN del compuesto 11

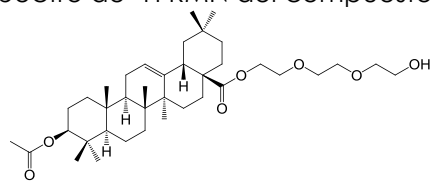

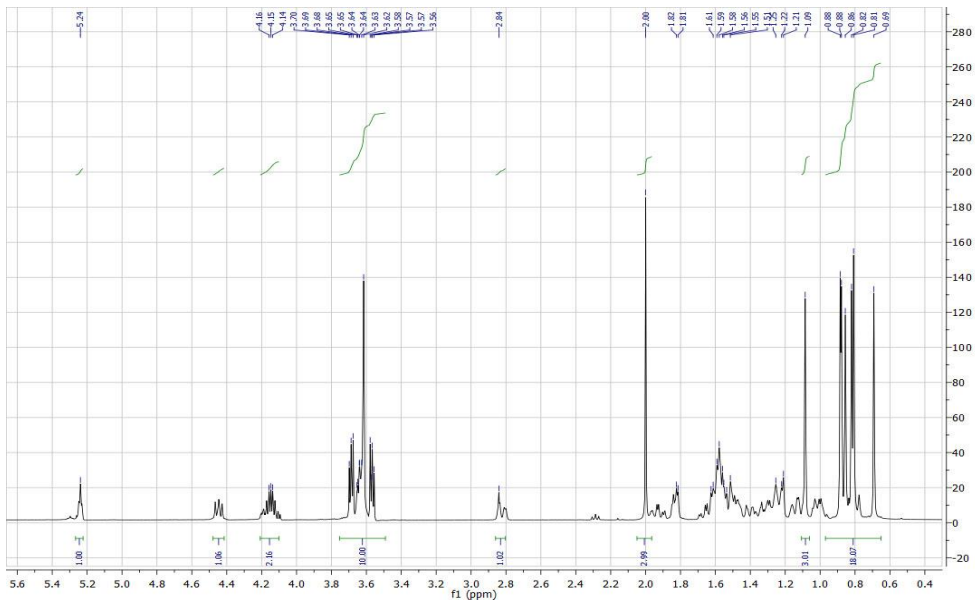

Espectro de ^{13}C RMN del compuesto 11

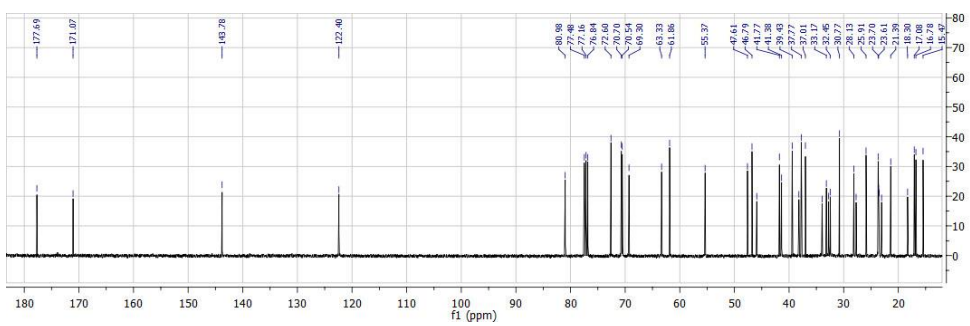

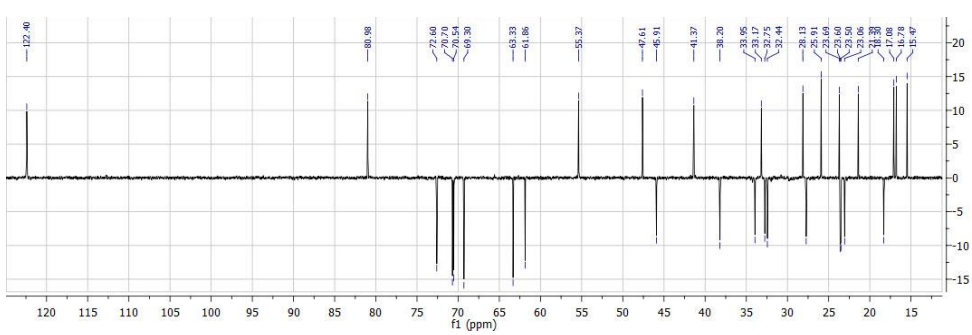

Espectro de ^{1}H RMN del compuesto 12

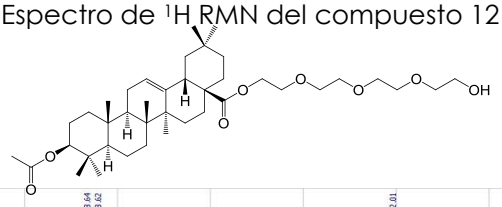

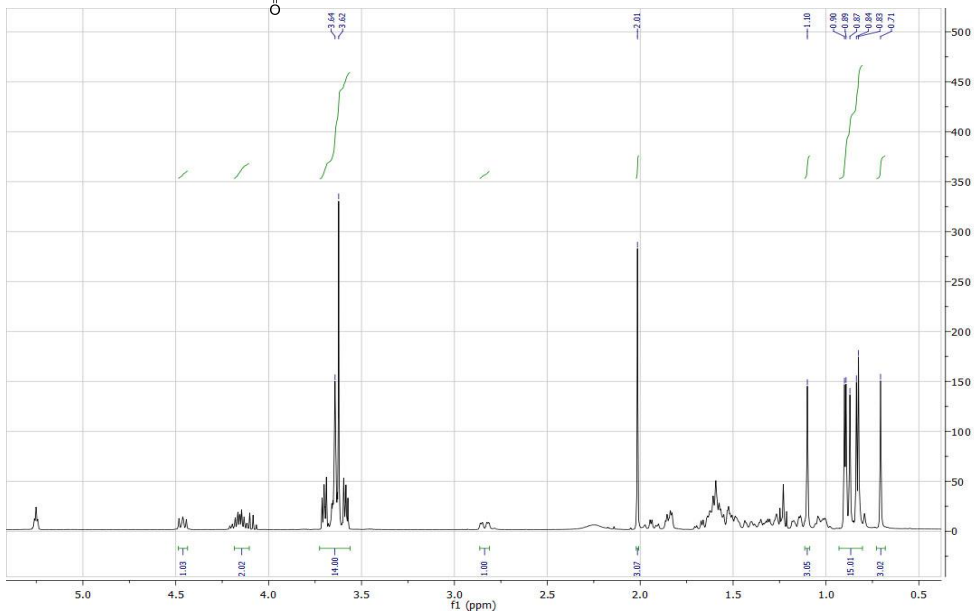

Espectro de ^{13}C RMN del compuesto 12

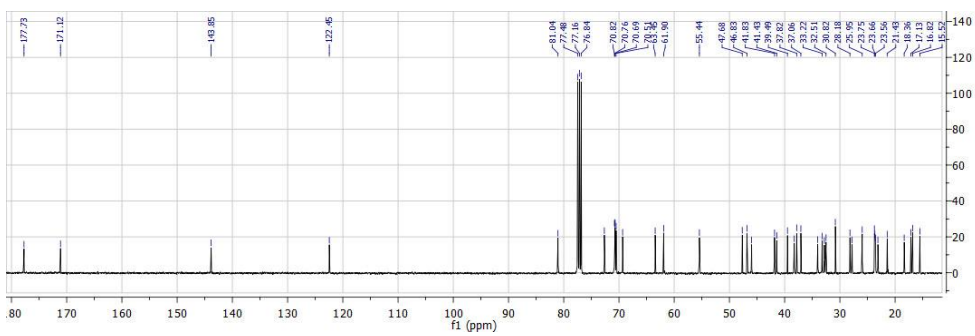

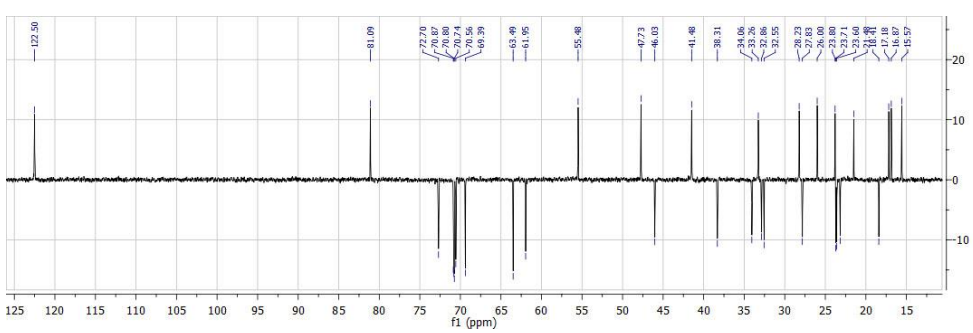

Espectro de ^{1}H RMN del compuesto 13

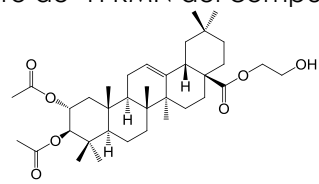

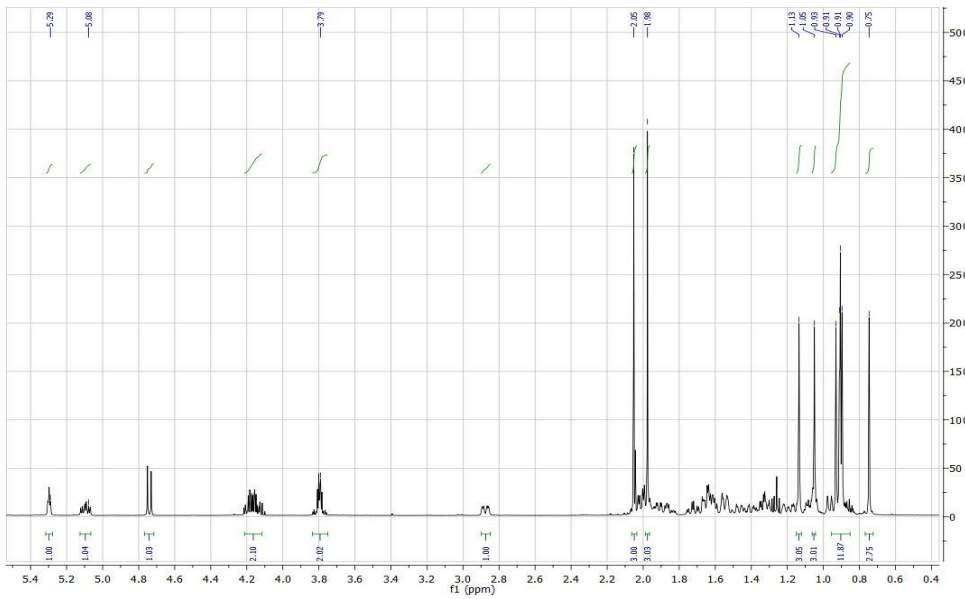

Espectro de ^{13}C RMN del compuesto 13

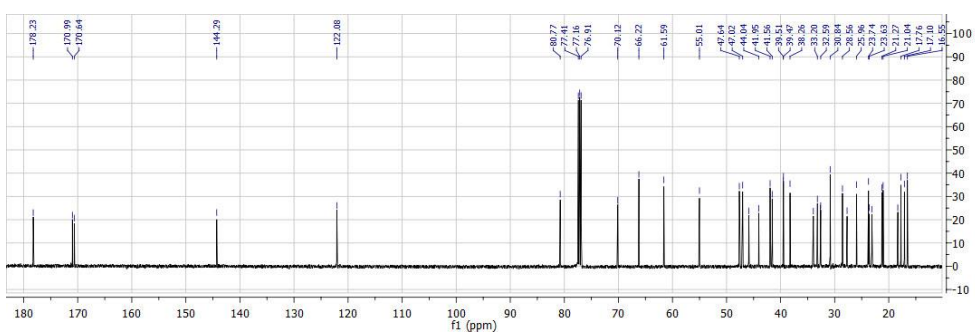

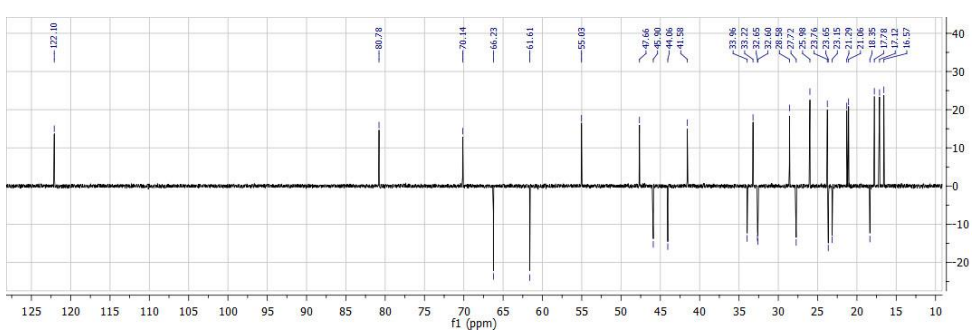

Espectro de ^{1}H RMN del compuesto 14

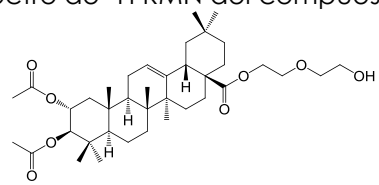

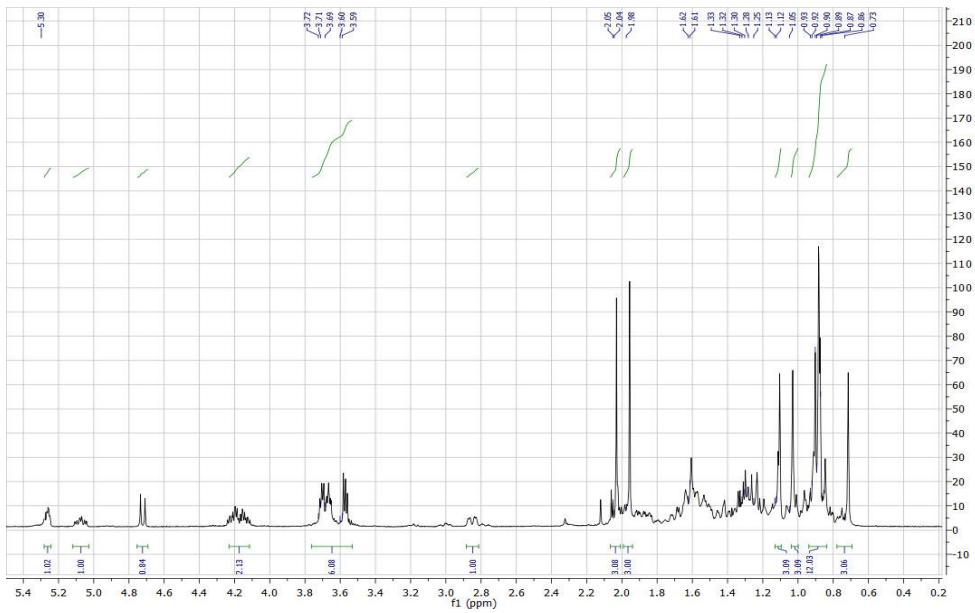

Espectro de ^{13}C RMN del compuesto 14

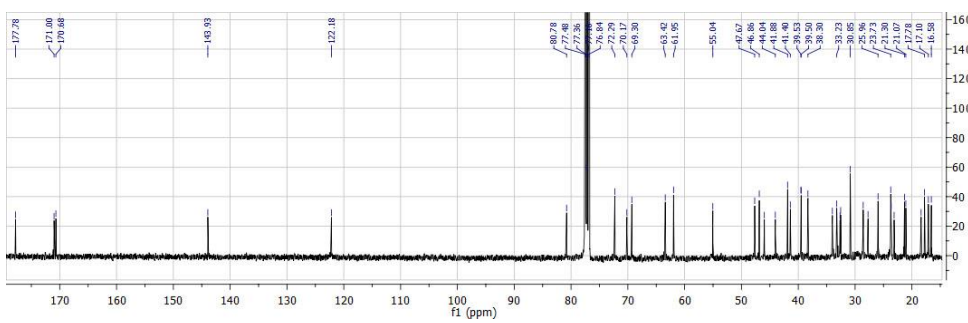

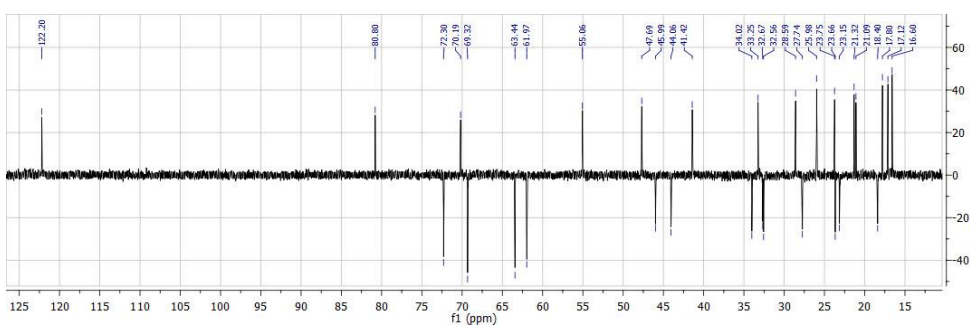

Espectro de ^{1}H RMN del compuesto 15

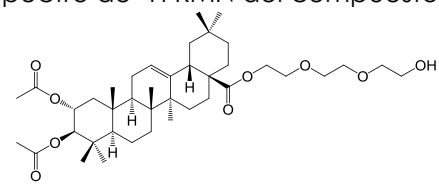

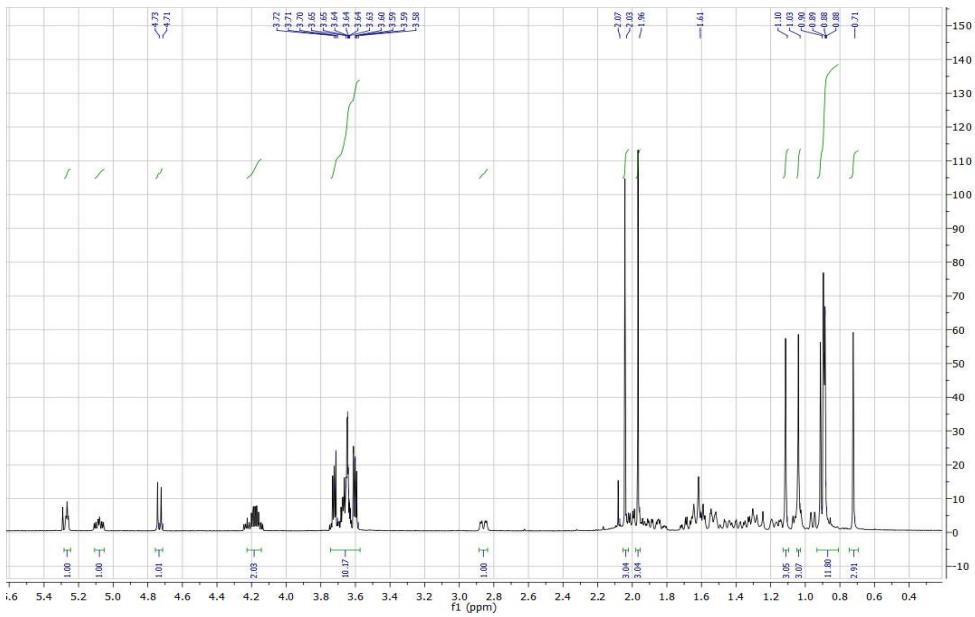

Espectro de ^{13}C RMN del compuesto 15

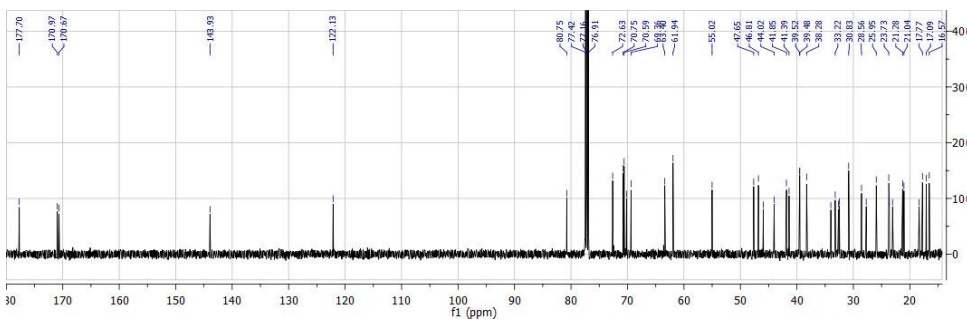

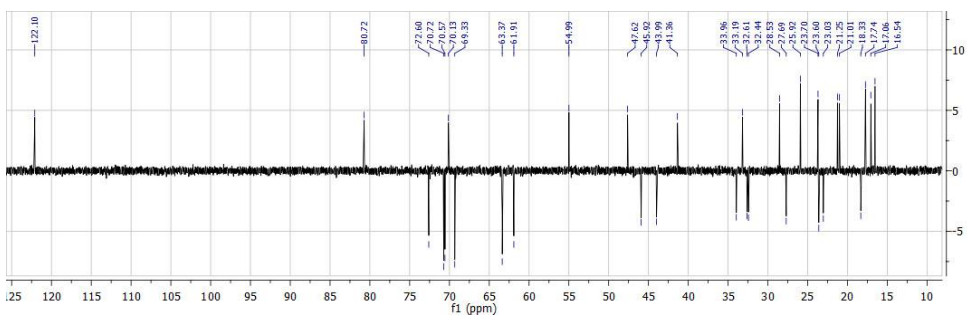

Espectro de ^{1}H RMN del compuesto 16

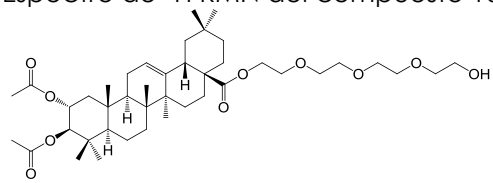

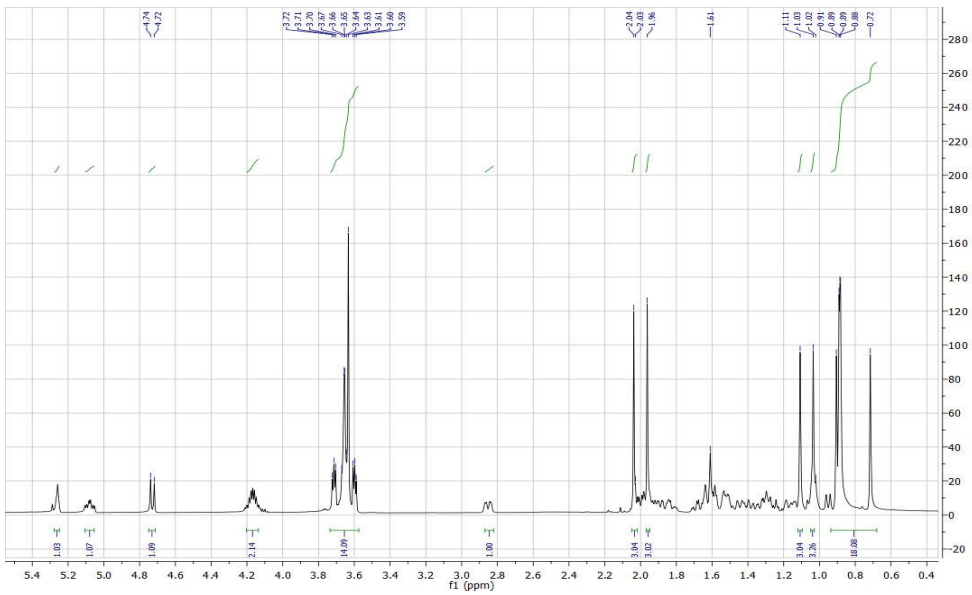

Espectro de ^{13}C RMN del compuesto 16

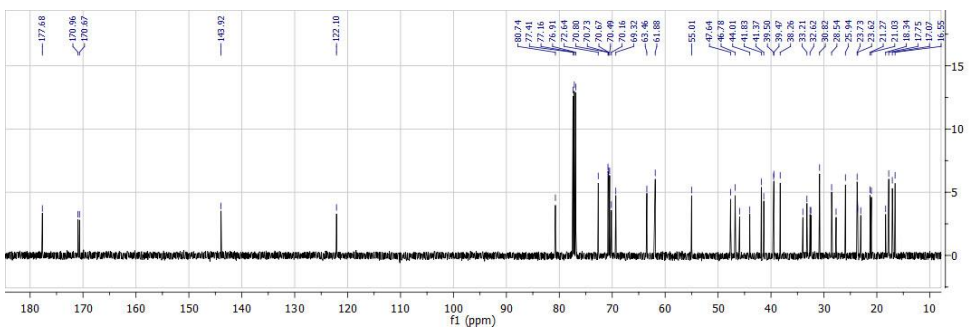

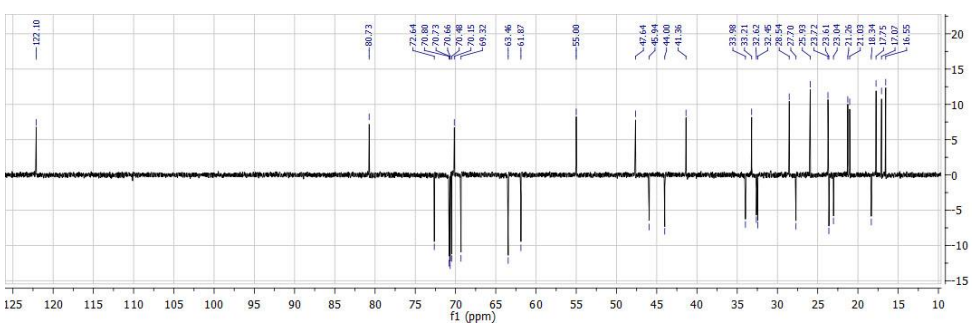

Espectro de ^{1}H RMN del compuesto 17

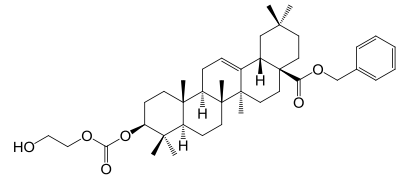

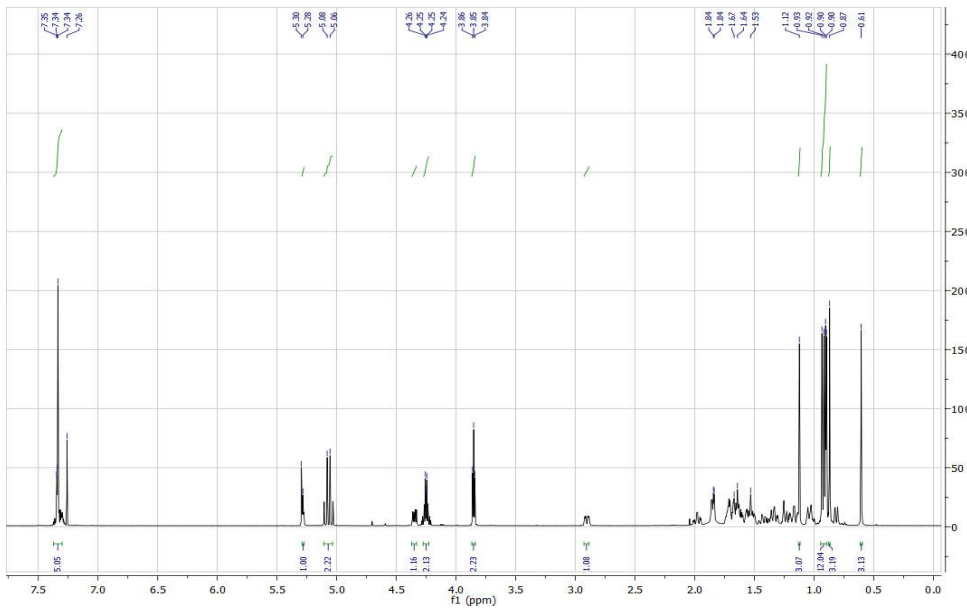

Espectro de ^{13}C RMN del compuesto 17

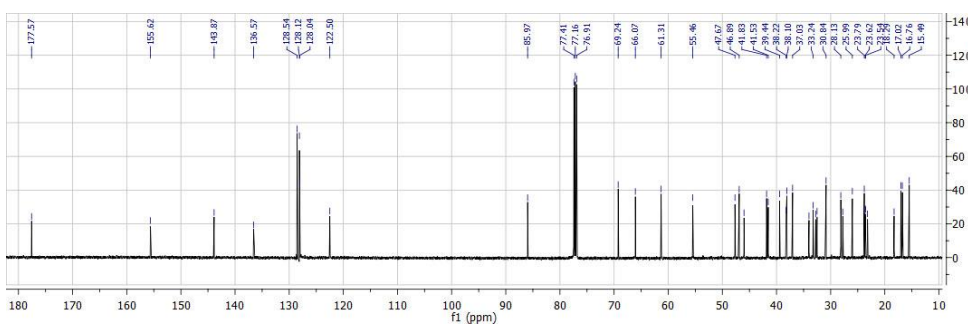

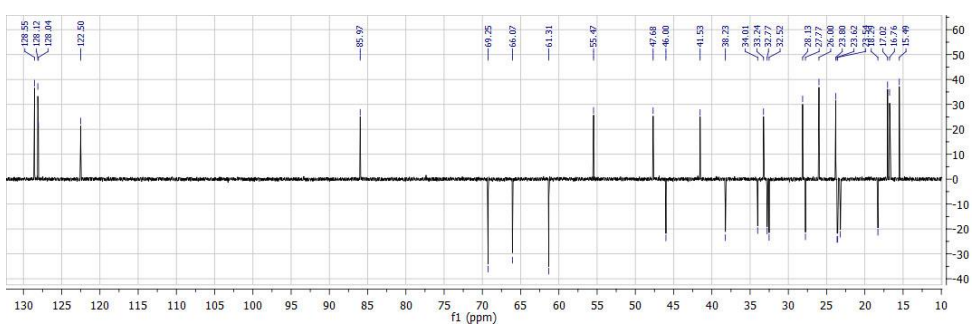

Espectro de ^{1}H RMN del compuesto 18

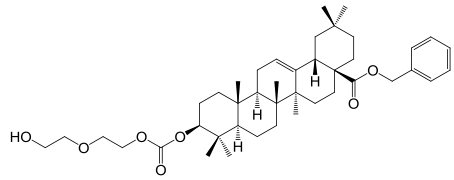

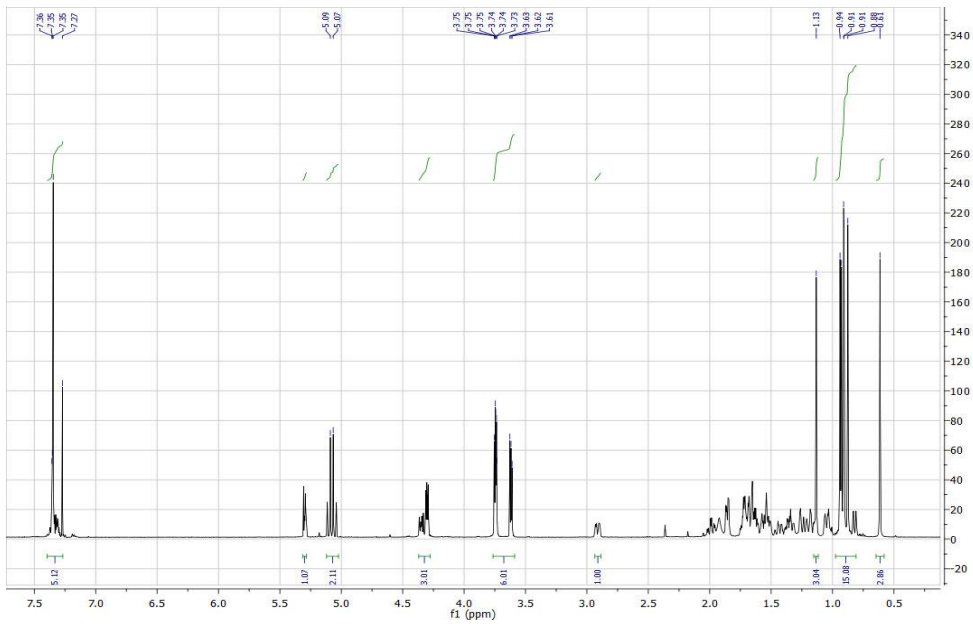

Espectro de ^{13}C RMN del compuesto 18

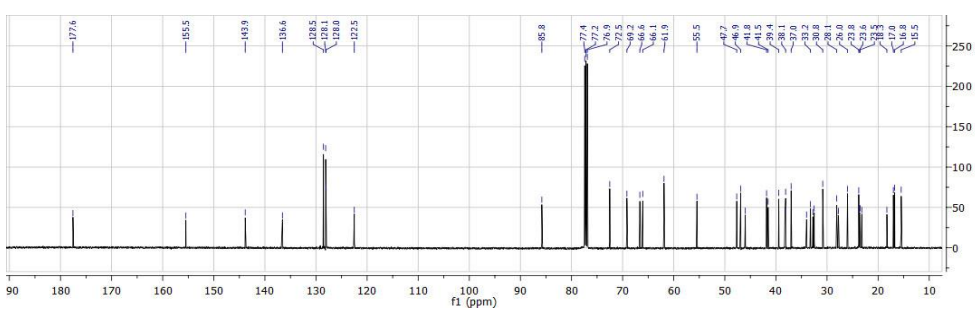

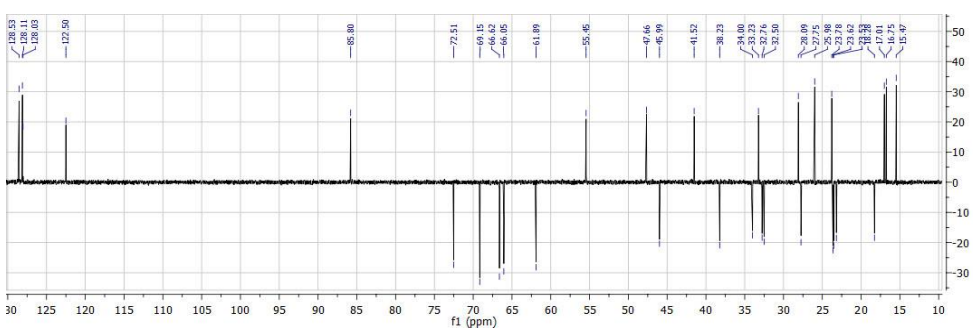

Espectro de ^{1}H RMN del compuesto 19

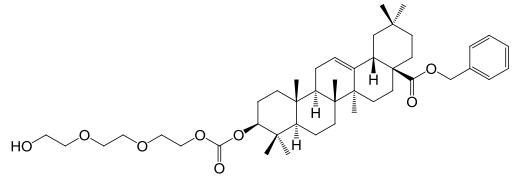

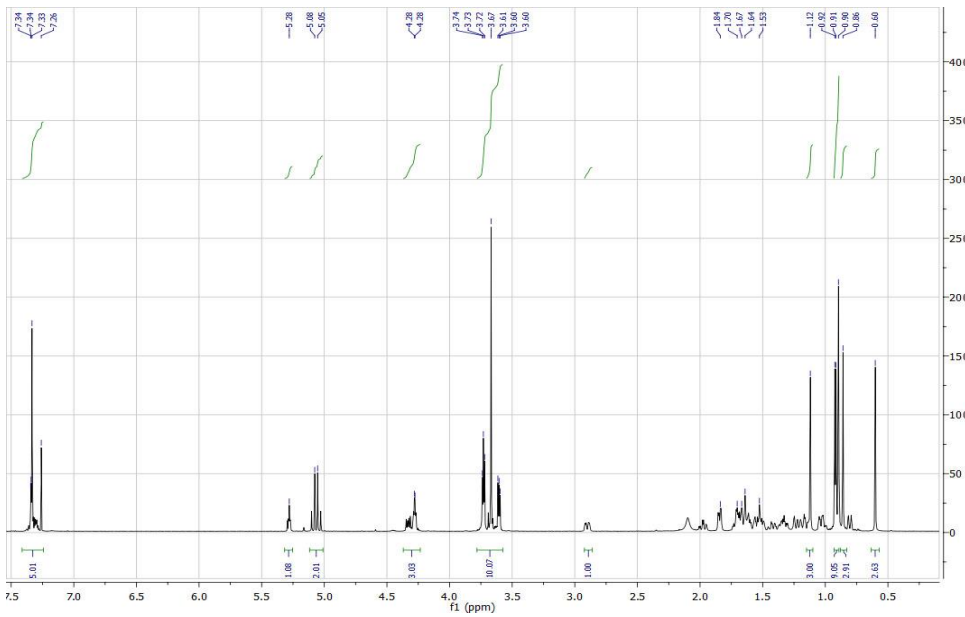

Espectro de ^{13}C RMN del compuesto 19

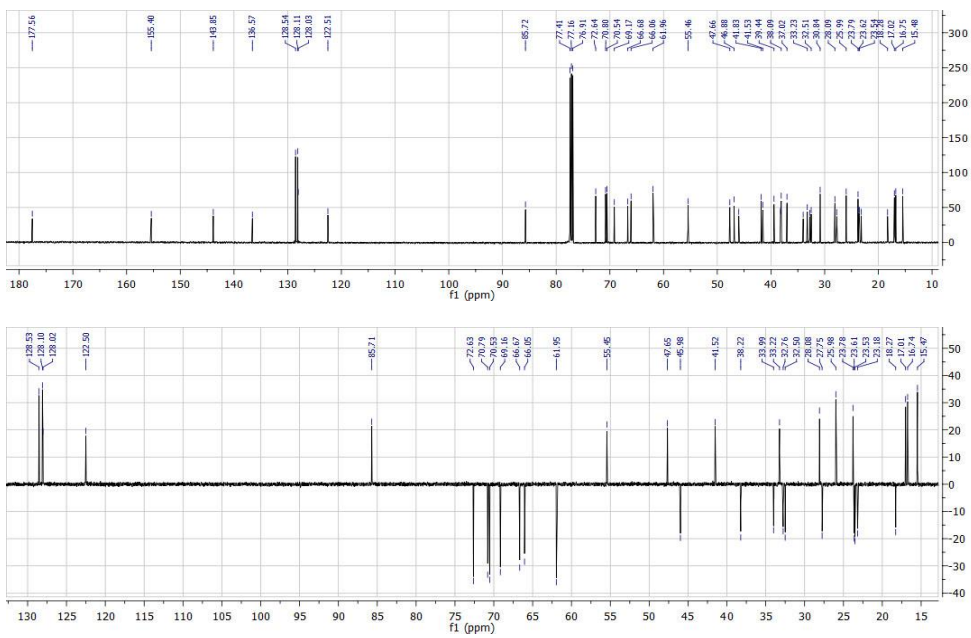

Espectro de ^{1}H RMN del compuesto 20

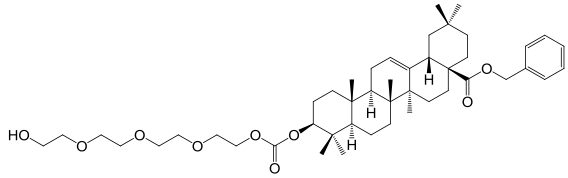

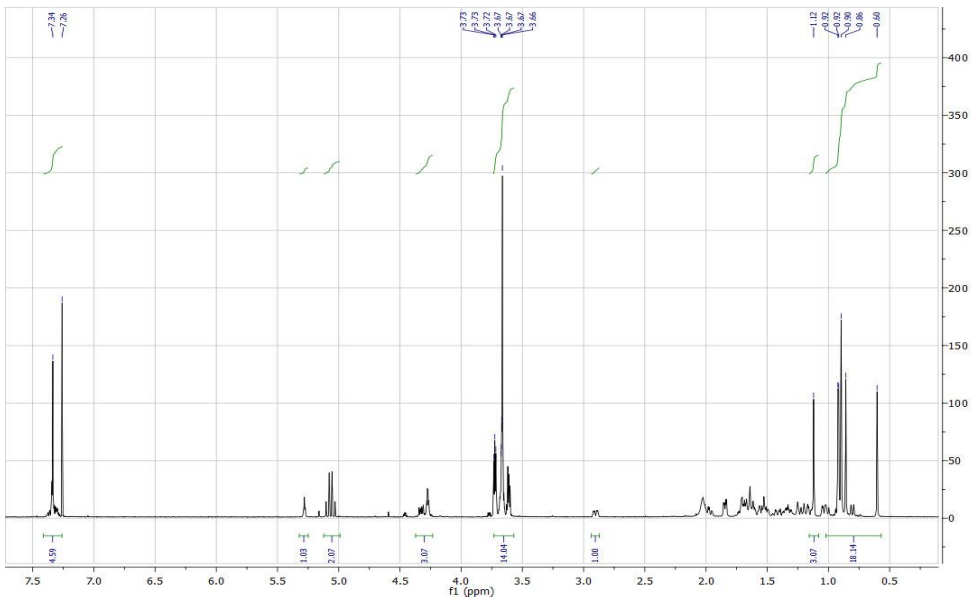

Espectro de ^{13}C RMN del compuesto 20

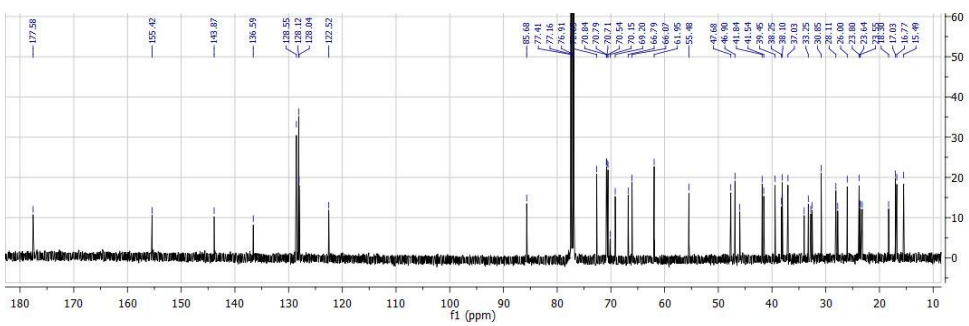

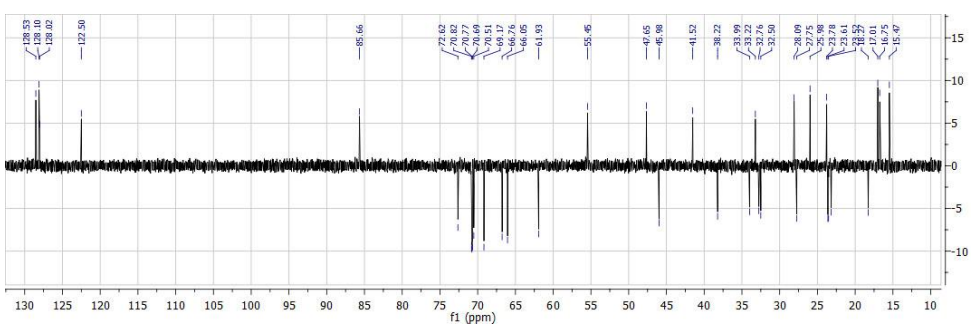

Espectro de ^{1}H RMN del compuesto 21

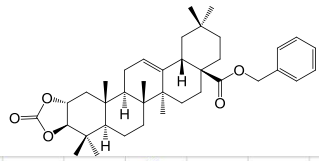

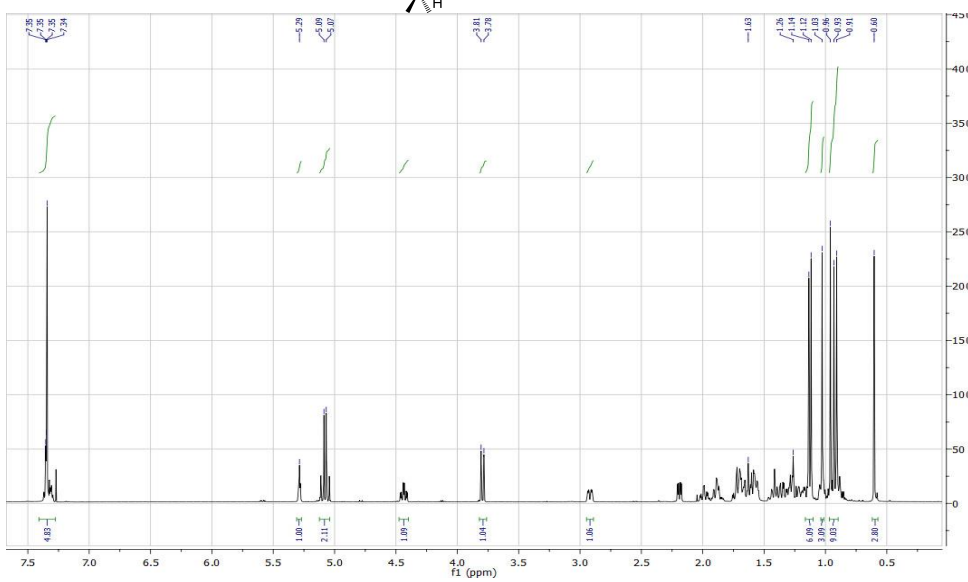

Espectro de ^{13}C RMN del compuesto 21

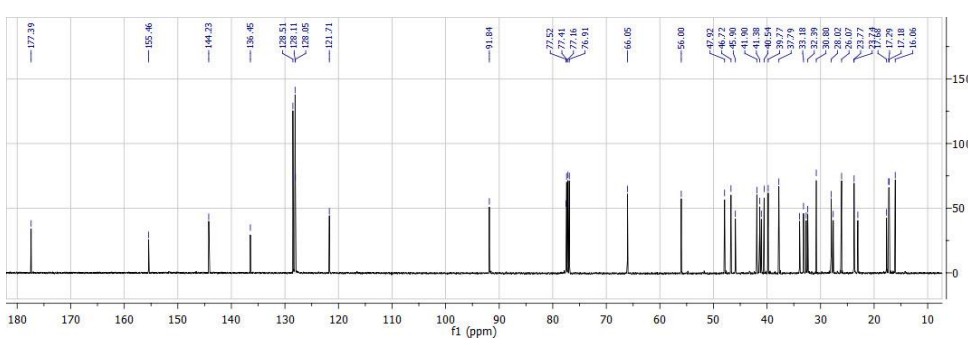

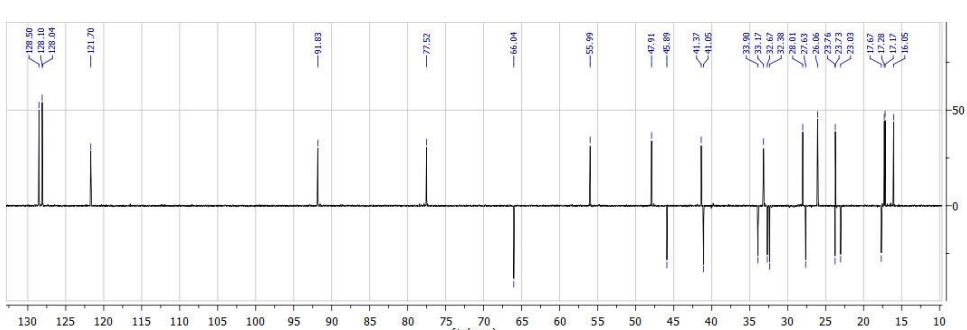

Espectro de ^{1}H RMN del compuesto 25

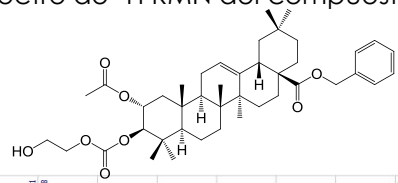

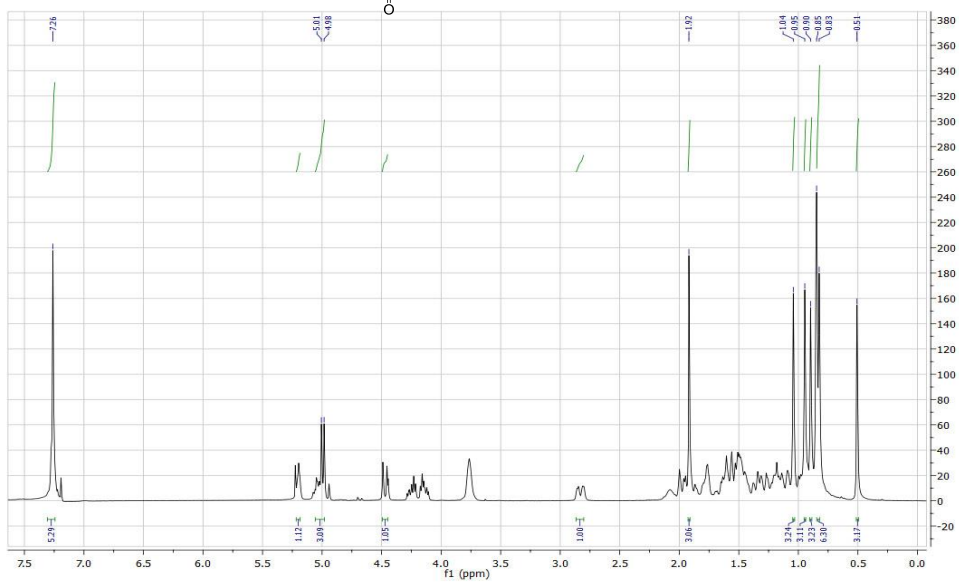

Espectro de ^{13}C RMN del compuesto 25

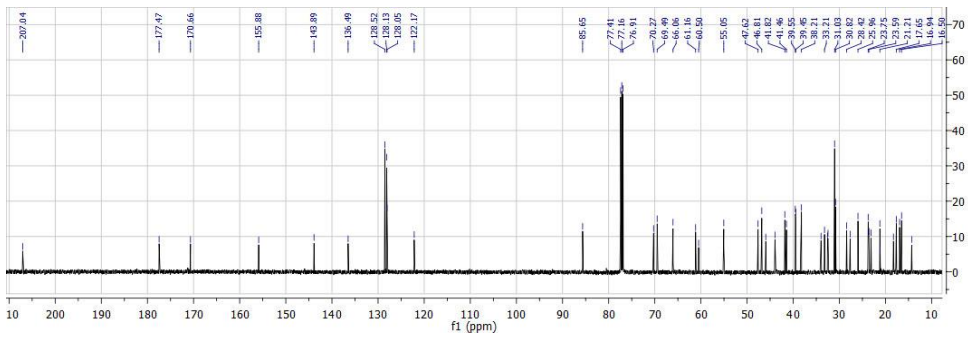

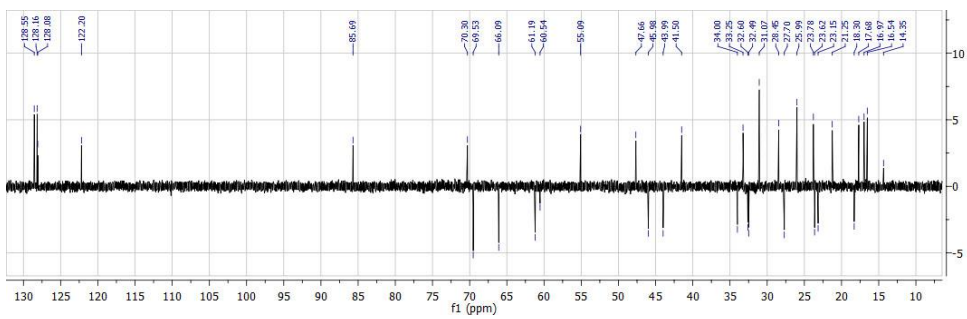

Espectro de ^{1}H RMN del compuesto 26

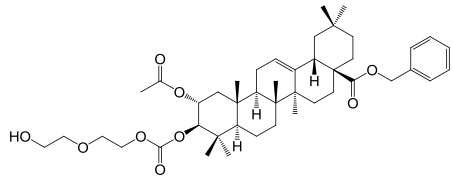

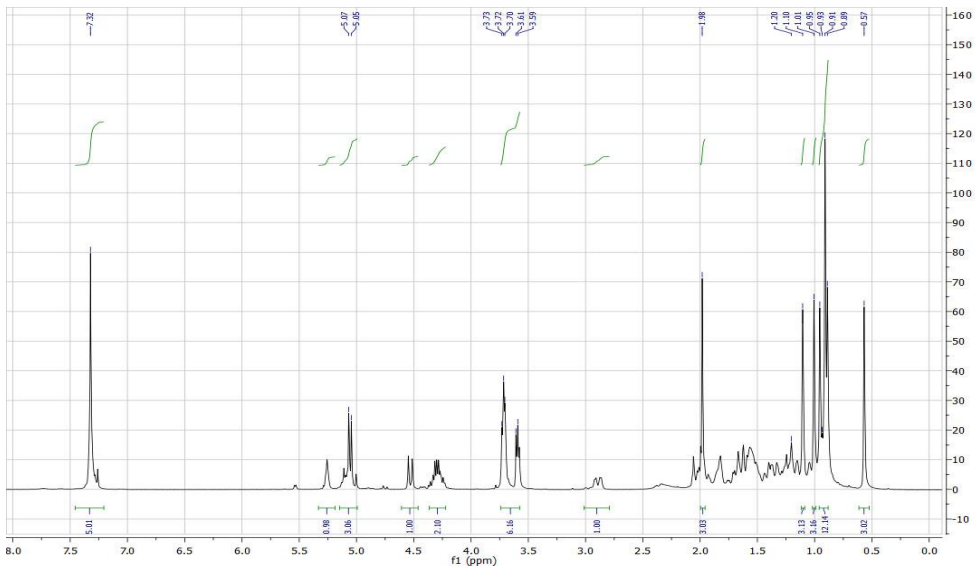

Espectro de ^{13}C RMN del compuesto 26

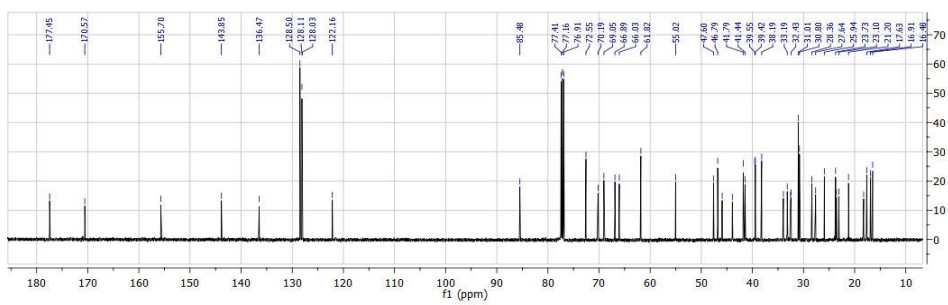

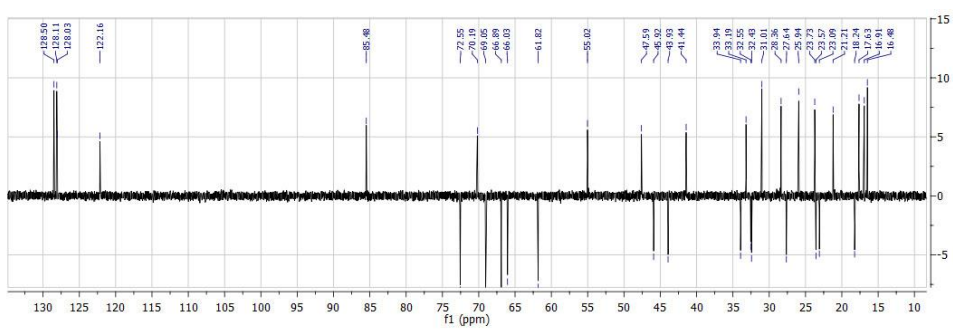

Espectro de ^{1}H RMN del compuesto 27

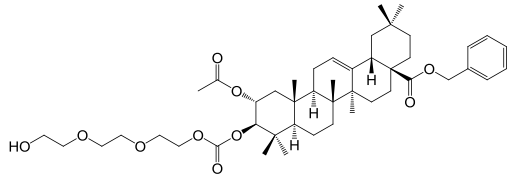

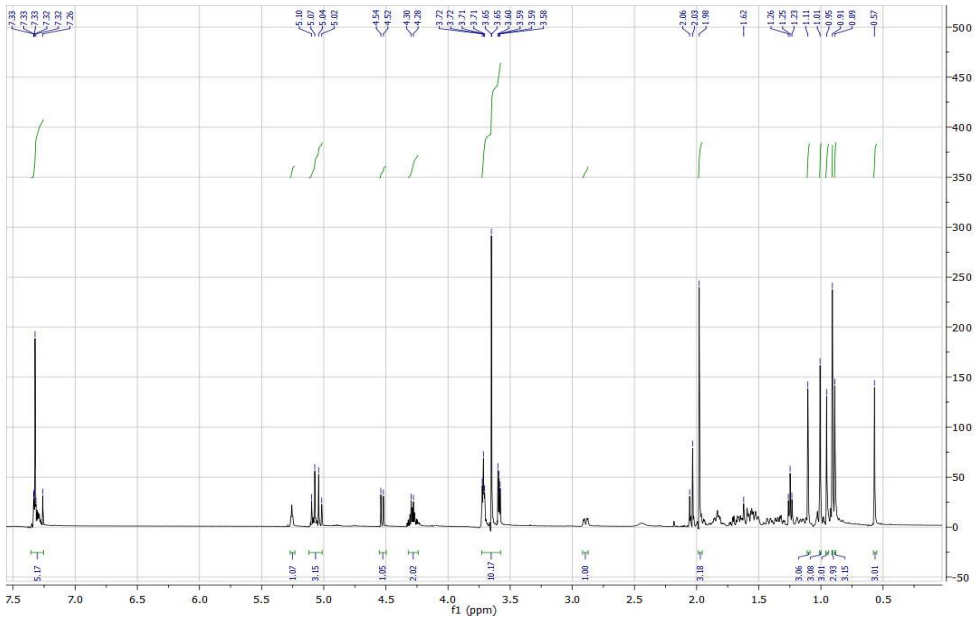

Espectro de ^{13}C RMN del compuesto 27

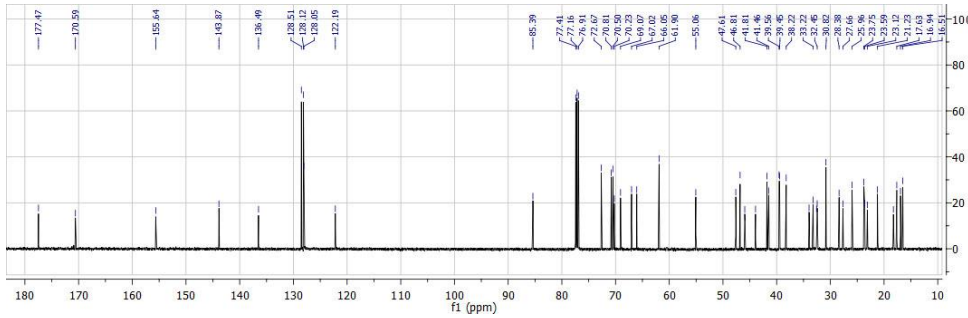

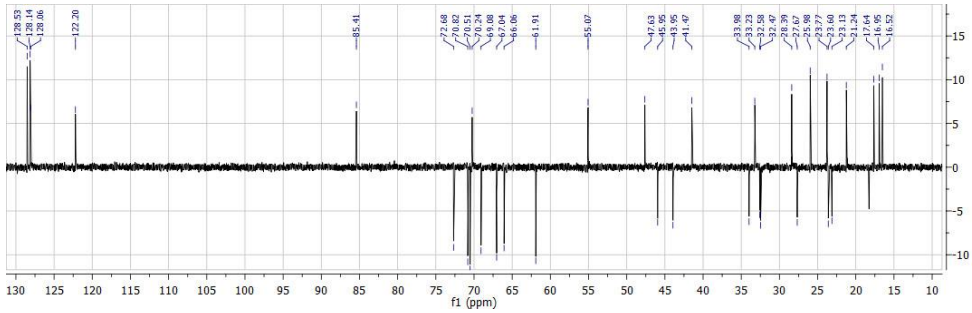

Espectro de ^{1}H RMN del compuesto 28

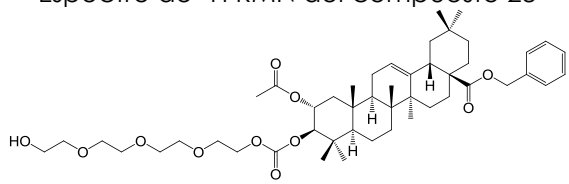

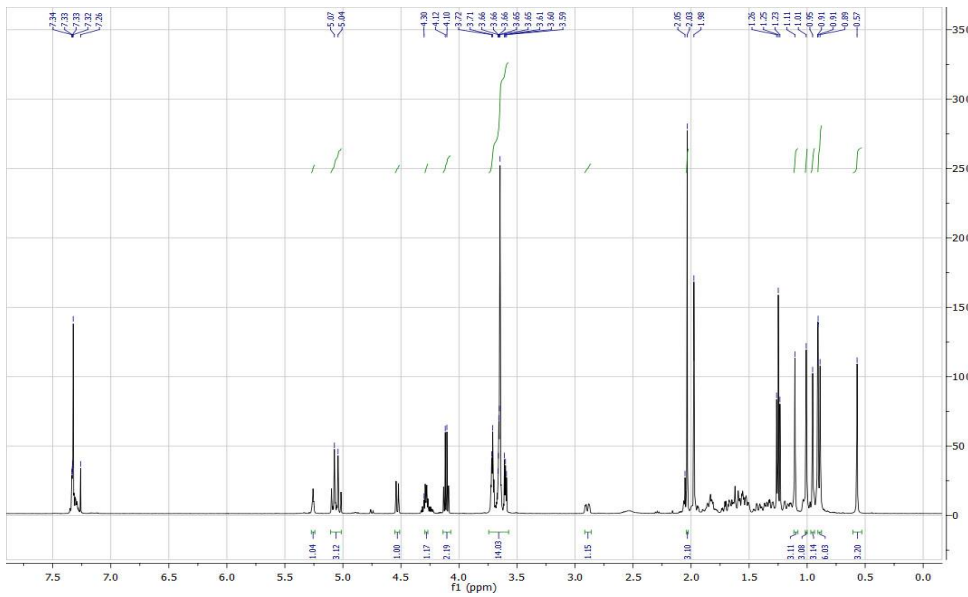

Espectro de ^{13}C RMN del compuesto 28

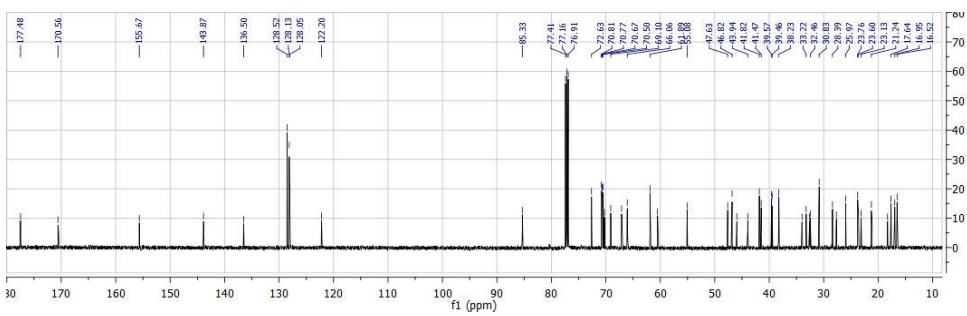

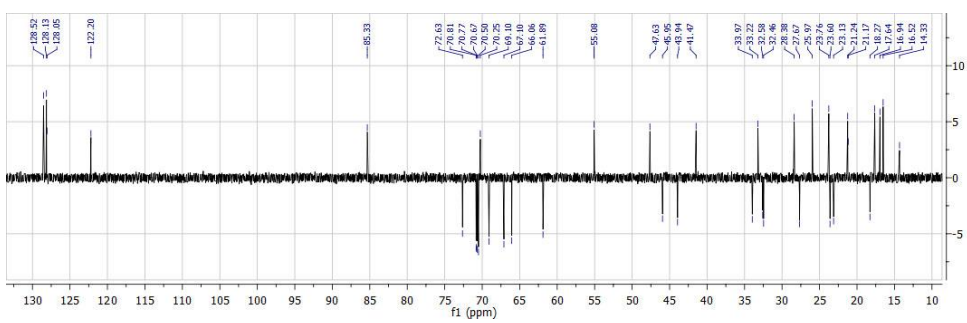

Espectro de ^{1}H RMN del compuesto 29

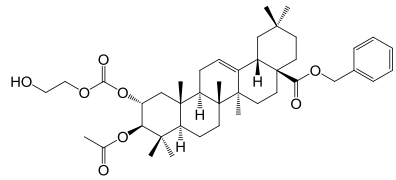

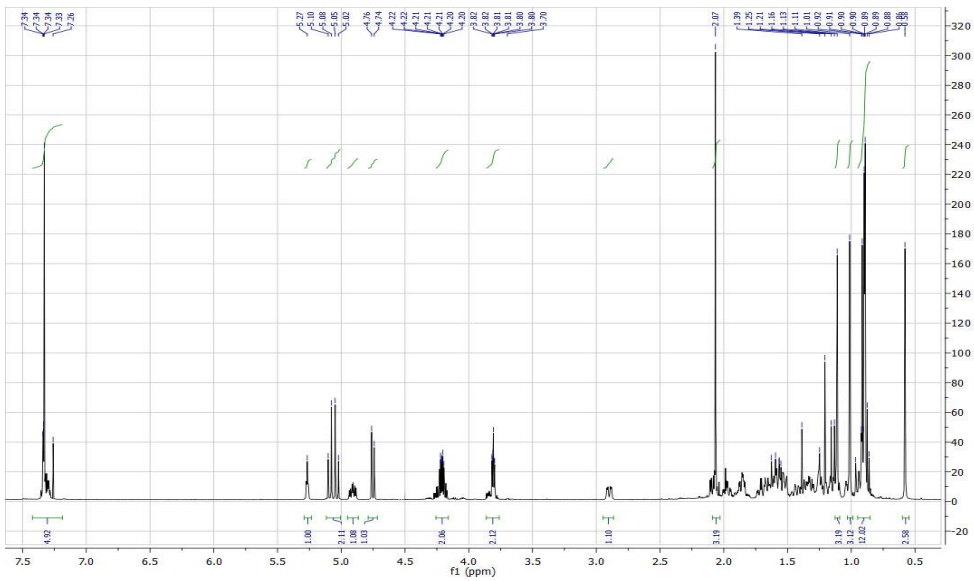

Espectro de ^{13}C RMN del compuesto 29

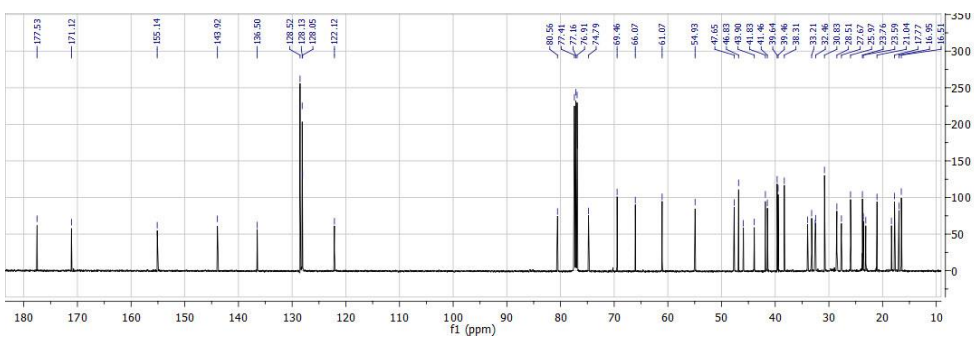

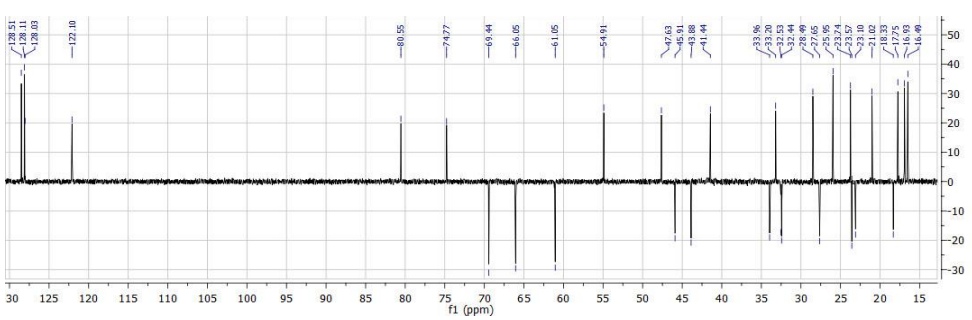

Espectro de ^{1}H RMN del compuesto 30

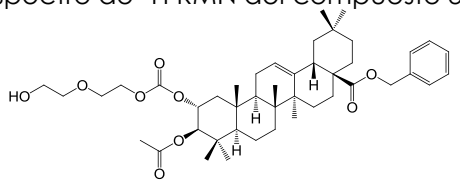

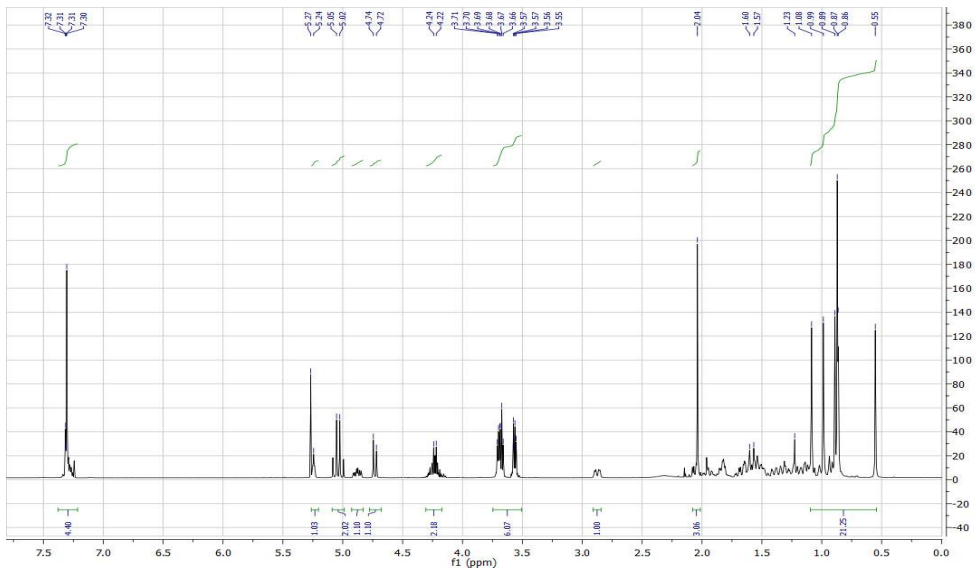

Espectro de ^{13}C RMN del compuesto 30

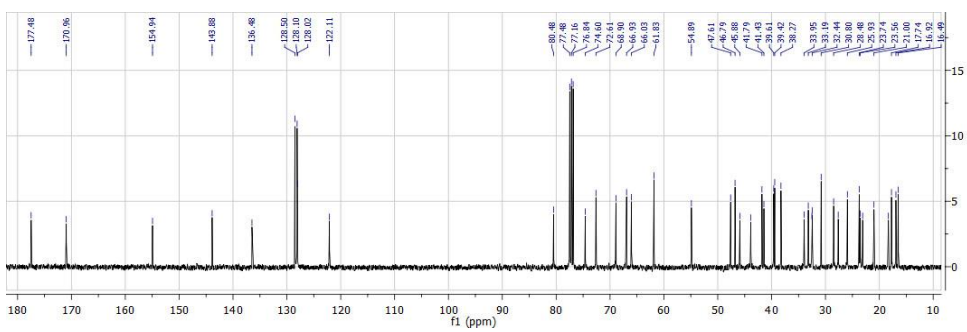

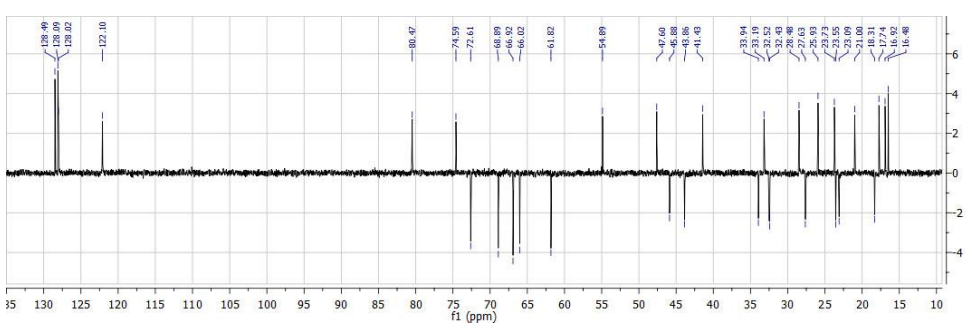

Espectro de ^{1}H RMN del compuesto 31

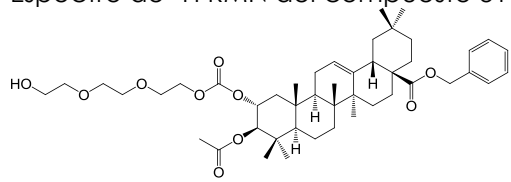

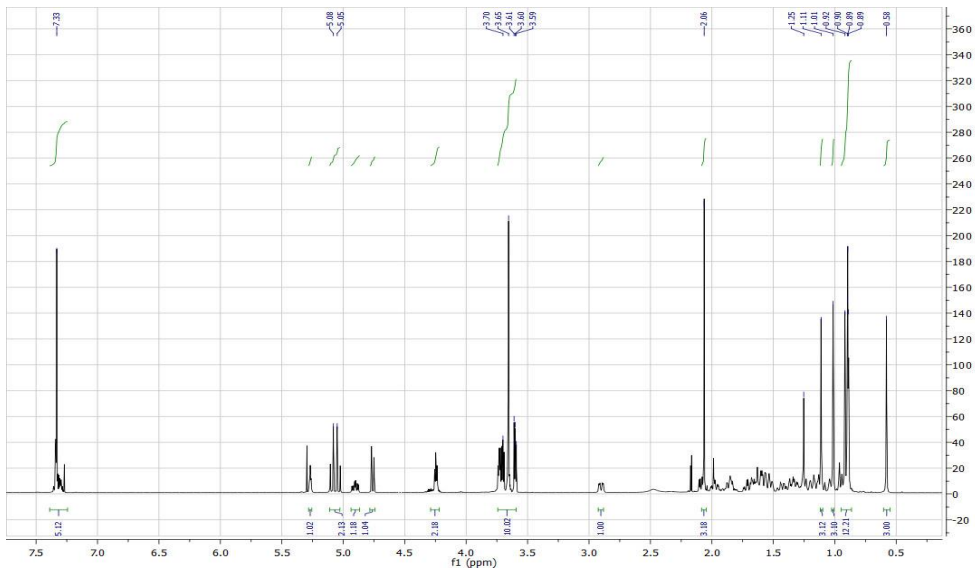

Espectro de ^{13}C RMN del compuesto 31

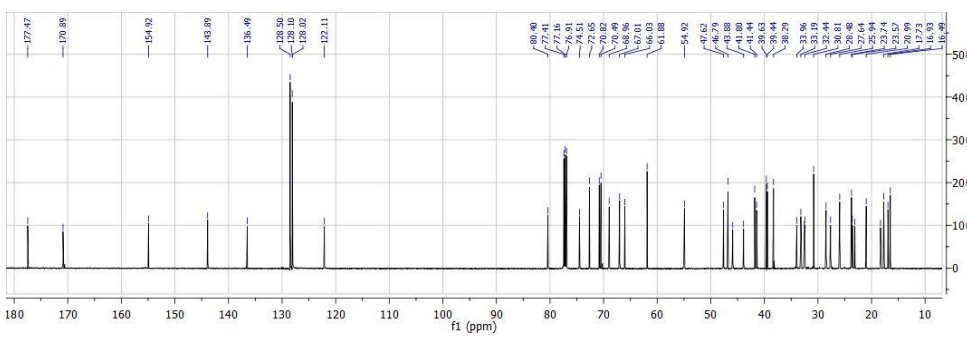

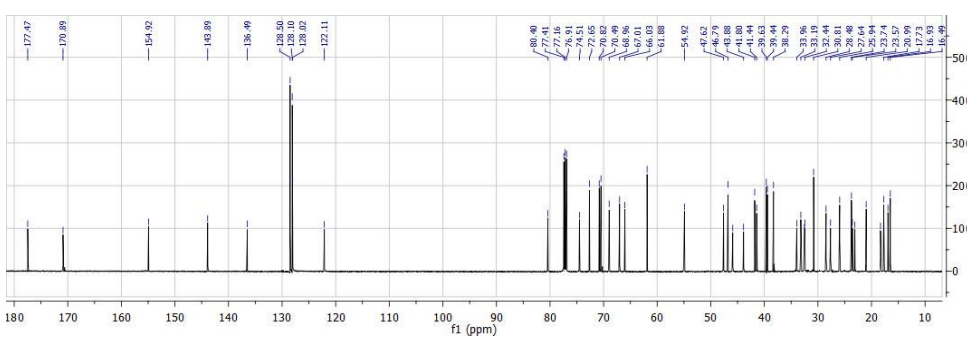

Espectro de ^{1}H RMN del compuesto 32

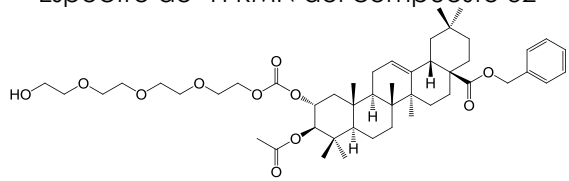

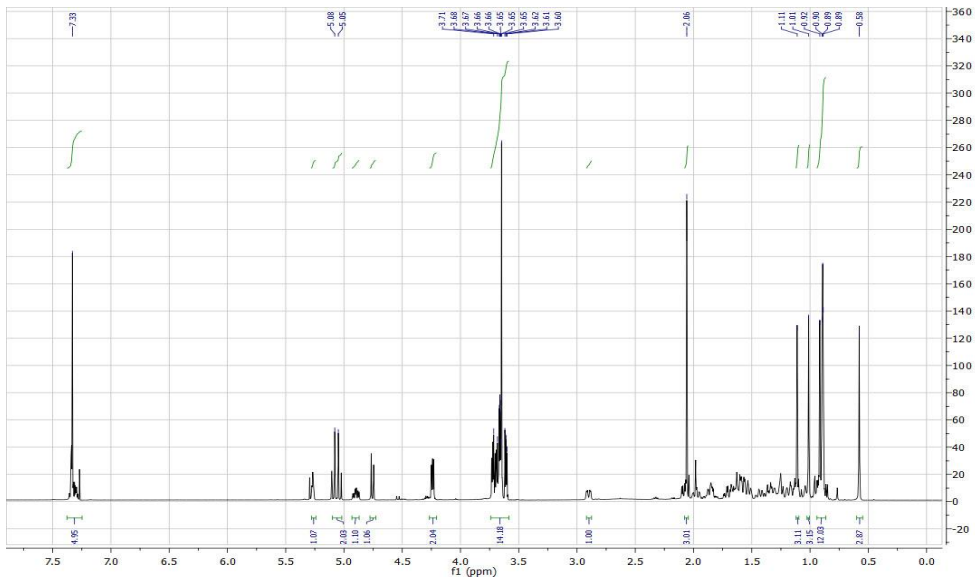

Espectro de ^{13}C RMN del compuesto 32

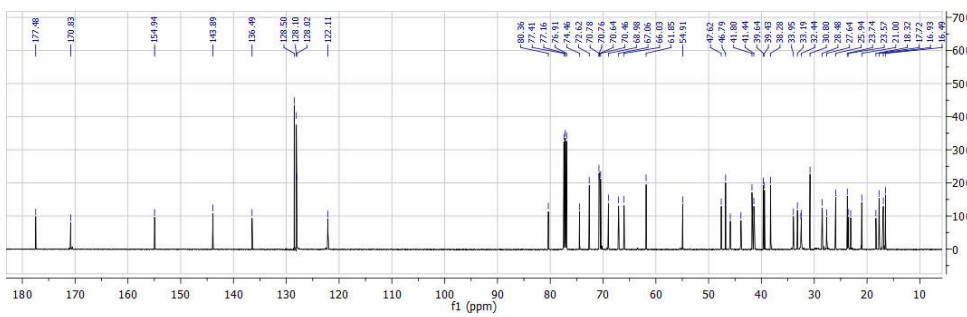

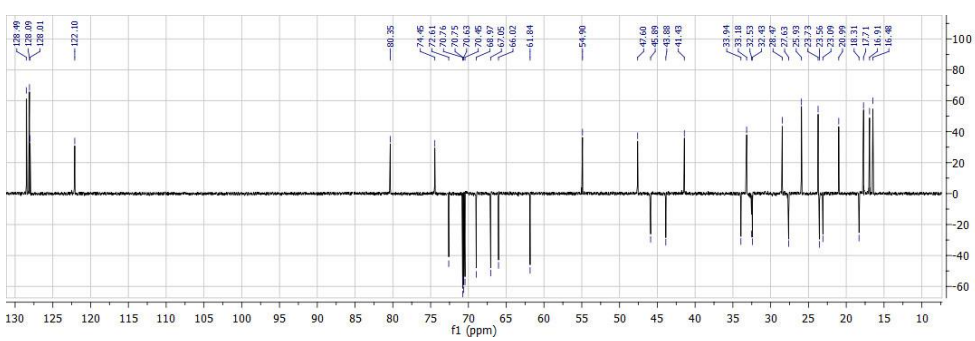

4. ESPECTROS RMN PUBLICACIÓN 4

Espectro de ^{1}H RMN del compuesto 1

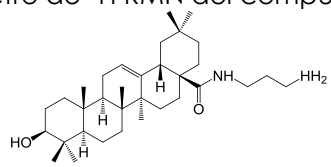

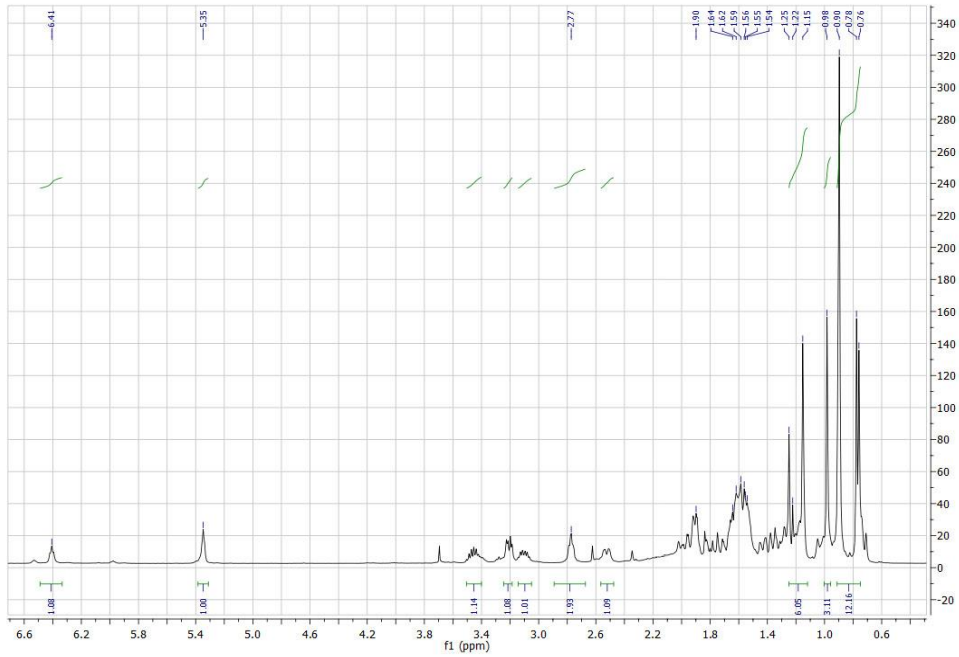

Espectro de ^{13}C RMN del compuesto 1

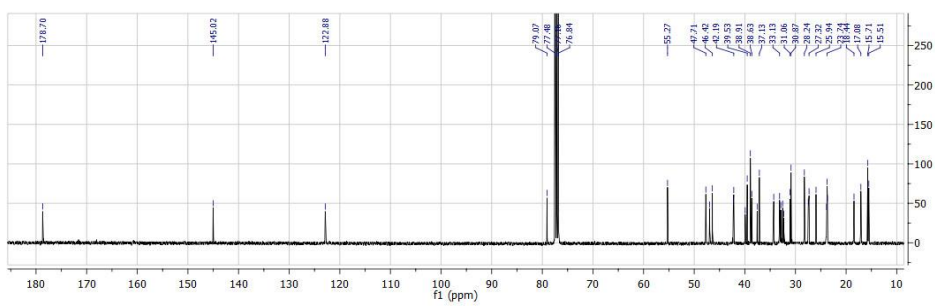

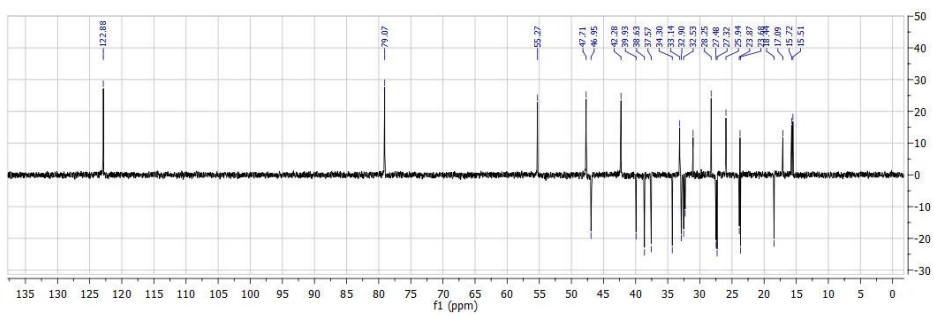

Espectro de ^{1}H RMN del compuesto 2

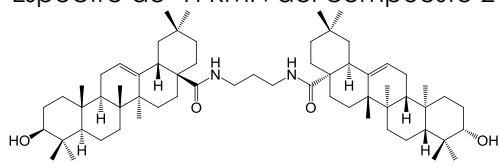

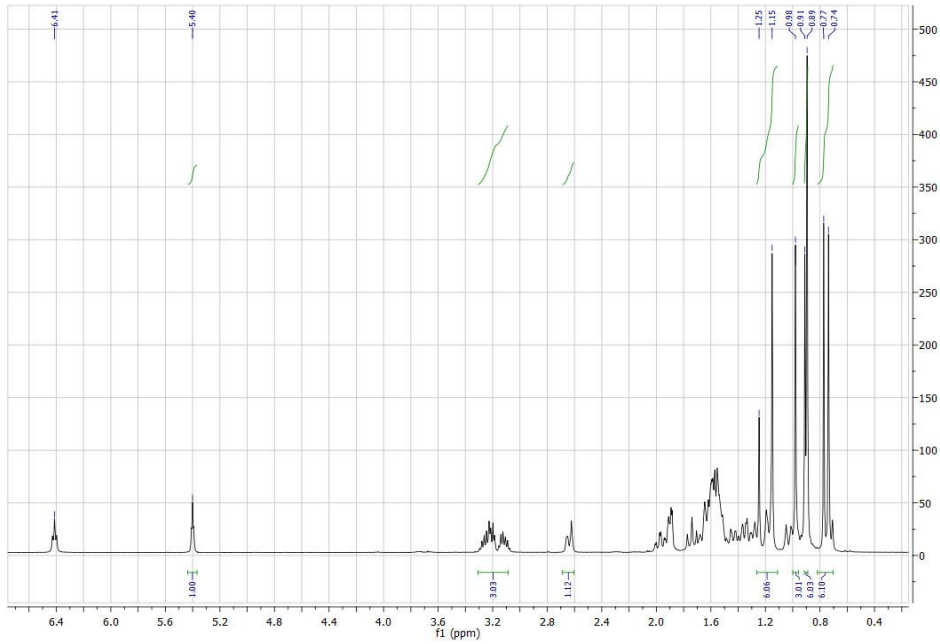

Espectro de ^{13}C RMN del compuesto 2

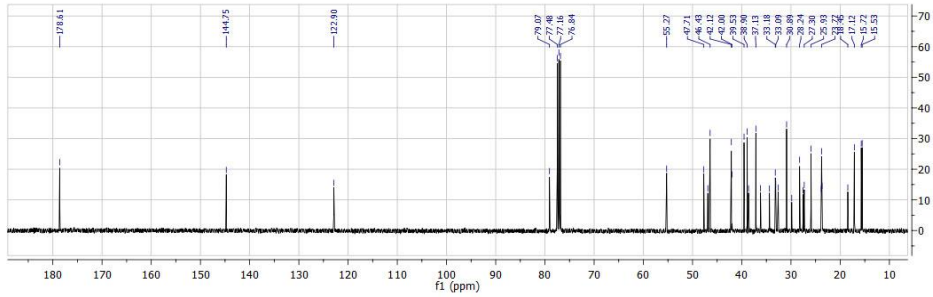

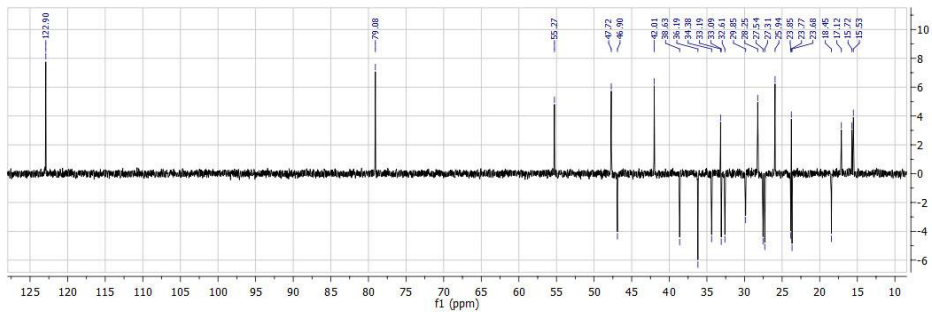

Espectro de ^{1}H RMN del compuesto 3

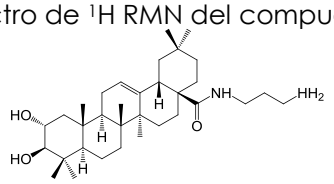

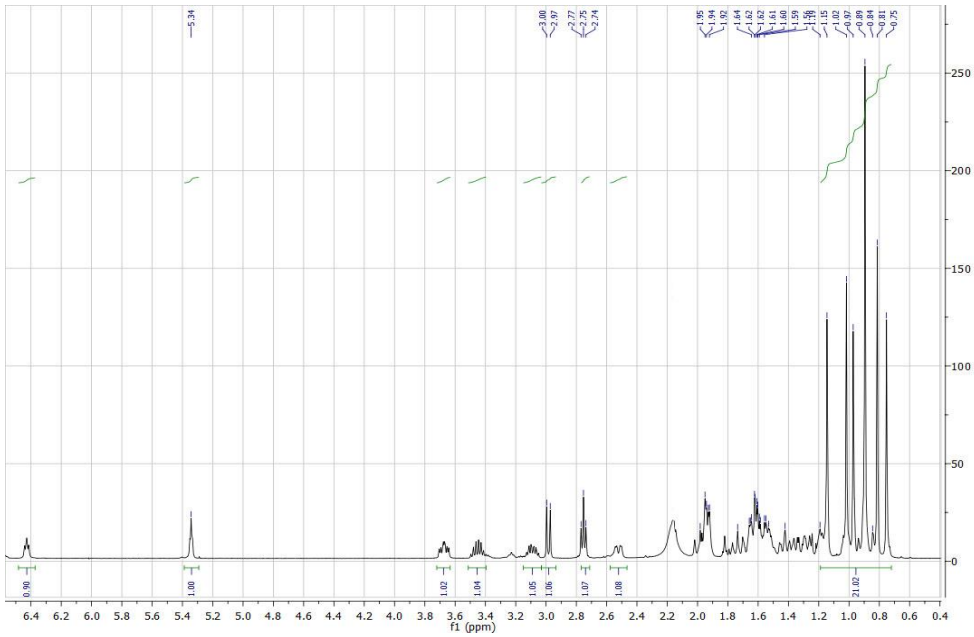

Espectro de ^{13}C RMN del compuesto 3

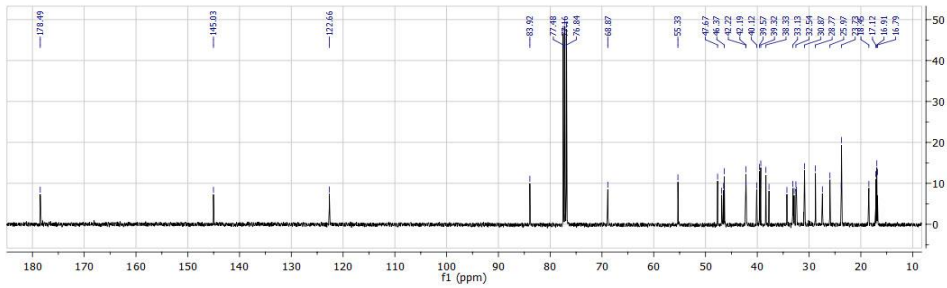

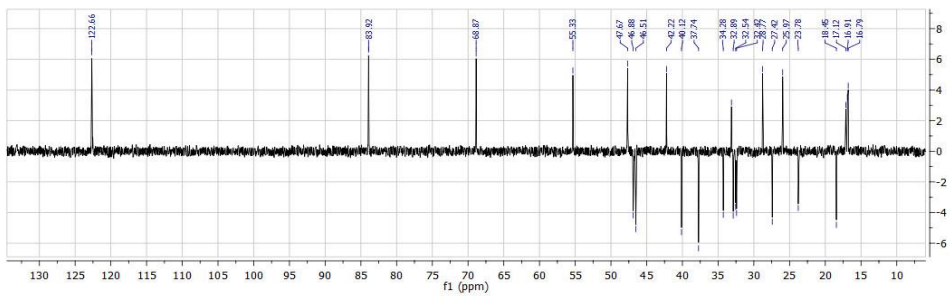

Espectro de ^{1}H RMN del compuesto 4

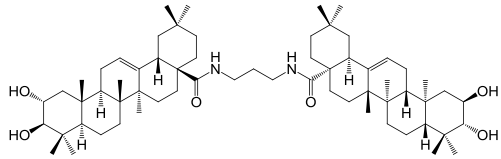

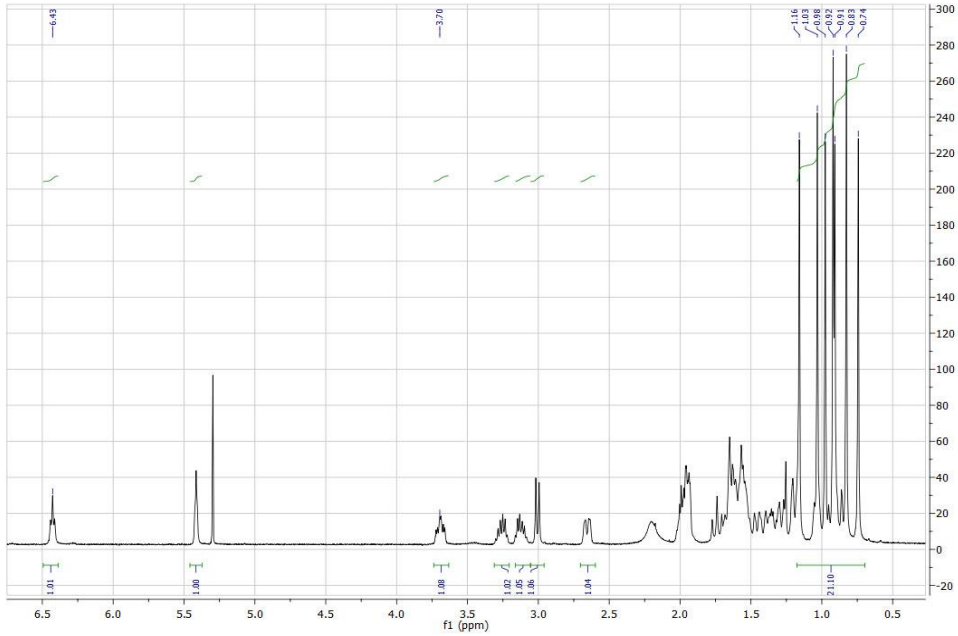

Espectro de ^{13}C RMN del compuesto 4

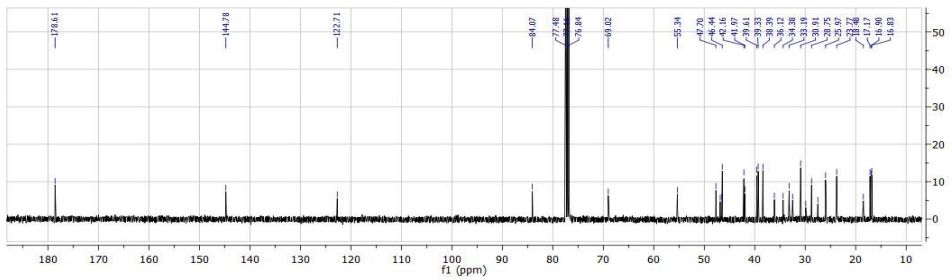

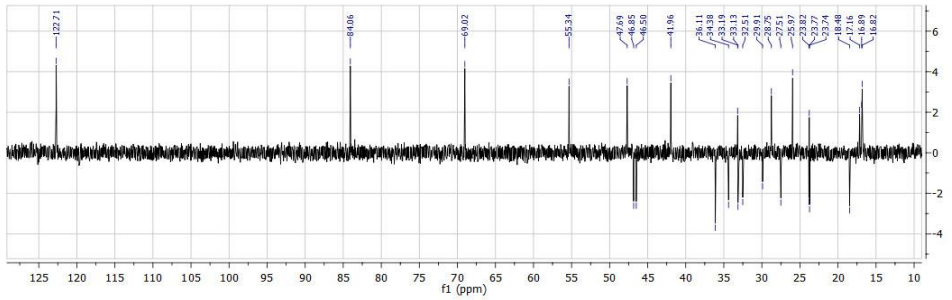

Espectro de ^{1}H RMN del compuesto 5

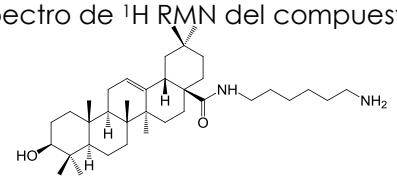

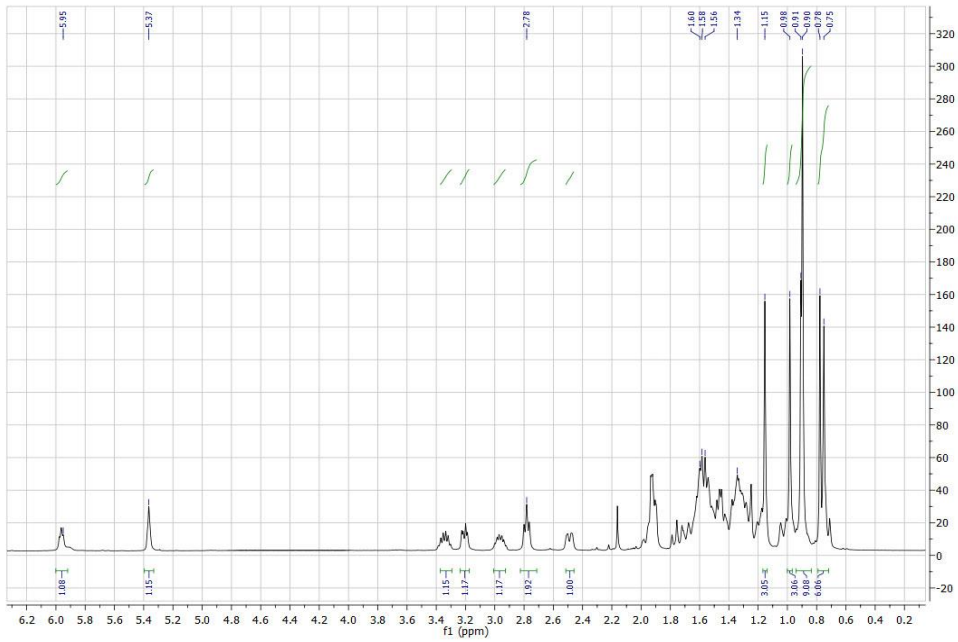

Espectro de ^{13}C RMN del compuesto 5

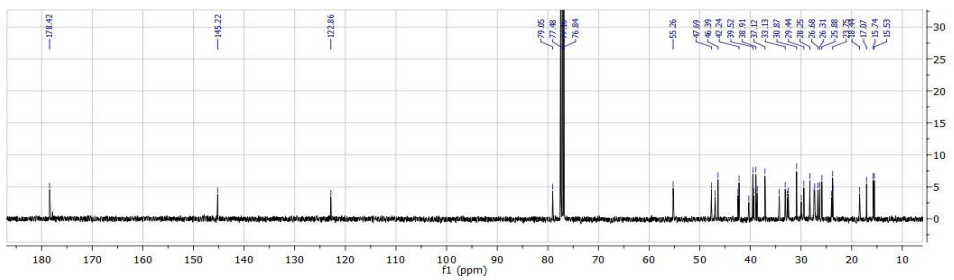

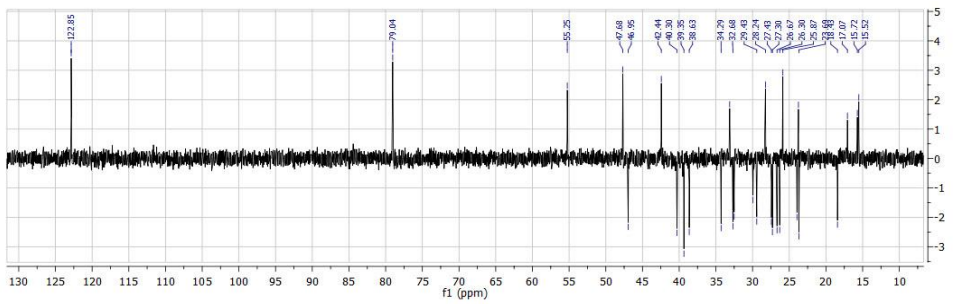

Espectro de ^{1}H RMN del compuesto 6

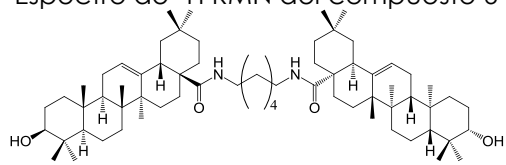

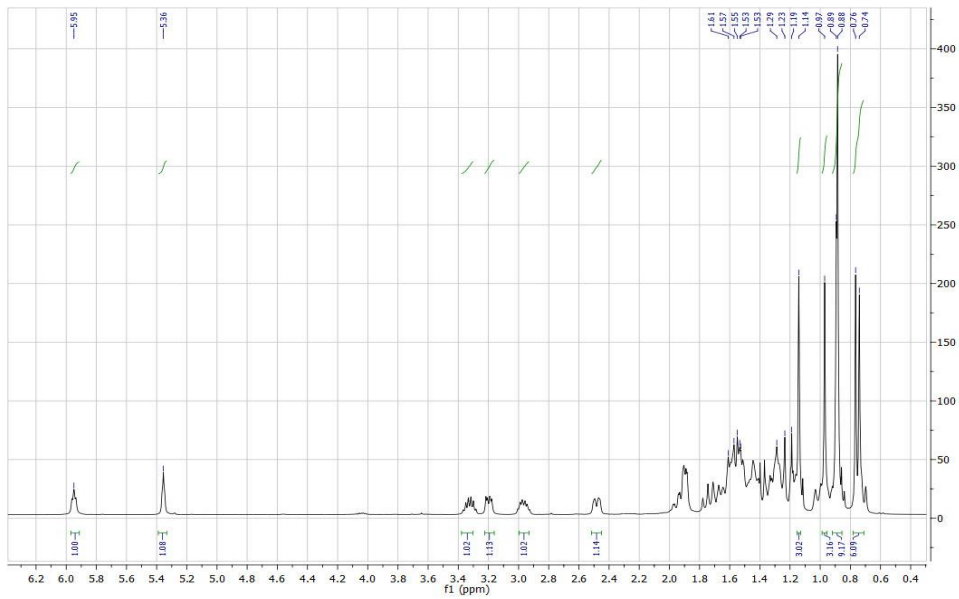

Espectro de ^{13}C RMN del compuesto 6

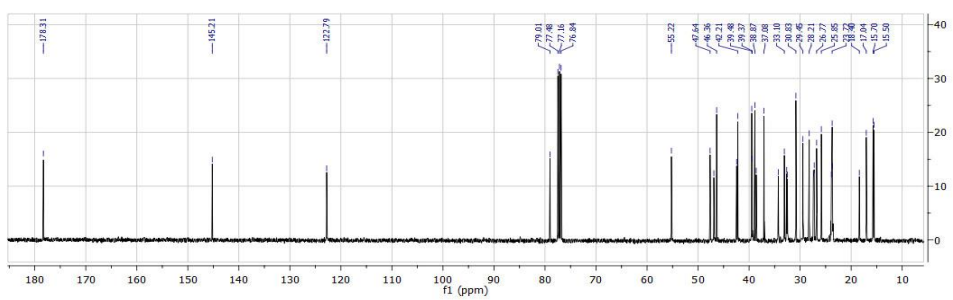

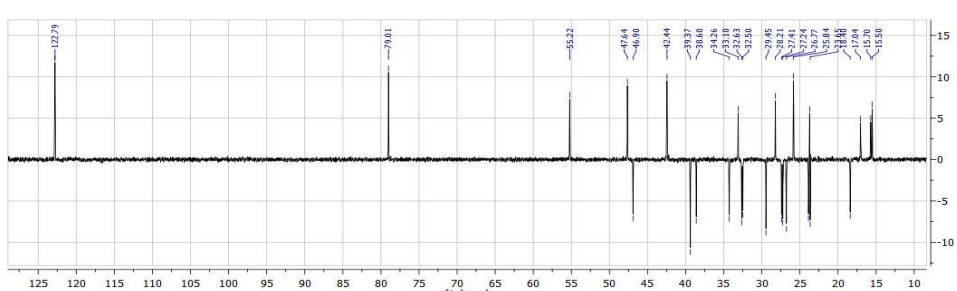

Espectro de ^{1}H RMN del compuesto 7

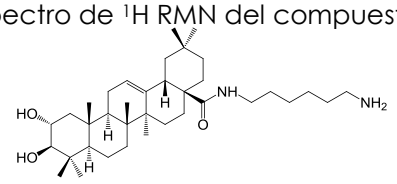

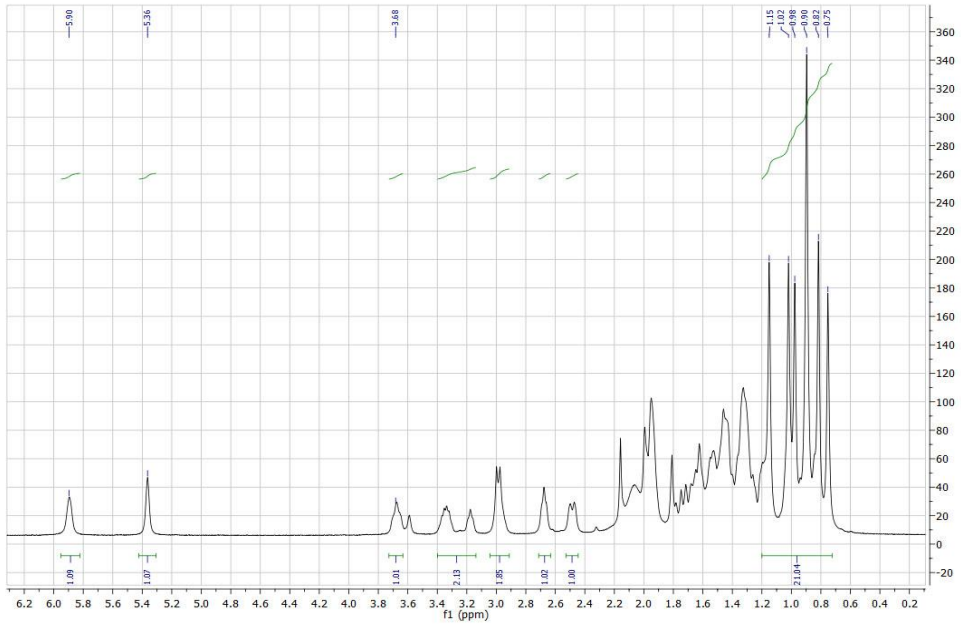

Espectro de ^{13}C RMN del compuesto 7

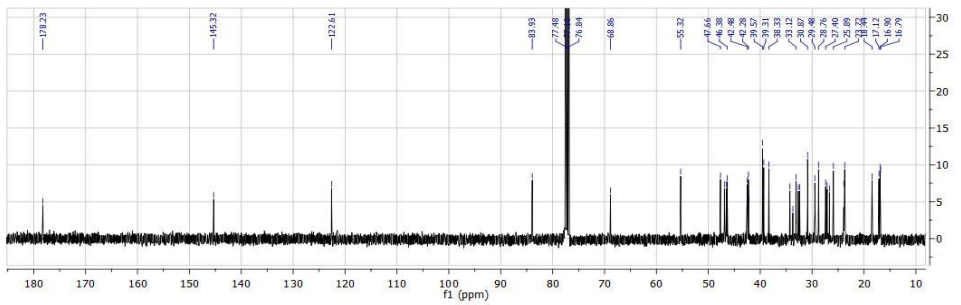

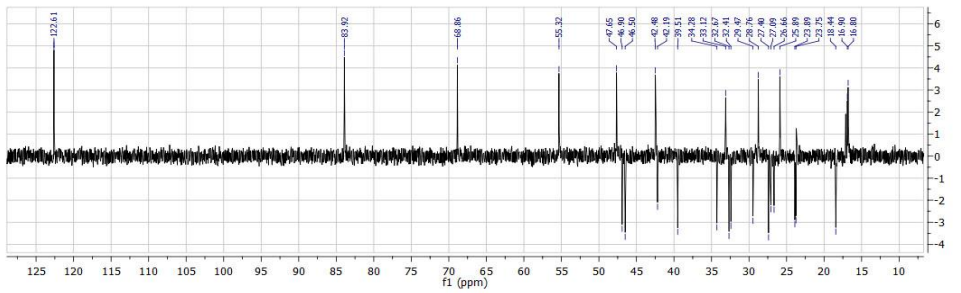

Espectro de ^{1}H RMN del compuesto 8

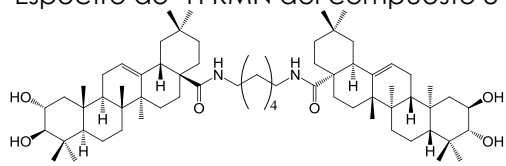

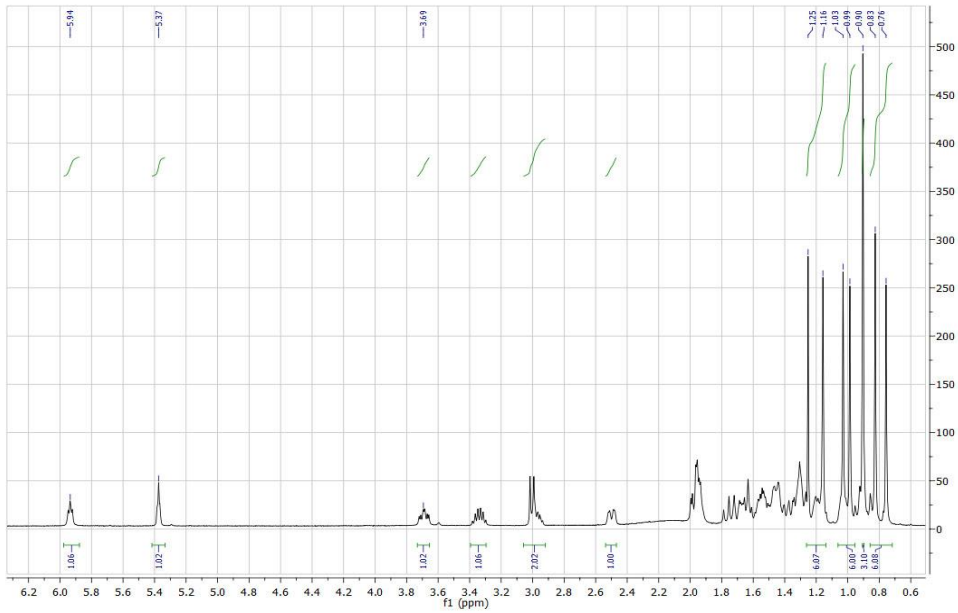

Espectro de ^{13}C RMN del compuesto 8

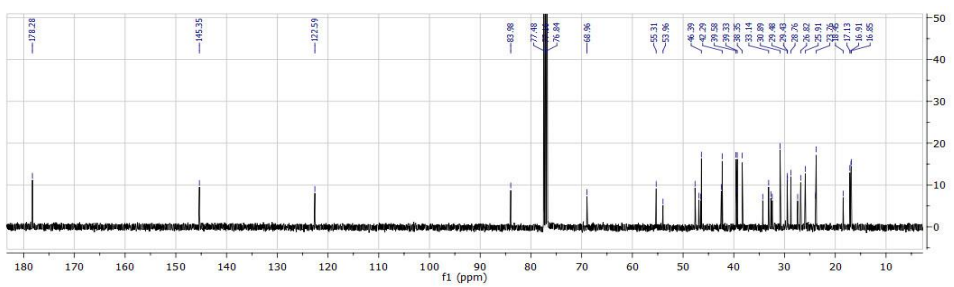

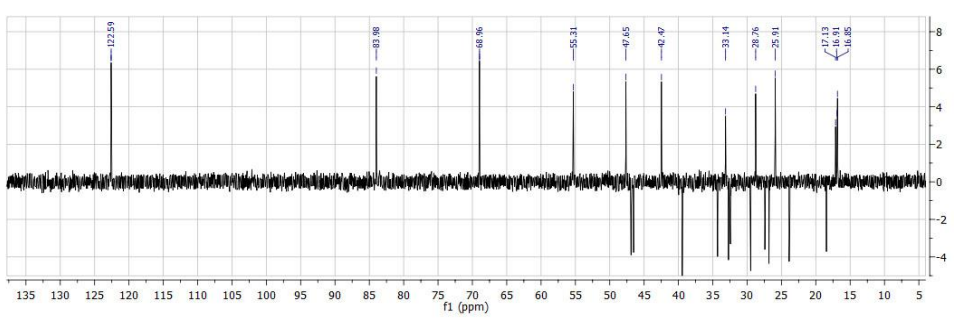

Espectro de ^{1}H RMN del compuesto 9

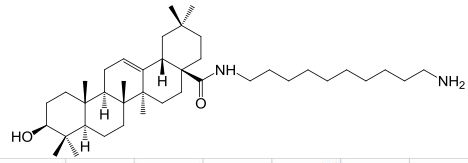

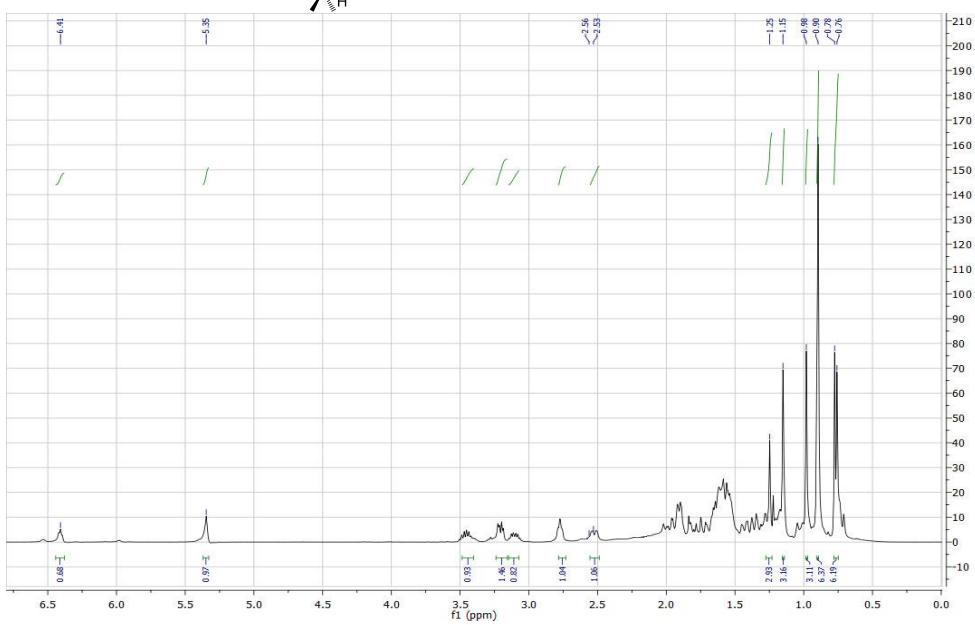

Espectro de ^{13}C RMN del compuesto 9

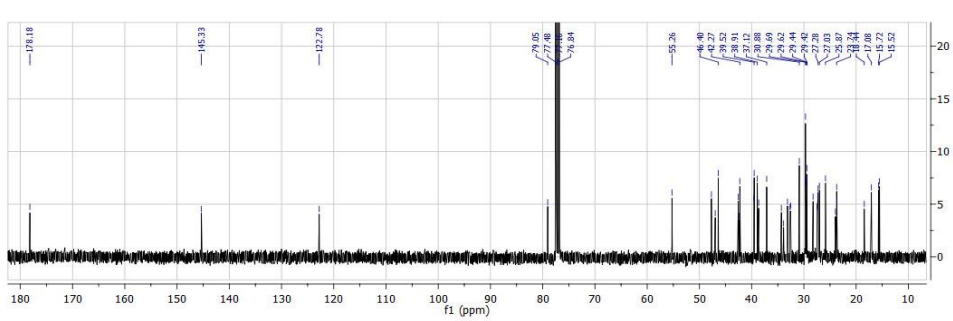

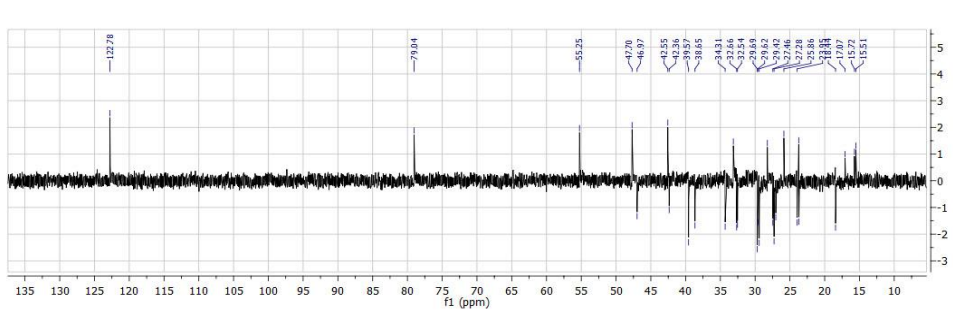

Espectro de ^{1}H RMN del compuesto 10

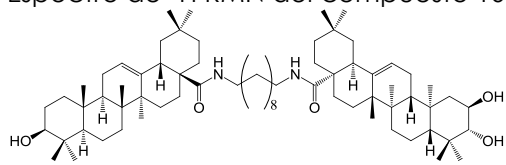

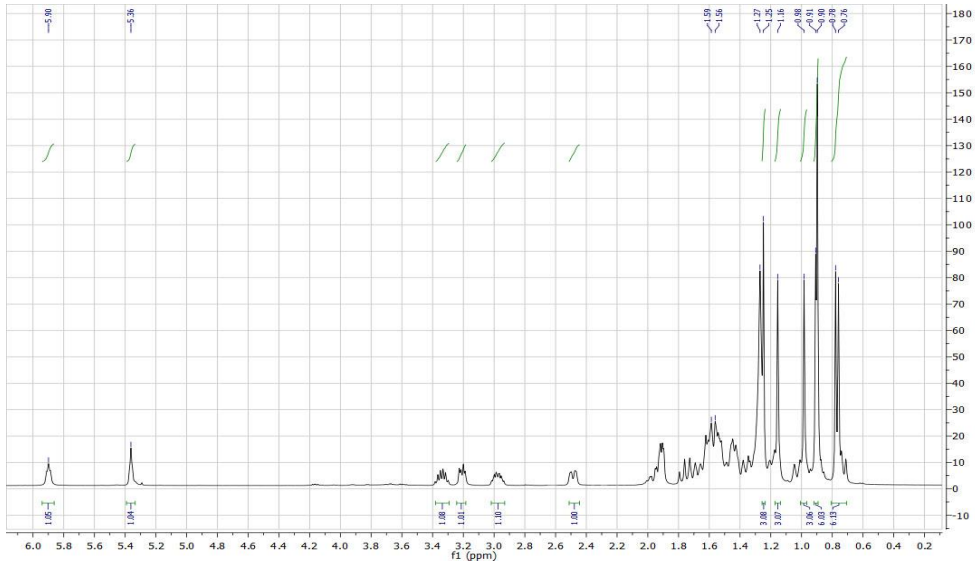

Espectro de ^{13}C RMN del compuesto 10

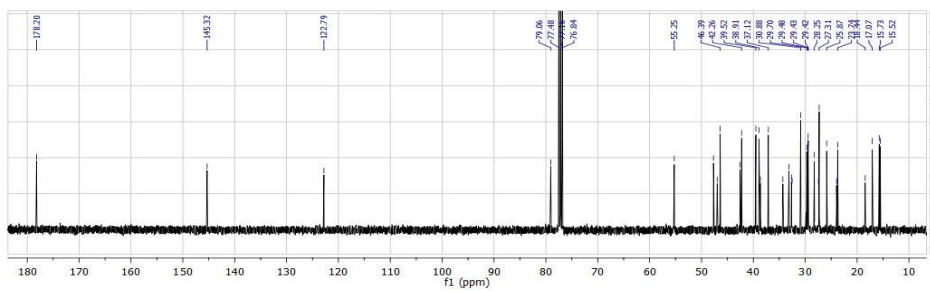

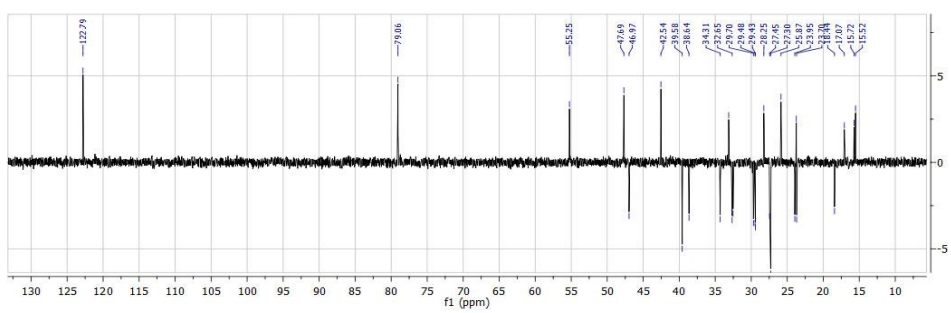

Espectro de ^{1}H RMN del compuesto 11

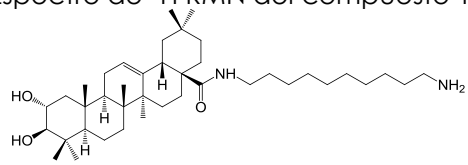

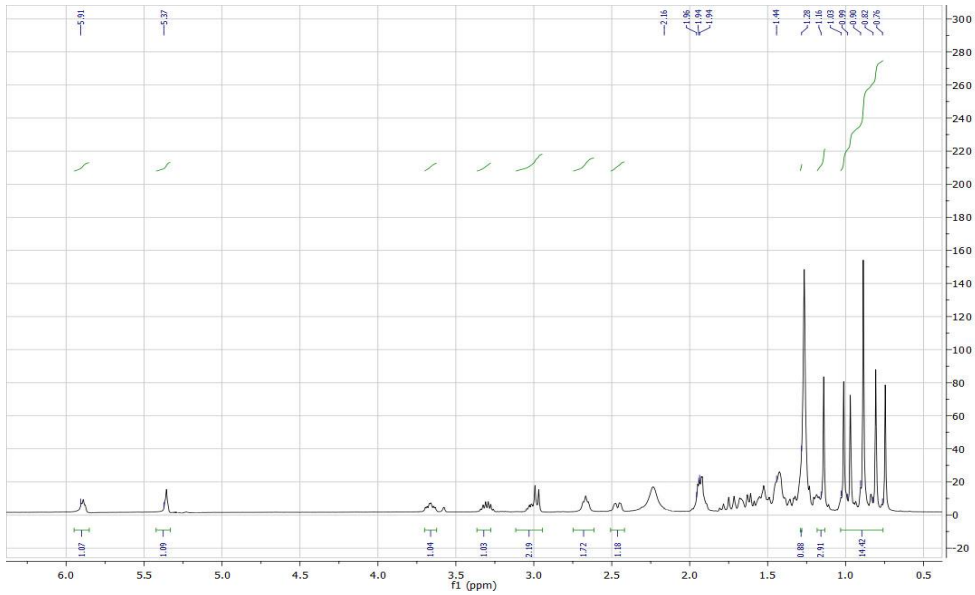

Espectro de ^{13}C RMN del compuesto 11

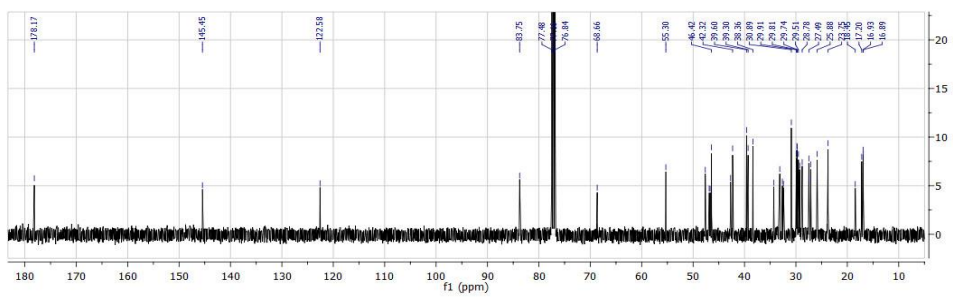

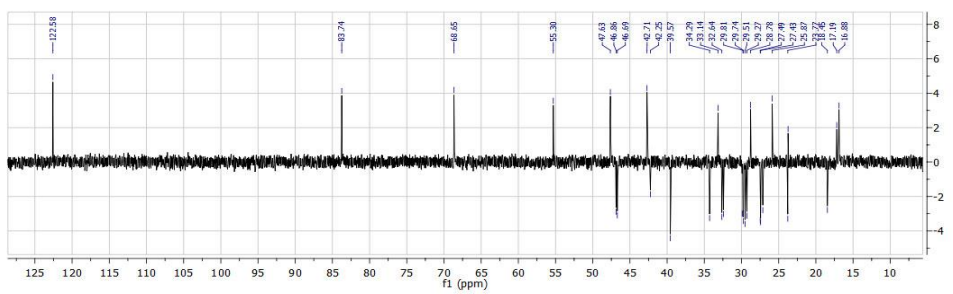

Espectro de ^{1}H RMN del compuesto 12

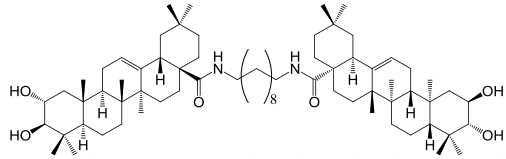

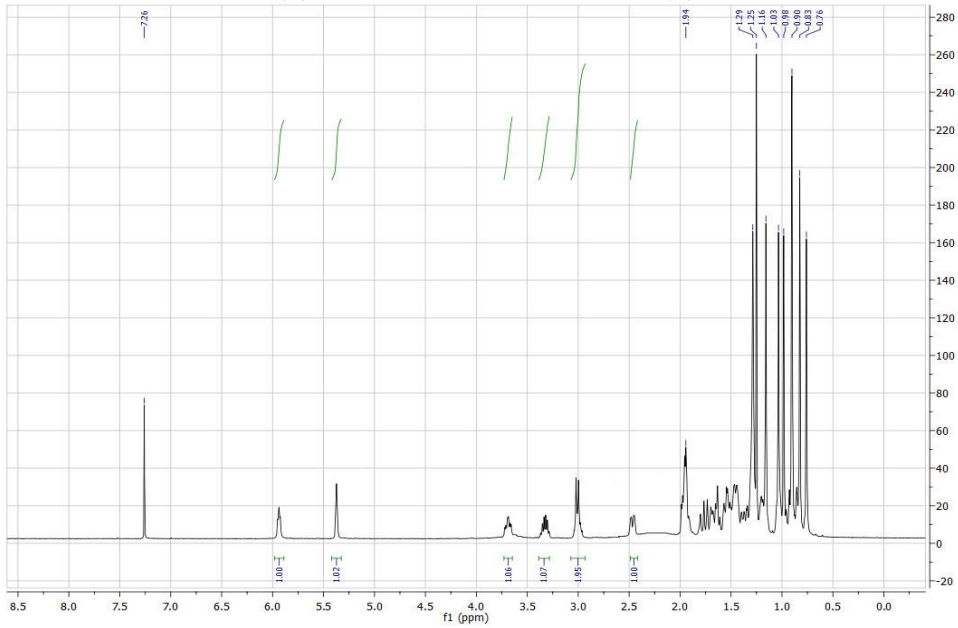

Espectro de ^{13}C RMN del compuesto 12

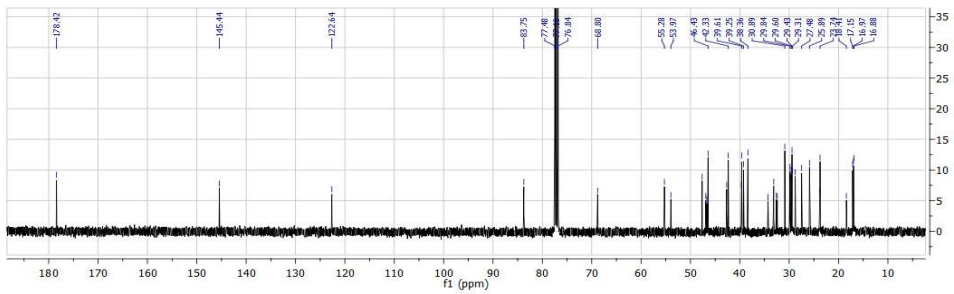

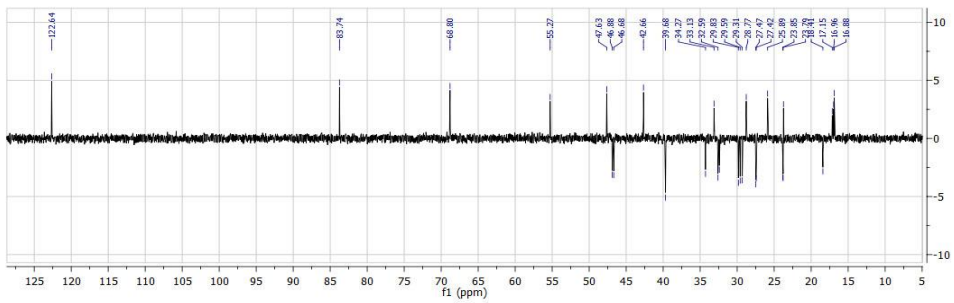

Espectro de ^{1}H RMN del compuesto 13

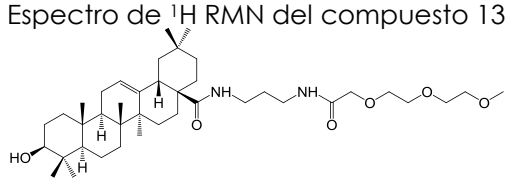

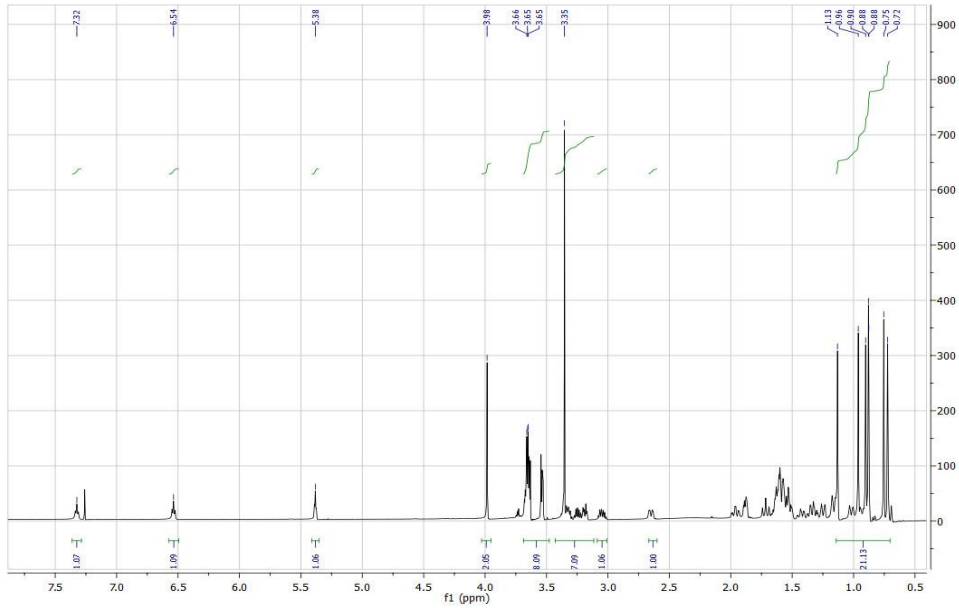

Espectro de ^{13}C RMN del compuesto 13

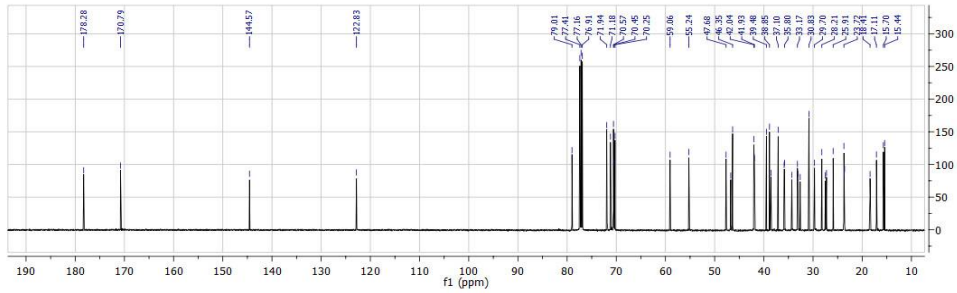

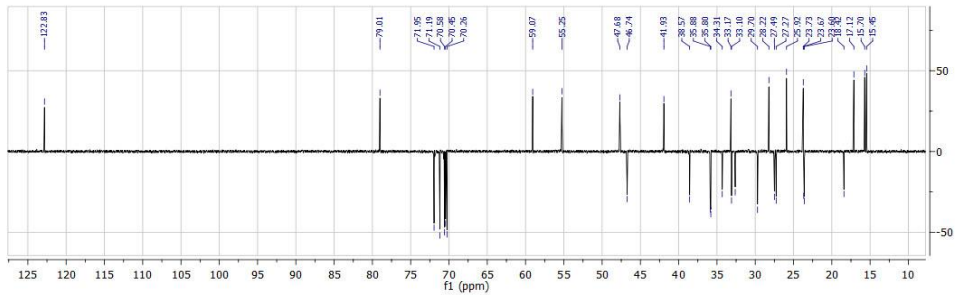

Espectro de ^{1}H RMN del compuesto 14

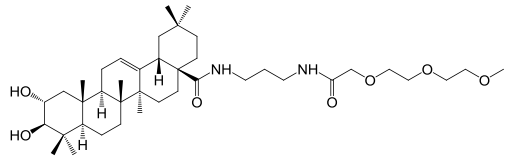

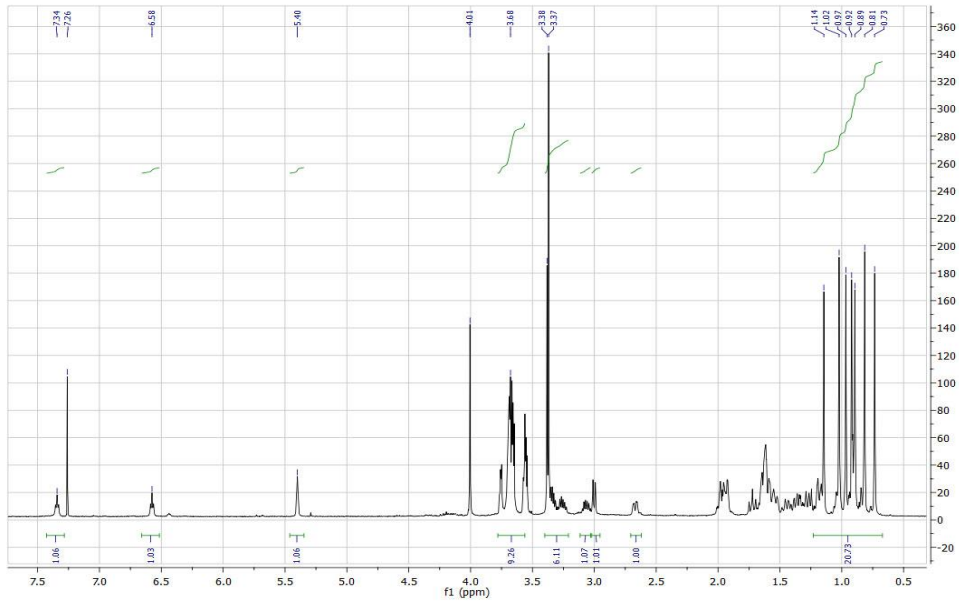

Espectro de ^{13}C RMN del compuesto 14

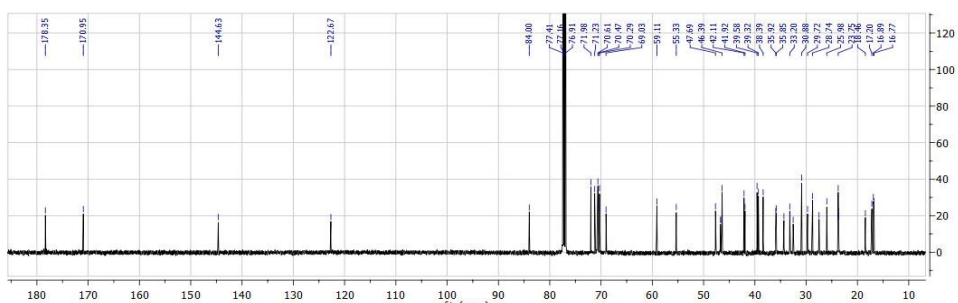

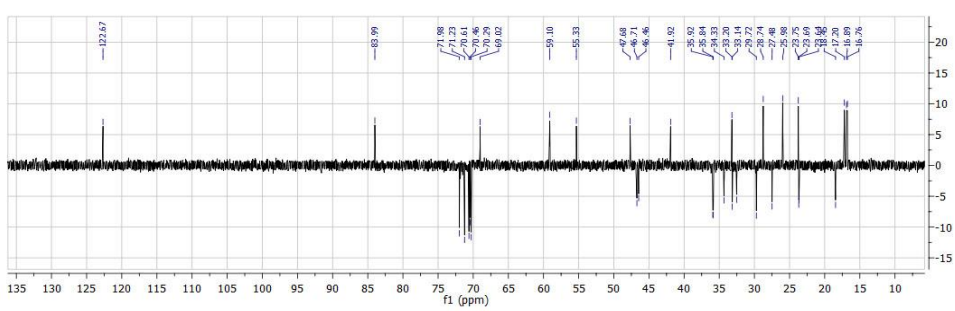

Espectro de ^{1}H RMN del compuesto 15

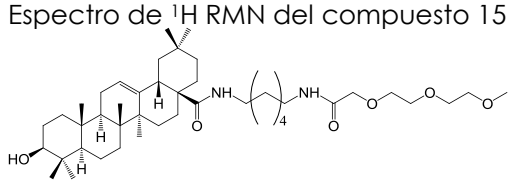

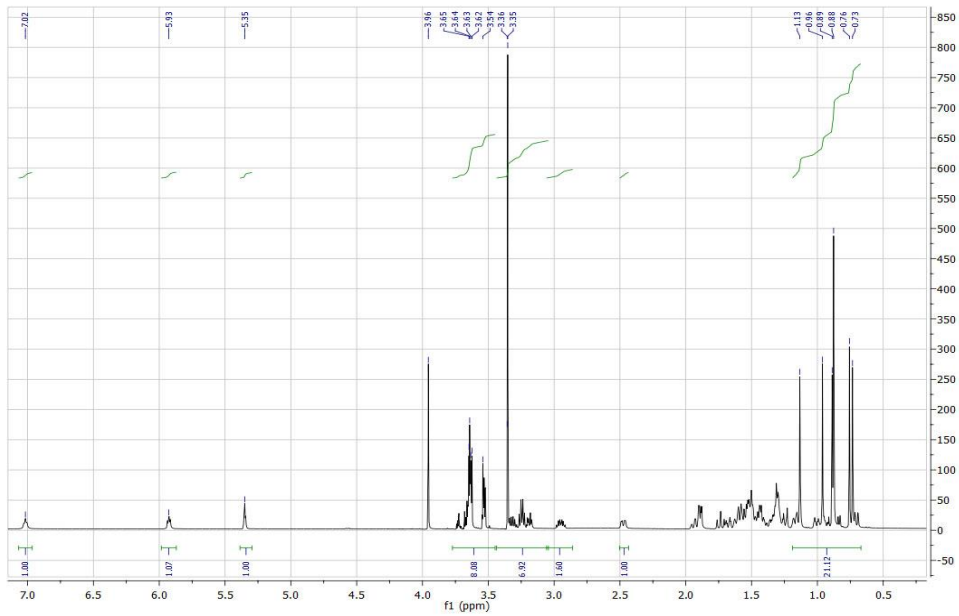

Espectro de ^{13}C RMN del compuesto 15

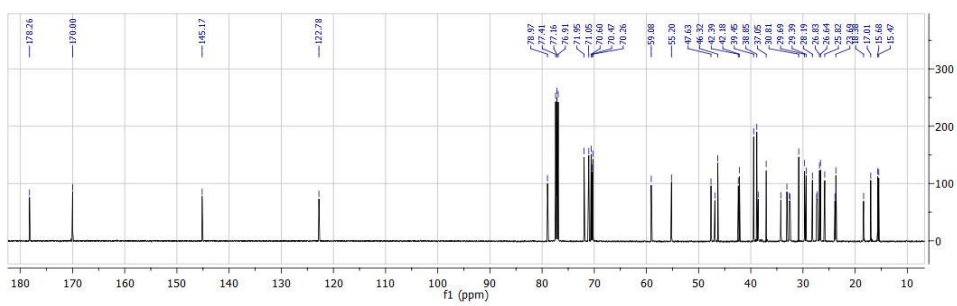

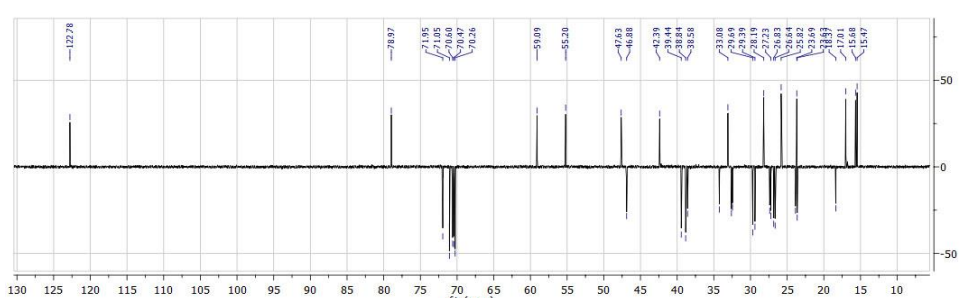

Espectro de ^{1}H RMN del compuesto 16

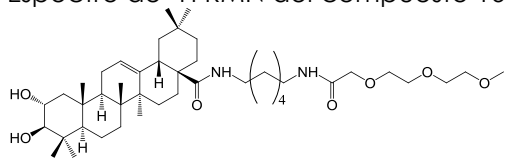

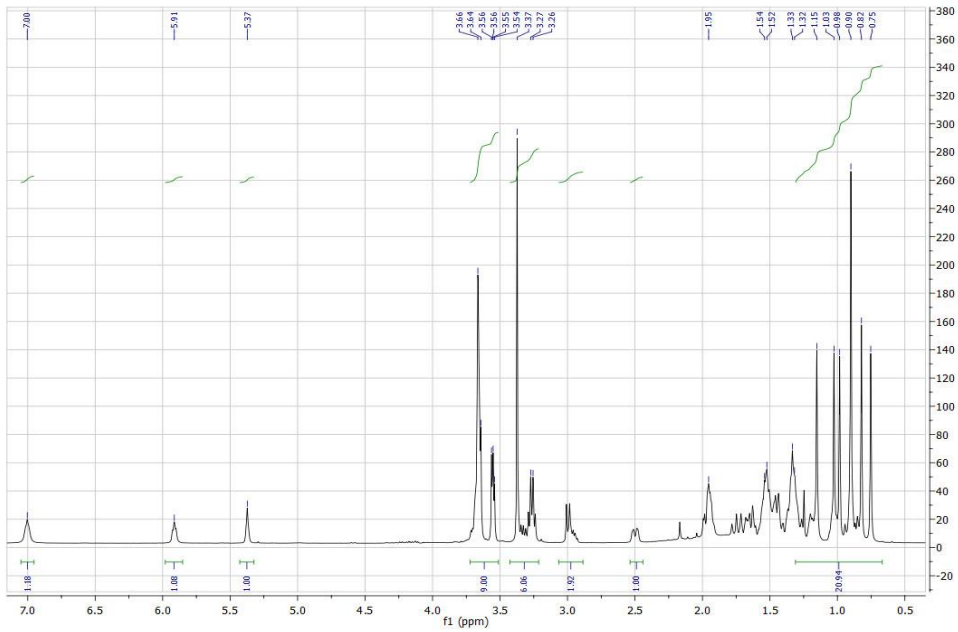

Espectro de ^{13}C RMN del compuesto 16

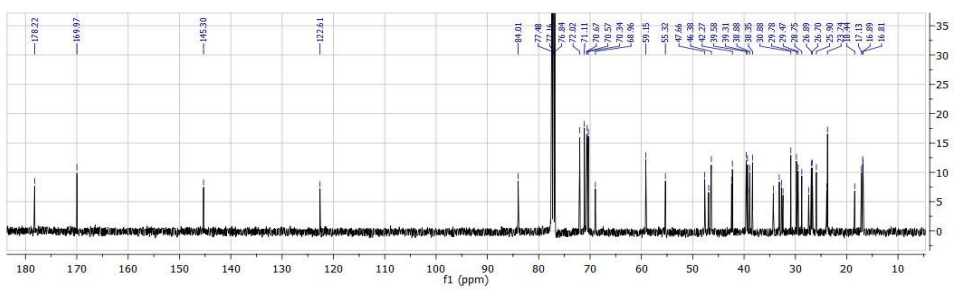

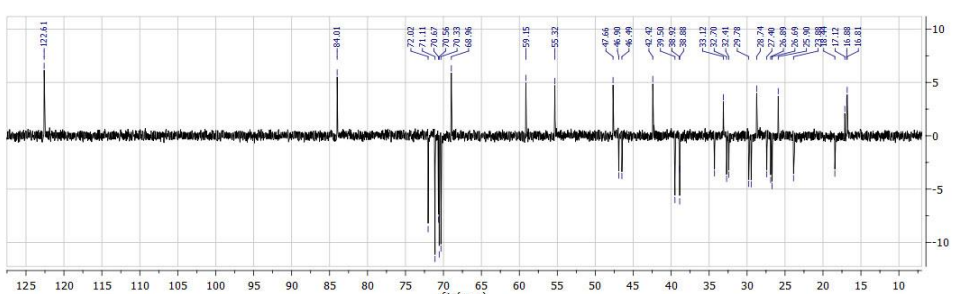

Espectro de ^{1}H RMN del compuesto 17

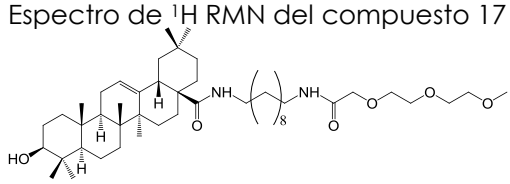

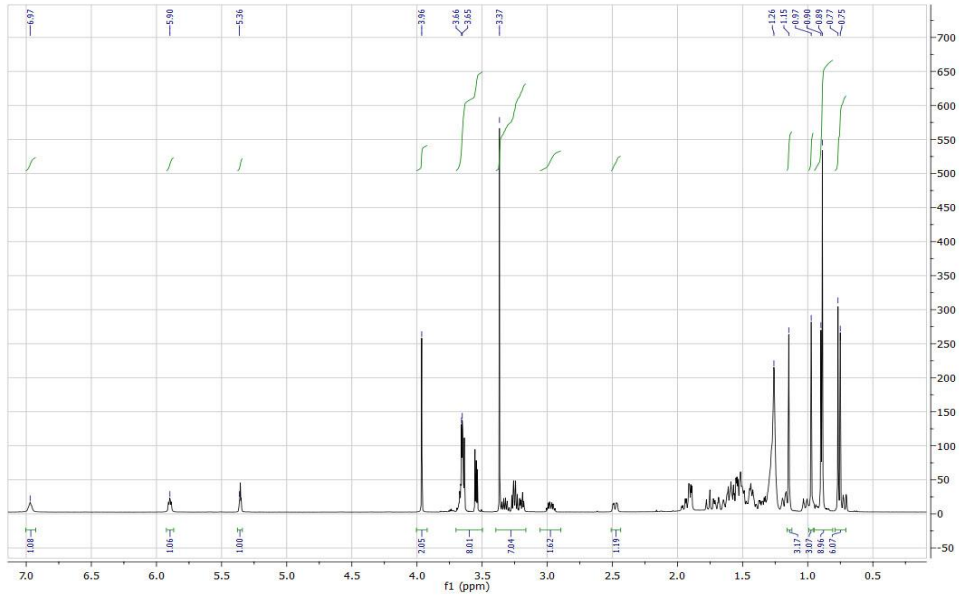

Espectro de ^{13}C RMN del compuesto 17

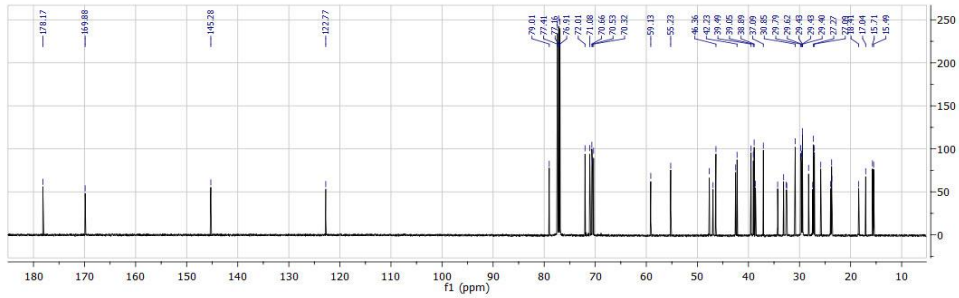

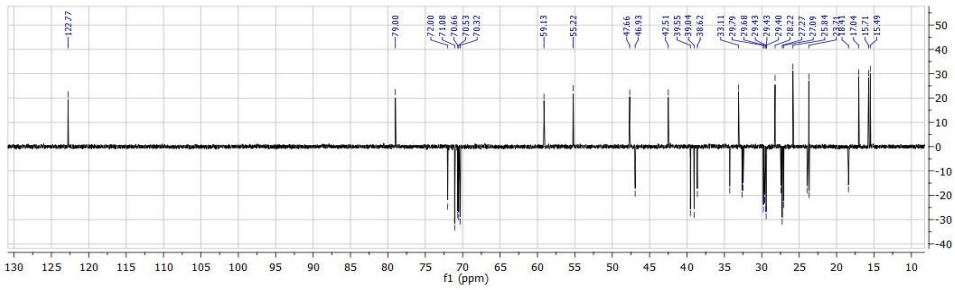

Espectro de ^{1}H RMN del compuesto 18

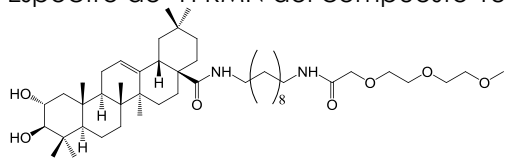

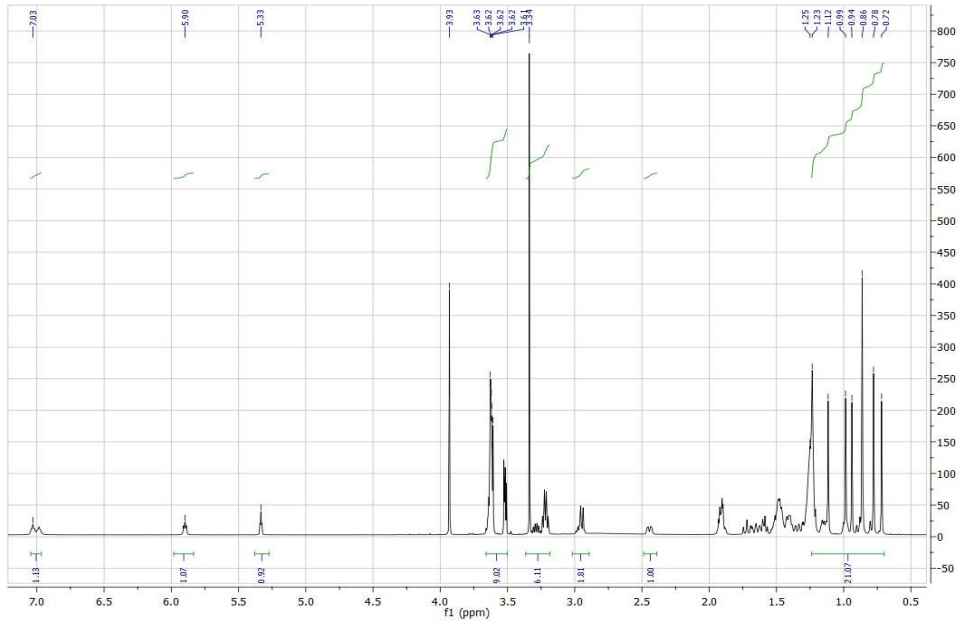

Espectro de ^{13}C RMN del compuesto 18

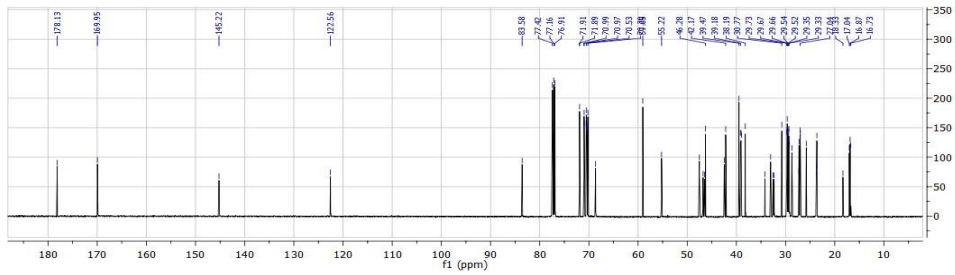

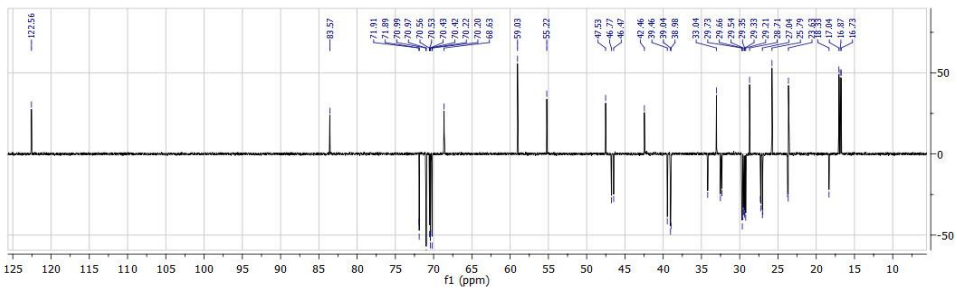

UNIVERSIDAD
DE GRANADA

FACULTAD DE CIENCIAS

Departamento de
Química Orgánica

TESIS DOCTORAL

Marta Medina O'Donnell

Granada, 2017